14 October 2005

Science

Vol. 310 No. 5746
Pages 177–388 $10

Deep Impact

125 YEARS OF GLOBAL Science

AAAS

Mx3005P™ System
Most Flexible

Mx3000P® System
Most Affordable

Performance runs in the family.

Choose the personal QPCR system that's right for you.

Stratagene now offers two affordable, fully-featured quantitative PCR (QPCR) systems. The new five-color Mx3005P™ QPCR System includes expanded features to support a wider range of real-time QPCR applications, such as simultaneous five-target detection and alternative QPCR probe chemistries. The Mx3000P® QPCR System is still the most affordably priced four-color 96-well system available.

- **A four- or five-color instrument, with user-selected filters**
- **Advanced optical system design for true multiplexing capability, and wider application support**
- **QPCR Software with enhanced data analysis and export functionality**

Need More Information? Give Us A Call:

Stratagene USA and Canada
Order: (800) 424-5444 x3
Technical Services: (800) 894-1304 x2

Stratagene Europe
Order: 00800-7000-7000
Technical Services: 00800-7400-7400

Stratagene Japan K.K.
Order: 03-5159-2060
Technical Services: 03-5159-2070

www.stratagene.com

STRATAGENE

Small Samples. Big Results.

A Better Choice.

Ambion's MagMAX™ kits deliver high quality RNA to maximize the success of your gene expression studies.

Advantages of MagMAX technology over glass filter methods:

- Rapid, high throughput isolation of total nucleic acid without cumbersome preprocessing steps
- Higher RNA yields due to more efficient binding and elution of the RNA
- No troublesome filter clogging
- More consistent RNA yields across a variety of sample types and from experiment to experiment
- Low elution volume concentrates RNA for convenient streamlining of downstream applications

Generate the Same High Quality Microarray Data as the "Gold Standard"

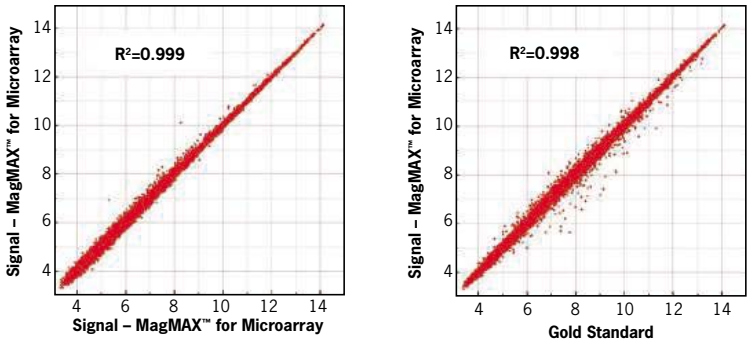

Scatter plot of normalized signal intensities of two mouse kidney total RNA samples using MagMAX™-96 for Microarrays and the Gold Standard. The correlation between samples is 0.999. The correlation between the two methods is 0.998. Greater than 60% percent Present calls were obtained for each method.

MagMAX™

Magnetic Bead-Based Nucleic Acid Isolation Kits

NEW MagMAX™-96 Blood RNA Isolation Kit

NEW MagMAX™-96 for Microarrays Total RNA Isolation Kit

MagMAX™-96 Total RNA Isolation Kit

MagMAX™-96 Viral RNA Isolation Kit

Learn more at
www.ambion.com/prod/magmax

Ambion®
THE RNA COMPANY®

Ambion, Inc.
U.S. 800-888-8804 • Canada 800-445-1161
fax +1-512-651-0201

Ambion (Europe) Ltd
tel +44 (0)1480-373-020
fax +44 (0)1480-373-010

Ambion K.K. (Japan)
tel +81 (0)3-5638-2181
fax +81 (0)3-5638-2182

For a list of Ambion direct free phone numbers and distributors in your country, go to www.ambion.com/contact

Systems Biology — Plasmid DNA Purification

Raising plasmid prep standards again — visual lysis control for greater confidence

New

Insufficient mixing of lysis buffer

Correct mixing of lysis buffer

Correct mixing of neutralization buffer

QIAGEN plasmid kits — now better than ever!

QIAGEN has consistently set the standard for plasmid purification, providing faster preps, higher throughput, more convenience, superior DNA quality for stringent applications, and contract production services. Now our enhanced plasmid prep kits offer even more:

- **Visual lysis control** — a simple color change during cell lysis (blue) and neutralization (colorless), ensures optimal mixing of buffers to give maximum yields of plasmid DNA
- **Color-coded buffer bottles** — easy identification of the correct buffer for added confidence
- **Streamlined handbooks and short protocols** — quickly find the information you need to get rapid results
- **Comprehensive plasmid resource site** — a one-stop Web site containing information on all aspects of plasmid purification at www.qiagen.com/goto/plasmidinfo

Purify your DNA with confidence — use QIAGEN plasmid kits with visual lysis control!

QIAGEN

Systems Biology — Whole Genome Amplification

REPLI-g — perfection in DNA replication: unlimited and precise throughout the whole genome

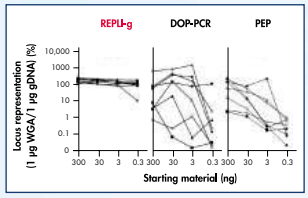

Superior locus representation compared to PCR-based techniques

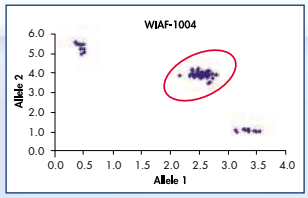

Reliable SNP genotyping

REPLI-g® Kits and Services provide unlimited and precise replication of genomic DNA, allowing precious samples to be expanded, shared, and banked.

- **Reproducible amplification from a variety of starting materials** — including genomic DNA, fresh or dried blood, buccal swabs, fresh or frozen tissue, and cells
- **Highly uniform amplification** — across the whole genome with minimal sequence bias
- **Get more data from your samples** — unlimited DNA for all your downstream applications including SNP genotyping, STR analysis, PCR, sequencing, and arrays
- **Standardized and consistent DNA yields** — enabling direct use in downstream applications without quantification

For perfect and reproducible results, use REPLI-g technology.
Find out more at www.qiagen.com/goto/wholegenomeamplification !

QIAGEN

GE Healthcare

Greater flexibility and binding capacity in histidine-tagged protein purification

Ni Sepharose™ products from GE Healthcare give you the greatest binding capacity available for histidine-tagged protein purification. They offer the flexibility to use a variety of formats and protocols, ensuring the highest possible purity. And with our His GraviTrap™ and HisTrap™ FF crude columns, you can now get pure histidine-tagged proteins directly from unclarified lysate in just 30 minutes.

Maximum target protein activity is assured with Ni Sepharose, thanks to its tolerance of a wide range of additives and negligible nickel ion leakage. With up to four times the capacity of competing products, dramatically increasing your yield while saving on time and resin/buffer costs is no longer pure imagination.

www.amershambiosciences.com/his

imagination at work

GE18-05

Science

Special Issue

Deep Impact

The collision of Deep Impact with the nucleus of Comet 9P/Tempel 1 as seen from the accompanying spacecraft. The nucleus is about 5 kilometers across, and several impact craters can be seen above the impact plume. Analysis of the debris plume by Deep Impact and dozens of telescopes worldwide showed that the nucleus had a low density and provided a view of the previously hidden interior of a comet. [Image: NASA/JPL/University of Maryland]

Volume 310
14 October 2005
Number 5746

Introduction

Research Articles

Reports

Departments

News of the Week

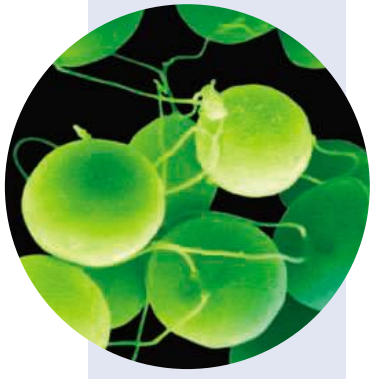

216

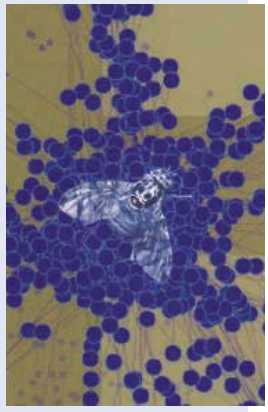

237

News Focus

Letters

Books *et al.*

Policy Forum

Contents continued

Molecular Biology Services

- **Normalization of full-length-enriched cDNA** to facilitate EST projects and functional screenings
- **cDNA depletion** of already analyzed sequences to accelerate expression cloning
- **Subtractive hybridization** to find differentially distributed sequences in cDNA and bacterial genomes
- **Custom construction of cDNA libraries** (from small quantity of RNA, normalized, subtracted cDNA libraries)
- **Gene synthesis, mutagenesis,** and all kinds of PCR and DNA cloning

Fluorescent reporters

- **TurboGFP,** bright green fluorescent protein with extra fast maturation rate
- **PhiYFP,** bright true-yellow fluorescent protein
- **JRed,** red fluorescent protein adapted for protein localization studies
- **PS-CFP2,** most contrast photoactivatable cyan fluorescent protein
- **KFP-Red,** kindling red fluorescent protein

p2FP-RNAi vector, dual color expression vector designed for RNA interference studies

Trimmer-direct, cDNA normalization kit

Evrogen JSC
Miklukho-Maklaya str, 16/10
117997, Moscow, Russia
Tel: +7(095) 4298020
Fax: +7(095) 4298520
E-mail: order@evrogen.com

EVROGEN
www.evrogen.com

Perspectives

Review

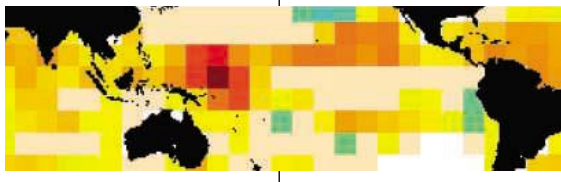

Science Express www.sciencexpress.org

Technical Comment Abstracts

Brevia

Reports

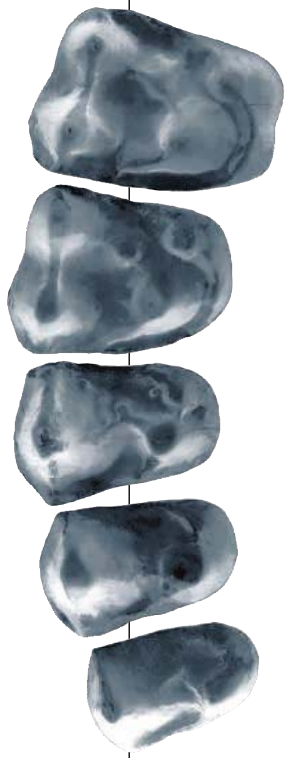

244 & 300

Contents continued

Most citations. Most trusted. Period.

Lipofectamine™ 2000 Transfection Reagent—confidence for success

- One reagent convenience for DNA or RNAi transfection
- Optimized protocols provided for widest range of cell types
- Overwhelmingly more publications cite Lipofectamine™ 2000 Reagent

Lipofectamine™ 2000 Reagent delivers DNA or siRNA with the highest transfection performance for protein expression, gene silencing, and functional assays. Superior efficiency, optimized protocols, and unparalleled success across a broad range of cell lines—Lipofectamine™ 2000 Reagent does it all. With more proven, published results (Figure 1) from apoptosis assays to RNAi pathway elucidation, you can trust Lipofectamine™ 2000 Reagent for your experiments.

Figure 1—Most widely cited transfection reagents

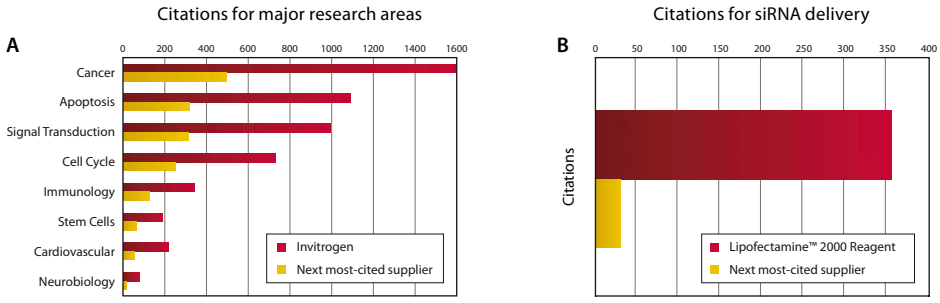

Invitrogen transfection reagents are the most cited in the scientific literature compared to all other suppliers. A. Citation results from the top two transfection reagent companies from January-June 2005 in major research fields. B. For siRNA delivery, Lipofectamine™ 2000 Reagent is cited over ten times more often than the next-cited reagent on the market. Data obtained through www.highwire.org.

Help shape the next generation of proven and trusted delivery technologies.
Visit **www.invitrogen.com/cellchallenge** and share your most challenging experiences with delivery.

invitrogen™

REPORTS CONTINUED

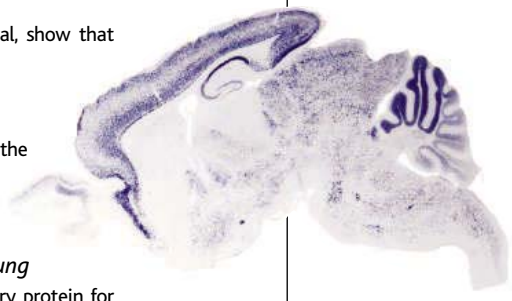

211 & 317

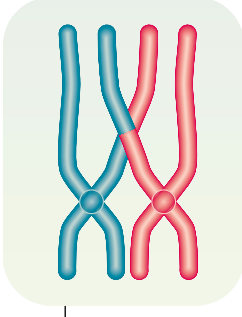

247 & 321

AAAS
ADVANCING SCIENCE, SERVING SOCIETY

SCIENCE (ISSN 0036-8075) is published weekly on Friday, except the last week in December, by the American Association for the Advancement of Science, 1200 New York Avenue, NW, Washington, DC 20005. Periodicals Mail postage (publication No. 484460) paid at Washington, DC, and additional mailing offices. Domestic individual membership and subscription (51 issues): $135 ($74 allocated to subscription). Domestic institutional subscription (51 issues): $550; Foreign postage extra: Mexico, Caribbean (surface mail) $55; other countries (air assist delivery) $85. First class, airmail, student, and emeritus rates on request. Canadian rates with GST available upon request, GST #1254 88122. Publications Mail Agreement Number 1069624. **Printed in the U.S.A.**

Change of address: allow 4 weeks, giving old and new addresses and 8-digit account number. **Postmaster:** Send change of address to *Science*, P.O. Box 1811, Danbury, CT 06813–1811. **Single copy sales:** $10.00 per issue prepaid includes surface postage; bulk rates on request. **Authorization to photocopy** material for internal or personal use under circumstances not falling within the fair use provisions of the Copyright Act is granted by AAAS to libraries and other users registered with the Copyright Clearance Center (CCC) Transactional Reporting Service, provided that $15.00 per article is paid directly to CCC, 222 Rosewood Drive, Danvers, MA 01923. The identification code for *Science* is 0036-8075/83 $15.00. *Science* is indexed in the *Reader's Guide to Periodical Literature* and in several specialized indexes.

Contents continued ▶

Make It Personal

Introducing the BioOdyssey™ Calligrapher™ miniarrayer from Bio-Rad. Now you can print the sample of your choice — DNA, proteins, or cell lysates — onto or into the substrate of your choice — slides, membranes, or 96-well plates — all from your laboratory benchtop.

Your Arrayer, Your Discovery

- Easy-to-use computer software to automatically create grids
- Flow-through wash station and vacuum
- Small footprint to fit easily on your benchtop
- Flexible options to empower your specific research needs — Humidity control module (HCM) to add and reduce humidity, a chilling unit for cooling the work surface, and a software upgrade to give total control of the robot

For more information on microarray systems from Bio-Rad, visit us on the Web at **www.bio-rad.com/ad/calligrapher/**

Visit us on the Web at **discover.bio-rad.com**
Call toll free at 1-800-4BIORAD (1-800-424-6723);
outside the US, contact your local sales office.

BIO-RAD

Science
www.scienceonline.org

Quarterly Author Index
www.sciencemag.org/feature/data/aindex.shl

sciencenow www.sciencenow.org Daily News Coverage

Eggs Won't Run on Empty
Supplying nutrients to egg cells staves off cell death.

Bright, Brief, but No Longer Baffling
Astronomers nail origins of short gamma ray bursts.

Why Only Three Dimensions?
Our reality may have had an evolutionary advantage over other worlds.

Changes in French research careers.

science's next wave www.nextwave.org Career Resources for Young Scientists

Europe: The New Pact for Research in France—What's in It for Young Scientists *E. Pain*
The French government has unveiled a new draft bill to make scientific careers more attractive.

Europe: Cretan Tales *A. Forde*
Two Marie Curie fellows describe their experiences on the island of Crete in Greece.

MiSciNet: No Pubs, No Postdoc? *MentorDoctor*
A chemist feels that his lack of first-author publications hurts his chances for a postdoctoral fellowship.

Career Development Center: Speaking from Experience *D. Houston*
Pharmacology professor Gary Johnson shares lessons from 29 years of academic research.

Career Development Center: International Funding *GrantDoctor*
The GrantDoctor answers questions about funding for scientists overseas.

science's sage ke www.sageke.org Science of Aging Knowledge Environment

Perspective: *C. elegans* Gives the Dirt on Aging *M. Hertweck*
Presentations at the 15th International *C. elegans* Meeting provide new insights on aging.

News Focus: Fatal Hunger *M. Leslie*
Aging eggs might starve to death.

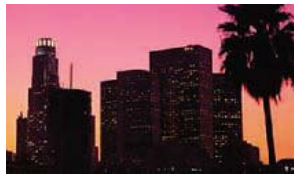

Los Angeles conference stars *C. elegans*.

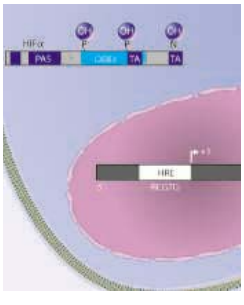

Coordinating the response to hypoxia.

science's stke www.stke.org Signal Transduction Knowledge Environment

Review: Integration of Oxygen Signaling at the Consensus HRE *R. H. Wenger, D. P. Stiehl, G. Camenisch*
Signaling pathways regulate hypoxia-inducible factor abundance and activity to coordinate the response to existing or anticipated hypoxia.

Forum: Open Discussion of Modeling and Computational Approaches to Cellular Signaling
Share your thoughts on how network analysis of protein interactions leads to discovery of new cell signaling participants.

Separate individual or institutional subscriptions to these products may be required for full-text access.

START AUTOMATING

with the fully automatic, bench-top instrument that purifies plasmid and genomic DNA... all with the push of a button.

The Mini-Prep 96

MacConnell RESEARCH

STOP MANUAL MINI PREPS START AUTOMATING

800.466.7949 www.macconnell.com

Faraway Planets

Since the mid-1990s, more than 150 planets have been discovered in orbit around stars outside the solar system. As a result of increased precision and power of planet-search surveys, a wide variety of these objects has been identified. **Santos *et al.*** (p. 251) review these findings and how they relate to theories of planet formation. As the database of exoplanets continues to grow, such observations should answer key questions about chemical and physical processes involved in formation of planetary systems.

Quantum Criticality in a 2DES

Experimental work on a variety of two-dimensional electron systems (2DESs) has shown that the observed metallic behavior is a robust phenomenon, contrary to the insulating behavior expected from scaling considerations. **Punnoose and Finkel'stein** (p. 289) now present a theoretical description of this behavior that includes electron-electron interactions and disorder in the vicinity of the metal-to-insulator transition (MIT). They used renormalization group theory to identify a quantum critical point that separates the metallic and insulating phases of the 2DES. This model can account for the observed anomalous transport and magnetic properties in the vicinity of the MIT.

Prions in Urine?

The factors enabling horizontal prion spread for diseases, including sheep scrapie and chronic wasting disease in deer and elk, have been discussed for many years. **Seeger *et al.*** (p. 324) have found that infectious urinary prions are consistently shed by mice suffering from chronic inflammatory kidney conditions (nephritis) long before any clinical symptoms of scrapie are seen. In the absence of kidney inflammation, or if inflammation occurs in other organs (such as the liver in hepatitis), urinary prion infectivity was never observed, even in transgenic mice that overexpress the prion protein. Thus, inflammation of excretory organs may be one of the cofactors responsible for the spread of prion diseases, and it may be important to screen biopharmaceuticals derived from urine.

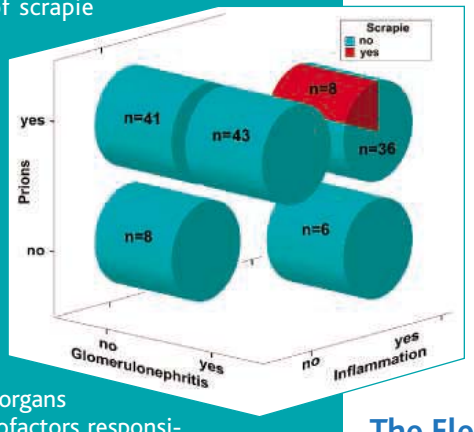

Carving a Steep Slope

Ion-beam irradiation is an important tool for the micro- and nanofabrication of steep sidewall features, but theoretical approaches to understanding the sputtering process are normally formulated as expansions in the opposite limit, that of very shallow slope. **Chen *et al.*** (p. 294) now present a theoretical model that allows for the control of slope during the sputtering process that has a mathematical form that resembles a shock equation. They demonstrate that features created by field-ion bombardment can be sharpened and increase in slope as they get smaller, rather than dissipate.

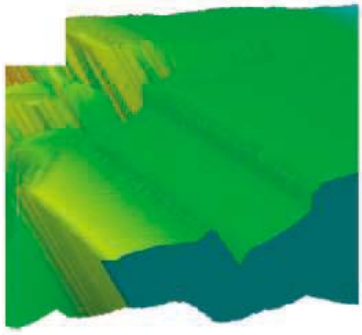

CREDITS (TOP TO BOTTOM): SEEGER *ET AL.*; CHEN *ET AL.*

Ups and Downs of Mantle Melting

Much of the dynamics on Earth are driven by differences in density among liquids or gases, or between liquids and solids. In Earth's deep mantle, dynamics depends on how the density of solid silicate minerals compares with that of likely melt phases. **Stixrude and Karki** (p. 297) have used molecular dynamics simulations to infer the structure of the melt of $MgSiO_3$ perovskite, the dominant mineral in Earth's lower mantle. Their simulations show that with increasing pressure, the coordination of Si in the melt changes from four to six (the solid is six-coordinated) and at pressures near the core, the melt with pure magnesium is nearly as dense as the solid.

Filling an Anthropoid Gap

Anthropoids, the clade that includes higher primates and humans, arose about 45 to 55 million years ago (Ma), but much of their history prior to about 35 Ma is poorly understood. **Seiffert *et al.*** (p. 300; see the Perspective by **Jaeger and Marivaux**) obtained two early anthropoid jaw fragments, with several teeth, from rocks in Egypt dating to about 37 million years ago. These specimens show derived features shared with the much earlier fossils dating to >45 Ma, as well as more abundant later fossils.

The Flexible Bird Catches the Worm

Climate change can lead to mismatches in the seasonal responses of predators and prey. During the last 30 years, the growing season for the caterpillar prey of Dutch great tits occurs earlier in the year, so that the peak of caterpillar abundance is reached before the predator chicks are at their most voracious. **Nussey *et al.*** (p. 304; see the news story by **Pennisi**) investigate whether the current mistiming could be restored. Phenotypic plasticity in egg-laying date would need to be both under selection and heritable, conditions that have not been demonstrated in the wild. The authors find that there is indeed heritable variation among females in their laying date plasticity, and that selection favors highly plastic females.

Illuminating Quantitative Biology

Efforts to model cell biological processes are hampered by a lack of quantitative information on reaction rates, concentration, and stoichiometry. **Wu and Pollard** (p. 310) measured protein concentrations directly in living cells using fluorescence microscopy. Global and local concentrations of 28 cytoskeletal and signaling proteins, fused to yellow fluorescent protein (YFP) in the fission

CONTINUED ON PAGE 193

Roche Applied Science

cOmplete Protease Inhibitor Cocktail Tablets

cOmplete protection.
cOmplete convenience.

EASYpack foil strips make using cOmplete Tablets even more convenient than ever before. Ask your Roche sales representative about this new and improved packaging.

Maximize the convenience of protease inhibition with **cOmplete Protease Inhibitor Cocktail Tablets**, now available in even more convenient *EASYpack* foil strips.

- Simply drop a tablet into your lysis buffer and eliminate the cumbersome job of weighing small amounts of different protease inhibitors.
- Deliver a stable, consistent dose of inhibitor every time.
- Inhibit serine, cysteine, and metalloprotease activity in tissue and cell extracts.
- Choose a tablet for either 10 ml or 50 ml of lysate, with or without EDTA.

For more information on our products for protease inhibition, visit ***www.roche-applied-science.com/proteaseinhibitor***

Product	Cat. No.	Glass Vial	Cat. No.	*EASYpack*
cOmplete	11 697 498 001 11 836 145 001	20 tablets 3 x 20 tablets	04 693 116 001	20 tablets
cOmplete, Mini	11 836 153 001	25 tablets	04 693 124 001	30 tablets
cOmplete, EDTA-free	11 873 580 001	20 tablets	04 693 132 001	20 tablets
cOmplete, Mini, EDTA-free	11 836 170 001	25 tablets	04 693 159 001	30 tablets

Roche Diagnostics

Roche Diagnostics GmbH
Roche Applied Science
68298 Mannheim
Germany

yeast *Schizosaccharomyces pombe*, were tracked. Used with caution, this method provides a precision measuring tool for quantitative biology.

Mitochondria and NO for Longer Life

Calorie restriction extends life span in organisms ranging from yeast to mammals. **Nisoli *et al.*** (p. 314) find that when mice are subjected to calorie restriction, endothelial nitric oxide synthase (eNOS) expression and 3′,5′-cyclic guanosine monophosphate formation are increased. This change is accompanied by mitochondrial biogenesis, increased oxygen consumption, adenosine triphosphate production, and expression of sirtuin 1, a protein previously implicated in mediating the effects of calorie restriction on life span. These effects are strongly attenuated in mutant mice lacking eNOS. Thus, NO may play a role in the processes induced by calorie restriction and in life-span expansion in mammals.

Genetic Clue to Tourette's Syndrome

Tourette's syndrome (TS) is a common psychiatric disorder that is associated with a complex array of behavioral disturbances, most notably motor and vocal tics, and considerable evidence suggests a role for genetic factors. **Abelson *et al.*** (p. 317) show that a small number of patients with TS carry sequence alterations in *SLITRK1*, a gene that is expressed in the brain and that encodes a poorly characterized protein that enhances neuronal differentiation in vitro. Intriguingly, the location of one of these sequence alterations suggests that the *SLITRK1* gene is regulated by microRNAs.

Artificial Transfer of *Wolbachia*

Some species of mosquito harbor the commensal rickettsia-like bacterium *Wolbachia*, which causes cytoplasmic incompatibility—fertile mating only occurs for infected female mosquitoes. Uninfected mosquitoes are eventually replaced by *Wolbachia*-infected mosquitoes within a population, an effect that could be exploited to facilitate control measures. Unfortunately, natural populations of *Aedes aegypti*, the vector for dengue and dengue hemorrhagic fevers, do not harbor *Wolbachia*. **Xi *et al.*** (p. 326) show that *A. aegypti* can be artificially infected in cage experiments with the bacterium obtained from *A. albopictus* and that such infections confer cytoplasmic incompatibility. The infections required an initial 20% infection frequency to obtain saturation after seven generations, with no evidence of maternal inheritance failure.

Extending the Reach of Mirror Neurons

A subset of neurons, the mirror neurons, is active both when an individual performs an action and when the individual observes another individual performing the same action. These findings were made in monkey cortical area F5 in single-neuron recordings. **Nelissen *et al.*** (p. 322; see the news story by **Olsen**), using functional magnetic resonance imaging in awake monkeys, show that such action representation in the frontal lobe is only a small part of the story. They found activity in area F5c that was responsive to full-body images involving grasping movements; diminished responses were seen in this region in response to more abstract images. However, there were responses to more abstract images of grasping movements in more rostral regions of area F5. They also observed responses to action observation as well as to images of objects in area 45B of prefrontal cortex. The authors speculate that monkey areas F5 and 45B, which are thought to be the homologs of human areas BA44 and BA45, may represent ancestral precursors of these speech-related areas in humans.

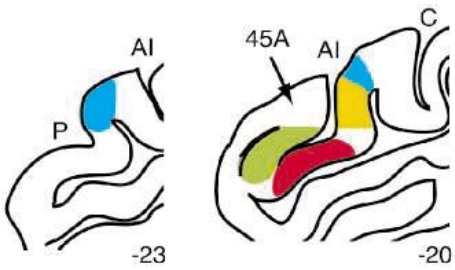

CREDIT: NELISSEN *ET AL.*

Your options are endless

for Protein and Nucleic Acid Detection

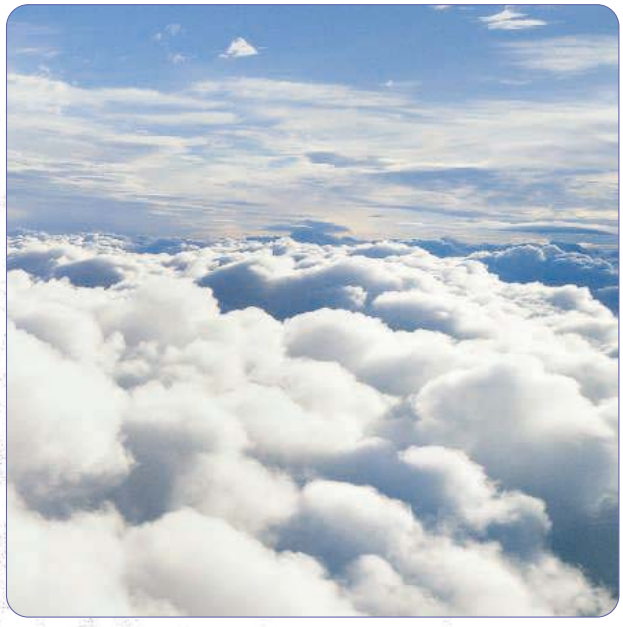

Introducing UltraAmp™

UltraAmp Multi-Assay Signal Amplifiers are revolutionary detection molecules that increase sensitivity in an assay by delivering more labels to a single target than standard labeling methods. UltraAmp reagents have improved signal/noise values up to 200-fold in several applications. With over 70 combinations of targeting moieties and labels, UltraAmp reagents fit into any assay you can create.

Here are just some of the possibilities: Bead-Based Assays, Protein Arrays, ELISA, FISH, Cellular Flow Cytometry, Tissue Arrays, and more...

For more information call: 877.888.3DNA or 215-996-3000 www.genisphere.com

Visit us at the American Society of Human Genetics October 25-29 Booth 702

Genisphere®

SIGNAL + SAMPLE AMPLIFICATION PRODUCTS

Better Never Than Late

Last week, this space contained an editorial by Phillip Sharp, dealing with the difficult problems raised by the publication of information about certain "dual-use" technologies. The term arises because papers dealing with modified human pathogens that are also "select agents" might yield great public health benefits but also could be used by terrorists against that same public. A U.S. National Academies committee chaired by Gerald Fink recommended in a 2003 report that a National Science Advisory Board for Biosecurity (NSABB) be established. As Sharp's editorial reported, that body was consulted with regard to *Science*'s publication of the paper by Tumpey *et al.* on the reconstruction of the 1918 Spanish influenza virus. It voted unanimously in favor of publication.

That may sound like a happy ending, but it wasn't entirely happy nor is it the whole story. The paper's history contains some lessons about how this kind of dual-use problem should be managed. We recognized that the work might raise questions about the propriety of publication, and we considered this during the process of scientific peer review. We followed an established procedure in which we solicit views from experts who have knowledge about security issues. The authors located at the U.S. Centers for Disease Control and Prevention (CDC) were urged to consult with CDC Director Julie Gerberding and with Anthony Fauci, director of the U.S. National Institute of Allergy and Infectious Disease. Amy Patterson, director of the Office of Biotechnology Activities (the office responsible for NSABB matters) at the National Institutes of Health, was also informed. All three felt that the public health benefits of the study far outweighed any biosecurity risks.

Having received these assurances by 16 September and thus confident about moving forward, we were prepared to send pages to the printer early in the week of 26 September. On that day, the editorial staff went off to *Science*'s annual retreat in West Virginia. Alas, on the evening of 27 September, a call was relayed from the Office of the Secretary of the U.S. Department of Health and Human Services (HHS), indicating belated concerns about the paper.

There followed a series of conference calls involving various HHS officials, including Patterson and Assistant HHS Secretary Stewart Simonson, who reported that HHS Secretary Michael Leavitt was insisting on review by the NSABB. I told them that in 24 hours the issue would be at the printer, and reminded them that the NSABB's own charter makes it clear that it does not screen individual papers. Simonson ordered that the NSABB committee be polled—just as the issue was being printed—and a day later, we learned of its approval. A virologist on the NSABB board suggested adding an editorial addressing some of the biosecurity issues. We gave them this page: Phillip Sharp was persuaded to write a piece on short notice, and produced splendidly. He and I did some final edits on Sunday night so that it could be squeezed into the issue at the last possible moment.

What can be learned from all this? To begin with, *Science* did the right thing in consulting with the proper authorities, both our own and those at HHS. The 11th-hour intervention from the secretary's office, it has been explained to us, was to give the NSABB a real experience with a "live" issue. That may have been a useful purpose, but it did cause some hardship to editors and authors alike. There are other issues in such cases that should concern the scientific community. First, there is a real question of authority here. Government officials can advise, and should be listened to thoughtfully. But they can't order the nonpublication of a paper just because they consider the findings "sensitive." No such category short of classification exists, as the Reagan-era Executive Order National Security Decision Directive 189, still in force, makes clear. If a paper should not be published because of biosecurity risks, then it should be classified. Second, the NSABB should regard this first exercise as a helpful one-off and turn to its mandate of developing principles rather than making decisions on individual papers.

So would I, given our own convictions, the timing, and what we had learned from our consultations with Gerberding, Fauci, and others, have published the paper even if the NSABB had voted otherwise? Absolutely—unless they had it classified.

Donald Kennedy
Editor-in-Chief

10.1126/science.1120965

CREDIT: SCIENCE

Who says there are no more Heroes?

The American Chemical Society is proud to honor the 2005 Heroes of Chemistry.

Through innovations founded on chemistry, these industrial scientists have created successful commercial products that attack conditions affecting the quality of millions of lives, improve our air and water quality, and enable technologies that make modern life possible.

Colgate-Palmolive Company | *Abdul Gaffar*
For the development of the technology for Colgate Total® toothpaste, the only toothpaste approved by the FDA for controlling dental diseases.

ExxonMobil Corporation | *Garland Brignac, Bruce Cook, Richard Demmin, John Greeley, Thomas Halbert, Jeffrey Kaufman, Mark Lapinski, Steve Mayo, Craig McKnight, and Kenneth Riley*
For the development of SCANfining and SCANfining II refinery processes that reduce sulfur in gasoline, thereby improving air and water quality.

IBM | *Hiroshi Ito and C. Grant Willson*
For the development of chemically-amplified resist materials which are the universal standard for creating smaller, denser chips and microprocessors.

Johnson & Johnson Pharmaceutical Research & Development | *Ludo Kennis*
For the development of Risperdal, a standard in the treatment of psychosis, revolutionizing anti-psychotic treatments.

Novartis Institutes for BioMedical Research | *Peter Graf, Ulrike Pfaar, Peter Traxler, and Jürg Zimmermann*
For the development of Gleevec, a treatment for chronic myeloid leukemia, which converts the disease into a treatable condition.

http://chemistry.org/heroes

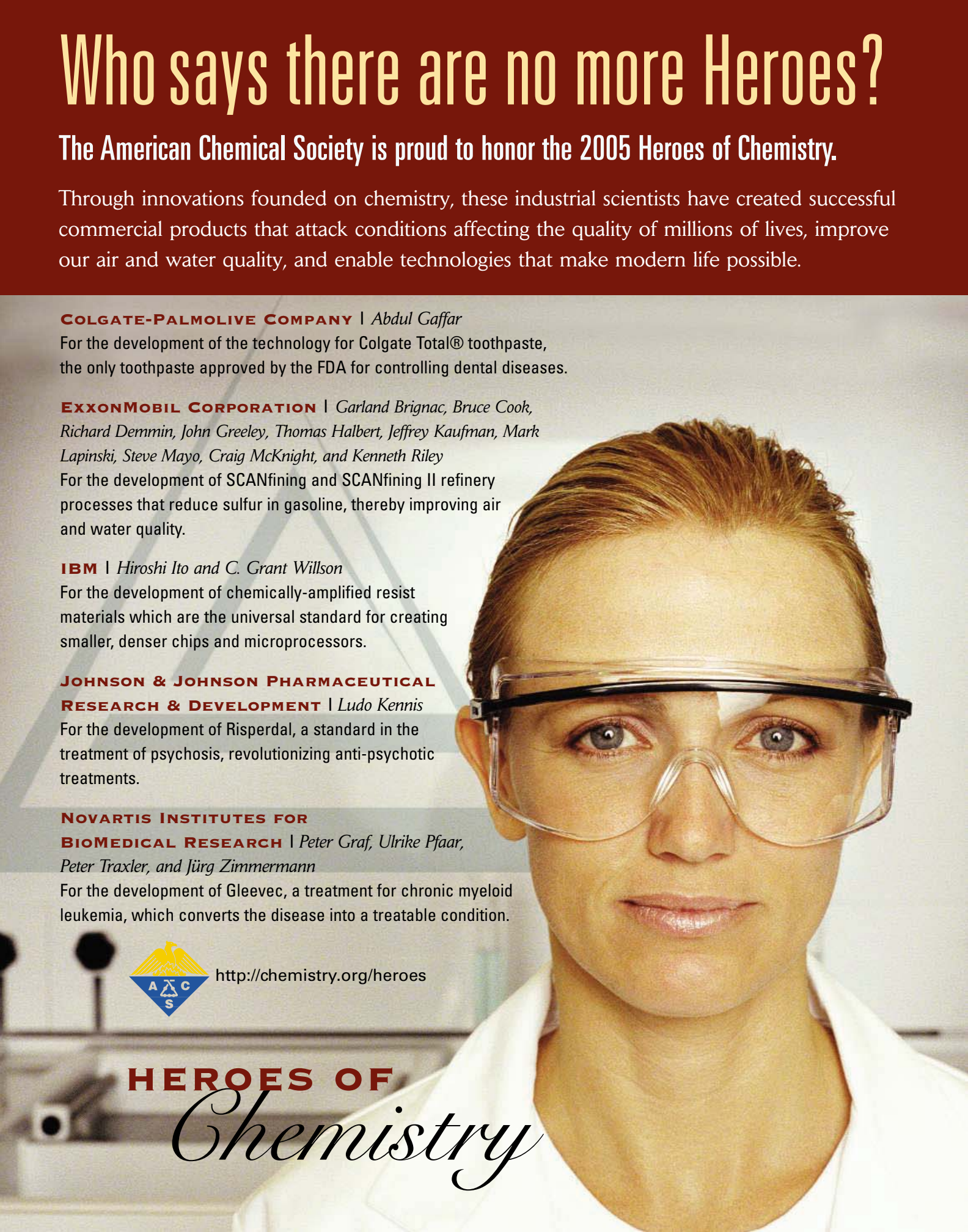

HEROES OF *Chemistry*

EDITORS' CHOICE

edited by Stella Hurtley

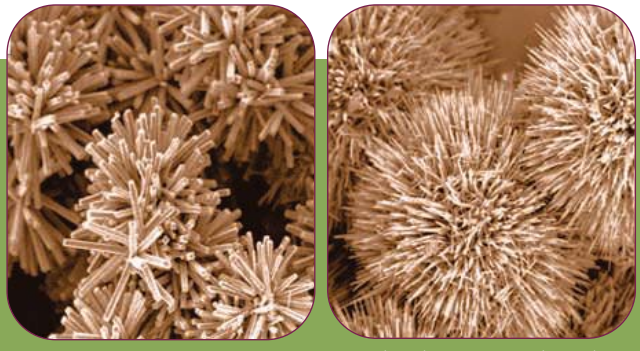

Dendritic structure produced at 120°C (left) and 180°C (right).

CHEMISTRY

Inorganic Dendrites

Manganese oxides are used in batteries, chemical separation, and catalysis because of their porosity, acidity, and ion exchange properties. Organic templates have been used to make complex architectures but require subsequent purification of the end product with the risk of residual organic material remaining as impurities. Manganese oxides have previously been fabricated into octahedral molecular sieves that possess microporous tunnel structures, but the particles have not possessed uniform shapes or any sort of three-dimensional ordering. Yuan *et al.* have now developed a synthesis protocol that mixes potassium dichromate and manganese sulfate monohydrate under mild hydrothermal conditions to generate defined three-dimensional structures. Control of the resulting structures is achieved solely by varying the autoclave temperature from 120° to 180°C. Smaller crystals form at the higher temperature, creating a dendritic structure with finer and denser needlelike branches. The key to the control comes from the fact that the redox potential of $Cr_2O_7^{2-}/Cr^{3+}$ is only slightly larger than that of Mn^{4+}/Mn^{2+}, so that the reaction is slow. This gives precise control over the nucleation and growth processes leading to highly uniform dendritic structures. — MSL

J. Am. Chem. Soc. 10.1021/ja053463j (2005).

BIOCHEMISTRY

Protein Waves

Molecular dynamics are essential to protein stability and function. Nuclear magnetic resonance methods can measure residual internuclear dipolar couplings, which report on the average orientations of internuclear vectors on the slow time scales that are important for many biological processes (up to milliseconds). Bouvignies *et al.* took an in-depth look at the dynamics of an immunoglobulin-binding domain of streptococcal protein G and identified a long-range network of correlated motions. In the β sheet, an alternating pattern of dynamics resembled a standing wave: Nodes were associated with strongly hydrophobic side chains buried in the core of the protein that probably anchor the backbone motions as they propagate across the β sheet. The motion was correlated across hydrogen bonds, suggesting that dynamic information is transmitted across hydrogen bond networks. Independent confirmation of the dynamic network was provided by hydrogen-bond scalar coupling analysis. The amplitude of motion increased across the sheet, so that the greatest flexibility was in the strand that interacts with the antigen-binding domain of immunoglobulin G. Similar processes of information transfer through hydrogen bond networks may be important in processes such as allosteric regulation. — VV

Proc. Natl. Acad. Sci. USA **102**, 13885 (2005).

ECOLOGY/EVOLUTION

Geography of Gene Swapping

Horizontal gene transfer between unrelated species has not been uncommon in the course of biological evolution. Recently discovered examples have included the transfer of mitochondrial genes from parasitic flowering plants to their flowering plant hosts, and vice versa. Davis *et al.* now document horizontal gene transfer between more distantly related plants: Part of the mitochondrial genome of the rattlesnake fern, *Botrychium virginianum*, appears to be derived from sequences characteristic of mitochondria of the parasitic sandalwoods and mistletoes. The angiosperm sequences are present across the entire Northern Hemisphere range of the rattlesnake fern but are absent from any of its close relatives. These and other biogeographic and life-history data suggest that the horizontal gene transfer occurred quite recently in the ancestry of *B. virginianum* and was followed by rapid expansion to its current wide distribution. How this transfer occurred remains speculative—plausible mechanisms include direct transfer from a now-extinct parasite to an ancestor of the fern, or indirect transfer via mycorrhizal fungi. — AMS

The rattlesnake fern, *B. virginianum*.

Proc R. Soc. London Ser. B 10.1098/rspb.2005.3226 (2005).

HUMAN GENETICS

An RNA of Stature

Human growth and stature are regulated in part by the signaling pathways that control cell division and growth. Molecular insights into these pathways have come from the analysis of human mutations that confer clinical abnormalities in stature. One interesting example is cartilage-hair hypoplasia (CHH), a mild form of dwarfism that has been traced to mutations in the RNA subunit of a ribonucleoprotein enzyme (MRP) that cleaves RNA but whose mechanistic role in pathogenesis has been unclear.

Thiel *et al.* now show that different mutations in MRP RNA cause anauxetic dysplasia, a rare genetic disorder characterized by extreme short stature (adult height <85 cm). After comparing the various mutant RNAs in functional assays, the authors suggest that the clinical differences may arise from differential effects of the mutations on two distinct cellular pathways. Whereas the anauxetic dysplasia mutations appear to severely disrupt processing of ribosomal RNA (presumably leading to inhibition of protein synthesis), the CHH mutations have a modest effect on this pathway but simultaneously disrupt the

CONTINUED ON PAGE 199

CREDITS: (TOP) YUAN *ET AL.*, *J. AM. CHEM. SOC.* 10.1021/JA053463J (2005); (BOTTOM) ROBBIN MORAN

MOVE BEYOND TRADITIONAL PCR LIMITATIONS

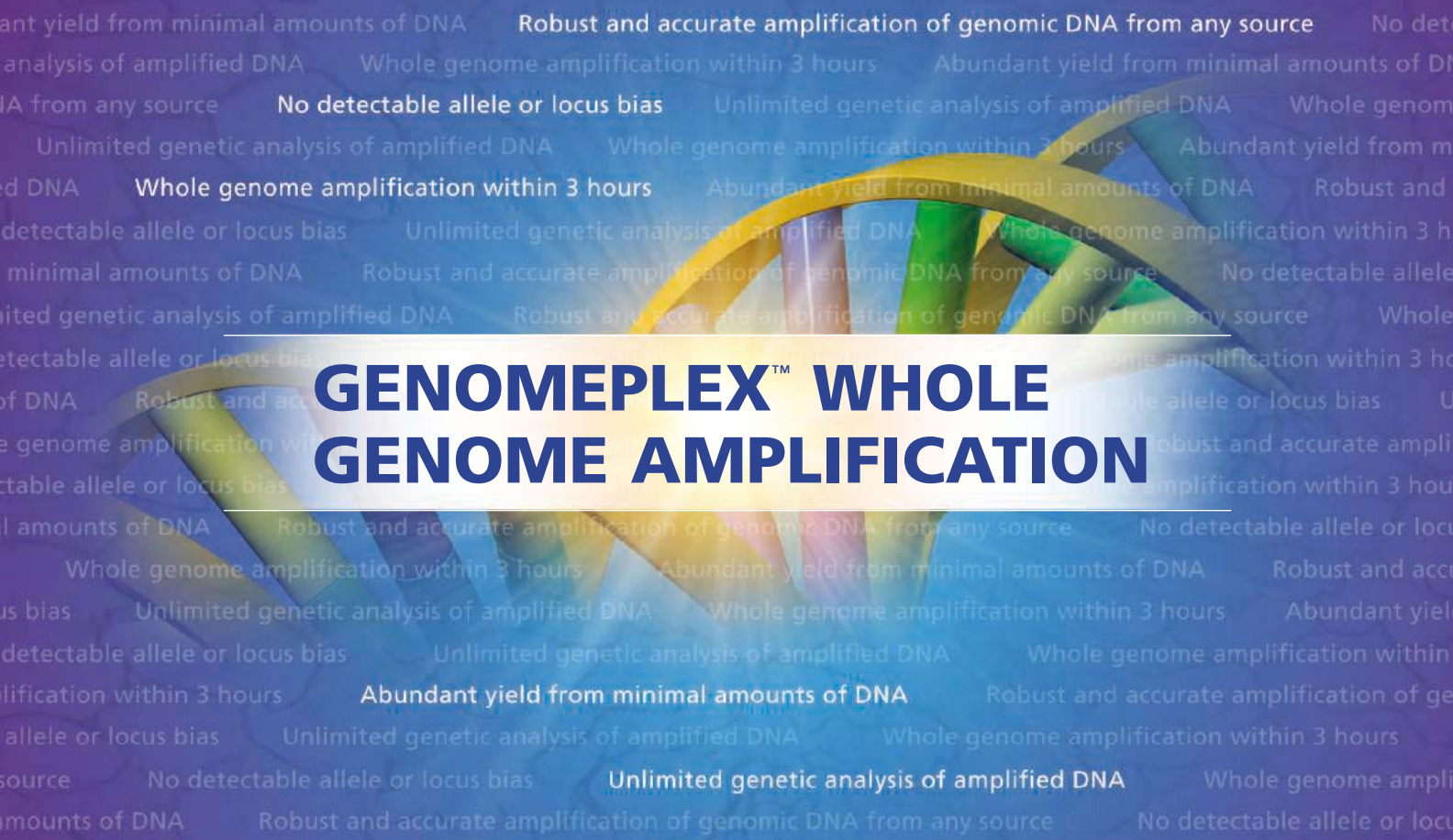

GENOMEPLEX™ WHOLE GENOME AMPLIFICATION

UNSURPASSED YIELD, UNLIMITED POTENTIAL

Sigma's GenomePlex Whole Genome Amplification (WGA) kit provides a rapid and straightforward method to preserve and expand very small amounts of precious DNA.

- **Robust and Accurate Amplification**
  Whole genome amplification with no detectable allele or locus bias within 3 hours
- **Ultimate Flexibility**
  Amplify DNA from virtually any source including blood, buccal swabs, cell culture, plants, and bacteria
- **Unlimited Genetic Analysis**
  GenomePlex WGA DNA is suitable for use with common downstream applications including TaqMan® and BeadArray® or may be stored at -20°C.

Product Code	Description
WGA-1	GenomePlex WGA Kit

Call **800-325-3010** to order or visit us on the web at **sigma-aldrich.com/swga**.

sigma-aldrich.com

LEADERSHIP IN LIFE SCIENCE, HIGH TECHNOLOGY AND SERVICE

SIGMA-ALDRICH CORPORATION • BOX 14508 • ST. LOUIS • MISSOURI 63178 • USA

SIGMA®

processing of an mRNA encoding a key cell-cycle regulator. — PAK

Am. J. Hum. Genet., in press.

ENGINEERING

Integrated Microfluidics

Microfluidics involves the handling and manipulation of very small fluid volumes, and there is much hope that small, portable, and low-cost devices can be designed for tackling global health problems. Pal *et al.* have been able to fabricate a complex device that integrates heaters, temperature sensors, and valves that can control nanoliter-volume reactors in series followed by an electrophoretic separation. Because the key components are electronically addressable, it should be possible to make the device operate autonomously. The device was used for a number of analyses, including the subtyping of two strains of influenza and the amplification of human DNA, mouse plasmid DNA, and plasmid DNA of one of the flu strains. Currently, the device costs about $7 per unit to make, but this can be reduced to below $1 by scaling down the features by an order of magnitude while retaining functionality. It remains to be determined whether sample preparation will be integrated into the device or remain offline and how portable the device will become. — MSL

Lab on a Chip **5**, 1024 (2005).

CHEMISTRY

Looking at SO_2

Optical sensors for SO_2, a colorless pollutant, have relied on secondary indicators, such as those that detect pH changes or detect byproducts of SO_2 reactions. Leontiev and Rudkevich have focused on a long-known but apparently little-used aspect of SO_2 chemistry: its ability to form adducts with amines by accepting their lone-pair electrons. Binding of amines such as piperidine or diethylamine to Zn-tetraphenylporphyrin in chloroform solution shifts its color from red to dark green. Addition of SO_2 displaces the amine and turns the solution back to red. Because of the specificity of adduct formation, molecules such as CO, CO_2, H_2O, or N_2O had no effect on the indicator, which is sensitive down to the low millimolar range. — PDS

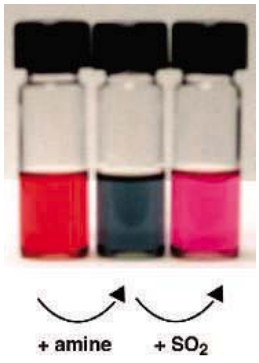

Color change from red to green and back to red

J. Am. Chem. Soc. 10.1021/ja053260v (2005).

CREDITS: LEONTIEV *ET AL.*, *J. AM. CHEM. SOC.* 10.1021/JA053260V (2005)

HIGHLIGHTED IN *SCIENCE*'S SIGNAL TRANSDUCTION KNOWLEDGE ENVIRONMENT

Science's STKE www.stke.org

Converting Repulsion to Attraction

Growth cones guide neurons to their targets by monitoring chemoattractive and chemorepellant cues. Many cues elicit localized increases in cytosolic free calcium concentration ($[Ca^{2+}]_c$) but, curiously, both attractive and repulsive diffusible cues can increase local $[Ca^{2+}]$ so that the growth cone turns toward (attraction) or away from (repulsion) the side with greater $[Ca^{2+}]_c$. Ooashi *et al.* used focal laser-induced photolysis of caged Ca^{2+} to transiently increase local $[Ca^{2+}]_c$ in the growth cones of dorsal root ganglion neurons grown on different substrates. Neurons grown on L1 or N-cadherin substrates turned toward, whereas neurons grown on laminin turned away from, the side on which $[Ca^{2+}]_c$ was greater. Neurons grown on L1 and N-cadherin substrates showed increased cyclic AMP (cAMP) binding to the regulatory subunits of cAMP-dependent protein kinase. Inhibition of cAMP signaling converted Ca^{2+}-mediated attraction to repulsion, whereas pharmacological activation of protein kinase A converted Ca^{2+}-mediated repulsion to attraction. Analysis of calcium signals and of the turning behavior of neurons from mice lacking the type 3 ryanodine receptor isoform (RyR3) implicated RyR3 in protein kinase A–dependent calcium-induced calcium release and attractive turning. The source of the cytosolic Ca^{2+} signal—rather than its amplitude—determined turning behavior. Thus, a Ca^{2+} signal that triggers calcium-induced calcium release from intracellular stores stimulates attractive turning, whereas a Ca^{2+} signal without calcium-induced calcium release elicits repulsion. — EMA

J. Cell Biol. **170**, 1159 (2005).

Visit the *PNAS in the News* web page at www.pnas.org/misc/news.shtml

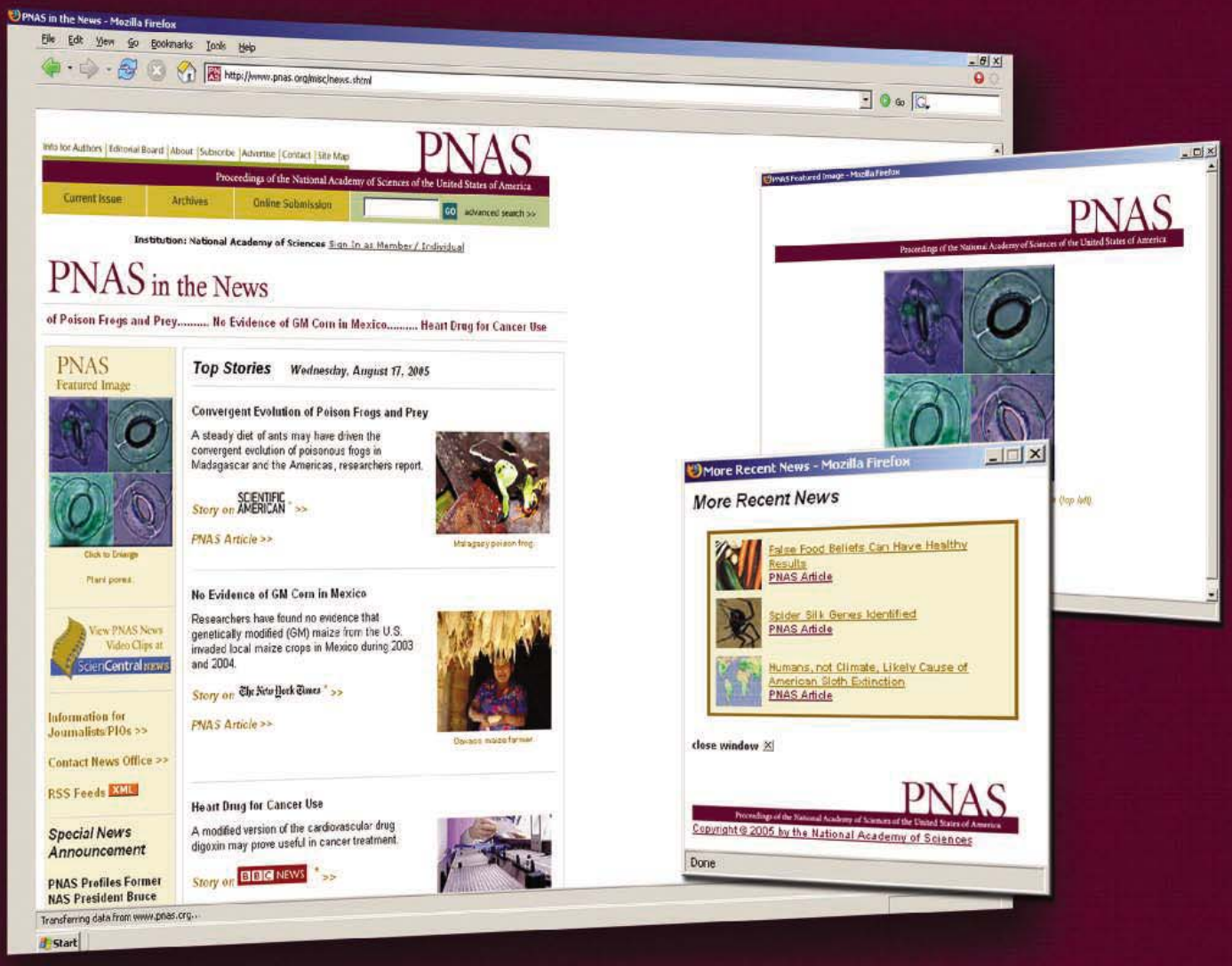

Visit the news page for frequent updates on:

- PNAS articles in the press.
- The latest news stories on PNAS research and how it affects science and the public.
- Eye-catching media images.

Also:

- Sign up for RSS feeds.
- Get information for journalists and press officers.
- Bookmark for frequent updates.

www.pnas.org PNAS

Proceedings of the National Academy of Sciences of the United States of America

Visit us at booth #403
ASHG Annual Meeting
Oct. 26-28

Patience?

Patients can't afford it.

And, if you're like our scientists, you want to help them now. The good news is, you can. By partnering with Perlegen, you can initiate whole genome association studies that analyze millions of unique SNPs in hundreds of cases and controls.

If you have access to DNA samples for a well-characterized phenotype, we can help you impact patient care now. Our scientists will collaborate with you to perform, analyze, and publish whole genome association studies in a matter of months, not years.

Patients are waiting.

To learn more, contact:
Partnerships21@perlegen.com
www.perlegen.com

Targeting today's drugs.
Discovering tomorrow's.™

PERLEGEN SCIENCES®

www.sciencemag.org

Science

1200 New York Avenue, NW
Washington, DC 20005
Editorial: 202-326-6550, FAX 202-289-7562
News: 202-326-6500, FAX 202-371-9227

Bateman House, 82-88 Hills Road
Cambridge, UK CB2 1LQ
+44 (0) 1223 326500, FAX +44 (0) 1223 326501

SUBSCRIPTION SERVICES For change of address, missing issues, new orders and renewals, and payment questions: 800-731-4939 or 202-326-6417, FAX 202-842-1065. Mailing addresses: AAAS, P.O. Box 1811, Danbury, CT 06813 or AAAS Member Services, 1200 New York Avenue, NW, Washington, DC 20005

INSTITUTIONAL SITE LICENCES please call 202-326-6755 for any questions or information

REPRINTS: Author Inquiries 800-635-7181
Commercial Inquiries 803-359-4578
Corrections 202-326-6501

PERMISSIONS 202-326-7074, FAX 202-682-0816

MEMBER BENEFITS Bookstore: AAAS/BarnesandNoble.com bookstore www.aaas.org/bn; Car purchase discount: Subaru VIP Program 202-326-6417; Credit Card: MBNA 800-847-7378; Car Rentals: Hertz 800-654-2200 CDP#343457, Dollar 800-800-4000 #AA1115; AAAS Travels: Betchart Expeditions 800-252-4910; Life Insurance: Seabury & Smith 800-424-9883; Other Benefits: AAAS Member Services 202-326-6417 or www.aaasmember.org.

science_editors@aaas.org (for general editorial queries)
science_letters@aaas.org (for queries about letters)
science_reviews@aaas.org (for returning manuscript reviews)
science_bookrevs@aaas.org (for book review queries)

Published by the **American Association for the Advancement of Science (AAAS)**, *Science* serves its readers as a forum for the presentation and discussion of important issues related to the advancement of science, including the presentation of minority or conflicting points of view, rather than by publishing only material on which a consensus has been reached. Accordingly, all articles published in *Science*—including editorials, news and comment, and book reviews—are signed and reflect the individual views of the authors and not official points of view adopted by the AAAS or the institutions with which the authors are affiliated.

AAAS was founded in 1848 and incorporated in 1874. Its mission is to advance science and innovation throughout the world for the benefit of all people. The goals of the association are to: foster communication among scientists, engineers and the public; enhance international cooperation in science and its applications; promote the responsible conduct and use of science and technology; foster education in science and technology for everyone; enhance the science and technology workforce and infrastructure; increase public understanding and appreciation of science and technology; and strengthen support for the science and technology enterprise.

INFORMATION FOR CONTRIBUTORS

See pages 135 and 136 of the 7 January 2005 issue or access www.sciencemag.org/feature/contribinfo/home.shtml

EDITOR-IN-CHIEF **Donald Kennedy**
EXECUTIVE EDITOR **Monica M. Bradford**
DEPUTY EDITORS **R. Brooks Hanson, Katrina L. Kelner**
NEWS EDITOR **Colin Norman**

EDITORIAL SUPERVISORY SENIOR EDITORS Barbara Jasny, Phillip D. Szuromi; **SENIOR EDITOR/PERSPECTIVES** Lisa D. Chong; **SENIOR EDITORS** Gilbert J. Chin, Pamela J. Hines, Paula A. Kiberstis (Boston), Beverly A. Purnell, L. Bryan Ray, Guy Riddihough (Manila), H. Jesse Smith, Valda Vinson, David Voss; **ASSOCIATE EDITORS** Marc S. Lavine, Jake S. Yeston; **ONLINE EDITOR** Stewart Wills; **CONTRIBUTING EDITOR** Ivan Amato; **ASSOCIATE ONLINE EDITOR** Tara S. Marathe; **BOOK REVIEW EDITOR** Sherman J. Suter; **ASSOCIATE LETTERS EDITOR** Etta Kavanagh; **INFORMATION SPECIALIST** Janet Kegg; **EDITORIAL MANAGER** Cara Tate; **SENIOR COPY EDITORS** Jeffrey E. Cook, Harry Jach, Barbara P. Ordway; **COPY EDITORS** Cynthia Howe, Alexis Wynne Mogul, Sabrah M. n'haRaven, Jennifer Sills, Trista Wagoner; **EDITORIAL COORDINATORS** Carolyn Kyle, Beverly Shields; **PUBLICATION ASSISTANTS** Ramatoulaye Diop, Chris Filiatreau, Joi S. Granger, Jeffrey Hearn, Lisa Johnson, Scott Miller, Jerry Richardson, Brian White, Anita Wynn; **EDITORIAL ASSISTANTS** E. Annie Hall, Lauren Kmec, Patricia M. Moore, Brendan Nardozzi, Michael Rodewald; **EXECUTIVE ASSISTANT** Sylvia S. Kihara; **ADMINISTRATIVE SUPPORT** Patricia F. Fisher

NEWS SENIOR CORRESPONDENT Jean Marx; **DEPUTY NEWS EDITORS** Robert Coontz, Jeffrey Mervis, Leslie Roberts, John Travis; **CONTRIBUTING EDITORS** Elizabeth Culotta, Polly Shulman; **NEWS WRITERS** Yudhijit Bhattacharjee, Adrian Cho, Jennifer Couzin, David Grimm, Constance Holden, Jocelyn Kaiser, Richard A. Kerr, Eli Kintisch, Andrew Lawler (New England), Greg Miller, Elizabeth Pennisi, Robert F. Service (Pacific NW), Erik Stokstad; Carolyn Gramling, Genevra Ornelas, Cathy Tran (interns); **CONTRIBUTING CORRESPONDENTS** Marcia Barinaga (Berkeley, CA), Barry A. Cipra, Jon Cohen (San Diego, CA), Daniel Ferber, Ann Gibbons, Robert Irion, Mitch Leslie (NetWatch), Charles C. Mann, Evelyn Strauss, Gary Taubes, Ingrid Wickelgren; **COPY EDITORS** Linda B. Felaco, Rachel Curran, Sean Richardson; **ADMINISTRATIVE SUPPORT** Scherraine Mack, Fannie Groom **BUREAUS:** Berkeley, CA: 510-652-0302, FAX 510-652-1867, New England: 207-549-7755, San Diego, CA: 760-942-3252, FAX 760-942-4979, Pacific Northwest: 503-963-1940

PRODUCTION DIRECTOR James Landry; **SENIOR MANAGER** Wendy K. Shank; **ASSISTANT MANAGER** Rebecca Doshi; **SENIOR SPECIALISTS** Jay R. Covert, Chris Redwood **PREFLIGHT DIRECTOR** David M. Tompkins; **MANAGER** Marcus Spiegler; **SPECIALIST** Jessie Mudjitaba

ART DIRECTOR Joshua Moglia; **ASSOCIATE ART DIRECTOR** Kelly Buckheit; **ILLUSTRATORS** Chris Bickel, Katharine Sutliff; **SENIOR ART ASSOCIATES** Holly Bishop, Laura Creveling, Preston Huey; **ASSOCIATE** Nayomi Kevitiyagala; **PHOTO RESEARCHER** Leslie Blizard

***SCIENCE* INTERNATIONAL**

EUROPE (science@science-int.co.uk) **EDITORIAL: INTERNATIONAL MANAGING EDITOR** Andrew M. Sugden; **SENIOR EDITOR/PERSPECTIVES** Julia Fahrenkamp-Uppenbrink; **SENIOR EDITORS** Caroline Ash (Geneva: +41 (0) 222 346 3106), Stella M. Hurtley, Ian S. Osborne, Stephen J. Simpson, Peter Stern; **ASSOCIATE EDITOR** Joanne Baker **EDITORIAL SUPPORT** Alice Whaley, Deborah Dennison **ADMINISTRATIVE SUPPORT** Janet Clements, Phil Marlow, Jill White; **NEWS: INTERNATIONAL NEWS EDITOR** Eliot Marshall **DEPUTY NEWS EDITOR** Daniel Clery; **CORRESPONDENT** Gretchen Vogel (Berlin: +49 (0) 30 2809 3902, FAX +49 (0) 30 2809 8365); **CONTRIBUTING CORRESPONDENTS** Michael Balter (Paris), Martin Enserink (Amsterdam and Paris); **INTERN** Michael Schirber

ASIA Japan Office: Asca Corporation, Eiko Ishioka, Fusako Tamura, 1-8-13, Hirano-cho, Chuo-ku, Osaka-shi, Osaka, 541-0046 Japan; +81 (0) 6 6202 6272, FAX +81 (0) 6 6202 6271; asca@os.gulf.or.jp **JAPAN NEWS BUREAU:** Dennis Normile (contributing correspondent, +81 (0) 3 3391 0630, FAX 81 (0) 3 5936 3531; dnormile@gol.com); **CHINA REPRESENTATIVE** Hao Xin, + 86 (0) 10 6307 4439 or 6307 3676, FAX +86 (0) 10 6307 4358; haoxin@earthlink.net; **SOUTH ASIA** Pallava Bagla (contributing correspondent +91 (0) 11 2271 2896; pbagla@vsnl.com); **ASIA** Richard Stone (rstone@aaas.org)

EXECUTIVE PUBLISHER **Alan I. Leshner**
PUBLISHER **Beth Rosner**

FULFILLMENT & MEMBERSHIP SERVICES (membership@aaas.org) **DIRECTOR** Marlene Zendell; **MANAGER** Waylon Butler; **SYSTEMS SPECIALIST** Andrew Vargo; **SPECIALISTS** Pat Butler, Laurie Baker, Tamara Alfson, Karena Smith, Vicki Linton; **CIRCULATION ASSOCIATE** Christopher Refice

BUSINESS OPERATIONS AND ADMINISTRATION DIRECTOR Deborah Rivera-Wienhold; **BUSINESS MANAGER** Randy Yi; **SENIOR BUSINESS ANALYST** Lisa Donovan; **BUSINESS ANALYST** Jessica Tierney; **FINANCIAL ANALYST** Michael LoBue, Farida Yeasmin; **RIGHTS AND PERMISSIONS: ADMINISTRATOR** Emilie David; **ASSOCIATE** Elizabeth Sandler; **MARKETING: DIRECTOR** John Meyers; **MARKETING MANAGERS** Darryl Walter, Allison Pritchard; **MARKETING ASSOCIATES** Julianne Wielga, Mary Ellen Crowley, Catherine Featherston; **DIRECTOR OF INTERNATIONAL MARKETING AND RECRUITMENT ADVERTISING** Deborah Harris; **INTERNATIONAL MARKETING MANAGER** Wendy Sturley; **MARKETING/MEMBER SERVICES EXECUTIVE:** Linda Rusk; **JAPAN SALES** Jason Hannaford; **SITE LICENSE SALES: DIRECTOR** Tom Ryan; **SALES AND CUSTOMER SERVICE** Mehan Dossani, Kiki Forsythe, Catherine Holland, Wendy Wise; **ELECTRONIC MEDIA: MANAGER** Lizabeth Harman; **PRODUCTION ASSOCIATES** Sheila Mackall, Amanda K. Skelton, Lisa Stanford, Nichele Johnston; **APPLICATIONS DEVELOPER** Carl Saffell

ADVERTISING DIRECTOR WORLDWIDE AD SALES Bill Moran

PRODUCT (science_advertising@aaas.org); **MIDWEST** Rick Bongiovanni: 330-405-7080, FAX 330-405-7081 • **WEST COAST/W. CANADA** B. Neil Boylan (Associate Director): 650-964-2266, FAX 650-964-2267 • **EAST COAST/E. CANADA** Christopher Breslin: 443-512-0330, FAX 443-512-0331 • **UK/EUROPE/ASIA** Tracey Peers (Associate Director): +44 (0) 1782 752530, FAX +44 (0) 1782 752531 **JAPAN** Mashy Yoshikawa: +81 (0) 33235 5961, FAX +81 (0) 33235 5852 **ISRAEL** Jessica Nachlas +9723 5449123 • **TRAFFIC MANAGER** Carol Maddox; **SALES COORDINATOR** Deiandra Simms

CLASSIFIED (advertise@sciencecareers.org); **U.S.: SALES DIRECTOR** Gabrielle Boguslawski: 718-491-1607, FAX 202-289-6742; **INSIDE SALES MANAGER** Daryl Anderson: 202-326-6543; **WEST COAST/MIDWEST** Kristine von Zedlitz: 415-956-2531; **EAST COAST** Jill Downing: 631-580-2445; **CANADA, MEETINGS AND ANNOUNCEMENTS** Kathleen Clark: 510-271-8349; **LINE AD SALES** Emnet Tesfaye: 202-326-6740; **SALES COORDINATORS** Erika Bryant; Rohan Edmonson Christopher Normile, Joyce Scott, Shirley Young; **INTERNATIONAL: SALES MANAGER** Tracy Holmes: +44 (0) 1223 326525, FAX +44 (0) 1223 326532; **SALES** Christina Harrison, Svitlana Barnes; **SALES ASSISTANT** Helen Moroney; **JAPAN:** Jason Hannaford: +81 (0) 52 789 1860, FAX +81 (0) 52 789 1861; **PRODUCTION: MANAGER** Jennifer Rankin; **ASSISTANT MANAGER** Deborah Tompkins; **ASSOCIATES** Christine Hall; Amy Hardcastle; **PUBLICATIONS ASSISTANTS** Robert Buck; Natasha Pinol

Precisely What You've Been Looking For

Real-Time PCR amplification plot of synthetic lin-4 miRNA.

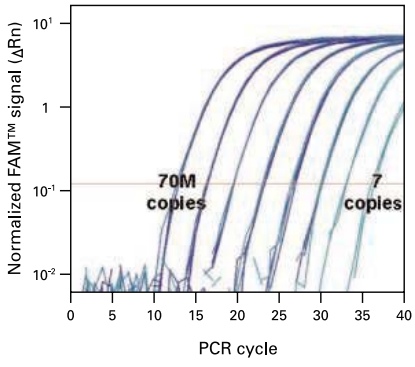

Correlation of copy number to C_T remains linear over seven orders of magnitude.

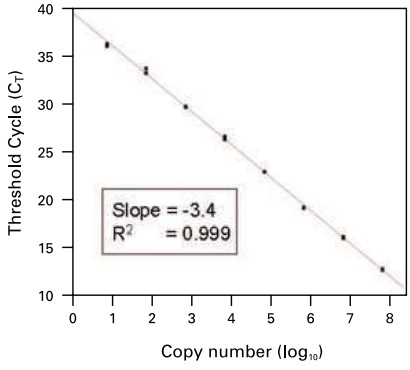

TaqMan® MicroRNA Assays

TaqMan® MicroRNA Assays bring the specificity, sensitivity, and simplicity of Real-Time PCR to miRNA detection and quantitation. Discover an unparalleled level of dynamic range in your research.

Highly specific – Quantitate only mature miRNAs, not inactive precursors

Fast, simple, and scalable – Two-step assay provides high-quality results in less than three hours

Sensitive – Conserves limited samples by requiring only 1-10 *nano*grams of total RNA or equivalent

Wide dynamic range – Up to seven logs

To find out more about TaqMan MicroRNA Assays visit
mirna.appliedbiosystems.com

Applied Biosystems

Integrated Solutions for Protein & Peptide Arrays

- **Protein localization**
- **Differential expression**
- **Interaction profiling**
- **Epitope mapping**
- **Phosphorylation profiling**

Sigma-Aldrich recognizes microarray technology as a central proteomic research tool and is committed to enabling accurate identification of your biological sample's interaction or function against a characterized set of proteins, peptides, antibodies, or tissue extracts.

The foundation of our microarray product line lies in novel and innovative technologies that ensures consistent representation and compatibility with a variety of probes such as DNA, protein, or small molecules. Whether you are screening for antibody expression or protein interaction, be confident your profile pattern is accurate. Discover the advantages of Sigma's microarrays today!

Product Description	Product Code
NEW Panorama Human Cancer Array v1 Microarray	**HPFM2**
Panorama Human p53 Protein Function Microarray	**HPFM1**
Panorama Antibody Microarray – Cell Signaling	**CSAA1**
NEW Panorama Antibody Microarray – Gene Regulation	**GRAA2**
NEW Panorama Antibody Microarray – MAPK & PKC Pathways	**MPAA3**
Panorama Mouse/Rat Tissue Extract Protein Array Kit	**MRPA1**
PEPscreen® Custom Peptide Libraries	*Contact Sigma-Genosys at* **www.sigma-genosys.com** *for details*

Learn more about Sigma's arrays and custom services at
sigma-aldrich.com/arrays

sigma-aldrich.com

LEADERSHIP IN LIFE SCIENCE, HIGH TECHNOLOGY AND SERVICE
SIGMA-ALDRICH CORPORATION • BOX 14508 • ST. LOUIS • MISSOURI 63178 • USA

SIGMA®

Advancing RNAi Technology.

Dharmacon...the world's most trusted siRNA resource

- The largest and most referenced siRNA supplier
- Target any unique human, mouse or rat gene
- Highest level of guaranteed silencing available
- Innovative technologies to enhance specificity
- Breakthrough siRNA transfection reagents
- Expert technical support

Leading RNAi researchers count on Dharmacon's state-of-the-art *SMART*selection™ and *SMART*pool® technologies for potent and specific gene silencing. Four individual siRNAs and a *SMART*pool siRNA reagent are available for over 66,000 unique human, mouse, and rat genes - each with the industry's best performance guarantee and backed by our expert technical support. Simply use our on-line si*GENOME*™ search tool to identify the siRNA reagents for your target gene.

No wonder Dharmacon is the most frequently referenced siRNA supplier in peer-reviewed journals!

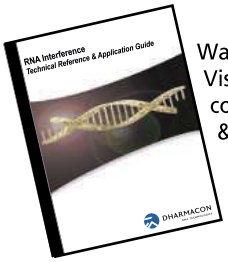

Want to know more about RNAi? Visit our website to request your FREE copy of the RNAi Technical Reference & Application Guide today.

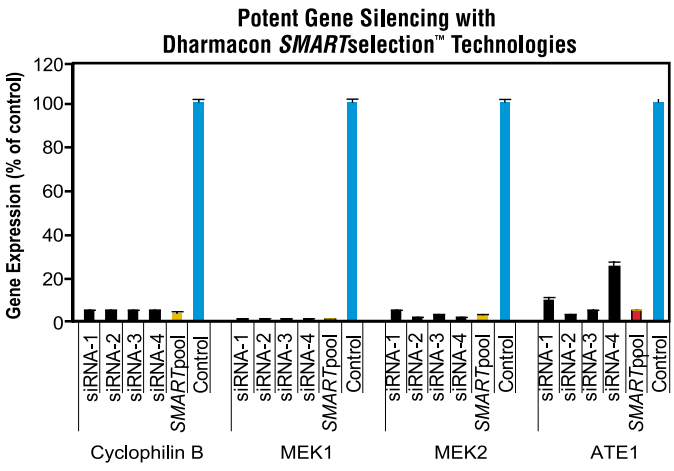

DHARMACON
RNA TECHNOLOGIES

www.dharmacon.com
Tel: 303-604-9499 or 800-235-9880 • Fax: 303-604-9680

For European offices and distributors, please visit www.perbio.com
PERBIO

NetWatch

edited by Mitch Leslie

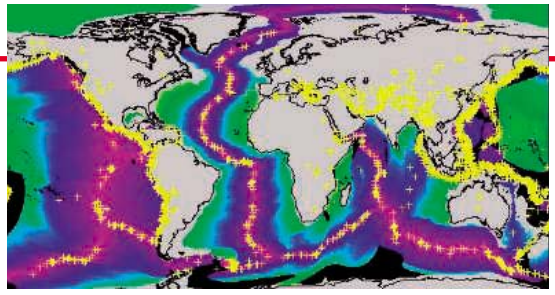

EDUCATION

The Silicon Planet

Students have the whole world in their hands—or at least in their computers—at the tutorial Discover Our Earth at the San Diego Supercomputer Center. Mapping exercises for high school and lower-division college classes explore plate tectonics, volcanic eruptions, earthquakes, and other geoscience fundamentals. The chart above, for instance, shows that many of the large quakes in the 1980s (yellow crosses) shook the youngest parts of the sea floor (magenta), the dynamic areas where new crust is extruding. Visitors can zip over volcanoes in Hawaii and the Cascade Range of the western United States and fire up interactive simulations. One covers the buoyancy of Earth's crust floating on the underlying mantle, which helps determine elevation.

www.discoverourearth.org

IMAGES

Charting Brain Receptors

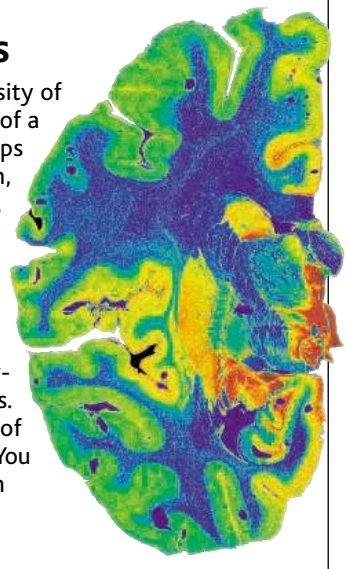

Red marks the spots with the highest density of serotonin transporters in this labeled slice of a human brain (right). The transporter helps recycle the neurotransmitter serotonin, which plays a role in schizophrenia, anxiety, and depression. Researchers studying the distribution of neurotransmitter receptors and transporters in the brain can get an eyeful at this new atlas from Columbia University. The images map the abundance of receptors that might contribute to psychiatric illnesses and neurological disorders. Users can view slices from various parts of the brain and from different orientations. You can also compare tagged brain slices with PET and MRI scans of patients.

cba.cpmc.columbia.edu

RESOURCES

Bioethics Conversation Starter

From the morality of tinkering with human genes to the complexities of determining the order of authors on a paper, tough ethical questions await tomorrow's biomedical researchers. This new Web site from the Howard Hughes Medical Institute (HHMI) aims to spur future scientists to think about these issues. The content complements a free DVD users can order from HHMI that features conversations with more than 30 scientists, ethicists, patients, and other commentators. Covering topics such as genetic alteration and scientific integrity, the site provides discussion questions, case studies, and reading lists.

www.hhmi.org/bioethics

EXHIBITS

Colonial Doctoring

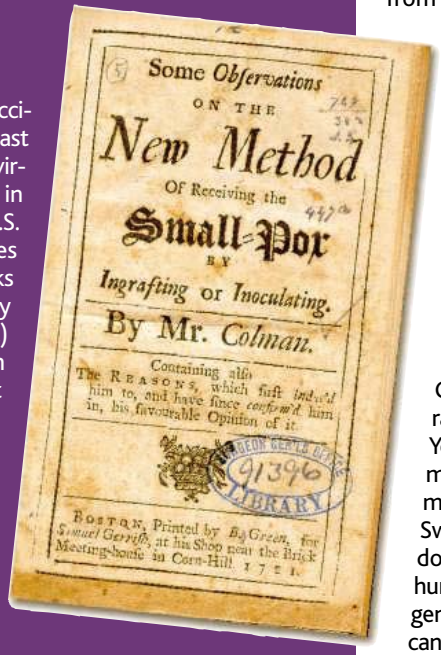

If you're tracing the history of smallpox vaccination in the United States or probing past inequalities in health care, reach for the virtual bookshelf at the new site Medicine in the Americas. The collection from the U.S. National Library of Medicine houses scanned versions of eight medical books published between the early 18th and early 20th centuries. This 1721 offering (right) advocates inoculating patients with material from smallpox sores to prevent a serious case of the disease. You can also browse a pioneering 1903 assessment of the health of the growing African-American urban population. In Atlanta, Georgia, the death rate from pneumonia and tuberculosis was 137% higher among African Americans than among whites, a disparity the report blamed partly on inadequate medical care: "Here in this city of push, pluck and Christian progress, there is not a decent hospital where colored people can be cared for." Curator Michael North plans to add 100 more titles on medicine throughout the Americas.

www.nlm.nih.gov/hmd/americas/americashome.html

DATABASE

Doing the Splits

Cell division involves intricate molecular choreography that would make Busby Berkeley envious. You can learn more about the genes that control mitosis, meiosis, and related processes at GermOnline, hosted by the University of Basel in Switzerland. Although data for brewer's yeast predominate, the site also offers information for humans and 10 other species. GermOnline builds on gene descriptions submitted by researchers. Users can scan the database by categories such as species, biological process, and molecular function. The resulting locus report includes links to gene and protein sequences and to studies or sites that hold gene activity measurements from microarrays.

www.germonline.org

Send site suggestions to netwatch@aaas.org. Archive: www.sciencemag.org/netwatch

CREDITS (TOP TO BOTTOM): DISCOVER OUR EARTH; COLUMBIA UNIVERSITY; NATIONAL LIBRARY OF MEDICINE

NEWS

This Week

PAGE 212
A trio of Nobel Prizes

213
A polio mystery

PALEOANTHROPOLOGY

New 'Hobbits' Bolster Species, But Origins Still a Mystery

Last year's announcement of an astonishingly tiny species of extinct human from the Indonesian island of Flores sent anthropologists reeling. News of the first, nearly complete skeleton ignited a debate about what evolutionary path might have led to humans who stood about 1 meter tall. A few researchers argued that the skeleton, dated to only 18,000 years ago, was simply a diseased modern human (*Science*, 12 November 2004, p. 1116).

This week, the original Australian-Indonesian discovery team unveiled new specimens of *Homo floresiensis*. Their paper in *Nature* describes bones of seven additional adults at least as small as the original, as well as a child's arm and leg bones so tiny that they snuggle neatly on a bank note (see photograph, p. 209). The new finds also include the right arm of the original skeleton and a lower jaw estimated at 15,000 years old. The age bolsters the case that the "hobbits" inhabited the Liang Bua cave for thousands of years.

"This destroys the argument that the first skeleton was an aberrant individual," says paleoanthropologist Russell Ciochon of the University of Iowa in Iowa City. "They have [found] a unique population of small-bodied hominids."

But a few researchers disagree. A Technical Comment in this week's issue of *Science* (p. 236) argues that it is possible that the single skull unearthed suffered from microcephaly, a pathological condition that causes small brains and may affect body shape. Daniel Lieberman of Harvard University says that the new bones make pathology unlikely but points out that no one has yet compared *H. floresiensis* with a wide range of microcephalics, so "everyone still has a right to ask that [microcephaly] question."

The discovery team, led by Michael Morwood of the University of New England in Armidale, Australia, found the latest bones in Liang Bua cave during the 2004 field season. The *H. floresiensis* specimens range from 12,000 to at least 74,000 years old, Morwood says. Stone tools, charred pebbles, and extinct animals were also found in the hominid-bearing layers. Because of a dispute with a leading Indonesian researcher (*Science*, 25 March, p. 1848), Indonesian officials postponed planned work at Liang Bua this year, Morwood says.

Hobbits multiply. Researchers have found more bones of *Homo floresiensis*, including a second jaw.

Researchers familiar with this week's paper say it underscores how strange the little Flores people were. The first skeleton uncovered, thought to be that of a 30-year-old female, has a tiny skull with a modern-looking face and teeth perched atop a short, chunky body. She has relatively long arms and short legs, and a bizarrely rotated upper arm bone not seen in any other ape. "They're so weird," says Lieberman.

Paleoanthropologist and team member Peter Brown, who described the bones, says the distinctive similarities among the specimens show that they are a new species rather than diseased moderns. For example, the two jaws both lack a chin, considered a hallmark of modern humans, and the long bones are unusually thick for their length.

Brown draws special attention to the right arm bone because it completes the skeleton of the little lady of Flores. He notes that her limb proportions differ from those of all other known members of *Homo* but match those of "Lucy," the 3-million-year-old *Australopithecus afarensis* from Africa, ▶

PAKISTAN EARTHQUAKE

A Seismic Murmur of What's Ahead for India

The death toll from last weekend's major earthquake was soaring past 30,000 at press time. But it could have been worse, seismologists say. And it probably will be.

The magnitude-7.6 quake ruptured 40 kilometers of the westernmost end of a 2500-kilometer fault zone that arcs from northern Pakistan across the top of India, through Nepal, to eastern India. This zone is where the Indian subcontinent—more than 40 million years after colliding with Asia—still dives into the mantle at a rate of 2 meters per century, pushing up the Himalayas in the process. Major quakes broke fault segments just to the east of the latest quake in 1885 and again in 1905, when 19,500 people were killed.

Longer segments have ruptured in the past 200 years, setting off several great quakes up to 30 times more powerful than last week's temblor, according to studies by seismologist Roger Bilham and tectonophysicist Peter Molnar of the University of Colorado, Boulder, and geoscientist Vinod Gaur of the Indian Institute of Astrophysics in Bangalore. But earthquakes have ruptured less than half of the Himalayan arc in that time. Meanwhile, the urban population in the Ganges Plain—which stretches along the Himalayan foothills—has increased by a factor of 10 since the 1905 earthquake. A quake that powerful on long-unbroken segments could kill 200,000 people, the trio wrote in 2001 (*Science*, 24 August 2001, p. 1442). A plausible great quake striking near a megacity such as Delhi, they estimated, could conceivably kill 2 million.

"Thankfully, the Earth has not delivered as immensely devastating a blow as was being forecast," says Valangiman Ramamurthy, secretary of the Department of Science and Technology in New Delhi. But the quake, he adds, is "a timely cue to get our act together for seismic planning." **–RICHARD A. KERR AND PALLAVA BAGLA**

CREDIT: PETER BROWN

who also stood about 1 meter tall. "There are so many similarities between the Liang Bua bones and australopithecines that I'm leaning toward the possibility that a small-brained, small-bodied hominid got [to Flores] and shrank further," he says. The hominid who first made landfall might have been as primitive as an australopithecine, he says.

However, many researchers are skeptical about that idea, because there's no evidence that such primitive hominids ever left Africa. In Ciochon's view, a more likely tale of hobbit origins starts with a relatively small *H. erectus* with a yen for travel. He notes that new *H. erectus* specimens from Dmanisi, Georgia, dated to about 1.7 million years ago, have statures of about 1.4 meters and brain sizes of 665 cubic centimeters (cc), or about half the size of a modern human brain. It's not far-fetched to imagine such a human settling on Flores and eventually shrinking to *H. floresiensis*'s 106 centimeters of height and 417-cc brain, he and others say.

Littlest human. A child's leg and arm bones fit easily on an Indonesian bank note.

Meanwhile, a few researchers find the notion of such a small-brained human creating sophisticated tools so outlandish that they remain open to the idea of microcephaly. Anthropologist Robert D. Martin of the Field Museum in Chicago, Illinois, points out that microcephaly often runs in families and that bones can be jumbled in caves, boosting the chances of finding several microcephalic individuals together. "I'm not 100% convinced it's microcephaly, but I am convinced that that brain size doesn't go with those tools," he says.

As opinions pour in, Fred Spoor of University College London notes that the first Neandertal skull dug up in the 19th century was labeled degenerate, too. "There's a long history of finding new human species and someone shouting, 'Pathology!' " he says. Lieberman calls for additional analyses of microcephalics and for more-detailed scaling studies. "This is fun," he says. "But we have a ways to go."

–ELIZABETH CULOTTA

PUBLIC HEALTH

Pandemic Flu Jitters Grip Washington

The pandemic prophets are finally being listened to—at least in the United States. Last week saw a flurry of political activity on influenza in Washington, D.C. Flu experts relish the high-level attention but want to see actions to back up the words. Meanwhile, new reports from Turkey and Romania raised alarms that the H5N1 avian influenza strain may sweep through European poultry. Tests were pending when *Science* went to press.

To address the looming shortage of influenza vaccine during a pandemic, President George W. Bush met with flu vaccine makers at the White House on 7 October. The same day, the State Department met with representatives from more than 80 countries to discuss collaboration on bird flu. Secretary of Health and Human Services (HHS) Michael Leavitt, meanwhile, embarked on a 10-day trip to bird-flu–stricken countries in Asia to discuss collaboration on surveillance and testing, accompanied by the World Health Organization's Director-General Lee Jong-wook and pandemic influenza chief Margaret Chan.

What prompted the Administration's sudden activity last week remains a mystery, although experts have cited factors including criticism about its slow response to Hurricane Katrina and recent papers claiming that the 1918 pandemic flu originated in birds (*Science*, 7 October, p. 28).

Exactly how the Bush Administration plans to handle a pandemic is the topic of its long-awaited preparedness plan, some details of which were revealed in an 8 October story in *The New York Times*; the paper reported, for instance, that the plan says the country should be able to produce 600 million doses of vaccine within 6 months. It's not clear, however, how the plan differs from a draft that has been posted on the HHS Web site for more than a year. An HHS spokesperson would not say when the final plan might be released. The Senate, meanwhile, voted last week to spend $3.9 billion to shore up defenses on bird flu, including $3 billion for antiviral drugs.

Bird watchers. HHS head Leavitt (*left*) and WHO chief Lee (*right*) talked with Thailand's Minister of Public Health Suchai.

Worries about a pandemic would ratchet up if H5N1 is found to be the cause of two new outbreaks in birds. Ducks in two villages in Romania are said to have died from what scientists there, based on antibody tests, believe may be bird flu; in Turkey, an outbreak that has killed approximately 1700 turkeys was caused by an H5 virus, Turkish officials say, although its neuraminidase (N) type isn't clear.

Virus samples from Turkey were slated to be analyzed this week at the Veterinary Laboratories Agency (VLA), a U.K. government lab in Weybridge, and an E.U. team traveled to Romania to help confirm the cause of its outbreak. The virus's genome sequence—as well as epidemiological investigations—should give clues to where the virus came from and how it reached Turkey, says VLA virologist Ian Brown.

On 11 October, French foreign affairs minister Philippe Douste-Blazy called for an urgent E.U. meeting on how to protect Europe's vast poultry sector. If there's evidence that migratory birds carried H5N1 to Turkey, European countries may ramp up measures to try to prevent their flocks from becoming infected, Brown says.

–MARTIN ENSERINK

CREDITS (TOP TO BOTTOM): PETER BROWN; CHAIWAT SUBPRASOM/REUTERS

ligation in a flash.

INTRODUCING THE

QuickLigation™ Kit

FROM NEW ENGLAND BIOLABS

Advantages

- *Fast* — 5 minutes for cohesive or blunt ends
- *Convenient* — ligation performed at room temperature
- *Flexible* — suitable for all common ligation reactions

NEB Quick Ligation Kit

#M2200S	30 reactions
#M2200L	150 reactions

Includes: Quick T4 DNA Ligase, 2X Quick Ligation Buffer, Protocols

Ligation in 5 minutes or less

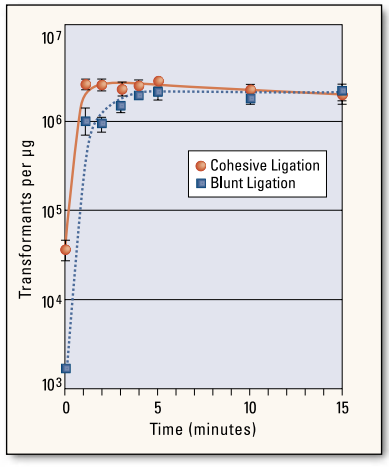

► *Using the Quick Ligation Kit protocol, blunt and cohesive inserts were ligated into LITMUS 28 vector cut with either EcoR V (blunt) or Hind III (cohesive). Ligation products were transformed into chemically competent E. coli DH-5α cells.*

PRODUCTS YOU TRUST.
TECHNICAL INFORMATION YOU NEED.
www.neb.com

- **New England Biolabs Inc.** 240 County Road, Ipswich, MA 01938 USA 1-800-NEB-LABS Tel. (978) 927-5054 Fax (978) 921-1350 info@neb.com
- **Canada** Tel. (800) 387-1095 info@ca.neb.com
- **Germany** Tel. 0800/246 5227 info@de.neb.com
- **UK** Tel. (0800) 318486 info@uk.neb.com
- **China** Tel. 010-82378266 beijing@neb-china.com

NEW ENGLAND BioLabs® Inc.
the leader in enzyme technology

DISTRIBUTORS: Argentina (11) 4372 9045; Australia (07) 5594-0299; Belgium (0800)1 9815; Brazil (11) 3622 2320; Czech Rep. 0800 124683; Denmark (39) 56 20 00; Finland (09) 584-121; France (01) 34 60 24 24; Greece (010) 5226547; Hong Kong 2649-9988; India (044) 220 0066; Israel (3) 9021330; Italy (02) 381951; Japan (03) 3272-0676; Korea (02) 556-0311; Malaysia 603-80703101; Mexico 52 5525 5725; Netherlands (033) 495 00 94; Norway 23 17 60 00; Singapore 67775366; Spain 902.20.30.70; Sweden (08) 30 60 10; Switzerland (061) 486 80 80; Taiwan (02) 28802913

MEDICINE

Teenager's Odd Chromosome Points To Possible Tourette Syndrome Gene

A bad break that apparently gave a young boy Tourette syndrome may turn out to be a lucky break for researchers studying the neuropsychiatric disorder.

Tipped off by a suspicious chromosomal rearrangement, a team led by geneticist Matthew State at Yale University Medical School reports on page 317 that it has identified a gene that the researchers believe causes Tourette syndrome when mutated. Although the gene is responsible for at most a small fraction of Tourette cases, it's the best lead yet in tracking down the genetic contributors to the syndrome. "This gives us a key clue to the potential biological pathways that are altered in this disorder," says neurologist Daniel Geschwind, director of the center for autism research at the University of California, Los Angeles (UCLA).

Traditional genetic analyses of people with Tourette and their families have fingered a half-dozen chromosomal regions that appear to be involved in the syndrome, which causes as many as 1 in every 100 people to involuntarily move or make sounds (*Science*, 3 September 2004, p. 1390). But difficulties in pinning down susceptibility genes in those regions led State to take a different approach. He has been looking in people with the syndrome for chromosomal breaks and rearrangements that might implicate specific genes.

Gene find. The potential Tourette syndrome gene *SLITRK1* is expressed (blue) in this piece of a human fetal brain.

CREDIT: J. ABELSON *ET AL.*, *SCIENCE*

A little over a year ago, a geneticist associated with a consortium organized by the Tourette Syndrome Association (TSA) told State about a boy who had an inversion in chromosome 13: A portion of his chromosome had an orientation opposite that of normal chromosomes. The boy was the only member of his family with Tourette syndrome and the only one with the inversion.

State and his colleagues found three genes close to the breakpoints of the inversion. Two had no plausible connection to Tourette syndrome, but the third immediately drew their attention. Known as *Slit and Trk-like family member 1* (*SLITRK1*), it was related to a group of genes known to be involved in neuronal growth, guidance, and branching.

To test the gene's association with the syndrome, State and his colleagues sequenced *SLITRK1* in 174 people with Tourette. They found one person with a missing nucleotide in the gene that resulted in a truncated protein. State's medical school colleague Nenad Sestan then cultured mouse neurons that expressed either the regular *SLITRK1* gene or the version with the missing nucleotide. The cells with the normal gene grew significantly longer dendrites—the portions of the cell that reach out to receive nerve impulses—than did neurons with the mutated gene. Although the link to Tourette syndrome remains to be determined, the gene appears to have a "functionally important" role in neuronal growth and differentiation, says Sestan.

Among the 174 people with the syndrome, State, Sestan, and their colleagues also found two unrelated individuals who had a change near the coding region of the gene. The change altered a binding site for a short RNA molecule, or microRNA, that regulates expression of the gene. And both the microRNA and *SLITRK1* are expressed in portions of the brain thought to be involved in Tourette syndrome.

State suspects that mutations in or near *SLITRK1* can cause Tourette syndrome when they block or reduce the expression of the gene during development. "This finding needs to be replicated," he says. "But we have multiple lines of evidence pointing to the involvement of this gene."

Other researchers warn that the findings, although interesting, remain tentative. "Each piece of the evidence is intriguing but not on its own conclusive," says UCLA geneticist Nelson Freimer. "To what degree can the pieces be combined to make a persuasive case? Opinions will differ on that."

To try to resolve the matter, TSA has given funding to State, Sestan, and their colleague neurobiologist Angeliki Louvi to produce a mouse in which *SLITRK1* has been knocked out and to study how the SLITRK1 protein functions. "If it holds up, it's a giant leap for Tourette research," says neuropsychiatrist Neal Swerdlow of the University of California, San Diego, School of Medicine.

–STEVE OLSON

Steve Olson is a writer in Bethesda, Maryland.

ScienceScope

Task Force: U.S. Needs New Nukes

A Department of Energy (DOE) task force report slams as "neither robust nor agile" the government's ongoing effort to certify aging bombs as reliable. The report, approved by the energy secretary's advisory committee last week, calls for new weapons that would be cheap to build, long-lasting, and hard to steal—without resuming nuclear testing.

DOE lawyers pushed the department's advisory committee to endorse the report last week rather than simply pass it on, according to chair Peter McPherson, former Michigan State University head. But one committee member, physics Nobelist Burton Richter of Stanford University, warned that building new bombs could geopolitically "stir up some kind of a hornets' nest." Voting unanimously to approve "the thrust of the report," committee members noted that they "did not have sufficient time to consider" some issues. Congress is expected to triple funding for a current preliminary design project, and the report is seen as aiding backers of new weapons. –ELI KINTISCH

Updates

■ Kazakh authorities last week announced that they had nearly finished converting 2.9 tons of highly enriched uranium (*Science*, 23 May, p. 1224) into low-grade material for civilian nuclear plants with U.S. help.

■ The U.S. Senate last week voted to double the size of a scholarship program aimed at attracting U.S. citizens into scientific careers within the Department of Defense to $20 million. The measure, aimed at spawning a new National Defense Education Act, the groundbreaking education program spurred by the 1957 Sputnik launch, is expected to garner House support in an upcoming conference.

■ NASA last week reversed its decision to shut down the $600 million Tropical Rainfall Measuring Mission, a joint mission with Japan, promising to keep the satellite operating at least through 2009 and possibly as long as 2012, when its fuel is likely to give out.

■ Despite losing the second of three gyroscopelike reactor wheels last week, Japanese officials say spacecraft Hayabusa (*Science*, 16 September, p. 1797) may still land on near-Earth asteroid Itokawa for a sample-return mission. The team is studying how the use of rockets for stability will affect fuel reserves.

NOBEL PRIZE: CHEMISTRY

Molecular Mystery Yields a Trio of Novel Matchmakers

Three chemists shared the Nobel Prize in chemistry last week for their roles in devising novel catalysts that act like molecular dance instructors, rearranging dance partners to make novel pairings. Such rearrangements are now a staple of organic chemists for producing everything from pharmaceuticals and pheromones to agrochemicals and plastics.

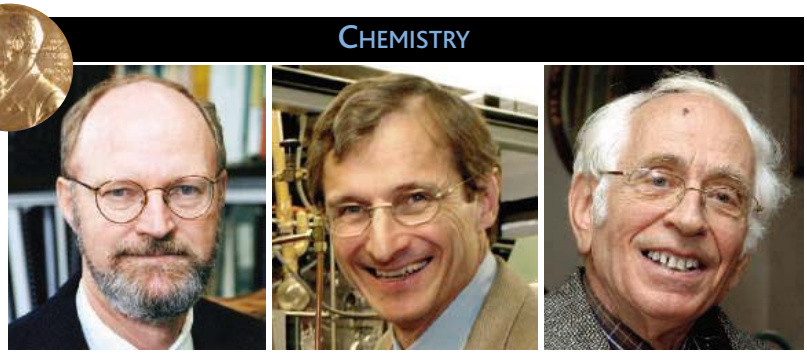

Agents of change. Robert Grubbs, Richard Schrock, and Yves Chauvin (*left to right*) discovered catalysts that have revolutionized synthetic chemistry.

Yves Chauvin, 74, of the French Petroleum Institute in Rueil-Malmaison will receive one-third of the $1.3 million prize for working out the details of the "metathesis" reaction, in which a metal catalyst causes carbon-containing molecules to break bonds and change partners. Richard Schrock, 60, of the Massachusetts Institute of Technology in Cambridge and Robert Grubbs, 63, of the California Institute of Technology in Pasadena each will receive another third for developing novel metathesis catalysts that were more efficient, stable, and environmentally friendly.

"This was a widely expected prize and well deserved," says Peter Stang, a chemist at the University of Utah in Salt Lake City. Even Schrock says he'd picked up hints: "I had heard rumors, of course. But it's something you don't ever expect to happen."

Carbon is central to synthetic chemistry because of the unique ability of its atoms to bind to one another with single, double, and triple bonds and to form chains, branches, and rings of different sizes. In the 1950s, chemists at DuPont and other companies hoped to exploit this molecular dexterity to make novel polymers and other materials. They found that adding certain metals bound to carbon to simple organic compounds known as olefins, which have double bonds between a pair of carbon atoms, caused the reactants to change shape. But how that happened remained more alchemy than science.

Clues to the mystery continued to trickle in through the 1960s. Chemists around the globe raced to explain the shape shifting. In 1971, Chauvin cracked the case, describing the steps by which certain transition metals bound to carbon could slice olefins apart. The electron-hungry metal, Chauvin found, homes in on an olefin's electron-rich ▶

NOBEL PRIZE: ECONOMICS

Two Honored for the Theory and Practice of Game Theory

Two players representing different ends of the spectrum in game theory will share this year's $1.3 million Nobel Prize in economics: Thomas Schelling of the University of Maryland, College Park, and Robert Aumann of Hebrew University in Jerusalem.

Game players. Robert Aumann (*left*) and Thomas Schelling win big.

Schelling, 84, is best known for analyses directly related to practical questions, such as arms control; Aumann, 75, a mathematician, is credited with more theoretical contributions. Economist Jeffrey Ely of Northwestern University in Evanston, Illinois, says work by Schelling, long admired for his accessible prose, could be characterized as "a user's guide for strategic interaction," whereas Aumann writes "a manual for specialists."

Schelling first came to prominence by using game theory to analyze the nuclear arms race in the 1950s. He "basically invented the scholarly study of arms control," according to the prize committee, offering such counterintuitive ideas as "uncertain retaliation is more credible and more efficient than certain retaliation."

"Tom's work is so rich and so varied that you could just about take any public policy and find some contribution he made to it," says fellow Maryland economist Jeffrey Lewis. Lewis says much of Schelling's work has focused on "how the preferences that individual people might have in interacting with others might produce surprising results"—for example, on how weak preferences for living in a mixed neighborhood can result in racial segregation.

Aumann was cited as "the first to conduct a full-fledged formal analysis of so-called infinitely repeated games"; that is, looking at outcomes not from a single interaction but over the long term. "The repeated-games approach clarifies the raison d'être of many institutions, ranging from merchant guilds and organized crime to wage negotiations and international trade agreements," said the committee.

Ely says he thinks Aumann's "most significant contribution" is in the area of "common knowledge": the fact that interactions from arms races to stock speculation are influenced not just by knowledge but by knowledge about the knowledge of the other players. Aumann also melds his religion with his economics, as in a 1985 paper entitled "Game-Theoretic Analysis of a Bankruptcy Problem From the Talmud."

–CONSTANCE HOLDEN

IAEA, ElBaradei Honored

The 2005 Nobel Peace Prize has been awarded to the United Nations International Atomic Energy Agency (IAEA) and its Director General Mohamed ElBaradei for work "of incalculable importance." Nobel laureate and physicist Burton Richter, an IAEA adviser, praised agency scientists for working "on their own time, with their own resources." For ElBaradei, a lawyer, the award sends "a very strong message: Keep doing what you are doing."

–JOHN BOHANNON

CREDITS: (TOP, LEFT TO RIGHT) CALTECH; DONNA COVENEY/MIT; CHRISTOPHE GAYE/REUTERS; (BOTTOM, LEFT TO RIGHT) RONEN ZVULUN/REUTERS; UNIVERSITY OF MARYLAND

double bond and grabs one of its carbons much as a dancer grabs a partner with two hands. When the catalyst encounters another olefin, it drops one "hand" with the first carbon and uses it to pull another pair of carbons into a ring of four. Finally, as the ring breaks, the metal grabs a new carbon by two hands, releasing its original partner to form a new compound.

The mechanism Chauvin discovered had a wide range of potential uses, such as turning linear compounds into rings, stitching linear chains together, and breaking rings open. "It's extremely versatile," says Dale Boger, a synthetic chemist at the Scripps Research Institute in San Diego, California.

At the time, however, the known metathesis catalysts were inefficient and fell apart when exposed to air or moisture. "Olefin metathesis was a very interesting curiosity until Grubbs and Schrock walked in," says Amir Hoveyda, a chemist at Boston University. In 1971, Schrock joined DuPont and began exploring tantalum-carbon compounds, whose chemistry was virtually unknown. "I thought that was a good place to look for new chemistry," says Schrock, who moved to MIT in 1975. He hit upon a metathesis catalyst that he later improved by switching the metal to tungsten and molybdenum.

Unfortunately, Schrock's catalysts were unstable in air or around moisture, because the metals at their core readily reacted with oxygen or water. Grubbs and colleagues solved the problem by substituting ruthenium, a less electron-hungry transition metal. The resulting catalysts typically don't work quite as fast as the molybdenum-based compounds, but they are stable in air, water, and a wide variety of other compounds, which has made them widely useful.

–ROBERT F. SERVICE

EPIDEMIOLOGY

Minnesota Polio Case Stumps Experts

Public health experts are mystified about how an unusual strain of poliovirus infected an infant in rural Minnesota—smack in the middle of a country that has been free of wild poliovirus since 1979. Genetic and epidemiological investigations are now under way to try to determine the source of the virus, detected just last week, and whether it poses a public health threat.

The genetic evidence available so far paints a confusing picture, indicating that the strain infecting the child is derived from the so-called Sabin virus used to make oral polio vaccine (OPV). Although the live, attenuated virus in the vaccine is known to revert and cause disease in rare instances, this 7-month-old infant has not been vaccinated. Indeed, while still commonly used in developing countries, OPV has not been used in the United States since 2000.

Mystery. How did a U.S. infant get infected with poliovirus?

CREDIT: WHO

Experts at the Centers for Disease Control and Prevention (CDC) in Atlanta, Georgia, speculate that this case represents a new and worrisome route of exposure that began in another country more than 2 years ago. "This is one of those scenarios you would never dream up because no one would believe it," says Mark Pallansch, who leads the CDC group that genetically analyzes poliovirus strains.

The mystery came to light last week when the Minnesota Department of Health was doing a virus check on a stool sample from an infant hospitalized for conditions related to a congenital immune disorder. The child has no symptoms of paralysis, so researchers were shocked when poliovirus turned up. "My initial response was that this can't be possible," says state epidemiologist Harry Hull, who used to run global polio-eradication efforts out of Geneva.

But it was, CDC confirmed last Thursday. The CDC group, led by Pallansch and Olen Kew, also confirmed that the child's virus is closely related to the OPV strain. By tallying up the number of genetic mutations in the virus—a measure of how much it has diverged from the original virus used to manufacture the vaccine—the CDC team deduced that the virus is older than the child. It seems to have originated in a person immunized with OPV about 2 years ago. The distinctive pattern of mutations also suggests, says Pallansch, that the person was either immune compromised or quickly spread the virus to an immune-compromised person who has been shedding the virus ever since.

While geneticists try to nail down the source and its connection to the infected child, epidemiologists in Minnesota are trying to determine whether the poliovirus has spread within the hospital—they are especially worried about other immune-compromised individuals—or in the child's community. Although the overall risk is low because of high U.S. immunization rates, the child is part of a religious community that avoids vaccination. That's why state epidemiologists are going door to door, in hope of collecting blood and stool samples and persuading community members to be immunized.

–LESLIE ROBERTS

ScienceScope

NIH Bolsters Clinical Research

The National Institutes of Health (NIH) this week announced a new initiative to move biomedical discoveries to the bedside. The competition will help institutions create new centers or departments for clinical and translational research—from testing discoveries in animals to moving treatments into practice, NIH says. NIH aims to expand the program from $41.5 million in research awards and planning grants in 2006 to $500 million by 2012. "[A] new, vital, and reinforced academic discipline" will result, writes NIH Director Elias Zerhouni in this week's *New England Journal of Medicine*. Proposals are due by 27 March 2006.

–JOCELYN KAISER

DARPA 'Bots Navigate Mojave

Armed with six Pentium M processors and radar, GPS, camera, and laser systems, a Stanford University–developed autonomous vehicle this week won this year's $2 million, 212-kilometer DARPA Grand Challenge race across the Mojave Desert in Nevada. Defense Advanced Research Projects Agency officials are thrilled with the competitor's technical achievements; four other vehicles completed the windy course, three within 40 minutes of Stanford's "Stanley," the speedy VW Touareg R5 that won in roughly 7 hours. Last year, the best 'bot went only 12 km. "At one point, we dodged a bird," said Stanford's Sebastian Thrun proudly.

–ELI KINTISCH

New German Government Pledges R&D Boost

BERLIN—A "grand coalition" agreement between Germany's two biggest political parties, usually bitter rivals, lists an increase in research funding as the first point of accord. Under the agreement, Germany should invest by 2010 at least 3% of its GDP on research and development; the current figure is 2.5%. Angela Merkel, who holds a Ph.D. in physical chemistry, will be chancellor (*Science*, 2 September, p. 1471).

Annette Schavan, a former state culture minister, is expected to be named science and education minister. Schavan studied education, philosophy, and Roman Catholic theology and is thought unlikely to support loosening Germany's prohibitions on embryo research. But Horst Seehofer, expected to be agriculture and consumer protection minister, could ease strict regulations on genetically modified plants.

–GRETCHEN VOGEL

More Published

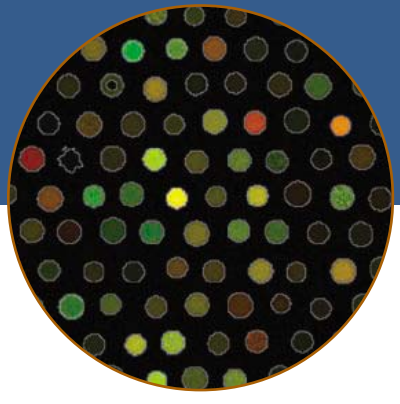

INSTRUMENTS

SOFTWARE

INFORMATICS

In a recent PubMed survey, more publications referenced GenePix® from Molecular Devices than any other slide-based microarray scanner platform. Why? Because researchers trust the results they get with GenePix scanners and Acuity® analysis software. When you trust the tools you use, you have the confidence to publish your results.

Obtaining reliable data requires high performance instruments and software that are easy to use and increase your productivity. With Molecular Devices' microarray scanning solutions, we give you that and more—so you can get more published.

Microarray Scanning

- GenePix Autoloader 4200AL: 36-slide capacity with automation
- GenePix Professional 4200A: four-laser flexibility and upgradeability
- GenePix 4000B: fastest two-laser scanner in existence
- GenePix Personal 4100A: affordable, quality two-laser scanning

Microarray Analysis Software

- GenePix Pro 6.0 microarray image analysis software
- Acuity 4.0 microarray informatics software

For more information, visit our web site or see us at the American Society of Human Genetics Annual Meeting, Booth #221.

Molecular Devices

tel. 800-635-5577 | www.moleculardevices.com

EVOLUTION

Better Habits Sometimes Heritable

When the price of gas skyrocketed in the U.S. last month, many commuters switched to public transportation. Others just couldn't bear to give up their cars. Those new bus and train riders who adjusted their mode of transport exhibited what evolutionary biologists call phenotypic plasticity.

Although no one would suggest that the children of either type of commuter would inherit a preference for cars or subways, researchers studying birds called great tits have evidence suggesting that phenotypic plasticity runs in families and, when it confers a survival advantage, that this trait will be selected for over time.

By reviewing 32 years of data, Daniel Nussey, a graduate student at the University of Edinburgh, U.K., and his colleagues have found that some great tits and their young have shifted the timing of when they lay their eggs, giving them an edge over other great tits in dealing with global warming. The results, reported on page 304, show that "plasticity plays a critical role in the ability of animals to cope with changing environments," says evolutionary ecologist Ben Sheldon of Oxford University in the U.K.

Over the past decade, evolutionary biologists working with plants and animals in the lab have established that plasticity depends in part on one's genes. Now, Nussey, working with ecologist Marcel Visser of the Netherlands Institute of Ecology in Heteren, has demonstrated this genetic link in natural populations; they have also shown that this plasticity is truly advantageous and thus should become more common with natural selection.

Early bird gets the … Flexible behavior is helping great tits cope with climate change.

Nussey and his colleagues analyzed data on great tits living in a national park in the Netherlands to see how the birds were dealing with the gradual warming the area was experiencing. Throughout the 1970s, females timed reproduction so that chicks hatched at a time when their food, caterpillars, was most plentiful. But during the 1980s, warming trends prompted ever-earlier springs and ever-earlier emergence of caterpillars—they now appear 2 weeks sooner than they did in 1985. Most of the birds did not adapt and maintained their original schedule, and the numbers of surviving offspring have begun to decline.

But there were some exceptions. Even in the 1980s, some individuals altered their behavior in accordance with the climate, laying eggs earlier in the warm years and later in the cool years. These climate-attuned females have twice as many surviving offspring. "The ability to adjust their timing allows [reproduction] to coincide with the best conditions," says Sheldon.

Although there are not yet enough long-term data to say for sure that great tits are evolving greater phenotypic plasticity, says Nussey, this advantage suggests that over time, the more flexible birds may win out, and eventually the population will be better able respond to climate changes.

–ELIZABETH PENNISI

WILDLIFE CONSERVATION

Kenyan Edict Threatens Famed Park

Kenya's President Mwai Kibaki threw Kenya's wildlife establishment into an uproar late last month when he announced that Amboseli National Park, one of the country's prime game reserves, will be turned over to local control. The move, if not reversed, opens the door for the government to do the same with all the country's wildlife and parks, says David Western, former director of the Kenya Wildlife Service (KWS), which has run the park since 1974. "It makes a mockery of our wildlife policies and the rule of law in Kenya," he says.

Conservation groups say the 29 September decision to relabel the 400-square-kilometer tract a "national reserve" flouts laws requiring consultation with KWS and approval by the National Assembly. The move has been widely interpreted as an attempt to curry favor with the Maasai people, who believe a proposed new constitution that Kenyans will vote on next month will strip them of control over some of their lands.

Conservation groups have set up a Web site (www.saveamboseli.net) for people to petition the government. Last week, the East African Wildlife Society and seven other groups held a press conference in Nairobi supporting KWS's continued management of the park. Amboseli would be run by the county council of the Kajaido region. Former KWS Director Richard Leakey says county councils don't have the expertise to administer reserves. He adds, "Why should donors like the World Bank provide support … when the government actively promotes the destruction of a major tourist attraction?"

Change afoot. Elephants gather near Mount Kilimanjaro.

Western says Amboseli was set up as an open wildlife park integrated into a 5000-square-kilometer ecosystem where migrations of zebras, elephants, wildebeests, and other animals would be preserved. It's the most remunerative one in Kenya, reportedly pulling in $3.4 million from tourism last year. "I've been saying all along that the Maasai should get more benefits from living [near] these wild animals, but this probably isn't the way to do it," says Cynthia Moss, who has been tracking Amboseli's elephants, now numbering 1400, since 1972.

Western, who now heads the African Conservation Center in Nairobi, says this sets a disastrous precedent: "Every other national park and reserve … risks being erased on a political whim at a moment's notice." KWS is not commenting on the situation, and its future role is unknown.

The immediate impact of the president's action has been permission for the Maasai to allow their cattle, hitherto mostly banned from the park, to graze on the land. Western reports that last week he counted 15,000 livestock. Moss says the tourists "are already complaining that they didn't spend several hundreds of dollars a day to come to Africa to look at cattle."

–CONSTANCE HOLDEN

CREDITS (TOP TO BOTTOM): © PHILLIP GIENAPP; CYNTHIA MOSS/ELEPHANT TRUST

With help from a single-celled alga, scientists are learning that cilia play unexpectedly crucial roles in human development and disease

Betting on Cilia

Patients with Bardet-Biedl syndrome have an odd combination of symptoms. The first signs appear at birth: They have extra fingers or toes, which are most often surgically removed. When patients are in their teens and early 20s, more ominous symptoms appear. Their kidneys fail, they start to lose their eyesight, and they become obese and develop diabetes. Some also suffer from mental retardation. For decades, the disease, which affects one in 100,000 people, was a stubborn puzzle for doctors who struggled to link the diverse maladies.

But as recent discoveries have made clear, the troubles of Bardet-Biedl can all be blamed on faults in the hairlike cellular projections called cilia. This and other surprises about cilia—and their longer cousins called flagella—are now pointing to a fundamental role for these underappreciated organelles, which are best known for propelling single-celled organisms or moving mucus in the airways.

Researchers have recognized for decades that individual cilium appear, at least temporarily, on most cells in the body, but most biologists either ignored them or dismissed them as evolutionary remnants of our single-celled days. Until recently, cilia were largely the purview of a small group of cell biologists whose favorite subject was the double-flagella–equipped alga *Chlamydomonas*, or Chlamy for short. "For a long time, cilia were in the backwater," says molecular geneticist Susan Dutcher of Washington University School of Medicine in St. Louis, Missouri.

That has changed dramatically. It is now clear that primary cilia—the single, immotile cilium on a cell—perform key tasks for a surprising variety of organs. When mutations interrupt their formation or their function, the consequences can be severe. Some cells grow too quickly; others die before their time. Other evidence suggests that some of the most important developmental signals—cues that shape the body axis, backbone, brain, and limbs—are transmitted, at least in part, through cilia.

Cilia, it seems, can serve not only as propellers but also as a sort of cellular antenna, picking up signals from the environment and helping pass them on to the cell's nucleus. In the brain, for example, neurotransmitters may signal nerve cells via cilia. This new understanding of the organelle is "really changing the way we view the cell. We are starting to recognize that inputs are not from random places on the [cell] membrane but at a discrete place" through the cilia, says molecular geneticist Nicholas Katsanis of Johns Hopkins University in Baltimore, Maryland. "It's turning a big chunk of molecular biology on its head."

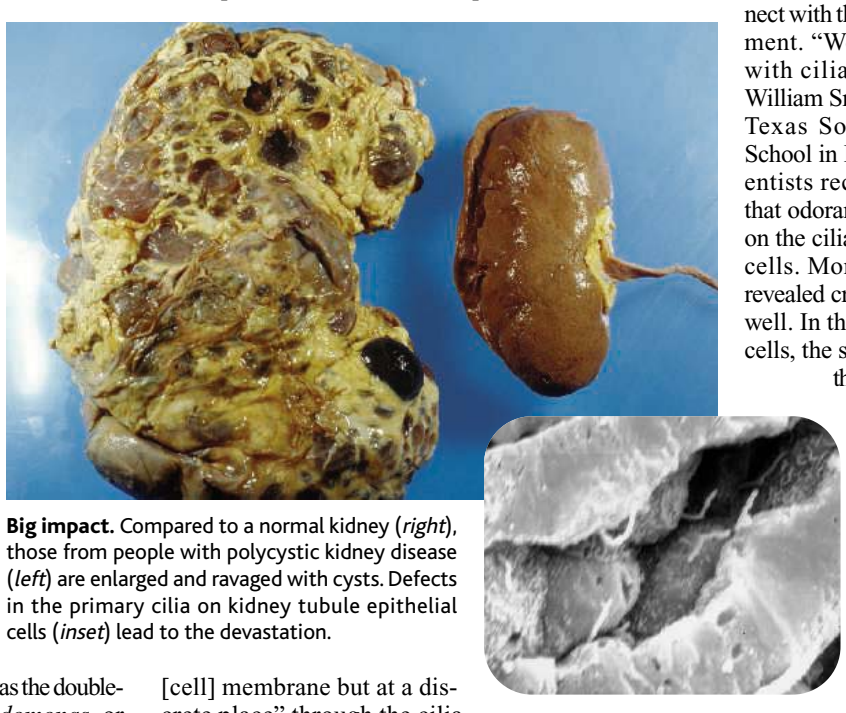

Big impact. Compared to a normal kidney (*right*), those from people with polycystic kidney disease (*left*) are enlarged and ravaged with cysts. Defects in the primary cilia on kidney tubule epithelial cells (*inset*) lead to the devastation.

And that has implications far beyond the rare Bardet-Biedl patients. Scientists are now contemplating whether ciliary defects have a broader role in obesity, high blood pressure, diabetes, and perhaps even cancer. "As more and more people realize that their favorite diseases are ciliopathies, this is going to be a bustling field," Katsanis predicts.

Making sense

Cilia are impressively sophisticated organelles, tiny machines of microtubules driven by the cell's fuel molecule ATP. They extend from the cell surface, anchored by another organelle called the basal body. The best known cilia beat in unison, moving mucus through the airways or moving a paramecium through the water. (The longer flagella are built the same way but move with a waving motion instead of short strokes.)

Evolution has frequently used cilia to connect with the surrounding environment. "We hear, see, and smell with cilia," says cell biologist William Snell of the University of Texas Southwestern Medical School in Dallas. In the nose, scientists recognized decades ago that odorant receptors congregate on the cilia of olfactory epithelial cells. More recent studies have revealed crucial roles in the eye as well. In the retina's rod and cone cells, the so-called outer segment that contains light-sensitive photoreceptors is a specialized form of cilia. In Bardet-Biedl syndrome, defects in the cilia kill the cells, leading to the degeneration that causes blindness.

Cilia can apparently sense touch as well, at least in the kidney—and that insight has offered a surprising explanation for polycystic kidney disease (PKD), one of the most common genetic disorders. Normal kidney cells have one cilium per cell, but like other primary cilia, they stay largely still, which led most experts to dismiss them as unimportant. But a strain of mutant mice with cysts in theirs kidneys prompted scientists to take a closer look. The rodents lacked a gene that scientists first called *Tg737*. Like patients with PKD, the mice also suffered from cysts in the pancreas and fibroids in the liver; for that reason, the

CREDITS (TOP TO BOTTOM): RICHARD KESSEL/VISUALS UNLIMITED; ARTHUR GLAUBERMAN/PHOTO RESEARCHERS; (INSET) G. PAZOUR *ET AL. J. CELL BIOL.* **151**, 709-718 (2000)

scientists who identified the mutant strain in 1994 suggested that the animal might serve as a model for the human disease.

In 2000, Gregory Pazour of the University of Massachusetts Medical School in Worcester, Douglas Cole of the University of Idaho in Moscow, and their colleagues, who were studying *Chlamydomonas*, found that one of the genes required for building the alga's flagella was strikingly similar to *Tg737*. And when they looked at the kidneys of the mutant mice, they found that the cilia were much shorter than normal.

That *Chlamydomonas* connection quickly shed new light on PKD. A few years before Pazour and Cole's discovery, cell biologist Joel Rosenbaum of Yale University and his colleagues found inside the alga's flagella a transport system ferrying proteins needed to lengthen or shorten the organelles in response to environmental conditions. The team showed that blocking the so-called intraflagellar transport system (IFT) causes the flagella to shrink. The protein product of the alga version of the *Tg737* gene, also called *polaris*, turned out to be part of the so-called IFT particle that carries cargo up and down the cilia.

Since then, the connections between cilia and disease have multiplied. Half a dozen human genes that cause PKD when mutated have been found to affect cilia function. It seems the kidney's cilia do not cause movement but instead detect it. In cultured kidney cells, bending each cell's cilium, either with a micropipette or by forcing a flow of liquid over the cells, triggers a strong release of calcium ions, a key sign of cell activation. How this explains PKD remains somewhat murky, but one possibility is that the kidney cilia sense the flow of fluid through the organ and regulate cell proliferation in response. If this cilia signal is missing, cells might divide too often or incorrectly, forming the cysts and enlarged kidneys typical of the disease.

Developing importance

Cilia also seem to help sense molecular signals. A few years ago, Snell and his colleagues showed that the *Chlamydomonas* IFT system was not only needed for assembly and disassembly of cilium; the alga also uses it to transport molecular messages during the mating process. Preliminary evidence now suggests that cilia might play a similar role in animal brain cells.

Scientists have known for decades that most brain cells, including neurons, have a single primary cilium. But until recently, says Snell, neuroscientists took little notice of these potential antennae, even after separate research teams reported in 1999 and 2000 that receptors for somatostatin and serotonin, two key brain signaling molecules, are on the cilia of rodent neurons.

Again, it has taken clues from Bardet-Biedl syndrome to awaken interest in the brain's cilia. The obesity and mental retardation that show up in connection with the syndrome are still a puzzle, but scientists suspect that the answer might lie in the cilium's role as a signal detector for nerve cells. The hypothalamus, a brain region that helps control appetite and metabolism, "has beautiful cilia," says Dutcher. And several teams have noticed that cilia are present on the brain cells involved in responding to leptin, a molecule involved in weight regulation.

One reason that the role of cilia in adult animals has been overlooked for so long is that embryos lacking cilia die very early in development. The developmental importance of cilia first came to light in 1999, when several teams showed that twirling cilia in a key embryonic structure called the node determine whether the heart, stomach, and liver develop on the body's left side or the right (*Science*, 2 July 1999, p. 23).

Many scientists were skeptical at first, but mouse mutants with defective cilia and hearts on the wrong side, along with microscopic videos that enabled scientists to glimpse the movement of the nodal cilia, eventually sealed the case. The connection also explained a long-mysterious genetic condition called Kartagener syndrome in which patients have immotile sperm and defective cilia in their airways—and in about half the cases, their hearts are on the right instead of the left.

This condition, called situs inversus, provided one of the early clues that cilia have a role in Bardet-Biedl syndrome as well. In one family affected by the disease, several members' hearts, livers, and stomachs are on the wrong side. Two years ago, Katsanis and his colleagues reported that the family carried mutations in a gene encoding a protein that sits at the base of a cell's cilium, providing the first hard evidence that defects in cilia explain the unusual suite of Bardet-Biedl symptoms. Subsequent studies have shown that seven additional genes that, when mutated, cause Bardet-Biedl are involved somehow in cilia's structure or function.

Recent work has also tied cilia to some of the most powerful molecules at work in the early embryo. The molecules called Hedgehog, Smoothened, and Wnt have roles in almost every major developmental process, from the earliest cell movements onward—and they seem to depend on cilia to get their messages across.

The first clues came from work by developmental biologist Kathryn Anderson of Memorial Sloan-Kettering Cancer Center in New York City and her colleagues. Anderson studies a signaling pathway that works through the Hedgehog family of proteins. This pathway plays a vital role in setting up the early body plan of animal embryos from flies to humans. They found that gene mutations interrupting IFT in the mouse embryo caused defects very similar to those caused by mutations in a gene called *Sonic hedgehog*.

Since then, several research teams have found evidence that other members of the pathway are also dependent on properly functioning primary cilia. For example, Jeremy Reiter and Didier Stainier of the University of California, San Francisco, reported online on 31 August in *Nature* that Smoothened, a protein that helps transmit the Hedgehog signal, seems to move to the cilia in response to Hedgehog signaling in both mouse and zebrafish embryos. A mutation that prevented the protein from reaching the cilia also shut down the signaling pathway.

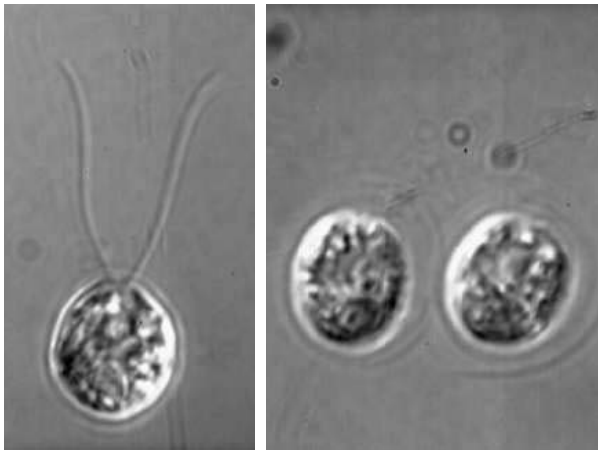

Algal insights. *Chlamydomonas* with mutations in the *IFT88* gene (*right*) lack the twin flagella of their wild-type cousins (*left*). Mutations in the gene cause kidney disease in humans.

More and more papers are implicating cilia in Hedgehog signaling, notes Katsanis, although the case is not yet open and shut. If confirmed, the link might help account for the extra fingers and toes of Bardet-Biedl patients: Hedgehog is vital for proper limb formation.

Another of the cell's most important signaling pathways—active in both embryos and adults—might also work through the cilia. The so-called Wnt pathway influences the expression of dozens of genes that control cell division and developmental processes as diverse as kidney formation and hair growth. And when the pathway goes awry after development, cells can divide out of control, causing tumors.

In May, Gerd Walz of the University Hospital Freiburg in Germany and his colleagues reported that *inversin*, a gene involved in left-right reversal, also plays a role in *Wnt* signaling. The team found that mice lacking a functional *inversin* gene not only had their hearts and livers on the wrong side but also had kid-

CREDITS: G. PAZOUR *ET AL.*, *J. CELL BIOL.* **151**, 709–718 (2000)

ney problems similar to those in mice with faulty *Wnt* signaling. In a series of experiments in mice, frogs, zebrafish, and cell cultures, the team built the case that the inversin protein enables the cell to switch from one type of *Wnt* signaling to another.

Katsanis estimates that hundreds of proteins will turn out to be dependent on cilia for their proper function. Although finding defective cilia might help explain a wide range of maladies, fixing the cilia may not be simple. "These are amazingly complex little machines," Dutcher says. Basal bodies alone involve at least 200 proteins according to the latest estimates, and the cilia themselves might use as many as 500.

Although correcting subtle defects in such complex and ubiquitous structures won't be easy, Katsanis notes that there are already drugs such as the anticancer drug Taxol that affect microtubules, the main building block of cilia. "It may be that some of these molecules could rescue ciliary function," he says, and some conditions might be corrected by tissue-specific treatments that could replace the missing ciliary signal.

Weighty question. Scientists can't yet explain why mutations in *BBS4*, a gene linked to cilia function and Bardet-Biedl syndrome, lead to obesity in mice (*left*) and humans.

At the moment, cilia biologists have more questions than answers. Dutcher points out that cilia have been spotted on dendritic cells that serve as the immune system's first responders to viruses and bacteria. "I don't think anyone has any idea what they're doing [there] yet," she says. And Snell notes that stromal cells in the prostate have prominent cilia—although no one has yet linked them to disease.

Given how new the field is, Katsanis predicts that the number of "ciliopathies" will only increase. "I will no longer be surprised if anyone comes to me with any cell type, from any tissue, and shows me they are ciliated," he says. His confidence has already paid off. Katsanis says he recently won "an excellent bottle of Chablis" from a wager with a neuroscientist who didn't believe that a certain class of neurons had cilia. It's a fairly good bet cilia will continue to surprise.

–GRETCHEN VOGEL

Stockpile Stewardship

Is the U.S. Getting Enough Bang From Los Alamos Tests?

A key facility for hydrodynamic tests faces questions that could impact a U.S. nuclear weapons complex in transition

Experts inside and outside the U.S. government agree that researchers at Los Alamos National Laboratory (LANL) are not blowing up stuff often enough.

For decades, scientists at the Department of Energy's (DOE's) nuclear weapons facility have filmed imploding simulated nuclear bomb parts to study how weapons perform. After the United States halted nuclear testing in 1992, these so-called hydrodynamic tests, or hydrotests, became a central duty for Los Alamos scientists, providing crucial clues about the readiness of aging weapons. The lab conducts the tests at its Dual Axis Radiographic Hydrodynamic Test Facility (DARHT), a half-hectare-sized machine that uses a pair of linear accelerators to create x-ray beams fired at right angles through the test site. The resulting x-ray movies, trained on explosions up to the equivalent of 68 kilograms of TNT, give scientists a glimpse of the inside of a nuclear weapon.

But all is not well at DARHT. Completed in 2003 to replace an older, less capable instrument, the $350 million facility has missed a series of technical deadlines. A report last month by the DOE inspector general (IG) says the problems could delay refurbishment of the W76, a warhead aboard submarines that officials worry might be degrading over time. "Without critical hydrotest data, scientists lose one of their most important tools for evaluating … the performance of key weapons components and the reliability of the stockpile," says the new IG report.* DOE officials disagree with the IG's assessment, saying the hydrotest program is on track and has provided outstanding data this year.

Targeting DARHT. Critics say more non-nuclear hydrodynamics tests are needed to validate aging weapons.

DARHT's ups and downs could have a ripple effect on the nation's nuclear weapons program. This year, Congress is expected to roughly triple DOE's funding to explore new bomb designs, which would need to be validated by hydrotesting. The new IG report also raises questions about the ability of the University of California (UC) to manage LANL on the eve of DOE's decision to either extend the university's contract or hand over management to a team led by Lockheed Martin and the University of Texas. "This could not come at a worse time," says Hugh Gusterson, a Massachusetts Institute of Technology anthropologist and expert on the labs, about the competition for the $2.2-billion-a-year lab. DARHT isn't the only major element of stockpile science managed by UC that's in hot water: Congress is currently debating shutting down the long-troubled National Ignition Facility, a $3.5 billion megalaser at Lawrence Livermore National Laboratory in California (*Science*, 2 September, p. 1479).

Blasts away

The IG's report raises several questions about whether DARHT is meeting its obligation to validate the nation's nuclear stockpile. One bone of contention is the work schedule. DOE says the second of the two linear accel-

* www.ig.doe.gov/pdf/ig-0699.pdf

CREDITS (TOP TO BOTTOM): VAL SHEFFIELD; LOS ALAMOS NATIONAL LABORATORY

erators that make up DARHT won't be ready until 2008, 5 years late. Of seven shots originally planned for the fiscal year that just ended, the lab conducted only three.

DOE officials say an 8-month shutdown of the lab last year, ordered by former director George "Pete" Nanos after computer disks with classified data were reported missing (*Science*, 23 July 2004, p. 462), forced them to alter their original plans. But they insist the facility remains on schedule. However, even the plan for six firings next year suggests that the lab could have trouble reaching the level of 11 per year called for by 2009. Last year, the lab conducted seven of 10 scheduled hydrotests, but only by relying on an older facility called PHERMEX, which provides much less data than DARHT does. PHERMEX was closed last year after officials decided it was redundant with a similar facility at Livermore.

Another major hurdle for the lab is containing debris from DARHT's open-air shots. The lab had hoped to have hard containers in place by 1999, DOE auditors say. But researchers are still developing a rigid, mobile container that doesn't disrupt x-rays. Meanwhile, foam-filled tents catch debris. Los Alamos officials acknowledged to the IG that the foam system extends the time needed to clean up after each test and prepare for the next one. But David Crandall, an official with DOE's National Nuclear Security Administration (NNSA), which oversees Los Alamos, says preparing the experiments, not the cleanup, is the limiting factor.

Planning and management challenges also loom large at DARHT. A 2003 report criticized the program for $58 million in cost overruns that other programs had to absorb. And the new report complains that administrators have "often dispersed responsibility for completing the work among several organizations, … lessening control and accountability for completing specific tasks." NNSA officials say they've implemented management changes that address these problems.

Shelving PHERMEX was another sign of poor planning, says Los Alamos experimentalist John Horne. It "should never have been closed," he says, arguing that the data, although not as rich as those from DARHT, would still have been very useful. "If you don't collect [hydrodynamics] data, you can't make changes if necessary." NNSA adviser Jeremiah Sullivan of the University of Illinois, Urbana-Champaign, said the problems with the program are not serious. But he agrees that "deadlines should be met" to maintain credibility.

Hydrotesting isn't the only element in the lab's effort to certify weapons. A prime distraction, says Raymond Jeanloz, a UC Berkeley physicist and member of an LANL oversight committee, is the Robust Reliable Warhead (RRW) program, a nascent effort by the weapons labs to redesign components of currently deployed weapons—or whole new bombs—instead of simply copying existing ones. Created by Congress last year, the RRW program is seen by lab managers as a way to mend what in May they declared was an "increasingly unstable" stockpile stewardship program.

Critics worry that designing new weapons would give foreign powers an excuse to build their own new weapons or lead to calls for nuclear testing to ensure the new designs actually work. The failure to perform routine tasks such as hydrotests is "going to add arrows to the quiver of proponents of the RRW," says John Pike, director of GlobalSecurity.org in Alexandria, Virginia.

NNSA officials say the IG report fails to account for routine adjustments to the DARHT program. Some of the shots originally planned for this year have turned out to be unnecessary, they say, and the two shots the lab fired provided "critical" hydrotest data for the W76 refurbishment. Los Alamos has cut the turnaround time between shots while using the foam, Crandall says, and a lab spokesperson says RRW work has not diverted resources from other missions, which are on schedule.

Spending panel staff from the House and Senate who oversee the lab say they are confident the program is heading in the right direction. But as U.S. policymakers debate the need for new weapons, they will also be wondering how well the nation is preserving existing ones.

–ELI KINTISCH

CREDIT: SKIDMORE, OWINGS & MERRILL LLP

Building Safety

Directing the Herd: Crowds and The Science of Evacuation

No skyscrapers are designed to be able to disgorge all their occupants in a dire emergency like the attack on the World Trade Center towers. Can they be made safer?

VIENNA, AUSTRIA—In the hour and 42 minutes that elapsed between the first airplane strike on the World Trade Center (WTC) on 11 September 2001 and the collapse of both towers, more than 2000 people failed to escape. Roughly 500 occupants are believed to have died immediately upon impact, and more than 1500 trapped in upper floors died in the aftermath. The toll might have been far worse, according to studies presented here at the International Conference on Pedestrian and Evacuation Dynamics on 28 to 30 September. Had the same attack come when the towers were at their full capacity of 20,000 people each, says Jason Averill, a fire safety engineer at the National Institute of Standards and Technology (NIST) in Gaithersburg, Maryland, the staircases would have quickly gridlocked, resulting in some 14,000 deaths.

Faulty tower? Experts say the proposed Freedom Tower would be as hard to evacuate as its destroyed predecessors.

No tall building is designed to be fully evacuated. Instead, regulations typically require that a few floors be emptied, assuming nothing worse than a localized fire. "This has to change," says Shyam Sunder, deputy director of NIST's Building and Fire Research Laboratory, "because in the lifetime of a building, there will be situations where you've got to get everyone out."

But getting everyone out of harm's way will require a deeper understanding of the collective behavior of crowds, says Jake Pauls, a veteran building safety consultant now based in Silver Spring, Maryland. Researchers are "just scratching the surface," says Averill, although they have made leaps and bounds over the past few years. Studies presented at the meeting offered a glimpse of how evacuations could be conducted more safely.

Modeling mobs

Until recently, there was little science in emergency planning, says Ed Galea, a fire safety engineer at the University of Greenwich, U.K. That is changing as scientists try to capture the behavior of crowds using computer simulations. A diverse effort is under way to refine these models with real-world

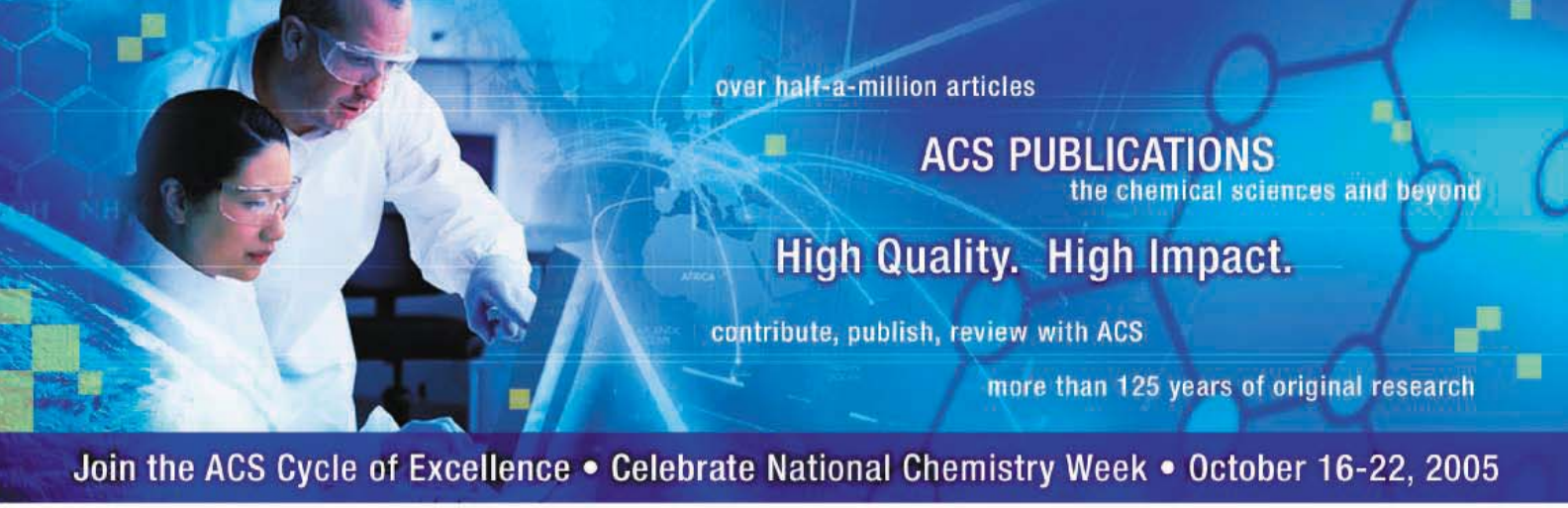

See the greatest hits of 2005 in the chemical and related sciences.

You're invited to see the ACS journal articles that have been accessed the most online during the first six months of 2005. Go to **http://pubs.acs.org/mostaccessed** and view the top 20 most-accessed articles from all 33 journals published by ACS. During National Chemistry Week, October 16-22, you can enjoy free access to the full text of the top three articles from all ACS journals!

Here's a sampling of the articles you can access at http://pubs.acs.org/mostaccessed from ACS high-impact journals:

Journal of Proteome Research (6.917 ISI impact factor)

• **Functions and Possible Provenance of Primordial Proteins-Part II: Microorganism Aggregation in Clouds Triggered by Climate Change**
Sommer, A. P.; Wickramasinghe, N. C
J. Proteome Res. **2005**, *4*(1), pp 180-184.
DOI: 10.1021/pr0498382

• **Probability-Based Evaluation of Peptide and Protein Identifications from Tandem Mass Spectrometry and SEQUEST Analysis: The Human Proteome**
Qian, W.-J.; Liu, T.; Monroe, M. E.; Strittmatter, E. F.; Jacobs, J. M.; Kangas, L. J.; Petritis, K.; Camp, D. G., II; Smith, R. D
J. Proteome Res. **2005**, *4*(1), pp 53-62.
DOI: 10.1021/pr0498638

• **Protein Staining Influences the Quality of Mass Spectra Obtained by Peptide Mass Fingerprinting after Separation on 2-D Gels. A Comparison of Staining with Coomassie Brilliant Blue and Sypro Ruby**
Lanne, B.; Panfilov, O
J. Proteome Res. **2005**, *4*(1), pp 175-179.
DOI: 10.1021/pr040005l

Journal of the American Chemical Society (6.903 ISI impact factor)

• **Mapping Long-Range Interactions in α-Synuclein using Spin-Label NMR and Ensemble Molecular Dynamics Simulations**
Dedmon, M. M.; Lindorff-Larsen, K.; Christodoulou, J.; Vendruscolo, M.; Dobson, C. M.
J. Am. Chem. Soc. **2005**, *127*(2), pp 476-477.
DOI: 10.1021/ja044834j

• **Catalysts for Suzuki-Miyaura Coupling Processes: Scope and Studies of the Effect of Ligand Structure**
Barder, T. E.; Walker, S. D.; Martinelli, J. R.; Buchwald, S. L.
J. Am. Chem. Soc. **2005**, *127*(13), pp 4685-4696.
DOI: 10.1021/ja042491j

• **Total Synthesis of Brasoside and Littoralisone**
Mangion, I. K.; MacMillan, D. W. C.
J. Am. Chem. Soc. **2005**, *127*(11), pp 3696-3697.
DOI: 10.1021/ja050064f

Nano Letters (8.449 ISI impact factor)

• **Bright and Stable Core-Shell Fluorescent Silica Nanoparticles**
Ow, H.; Larson, D. R.; Srivastava, M.; Baird, B. A.; Webb, W. W.; Wiesner, U.
Nano Lett. **2005**, *5*(1), pp 113-117.
DOI: 10.1021/nl0482478

• **High-Density Silver Nanoparticle Film with Temperature-Controllable Interparticle Spacing for a Tunable Surface Enhanced Raman Scattering Substrate**
Lu, Y.; Liu, G. L.; Lee, L. P.
Nano Lett. **2005**, *5*(1), pp 5-9.
DOI: 10.1021/nl048965u

• **Controlled Growth of Si Nanowire Arrays for Device Integration**
Hochbaum, A. I.; Fan, R.; He, R.; Yang, P.
Nano Lett. **2005**, *5*(3), pp 457-460.
DOI: 10.1021/nl047990x

Following National Chemistry Week, you can continue to access the top ACS journal articles. Check back for ongoing updates. Find out which articles are being accessed the most by scientists worldwide—and gain valuable insights on hot topics and new trends in research.

Go to http://pubs.acs.org/mostaccessed and view the most accessed articles for all ACS journals.

JOIN THE ACS CYCLE OF EXCELLENCE

contribute | *publish* | *review*

ACS PUBLICATIONS
HIGH QUALITY. HIGH IMPACT.

data. For example, a team led by Jean Berrou, a computer scientist at the Maia Institute in Monaco, has been secretly filming pedestrians in 10 different cities around the world, analyzing nearly 1000 hours of video to measure different cultural patterns of walking. For example, he says, "pedestrians in London are faster than those in New York."

The goal is to find rules that individual pedestrians unconsciously follow to navigate crowded spaces. "What's amazing is that people don't collide with each other more often on a typical city sidewalk," says Jon Kerridge, a computer scientist at Napier University in Edinburgh, U.K. On a scale of microseconds, people negotiate priority with cues transmitted through body language. "If we can understand how that works," he says, we might learn why certain geometries of corridors and portals work better than others.

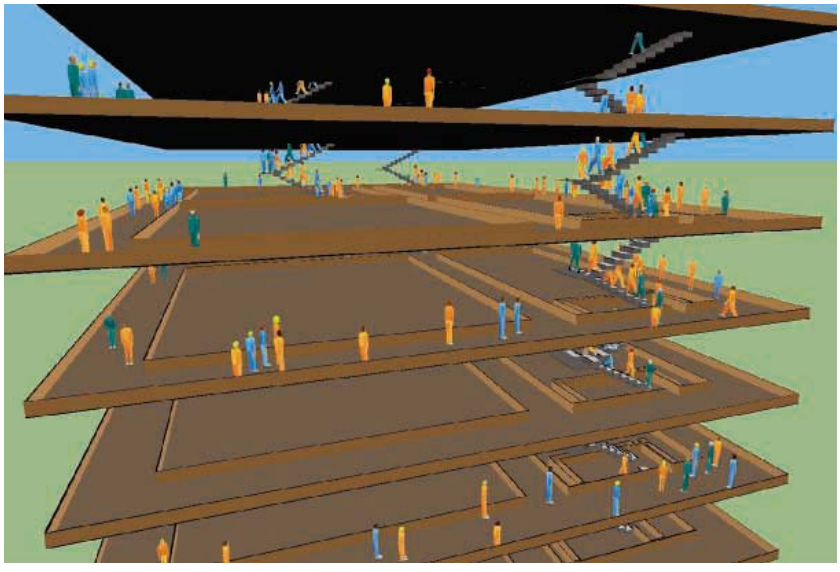

Built-in catastrophe? Computer modeling of the World Trade Center reveals the inherent risks of today's tall buildings when the entire structure must be evacuated.

The next step is to understand how an emergency changes everything. Researchers use a parameter called drive to define the level of motivation people have to go from A to B. "This is where things get very difficult to model," says Kerridge, "because we're talking about innate, personal factors."

Strange things happen when fear is added to the mix. Take the paradox that the more urgently people want to leave a crowded room with a narrow exit, the longer it takes to get out. That occurs in part because of a breakdown in normal communications. Daniel Parisi and Claudio Dorso, computer scientists at the University of Buenos Aires, Argentina, have found that the optimum exit speed is a fast walk of about 1.38 meters per second.

Such studies reveal that "the fundamental unit of a crowd is not the individual but the cluster," says Kerridge. This is because "the first thing we do in an emergency situation is look to each other for support and information." But that response slows movement dramatically. On a larger scale, people form groups similar to animal herds in which individuals let the crowd do the navigating, often passing right by exits within clear view.

Learning to predict and control these behaviors may save lives—and not just in big buildings. The main killer when people mass is not trampling, as is commonly thought, but "crowd crush." When two large groups merge or file into a dead end, the density makes it impossible to fall down, says Pauls. But the accumulated pushing creates forces that can bend steel barriers. "The situation is horrible," he says: "Suddenly everything goes quiet as peoples' lungs are compressed. No one realizes what's happening as people die silently." Dangers like these make designing architecture and procedures for evacuation like a tightrope walk, says Pauls: "You have to get people out fast, but safely."

Revisiting 9/11

Armed with these insights, two separate groups have been trying to model the WTC evacuation to see what lessons can be learned. In 2002, the U.S. Congress ordered NIST to investigate the WTC safety and emergency response, and the U.K. government commissioned a team led by Galea, which has paved the way for a larger study called HEED. "This was one of the largest full-scale evacuations of people in modern times," says Galea.

To build a minute-by-minute chronology of the event, the NIST team has conducted more than 1000 interviews with survivors by telephone, and Galea's team is set to do up to 2000 face-to-face interviews next year. One of the most surprising discoveries, says Galea, is the long lag time between the first attack and the start of evacuation. Galea's team found that although 77% of survivors began the egress within 5 minutes of the impact, it took another hour for the next 19% to get going, and 4% stayed in their offices for over an hour. "In some cases people were more worried about saving their computers," he says.

Both teams have incorporated these data into a model called EXODUS, designed by Galea. When the NIST team used the model to play out the WTC disaster with full occupancy, it estimated roughly 14,000 deaths, most among those stuck on the stairs. This didn't surprise Pauls.

"Those stairs were not designed to handle a full evacuation," he says. "In fact, no tall building is prepared for it." Sunder says NIST is pushing to include full evacuation for many tall buildings in the next review of U.S. building codes in 2008. "There is a lot of resistance" to requiring full evacuation capability even after the WTC attacks because people "believe that was a one-time-only event," he says. But he notes that a building's typical lifetime is a century; designers should be preparing for other "extreme events" like multifloor fires, earthquakes, and hurricanes.

Until the existing tall buildings are replaced with a new generation, experts say, improvements will have to come through better emergency procedures and retrofitting. For one, elevators should be made usable during emergencies, says Sunder. WTC tower number 2 emptied far more efficiently than tower 1 because its elevators were available before it was hit by the second plane, the studies found. New elevator systems that include independent power supplies and computers that prevent them from opening on a burning floor will be available within a few years, says Averill. Galea suggests another possible innovation: adding sky bridges to create new escape routes linked to other buildings. His simulation of a WTC evacuation with the towers linked by a bridge was far more efficient.

Evacuation experts say they are continuing to look at all kinds of evacuation backups, even far-out ones. For example, a pole system that can be attached to the outside of buildings is being tested. By strapping into a vest attached to the pole, people could slide down safely using electromagnetic brakes. Another option: People could jump into fabric tubes and bounce their way down to the bottom—although this would likely cause friction burns. Even parachutes have been proposed as a last chance resource.

"But really, the best thing we can do to make these buildings safer," says Pauls, "is to focus on the basics." That means better stairs, elevators, and fire drills.

—JOHN BOHANNON

CREDIT: FSEG/UNIVERSITY OF GREENWICH

New Leaders for MIT and BU Herald Fresh Era in Boston

A scientist and an engineer are charting new courses for their institutions, drawing on their insider status and progressive social views about modern universities

BOSTON—This city and environs are flush with 5000 life scientists, $1.5 billion in National Institutes of Health funding, and dozens of pharmaceutical giants and small biotechnology firms. At the core of what attracts the people, funding, and business to this region is its wealth of universities. Two former bench scientists are now at the helms of two of the largest and most prestigious schools, and they are revving up their universities' research engines to break down the walls between biology and other disciplines. They also are quietly advocating a social agenda designed to make their campuses more hospitable to women scientists and engineers—and more competitive in netting the best brains in a tough market.

Both Susan Hockfield—a Yale neuroscientist who last December became president of the Massachusetts Institute of Technology—and former MIT engineer Robert Brown, who last month crossed the Charles River to take the reins at Boston University (BU)—are technically savvy academic insiders with reputations for collegiality. Their backgrounds and personalities stand in sharp contrast to those of Brown's predecessor John Silber and the current president of the academic colossus down the road, Harvard's Lawrence Summers. Both Silber and Summers are social scientists notorious for their bluntness, political connections, and autocratic styles.

As they settle into their jobs, both new presidents face formidable challenges. Brown's task is to restore BU's battered reputation, build its small endowment, and vault it into the top tier of U.S. research universities. Hockfield's assignment is just as tough: Keep MIT in that top rank amid stiff competition for the best brains and become a national spokesperson for the science and technology community. *Science* recently spoke with both novice presidents about what they hope to accomplish.

Close watch. MIT's Susan Hockfield (*above*) hopes the life sciences will inform other disciplines, including computer science, housed in this new Frank Gehry–designed building (*right*).

Susan Hockfield: Finding her voice

Hockfield scored two firsts in succeeding Charles Vest, a mechanical engineer whose 14-year tenure featured a seat on the President's Council of Advisors on Science and Technology (PCAST) along with a host of other national organizations. She is the first woman and the first biologist to run MIT, a momentous change at an institution long dominated by male engineers.

Her appointment reflects MIT's deliberate effort to retool itself in two key areas: equal opportunity and biological research. An internal report released in 1999 found that women at MIT—even senior professors—faced career impediments. MIT responded quickly, bringing more women into senior administrative positions, providing better daycare and more flexible family options, and closely monitoring faculty appointments. At the same time, MIT moved to integrate some of its fiercely independent fiefdoms to take advantage of the biological revolution. This fall, a new building housing cross-disciplinary neuroscience studies will open its doors, and a new computational and systems biology initiative now pulls together some 80 biologists, computer scientists, and engineers from 10 separate academic units.

Although Hockfield is helping MIT move in new directions, she says she has had little direct experience either with professional discrimination or interdisciplinary work. She spent 20 years at Yale studying brain development in mammals, in particular deadly brain tumors called gliomas. Previously, she had worked under James Watson at Cold Spring Harbor Laboratory in New York.

Given MIT's reputation as an engineering center, Hockfield acknowledges that the appointment of a life scientist as president raised eyebrows. But she sees it as an example of MIT's eagerness to adapt to the rapidly changing research environment. Beginning in the 1930s, she notes, the institute chief brought in top-ranked physicists despite skepticism from engineers. That influx "provided an understanding of the nuts and bolts of the physical universe," she says, making the institution "a vehicle" for better engineering. The blossoming of engineering science in the 1950s revolutionized the field. A half-century later, she says, molecular genetics is providing a "similar convergence of life sciences with engineering."

Discrimination is not part of her professional experience, says 54-year-old Hockfield, although she has been subject to "the subtle or not-so-subtle slights that women suffer." Still, she's not afraid to speak out on the subject. In February, she co-authored an editorial in *The Boston Globe* that roundly criticized Summers's widely publicized remarks that genetic differences might explain why men outrank women in science (*Science*, 28 January, p. 492). "The question we must ask as a society is not 'Can women excel in math, science, and engineering?'—Marie Curie exploded that myth a century

CREDITS (LEFT TO RIGHT): 2005 DONNA COVENEY/MIT; BIZUAYEHU TESFAYE/AP PHOTO

ago—but 'How can we encourage more women with exceptional abilities to pursue careers in these fields?' " she asserted. "Colleges and universities must develop a culture, as well as specific policies, that enable women with children to strike a sustainable balance between workplace and home."

One of Hockfield's first initiatives is to tackle the problem of energy. Based on feedback from students, faculty, and alumni, she recently organized a council to lay out what energy research is being conducted at MIT and "to design programs and figure out what we need. I expect a report in early spring." She says that the post–9/11 visa restrictions on foreign students have been significantly eased, but she is worried about assuring an adequate supply of U.S. scientists and engineers. "Eighty-five percent of our undergraduate degrees are in science and engineering," she says. "Nationwide, it is 17%. At the undergraduate level in Singapore, it is 68%. … I am very concerned about the position of America in the global economy."

Hockfield is more cautious about her role as a spokesperson for science on the national stage, where the MIT president has traditionally loomed large. (In addition to his current spot on PCAST, Vest is past chair of the 62-member Association of American Universities in Washington, D.C.) Although she joined the upper echelon of U.S. academia when she became Yale's provost in 2003, national politics has been outside her field of vision. "This is a new area to me," she says.

Hockfield meets at least monthly with federal lawmakers and Administration officials in Washington. She's also been quietly talking with other presidents of major research universities about how to deal with a range of hot-button issues, from intelligent design to global warming to stem-cell research, in a coordinated fashion. But she weighs her words carefully when asked whether Republicans are waging a "war" on science. "I have no idea; I'm not in a position to judge that," she says, adding: "I'm very concerned when interesting and dynamic science … gets subverted by political agendas."

Hockfield says one of her primary concerns is that government support for science is not keeping up with the expanding opportunities. She also acknowledges widespread concerns about the potential for private funding to alter or quash research results. Hockfield says that "my sense is that we are not overly swayed by the interests of any funder—but one has to be always vigilant." While praising the "entrepreneurial spirit" of MIT faculty, she recently warned her deans to adhere closely to the institution's ethical policies.

Robert Brown: Aiming for the top

When Bob Brown looks out the wall of glass behind his desk, his view of the spires, domes, and high rises of Harvard and MIT across the Charles River remind him what he faces in putting BU on the list of major research universities. The institution he now leads has spent the past 3 years lurching from crisis to controversy. "BU is a very fine university that just tends to get itself into the paper," he says diplomatically. It is, he insists, "much better than its public image."

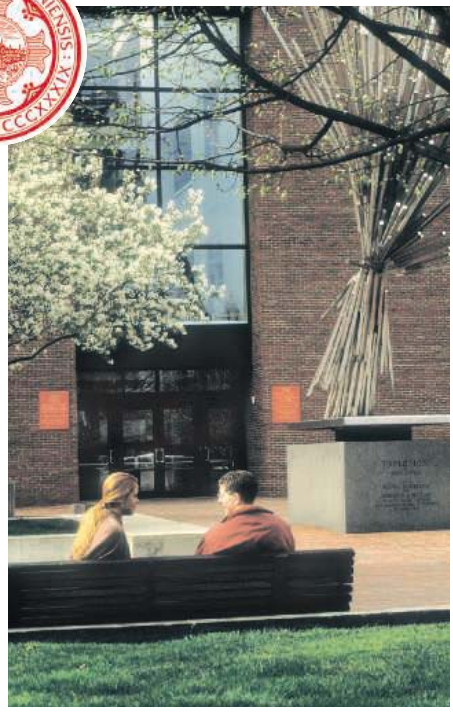

During his 30 years as BU's president ending in 2002, Silber turned a lackluster commuter school into the country's fourth-largest private university. His extensive political connections helped attract the resources needed to build national reputations in high-energy physics, photonics, and medicine. But Silber also frequently angered faculty members by his involvement in what was taught in the classroom and by his public comments against feminists and homosexuals. He also faced criticism for leaving the school with a modest endowment of $620 million in 2003, 73rd in the nation. MIT, by contrast, had a $5.1 billion endowment, and Harvard's $25.9 billion rules the academic roost.

Silber's departure was as controversial as his tenure. He stepped aside to become chancellor in 1996, only to resume the presidency when his handpicked successor abruptly resigned in 2002. A long search for a successor produced former NASA chief Daniel Goldin, who immediately began discussing plans for radical changes in senior management. Alarmed trustees rescinded their offer 1 day before Goldin was to start work, paying him a $1.8 million settlement. Alluding to the recent difficult years, Brown says, "My sense is that many people believe we lost" track of the university's principles. "A lot of faculty have put their head down, done great research and teaching, but are very quiet about where they work."

Although Brown praises Silber for many accomplishments, he says he hopes to graft what he learned at MIT onto his new institution. At MIT, he says, "there was a feeling that being critical was not being disloyal." He also intends to make his administration more transparent. "I am more open about data, about processes, trying to get people around the table to talk and work together to create a consensus," he says. "But I'm not looking for a vote to drive the university forward, because that won't lead to a great university either."

Lab gamble. Robert Brown (*above*) is betting that a controversial new biomedical lab will pay big benefits for Boston University, which used congressional earmarks to build its photonics lab (*left*).

One immediate test of leadership will be the construction of an advanced laboratory to study dangerous biological agents in the heart of the university's medical center in the middle of the city. Although BU sees the planned facility as key to expanding its research portfolio, community activists fear it might release toxins or draw a terrorist attack.

Brown insists that BU is doing "a superb job of being responsive to concerns" and disputes any damage to its reputation as a community-based organization. "BU is taking on an initiative to build a great research infrastructure and a great group working on infectious disease in all kinds of contexts, not just bioterrorism," he says. And he argues that its location is an asset. "How much synergy can you get by putting it in the middle of a health science complex? What we're banking on is that you get a lot."

Given BU's myriad difficulties, Brown's decision to take the job stunned many faculty members. "Why would he choose to come here?" asked one incredulously. "He's really good!" University sources say he was gunning for the top MIT job after Vest's departure last year, rejecting overtures from the University of California, Berkeley, and Rice University in Houston, Texas. Brown declines comment.

The 53-year-old Brown arrived at MIT as a chemistry professor in 1979, and by 1998 he had become provost. While Vest met with policymakers in Washington, D.C., and wooed donors around the world, Brown stayed in Cambridge and quietly revolutionized the 140-year-old school. As engineering dean, he cannily asserted control over empty faculty slots. "If that hadn't happened, there would not be a biological engineering division today," he says. That control, Brown adds, allowed MIT to reshape itself to address the increasingly interdisciplinary nature of biology, engineering, and the physical sciences.

It's an area in which Brown expects BU can shine, too. "When you have the top five departments in the world, the tendency to want to interact outside that department is less. BU hasn't had the luxury of those very, very strong departments, so you see an enormous amount of interaction between faculty. The best example is the new engineering and life sciences building, which is not owned by a department. The floors are laid out in terms of research areas. At one of these great top-tier universities, [such synergy] would be very difficult."

At MIT, Brown also oversaw construction of a flashy computer science and artificial intelligence center designed by Frank Gehry, and he brokered a difficult and time-consuming deal with Harvard to create the Broad Institute to combine genomics with medical research. He's also been a leading advocate for revamping the way women scientists are treated in academia.

Does BU have a similar problem? "I have no data, but it is definitely on the radar screen," he says. Brown is organizing a group that would do for BU what the 1999 report did for MIT. "There are some [issues] that are easy, such as daycare," he says, but to standardize hiring procedures across units is more difficult. He says he soon will set up a committee charged by the president and provost to gather data and propose changes.

In the meantime, Brown must compete with other Boston-area universities and industry for top science and engineering faculty. He knows that, without a huge endowment, he's starting at a disadvantage. "I can't see how you easily ever make it up. You are going to need to build a philanthropic tradition that has not been in this institution." He also knows that those domes and spires across the river can't be ignored. "Will Harvard always cast a shadow?" he asks. "Yes."

–ANDREW LAWLER

Science Education

New Curricula Aim to Make High School Labs Less Boring

A cadre of education researchers is remaking science labs to give students a taste of the real thing

This year, Barrington Ross made cell division a life-or-death matter for his seventh-grade class at Shepherd Middle School in Durham, North Carolina. Instead of peering into a microscope or acting out the process, the students worked through a series of computer simulations to select which of three plant extracts is most likely to be active against the unchecked proliferation of cells that is the hallmark of cancer. Then they defended their choice in an online debate. "Having an authentic problem to work on made them think and feel like real scientists," says Ross, noting that some students added personal dimensions to the exercise by talking about family members suffering from cancer.

Ross doesn't expect all his students to become scientists. But he does want them to understand the scientific method—and what it's like to develop and test a hypothesis. Those goals are rarely achieved in secondary school science labs, says a new report* by the National Academies. The study, requested by the National Science Foundation, found that most labs focus on mechanical procedures such as slide preparation and pH measurement instead of scientific principles. "For many students," says Vincent Lunetta, an education researcher at Pennsylvania State University, University Park, "lab work is manipulating equipment, not ideas."

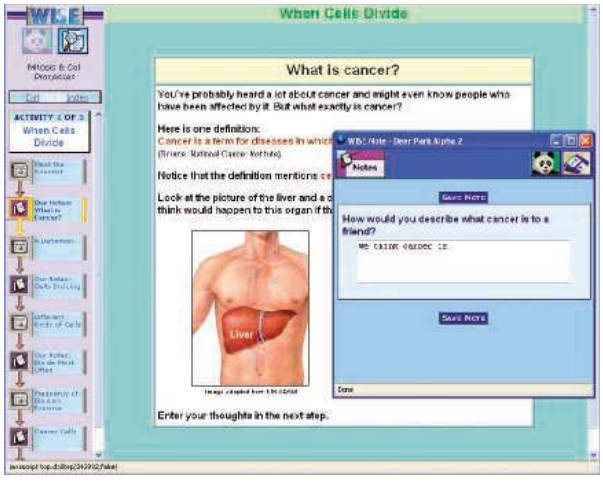

Forming ideas. This Web-based exercise on cell division, developed at UC Berkeley, encourages students to develop and test their own hypotheses.

CREDIT: WISE

A growing number of education researchers are trying to change that pattern. Some of the new materials take students beyond the traditional tasks of observation and data collection into the realms of theory-building and scientific reasoning. "The goal is to put students through a process that mirrors what scientists do," says Marcia Linn, an education professor at the University of California (UC), Berkeley.

Embrace the unknown

The academy is not the first to conclude that most science labs are dull, dry affairs in which students are told ahead of time what they will learn. Many teachers aren't sufficiently trained to conduct open-ended, inquiry-based labs, for one, and few have the time and resources needed to go beyond the cookbook approach. There's also little incentive for schools to transform labs when state assessment tests—the real drivers of curriculum change—emphasize factual knowledge rather than scientific reasoning. "Following instructions out of a textbook is much easier" for teachers, says Joseph Kracjik, a professor of science education at the University of Michigan, Ann Arbor.

The new wave of education materials is meant to be more appealing to students without being more difficult

*America's Lab Report: Investigations in High School Science, 2005 (www.nap.edu/books/0309096715/html)

for teachers. In one exercise designed by Norman Lederman, a science and math education researcher at the Illinois Institute of Technology in Chicago, students are asked to study the effect of temperature on the heart rate of the water flea—a translucent crustacean—without being given any specific instructions. "All they know is that the water flea is a cold-blooded organism that has to adapt to cold conditions," Lederman says. Each group must figure out how many beakers of water to use and what the water temperature should be in each one. "In many labs, students know the research question, the procedure, and even the answer in advance," he says. "Our goal is to take it all away" and let them figure it out on their own.

Through repeated observations, students discover the minimum temperature difference between water samples that's needed to have a discernible effect on heart rate; they also learn that they might miss important data points if they set the temperatures too far apart. Lederman says the experience helps students realize a fundamental principle: that experimental design can have an impact on the findings of a study.

Another ingredient of scientific inquiry absent from most traditional labs is hypothesis development and testing, says Linn, who along with her colleagues at UC Berkeley has designed a dozen Web-based exercises to address that shortcoming (wise.berkeley.edu). The cancer lab that Ross used was one such project, presented in a set of four 45-minute lessons.

Another exercise, on heat and temperature, begins by asking students to predict the temperature of different objects. Many mistakenly think that metallic objects will be colder than wooden ones because metal feels colder. After discovering that everything is at room temperature, the students are asked to propose their own explanations for why objects feel different to the touch.

Then, after watching a simulation of heat flow from the hand into metal and wood, students revise their explanations and "reconcile their sensory experience with the empirical evidence (observed temperatures) and a visualization of heat flow," says Linn. The exercise drives home two fundamental principles: Objects in the same surroundings will reach the same temperature in the absence of a heat source, and heat flows faster through certain materials (conductors) than through others (insulators). Diane Drazinski, a science teacher at Mesquite High School in Gilbert, Arizona, says the activity has helped her students nail down the distinction between heat and temperature, an Achilles' heel in high school physics learning.

In the same vein, to illustrate how ground cover affects climate, Daniel Edelson, a researcher at Northwestern University in Evanston, Illinois, asks high school students first to study the reflectivity of different colored envelopes under a lamp and then predict the reflectivity of grass, sand, and ice. Finally, the students analyze global remote-sensing data that show how deserts reflect more heat than forests. "The sequence enables them to go from direct experience of reflectivity to an analysis of its implications in the actual world," says Christine Nichols, a teacher at Englewood High School in Colorado, who used the activity last year.

Learning by doing. Researchers say training teachers to lead inquiry-based activities is essential to any reform of classroom labs.

CREDIT: JIM ZIV

Pressed for time

Even the most artfully designed inquiry-based lab, however, must compete for time in a crowded academic schedule. Theresa Dzoga-Borg, who teaches at Roberto Clemente High School in Chicago, Illinois, discovered that hard fact recently when she tried to teach her ninth-grade environmental science class the relation between potential and kinetic energy. She gave the students marbles of different sizes, ramps of different heights, and milk cartons; the activity involved rolling marbles down the ramps and measuring how far a carton placed at the bottom of the ramp traveled upon impact.

The exercise engaged the students, she admits. But she and her students were foiled by the clock on the wall. "By the time some of the kids figured out that the distance moved by the carton depended on both the weight of the marble and the height of the ramp, we had only 10 minutes left," says Dzoga-Borg. "They were far from setting up an experiment and recording observations in a systematic way, which would have allowed them to compare their results. We also never got to the point of discussing the conservation of energy in the environment, which was the whole purpose of the exercise." With so much else to cover in subsequent classes, Dzoga-Borg reluctantly abandoned the effort and went back to the textbook.

To help teachers deliver the goods within the allotted time, Michael Lach, director of science for Chicago Public Schools, recommends ongoing professional development. He started an initiative 3 years ago that provides Chicago science teachers with 60 hours of training every year—much of it focused on inquiry-based labs. Schools also need systems in place to facilitate quality lab instruction, says Stephen Flisk, a former science teacher who is now principal of Walsh Elementary School in Chicago. "Ordering supplies, maintaining equipment, setting up the lab at the beginning of each class, cleaning up after—the materials management alone can be overwhelming," Flisk says. "Unless the school dedicates staff for those duties, teachers are more likely to demonstrate the activity instead of having every student do it."

Initiating such sweeping changes, however, won't be easy, reformers acknowledge. "Schools are complicated places with lots of people, traditions, and histories, and it's hard to change them overnight," says Lach.

But some schools appear to be making progress. Pre- and posttests given to Ross's students showed considerable learning gains from the cell division unit. Encouraged by Ross's experience, two fellow science teachers at the middle school are now taking Web-based tutorials so they can teach similar units to their students this school year.

"Hopefully, this is the start of a paradigm shift in how we teach labs," Ross says. He plans to squeeze out more time from classroom instruction for inquiry-based labs next year and to recommend them to teachers at other schools in his district.

–YUDHIJIT BHATTACHARJEE

Roche Applied Science

Genome Sequencer 20 System

First to the Finish

Revolutionize your research with the newest innovation in rapid whole genome sequencing and assembly — the new **Genome Sequencer 20** from Roche Applied Science. Perform genomic analyses not currently possible due to the cost and time constraints of current methods.

- **Generate data fast**
  Sequence at least 20 million bases in one 4.5 hour run.
- **Spend less per base**
  Reduce cost per raw base with rapid, efficient amplification and sequencing through picoliter format with massive parallelization.
- **Simplify sample preparation**
  Eliminate cloning and colony picking with single-tube library preparation per genome.
- **Expand your versatility**
  Perform a wide variety of projects with *de novo* assembly and mapping software.

Be first to the finish! Explore the power of the newest revolution in sequencing today — visit ***www.roche-applied-science.com/sis/sequencing/genome/*** or contact your local sales representative.

454 LIFE SCIENCES

Roche Diagnostics

Roche Diagnostics GmbH
Roche Applied Science
68298 Mannheim
Germany

Edited by Constance Holden

Brane Teaser

String theorists claim there are at least nine dimensions to the universe. So why is our world in only three?

String theory describes subatomic particles as infinitesimally tiny bits of vibrating string. It also predicts extra spatial dimensions, which are hidden because they are tightly curled up or because matter and forces are barred from them.

Nothing in the theory dictates the number of accessible dimensions, though. Now, Andreas Karch of the University of Washington, Seattle, and Lisa Randall of Harvard University have done an analysis that they say shows why a 3D world is the most likely. The researchers assumed that the universe began as a nine-dimensional volume filled with surfaces, or "branes," of every possible dimensionality: from 1D strings to 9D hypercubes. As this universe expanded, any branes that collided would be annihilated, like what happens when matter and antimatter meet. But 3D branes may have survived because geometrically they have a harder time "finding" each other, says Randall. The only alternative reality would be 7D branes, which compensate for self-destruction by filling up more space, she and Karch conclude in the October edition of *Physical Review Letters*. But, notes Karch, gravity is too weak in 7D to hold planets in orbit.

Theoretical physicist David Tong of Cambridge University in the U.K. says the researchers have yet to explain how gravity—the one force that can radiate into extra dimensions—becomes confined to the 3D brane. But if that can be worked out, Tong thinks brane evolution could be a fruitful new line of research.

Mini-Explorer

This photo, entitled "A space shuttle exploring the moon," is actually a picture of a 24-day-old, eight-armed sea urchin larva (*Paracentrotus lividus*) in a petri dish. The image, by Italian biologist Rosa Bonaventura, won first prize last month in a contest organized by Marine Genomic Europe, a 16-country research network.

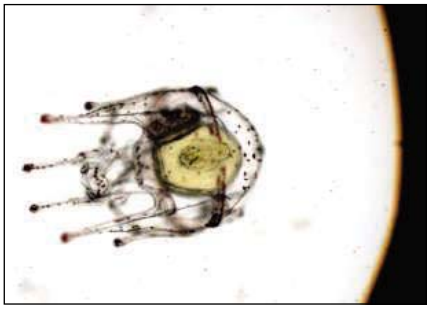

The Talk Landscape

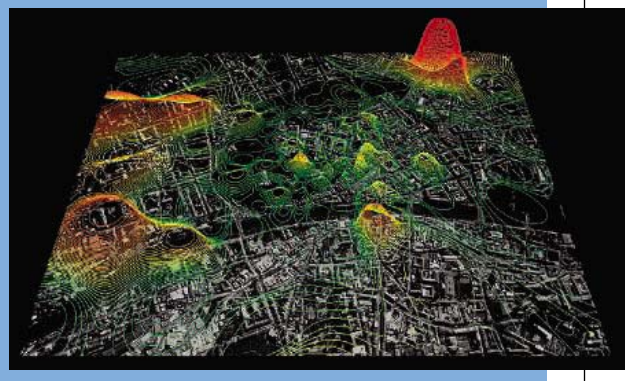

Researchers at the Massachusetts Institute of Technology (MIT) have managed to come up with a unique look at urban personal communication by mapping cell phone usage in Graz, Austria. Created with data from subscribers who agreed to allow their phones to be monitored, the map is part of MIT's Mobile Landscapes project, which generates images that can be overlaid on city maps to "visualize the full dynamics of a city in real time," according to MIT architect and engineer Carlo Ratti. The continuously changing displays, on view at the Kunsthaus Graz exhibit hall until January, will generate "new possibilities for urban studies and planning," he says. The big red hump marks the Dietrichsteinplatz, a major tramway intersection.

A Lying Matter

Rather than longer noses, compulsive liars have about 25% more white matter in the prefrontal cortex, according to a study at the University of Southern California (USC) in Los Angeles.

Researchers have long known that brain activity changes, causing peripheral symptoms such as sweating, during the act of lying. But the new study is the first to look at pathological liars and whether they exhibit differences in brain structure.

A team led by Adrian Raine and Yaling Yang, neuroscientists at USC, used magnetic resonance imaging to compare brain structures in 12 pathological liars, 16 people with antisocial problems other than lying, and 21 normal controls. The liars had more white matter—the fibers connecting neurons—in areas behind the forehead responsible for personality, judgment, and complex planning, the team reports in the October issue of the *British Journal of Psychiatry*.

Raine says more white matter implies more neural connectivity. That, he speculates, may facilitate lying, which is "harder than telling the truth." But the liars also had about 15% less gray matter in the region, meaning they have fewer neurons—possibly relating to "disinhibited, antisocial behavior," says Raine.

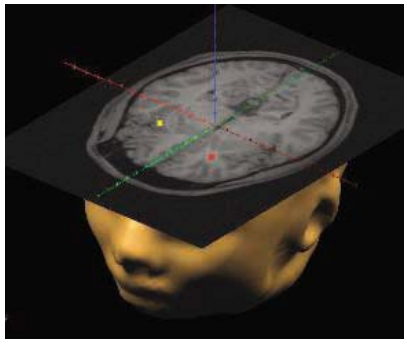

Cutaway skull showing brain of chronic liar.

The study may have "profound consequences for the way we view immoral [behavior]," says Sean Spence, a psychiatrist at the University of Sheffield, U.K., because it shows that a fundamental moral quality "is constrained by biology." Whether lying changes the brain—or whether brain peculiarities make one more prone to lying—is still an open question.

CREDITS (TOP TO BOTTOM): MOBILE LANDSCAPE, GRAZ IN REAL TIME/MIT, SENSEABLE CITY LABORATORY M-CITY EXHIBITION, GRAZ KUNSTHAUS, 2005; YALING YANG/USC; ROSA BONAVENTURA/CONSIGLIO NAZIONALE DELLE RICERCHE, ITALY

Spend less time looking for antibodies and more time doing research...

FREE!

Find Antibodies Online

Search over 130,000 antibodies from over 100 companies by antigen, species reactivity, and application... free and online.

- Over 130,000 Antibodies
- Over 100 Antibody Companies
- No Registration Required
- Full Product Specifications
- Over 225,000 Research Products and Instruments
- Direct Access to Product Pages on Company Websites

biocompare®

The Buyer's Guide for Life Scientists™

www.biocompare.com

Edited by Yudhijit Bhattacharjee

AWARDS

The IgNobels. Although bypassed by Swedish authorities, artificial dog testicles and a study of how penguins poop collected IgNobel Prizes last week at a ceremony in Cambridge, Massachusetts. Half of the 10 awards, given out by the *Annals of Improbable Research* for accomplishments "that cannot or should not be reproduced," went to researchers from Australia or New Zealand.

John Mainstone and the late Thomas Parnell of the University of Queensland, Australia, won the physics prize for patience: Since 1927, the team has monitored one

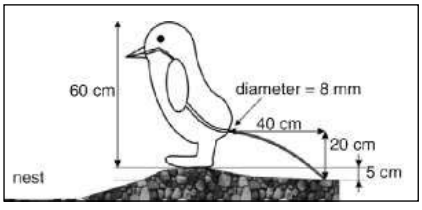

drop of sticky black pitch dripping through a funnel every 9 years. Edward Cussler and Brian Gettelfinger of the universities of Minnesota and Wisconsin captured the chemistry award for determining that people can swim as fast in syrup as in water.

A team from Germany, Finland, and Hungary, who calculated that penguins build up 450 mm Hg of pressure in their bellies to expel excrement the consistency of olive oil away from their nests, could not obtain visas to attend the ceremony. "Let's hope it had nothing to do with the explosive nature of our work," they said in a videotaped acceptance speech.

JOBS

Thinking big. Britain's Environment Agency (EA) has named its first chief scientist and asked him to think more about long-term research questions. Toxicologist Michael Depledge, who has studied endocrine disrupters and continues to do research at Oxford University and at the Plymouth Environmental Research Centre in the southwestern U.K., got the new title last week after the agency agreed with a review he led last year that concluded the agency needs to look farther down the road.

"I like to straddle the boundary" between academic science and action, says Depledge, who also leads EA's 200-person scientific staff. Topics on his study list include nanotechnology, air pollution, mixed chemical effluents, genotoxicity, climate change, and poverty-linked environmental harm.

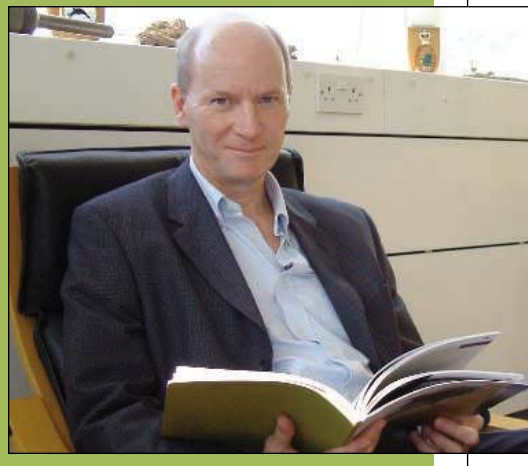

Physics prizes. Mike Gillan of University College London (UCL) last week won the Dirac Medal, the U.K.'s highest honor for theoretical physics. The prize, from the Institute of Physics, recognizes his work on computer simulations to solve many-body quantum mechanical problems, including a calculation of the constraints on the temperature and composition of Earth's core.

The institute's Guthrie Medal goes to Marshall Stoneham, also from UCL, for research in areas from quantum-mechanical defects in semiconductors to the sense of smell. Stoneham, former chief scientist at the U.K. Atomic Energy Authority, is working on a room-temperature quantum computer—an idea often met with "looks of disbelief," he says.

The Glazebrook Medal goes to Andrew Taylor, head of the ISIS facility at the Rutherford Appleton Laboratory, for his contributions to neutron-scattering physics.

Got any tips for this page?
E-mail people@aaas.org

THEY SAID IT

"Darwin pulled off quite a feat, and it remains one of the very great works of intellectual history."

—Cardinal Christoph Schönborn, the Roman Catholic archbishop of Vienna, in a lecture last week. Schönborn offered his remarks as a clarification to a 7 July op-ed he wrote in *The New York Times* that argued in favor of intelligent design.

CELEBRITIES

Toxic award? Harvard's School of Public Health (HSPH) has stirred controversy by awarding its top honor to celebrity activist Erin Brockovich-Ellis (below). As a file clerk at a law firm, Brockovich-Ellis uncovered a case of industrial pollution that led to a $333 million settlement in 1996 and inspired an eponymous Hollywood blockbuster. But critics say the award endorses a "symbol of junk science."

Facilities owned by Pacific Gas and Electric leaked the carcinogen chromium-6 into drinking water for decades. In an invitation to the 18 October awards ceremony, HSPH Dean Barry Bloom lauded Brockovich "for her efforts on behalf of all of us, and especially the residents of Hinkley, California, whose health was adversely affected by toxic substances dumped by a utility company."

But Harvard physicist Richard Wilson, who has studied arsenic poisoning in Bangladesh, objects: "If you have the dean saying that this harmed the residents of Hinkley, that's false." And Elizabeth Whelan, an HSPH alumnus and president of the American Council on Science and Health, who is boycotting the ceremony, says there's no evidence that ingesting chromium-6 causes cancer.

Brockovich gets an endorsement from Lynn Goldman of Johns Hopkins School of Public Health in Baltimore, Maryland, however, who points out that chromium-6 can be carcinogenic when inhaled, say from water vapors.

CREDITS (TOP TO BOTTOM): PLYMOUTH MARINE LABORATORY; VICTOR BENNO MEYER-ROCHOW, JOZSEF GAL, *POLAR BIOL* 27 (2003); ERIN BROKOVICH-ELLIS

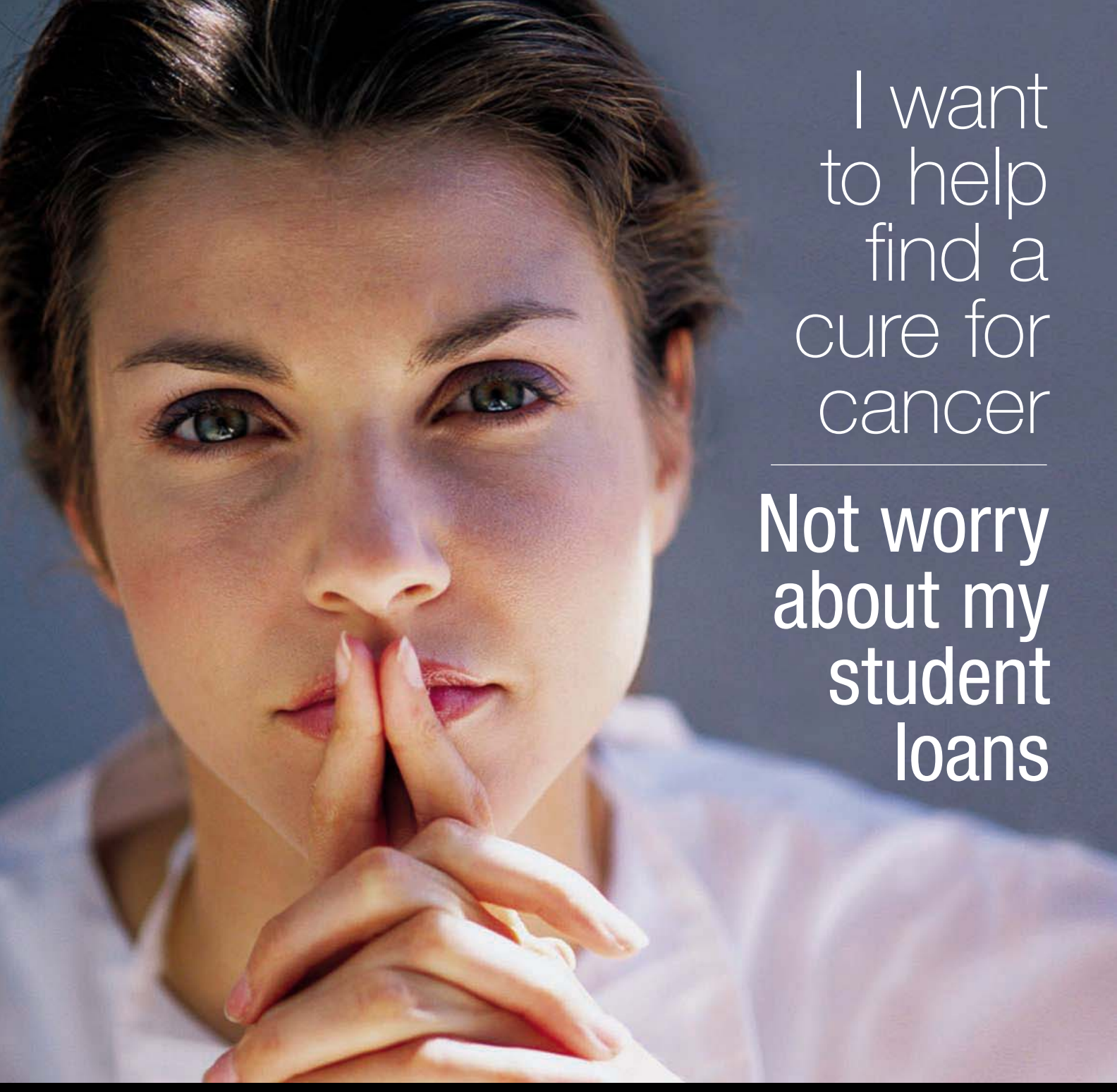

I want to help find a cure for cancer

Not worry about my student loans

If you're interested in a biomedical research career, you should know that the National Institutes of Health Loan Repayment Programs may repay up to $35,000 per year of your qualified educational loan debt.

Deadline for Applications is December 1

For more information, visit www.lrp.nih.gov or call 1–866–849–4047

The NIH Loan Repayment Programs | *Healthier Futures Through Research*

Debate Over a GM Rice Trial in China

In their Report "Insect-resistant GM rice in farmers' fields: assessing productivity and health effects in China" (29 Apr., p. 688), J. Huang *et al.* found that farmers growing insect-resistant GM rice obtained higher yields with less use of insecticides than farmers growing conventional varieties. Huang *et al.*'s methodology does not, however, permit discrimination between two alternative hypotheses explaining the farmers' decision to spray Bt/Ti rice less often: (i) farmers sprayed Bt/Ti rice less often because they observed fewer lepidopterans (the main insect pests that would be affected); or (ii) because the farmers knew beforehand which variety they were growing, they decided a priori to spray Bt/Ti rice less often.

Were farmers responding to real effects of Bt/Ti rice, or were they acting on faith that they needed to spray conventional varieties frequently but Bt/Ti rice only occasionally? To test for real effects, a subset of farmers should not know which type of rice they are growing. This can be accomplished by conducting a double-blind study or by adding a placebo treatment. To assess farmers' responsiveness to pest infestation, pest levels should also be analyzed.

The influence of farmers' perceptions on pest management in rice is well known. Farmers tend to spray more insecticides than needed (*1*–*4*) unless their perceptions are changed. Spraying has been successfully reduced without yield loss and without adoption of Bt/Ti technology by rice farmers under a number of different circumstances (*5*–*8*). Perhaps the Chinese farmers in this study could also have reduced spraying of the conventional varieties without yield loss.

In the precommercialization evaluation of the impact of insect-resistant GM food crops on productivity, health, and the environment, we stress the importance of distinguishing between perceived and real effects of the transgenic variety.

A Chinese researcher looks at seedlings of a GM rice strain in south China's island province of Hainan.

CREDIT: REUTERS/CHINA NEWSPHOTO

K. L. Heong,[1] Yolanda H. Chen,[1] David E. Johnson,[2] Gary C. Jahn,[1] Mahabub Hossain,[3] Ruaraidh Sackville Hamilton[4]

[1]Entomology and Plant Pathology Division, [2]Crop, Soil, and Water Sciences Division, [3]Social Sciences Division, [4]Genetic Resources Center, International Rice Research Institute, DAPO Box 7777, Metro Manila, Philippines.

References

1. J. W. Bentley, *Agric. Hum. Values* **6**, 25 (1989).
2. J. Mumford, G. A. Norton, *Annu. Rev. Entomol.* **29**, 157 (1984).
3. H. Waibel, *The Economics of Integrated Pest Control in Irrigated Rice* (Springer, Berlin, 1986).
4. A. Rola, P. L. Pingali, *Pesticides, Rice Productivity and Farmers' Health—An Economic Assessment* (International Rice Research Institute, Los Baños, Philippines, 1993).
5. K. L. Heong, M. M. Escalada, *J. Appl. Commun.* **81**, 3 (1997).
6. M. M. Escalada, K. L. Heong, *Crop Prot.* **18**, 315 (1999).
7. P. C. Matteson, *Annu. Rev. Entomol.* **45**, 549 (2000).
8. M. Escalada *et al.*, *J. Appl. Commun.* **83**, 7 (1999).

It was with some astonishment that we read the Report by J. Huang *et al.* about the trials of GM rice in farmers' fields in China ("Insect-resistant GM rice in farmers' fields: assessing productivity and health effects in China," 29 Apr., p. 688). Just two weeks before this Report was published, Greenpeace revealed (*1*) the illegal sale and cultivation of GM rice varieties in China. At least one of these illegal GM varieties, Bt Xianyou (or Shanyou) 63, appears to have been used in Huang *et al.*'s study. What measures were taken to contain the GM rice (e.g., separation barriers from conventional rice), and how was the GM rice harvest collected?

Reducing the use of pesticides in agriculture is certainly a worthwhile goal. However, this short-term study did not consider the medium- to long-term aspects of Bt crop management, such as the practicalities of Bt refugia required to delay insect resistance to Bt crops. The Report also omitted any food safety concerns regarding the GM rice and did not consider potential ecological impacts such as adverse effects on nontarget organisms.

In addition to the wider biosafety issues concerning GM crops, this research raises serious ethical concerns for those involved in GM crop trials. We suggest that, in the future, safeguards aiming to prevent GM contamination should be made a prerequisite of any such GM crop trials and a precondition of publication of their results.

Pang Cheung Sze[1] and Janet Cotter[2]

[1]Greenpeace China, 3/F, Seaview Commercial Building, 21-24 Connaught Road West, Sheung Wan, Hong Kong. E-mail: Pang.Cheung.Sze@hk.greenpeace.org. [2]Greenpeace Research Laboratories, Department of Biological Sciences, University of Exeter, Exeter EX4 4PS, UK. E-mail: J.Cotter@exeter.ac.uk.

Reference

1. See www.greenpeace.org/raw/content/international/press/reports/RiceatRiskTestResults.pdf.

In their Report ("Insect-resistant GM rice in farmers' fields: assessing productivity and health effects in China," 29 Apr., p. 688), J. Huang *et al.* show reduced pesticide use and higher yields of Bt rice in preproduction trials in China, supporting the suggestion that GM crops could help reduce hunger, which may influence commercialization globally. This study does not discuss potential costs. One estimate of the cost to develop a GM variety is 50 times that of a conventional variety (*1*). Other costs include refuges and resistance monitoring to manage evolution of resistance (for pesticidal crops like Bt rice) and containment measures to reduce gene flow, especially in centers of crop origin and diversity (*2*). Significant gene flow from domestic rice to wild and weedy relatives has been documented (*3*); transgene flow from herbicide-tolerant or Bt crops may increase weed resistance (*4*), negatively affect nontarget species (*5*), compromise refuge efficacy (*6*), or increase social costs (*7*, *8*).

However, comparing existing conventional varieties with GM varieties is not enough. Investments in alternative approaches to reducing hunger with possibly higher benefits and costs need to be considered (*7*). As with the green revolution (*9*), alternative strategies could have higher net benefits. For example, increasing rice diversity through intercropping in small-scale agriculture in China significantly reduced plant disease and increased yields while conserving genetic diversity at minimal cost (*10*, *11*). Greater participation of small-scale farmers will be critical in assessing the potential of GM crops and alternatives to reduce

hunger—these farmers produce food in systems that are very different from those for which GM crops have so far been developed, and they may have preferences for different possible scenarios (*8*, *12*).

DAVID A. CLEVELAND AND DANIELA SOLERI
Department of Environmental Studies, University of California, Box 4160, Santa Barbara, CA 93106–4160, USA.

References

1. M. M. Goodman, *Crop Sci.* **44**, 1913 (2004).
2. National Research Council, *Biological Confinement of Genetically Engineered Organisms* (National Academies Press, Washington, DC, 2004).
3. L. J. Chen, D. S. Lee, Z. P. Song, H. S. Suh, B. R. Lu, *Ann. Bot.* **93**, 67 (2004).
4. D. R. Gealy, D. H. Mitten, J. N. Rutger, *Weed Technol.* **17**, 627 (2003).
5. D. A. Andow, A. Hilbeck, *Bioscience* **54**, 637 (2004).
6. C. F. Chilcutt, B. E. Tabashnik, *Proc. Natl. Acad. Sci. U.S.A.* **101**, 7526 (2004).
7. National Research Council, *Environmental Effects of Transgenic Plants: The Scope and Adequacy of Regulation* (National Academy Press, Washington, DC, 2002).
8. D. A. Cleveland, D. Soleri, *Ecol. Soc.* **10** (no. 1), Article 9 (2005) (available at www.ecologyandsociety.org/vol10/iss1/art9/).
9. N. W. Simmonds, J. Smartt, *Principles of Crop Improvement* (Blackwell Science, Oxford, UK, ed. 2, 1999), p. 352.
10. Y. Zhu, Y. Wang, H. Chen, B.-R. Lu, *Bioscience* **53**, 158 (2003).
11. Y. Y. Zhu *et al.*, *Nature* **406**, 718 (2000).
12. D. Soleri *et al.*, in preparation.

Response

HEONG *ET AL.* ARE CONCERNED THAT WE ARE not properly isolating the effect of GM rice on insecticide use. Heong *et al.* suggest that because GM rice in China is called "insect-resistant rice," farmers are being given the message that with this new variety of rice they do not need to use any pesticides, and that because of this, our results overstate the GM effect by attributing the entire decline in pesticide use to the adoption of GM rice. They implicitly claim that similar declines in pesticide use would have occurred in non-GM rice had similar extension efforts promoting varieties that need low applications of pesticides been made.

When we designed our study, in fact, we were concerned with isolating the GM effect from the perception effect (see our SOM). We included a measure of the perception of farmers of the loss that would occur due to not using pesticides. The magnitude of the perception effect is relatively small. If we make the most extreme assumption and assume that there is a perception effect for conventional rice but no perception effect for GM rice (Heong *et al.*'s assumption), this would account for 21% (or 4.13/19.2) of the difference between the pesticide used on conventional and GM rice. The GM effect, however, is much larger (–16.77 or 88%).

Sze and Cotter allege that the farmers may have been producing GM rice illegally and that we did not address the medium- to long-term aspects of Bt crop management, such as the issue of refugia for GM rice in China.

It is not true that farmers in our sample areas were illegally growing GM rice. In fact, after being approved in both the field trial and environmental release trial phases of the biosafety procedures before 2000, China's Biosafety Committee mandated that the newly approved varieties (GM Xianyou 63 and GM II–Youming 86) undergo further testing in preproduction trials. The main purpose of preproduction trials was to assess how well the new varieties perform under actual field conditions. Following the directions of the Biosafety Committee, the scientific teams that developed the new GM rice varieties provided seeds to farmers in a set of specified villages. After obtaining permission from the scientific teams, our research group visited the preproduction villages and randomly selected a sample of farmers for the study from a list of all farmers in the village, some of whom were producing GM varieties and some of whom were not.

The main focus of our paper was to examine the impact of GM rice (i) on the use of chemical pesticide use; (ii) on rice yields; and (iii) on the health of producers. Using descriptive statistics and standard econometric methods, we discovered that holding all other factors constant, GM rice improved the productivity of rice production by reducing pesticide use and raising yields. We agree that there also is a need to examine whether China will need to implement a refuge policy if the nation decides to commercialize GM rice. Given the nature of our sample, however, this was not an appropriate topic of study.

Sze and Cotter also suggest that "safeguards aiming to prevent GM contamination should be made a prerequisite of any such GM crop trials and a precondition of publication of their results." Although this is an important point, this would seem to be a matter that needs to be addressed by China's Biosafety Committee and the individual research teams.

Cleveland and Soleri raise a number of issues that they suggest may affect the ultimate net benefit of commercialization of GM rice. Specifically, they suggest that there are other costs that need to be considered: the increased cost of developing GM rice compared with that of conventional rice varieties, refuge costs, and the costs associated with biosafety regulation. We agree that it is important to research these issues. However, these issues were beyond the scope of our paper. We also agree that governments and international donors need to make a number of alternative investments—not just in GM crops—in their battle against hunger and poverty. Our research, however, shows that the commercialization of GM rice would help reduce poverty. In fact, in our work on producer effects of Bt cotton in China, we show that there is rapid adoption by small, relatively poor farmers who improve productivity and health (*1*). In other work, we show that the rate of return for both Bt cotton and GM rice inside China is high (*2*).

JIKUN HUANG,[1] RUIFA HU,[1] SCOTT ROZELLE,[2] CARL PRAY[3]

[1]Center for Chinese Agricultural Policy, Institute of Geographical Sciences and Natural Resource Research, Chinese Academy of Sciences, Jia 11, Datun Road, Beijing 100101, China. [2]Department of Agricultural and Resource Economics, University of California Davis, 1 Shields Avenue, Davis, CA 95616, USA. [3]Department of Agricultural, Food, and Resource Economics, Rutgers University, 55 Dudley Road, New Brunswick, NJ 08901–8520, USA.

References

1. J. Huang, C. Pray, S. Rozelle, Q. Wang, *Science* **295**, 674 (2002).
2. J. Huang, R. Hu , H. van Meijl, F. van Tongeren, *J. Dev. Econ.* **75**, 27 (2004).

AMPA Receptor Trafficking and GluR1

IN THEIR RESEARCH ARTICLE "POSTSYNAPTIC receptor trafficking underlying a form of associative learning" (1 Apr., p. 83), S. Rumpel *et al.* draw the important conclusions that "encoding of memories in the lateral amygdala is mediated by AMPA receptor trafficking" and that "synaptic incorporation of AMPARs is necessary for learning." The key experiment used to test the importance of the AMPA receptor trafficking involved the overexpression of a recombinant AMPA receptor fragment comprising 81 amino acids of the COOH-terminus of GluR1 and is referred to as the "plasticity-block" vector. This fragment is rich in protein-protein interaction sites (including PDZ, Forkhead-associated, 14-3-3 domain, and ERK and PDK docking sites) and phosphorylation sites for several kinases (PKA, PDK1, CamKII). The overexpression of this plasticity block vector will interfere with these kinases and protein interactions. Because these kinases and protein interactions are well known to regulate many synaptic (and nonsynaptic) substrates other than GluR1, it should not be assumed that only AMPA receptors are inhibited by the plasticity block vector. For example, PKA and CamKII phosphorylate multiple ion channels, enzymes, and scaffold proteins (*1*, *2*). These experiments do not therefore prove that AMPA trafficking is either necessary or sufficient for learning. A possible conclusion would be that AMPA receptor trafficking can occur with learning, and further work is necessary before its role in learning is established.

SETH G. N. GRANT
The Wellcome Trust Sanger Institute, Hinxton, Cambridge, Cambridgeshire CB10 1SA, UK.

References
1. T. Yamauchi, *Mass Spectrom. Rev.* **21**, 266 (2002).
2. M. O. Collins *et al.*, *J. Biol. Chem.* **280**, 5972 (2005).

Response

GRANT'S IN SILICO ANALYSIS SUGGESTS THAT overexpression of the GluR1-c-tail construct could perturb processes unrelated to GluR1 trafficking and thereby block plasticity.

None of the interactions predicted by Grant with in silico methods have been identified with experimental approaches to isolate GluR1 interactors, such as the yeast two-hybrid and proteomic methods. Conversely, the experimentally demonstrated CaMKII phosphorylation site on GluR1-c-tail is not predicted by such methods. Indeed, GFP is predicted in silico to have up to 15 kinase or protein interaction sites (many of the same as predicted

for GluR1-c-tail). More importantly, the only proteins experimentally demonstrated to interact with GluR1-c-tail (i.e., 4.1 and SAP-97) have been shown to affect GluR1 trafficking to synapses during plasticity (*1*, *2*).

The kinases mentioned by Grant (as potentially inhibited by GluR1-c-tail) affect function of NMDA receptors, K channels, Na channels, etc. We have shown that 1 or 2 days' expression of GluR1-c-tail produces no effect on synaptic NMDA currents, input resistance, resting potential, or action potential firing [(*3*), our Report]. Thus, GluR1-c-tail does not significantly affect these kinases or any protein-protein interactions controlling these processes.

We agree that the exact mechanism by which GluR1-c-tail blocks plasticity is not established. However, several studies now show that GluR1 is driven into synapses during plasticity [(*3, 4*), our Report], and mutagenesis studies show that the GluR1-c-tail plays a crucial role in controlling synaptic trafficking of GluR1 (*3*, *4*). It is thus logical that overexpression of the GluR1-c-tail would perturb plasticity by blocking GluR1 trafficking. Similar strategies have been used to show that fragments of GluR2 perturb GluR2 trafficking (*3*, *5*–*10*).

Most of the results of our study do not depend on the GluR1-c-tail construct specifically affecting AMPA receptor trafficking. We showed that learning drives GluR1 into synapses, demonstrating that learning modifies synapses, a long-held conjecture and a result independent of the GluR1-c-tail construct. Our finding that synaptic modifications are widely distributed is also independent of this construct. And lastly, finding that learning is very sensitive to plasticity block is independent of the mechanism by which GluR1-c-tail blocks plasticity.

ROBERTO MALINOW,[1] SIMON RUMPEL,[1] ANTHONY ZADOR,[1] JOSEPH LEDOUX[2]

[1]Cold Spring Harbor Laboratory, Cold Spring Harbor, NY 11724, USA. [2]New York University, New York, NY 10003, USA.

References

1. L. Shen, F. Liang, L. D. Walensky, R. L. Huganir, *J. Neurosci.* **20**, 7932 (2000).
2. T. Nakagawa *et al.*, *Neuron* **44**, 453 (2004).
3. S. Shi, Y. Hayashi, J. A. Esteban, R. Malinow, *Cell* **105**, 331 (2001).
4. Y. Hayashi *et al.*, *Science* **287**, 2262 (2000).
5. C. H. Kim, J. E. Lisman, *J. Neurosci.* **21**, 4188 (2001).
6. C. Luscher *et al.*, *Neuron* **24**, 649 (1999).
7. A. Luthi *et al.*, *Neuron* **24**, 389 (1999).
8. A. Nishimune *et al.*, *Neuron* **21**, 87 (1998).
9. J. Noel *et al.*, *Neuron* **23**, 365 (1999).
10. C. H. Kim, H. J. Chung, H. K. Lee, R. L. Huganir, *Proc. Natl. Acad. Sci. U.S.A.* **98**, 11725 (2001).

Avian Flu: In Taiwan or Not?

IN THE BREVIA "HIGHLY PATHOGENIC H5N1 influenza virus infection in migratory birds" (J. Liu *et al.*, 19 Aug., p. 1206), Fig. 1 showed Taiwan as one of the areas affected by the avian influenza virus H5N1. This figure is incorrect. A surveillance program for monitoring avian influenza virus has been active in Taiwan since 1998, and H5N1 has not been found. Taiwan is also recognized as being free from avian influenza by the World Organization for Animal Health (OIE).

WATSON H. T. SUNG

Director General, Bureau of Animal and Plant Health Inspection and Quarantine, Council of Agriculture, Executive Yuan, SF, 51, Section 2, Chungching South Road, Taipei 100, Taiwan.

Response

THE INFORMATION ON H5 AVIAN INFLUENZA virus in Taiwan came from two Web sites (*1*, *2*). The first Web site claimed the identification of H5N1 from red-faced ducks (Muscovy ducks) in Kim-meng (Jinmen), Taiwan (*1*), and the second claimed that H5N2 viruses were isolated from chicken

farms in the counties of Changhwa (Zhanghua) and Tainan, Taiwan. Therefore, we believe that our figure is correct.

GEORGE F. GAO
Institute of Microbiology, Chinese Academy of Sciences, Beijing 100080, China. E-mail: gao@im.ac.cn

References
1. See http://news.tom.com/1002/3293/20040101-564295.html.
2. See http://www.fx120.net/news/news-zt/rdzt-qlg/nd/20040215090059.htm.

CORRECTIONS AND CLARIFICATIONS

Reports: "Triangular and Fibonacci number patterns driven by stress on core/shell microstructures" by C. Li *et al.* (5 Aug., p. 909). Reference (*9*) was wrongly cited. It should be "X. N. Zhang, C. R. Li, Z. Zhang, Z. X. Cao, *Appl. Phys. Lett.* **85**, 3570 (2004)." The new reference (*9*) should be cited in the sentence "As expected, the densest pattern is observed in the shell structure shown in Fig. 1A (*9*), which has the best image quality because the SiO_x layer is very thin." This sentence appears on page 910, second column, line 8.

TECHNICAL COMMENT ABSTRACTS

COMMENT ON "The Brain of LB1, *Homo floresiensis*"

Jochen Weber, Alfred Czarnetzki, Carsten M. Pusch

Falk *et al.* (Reports, 8 April 2005, p. 242) presented new data on the brain of the type specimen of *Homo floresiensis*, LB1. We argue that the size, proportions, and shape of the LB1 endocast fall within the range of variation observed for microcephalics. This specimen might therefore represent a pathological human being rather than a new hominid species.

Full text at www.sciencemag.org/cgi/content/full/310/5746/236b

RESPONSE TO COMMENT ON "The Brain of LB1, *Homo floresiensis*"

Dean Falk, Charles Hildebolt, Kirk Smith, M. J. Morwood, Thomas Sutikna, Jatmiko, E. Wayhu Saptomo, Barry Brunsden, Fred Prior

Weber *et al.* claim to have one microcephalic individual whose endocast shape is essentially identical to that of LB1, but they fail to provide its absolute measurements or illustrate it properly. We show that images of their microcephalic endocasts resemble those of the microcephalic we compared to LB1.

Full text at www.sciencemag.org/cgi/content/full/310/5746/236c

Letters to the Editor

Letters (~300 words) discuss material published in *Science* in the previous 6 months or issues of general interest. They can be submitted through the Web (www.submit2science.org) or by regular mail (1200 New York Ave., NW, Washington, DC 20005, USA). Letters are not acknowledged upon receipt, nor are authors generally consulted before publication. Whether published in full or in part, letters are subject to editing for clarity and space.

SYSTEMS BIOLOGY

The Origins of Stability

Greg Gibson

Robustness and Evolvability in Living Systems
by Andreas Wagner

Princeton University Press, Princeton, NJ, 2005. 383 pp. $49.50, £32.50. ISBN 0-691-12240-7. Princeton Studies in Complexity.

In the last few months, five airliners have crashed in various places around the world, apparently due to unrelated failures. On reflection, this is not so surprising—considering the amount of time that I spend sitting on tarmacs waiting for cockpit warning lights to be heeded. Manifold failures must be occurring frequently, so I assume that engineers have built in fail-safe mechanisms that allow planes to cope with them. So too must organisms be robust to genetic and environmental perturbations. Only instead of having been designed to be robust, they have evolved that way. In *Robustness and Evolvability in Living Systems*, Andreas Wagner synthesizes the mechanisms and consequences of such biological buffering. The book, a volume in the Princeton Studies in Complexity series, is sure to lay the foundation for growth of research in this underappreciated field of study.

In the first half of the book, Wagner (a computational and theoretical evolutionary biologist at the University of New Mexico) provides a masterful survey of the literature on robustness at all levels of biological organization, from the genetic code through RNA and protein structure to metabolic organization and pattern formation during development. Biologists and engineers alike will find snippets of interest in these chapters, and taken together they ought to convince even the most skeptical reader that robustness to perturbation is a pervasive aspect of biology. In the book's second half, Wagner reviews the theory of robustness. His readily comprehensible account uses only such mathematics as is essential to convey the key concepts. Wagner offers some new theory, but for the most part his treatment is synthetic. Nonetheless, it certainly provokes thought in new directions.

Perhaps the most crucial chapter of *Robustness* is the one that hinges the book's two main parts, in which Wagner introduces the concept of a neutral space. Rather than being defined in terms of adaptive value, the term neutral is used more loosely in reference to the observation that there are always multiple different ways to achieve any objective: all of the equivalent solutions occupy a neutral space. For example, the long neck of a giraffe could have evolved either by addition of extra cervical vertebrae or by lengthening of the existing ones. Or, considering changes at the molecular level, any given RNA or protein secondary structure can be achieved by hundreds of different sequences so long as substitutions don't disrupt the folding energy. Wagner makes three observations about neutral spaces: (i) They are ubiquitous at all levels of organization from molecule to organism. (ii) Different points in neutral space will generally vary in their robustness to perturbation. (iii) Natural selection will tend to favor the most robust solution.

It may seem intuitive to conclude from these observations that the evolution of robustness is inevitable, but Wagner recognizes and explores two reasons why this is not actually the case. First, the most robust solution may not be accessible from all places in the neutral space. (Adding and growing cervical vertebrae are completely different developmental mechanisms; once one has been settled on, it is almost impossible to explore the alternative.) Second, selection only leads to evolution if the variation is heritable. Unfortunately, quantitative genetics—which is central to understanding the capacity for genetic components of robustness to evolve under selection—is the one aspect of the theory of robustness that the author does not treat in much detail in the book.

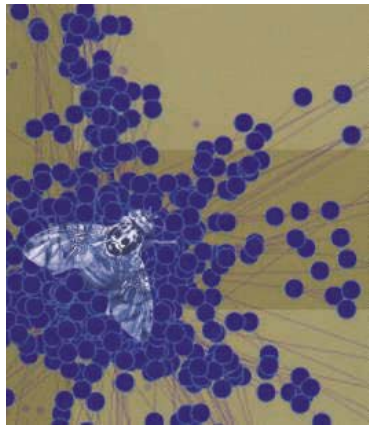

Nevertheless, Wagner does a wonderful job of outlining the parameters of the debate. He recognizes two basic difficulties. One is a catch-22: the more robust a system becomes, the less variable it is (by definition), and the less raw material there is available for selection to act on. A possible—but as yet unsubstantiated—solution to this dilemma is that environmental variation is always present. Thus, so long as selection acts to reduce environmental noise, genetic robustness might be expected to evolve in parallel. A more basic conundrum is that robustness must involve non-additive genetic interactions, but quantitative geneticists have—for the better part of a century—generally accepted that it is only the additive component of genetic variation that responds to selection. Consequently, we are faced with the observation that biological systems are pervasively robust but find it hard to explain exactly how they evolve to be that way.

Wagner's provocative suggestion is that very often the robustness may be an intrinsic property of biological systems, an inevitable consequence of processes that make order out of chaos. He considers two basic buffering mechanisms, redundancy and distributed robustness, and he concludes that the latter is much more commonly responsible for robustness. That is, whereas gene duplication (for example) certainly provides fail-safe switches on occasion, it does not appear to be the general solution we might naïvely expect. Rather, we should look to the capacity of whole systems to absorb the effects of environmental noise and genetic mutation, whether through compensatory nucleic acid or amino acid interactions or by shunting metabolites through alternate components of the network. Perturbation is distributed, and robustness is built into the very structure of biochemical and physiological organization.

Several years ago, Stuart Kauffman prefaced *The Origins of Order* with the observation that "no body of thought incorporates self-organization into the weave of evolutionary theory" (*1*). *Robustness and Evolvability in Living Systems* adds an extra dimension to this endeavor. Wagner contributes significantly to the emerging view that natural selection is just one, and maybe not even the most fundamental, source of biological order. His two-page epilogue throws out seven open questions for systems biologists and neo-Darwinians to consider; hopefully they will do so.

The reviewer is in the Department of Genetics, North Carolina State University, Raleigh, NC 27695–7614, USA. E-mail: ggibson@unity.ncsu.edu

Reference
1. S.A. Kauffman, *The Origins of Order: Self-Organization and Selection in Evolution* (Oxford Univ. Press, New York, 1993).

10.1126/science.1119501

Finish your research projects in record time

with 454 sequencing services

Take the inside track with fast, accurate and cost-effective whole genome sequencing. Using proprietary technology, we can sequence over 20 mbps in a 4-hour run at a cost that makes whole genome sequencing practical for a wider range of your projects.

Choose from our full range of high-speed sequencing services including:

- Microbial strain variant comparison
- Resequencing for mutation identification
- Raw reads for a variety of sample types
- Whole genome de novo sequencing and assembly of microbial genomes

You supply the sample. We do the work, and provide you with high-quality data in industry-standard format.

Complete your research in record time. Put 454 Life Sciences Measurement Services to work on your next sequencing project. Call 203-871-2300 or email msc@454.com

454 LIFE SCIENCES

get there faster

454 Life Sciences Measurement Services
203-871-2300 | msc@454.com

INTELLECTUAL PROPERTY

Intellectual Property Landscape of the Human Genome

Kyle Jensen and Fiona Murray*

Gene patents are the subject of considerable debate and yet, like the term "gene" itself, the definition of what constitutes a gene patent is fuzzy (*1*). Nonetheless, gene patents that seem to cause the most controversy are those claiming human protein-encoding nucleotide sequences. This category is the subject of our analysis of the patent landscape of the human genome (*2*).

Enhanced online at www.sciencemag.org/cgi/content/full/310/5746/239

Critics describe the growth in gene sequence patents as an intellectual property (IP) "land grab" over a finite number of human genes (*3*, *4*). They suggest that overly broad patents might block follow-on research (*5*). Alternatively, gene IP rights may become highly fragmented and cause an anticommons effect, imposing high costs on future innovators and underuse of genomic resources (*6*). Both situations, critics argue, would increase the costs of genetic diagnostics, slow the development of new medicines, stifle academic research, and discourage investment in downstream R&D (*7*–*11*).

In contrast, the classic argument in support of gene patenting is that strong IP protection provides incentives crucial to downstream investment (*12*, *13*) and the disclosure of inventions. Patents are also regarded as the cornerstone of vibrant markets for ideas (*14*) and central to the biotech boom of the 1980s and 1990s (*15*).

Policy-makers are hampered by the lack of empirical data on the extent of gene patenting. Most analyses have relied on anecdotal evidence (*11*, *16*–*18*) and empirical analyses have been hindered by (i) limited (and poorly defined) coverage of DNA sequence patents (*17*, *19*); (ii) difficulty separating patents that claim gene sequences per se from those merely disclosing DNA sequences (*20*–*22*); and (iii) distinguishing patents on the human genome from those on other species (*23*).

Our detailed map was developed using bioinformatics methods to compare nucleotide sequences claimed in U.S. patents to the human genome. Specifically, this map is based on a BLAST (*24*) homology search linking nucleotide sequences disclosed and claimed in granted U.S. utility patents to the set of protein-encoding messenger RNA transcripts contained in the National Center for Biotechnology Information (NCBI) RefSeq (*25*) and Gene (*26*) databases. This method allows us to map gene-oriented IP rights to specific physical loci on the human genome (*27*) (see figure, right). Our approach is highly specific in its identification of patents that actually claim human nucleotide sequences. However, by limiting the search to patents using the canonical "SEQ ID NO" claim language we do not consider claims on genes defined through amino acid sequences. (See table S1 for a sensitivity analysis.)

Our results reveal that nearly 20% of human genes are explicitly claimed as U.S. IP. This represents 4382 of the 23,688 of genes in the NCBI's gene database at the time of writing (see figure, right). These genes are claimed in 4270 patents within 3050 patent families (*28*). Although this number is low compared with prior reports, a distinction should be made between sequences that are explicitly claimed and those that are merely disclosed, which outnumber claimed sequences roughly 10:1. The 4270 patents are owned by 1156 different assignees (with no adjustments for mergers and acquisition activity, subsidiaries, or spelling variations). Roughly 63% are assigned to private firms (see figure, above). Of the top ten gene patent assignees, nine are U.S.-based, including the University of California, Isis Pharmaceuticals, the former SmithKline Beecham, and Human Genome Sciences. The top patent assignee is Incyte Pharmaceuticals/Incyte Genomics, whose IP rights cover 2000 human genes, mainly for use as probes on DNA microarrays.

Although large expanses of the genome are unpatented, some genes have up to 20 patents asserting rights to various gene uses and manifestations including diagnostic uses, single nucleotide polymorphisms (SNPs), cell lines, and constructs containing the gene. The distribution of gene patents was nonuniform (see figure, page 240, top right): Specific regions of the genome are "hot spots" of heavy patent activity, usually with a one-gene-many-patents scenario (see figure, below). Although less common, there were cases in which a single patent claims many genes, typically as complementary DNA probes used on a microarray (see figure, p. 240, bottom).

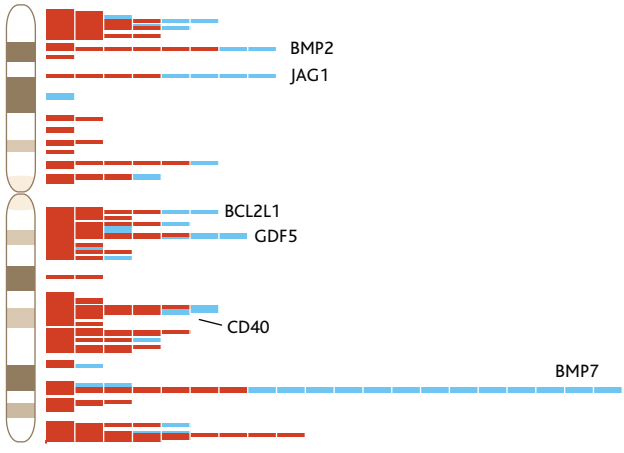

Physical mapping of patent activity on chromosome 20, divided into 300-kb segments. Each horizontal bar represents a unique patent claiming a gene sequence located in that region. Orange represents the number of unique patent families in a region (*28*). Labels show the loci of highly patented genes (see table S1).

BMP7, an osteogenic factor, and CDKN2A, a tumor suppressor gene, were the most highly patented genes in the genome [their sequences were each claimed in 20 patents (table S2)]. The patents on CDKN2A are distributed between nine different assignees and, collectively, claim all three splice variants of the gene. Nearly all of these patents are directed toward diagnostic applications. In contrast, the patents on BMP7 are for the use of BMP7 proteins in implants to stimulate bone growth. However, a number are directed towards more speculative utilities, such as drug-screening probes, which suggests a strategy of "science-

K. Jensen is in the Department of Chemical Engineering, F. Murray is in the Sloan School of Management, Massachusetts Institute of Technology, Cambridge, MA 02139, USA.

*Author for correspondence. E-mail: fmurray@mit.edu

based" rather than "disease-based" patenting.

Unsurprisingly, other heavily patented genes tended to have relevance to human health and diseases: e.g., BRCA1 (breast cancer), PIK3R5 (diabetes), and LEPR (obesity). Of the 291 cancer genes reviewed by Futreal *et. al.* (*29*), 131 are patented—significantly more than expected for a random sample of genes ($P = 1.2^{-32}$ based on binomial distribution). Moreover, these genes contain a higher number of patents per gene than expected by chance ($P = 9.4^{-11}$ based on a chi-squared test) (*30*).

Of the 4000+ patented genes, at least 3000 have only a single IP rights holder. For the remainder, we examined whether IP ownership was fragmented by constructing a measure based on the Herfindahl index (*31*) (see figure, top right; part C). The two genes with the most fragmented ownership were PSEN2, the amyloid precursor protein (8 assignees for 9 patents), and BRCA1, the early onset breast cancer gene (12 assignees for 14 patents). Such fragmentation raises the possibility that innovators may incur considerable costs securing access to genes via structuring complex licensing agreements.

Our analysis suggests a number of avenues for further research: It would be valuable to examine whether current practice in patent examination has allowed multiple conflicting patents on the same gene. In addition, genes with multiple patents and IP owners provide a valuable context in which to explore the variety of arrangements used to facilitate or block access to gene-based research and the impact of these arrangements on future innovators. Finally, whereas our study includes only protein-coding genes, future studies should characterize the nature and extent of the rapidly growing IP surrounding non–protein coding components of the human genome, such as microRNAs, ribozymes, and cis-regulatory elements.

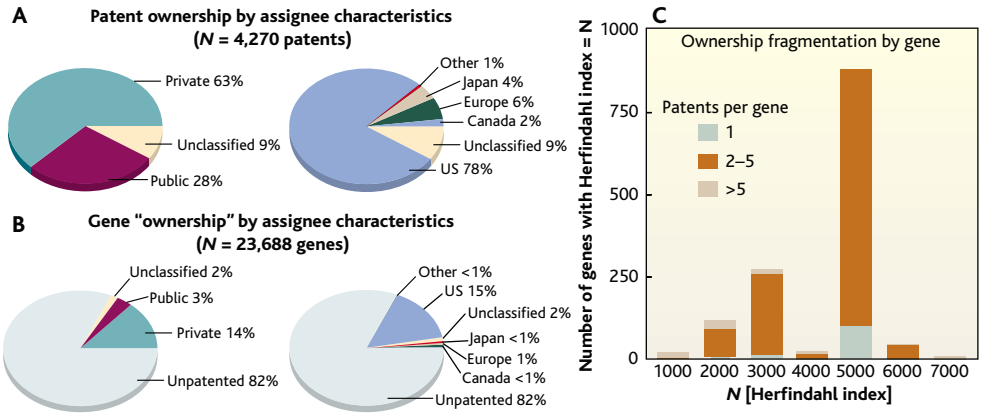

Patent and gene ownership characteristics. (**A**) and (**B**) Distribution of gene patent assignees "public" includes governments, schools, universities, research institutions, and hospitals. (A) Ownership breakdown for the 4270 human gene patents. Fractional ownership is based on the number of assignees on a single patent or the number of patents on a gene. (B) "Ownership" breakdown of the genes in the human genome. (**C**) The fragmentation of gene ownership by the Herfindahl index, rounded to the nearest 1000. (*31*). (The 3002 genes with an index of 10,000 are not shown; those for 8000 to 9000 would not be visible on the graph.) The assignee names were used as listed on the patents by the European Patent Office. As such, the Herfindahl indices are likely to overestimate the "true" fragmentation because they do not reflect assignee name changes, mergers, acquisitions, splits, partnerships, or other events that usually lead to a consolidation of IP rights.

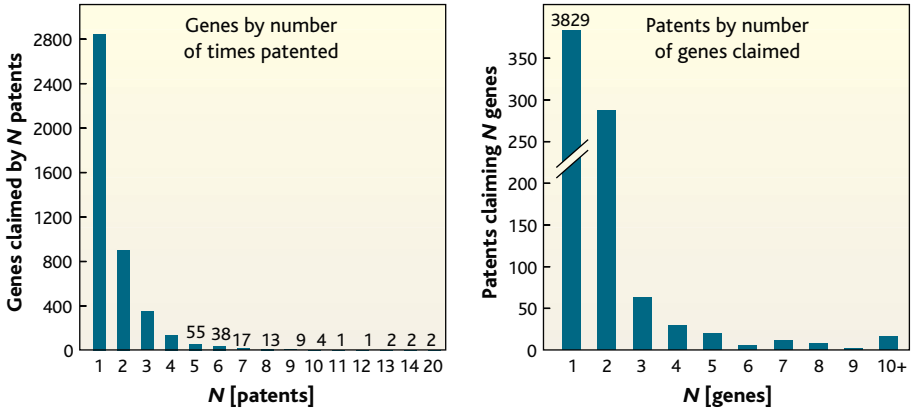

Global characteristics of the patent map. (**Left**) Distribution of genes by the number of times they are patented. (**Right**) Distribution of patents by the number of unique genes they claim.

References and Notes

1. E. F. Keller, *The Century of the Gene* (Harvard Univ. Press, Cambridge, MA, 2000).
2. We use the term "gene" to mean a set of cotranscribed protein-encoding exons. Here, "gene patent" means a patent disclosing and claiming a human gene sequence or some fraction thereof.
3. D. Crease, G. Schlich, *Nat. Rev. Drug Discov.* **2**, 407 (2003).
4. T. Hollon, *Nat. Med.* **6**, 362 (2000).
5. S. Scotchmer, *J. Econ. Perspect.* **5**, 29 (1991).
6. M. A. Heller, R. S. Eisenberg, *Science* **280**, 698 (1998).
7. U. S. Patent and Trademark Office, *Fed. Regist.* **66** (4), 1092 (January 2001).
8. Nuffield Council on Bioethics, "The ethics of patenting DNA" (Tech. rep., Nuffield Council on Bioethics, London, UK, 2002).
9. T. Caulfield, E. Gold, M. Cho, *Nat. Rev. Genet.* **1**, 227 (2000).
10. L. Andrews, *Nat. Rev. Genet.* **3**, 803 (2002)
11. S. M. Thomas, M. M. Hopkins, M. Brady, *Nat. Biotechnol.* **20**, 1185 (2002).
12. M. Stott, J. Valentine, *Nat. Rev. Drug Discov.* **3**, 364 (2004).
13. J. J. Doll, *Science* **280**, 689 (1998).
14. J. Gans, S. Stern, *J. Econ. Manage. Strat.* **9**, 485 (2000).
15. R. Levin, A. K. Klevorick, R. R. Nelson, S. G. Winter, *Brookings Pap. Econ. Act.* **3**, 783 (1987).
16. R. Eisenberg, *C. R. Biol.* **326**, 1115 (2003).
17. M. Stott, J. Valentine, *Nat. Biotechnol.* **21**, 729 (2003).
18. J. P. Walsh, A. Arora, W. M. Cohen, *Science* **299**, 1021 (2003).
19. G. Xu, A. Webster, E. Doran, *World Patent Inform.* **24**, 95 (2002).
20. G. Dufresne, M. Duval, *Nat. Biotechnol.* **22**, 231 (2004).
21. Georgetown University Kennedy Institute of Ethics, DNA patent database (http://dnapatents.georgetown.edu/).
22. National Genome Information Center, Patome database (http://bach.ngic.re.kr:8000/patent/en/).
23. G. Dufresne, L. Takacs, H. C. Heus, J.-J. Codani, M. Duval, *Nat. Biotechnol.* **20**, 1269 (2002).
24. S. Altschul, G. Warren, W. Miller, E. Myers, D. Lipman, *J. Mol. Biol.* **215**, 403 (1990).
25. K. D. Pruitt, T. Tatusova, D. R. Maglott, *Nucleic Acids Res.* **33** (database issue), 501 (2005).
26. D. Maglott, J. Ostell, K. D. Pruitt, T. Tatusova, *Nucleic Acids Res.* **33** (database issue), 54 (2005).
27. Materials and methods are available as supporting material on *Science* Online.
28. We use the definition of patent family recommended by the International Patent Documentation Center: Any two patents linked directly or indirectly by a priority document are in the same family.
29. P. A. Futreal *et al.*, *Nat. Rev. Cancer* **4**, 177 (2004).
30. We found similar patenting rates for the 1456 genes listed in the Online Mendelian Inheritance in Man (*32*) with a well-characterized association to disease phenotypes (517 of 1456, *P* value = 1.6^{-67}).
31. The Herfindahl index is the sum of the squares of the patent shares (in percentage terms) of each patent assignee (range 0 to 10,000), where 10,000 represents a "monopolist" with 100% of patents owned by one assignee and low numbers representing more fragmentation.
32. Online Mendelian Inheritance in Man, OMIM, McKusick-Nathans Institute for Genetic Medicine, Johns Hopkins University (Baltimore, MD) and National Center for Biotechnology Information, National Library of Medicine (Bethesda, MD), 2000.

Supporting Online Material
www.sciencemag.org/cgi/content/full/310/5746/240DC1

10.1126/science.1120014

SCIENCE AND LAW

When Should Judges Admit or Compel Genetic Tests?

Diane E. Hoffmann and Karen H. Rothenberg

During the past two decades, the use of DNA tests has revolutionized court proceedings in criminal and paternity cases. The tests' availability has arguably eliminated the need for "judging" as the tests provide virtually conclusive evidence of identity. On the horizon is a new challenge for judges—whether to admit or compel genetic tests to confirm or predict genetic diseases and conditions in other judicial contexts, including decisions regarding culpability, sentencing, liability, causation, and damages. Although the bulk of these new uses of genetic tests are in the torts area (*1*, *2*), their use has also been reported or proposed in criminal, family law, employment, and discrimination cases (*3*).

In civil cases, courts may compel a genetic test pursuant to Rule 35 of the Federal Rules of Civil Procedure or comparable state law. Rule 35 allows a court to order physical or mental examinations if the person subject to examination has placed her mental or physical condition "in controversy" and if "good cause" exists for the examination. "Good cause" depends on relevance and need, including whether the information may be obtained by other means. In personal injury actions, failure to comply with an order for a medical exam may result in dismissal of the case.

In criminal cases, a request to compel a saliva sample for purposes of genetic testing has been determined to constitute a search under the Fourth Amendment. Such searches must be reasonable, i.e., strike a balance between individual privacy interests and law enforcement needs.

Sometimes, the test result may already exist as a result of medical care, and the judge must decide whether to admit the information. In addition to meeting the standard for admissibility of scientific evidence in a given jurisdiction, the evidence must be relevant (make some fact that is of consequence to the outcome of the case more or less probable). The probative value of a genetic test result may depend on a variety of factors, including the accuracy and reliability of the test, the penetrance of the gene, the severity of the disease, and the impact of environmental causes. Even relevant evidence may be excluded, however, if the judge concludes that its admission risks inflaming or confusing the jury, is cumulative of other evidence, or would unduly delay the case.

To better understand judicial perspectives about the value of genetic information, we conducted a survey of all trial court judges (state and federal) in Maryland. Among other questions, judges were given several hypothetical cases and asked whether they would admit or compel a genetic test in a variety of scenarios (*4*). The hypotheticals (some based on actual cases) (*5*–*8*) were designed to glean information about the importance of different contextual factors, including whether the request was to admit or compel, the purpose of the information, and the characteristics of the genetic condition and test.

Two hypotheticals were based on criminal cases. Respondents were first asked whether they would admit a positive genetic test for schizophrenia to establish that the defendant did not have the necessary criminal intent (*mens rea*) to commit the crime. Respondents were also asked whether, in a sentencing proceeding, they would compel a test for a condition that predisposes an individual to bouts of rage (proclivity to "future dangerousness").

Four hypotheticals involved civil cases: two in the context of causation for tort liability and two involving determination of damages. In the causation cases, the defendant sought to have the judge compel a genetic test to show that the plaintiff's developmental disabilities were due to a genetic defect rather than the defendant's negligence. The first was a malpractice case against an obstetrician for a birth injury. The second was a toxic torts case against a solvent manufacturer in which the genetic condition manifested only as a result of having both a gene mutation and exposure to a chemical solvent. In both cases the injured parties were children.

In the first damage case, the defendant asked the judge to compel the plaintiff to have a genetic test for neurofibromatosis type 2 (NF2), which would significantly shorten the plaintiff's life expectancy and thus the amount the defendant would be required to pay in damages. In the second damage case, the plaintiff requested that the judge admit a genetic test to show that he had a heightened sensitivity to pain and thereby potentially increase his damage award. In each case, respondents were asked, assuming the relevant scientific evidentiary standard had been met, whether they would admit or compel the test. If they answered no, they were asked to provide the reasons for their decision.

Of 140 state trial court judges in Maryland, 101 responded to the written survey and 16 of the 25 federal district court judges in the state responded. After the results were tabulated, we met with groups of judges in five of the state circuits and the federal district court to share our findings and to solicit their reactions (see table, above).

The judges were almost equally divided on whether they would admit a positive test for schizophrenia in a criminal case to dis-

NUMBER OF RESPONSES TO SURVEY QUESTIONS – RAW DATA*

Survey question	State judges		Federal judges	
	Yes	No	Yes	No
Criminal cases				
Admit genetic test for schizophrenia?	50	42	5	8
Compel genetic test for condition leading to bouts of rage?	17	75	2	11
Civil tort cases: Causation				
Compel test for Fragile X syndrome?	77	14	9	3
Compel test for complex genetic condition caused by combination of environmental and genetic factors?	65	26	10	3
Civil tort cases: Damages				
Compel test for neurofibromatosis type 2?	39	50	5	8
Admit test for pain?	73	16	8	5

*Not all judges responded to each question.

The authors are at the University of Maryland School of Law, Baltimore, MD 21210, USA.

*Author for correspondence. E-mail: dhoffman@law.umaryland.edu

prove *mens rea*. Several described this as a "gray area" where the ultimate question would be whether the information would be more prejudicial than probative. The judges differed on how a jury would interpret the test result: some thought a jury would give it more weight than it deserves; others felt that an expert could help jurors interpret the test results.

A large majority of judges said they would not compel a genetic test for a condition leading to bouts of rage in a criminal sentencing. Respondents felt that the test was an "inexact" instrument that could brand someone for life and would be especially stigmatizing in the context of mental health. A few judges, however, argued that because the defendant had been convicted, his privacy interest was already diminished. Furthermore, they reasoned, because judges must assess risk, this information might assist them in predicting future dangerousness, especially when the defendant has no prior criminal record.

In contrast to the criminal cases, the large majority of judges in the civil cases for tort liability would compel a test to establish that the defendant's negligence was not the cause of the plaintiff's injury. The judges reasoned that since the plaintiff's health was at issue, the defendant had a right to use this information to show that it was the plaintiff's genetic condition that caused the injury. Moreover, they commented that the test was being used to confirm a diagnosis, not for prediction, and that compelling medical tests in these circumstances was well established.

In the first torts case involving damages, the judges were almost evenly divided on whether they would compel a genetic test for neurofibromatosis for an asymptomatic 21-year-old plaintiff with a family history of NF2. Reasons for not compelling the test varied but focused on the psychological impact of predictive testing in the context of a damage calculation. Some judges indicated that a jury would have difficulty understanding the information; others, however, felt that life tables could be used with an instruction about the meaning of the test. Those troubled by compelling the test raised the specter of predictive tests being used for breast cancer, heart disease, or other late-onset disorders. Some judges, in contrast, commented that they might admit predictive information in some cases, for example, when the plaintiff smokes and statistically has a reduced life expectancy.

The majority of judges agreed to admit, at the plaintiff's request, a positive genetic test for heightened sensitivity to pain. A few judges thought it would be very helpful to have an "objective" test for pain. Others said they were more likely to admit a test than to compel one. The few who would not admit the test expressed concern that the "test was not sufficiently predictive" or that the jury would weigh the test result inappropriately.

In sum, while many of the judicial respondents recognized the complexity of these decisions, these cases raise new challenges for judges. In addition to the concerns raised by respondents about relevancy and juror understanding, these genetic tests have impacts that are distinct from genetic tests used only for purposes of identity. Many genetic tests for health and behavioral traits have the potential to predict diseases and conditions that have no prospect of treatment or cure, as well as the ability to affect both family members and individuals. We therefore recommend that judges scrutinize the admitting or compelling of each of these new tests in the context in which its use is proposed. This scrutiny is particularly important because, if compelled, individuals and their families are forced to obtain genetic information without consent. Furthermore, for those individuals who have chosen to be tested in a medical setting, the informed consent process for genetic testing does not currently take into consideration the risk that genetic information may be admitted in future court proceedings.

We encourage judges to be cautious and to consider the following when evaluating the need for genetic information in legal cases:

1) What is the evidentiary context? Is it to admit or compel the test? Is it a civil or criminal case? Is it being requested by the prosecution or the defense or the plaintiff or defendant? Whereas a decision to admit requires an understanding of the scientific value of the test in the context of a specific case, a request to compel deserves elevated scrutiny in light of the involuntary nature and psychological impact of the testing. Moreover, given the potential constitutional infringement and impact on individual liberty, requests by a prosecutor to admit or compel a test in a preconviction criminal case should require a higher showing of "need" and "probative value" before the request is granted.

2) What is the nature of the genetic condition at issue? Is it a mental or physical condition? Is it congenital or late onset? How serious are the symptoms? Is there a cure or treatment? Information regarding a mental condition may raise heightened concerns about privacy and stigma, whereas information about the possibility of developing a serious, incurable disease in the future may have a serious psychological impact on an individual or their relatives who may not wish to know their own genetic status. Furthermore, if the party to be tested is a child, unable to provide informed consent, additional consideration should be given to the psychological impact and stigma associated with disclosure of the information.

3) How predictive is the test for the genetic condition? Is the condition caused by a single gene mutation or is it a more complex disorder resulting from interaction between gene mutations and environmental factors? For a late-onset disease, use of the test for predictive purposes requires greater caution as, for most complex genetic disorders, the test will only indicate that an individual has a susceptibility to a disease; it will not be determinative. Even if a test indicates that someone has a high probability of developing the genetic disease or condition, it cannot be used to determine the age at which someone will exhibit symptoms or the seriousness with which the condition will manifest. Moreover, although a positive genetic test may not rule out negligence or environmental factors as the cause of a developmental disability, it may change the damage calculation in torts cases and challenge the ability of medical experts and scientists to determine the degree of damage attributable to different causes.

4) What are the social policy implications of judges routinely compelling or admitting health-related genetic tests? Will this impact the willingness of individuals to obtain beneficial genetic tests in the health care setting or participate in genetic research? Will it validate claims of genetic determinism and contribute to the development of an unintended social norm regarding the meaning of genetic makeup?

In conclusion, decision-making in these cases will be complex and will require judges to simultaneously consider multiple factors. We hope that these recommended questions for consideration will provide guidance to judges as they are increasingly asked to decide whether to admit or compel this new generation of genetic tests.

References and Notes

1. See, e.g., A. S. Niedwiecki, *Univ. of San Francisco L. Rev.* **34**, 295 (2000).
2. G. E. Marchant, *Seton Hall L. Rev.* **31**, 949 (2001).
3. See, e.g., D. K. Casey, *Judicature* **83**, 105 (1999).
4. The full text of the questions are available as supporting material on *Science* Online.
5. *Bennett* v. *Fieser*, No. 93-1004-MLB, 1994 U.S. Dist. LEXIS 4050 (D. Kan. 25 February 1994).
6. *Harris* v. *Mercy Hospital*, 231 Ill. App. 3d 105; 596 N.E. 2d 160 (1992).
7. Wintz v. Northrop Corp., 110 F.3d 508 (7th Cir. 1997).
8. *Mobley* v. *State*, 265 Ga. 292, 455 S.E. 2d 261 (Ga. 1995).

Supporting Online Material

www.sciencemag.org/cgi/content/full/310/5746/241 DC1

10.1126/science.1117972

ECOLOGY

Interrelated Causes of Plant Invasion

Dana Blumenthal

An occasional stem of leafy spurge in the prairie would not threaten native species. Nor would it bother ranchers. But the millions of hectares of this Eurasian species that inhabit western North America have displaced native plant species and reduced forage for both wild and domestic animals, costing hundreds of millions of dollars annually (*1*). The problems caused by such invasive species are the direct result of their success in colonizing new habitats, and understanding why they are so successful is essential to controlling their spread. Although there are many competing ideas to explain invasion, it is possible that two of the most important are interrelated: The plant species that benefit the most from high resource availability may also gain the most from escaping enemies upon moving to a new range. This proposal predicts that resources may influence the success of biological control (the introduction of enemies from an invader's native range). It also implies that anthropogenic increases in plant resources may play a larger role in invasion than previously thought.

Due to the enormous variety of invasive plants, attempts to explain invasion have led to an array of partially overlapping hypotheses. Hypotheses explaining the exceptional success of exotic species are based upon ways in which a species' new range differs from its native range: fewer insects and diseases (*2, 3*), less competitive environments (*4*), and competitors that are more susceptible to chemicals produced by the invader (*5*). Hypotheses explaining colonization in general, irrespective of whether the colonizing species are native or exotic, rely on characteristics of the colonizer or the colonized plant community. For example, fast-growing species with high seed production make good colonizers (*6, 7*). Plant communities with lots of disturbance, high resource availability, or reduced species diversity tend to be easily colonized (*4, 8*).

Of primary interest are two mechanisms of invasion that are particularly well supported by existing studies of plant invasions: release from natural enemies and increased resource availability (*2–4, 8*). The enemy release hypothesis attributes the success of exotic species to their escape from diseases and herbivores upon moving to a new range (*2, 3*). This gives them an advantage when competing with native species still burdened by enemies. Not only are enemies missing in exotic species' new ranges, but the absence of enemies is correlated with invasiveness (*3, 9*). Enemy release provides the greatest benefit to exotic species that are highly susceptible to enemies in their native range (*2*).

The resource hypothesis suggests that plant invasion is caused by availability of resources such as light, water, and soil nutrients (*8*). Resources become available when resource supply increases, as with atmospheric nitrogen deposition, or when resource capture by other plants decreases, as with disturbances such as fire or plowing (*8*). High resource availability benefits fast-growing native or exotic species.

The reason that enemy release and resource availability may interact is that fast-growing, high-resource species also tend to be highly susceptible to enemies. When introduced to a new range, these species are likely to benefit from both high resource availability and enemy release. Where resources necessary for plant growth are scarce, growth is slow and the metabolic cost of producing new plant tissue is high; therefore, plants from such habitats have evolved defenses to protect that tissue (*10*). Conversely, plants from high-resource habitats grow quickly, produce tissue at low metabolic cost, and invest little in defense (*10, 11*). Such high-resource species are also nutritious, with little structural material and high tissue nutrient concentrations (*11, 12*). Poorly defended, nutritious, high-resource species tend to be preferred by herbivores (*10, 13*), to lose more tissue to herbivory (*14*), and to be more strongly regulated by herbivory (*13, 15*) than low-resource species. They may also be particularly susceptible to pathogens (*16*).

If, as the evidence indicates, high-resource plant species are more strongly affected by enemies than are low-resource species, they should also gain more from leaving those enemies behind. The effect of enemy release in a new environment should therefore increase with the resource availability to which a species is adapted (see the figure, left). This concept, referred to here as the resource–enemy release hypothesis, predicts that enemy release and increased resource availability may act in concert to cause invasion (see the figure, right). Consequently, successful management of plant invasions may require both biological control, which aims to reduce enemy release by introducing enemies from an invader's native range, and methods aimed at limiting or reducing resource availability.

Explaining plant invasions is likely to involve not only multiple mechanisms of invasion, but also understanding the conditions under which each mechanism tends to be important. The resource–enemy release hypothesis predicts those conditions for two of the principal mechanisms of invasion, and in turn suggests how we could manage invasive species. For example, the effects of enemy release may be strongest for high-resource species. It follows that biological control may be most effective against high-resource invaders. Furthermore, unlike the resource hypothesis which

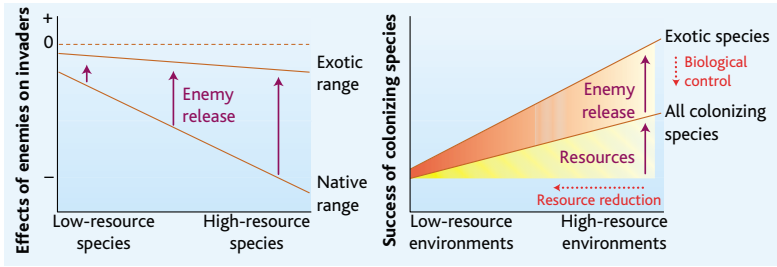

Resources and enemy release may interact to cause invasion. (Left) Species adapted to high resource availability are inhibited by enemies in their native range, and therefore have great potential to benefit from escaping those enemies in their exotic range. **(Right)** Although all high-resource species will benefit from high resource availability, high-resource exotic species will also benefit from enemy release. Therefore, increasing resource availability will increase the advantage of exotic over native species.

The author is at the U.S. Department of Agriculture–Agricultural Research Service Rangeland Resources Research Unit, Crops Research Laboratory, 1701 Center Avenue, Fort Collins, CO 80526, USA. E-mail: dana.blumenthal@ars.usda.gov

applies equally to native and exotic species (*8*), the resource–enemy release hypothesis predicts that high resource availability will help exotic species more than native species (see the figure, right). Consequently, anthropogenic increases in resource availability, ranging from small-scale disturbances to global climate change, may not just facilitate invasion, but facilitate invasion by exotic species in particular. In fact, exotic species tend to outperform native species in high- but not low-resource environments (*17*). Humans may therefore play an even larger role in invasions by exotic species than previously thought.

References

1. J. M. DiTomaso, *Weed Sci.* **48**, 255 (2000).
2. R. M. Keane, M. J. Crawley, *Trends Ecol. Evol.* **17**, 164 (2002).
3. C. E. Mitchell, A. G. Power, *Nature* **421**, 625 (2003).
4. K. Shea, P. Chesson, *Trends Ecol. Evol.* **17**, 170 (2002).
5. R. M. Callaway, E. T. Aschehoug, *Science* **290**, 521 (2000).
6. H. G. Baker, in *The Genetics of Colonizing Species*, H. G. Baker, D. L. Stebbins, Eds. (Academic Press, New York, 1965), pp. 147–172.
7. E. Grotkopp, M. Rejmanek, T. L. Rost, *Am. Nat.* **159**, 396 (2002).
8. M. A. Davis, J. P. Grime, K. Thompson, *J. Ecol.* **88**, 528 (2000).
9. S. J. Dewalt, J. S. Denslow, K. Ickes, *Ecology* **85**, 471 (2004).
10. P. D. Coley, J. P. Bryant, F. S. Chapin, *Science* **230**, 895 (1985).
11. J. P. Grime *et al.*, *Oikos* **79**, 259 (1997).
12. W. J. Mattson, *Annu. Rev. Ecol. Syst.* **11**, 119 (1980).
13. L. H. Fraser, J. P. Grime, *J. Ecol.* **87**, 514 (1999).
14. J. Cebrian, C. M. Duarte, *Funct. Ecol.* **8**, 518 (1994).
15. P. V. A. Fine, I. Mesones, P. D. Coley, *Science* **305**, 663 (2004).
16. E. Hoffland *et al.*, *Plant Cell Environ.* **19**, 1281 (1996).
17. C. C. Daehler, *Annu. Rev. Ecol. Syst.* **34**, 183 (2003).

10.1126/science.1114851

PALEONTOLOGY

Shaking the Earliest Branches of Anthropoid Primate Evolution

Jean-Jacques Jaeger and Laurent Marivaux

Although chimpanzees are our closest living relatives, humans also share many important anatomical and biochemical characteristics with a large group of extant and fossil primates that taxonomists have named "anthropoids." All living humans, apes, baboons, macaques, leaf monkeys, and New World monkeys, together with numerous fossil anthropoids, share a common ancestor that originated in either Africa or Asia, both continents having yielded primitive fossil representatives of this group (see the figure). In Africa, mostly through the work of Simons and his team in the Fayum desert in Egypt, numerous distinctive taxa of primitive anthropoids have been described from sediments dated at between 35 and 32 million years old (*1*). Not only did Simons discover *Aegyptopithecus*, the ancestor of later and more derived anthropoids (catarrhines, which includes the Old World monkeys), but he also recovered and described a diversity of more primitive anthropoid taxa, some of which appear to be endemic to North Africa while others are considered to be closely related to New World monkeys (*2*). Therefore, for several decades, North Africa was considered as the center of anthropoid origin and early diversification. But this classical Fayum record begins abruptly, at about 35 million years ago, when an ecologically diverse anthropoid community was already in place. Very little was known about earlier African anthropoids dating from closer to the beginning of the African anthropoid radiation.

The authors are at the Laboratoire de Paléontologie, Institut des Sciences de l'Évolution, Université Montpellier II, F-34095 Montpellier Cedex 05, France. E-mail: jaeger@isem.univ-montp2.fr, marivaux@isem.univ-montp2.fr

Now, on page 300 of this issue, Seiffert *et al*. (*3*) describe the most complete known remains of the earliest African anthropoids from the oldest fossiliferous level of the Fayum desert, Birket Qarun Locality 2 (BQ-2), precisely dated from 37 million years ago. These anthropoids are represented by two distinct and small species of the genus *Biretia* (*4*) whose body masses have been estimated to be 273 and 376 g, respectively. Their dental morphology agrees with what had been predicted for a common ancestor of later African anthropoids. It is also one step more evolved than that of any contemporaneous Asian anthropoid. The smaller of these two new species (*Biretia fayumensis*) is similar to a contemporaneous Algerian species (*Biretia piveteani*) from the Bir-El-Ater locality, which is known from a single tooth (*4*). But the larger of these new species, *Biretia megalopsis*, whose dentition is very similar to that of the smaller one, displays a surprising and unexpected specialization. Its ocular orbits are strongly enlarged, being similar in size and morphology to those of *Tarsius*, a modern small-bodied nocturnal primate from Southeast Asia, suggesting that *Biretia* displayed a nocturnal activity pattern as well.

Unfortunately, in the smaller new species this bony area below the orbit is not preserved. The enlarged orbits of *Biretia megalopsis* conflict with the classical notion that the earliest anthropoids were diurnal primates with well-developed stereoscopic and color vision (*5*), and with the oldest Asian fossil record. Seiffert *et al*. (*3*) consider this species as a specialized, early branch of African anthropoids, because no later Fayum anthropoid displays such a character. For these authors, *Biretia* suggests an ancient evolutionary history in Africa that allowed enough time for some anthropoids to develop such specialized adaptations. Alternatively, all of the Algerian and Egyptian anthropoids of this age may have shared enlarged orbits, because their similar dental characters suggest that they are closely related. But such a specialized adaptation would then exclude these fossils from the ancestry of their later Fayum relatives. Nevertheless, the dental morphology of these fossils undoubtedly documents an early stage of African anthropoid evolution, pinpointed by some uniquely shared specialized characters.

In addition to the description of these two new species, Seiffert *et al*. (*3*) present the results of an outstanding cladistic analysis using 360 morphological characters of 102 extant and fossil primate taxa, which supports some interesting hypotheses. The two new Fayum species appear as the sister groups of a well-known extinct anthropoid family, the Parapithecidae, which is only known from North Africa. They derive, according to that cladistic analysis, from an older Saharan primate, *Algeripithecus*, which was described several years ago on the basis of a couple of teeth (*6*), as the earliest (more than 45 million years old) and most primitive African anthropoid. In addition, both new Fayum species and *Algeripithecus* are considered as related to a late Paleocene (60 million years ago) Moroccan primate, *Altiatlasius*, known only from a dozen isolated teeth (*7*). According to that result, the anthropoids would have had a very long evolutionary history on the African continent, and this ancient origin is supported by several molecular analyses that suggest similar antiquity for the branching events between extant anthropoid lineages. Unfortunately, these older African putative "anthropoids" are extremely fragmentary, and many of their morphological characters remain undocumented. Needless to say, this hinders efforts to obtain a strong and accurate phylogenetic tree, and convergent evolution is a common pitfall of cladistic analyses.

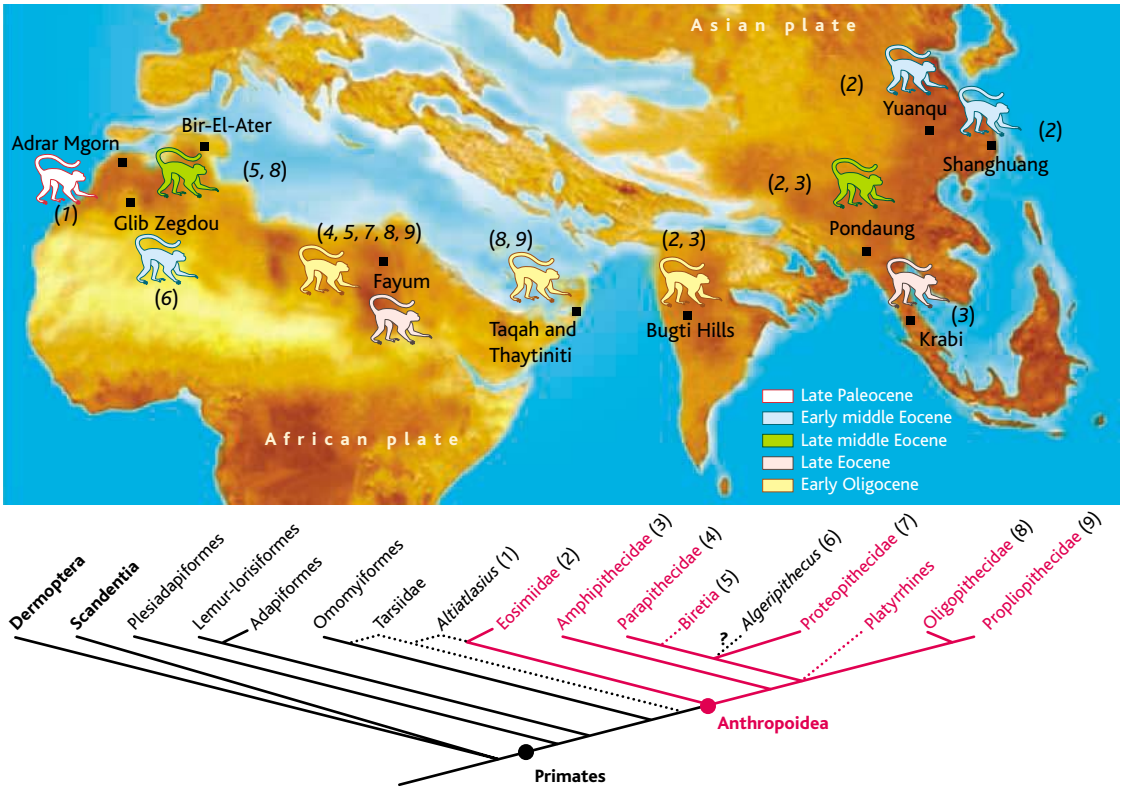

Early anthropoids. (**Top**) Paleogeographic reconstruction of South Asia and North Africa at the mid-Paleogene showing the fossiliferous localities that have yielded fossil anthropoid primates [map adapted from (*18*)]. (**Bottom**) Current consensus of anthropoid primate phylogeny. [Adapted from (*3*, *9*)]

Another interesting result of the analysis of Seiffert *et al.* (*3*) is the phylogenetic position of the Asian anthropoids, Eosimiidae and Amphipithecidae. For many years, their anthropoid nature was controversial, but with a recently enriched fossil record, amphipithecids are now recognized as stem anthropoids and as the sister group of the African anthropoids (*8*, *9*). The less specialized eosimiids appear now as the sister group of all anthropoids, pointing to an Asian origin of anthropoids (*10*). The phylogenetic results reported by Seiffert *et al.* closely mirror those that have recently been published by others (*9*), and this present phylogenetic framework appears to be the current consensus of primate phylogeny.

This marks the end of a long controversy and opens the way for deeper understanding of the phylogenetic relationships among these earliest Asian and African anthropoids. However, a major gap in our knowledge remains, both in Asia and in Africa, regarding the anthropoid faunas of the early and middle Eocene (57 to 40 million years ago), a time interval that is believed to correspond to a period of active intercontinental exchange of land mammals (*11*). The Eosimiidae, the oldest and most primitive anthropoids currently known, were originally described from the middle Eocene of China [45 million years ago (*12*)] and have subsequently been discovered in Myanmar in a 37-million-year-old dated locality (*13*), and recently also in Pakistan (*9*) from a more recent layer (32 million years ago), thereby testifying to their wide stratigraphic and geographic range. As stem anthropoids, they are now recognized as phylogenetically related to the African ones, but they have not yet been discovered in Africa. According to Beard (*10*) and Seiffert *et al.* (*3*), the earliest African anthropoids immigrated from Asia at a very early date, probably before the late Paleocene.

However, a later immigration age scenario remains possible, and in such a case, the scarce Moroccan and Algerian earlier anthropoid record will have to be reinterpreted differently on the basis of a more complete fossil record. In the Algerian Bir-El-Ater locality, roughly coeval to the new Fayum locality (BQ-2), *Biretia* has been found in association with two rodent families, anomaluroids and baluchimyines, whose fossil record is well documented in southern Asia (*14*, *15*), together with anthracotheres, a piglike mammalian family of undoubted Asian origins (*16*).

Therefore, African anthropoid ancestors may have immigrated from Asia together with these other Asian mammals just before 37 million years ago (*9*, *17*). But, as suggested by Seiffert *et al.* (*3*), a more complicated scenario is also possible, with several waves of Asian immigrations and exchanges between both continents. To choose between these alternative scenarios, we need a more complete fossil record and to discover new Eocene anthropoid localities in Asia and in Africa.

Understanding the first steps of our own fossil record and deciphering the various immigration events between Asia and Africa is now improving rapidly, and represents a great challenge for future research. Surprisingly, solving this problem may provide a model for the understanding of another critical period of human evolution, the origin and evolution of extant great apes and humans, whose biogeographical background also involves several geographic areas, including Southern Asia and Africa, and also probable multiple immigration events between both continents. The tree of human evolution, when shaken by new discoveries, often changes its branching pattern—a strong argument to stimulate further research in that fascinating field.

References and Notes

1. E. L. Simons, *Yearb. Phys. Anthropol.* **38**, 199 (1995).
2. E. R. Miller, E. L. Simons, *Proc. Natl. Acad. Sci. U.S.A.* **94**, 13760 (1997).
3. E. R. Seiffert *et al.*, *Science* **310**, 300 (2005).
4. L. Bonis de, J.-J. Jaeger, B. Coiffait, P.-E. Coiffait, *C. R. Acad. Sci.* **306**, 929 (1988).
5. C. P. Heesy, C. F. Ross, in *Anthropoid Origins: New Visions*, C. F. Ross, R. F. Kay, Eds. (Plenum, New York, 2004), pp. 665–698.
6. M. Godinot, M. Mahboubi, *Nature* **357**, 324 (1992).
7. B. Sigé, J.-J. Jaeger, J. Sudre, M. Vianey-Liaud, *Palaeontographica* **214**, 31 (1990).
8. L. Marivaux *et al.*, *Proc. Natl. Acad. Sci. U.S.A.* **100**, 13173 (2003).
9. L. Marivaux *et al.*, *Proc. Natl. Acad. Sci. U.S.A.* **102**, 8436 (2005).
10. K. C. Beard, *The Hunt for the Dawn Monkey: Unearthing the Origins of Monkeys, Apes, and Humans* (Univ. of California Press, Berkeley, 2004).
11. E. Gheerbrant, *Palaeontographica* **237**, 39 (1995).
12. K. C. Beard, T. Qi, M. R. Dawson, B. Wang, C. Li, *Nature* **368**, 604 (1994).
13. J.-J. Jaeger *et al.*, *Science* **286**, 528 (1999).
14. L. Marivaux, J.-L. Welcomme, M. Vianey-Liaud, J.-J. Jaeger, *Zool. Scr.* **31**, 225 (2002).
15. L. Marivaux *et al.*, *J. Vertebr. Paleontol.* **25**, 214 (2005).
16. S. Ducrocq, *Stuttg. Beitr. Naturkd. Ser. B* **250**, 1 (1997).
17. R. F. Kay, B. A. Williams, C. F. Ross, M. Takai, N. Shigehara, in *Anthropoid Origins: New Visions*, C. F. Ross, R. F. Kay, Eds. (Plenum, New York, 2004), pp. 91–135.
18. R. Blakey, http://jan.ucc.nau.edu/~rcb7/RCB.html.
19. This Perspective is an Instit des Sciences de l'Évolution-Montpellier publication 2005-086.

10.1126/science.1118124

PIERCE

Grasp the Proteome®

Plays well with others.

IT'S BETTER … THE NEWEST BCA™ PROTEIN ASSAY KIT FROM PIERCE IS NOW COMPATIBLE WITH REDUCING AGENTS

Highlights:

- Compatible with up to 5 mM DTT, 35 mM 2-mercaptoethanol or 10 mM TCEP
- Linear working range: 125-2,000 µg/ml
- Sample volume: 25 µl
- Compatible with most ionic and nonionic detergents
- Significantly less (14-23%) protein:protein variation than coomassie (Bradford)-based methods
- Colorimetric method; measure at 562 nm
- Easy-to-use protocol

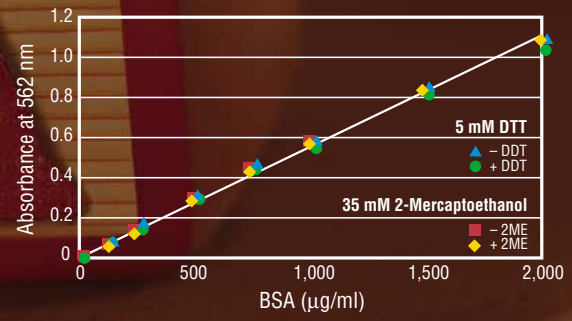

BCA™ Protein Assay – Reducing Agent Compatible produces a linear standard curve in the presence of reducing agents. Color response curves for BSA after treatment with Reducing Agent Compatible Reagent in the presence and absence of 5 mM DTT and 35 mM 2-mercaptoethanol. For data on 10 mM TCEP, visit our web site.

Ordering Information

Product #	Description	Pkg. Size
23250	BCA™ Protein Assay Kit – Reducing Agent Compatible *Sufficient reagents to perform 250 standard tube assays.*	Kit

Please visit our web site www.piercenet.com *for complete kit components.*

HURRY! Purchase the BCA™ Protein Assay Kit – Reducing Agent Compatible (Product # 23250) direct from Pierce by Oct. 31, 2005, and receive a FREE Pierce protein-patterned T-shirt. Mention this ad when placing your order. Offer valid in U.S. only. Void where prohibited.

www.piercenet.com/brac22j

PIERCE

Tel: 815-968-0747 or 800-874-3723 • Fax: 815-968-7316 • Technical Assistance E-mail: TA@piercenet.com • Customer Assistance E-mail: CS@piercenet.com

Outside the United States, visit our web site or call 815-968-0747 to locate your local Perbio Science branch office (below) or distributor

Belgium & Dist.:	China:	France:	Germany:	Hong Kong:	The Netherlands:	United Kingdom:	Switzerland:
Tel +32 53 85 7184	Tel +86 10 8049 9033	Tel 0800 50 82 15	Tel 0228 9125650	Tel 852 2753 0686	Tel 076 50 31 880	Tel 0800 252185	Tel 0800 56 31 40
euromarketing@perbio.com	support@perbio.com.cn	euromarketing@perbio.com	de.info@perbio.com	SalesHK@perbio.com	euromarketing@perbio.com	uk.info@perbio.com	euromarketing@perbio.com

PERBIO

GENETICS

Motivating Hotspots

Molly Przeworski

An estimated 10 to 30% of fertilized human ova have more or fewer than the normal number of 46 chromosomes (*1*). Most cases of aneuploidy (that is, having an abnormal number of chromosomes) result from a reduced number of recombination events (less than one per chromosome arm) or an unusual placement of such events along the chromosome (*2*). Recombination between nonallelic copies can also lead to chromosomal rearrangements and deletions, many of which have been associated with disease (*2*). Despite its importance, much remains unknown about the process of recombination, especially for mammals. In particular, no sequences or chromosome structures that influence human recombination rates have been identified. On page 321 in this issue, Myers *et al.* (*3*) present a fine-scale recombination map for the human genome and use it to identify the first set of candidate motifs.

Estimates of recombination rates for the entire genome have previously come from comparisons of physical maps to genetic maps based on pedigrees. Such comparisons revealed higher recombination rates in females than in males and suppressed recombination near centromeres, among other features, but lack the resolution to be informative about genetic distances below a centimorgan (*2*). To estimate finer-scale rates, there are currently two approaches: sperm-typing and analyses of linkage disequilibrium. Sperm-typing experiments provide direct estimates of recombination rates in regions from one to several hundred kilobases (kb) in length (*4*). The dozen regions examined by this technique show extensive heterogeneity in fine-scale recombination rates, with most crossover resolutions concentrated in segments of 1 to 2 kb called "hotspots." These findings therefore suggested that hotspots may be an extremely common feature of the human recombination landscape (*5*), as they are in yeast (*6*). Unfortunately, sperm-typing is labor intensive and not feasible on a genome-wide scale.

The alternative is to estimate fine-scale recombination rates indirect from levels of linkage disequilibrium, the nonrandom association of alleles on chromosomes. Patterns of linkage disequilibrium observed in extant individuals reflect recombination events that have occurred in the ancestors of the individuals from whom the sample was obtained. More recombination in the ancestral lineages tends to result in weaker associations between alleles (that is, less linkage disequilibrium), and vice versa. Given a model of recombination and population history, one can therefore use linkage disequilibrium data to estimate the recombination rates along a chromosome and to test for the presence of hotspots (that is, for a local increase in the rate of recombination relative to that expected by chance, under a model of uniform rates). What one obtains is a population rate of recombination, averaged over both male and female ancestors, in the time frame reflected by linkage disequilibrium—less than 1 million years for humans. When applied to the X chromosome, the approach provides estimates of fine-scale rates of recombination in females (which sperm-typing obviously cannot do). Despite the dependence on an oversimplified model, linkage disequilibrium–based estimates of recombination produce a fairly reliable characterization of rate variation, both in simulations and when compared to sperm-typing data from the region encoding the major histocompatibility complex and to genetic map–based estimates (*7*–*9*). Moreover, they can be readily applied to any chromosomal region for which there are genetic variation data.

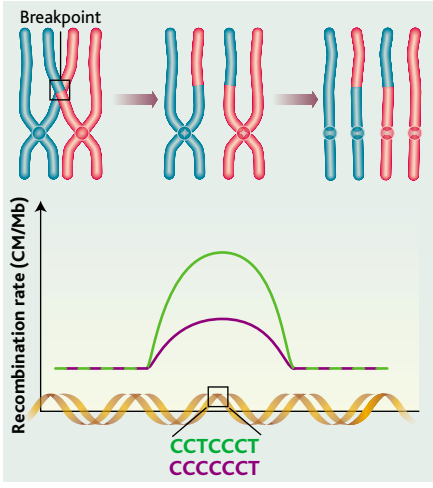

Sequence motifs in the human genome affect hotspot activity. (**Top**) Recombination refers to the exchange of DNA between chromosomes during meiosis. Shown here is a crossing-over event in which sections of homologous chromatids are exchanged. Recombination is necessary for the proper segregation of chromosomes in meiosis. (**Bottom**) Recombination rates vary along a chromosome, with most crossover events occurring in hotspots. Myers *et al.* identify sequence motifs in the hotspots that may influence their activity, with some alleles leading to greater intensity than others.

With the release of genome-wide genotyping data, it has therefore become possible to construct a fine-scale genetic map for most of the human genome. Myers *et al.* do so by applying their linkage disequilibrium–based estimator to publicly available genotyping data for 1.6 million single nucleotide polymorphisms distributed over most of the human genome (*10*). Confirming sperm-typing studies and analyses of linkage disequilibrium for subsets of the genome (*7*, *8*, *11*), they find extensive rate heterogeneity over the scale of kilobases. They further estimate that there is a hotspot every 50 kb or so in the human genome, with ~80% of the recombination events occurring in 10 to 20% of the sequence. Their analyses of the X chromosome demonstrate that this heterogeneity is a feature of female as well as male recombination landscapes.

This high-resolution genetic map of the human genome will be an important resource for the design of association studies for complex diseases (*4*). Beyond its descriptive value, however, the map is a fantastic tool to begin understanding the determinants of recombination rates. For example, in yeast, hotspots have been classified into three groups: α-hotspots, where the recombination machinery is recruited to transcription factor binding sites; β-hotspots, found in nuclease-sensitive regions; and γ-hotspots, associated with elevated GC nucleotide content (*6*). As the Myers *et al.* study reveals, two of these cases don't seem to be widespread in humans. Recombination rates tend to be lower, not higher, near coding regions, increasing (on average) for about 30 kb from the start codon, and GC content is not a strong predictor of fine-scale rate variation. Whether hotspots tend to lie in nuclease-sensitive regions or whether a new model is warranted for humans remains to be determined.

With more than 25,000 putative hotspots at their disposal, Myers *et al.* also find the first set of sequence features substantially overrepresented in hotspots relative to coldspots. Although the motifs are neither necessary nor sufficient for hotspot activity, their top-scoring candidate alone may play a role in a substantial proportion (11%) of them. The motif is a seven-nucleotide oligomer (CCTCCCT) and its effect on recombination is strongest when it lies within a specific mobile element (namely, within the long terminal repeats of a retrovirus-like retrotransposon). Low–copy number repeats are thought to play an important role in the generation of

The author is in the Department of Human Genetics, University of Chicago, 920 East 57th Street, 507F CLSC, Chicago, IL 60637, USA. E-mail: mfp@uchicago.edu

recombination events between nonallelic copies. The finding of a recombinagenic motif within the repeats may therefore help to explain the observation that the breakpoints of nonallelic recombination events are often clustered (*12*). The overall influence of mobile DNA elements on recombination remains unclear, however, with some over- and some underrepresented within hotspots.

The seven-nucleotide motif is not among those previously associated with recombination in other species. However, its role in influencing recombination is supported by sperm-typing experiments, as is the role of another nine-nucleotide motif motif (CCCCACCCC) identified by the authors. Indeed, at a subset of hotspots in humans, mouse, and yeast, variation in hotspot intensity among individuals has been shown to depend on particular alleles, with recombination events occurring more often initiating on the background of the "hot" variant. When Myers *et al*. examined the sequence context of two human hotspots whose intensity has been shown to vary among alleles, they found that the "hot" alleles were their top-scoring seven and nine oligomer motifs and that in both cases, the "colder" alleles were a mutation away from that motif. This result strongly suggests that these sequences modulate hotspot activity (see the figure). Further evidence will come from sperm-typing studies of other hotspots polymorphic at the same motifs, as well as at other candidate sequences.

In light of recent reports that hotspot locations are largely discordant in humans and chimpanzees (*9*, *13*), the discovery of human motifs that appear to influence hotspot activity raises a number of additional questions: Can changes to sequence motifs explain most of the interspecies differences, or do other genomic features, such as chromatin accessibility or transposable element activity, explain their rapid evolution? Given that most recombination events take place within hotspots, and hotspot locations appear to be rapidly evolving, is there any constraint on recombination rates below that of a chromosomal arm? For example, are the density and intensity of hotspots constrained within circumscribed regions of the genome? With more sperm-typing experiments and extensive linkage disequilibrium data collection in close evolutionary relatives of humans, answers to these questions should no longer be elusive.

References

1. T. Hassold, P. Hunt, *Nat. Rev. Genet.* **2**, 280 (2001).
2. A. Lynn, T. Ashley, T. Hassold, *Annu. Rev. Genomics Hum. Genet.* **5**, 317 (2004).
3. S. Myers, L. Bottolo, C. Freeman, G. McVean, P. Donnelly, *Science* **310**, 321 (2005).
4. N. Arnheim, P. Calabrese, M. Nordborg, *Am. J. Hum. Genet.* **73**, 5 (2003).
5. L. Kauppi, A. J. Jeffreys, S. Keeney, *Nat. Rev. Genet.* **5**, 413 (2004).
6. T. D. Petes, *Nat. Rev. Genet.* **2**, 360 (2001).
7. D. C. Crawford *et al.*, *Nat. Genet.* **36**, 700 (2004).
8. G. A. McVean *et al.*, *Science* **304**, 581 (2004).
9. S. E. Ptak *et al.*, *Nat. Genet.* **37**, 429 (2005).
10. D. A. Hinds *et al.*, *Science* **307**, 1072 (2005).
11. P. Fearnhead, N. G. C. Smith, *Am. J. Hum. Genet.*, www.journals.uchicago.edu/AJHG/home.html.
12. J. R. Lupski, *Genome Biol.* **5**, 242 (2004).
13. W. Winckler *et al.*, *Science* **308**, 107 (2005).

10.1126/science.1120154

ATMOSPHERIC SCIENCE

Weather Forecasting with Ensemble Methods

Tilmann Gneiting and Adrian E. Raftery

A radical change has occurred in the practice of numerical weather prediction over the past decade. Until the early 1990s, atmospheric scientists viewed weather forecasting as an intrinsically deterministic endeavor: For a given set of "best" input data, one "best" weather prediction is generated. Armed with sophisticated computing resources (including supercomputers), weather centers ran carefully designed numerical weather prediction models to produce deterministic forecasts of future atmospheric states. Although this is still the case today, weather prediction has been transformed through the implementation of ensemble forecasts. An ensemble forecast comprises multiple (typically between 5 and 100) runs of numerical weather prediction models, which differ in the initial conditions and/or the numerical representation of the atmosphere, thereby addressing the two major sources of forecast uncertainty.

Realizing the full potential of an ensemble forecast requires statistical postprocessing of the model output, in that model biases, insufficient representations of forecast uncertainty, and the differing spatial scales of model gridboxes and observations need to be addressed. In concert with statistical postprocessing, ensembles provide flow-dependent probabilistic forecasts in the form of predictive probability distributions over future weather quantities or events. Probabilistic forecasts allow one to quantify weather-related risk, and they have greater economic value than deterministic forecasts in a wide range of applications, including electricity generation, aircraft and ship routing, weather-risk finance, and disease modeling (*1*).

A maturing area is that of medium-range probabilistic forecasting at prediction horizons up to 10 days, which involves ensembles of global numerical weather prediction models (*1*, *2*). Three operational methods for the generation of medium-range initial condition ensembles have been developed. The U.S. National Centers for Environmental Prediction (NCEP) and the European Centre for Medium-Range Weather Forecasts (ECMWF) seek directions of rapid error growth in selective sampling procedures, known as the bred-vector perturbation method (*3*) and the singular-vector technique (*4*), respectively. The Meteorological Service of Canada (MSC) uses the Monte Carlo–like perturbed-observation approach (*5*), in which the model physics parameterizations vary as well. Ensemble forecasting and atmospheric data assimilation (the melding of weather observations into a numerical model) can mutually benefit from each other, and there are promising options for a linked system (*6*). A recent comparative study suggests that the ECMWF data assimilation, numerical modeling, and ensemble generation system has the best overall performance, with the NCEP system being competitive during the first few days, and the MSC system during the last few days, of the 10-day forecast period (*7*). The successful operation of forecast ensembles on the global scale has motivated the development of limited-area short-range ensembles driven by initial and boundary conditions supplied by different weather centers, such as the University of Washington ensemble system (*8*–*10*) over the North American Pacific Northwest (see the figure).

Probabilistic forecasting has become an integral part of seasonal prediction as well (*1*, *11*). Forecasts on seasonal to interannual time scales rely on comprehensive global coupled ocean-atmosphere models and have become feasible with an improved understanding of the coupling between sea surface temperature anomalies and atmospheric circulation patterns. A recent special issue of *Tellus* (*12*) is dedicated to results from the European Union–spon-

The authors are in the Department of Statistics, University of Washington, Box 354322, Seattle, WA 98195, USA. E-mail: tilmann@stat.washington.edu

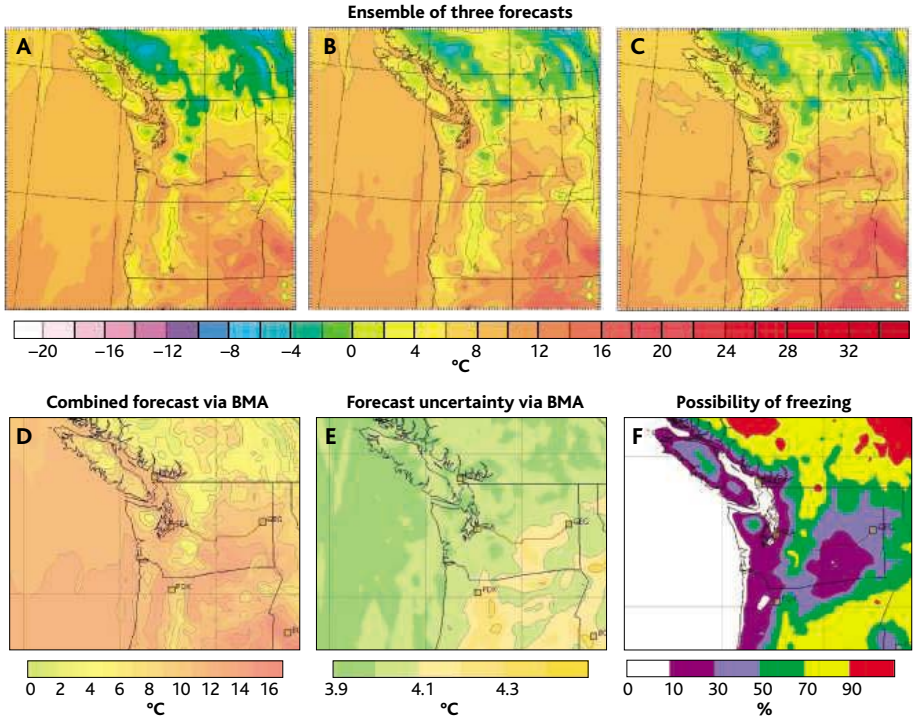

An improved forecast. Ensemble forecast of surface temperature over the North American Pacific Northwest, with postprocessed probabilistic forecast products derived by Bayesian model averaging (BMA) (*14*). (**A** to **C**) The ensemble consists of nine 48-hour forecasts (of which three are shown) valid at 4 p.m. local standard time on 2 April 2005, using the MM5 mesoscale model with initial conditions provided by different weather centers (*8–10*). (**D**) The BMA combined forecast is a weighted average of the bias-corrected ensemble members (*10*, *14*). (**E**) The uncertainty plot is a map of the half-width of the BMA forecast intervals. Higher values correspond to more uncertainty. (**F**) The BMA probability of freezing refers to the 24-hour period ending at the valid time.

sored DEMETER (Development of a European Multimodel Ensemble system for seasonal to inTERannual prediction) project. A single supercomputer hosted seven independent state-of-the-art models, which produced a series of 6-month ensemble reforecasts with common archiving systems and diagnostics. Each model was run nine times with different initial conditions, resulting in global multimodel, multi–initial condition ensemble reforecasts over the past 50 years. The DEMETER ensemble improved both deterministic and probabilistic forecast skill when compared to the single-model ensembles, in ways that cannot be attributed to the increase in ensemble size only. Applications to malaria incidence and crop yield prediction have shown the benefits of linking seasonal forecast ensembles to end-user models that are also run in ensemble mode. Building on the success of the DEMETER project, an operational real-time seasonal ensemble prediction system has been established at ECMWF.

Current challenges include the representation of forecast uncertainty due to the use of imperfect numerical models. Model uncertainty can be addressed through the use of multimodel ensembles (in which each single model run is deterministic), or through stochastic representations of parameterized physical processes, as implemented in the ECMWF medium-range ensemble, thereby introducing randomness into the model runs (*13*). Both options link flow-dependent forecast uncertainty and model-related errors, and it remains to be seen whether they are superior in any way to approaches based purely on statistical postprocessing (*7*, *14*). Nor has the debate on selective versus Monte Carlo sampling of initial condition uncertainty been resolved, although it may evolve in novel directions as operational experience with various methods of sequential data assimilation accrues.

From daily to seasonal time scales, probabilistic forecasts based on ensembles have become a prominent part of numerical weather prediction. The ability of ensemble systems, in concert with statistical postprocessing, to improve deterministic forecasts—in that the ensemble mean forecast outperforms the individual ensemble members—and to produce probabilistic and uncertainty information to the benefit of weather-sensitive public, commercial, and humanitarian sectors has been convincingly established. More work needs to be done to routinely provide fully reliable, flow-dependent probabilistic forecast distributions, particularly of weather fields, as opposed to forecasts at individual sites. In keeping with the remarkable pace of progress since the early 1990s, we anticipate notable improvements in deterministic and probabilistic forecast skill through the continued development of multimodel, multi–initial condition ensemble systems and advanced, grid-based statistical postprocessing techniques.

Additional effort is required in the communication, visualization, and evaluation of probabilistic forecasts, and differing interpretations of probability need to be reconciled, to avoid the risk of perfecting ensemble methodologies without a clear aim (*15*, *16*). To this end, the paradigm of maximizing the sharpness of the probabilistic forecasts under the constraint of calibration may offer guidance. Calibration refers to the statistical consistency between the probabilistic forecasts and the observations; sharpness refers to the spread of the predictive distributions and is a property of the forecasts only. The goal is to increase sharpness in the forecasts, without compromising the validity of the probability statements.

References and Notes

1. T. N. Palmer, *Q. J. R. Meteorol. Soc.* **128**, 747 (2002).
2. For real-time ensemble forecasts, see NCEP Operational Ensemble Forecasts (www.cdc.noaa.gov/map/images/ens/ens.html) and MSC Ensemble Forecasts (http://weatheroffice.ec.gc.ca/ensemble/index_e.html).
3. Z. Toth, E. Kalnay, *Bull. Am. Meteorol. Soc.* **74**, 2317 (1993).
4. F. Molteni, R. Buizza, T. N. Palmer, T. Petroliagis, *Q. J. R. Meteorol. Soc.* **122**, 73 (1996).
5. P. L. Houtekamer, L. Lefaivre, J. Derome, H. Ritchie, H. L. Mitchell, *Mon. Weather Rev.* **124**, 1225 (1996).
6. G. Evensen, *J. Geophys. Res.* **99**, 10143 (1994).
7. R. Buizza *et al.*, *Mon. Weather Rev.* **133**, 1076 (2005).
8. E. P. Grimit, C. F. Mass, *Weather Forecast.* **17**, 192 (2002).
9. F. A. Eckel, C. F. Mass, *Weather Forecast.* **20**, 328 (2005).
10. Real-time forecast products are available at the University of Washington Mesoscale Ensemble (www.atmos.washington.edu/~ens/uwme.cgi) and Bayesian Model Averaging (http://isis.apl.washington.edu/bma/index.jsp) sites.
11. T. N. Palmer *et al.*, *Bull. Am. Meteorol. Soc.* **85**, 853 (2004).
12. T. N. Palmer, Ed., Special issue on the DEMETER project, *Tellus A* **57** (May 2005), pp. 217–512.
13. R. Buizza, M. Miller, T. N. Palmer, *Q. J. R. Meteorol. Soc.* **125**, 2887 (1999).
14. A. E. Raftery, T. Gneiting, F. Balabdaoui, M. Polakowski, *Mon. Weather Rev.* **133**, 1155 (2005).
15. I. T. Jolliffe, D. B. Stephenson, *Forecast Verification: A Practitioner's Guide in Atmospheric Science* (Wiley, New York, 2004).
16. R. de Elía, R. Laprise, *Mon. Weather Rev.* **133**, 1129 (2005).

17. While preparing this Perspective, T.G. was on sabbatical leave at the Soil Physics Group, Universität Bayreuth, Germany. We thank C. Mass for comments; J. Baars, E. Grimit, and P. Tewson for assistance in preparing the figure; and the U.S. Department of Defense Multidisciplinary Research University Initiative (MURI) for financial support.

10.1126/science.1115255

Paving the way to a new era in cell counting - INCYTO

Simple, Accurate, Economical and Contamination Free – Everything for Cell Counting

Direct customer confirmation of counted cell images
No Calibration, Minimization of human count error
Complete customer-oriented service

Distributors & OEM Welcome

C-Chip Disposable Hemocytometer

Exact volume control & Easy to use!
No need coverslip, just drop & count

- DHC-N01 with Neubauer Improved
- DHC-F01 with Fuchs-Rosenthal
- DHC-S01 for semen test
- Other grid types are available

C-Reader Automatic Microchip Type Hemocytometer

Accurate & Easy Cell viability test / Cell counting!

LAB Type

- CRV-200 for mamallian cell (X40)
- CRM-350 for yeast cell (X100)
- CRD-200 for somatic cell (X40)

Portable Type

- CRP-200 for somatic cell (X40)
- CRP-300 for cell viability test (X40)
- CRP-400 for yeast count & cell viability test (X40, X100)

Head Office

Kyobo Tower Bldg., 1303 -22, Seocho4-dong, Seocho-gu, Seoul, 137-070, Korea
Tel : +82-2-3787-1964,5 / Fax : +82-2-537-2649 / E-mail : sales@incyto.com

Distribution Networks

US : +1-678-342-1651 (SKC America)
Japan : +81-3-5954-8570 (QDJ)
U.K. & Ireland : +44-1273-814888 (Labtech)
Turkey : +90-216-658-7840 (VitroLab)
Singapore : +65-6464-1361 (Biofrontier)
Hong Kong : +852-2628-1221 (Chinetek)
Taiwan : +886-2-8780-5228 (QDT)

iNCYTO

www.incyto.com

CE

Extrasolar Planets: Constraints for Planet Formation Models

Nuno C. Santos,[1,3]* Willy Benz,[2] Michel Mayor[3]

Since 1995, more than 150 extrasolar planets have been discovered, most of them in orbits quite different from those of the giant planets in our own solar system. The number of discovered extrasolar planets demonstrates that planetary systems are common but also that they may possess a large variety of properties. As the number of detections grows, statistical studies of the properties of exoplanets and their host stars can be conducted to unravel some of the key physical and chemical processes leading to the formation of planetary systems.

In 1992, Wolszczan and Frail made the discovery that planets far from our own solar system were in orbit around the pulsar PSR 1257+12 (*1*). After years of false starts and retracted announcements, it was thrilling that definitive evidence had finally been found for smaller orbiting bodies in distant stellar environments. At the same time, pulsars are not anything like our own Sun, and any planets orbiting them would not be expected to harbor life as in our solar system. For this reason, researchers had long been eager to observe planets in orbit around Sun-like stars, and in 1995, a first planet was detected around the star 51 Pegasi (*2*, *3*). Since then, more than 150 other planets have been found, most of these discovered, or at least confirmed, with radial-velocity techniques (*4*), in which the stellar wobble of the star moving about the center of mass of the star-planet system is measured with spectral Doppler information. These discoveries have advanced our understanding of planet dynamics and planet formation.

The increase in precision and continuity of the current radial-velocity surveys has given astronomers the possibility of unveiling a large variety of planets. In less than 10 years, the lowest known detectable planetary mass has decreased by more than one order of magnitude (Fig. 1), reflecting the jump in measurement precision from ~10 m s^{-1} to ~3 m s^{-1} at the end of the century (*5*), and more recently crossing the barrier of 1 m s^{-1} precision with state-of-the-art spectrometers such as the High Accuracy Radial Velocity Planet Searcher (HARPS) (*6*).

About 10% of the discovered exoplanets have an orbital period of less than 5 days. These planets are easier to detect because they require less observational time. However, these short-period planets were unexpected, because giant planets were thought to have formed on orbits beyond the ice line, the point where the nebula becomes cold enough for ices to condensate, thereby maximizing the density of solids available for accretion (*7*). Continuous planet searches have revealed giant planets with orbital periods as short as 1.2 days (*8*) or as long as ~10 years (*9*), although this upper limit is probably due to observational limitations. Some of the planets are on ec-

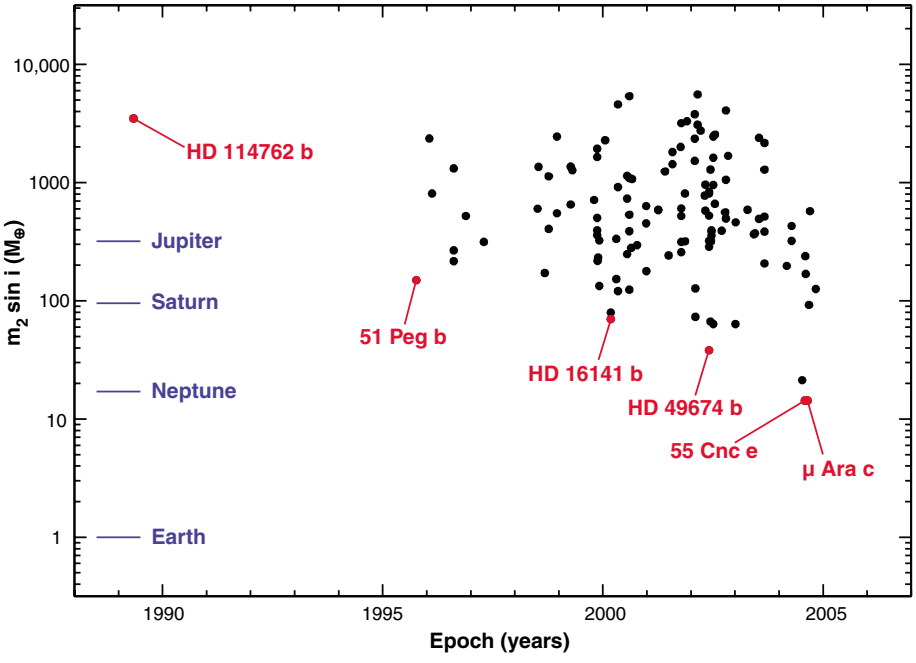

Fig. 1. Minimum mass of the known extrasolar planets orbiting solar-type stars, in Earth masses as a function of the year of the discovery. The masses of Jupiter, Saturn, Neptune, and the Earth are marked for comparison (blue lines). A few benchmark cases (red dots) are labeled: the probable brown-dwarf companion to HD 114762 (*65*), 51 Peg b (*2*), HD 49674 b (*66*), and the record-holders, recently discovered very low mass companions to 55 Cnc and μ Ara (*11*, *12*). Data are as of June 2005.

Table 1. Extrasolar planets transiting their host stars, as confirmed in June 2005. Other candidates exist, although their characteristics are still not well constrained (e.g., OGLE-TR-10).

System	Planet mass (M_{Jup})	Planet radius (R_{Jup})	Orbital period (days)	Reference
HD 209458	0.69 ± 0.05	1.35 ± 0.06	3.52	(*46*, *67*)
OGLE-TR-56	1.45 ± 0.23	1.23 ± 0.16	1.21	(*8*, *68*)
OGLE-TR-111	0.53 ± 0.11	$1.00 \pm {}^{0.13}_{0.06}$	4.02	(*48*)
OGLE-TR-113	1.35 ± 0.22	$1.08 \pm {}^{0.07}_{0.05}$	1.43	(*40*)
OGLE-TR-132	1.19 ± 0.13	1.13 ± 0.08	1.69	(*40*, *69*)
TrEs-1	0.75 ± 0.07	$1.08 \pm {}^{0.18}_{0.04}$	3.03	(*49*)

[1]Centro de Astronomia e Astrofísica da Universidade de Lisboa, Observatório Astronómico de Lisboa, Tapada da Ajuda, 1349-018 Lisboa, Portugal. [2]Physikalisches Institut, Universität Bern, Sidlerstrasse 5, CH-3012 Bern, Switzerland. [3]Observatoire de Genève, 51 chemin des Maillettes, 1290 Sauverny, Switzerland.

*To whom correspondence should be addressed. E-mail: nuno.santos@oal.ul.pt

centric orbits (*10*) more typical of some comets in the solar system, whereas others are in multiple planet systems (*11*). Finally, although the most recently discovered planets have masses only one order of magnitude larger than Earth (*11*–*13*), some behemoths have more than 15 times the mass of Jupiter (*14*). It is not clear whether the more massive of these companions should be classified as planets at all. According to the pre-1995 planet formation theories, none of these objects were supposed to exist.

To understand the meaning of these observations, models of planetary system formation and evolution are required. One giant planet formation scenario is the core accretion model. In this model, a solid core is first formed by the accretion of planetesimals. As the core grows, it eventually becomes massive enough to gravitationally bind some of the nebular gas, thus surrounding itself with an envelope. The subsequent evolution of this core-envelope structure has been studied in detail (*7*), and it has been shown that the solid core and the gaseous envelope grow in mass, the envelope remaining in quasistatic and thermal equilibrium. During this phase, the energy radiated by the gas is supplied by energy released from the accretion of planetesimals. As the core mass reaches a critical value [of the order of 15 Earth masses ($M_\oplus$) at 5 astronomical units (AU), but depending on different physical parameters, such as the solid accretion rate onto the core], radiative losses can no longer be offset by planetesimal accretion and the envelope starts to contract. This increases the gas accretion rate, which in turn raises the radiative energy losses, causing the process to accelerate, leading to the very rapid buildup of a massive envelope.

Paramount to this model is the growth of a critical core before the disappearance of the protoplanetary disk. The lifetime of these disks can be estimated from astronomical observations by relating the total mass of the disks (*15*) to the mass accretion rate (*16*). This yields a lifetime for these objects of 1 to 10 million years, in agreement with the frequency of disks in open clusters of different ages (*17*). Because this lifetime is of the same order, if not smaller, than the planet formation time scale, a fast growth of the core beyond the critical mass is essential. Calculations by Pollack *et al.* (*7*) showed that this formation time scale is extremely sensitive to the assumed disk surface density and that only relatively high values will yield giant planets within the disk's lifetime. Recent extensions of the core accretion model, including disk evolution and planet migration (*18*), have shown that, provided the planet survives, migration speeds up core growth, resulting in giant planet formation well within the inferred disk lifetimes.

In the direct collapse scenario (*19*), giant planets form directly from the gravitational fragmentation and collapse of the protoplanetary disk within a few dynamical time scales. Although this is an appealing feature that greatly simplifies a number of complicated processes, this model has its own difficulties as well. For example, high-resolution simulations of this process show that planets tend to form on elliptical orbits at distances of several astronomical units and masses between 1 and 7 Jupiter masses (M_{Jup}). Smaller mass planets would result from the evaporation of these objects by nearby hot type O and B stars (*20*). Furthermore, the enrichment in heavy elements as measured in the atmospheres of Jupiter and Saturn might be difficult to explain, as massive bodies eject many more planetesimals than they actually accrete (*21*). Finally, any sizable inner core will have to be built by the accretion of very large objects, because smaller ones will invariably be destroyed while plunging through the envelope.

In summary, two formation paradigms are currently being critically examined. The core accretion model is sufficiently advanced to begin to allow quantitative calculations to be made and thus permits a direct comparison with giant planets in (*22*) and outside (*21*) our solar system. The direct collapse model is in a state where only qualitative statements can be made without the possibility to compare quantitatively with observations.

Having at first painfully exposed our still sizable lack of understanding, the growing number of exoplanets discovered is now allowing a statistical analysis of their properties (*10*, *23*–*26*) as well as those of their host stars (*27*, *28*), thereby providing invaluable constraints on the physical and chemical processes involved in the formation of these systems.

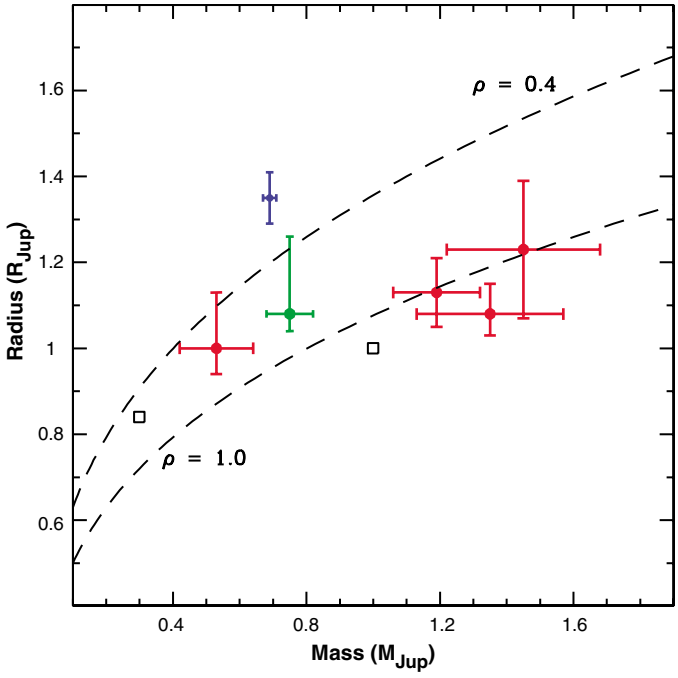

Fig. 2. Mass-radius diagram for the giant planet companions for which a transit event has been detected. Red symbols denote planets discovered by the OGLE survey (*8*, *40*, *48*), the green symbol denotes the planet orbiting the star TrEs-1 (*49*), and the blue symbol denotes HD 209458 b (*46*). The positions of Jupiter and Saturn are also marked (black open squares). Two isodensity curves, with densities ρ of 0.4 and 1.0 g cm^{-3}, are also shown for comparison. The planet orbiting HD 209458 presents the most anomalous (low) mean density.

Statistical Properties of Exoplanets

Before 1995, all our understanding of planet formation was based on studies of one system, the solar system. The failure of our theories to explain the diversity of the more than 150 exoplanets has markedly shown the necessity for further observational guidance. In the case of the solar system, this guidance is provided by in situ measurements that allow a detailed study of structure, composition, isotopic abundances, and often time scales. In the case of the exoplanets, this guidance is provided by a careful statistical analysis of the distribution of masses, periods, and orbital eccentricity, as well as of the chemical properties of the host star. Both approaches are needed.

The existence of giant planets with orbital periods of less than ~10 days, the so-called "hot Jupiters," poses important difficulties to conventional as well as unconventional giant planet formation scenarios. The most important is related to the high temperatures in these regions, which either prevent the condensation of enough solids to form a core capable of accreting several hundred Earth masses of gas during the lifetime of the disk or simply inhibit direct collapse. To circumvent this, migration of planets over relatively large distances is often invoked. Close-in planets may have formed at large distances and then migrated inward. Thus, the existence of "hot Jupiters" has forced on us the concept that the current locations of planets may have little to do with their birthplaces.

Migration can be due to several physical processes such as gravitational scattering in multiple systems (*29*) or gravitational interactions between the gaseous and/or the

planetesimal disk and the planet (*30*, *31*). These two mechanisms must necessarily occur, and interactions between an embedded planet and a gaseous disk were discussed before the discovery of the first exoplanet (*32*). The question is therefore not whether migration takes place or not but rather what its direction and amplitude are.

Two types of migration modes have been identified, depending on whether the planet is massive enough to open a gap in the disk (type II migration) or not (type I migration) (*30*, *33*–*35*). All these migration models conclude that planets are migrating mostly inward toward the star, over large distances and fast. In fact, migration time scales obtained so far are so short (especially for type I migration) that, in almost all cases, planets should not survive but should fall into their host star (*36*, *37*). Because planets are actually observed in large numbers and at various distances to their stars, two conclusions can be drawn: Either our migration theory is still incomplete or core accretion is not the way most planets form. Because new ideas for slowing down migration are emerging (*21*) and because core accretion models based on a slower rate are capable of meeting quantitative tests (*22*), we rather favor the first hypothesis.

Evidence of a mechanism halting the inward migration of planets at short distances may be deduced from the observed overabundance of systems with periods around 3 days, whereas for smaller orbital periods, only a few cases exist (*38*). This result contrasts with the period distribution of stellar companions for which periods much shorter than 3 days exist.

The physical mechanism responsible for halting and parking the planet at short distances from the host star is still being debated. Possible mechanisms include the existence of a central cavity in the disk, tidal interaction with a fast-spinning host star, or even Roche lobe overflow (*36*). Another possibility is that planets venturing closer are photoevaporated by the radiation field emitted by the host star, thus becoming too small to be detected or vanishing altogether (*39*). The case of the few new OGLE (Optical Gravitational Lensing Experiment) transiting planets (*8*, *40*) having orbital periods of less than 2 days may in this context be interpreted as the tail of the short-period planets distribution (*38*).

Although these stopping mechanisms are relevant at short distances, they do not explain why giant planets are found at intermediate distances (e.g., with periods around 1 year) nor why Jupiter, for example, has apparently remained beyond 5 AU. In fact, the recent addition of disk evolution and planetary migration mechanisms into the core-accretion models suggests that planets essentially migrate until the disk disappears (in fact, until the disk becomes much less massive than the planet) (*18*, *21*). In this picture, the diversity results from the distribution of parameters such as the disk masses, lifetimes, disk processes, photoevaporation, and number of planets formed. Unfortunately, none of these parameters are precisely known, and it may even be that planetary formation itself is providing a feedback mechanism (*41*).

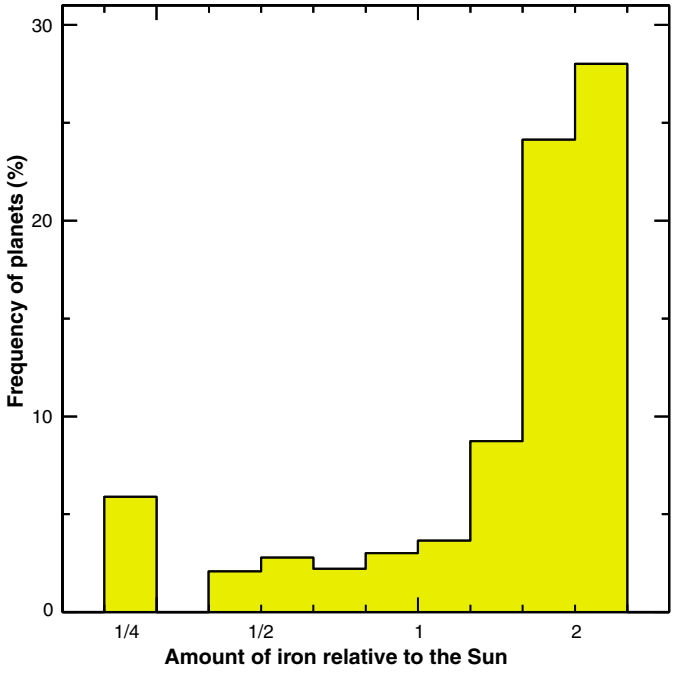

Fig. 3. Percentage of stars that were found to have planets among the Geneva planet search survey sample as a function of the relative amount of iron (i.e., metallicity) with respect to the Sun. This figure shows that ~25% of the stars with twice the solar metallicity harbor a planetary mass companion, whereas this percentage decreases to below 5% for stars with the same metal content as our Sun (*53*).

The observed period distribution of planetary companions may be telling us something about these issues (*23*, *25*). There seems to be a paucity of high-mass planetary companions with orbital periods shorter than ~40 days. Current statistical analysis suggests that the migration of a planet may be strongly related to its mass or even to the presence of other stellar companions (*24*, *25*).

The analysis of the mass distribution of companions to solar-type stars with orbital periods shorter than 3000 days indicates that although the radial-velocity technique is more sensitive to massive companions, the frequency of discovered planets increases as a function of decreasing mass (*42*). Furthermore, this distribution falls to a value close to zero for masses between about 10 and 20 times the mass of Jupiter. From 20 to 60 M_{Jup}, there is then a scarcity of companions to solar-type stars. This gap, usually called the brown dwarf desert (*43*), separates the lower mass planetary companions from their higher mass stellar counterparts, including brown dwarfs, considered to be failed stars. Together with the shape of the mass distribution, this suggests a different formation mechanism between low-mass companions to solar-type stars and planetary systems.

The analysis of the orbital eccentricity distribution also indicates that the measured values range from ~0 to more than 0.9, a range similar to the one found in binary stars. However, recent analysis (*10*) suggests that planetary systems have on average a lower eccentricity than multiple stellar systems. Although this might be interpreted as the signature of a different formation mechanism, it is worth pointing out that these high eccentricities cannot be accounted for in the standard formation model of giant planet formation. Eccentricity pumping mechanisms such as interactions in multiple systems (*44*, *45*) or the interactions between the planet and the disk of planetesimals (*45*) have to be invoked to explain these high eccentricities.

Transiting Planets: Probing the Planet Structure

So far, most of the known extrasolar planets have been detected with radial-velocity techniques. Alone, this gives us information only about the orbital parameters of the planets and their minimum masses but nothing about their physical properties such as radius or mean density. Fortunately, the recent detection of several cases (*8*, *40*, *46*–*49*) of photometric transits as the planets pass in front of their host stars, thus blocking part of the stellar light, has provided us with additional information to derive these quantities (Table 1).

These discoveries have also raised further interesting and troubling issues. For example, among the six confirmed transiting planets, HD 209458 has a mean density much smaller than that of the others (Fig. 2). Furthermore, the planets with shorter orbital periods are also the most massive ones, indicating that there might be a relation between planet mass and orbital period (*50*).

In addition to the internal structure, the detection of transiting planets opens a new possibility to study planetary atmospheres.

When a planet crosses the stellar disk, its upper atmosphere acts as a filter, absorbing the light coming from the star at preferential wavelengths that correspond to atomic or molecular transitions occurring in its atmosphere. Because of this effect, sodium absorption features were detected in the atmosphere of the planet orbiting HD 209458 (*51*). Further observations have also recently suggested that this giant planet is evaporating, as carbon and oxygen atoms are blown away along with its hydrodynamically escaping hydrogen atmosphere (*52*).

The Stars Hosting Planets

The study of the stars hosting planets has also found an unexpected correlation, the importance of which to planet formation is recognized even though its full implications have not yet been understood. Host stars have, on average, a higher metal content than stars with no planetary companions detected (*27*, *28*). In other words, these stars have a higher ratio of heavy elements to hydrogen than that observed in average solar-type field stars. The most recent studies have confirmed this correlation and shown that the observed trend cannot be due to any sampling or observational bias (*53*). More than 20% of stars with metallicity greater than two times the solar metallicity harbor a planet, whereas only ~3% of stars with solar metallicity have a giant planet (Fig. 3) (*28*, *53*, *54*). However, this does not imply that giant planets cannot be formed around more metal-poor stars. Rather, it suggests that the probability of formation in such a case is substantially lower (*55*). Indeed, there is a hint that, for lower metallicity values, the frequency of planets may remain relatively constant (*53*) as a function of the stellar metallicity. Whether this reflects the presence of two different regimes of a low metallicity tail is currently under debate, and more data will be needed before this question can be answered.

Although pollution of the star by infalling planetary material has been suggested to explain the higher metallicities (*27*, *56*), it is now believed that the stellar surface abundance is a relic of the original elemental abundance in the gas clouds that gave birth to the stars and the planets (*57*). In other words, this implies that planetary formation, at least for the kind of planets that have been discovered so far, is far more likely in a metal-rich environment. Alternatively, the metallicity could be increasing the migration rates of the giant planets. In such a case, we could be simply discovering those planets with periods that are relatively short, and thus, those bodies orbiting metal-rich stars. This possibility receives some support from the possible (weak) correlation found between the stellar metal content and the orbital period of the planets (*27*, *58*). However, recent models suggest that such an influence is probably not strong enough to effectively change the migration rates (*59*), which are already much faster than the traditional planet formation process itself.

More heavy elements should, in principle, lead to faster core growth and therefore to an easier formation of giant planets in the core accretion scenario. Models have been proposed that claim to explain quantitatively this correlation (*55*), even though many details are still not clearly accounted for. In the direct collapse model, the connection would need to be a more subtle one in which metallicity affects the ability to collapse, that is, to radiate energy. So far, calculations (*19*) indicate that collapse is insensitive to metallicity. Therefore, in this formation scenario, the observed correlation between stellar metallicity and likelihood of hosting a planet would have to be due to pollution by ingested planetary material. As a consequence, it seems that current results support core accretion as the main process leading to the formation of the now-discovered planets. However, disk instability is not excluded as a viable way to form planets, in particular around metal-poor stars.

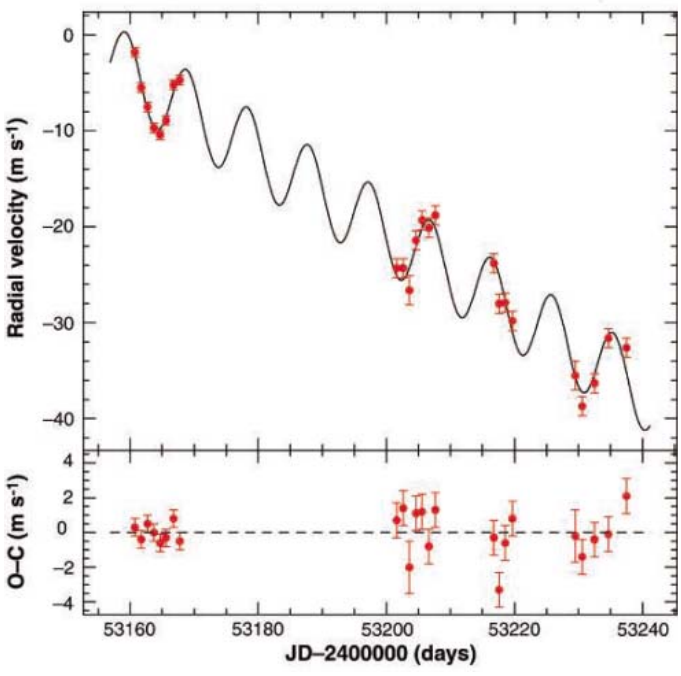

Fig. 4. Radial-velocity measurements of μ Ara as a function of time, as obtained with the HARPS spectrograph (*6*). The solid line represents the best fit to the data, obtained with the sum of a Keplerian function and a linear trend. This latter represents the effect of the long-period companions to the system (one, or possibly two other giant planets are known to orbit this star). The residuals of the fit, with a root mean square of only 0.9 m s^{-1}, are shown in the lower panel. [Adapted from Santos *et al.* (*12*)]

After All, What Is a Planet?

All these odd properties of the exoplanets have contributed to a change in the definition of planet. The answer to the question ''what is a planet?'' is not even clear at this moment. For example, the dividing line between low-mass stars (e.g., brown dwarfs) and planets seems to be rather uncertain, and it may be that bodies formed as planets may have a mass in the brown-dwarf regime (≥13 M_{Jup}) (*60*), and vice versa.

Although no consensus exists, and a clear definition of planet has not been agreed on, the International Astronomical Union (IAU) has proposed a working definition (*61*), based on three major points: (i) Objects with masses below the limiting mass for thermonuclear fusion of deuterium, currently calculated to be near 13 M_{Jup} for objects of solar metallicity (*60*), that orbit stars or stellar remnants are planets (no matter how they formed). The minimum mass or size required for an object to be considered a planet should be the same as that used in the solar system. (ii) Substellar objects with masses above the limiting mass for thermonuclear fusion of deuterium are brown dwarfs, no matter how they formed or where they are located. (iii) Free-floating objects in young star clusters with masses below the limiting mass for thermonuclear fusion of deuterium are not planets but are sub–brown dwarfs (or whatever name is most appropriate).

We should mention that, according to this definition, a very low mass object formed by the gravitational collapse of a molecular cloud, separated by ~50 AU from a low mass star, should be considered a planet. These kinds of objects have been found, and if we take this definition strictly, the first image of a planet orbiting another star may have been obtained (*62*). However, it seems unlikely that a giant planet could have been formed in a low mass disk at such a large distance from its host star, in this case (*62*) a brown dwarf itself, in a reasonable time scale (*7*). The 13-M_{Jup} limit also seems to us to be no more than an arbitrary limit used as a possible ''definition''

and is probably not related to the planetary/stellar formation physics.

Toward Other Earths

The discovery of numerous giant planets orbiting other solar-type stars has demonstrated that planet formation is a common process. By extension, these detections suggest that Earth-like planets might be just as common. Although the detection of an Earth-like planet is probably beyond the reach of current techniques, the discovery in August 2004 of two planets (*11*, *12*) with a minimum mass of ~14 $M_{\oplus}$ orbiting Sun-like stars (μ Ara c and 55 Cnc e) (Fig. 4), as well as of a slightly more massive exoplanet orbiting the M dwarf GJ 436 (*13*) (with a minimum mass of 21 $M_{\oplus}$), implies that we are only a factor of 10 in mass away from this goal. The former two of these planets have short-period (10-day) orbits and circle metal-rich solar-type dwarfs. Their orbital characteristics and masses, together with state-of-the-art models of planet formation (*18*), suggest that there might be two channels to account for their existence: one in which a large mass object has been evaporated to the present mass and another one in which the object never grew larger. In the latter case, because these objects probably could not have migrated too far, the exact location of the ice line during their accretion, which might be closer to the star than previously thought (*63*), is required to infer their composition.

μ Ara and 55 Cnc were the only two stars that were surveyed with high enough precision to allow the detection of such low-mass bodies around a ''solar mass'' star. This may imply that low-mass short-period planets are common. Very low mass planets like the ones orbiting μ Ara c and 55 Cnc e will be the prime targets for satellites like Convection Rotation and Planetary Transits (COROT) and Kepler (*64*).

Once Earth-like planets orbiting in the habitable zone are known, the search for life in these systems will undoubtedly follow. The question of the existence of life is too important to be ignored even if the technology required and the cost involved are currently still staggering. Hence, future space missions will have to be launched that are capable of remotely sensing the presence of life. The space interferometers Darwin (ESA) and the Terrestrial Planet Finder (NASA) are precisely such missions. Using optical coronography and nulling interferometry techniques (to remove the light from the target stars, leaving only the photons coming from the planet), these missions will be capable of detecting the spectroscopic signatures of life in the atmospheres of these planets.

References and Notes

1. A. Wolszczan, D. A. Frail, *Nature* **355**, 145 (1992).
2. M. Mayor, D. Queloz, *Nature* **378**, 355 (1995).
3. The previously discovered radial-velocity companion around HD 114762 (*65*) has a minimum mass above 10 M_{Jup}. For an updated list of known exoplanets, see the table available at http://obswww.unige.ch/Exoplanets. Pulsar planets are probably mostly second-generation planets; hypothetical planets existing by the time of the supernova explosion that gave origin to the pulsar would most probably have disapeared.
4. J. J. Lissauer, *Nature* **419**, 355 (2002).
5. S. S. Vogt, G. W. Marcy, R. P. Butler, K. Apps, *Astrophys. J.* **536**, 902 (2000).
6. M. Mayor *et al.*, *The Messenger* **114**, 20 (2003).
7. J. Pollack *et al.*, *Icarus* **124**, 62 (1996).
8. M. Konacki, G. Torres, S. Jha, D. Sasselov, *Nature* **421**, 507 (2003).
9. G. W. Marcy *et al.*, *Astrophys. J.* **581**, 1375 (2002).
10. J. L. Halbwachs, M. Mayor, S. Udry, *Astron. Astrophys.* **431**, 1129 (2005).
11. B. E. McArthur *et al.*, *Astrophys. J.* **614**, L81 (2004).
12. N. C. Santos *et al.*, *Astron. Astrophys.* **426**, L19 (2004).
13. R. P. Butler *et al.*, *Astrophys. J.* **617**, 580 (2004).
14. S. Udry *et al.*, *Astron. Astrophys.* **390**, 267 (2002).
15. S. V. W. Beckwith, A. I. Sargent, *Nature* **383**, 139 (1996).
16. L. Hartmann, N. Calvet, E. Gullbring, P. D'Alessio, *Astrophys. J.* **495**, 385 (1998).
17. K. E. Haisch, E. A. Lada, C. J. Lada, *Astrophys. J.* **553**, L153 (2001).
18. Y. Alibert, C. Mordasini, W. Benz, C. Winisdoerffer, *Astron. Astrophys.* **434**, 343 (2005).
19. A. P. Boss, *Astrophys. J.* **567**, L149 (2002).
20. A. P. Boss, G. W. Wetherill, N. Haghighipour, *Icarus* **156**, 291 (2002).
21. S. Ida, D. N. C. Lin, *Astrophys. J.* **604**, 388 (2004).
22. Y. Alibert, O. Mousis, C. Mordasini, W. Benz, *Astrophys. J.* **626**, L57 (2005).
23. A. Cumming, G. W. Marcy, R. P. Butler, *Astrophys. J.* **526**, 890 (1999).
24. S. Zucker, T. Mazeh, *Astrophys. J.* **568**, L113 (2002).
25. S. Udry, M. Mayor, N. Santos, *Astron. Astrophys.* **407**, 369 (2003).
26. A. Eggenberger, S. Udry, M. Mayor, *Astron. Astrophys.* **417**, 353 (2004).
27. G. Gonzalez, *Astron. Astrophys.* **334**, 221 (1998).
28. N. C. Santos, G. Israelian, M. Mayor, *Astron. Astrophys.* **373**, 1019 (2001).
29. F. Marzari, S. J. Weidenschilling, *Icarus* **156**, 570 (2002).
30. D. N. C. Lin, P. Bodenheimer, D. C. Richardson, *Nature* **380**, 606 (1996).
31. N. Murray, B. Hansen, M. Holman, S. Tremaine, *Science* **279**, 69 (1998).
32. P. Goldreich, S. Tremaine, *Astrophys. J.* **241**, 425 (1980).
33. D. N. C. Lin, J. Papaloizou, *Astrophys. J.* **309**, 846 (1986).
34. W. Ward, *Astrophys. J.* **488**, L211 (1997).
35. H. Tanaka, T. Takeuchi, W. R. Ward, *Astrophys. J.* **565**, 1257 (2002).
36. D. Trilling *et al.*, *Astrophys. J.* **500**, 428 (1998).
37. Y. Alibert, C. Mordasini, W. Benz, *Astron. Astrophys.* **417**, L25 (2004).
38. B. S. Gaudi, S. Seager, G. Mallen-Ornelas, *Astrophys. J.* **623**, 472 (2005).
39. I. Baraffe *et al.*, *Astron. Astrophys.* **419**, L13 (2004).
40. F. Bouchy *et al.*, *Astron. Astrophys.* **421**, L13 (2004).
41. R. Sari, P. Goldreich, *Astrophys. J.* **606**, L77 (2004).
42. A. Jorissen, M. Mayor, S. Udry, *Astron. Astrophys.* **379**, 992 (2001).
43. J. L. Halbwachs, F. Arenou, M. Mayor, S. Udry, D. Queloz, *Astron. Astrophys.* **355**, 581 (2000).
44. F. Rasio, E. Ford, *Science* **274**, 954 (1996).
45. N. Murray, M. Paskowitz, M. Holman, *Astrophys. J.* **565**, 608 (2002).
46. D. Charbonneau, T. Brown, D. Latham, M. Mayor, *Astrophys. J.* **529**, L45 (2000).
47. G. W. Henry, G. W. Marcy, R. P. Butler, S. S. Vogt, *Astrophys. J.* **529**, L41 (2000).
48. F. Pont *et al.*, *Astron. Astrophys.* **426**, L15 (2004).
49. R. Alonso *et al.*, *Astrophys. J.* **613**, L153 (2004).
50. T. Mazeh, S. Zucker, F. Pont, *Mon. Not. R. Astron. Soc.* **356**, 955 (2005).
51. D. Charbonneau, T. M. Brown, R. W. Noyes, R. L. Gilliland, *Astrophys. J.* **568**, 377 (2002).
52. A. Vidal-Madjar *et al.*, *Astrophys. J.* **604**, L69 (2004).
53. N. C. Santos, G. Israelian, M. Mayor, *Astron. Astrophys.* **415**, 1153 (2004).
54. I. N. Reid, *Publ. Astron. Soc. Pac.* **114**, 306 (2002).
55. S. Ida, D. N. C. Lin, *Astrophys. J.* **616**, 567 (2004).
56. S. Vauclair, *Astrophys. J.* **605**, 874 (2004).
57. M. H. Pinsonneault, D. L. DePoy, M. Coffee, *Astrophys. J.* **556**, L59 (2001).
58. A. Sozzetti, *Mon. Not. R. Astron. Soc.* **354**, 1194 (2004).
59. M. Livio, J. E. Pringle, *Mon. Not. R. Astron. Soc.* **346**, L42 (2003).
60. D. Saumon *et al.*, *Astrophys. J.* **460**, 993 (1996).
61. For more details, we point the reader to the *Science* magazine debate available at www.sciencemag.org/cgi/eletters/291/5508/1487b?ck=nck and to the IAU/UAI position statement at www.ciw.edu/boss/IAU/div3/wgesp/definition.html.
62. G. Chauvin *et al.*, *Astron. Astrophys.* **425**, L29 (2004).
63. D. D. Sasselov, M. Lecar, *Astrophys. J.* **528**, 995 (2000).
64. For more information on these missions, see http://smsc.cnes.fr/COROT and http://www.kepler.arc.nasa.gov, respectively.
65. D. Latham, R. Stefanik, T. Mazeh, M. Mayor, G. Burki, *Nature* **339**, 38 (1989).
66. R. P. Butler *et al.*, *Astrophys. J.* **582**, 455 (2003).
67. T. M. Brown, D. Charbonneau, R. L. Gilliland, R. W. Noyes, A. Burrows, *Astrophys. J.* **552**, 699 (2001).
68. G. Torres, M. Konacki, D. D. Sasselov, S. Jha, *Astrophys. J.* **609**, 1071 (2004).
69. C. Moutou, F. Pont, F. Bouchy, M. Mayor, *Astron. Astrophys.* **424**, L31 (2004).

70. We would like to thank the members of the Geneva extrasolar planet search group, D. Naef, A. Eggenberger, C. Lovis, F. Pepe, D. Queloz, and S. Udry, as well as G. Israelian, R. Rebolo (from the Instituto de Astrofisica de Canarias), Y. Alibert, and C. Mordasini, who have largely contributed to the results presented here. We wish to thank the Swiss National Science Foundation for its continuous support to this project. Support from Fundação para a Ciência e Tecnologia, Portugal, to N.C.S. in the form of a scholarship is gratefully acknowledged.

10.1126/science.1100210

Shrimp Alkaline Phosphatase – My Requirements:

1. Must have high activity
2. 100% heat-inactivation...quickly
3. Cost effective and works in many different buffers and applications
4. An enzyme I can completely trust

Want proof? Visit www.getsapfacts.com

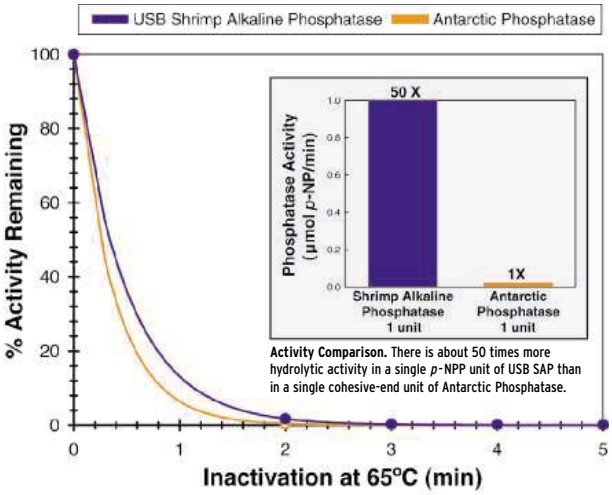

Activity Comparison. There is about 50 times more hydrolytic activity in a single *p*-NPP unit of USB SAP than in a single cohesive-end unit of Antarctic Phosphatase.

Heat inactivation of USB Shrimp Alkaline Phosphatase (SAP) and Antarctic Phosphatase. 20 cohesive-end units (0.2 *p*-NPP units) of each enzyme were diluted into assay buffer and incubated at 65°C. Percent activity remaining at indicated time points was measured by *p*-NPP assay. Complete heat-inactivation occurs within 5 minutes.

USB Shrimp Alkaline Phosphatase – The Benchmark Heat-Labile Alkaline Phosphatase.

Shrimp Alkaline Phosphatase was introduced by USB in the early 1990s as a novel enzyme that was every bit as active as calf intestinal alkaline phosphatase, but much easier to heat-inactivate. This feature of SAP made it the enzyme of choice because it is used directly in place of CIAP – with no need to change buffers or reaction conditions. SAP can be used directly in restriction enzyme digestions or with PCR products* prior to SNP analysis or DNA sequencing. Dephosphorylated vectors may be ligated without further purification. At USB, we know you need products made with integrity. Products that help you be more productive in the lab. Products like USB SAP. To get the facts on USB SAP, please visit www.getsapfacts.com.

usb
Fueling Innovation™

*ExoSAP-IT and the Exonuclease I/Shrimp Alkaline Phosphatase Method are covered by US Patent Nos. 5,741,676 and 5,756,285 and related patents. ExoSAP-IT is covered by US Patent Nos. 6,379,940 and 6,387,634.

800.321.9322 | www.usbweb.com

INTRODUCTION

Inside Out; Outside In

Comets harbor ice and organic material that formed early in our solar system and was partly incorporated into the planets, including ours. They often appear to be huge in the sky, but this is deceptive—their visible coma is produced from a relatively small nucleus, typically a few tens of kilometers across or less. Their small size may have helped to preserve a pristine record of early solar system chemistry. On 3 July 2005, Deep Impact penetrated the nucleus of comet 9P/Tempel 1, ejecting dust and debris from inside the nucleus that was studied by a nearby spacecraft and dozens of other telescopes and spacecraft worldwide. Results from the observations of this truly international experiment (originally published online on 8 and 15 September 2005) are described in six papers in this special section.

Our solar system has two populations of comets: One now resides in a region near and just beyond the orbit of Pluto (the Kuiper Belt), and one group of these (including comet 9P/Tempel 1) gets scattered into orbits that bring them closer to the Sun and Earth; another population now resides much farther out in the Oort Cloud and includes many of our famous comets (Halley, for example). Although now far distant, it is thought that the Oort comets originated near Neptune and Uranus—closer in than the Kuiper Belt comets—but were flung outward (many may have left our solar system entirely) as these and the other giant planets formed.

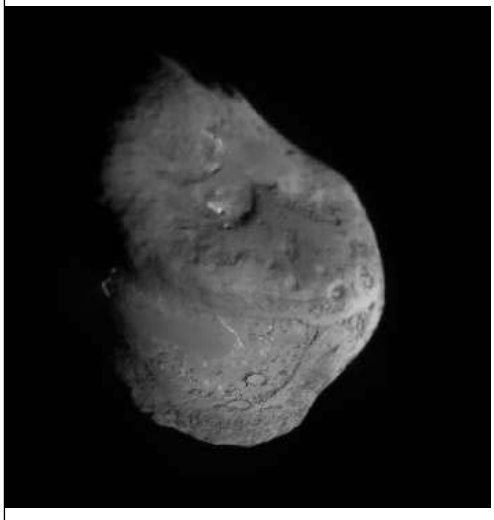

CREDIT: NASA/JPL/UNIVERSITY OF MARYLAND

As discussed in these papers, the Deep Impact experiment revealed several surprises about the nature of the nucleus of Tempel 1 and the origin of comets (see also the News story by Kerr in the 9 September 2005 issue of *Science*). On approach, Deep Impact found that the nucleus contained regions with different layering, perhaps suggesting the amalgamation of two or more separate pieces. Observations from the supporting telescopes, and later from the spacecraft, revealed several episodic outbursts of material from the nucleus. Its surface also contained impact craters, the first seen on a cometary nucleus. Data from the impact itself imply that the nucleus was loosely consolidated and had a low density, consistent with porous ice. Clear evidence of some complex internal layering in the nucleus was not evident. Together these observations reveal a complex history and help tie in features of the nucleus to the formation of its coma. Analysis of the debris cone identified organic molecules, water ice, and silicate-rich dust. Interestingly, the composition and relative abundance of these gases and particles in this Kuiper Belt comet are similar to those of several Oort comets previously studied. If so, then at least some Kuiper Belt comets may have originated close to or within the giant-planet region, implying a more common origin for now-distant comets and suggesting interesting dynamics within this region of the early solar system.

–BROOKS HANSON

CONTENTS

Science

RESEARCH ARTICLE

Deep Impact: Excavating Comet Tempel 1

M. F. A'Hearn,[1]* M. J. S. Belton,[2] W. A. Delamere,[3] J. Kissel,[4] K. P. Klaasen,[5] L. A. McFadden,[1] K. J. Meech,[6] H. J. Melosh,[7] P. H. Schultz,[8] J. M. Sunshine,[9] P. C. Thomas,[10] J. Veverka,[10] D. K. Yeomans,[5] M. W. Baca,[9] I. Busko,[11] C. J. Crockett,[1] S. M. Collins,[5] M. Desnoyer,[10] C. A. Eberhardy,[8] C. M. Ernst,[8] T. L. Farnham,[1] L. Feaga,[1] O. Groussin,[1] D. Hampton,[12] S. I. Ipatov,[1] J.-Y. Li,[1] D. Lindler,[13] C. M. Lisse,[1,14] N. Mastrodemos,[5] W. M. Owen Jr.,[5] J. E. Richardson,[7,10] D. D. Wellnitz,[1] R. L. White[11]

Deep Impact collided with comet Tempel 1, excavating a crater controlled by gravity. The comet's outer layer is composed of 1- to 100-micrometer fine particles with negligible strength (≤65 pascals). Local gravitational field and average nucleus density (600 kilograms per cubic meter) are estimated from ejecta fallback. Initial ejecta were hot (>1000 kelvins). A large increase in organic material occurred during and after the event, with smaller changes in carbon dioxide relative to water. On approach, the spacecraft observed frequent natural outbursts, a mean radius of 3.0 ± 0.1 kilometers, smooth and rough terrain, scarps, and impact craters. A thermal map indicates a surface in equilibrium with sunlight.

Our knowledge of the interior structure of comets, particularly of the evolution of the outer layers at successive perihelion passages, is almost unconstrained by data and relies instead primarily on theoretical models. Thus, the relation of the coma's composition to the solid composition of the nucleus is uncertain. The Deep Impact (DI) mission, in which a spacecraft would collide with and excavate a cometary nucleus, was conceived, proposed to, and selected by NASA to address this very point (*1*). DI delivered an impact of 19 GJ of kinetic energy to the nucleus of comet 9P/Tempel 1 on 4 July 2005 at about 05:44:36 UT (Earth-received time 05:52:02 UT).

The primary goals of the mission were to determine the differences between the surface of a comet with its ambient outgassing and its interior, which might contain enhanced volatiles, and to determine the structural properties and strength of the surface layers.

DI consisted of two fully functional spacecraft: an impacting spacecraft weighing 364 kg (plus 6.5 kg of unused hydrazine fuel, N_2H_4, at time of impact) and a flyby spacecraft for observing the impact and relaying data from the impactor. The impactor used an autonavigation system to analyze images of the comet and target the impactor at a site on the nucleus that would be in sunlight and visible from the flyby spacecraft. Impact speed was 10.3 km/s. The impactor was 49% copper to minimize chemical reactions with water in the comet that would lead to bright emission features. The two spacecraft separated 24 hours before impact, at which point the flyby spacecraft diverted to miss the nucleus by 500 km and slowed down by 100 m/s to provide an 800-s viewing window after impact. At 500 km before closest approach, the flyby spacecraft froze in an attitude that kept its dust shields in the proper orientation. After passing through the innermost coma, the spacecraft turned and looked back at the comet to take additional data (*2*, *3*). The event was also recorded at nearly all the world's remote observing facilities, both ground-based and space-based, to provide more extensive coverage in both time and space than was possible from a flyby mission (*4*).

The Comet Before Impact

The nucleus. The comet was observed by the flyby spacecraft almost continuously from several days before impact until impact and at 4-hour intervals for weeks before the nearly continuous observing. In addition, the impactor obtained images beginning shortly after release from the flyby until ~4 s before impact. The only comet that has been comparably well studied is comet Halley at its 1986 apparition. Figure 1 shows a composite of several images from the impactor, with the highest resolution in the vicinity of the impact site.

The shape of the nucleus is incompletely determined because the slow rotation period, 40.7 hours, and the high velocity of the flyby resulted in only slightly more than half the surface being illuminated and resolved. However, the nucleus was in full silhouette after the flyby, backlit by ejecta from the impact, which strongly constrains the mean radius. Images from the medium resolution instrument (MRI) covered ~25% of the object with sufficient stereo convergence and resolution to solve for 70 control points in 43 images, with an average relative uncertainty of <30 m. The positive spin pole was determined to be within 10° of RA = 5°, Dec = 78°. This solution compares favorably with a pre-encounter measurement of RA = 46°, Dec = 73° based on light curve analysis (*5*). The spin vector was constrained by the projected spin axis found in approach images, combined with matching outlines of the body in images before and after the encounter.

The control points, in combination with limb outlines, restrict the shape for slightly more than half the area, but some longitudes remain unobserved. The mean radius of the model is estimated to have been 3.0 ± 0.1 km in

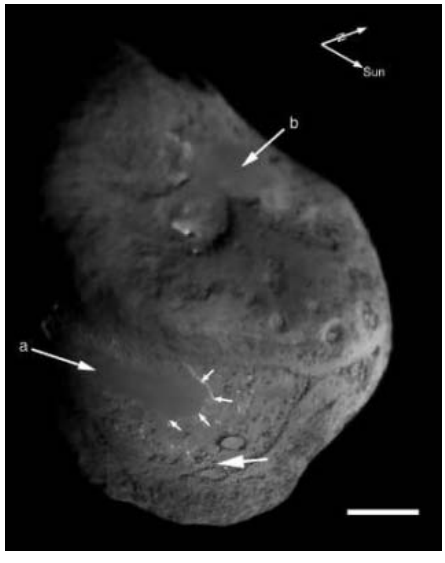

Fig. 1. Composite of ITS images. The Sun is to the right and celestial north is toward the upper right, near the rotational pole. Ecliptic north is another 20° counterclockwise from the north pole. Arrows a and b point to the large, smooth areas. The impact site is indicated by the other large arrow. The small arrows highlight the scarp, bright due to the illumination angle, which shows the smooth area to be elevated above the extremely rough terrain. The scale bar is 1 km, and the two arrows above the nucleus point to the Sun and to the rotational axis of the nucleus. Celestial north is near the rotational pole; ecliptic north is more nearly upward.

[1]University of Maryland, College Park, MD 20742, USA. [2]Belton Space Exploration Initiatives, Tucson, AZ 85716, USA. [3]Delamere Support Services, Boulder, CO 80301, USA. [4]Max-Planck-Institute for Solar System Research, Katlenburg-Lindau, D37191 Germany. [5]Jet Propulsion Laboratory, Pasadena, CA 91109, USA. [6]University of Hawaii, Honolulu, HI 96822, USA. [7]University of Arizona, Tucson, AZ 85721, USA. [8]Brown University, Providence, RI 02412, USA. [9]SAIC, Chantilly, VA 20151, USA. [10]Cornell University, Ithaca, NY 14853, USA. [11]Space Telescope Science Institute, Baltimore, MD 21218, USA. [12]Ball Aerospace and Technology Corporation, Boulder, CO 80301, USA. [13]Sigma Scientific, Greenbelt, MD 20771, USA. [14]Applied Physics Laboratory, Johns Hopkins University, Laurel, MD 20723, USA.

*To whom correspondence should be addressed. E-mail: ma@astro.umd.edu

good agreement with pre-encounter estimates (*5*, *6*); the longest dimension is 7.6 km and the shortest is 4.9 km, which implies much less elongation than pre-encounter estimates (*5*, *6*).

The shape model indicates that the incidence angle of the impactor was 34° from the local horizontal, slightly higher than estimated from the foreshortening of the large features near the impact site if one assumes that they are circular. However, our present shape model is not as well constrained at the impact site by control points as is the rest of the visible area, because it was obscured by the ejecta after impact.

DI high-resolution images cover about 30% of the nucleus at <10 m/pixel. A region about 2 km across, including the impact site, was imaged at slightly better resolution by the impactor targeting sensor (ITS) shortly before impact.

The observed part of the nucleus contains several regions of distinct morphology, which suggests considerable variation of exposed materials, geologic processes, and ages. Two different areas, basically the top and bottom halves of Fig. 1, display several dozen apparently circular features, ranging from 40 to 400 m. The cumulative size-frequency distribution of these features is consistent with impact crater populations. Those features in the bottom part of Fig. 1, near the impact site, appear to be expressed both topographically as circular ridges and as slightly darker material. Those in the top half of the vicinity of the impact site are expressed as depressions, with smooth, unraised rims. The size distribution of these features is different from that of circular depressions on comet Wild 2, the target of the Stardust mission (*7*). The morphology of the Tempel 1 round forms is also distinct from those on Wild 2.

The very bottom of the comet in Fig. 1 appears rough at high emission angles, and it may contain some circular features, but this area cannot be easily interpreted.

Two regions of smooth surface exist (arrows a and b in Fig. 1). One smooth region (arrow a) is bounded to the north by a scarp ~20 m in height. In combination with the appearance of the area to the north, which shows circular features, and the distinctly rougher terrain east and west of the smooth area, the scarp strongly suggests removal by backwasting of a 20-m layer, leaving an exhumed surface containing the circular features. The other smooth area (b) embays two areas of arcuate scarps, possibly bounding degraded circular forms. Both smooth areas are in gravitational lows and area a, at least, is approximately level. The smoothness is reminiscent of the plateau seen on comet Borrelly (*8*), but the surroundings are different.

The smooth surfaces and bounding scarp imply that the nucleus is layered. Banding of albedo, running nearly horizontally in Fig. 1 and at a high angle to the smooth surfaces, suggests either stripping of other layers or exposure of different kinds of layers within the comet.

Overall, the surface of Tempel 1 is remarkably homogeneous in albedo and color. Albedo variations are within 50% of an average of 0.04 (visible wavelength). The brightest small areas are no more than twice as bright as the bulk of the surface. Color ratios between 300 and 1000 nm are uniform to <±2%. No exposures of clean ice or frost have been identified on the basis of albedo or color. It is estimated that Tempel 1 loses some 10^9 kg of material per perihelion passage (*9*). Such a mass, if lost from 10% of the 100 km^2 area of the comet, would lower the surface (density = 1000 kg m^{-3}) by 10 cm per perihelion passage. Alternatively, all of the mass could be supplied by retreat by 50 m of a 1-km-long, 20-m-high scarp. Because there are probably at least several kilometers of such scarps, the observed mass loss could plausibly come from a few meters of retreat of scarps per perihelion passage.

With the infrared (1.05 to 4.8 μm) spectrometer of DI, we obtained three spatial scans of the nucleus that allowed us to map its temperature. We obtained (i) a scan of ~90% of the part of the nucleus visible from DI, ~19 min before impact, with a resolution of ~200 m/pixel, (ii) a scan of 100% of the part of the nucleus visible from DI, ~12 min before impact, with a resolution of ~160 m/pixel, and (iii) a scan of ~50% of the part of the nucleus visible from DI, ~6 min before impact, with a resolution of ~120 m/pixel.

For each scan, we derived the temperature by fitting the data with a model that includes two components: the scattered light from the Sun and a thermal component. For the scattered light, we used a solar spectrum (*10*) reddened by 4% per μm to match the data and normalized between 1.8 μm and 2.2 μm, where we have a good signal-to-noise ratio. The thermal component is a Planck function times the infrared emissivity of the nucleus, which we set to 0.95.

The derived temperature (Fig. 2) varies from 260 ± 6 K to 329 ± 8 K on the sunlit side. The uncertainty is due to an absolute calibration uncertainty of ~20%. The three scans are consistent with each other. The temperature map matches the topography of the nucleus: Shadows are the coolest areas, whereas the hottest areas are close to the subsolar point. This is a good indication that the thermal inertia is low. The maximum temperature of 326 ± 6 K is in excellent agreement with the subsolar point temperature of 325 K for a standard thermal model with no beaming factor (*11*). This agreement is another argument for a low thermal inertia, most probably lower than 100 MKS (MKS = $W/K/m^2/s^{1/2}$), in agreement with our own pre-encounter estimate for Tempel 1 (*12*) and with the inferred low (<15 MKS) thermal inertia on small bodies like Chiron and Chariklo, Asbolus, or main-belt asteroids (*13*–*15*). With our resolution, we do not see areas on the sunlit surface colder than 260 K, well above the temperature expected for sublimation of volatiles on the surface, such as H_2O, CO_2, and/or CO. Therefore, volatiles probably sublime below the surface.

Activity. Precise knowledge of the spin state of the nucleus is the key to linking remotely observed coma phenomena to specific locations on the nucleus. We derived information about the spin of the nucleus from two sources: the fully resolved images and time-series photometry of the unresolved nucleus on approach. The fully resolved

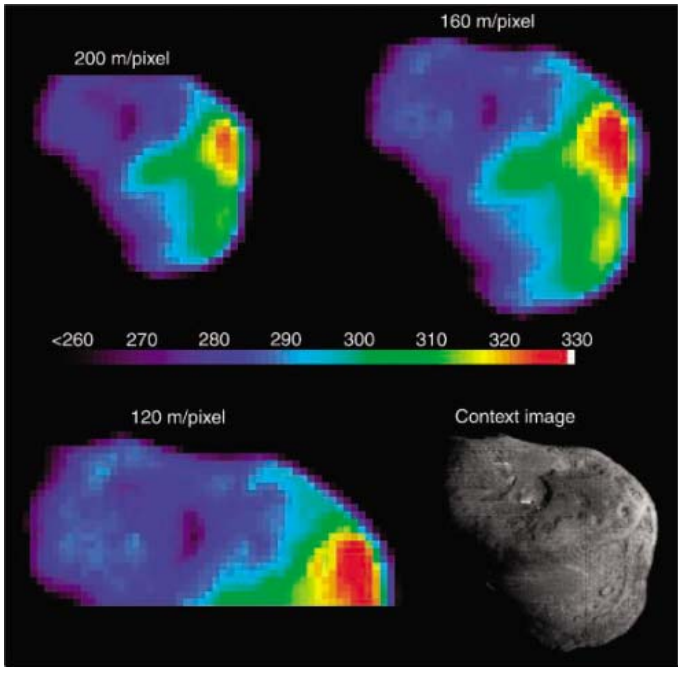

Fig. 2. Temperature maps of the nucleus with different resolutions. The context image is a deconvolved HRI image taken just before impact. The color bar in the middle gives temperatures in kelvins. The last spatial scan, in lower left, was interrupted to begin the sequence of impact observations. The Sun is to the right in all images.

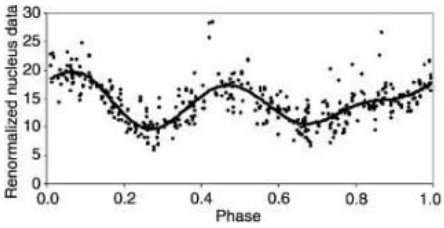

Fig. 3. Renormalized photometric model of the spinning nucleus, based on a four-harmonic least-squares fit to the MRI approach photometry. Zero phase is at the time of impact, JD 2453555.73932. Approach data are phased to $P = 1.701$ days. Most of the scatter comes from variations in the coma signal whose trend has been removed.

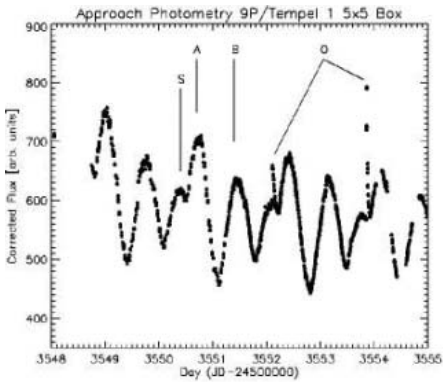

Fig. 4. Normalized rotational light curve immediately preceding encounter. S indicates the shoulder on the increase to peak A. Peak B is much smaller and has no shoulder. O indicates the last two outbursts before impact (at 3555.74 on this scale). Earlier outbursts occur either at this same rotational phase or at the two peaks.

images, using control point geodesy, provide the best estimate of the direction of the spin axis and sense of spin, whereas harmonic analysis of the approach photometry gives the best determination of the spin period.

Photometric coverage of the unresolved cometary nucleus in various color filters began 63.4 days before impact [(I), taken as JD2453555.73932], with samples taken, when possible, about every 4 hours using both the MRI and the high resolution instrument (HRI). At I – 19 days (phase angle 51.3°), a new sequence of images, more densely sampled, was begun for navigational purposes and continued through I – 0.6 days. These two independent databases provide excellent coverage for studies of coma activity, the spin state, and the dependence of nuclear brightness on solar phase angle. An extensive analysis was carried out using MRI data taken through the clear filters and based on 5 by 5 and 15 by 15 pixel arrays centered on the nucleus (*3*).

The resultant rotational variation of the nucleus is shown in Fig. 3, where the fitted curve has a period of 1.701 ± 0.014 days (40.832 ± 0.33 hours) and four harmonics. This should be compared with the pre-encounter prediction of 1.744 ± 0.006 days based on Earth-based observations (*5*). The difference corresponds to a half-cycle or whole-cycle shift between different observing runs.

Observations of the comet before impact detected numerous brief outbursts from the comet. The ambient outgassing results in a coma that is fainter, relative to the nucleus, than the coma of Wild 2 (*1*, *6*, *7*, *16*, *17*), making study of the ambient coma harder but the study of small outbursts easier. Many, but not all, of the outbursts appear to be from one part of the surface (Table 1). Outbursts like these are probably common occurrences for most comets near the Sun. Two obvious outbursts occurred in the week immediately before impact (Fig. 4). Analysis of the rotational phase of the outbursts shows that certainly three and probably four of the outbursts occurred near the start of the "shoulder" feature on the rotational light curve (Fig. 4 and Table 1). This corresponds very roughly to the time of sunrise on the upper surface in Fig. 1, and images taken at the time of the outburst show the ejecta primarily in the northeast quadrant from the nucleus, as expected from the orientation of that face at sunrise. Two outbursts, however, occurred near the two peaks of the light curve, one near each. We therefore see two active areas, one on the well-studied side of the nucleus and the other likely on the unstudied side.

Table 1. Outbursts detected by Deep Impact. Onset occurs at the given Julian day and the corresponding UT date. The height is in arbitrary units and is useful only for estimating a rough amplitude relative to each other and relative to rotational variations of about 250 units from peak A to the subsequent trough (*28*).

Julian day	UT	Height	Rotational phase
2453506.053	May 15 13:16		shoulder?
2453524.888	Jun 3 09:19	300	shoulder
2453536.055	Jun 14 13:19	<100	Peak B
2453543.884	Jun 22 09:13	75	Peak A
2453552.105	Jun 30 14:31	80	shoulder
2453553.857	Jul 2 08:34	240	shoulder

All of the well-observed outbursts are characterized by a very sharp rise (<10 min for the best sampled outburst) (Fig. 5) followed by a slow increase and gradual decay (or dissipation) over roughly an hour, although some signs of the large outbursts can be seen for a considerable portion of a day. We interpret the outburst as being nearly instantaneous (a few minutes or less), followed by some increase in brightness due to decreasing optical depth, with the particles that are dragged out evaporating and/or dispersing into the ambient coma outside the box over which we integrate the brightness on a time scale of a few hours. There is sometimes a residual brightness, no more than about 10% of the peak brightness, which can persist for up to 18 hours. Whether the particles also evaporate is still an open question.

The Cratering Experiment: Morphological Analysis

Impact site and crater. The impactor struck the nucleus near its southern (ecliptic) limb as seen on approach, leading to an oblique impact and the resultant phenomenology. The impact site was determined by analyzing a combination of all images from the impactor and its attitude telemetry (see Fig. 1 and, at higher resolutions, Fig. 6). At about 20 s before impact, a large dust particle hit the impactor, causing the pointing to rapidly slew away. The attitude-control system brought the pointing back more slowly, centering on the impact site again at ~10 s before impact, when another dust particle deflected it again. The last image pointed at the impact site had a scale of 1.2 m/pixel, but the image appears to have a resolution no better than 3 m, which indicates that sandblasting by dust may have degraded the optical quality of the ITS (change of scale during the 100-msec exposure is only about 1% of the actual scale; the degradation does not fit well with smear because of motion). The last image transmitted to Earth was taken about 4 s before impact, but at this time the camera was pointed more than a field of view away from the impact site.

The time of impact was not directly measured but can be inferred. The earliest possible time of impact is constrained by an analysis of the increase of scale in the ITS images and is roughly 05:44:35.4 UTC. The latest possible time of impact is constrained by the appearance of the flash in the high-speed imaging sequence with MRI (Fig. 7), which requires that impact occurred before about 05:44:36.2. Both times are as seen at the spacecraft. Allowing for the light travel time to Earth of 7:26.1, the window

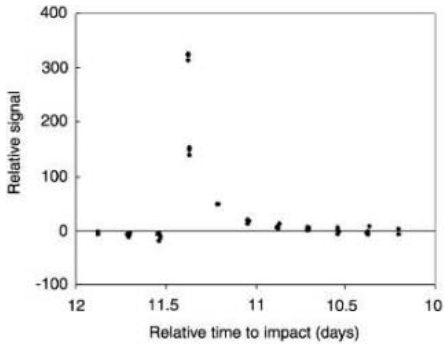

Fig. 5. Brightness profile of outbursts. Data on the two strongest outbursts are combined by applying scaling factors and time shifts. The abrupt rise occurs within 18 min. The brightness falls rapidly at first, followed by a more gradual falloff that clears in ~18 hours.

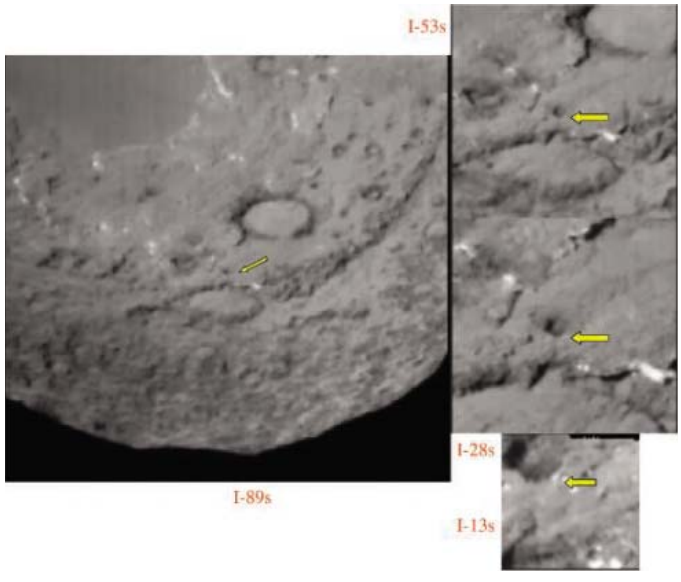

Fig. 6. Impact site at successively higher resolutions. The images were all taken by the impactor at the indicated times before impact. The impact site is indicated by the yellow arrow in each frame.

for the impact time as observed at Earth is 05:52:01.5 to 05:52:02.3.

The final crater has not yet been directly measured because of a large amount of fine dust in the ejecta obscuring our view.

Flash, plume, and early ejecta. The impact was oblique, 20° to 35° from horizontal, and the effects of obliquity appear in several ways. The initial flash (Fig. 7, panels 4 and 5) lasted <200 ms and may have been visible at the entry hole, or it may have been transmitted through the undisturbed layer under which the impactor tunneled. It is probably associated with vaporization of the impactor and part of the comet. The second flash (Fig. 7, panels 6 to 8, and Fig. 8, panel 2) was displaced downrange and saturated the detectors of both cameras for one HRI frame and two MRI frames covering 120 ms leading to the horizontal ''bleeding'' of charge (Fig. 7, panels 7 and 8, and Fig. 8, panel 2). This may be associated with the first eruption of material at the surface. A plume of hot material (see subsequent discussion of spectra) moved outward (Fig. 7, panels 7 to 10) at a projected velocity of 5 km/s. Depending on the angle with respect to the surface, the true velocity is likely to have been 7 to 10 km/s. This is consistent with laboratory experiments (*18*), which show downrange plumes moving at a speed comparable to that of the impactor. The plume expanded at ~3 km/s, consistent with gas-driven expansion in those laboratory experiments. The temperatures deduced below from spectroscopy suggest that this plume was self-luminous.

The mechanically excavated cone (Fig. 7, panels 9 to 12, and Fig. 8, panels 3 to 8) arises as the second flash drops below saturation, is displaced farther downrange, and consists of much more slowly moving material. Even as the ejecta expand rapidly above the surface, they remain optically thick, as is clear from the shadow cast on the nucleus by the ejecta. The shadow is highlighted by the red arrows in panels 3 and 7 of Fig. 8 (also visible in panels 4 to 6), showing that even many seconds after the start the ejecta are still optically thick. The optical depth producing the initial shadow is $\gg 1$. This is likely because the ejecta are primarily in the form of very small grains, which maximize the cross section per unit mass. The shadow is >300 m across at its base, which is much wider than the expected size of the crater at this early stage; this is undoubtedly due to a spread in the angle of ejection as seen in laboratory experiments.

The peak radiance from the ejecta occurred 3 to 4 s after the impact, and the brightness peak moves downrange at roughly 100 m/s, reflecting the excess of ejecta in the downrange direction. Several rays become obvious (Fig. 8, panels 4 to 8), and they persist until long after the encounter and are initiated at the very beginning of the excavation phase. There are no prominent rays toward the top of the figures. This reflects both the perspective from the spacecraft and an uprange zone of avoidance, with relatively little ejecta, indicated by the yellow arrow in panel 8 of Fig. 8, which is characteristic of oblique impacts (*19*). There is also a highly foreshortened uprange plume visible in Fig. 7 in the first second, similar to plumes seen in laboratory experiments with hypervelocity impact into porous material (*20*). In the experiments, this usually reflects flow back up the entry path. As late as 13 min after impact, the optical depth in ejecta near the limb of the nucleus has dropped only to the range of 2 to 3.

Later ejecta and fallback. The ejecta cone remained attached to the surface throughout the encounter and even through the look-back imaging (Fig. 9). The observation that the ejecta cone remained attached to the surface indicates that formation of the crater was controlled by gravity rather than by strength (*20*, *21*). The volume of ejecta then argues against deep burial of the impactor or compression control of the crater formation (*22*). The geometry in the look-back images is such that the curtain or cone can be no higher than 500 ± 250 m above the surface. With worst-case assumptions for all parameters (height of 750 m at 1 hour after impact, sandlike surface density of 1500 kg m^{-3}), we find an upper limit of 65 Pa (an extremely weak, powderlike substance) for the shear strength of the moderately shocked region around the rim of the final crater.

These look-back images also allowed us to observe the lateral expansion of the conical ejecta curtain for nearly half an hour, as the individual particles that make up the curtain follow ballistic paths in Tempel 1's gravitational field. The curtain itself marks the locus of the solid ejecta in flight at any given time: Its bottom region is composed of particles near the end of their flight and about to land on the surface; its middle region is composed of particles reaching their maximum height above the surface and traveling radially from the center of the cone (and thus parallel to the surface); and the upper portions are composed of particles that have not yet reached their apex, and the uppermost ones are on escape trajectories (*23*). If we assume (i) that the middle and late stages of excavation are not affected by the obliquity of the impact (the cone has become more nearly axially symmetric) as observed in experiments, (ii) that the laboratory-derived scaling relation-

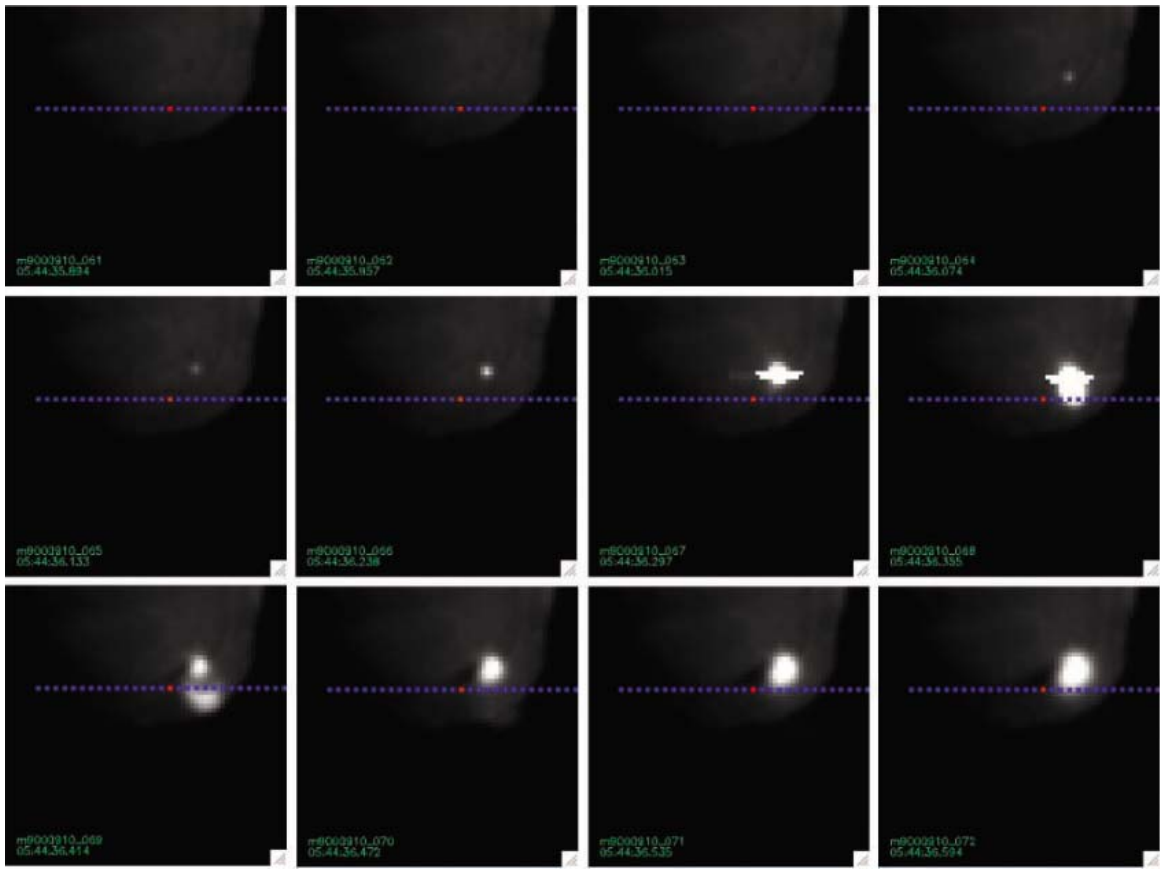

Fig. 7. Images of impact taken with MRI. The blue dotted line is the position of the spectrograph slit. The red point on the blue dotted line is the position along the slit for the spectrum shown in Fig. 11. Panels 1 (top left) through 12 (bottom right) are labeled with time of end of 50-ms exposure, and all images were taken during the exposure of the spectrum.

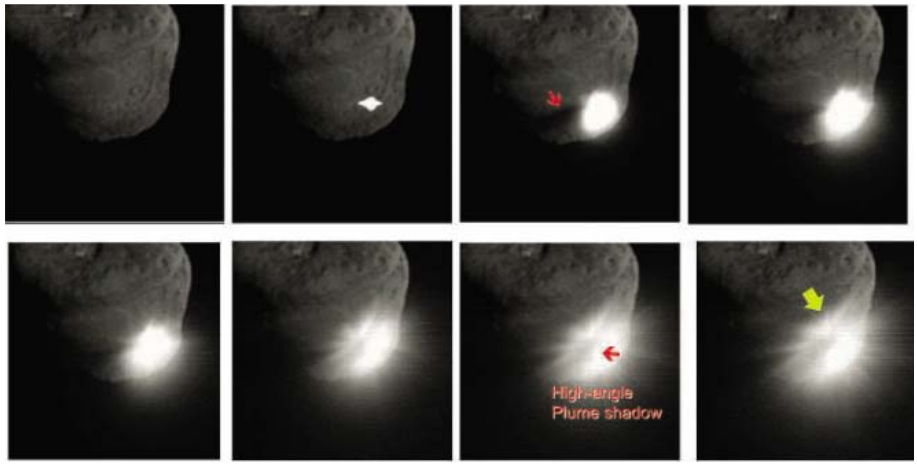

Fig. 8. HRI sequence showing the development of the ejecta. Red arrows highlight shadows due to opacity of the ejecta, whereas the yellow arrow indicates the zone of avoidance in the uprange direction. HRI frames 9000910_005 through 9000910_012 are 100-ms exposures spaced by 0.84 s, ending at 05:44:35.47 through 05:44:41.32.

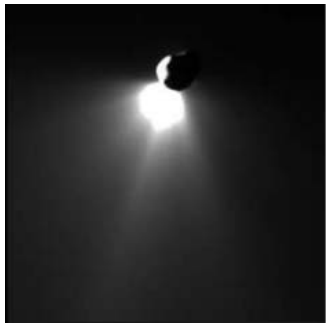

Fig. 9. Look-back image of comet taken 45 min after impact. The ejecta plume is still connected to the nucleus (the impact site is close to the limb on the far side). The image has been stretched to show the rays at large distances, and this causes the limb of the nucleus and the innermost ejecta cone to saturate.

ships for gravity-dominated cratering (*24*) are valid for our experiment, and (iii) that ejecta flow properties (*25*) extrapolate reasonably well to this particular impact, then the expansion of the base of the conical ejecta can be used to estimate the strength of gravity, as shown in Fig. 10.

Although the shape of the nucleus is far from spherical, this calculation gives a good first approximation to the local gravity at the impact site, 50 + 34/–25 mgal. We then use the preliminary shape model described above to find the uniform density, and thus mass, required to produce the local gravity field, deriving a total mass for the nucleus of 7.2×10^{13} ($+4.8/-3.8 \times 10^{13}$) kg and a bulk density of 620 + 470/–330 kg m^{-3}. In principle, the scaling laws can also be used to predict the size of the crater, but the result depends on assuming a value for the density of the surface layers, which may be different from the bulk density.

The Cratering Experiment: Spectral Analysis

A small subset of the spectra has been carefully calibrated. At the time of impact, the slit was positioned downrange of the impact site (Fig. 7), and spatially resolved spectra were taken as rapidly as possible while material flowed past the slit. The position sampled for the spectrum in Fig. 11 (red dot in Fig. 7) is roughly 85 m

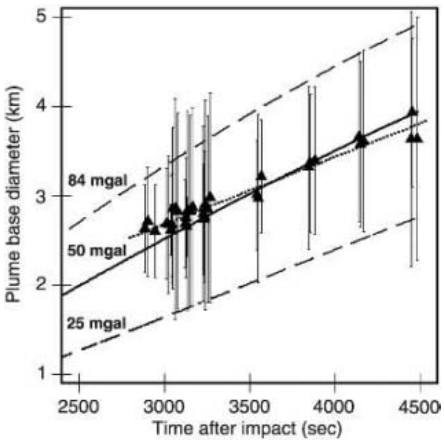

Fig. 10. Expansion of ejecta cone. Measurements of the width of the base of the ejecta cone in look-back images, with a correction of 250 m for the inability to see the actual base of the cone. The curves are numerical calculations (*20*) for various gravitational fields on a spherical nucleus.

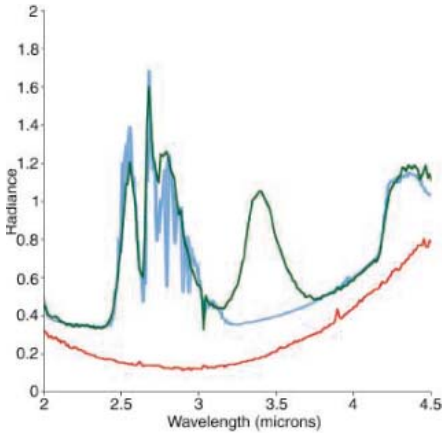

Fig. 11. Spectrum of vapor plume (green) at ~1 + 0.6 s. The blue line is the model described in the text. The model does not include species that contribute to the organic feature at 3.4 μm. The red line is the nuclear spectrum taken 0.7 s earlier.

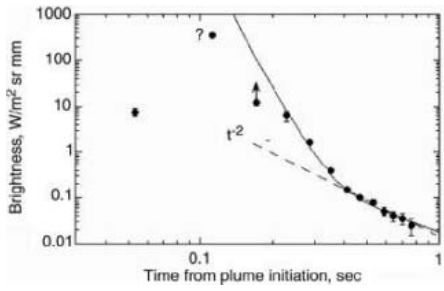

Fig. 12. Brightness of the peak pixel in the plume versus time in MRI frames mv9000910066-78. The point marked ? is a guess at the value for the saturated pixel. The dashed curve is what is expected for uniformly expanding particles reflecting sunlight. The solid curve is the model described in the text. The origin of time is based on extrapolating the motion of the plume back to its origin at constant velocity.

on a side at the comet, centered 0.46 km downrange from the impact site and 0.34 km to the side of the downrange direction. The side of the fast, hot vapor plume was present in the slit only for the last 200 msec of the exposure. The excavated ejecta from the event may be in the field of view for the last 50 msec. The immediately previous spectrum at this pixel, shown in red in Fig. 7, can be adequately described by a combination of reflected light, slightly reddened, and thermal emission at 285 K from the nucleus alone. Any foreground coma is minor compared with the dust and gas in subsequent spectra.

Emission features in the spectrum include those of H_2O, HCN, CO_2, and what is normally called the ''organic feature,'' which corresponds to the C-H stretching-mode vibration in several commonly seen molecules, including H_2CO (formaldehyde) and CH_3OH (methanol). Our spectral resolution is, in general, not sufficient to separate the individual species in the organic feature. Superimposed on the observed spectrum is a model spectrum that includes the observed nuclear spectrum shown in red, hot (850 K) dust, and the three identified species. Organics are not included in the model. The model assumes a rotational excitation temperature of 1400 K, but both the H_2O and the CO_2 can be adequately fit with a wide range of temperatures, roughly 1000 K to 2000 K. A calculation of fluorescent emission shows that the emissions are optically thick, requiring an extensive model to separate temperature broadening from optical depth and to determine relative abundances.

In the succeeding spectrum, for which the plume was not present and only ejecta were moving across the slit, the reflected continuum decreased by a factor of 2 but then, over the next 15 s, increased again by a similar factor as more of the excavated ejecta move into the beam. The color temperature of the thermal emission from the dust is at least a factor of 2 cooler than in Fig. 11. Ejecta fill the slit at the start of the integration, having left the nucleus roughly a half second earlier. By the end of the integration, the slit is sampling material that could have left the nucleus as much as 1.3 s earlier traveling at lower velocity (these correspond to projected velocities on the order of 1 km/s). The succeeding spectrum shows that H_2O and CO_2 have decreased in intensity by a factor of 20 and also have become rotationally much cooler, whereas the level of the organic feature has decreased only by a factor of 6. The very strong organic feature (compared with Earth-based measurements of comets) suggests that we may be vaporizing organics that would not normally be vaporized in comets.

The observed temperature of the continuum (850 K) suggests that the center of the plume is even hotter and that the light we see in the MRI images is thermal emission. The peak brightness in the plume, i.e., the brightest part of the arch near the bottom of panels 9 and 10 in Fig. 7, can be used to constrain the nature of the ejecta. The initial decay in brightness is far too steep for simple expansion at constant velocity. Only after 0.42 s, i.e., beyond the end of the sequence in Fig. 10, does the brightness decay as t^{-2}, as would be expected for expansion at constant velocity of particles reflecting sunlight. The observed decline shown in Fig. 12 is consistent with blackbody radiation from a cloud of cooling particles. We modeled the plume as a 4000-kg cloud of liquid silicate droplets of 150 μm diameter, albedo 0.1, density 2.5 g cm^{-3}, expanding at 1.7 km/s, and with initial temperature 3500 K. The observed temperature of 850 K at the lateral boundary of the plume is consistent with this model (solid line in Fig. 12), because the temperature at the peak drops rapidly to 1000 K at the break in the solid curve near 0.3 s after the start of the plume. The model predicts that the hot plume would be optically thin after 0.03 s.

To measure compositional differences between the interior and the surface of the comet, we compare two spectra (Fig. 13) taken just off the limb of the nucleus, one 10 min before impact (ambient outgassing) and the other 4 min after it (excavated subsurface material). For both spectra, the slit was positioned roughly one nuclear radius, 3 km, from the southerly limb of the nucleus, with the slit oriented perpendicular to the radial direction and with width subtending 150 m and 57 m, respectively. The extracted spectra correspond to the median of 15 pixels along the slit on both sides of the antisaturation filter. These pixels correspond to positions roughly 1 km on both sides of the center of the slit for the preimpact spectrum and 400 m on both sides of the center of the slit for the postimpact spectrum. A continuum due to dust has been removed from the spectra in Fig. 13 to show the gaseous features. The dust spectrum consists of a slightly reddened solar-reflection spectrum, dominant at the shorter wavelengths, and postimpact thermal emission at 380 K, dominant at the longer wavelengths. Because this relatively late stage of excavation should be cool, the temperature excess above that of an isothermal black body at this distance (230 K) is likely due at least in part to the superheat required for particles that are small compared with the wavelength of peak thermal emission (*26*). The superheat would be larger than seen in other comets and suggests either the complete predominance of small particles compared with a component of large (cooler) particles in the ambient comae of other comets, or some residual heat from excavation, or a combination of the two.

The individual spectra of the gas (Fig. 13) had low signal-to-noise ratio compared with the

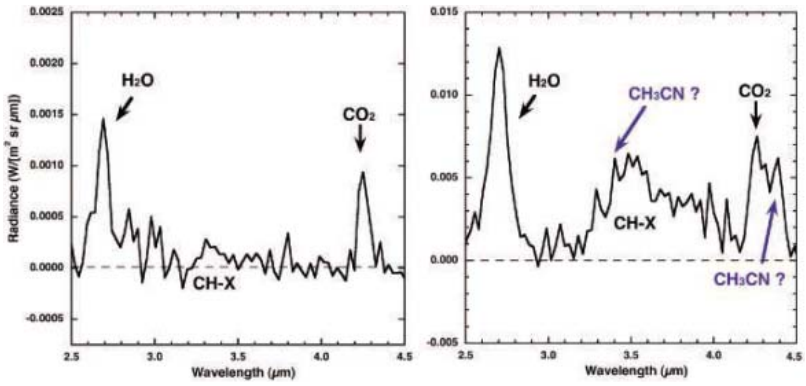

Fig. 13. Preimpact (–10 min, left) and postimpact (+4 min, right) spectra 3 km beyond the limb of the nucleus. The intensity scale differs by a factor of 6 between the two spectra. The abundance of organics relative to water increased substantially in the postimpact measurement.

signal of the nucleus, and the accuracy is limited primarily by the subtraction of the dark signal and the dust. The strong emission features are the same as those seen in the spectrum of the vapor plume, although relative abundances are different and the temperatures of the gases are much lower than those of the gases in Fig. 11. Even these emission features are optically thick in individual lines, so that absolute abundances cannot be obtained directly.

The most dramatic difference between the ambient outgassing and the excavated material was the large increase in organics. The abundances of HCN and CO_2 relative to H_2O also increased, but not as dramatically. Because the projected distance from the impact site to the field of view of the spectrometer was on the order of 4 km, material moving as slowly as 25 m/s (still well above escape speed) would have been excavated at 2 to 3 min into the excavation process and thus is material from far below the surface.

The feature at 4.40 μm is attributed to the ν_2 (CN stretch) band of methyl cyanide (CH_3CN). This species should also have its ν_1 (CH stretch) band at 3.38 μm, and this could correspond to the peak at that wavelength in the organic feature, a peak that is much weaker (and coincident with a methanol peak) in the preimpact spectrum. Other species with bands at 4.40 μm include HC_3N and HNCO. These are both ruled out by the absence of bands that should appear at other wavelengths. Nevertheless, we consider this identification very tentative because it appears to imply an excessively high abundance, although this may be due to optical depth effects. Ulich and Conklin (*27*) had identified methyl cyanide in a natural outburst of comet Kohoutek, but this result has been considered spurious. It is possible that the high abundance is incorrect as a result of errors in the assumed excitation of the molecule.

Summary and Conclusions

Comet Tempel 1 was thought to be a typical member of Jupiter's family of comets. The fact that the shapes and topographies of three comets in Jupiter's family (Borrelly, Wild 2, and Tempel 1) are so different from one another raises the question of whether any comet is typical when looked at closely. Both Borrelly and Tempel 1 have had long lifetimes in the inner solar system, whereas Wild 2 has not, but the differences between Borrelly and Tempel 1 are just as great as the differences between either of them and Wild 2. Tempel 1 is the first comet to show evidence for many classical impact craters. Tempel 1 also exhibits distinct layers with different topographic characteristics, a feature that may be common to all three of these comets. Tempel 1 exhibited frequent small outbursts, many of which were associated with an area near local sunrise. Because the nucleus also has little thermal inertia, this activity must be driven by material that is near the surface. We suspect that such activity may be common on other comets, but there are not sufficient data for any other comets to confirm this presumption. Although the surface temperatures, colors, albedos, and spectra indicate no ice on the surface, the rapid appearance of large amounts of volatiles in the earliest ejecta implies that ices are near the surface

The impact excavated a large volume of very fine (microscopic) particles, too many to have been pulverized in the impact itself; thus, they were preexisting either as very fine particles or as weak aggregates of such particles. This fine material must be tens of meters deep. From studying the ejecta at very late stages, the overall strength of the excavated material was determined to be <65 Pa, and the bulk density of the nucleus is estimated at roughly 0.6 g cm^{-3}. Initial ejecta were considerably hotter than 1000 K, but later stage ejecta were much cooler. The fastest material was moving at ~5 km/s, projected in the plane of the sky as seen from the spacecraft. The amount of organics relative to water increased considerably at the beginning of the outburst and, as the event progressed, the reduction in organics was much less than the reduction in H_2O and CO_2. The variation of CO_2 was similar but smaller. We have identified hydrogen cyanide (HCN) in the plume and suggest that methyl cyanide (acetonitrile, CH_3CN) could be present in the ejecta.

References and Notes

1. M. F. A'Hearn, M. J. S. Belton, A. Delamere, W. H. Blume, *Space Sci. Rev.* **117**, 1 (2005).
2. W. H. Blume, *Space Sci. Rev.* **117**, 23 (2005).
3. Information on instruments, data processing, and analysis is available on *Science* Online.
4. K. J. Meech *et al.*, *Science* **310**, 265 (2005).
5. M. J. S. Belton *et al.*, *Space Sci. Rev.* **117**, 137 (2005).
6. C. M. Lisse *et al.*, *Astrophys. J.* **625**, L139 (2005).
7. D. E. Brownlee *et al.*, *Science* **304**, 1764 (2004).
8. D. T. Britt *et al.*, *Icarus* **167**, 45 (2004).
9. C. Lisse, *Earth Moon Planets* **90**, 497 (2002).
10. A solar spectrum synthesized from various sources is available at the MODTRAN Web site (http://rredc.nrel.gov/solar/spectra/am0/modtran.html).
11. L. A. Lebofsky, J. R. Spencer, in *Asteroids II*, R. Binzel, Ed. (Univ. of Arizona Press, Tucson, AZ, 1989), pp. 128–147.
12. C. M. Lisse *et al.*, *Astrophys. J.* **625**, L139 (2005).
13. O. Groussin, P. Lamy, L. Jorda, *Astron. Astrophys.* **413**, 1163 (2004).
14. Y. R. Fernández, D. C. Jewitt, S. S. Sheppard, *Astron. J.* **123**, 1050 (2002).
15. J. R. Spencer, L. A. Lebofsky, M. V. Sykes, *Icarus* **78**, 337 (1989).
16. D. E. Brownlee *et al.*, *Science* **304**, 1764 (2004).
17. Z. Sekanina, D. E. Brownlee, T. E. Economou, A. J. Tuzzolino, S. F. Green, *Science* **304**, 1769 (2004).
18. P. H. Schultz, *J. Geophys. Res.* **101**, 21,117 (1996).
19. J. L. B. Anderson, P. H. Schultz, J. T. Heineck, *Meteorit. Planet. Sci.* **39**, 303 (2003).
20. P. H. Schultz, C. M. Ernst, J. B. Anderson, *Space Sci. Rev.* **117**, 207 (2005).
21. J. E. Richardson, H. J. Melosh, A. Artemeiva, E. Pierazzo, *Space Sci. Rev.* **117**, 241 (2005).
22. K. R. Housen, K. A. Holsapple, M. E. Voss, *Nature* **402**, 155 (1999).
23. H. J. Melosh, *Impact Cratering: A Geologic Process* (Oxford Univ. Press, New York, 1989).
24. R. M. Schmidt, K. R. Housen, *Int. J. Impact Eng.* **5**, 543 (1987).
25. K. R. Housen, R. M. Schmidt, K. A. Holsapple, *J. Geophys. Res.* **88**, 2485 (1983).
26. L. Kolokolova, M. S. Hanner, A.-Ch. Levasseur-Regourd, B. Å. S. Gustafson, in *Comets II*, M. C. Festou, H. U. Keller, H. A. Weaver, Eds. (Univ. of Arizona Press, Tucson, AZ, 2004), pp. 577–604.
27. B. L. Ulich, E. K. Conklin, *Nature* **248**, 121 (1974).
28. The outburst of June 14 was first reported on the DI Collaborators' Network by L.-M. Lara, based on observations at Calar Alto. It was then found easily in the data from the spacecraft. The later ones were found in near-real time in the spacecraft data. The outburst of June 22 was observed simultaneously and serendipitously with the Hubble Space Telescope. The earlier outbursts were found during the rotational analysis.
29. This work was funded by NASA through its Discovery Program, with a contract to the University of Maryland and a task order to the Jet Propulsion Laboratory. In addition to the referees, M. Mumma and D. Bockelée-Morvan provided helpful comments.

Supporting Online Material
www.sciencemag.org/cgi/content/full/1118923/DC1
Materials and Methods
Fig. S1
Table S1
References

16 August 2005; accepted 1 September 2005
Published online 8 September 2005;
10.1126/science.1118923
Include this information when citing this paper.

Deep Impact: Observations from a Worldwide Earth-Based Campaign

K. J. Meech,[1]* N. Ageorges,[2] M. F. A'Hearn,[3] C. Arpigny,[4] A. Ates,[5] J. Aycock,[6] S. Bagnulo,[2] J. Bailey,[7] R. Barber,[8] L. Barrera,[9] R. Barrena,[10] J. M. Bauer,[11] M. J. S. Belton,[12] F. Bensch,[13] B. Bhattacharya,[14] N. Biver,[15] G. Blake,[14] D. Bockelée-Morvan,[15] H. Boehnhardt,[16] B. P. Bonev,[17] T. Bonev,[18] M. W. Buie,[19] M. G. Burton,[20] H. M. Butner,[21] R. Cabanac,[22] R. Campbell,[6] H. Campins,[23] M. T. Capria,[24] T. Carroll,[21] F. Chaffee,[6] S. B. Charnley,[25] R. Cleis,[26] A. Coates,[27] A. Cochran,[28] P. Colom,[15] A. Conrad,[6] I. M. Coulson,[21] J. Crovisier,[15] J. deBuizer,[29] R. Dekany,[14] J. de Léon,[10] N. Dello Russo,[30] A. Delsanti,[1] M. DiSanti,[31] J. Drummond,[26] L. Dundon,[1] P. B. Etzel,[32] T. L. Farnham,[3] P. Feldman,[33] Y. R. Fernández,[23] M. D. Filipovic,[34] S. Fisher,[35] A. Fitzsimmons,[36] D. Fong,[37] R. Fugate,[26] H. Fujiwara,[38] T. Fujiyoshi,[39] R. Furusho,[40] T. Fuse,[39] E. Gibb,[41] O. Groussin,[3] S. Gulkis,[11] M. Gurwell,[37] E. Hadamcik,[42] O. Hainaut,[2] D. Harker,[43] D. Harrington,[1] M. Harwit,[44] S. Hasegawa,[45] C. W. Hergenrother,[46] P. Hirst,[21] K. Hodapp,[1] M. Honda,[45] E. S. Howell,[47] D. Hutsemékers,[4] D. Iono,[37] W.-H. Ip,[48] W. Jackson,[49] E. Jehin,[2] Z. J. Jiang,[50] G. H. Jones,[16] P. A. Jones,[51] T. Kadono,[52] U. W. Kamath,[53] H. U. Käufl,[2] T. Kasuga,[54] H. Kawakita,[55] M. S. Kelley,[56] F. Kerber,[2] M. Kidger,[10] D. Kinoshita,[48] M. Knight,[3] L. Lara,[57] S. M. Larson,[46] S. Lederer,[58] C.-F. Lee,[37] A. C. Levasseur-Regourd,[42] J. Y. Li,[3] Q.-S. Li,[50] J. Licandro,[10,59] Z.-Y. Lin,[48] C. M. Lisse,[30] G. LoCurto,[2] A. J. Lovell,[60] S. C. Lowry,[36] J. Lyke,[6] D. Lynch,[61] J. Ma,[50] K. Magee-Sauer,[62] G. Maheswar,[53] J. Manfroid,[4] O. Marco,[2] P. Martin,[22] G. Melnick,[37] S. Miller,[8] T. Miyata,[38] G. H. Moriarty-Schieven,[21] N. Moskovitz,[1] B. E. A. Mueller,[63] M. J. Mumma,[31] S. Muneer,[53] D. A. Neufeld,[33] T. Ootsubo,[64] D. Osip,[65] S. K. Pandea,[53] E. Pantin,[66] R. Paterno-Mahler,[5] B. Patten,[37] B. E. Penprase,[5] A. Peck,[37] G. Petitas,[37] N. Pinilla-Alonso,[67] J. Pittichova,[1] E. Pompei,[2] T. P. Prabhu,[53] C. Qi,[37] R. Rao,[37] H. Rauer,[68] H. Reitsema,[69] S. D. Rodgers,[25] P. Rodriguez,[70] R. Ruane,[26] G. Ruch,[56] W. Rujopakarn,[71] D. K. Sahu,[53] S. Sako,[38] I. Sakon,[38] N. Samarasinha,[63] J. M. Sarkissian,[51] I. Saviane,[2] M. Schirmer,[59] P. Schultz,[72] R. Schulz,[73] P. Seitzer,[71] T. Sekiguchi,[54] F. Selman,[2] M. Serra-Ricart,[10] R. Sharp,[74] R. L. Snell,[75] C. Snodgrass,[36] T. Stallard,[8] G. Stecklein,[5] C. Sterken,[76] J. A. Stüwe,[77] S. Sugita,[38] M. Sumner,[14] N. Suntzeff,[63] R. Swaters,[3] S. Takakuwa,[37] N. Takato,[39] J. Thomas-Osip,[65] E. Thompson,[26] A. T. Tokunaga,[1] G. P. Tozzi,[78] H. Tran,[6] M. Troy,[11] C. Trujillo,[29] J. Van Cleve,[69] R. Vasundhara,[53] R. Vazquez,[79] F. Vilas,[80] G. Villanueva,[16] K. von Braun,[81] P. Vora,[82] R. J. Wainscoat,[1] K. Walsh,[3] J. Watanabe,[54] H. A. Weaver,[33] W. Weaver,[26] M. Weiler,[68] P. R. Weissman,[11] W. F. Welsh,[32] D. Wilner,[37] S. Wolk,[37] M. Womack,[83] D. Wooden,[25] L. M. Woodney,[58] C. Woodward,[56] Z.-Y. Wu,[50] J.-H. Wu,[50] T. Yamashita,[39] B. Yang,[1] Y.-B. Yang,[50] S. Yokogawa,[37] A. C. Zook,[5] A. Zauderer,[3] X. Zhao,[50] X. Zhou,[50] J.-M. Zucconi[84]

On 4 July 2005, many observatories around the world and in space observed the collision of Deep Impact with comet 9P/Tempel 1 or its aftermath. This was an unprecedented coordinated observational campaign. These data show that (i) there was new material after impact that was compositionally different from that seen before impact; (ii) the ratio of dust mass to gas mass in the ejecta was much larger than before impact; (iii) the new activity did not last more than a few days, and by 9 July the comet's behavior was indistinguishable from its pre-impact behavior; and (iv) there were interesting transient phenomena that may be correlated with cratering physics.

The Deep Impact mission was designed so that much of the mission-critical science would be done from Earth-based telescopes. These facilities would observe the comet before, during, and after impact to follow the evolution of the comet in wavelength regimes and time scales inaccessible to the spacecraft. Observations began in 1997 to characterize the nucleus of comet 9P/Tempel 1 for mission planning and to establish a baseline of normal behavior against which impact-induced changes could be assessed (*1*, *2*). From 1997 through 2004, observations on 229 nights were obtained from 14 telescopes at nine observatories. In 2005, since the comet came out of solar conjunction, the worldwide collaboration has involved more than 550 whole or partial nights of observation using 73 Earth-based telescopes at 35 observatories (Fig. 1), plus many (Earth-orbital and Sun-orbital) space-based facilities.

Here we give an overview of the scientific conclusions and collective observations from the Earth-based campaign (*3*). As seen from Earth, the Deep Impact event did not create a new period of sustained cometary activity, and in many ways the artificial impact looked very much like a natural outburst. There were some observable changes after impact in the chemistry of the observed dust and gas as well as in the physical properties of the dust, which may suggest that the material beneath the surface was different in composition from the surface materials.

Ejecta cloud. The ejecta cloud was first resolved ~20 min after impact by Earth-orbiting telescopes at visible and ultraviolet wavelengths. Later, ground-based telescopes worldwide imaged the southwesterly-expanding cloud of dust and gas in the visible and infrared (IR) wavelength regime (λ = 0.3 to 13 μm). Generally, the visible and near-IR wavelengths (0.3 to 2.5 μm) achieved the best spatial resolution and sensitivity; that is, most observations were sampling the reflected sunlight from dust in the cloud, with some contribution from the gas in emission bands (<0.6 μm).

About 1 hour after impact, the ejecta was semicircular and extended across position angles 145° to 325°. The ejecta cloud had a nonuniform light distribution. During the first 20 hours after impact, the time series of images showed the leading edge of the dust cloud expanding outward at a projected speed of ~200 ± 20 m/s (although varying with azimuth). The southward orientation of the ejecta indicates that the impact occurred below the orbital plane of the comet.

From 6 July 2005 (all dates are UT) onward, the expanding dust cloud increasingly changed shape because of the push of solar radiation pressure, forcing the particles into the tail (i.e., antisolar) direction at a position angle of 110°.

Roche Applied Science

Genome Sequencer 20 System

First to the Finish

Revolutionize your research with the newest innovation in rapid whole genome sequencing and assembly — the new **Genome Sequencer 20** from Roche Applied Science. Perform genomic analyses not currently possible due to the cost and time constraints of current methods.

- **Generate data fast**
  Sequence at least 20 million bases in one 4.5 hour run.
- **Spend less per base**
  Reduce cost per raw base with rapid, efficient amplification and sequencing through picoliter format with massive parallelization.
- **Simplify sample preparation**
  Eliminate cloning and colony picking with single-tube library preparation per genome.
- **Expand your versatility**
  Perform a wide variety of projects with *de novo* assembly and mapping software.

Be first to the finish! Explore the power of the newest revolution in sequencing today — visit ***www.roche-applied-science.com/sis/sequencing/genome/*** or contact your local sales representative.

454 LIFE SCIENCES

Roche Diagnostics

Roche Diagnostics GmbH
Roche Applied Science
68298 Mannheim
Germany

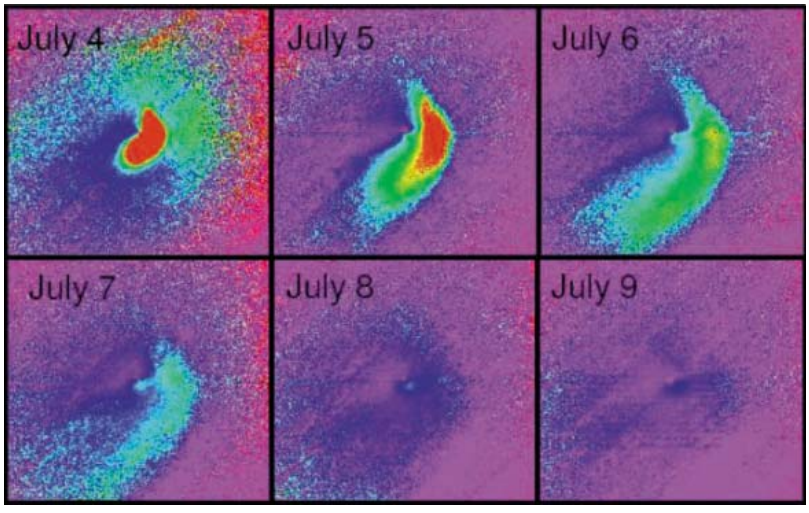

Fig. 2. Sequence of processed post-impact *R* band images of the dust coma of 9P/Tempel 1 acquired from the Nordic Optical Telescope. North is up and east is left. Dates are UT; the first image was taken ~16 hours after impact, and succeeding images were taken around the same time of day on the following nights. The width of each panel is ~120,000 km at the comet. Each image has been divided by a pre-impact 3 July image to accentuate structure in the coma. The evolution of the ejecta cloud is clearly seen.

features are interpreted as a fan coma emanating from localized sources on the nucleus, with the observer point of view being outside the emission cone (*4*, *5*). Neither the number of jets and fans nor their orientations changed during the impact period. In particular, no new long-lived jet or fan has been identified as being from the newly excavated crater.

Fluctuations that were observed in the intensity of some coma structures are possibly related to the impact event itself but could also be due to natural variations in activity. A southwesterly jetlike feature seen one-half rotation period after impact was observed to be brighter than it had been before impact. This could have been caused by gas production from the ejecta dust grains themselves. By just one full rotation period after impact (41 hours), the coma morphology had returned to its pre-impact state, which suggests that the impact site was by this time beginning to cease its activity.

Gas production. The gas species commonly monitored at visible wavelengths in cometary comae—CN, C_2, C_3, NH_2, and CH—were observed in 9P/Tempel 1 before and after impact. During the first 2 days after impact, observations showed the intensity of the species' emission bands increasing by a factor of ~1.5 to 5. An example of the increase in CN as seen through spectroscopy is shown in Fig. 3. Photometry was also used by some groups (*6*). The abundance ratios among the common species stayed at pre-impact levels (*5*). In particular, the C_2-to-CN abundance ratio of ~0.8 classifies 9P/Tempel 1 as a "typical" comet (*7*), as it was before impact. Gas production was back to its pre-impact level by 9 July.

In the near-IR, species not directly detectable before impact—H_2O, C_2H_6, CH_3OH, C_2H_2, and HCN—appeared after impact (*8*). The abundance ratios among these species were consistent with those of typical Oort cloud comets (*8*), although 9P/Tempel 1 is a Jupiter-family comet. There have been relatively few studies of these species among members of the Jupiter family.

Measurements of the CN (0-0) band in the visible spectra revealed isotopic abundances of carbon and nitrogen: The $^{12}C/^{13}C$ ratio was close to the solar value (which is 89), and the $^{14}N/^{15}N$ ratio was half that of Earth's value (which is 272). Hence, comet 9P/Tempel 1 shows the same low nitrogen isotopic ratio that was recently detected in other Jupiter-family comets (*9*).

In addition to near-IR detections of water, other groups monitored the submillimeter transitions of H_2O and the near-ultraviolet transitions of OH. For example, spacecraft observing the 557-GHz transition of water reported a 20% increase in the hours after impact. However, the natural variations in water production that were seen before impact could account for this. On the other hand, there was also a factor of 3 increase in OH production. The reconciliation of these data awaits further analysis.

Several species were monitored from ground-based radio telescopes. HCN at 88.6 and 265.9 GHz and CH_3OH at 145 GHz were detected for only a few days after impact; the production rates later returned to or fell below pre-impact levels. The abundance ratios of HCN and CH_3OH relative to water were similar to those observed in other comets. Post-impact upper limits to production rates were derived for CO, CS, H_2CO, and H_2S; pre-impact upper limits were obtained for OH, CH_3OH, and HCN. All radio detections and upper limits with space-based and ground-based telescopes indicated very little effect on molecular gas production as a result of the impact, whereas somewhat larger effects were noticeable in H-, C-, and N-bearing molecules and in the dust detectable in the visible and near-IR wavelength region. A possible explanation for this different behavior could be gas released from the ejected cometary dust as a consequence of dust fragmentation due to the sublimation of intergrain ices.

Wide-angle imaging in narrowband filters tuned to the fluorescence of H_2O^+ and CO^+ in visible wavelengths was performed. The observations did not reveal any signatures of substantial ion production that could be attributed to the impact.

X-ray observations (0.1 to 1.0 keV) were performed at impact time and afterward. Comets produce x-rays by charge-exchange reactions between the solar wind's highly ionized minor ion population and the neutral cometary gas species (*10*). A ~30% increase in the x-ray counts, lasting for about 1 day, was seen by Earth-orbiting x-ray telescopes after impact. This is interpreted as due to excursions in the comet's gas production rate for a collisionally thin charge-exchange system.

Dust properties. Mid-IR observations can be used to constrain fundamental properties of cometary dust, and 9P/Tempel 1 was no exception, at least after impact. Because of the comet's faintness, pre-impact mid-IR spectra (λ = 8 to 13 μm) obtained from the ground were essentially flat and featureless. Space-based observations gave better signal but yielded a similar pre-impact picture. The grains were generally large (>1 μm) and the 8- to 13-μm emission band was very weak, consistent with previous apparitions (*11*).

Immediately after impact, a short barlike structure extending ~1 arc sec at a position angle of ~225° was seen from ground-based mid-IR imaging. Over the next several hours, the mid-IR flux of the central coma brightened by a factor of ~2 (Fig. 4). Note that the increase in total dust flux (compared to the apparently more modest increase in gas flux) implies that the ratio of dust mass to gas mass in the ejecta was not the same as that seen before impact. This was a dusty impact.

Ground-based mid-IR spectroscopy revealed a substantial growth in the 8- to 13-μm silicate emission feature after impact. The strength of that emission band suggests an emission dominated by submicrometer (0.5 to 1 μm) dust grains. The small size of the grains is consistent with the reports from the spacecraft imaging (*12*). The composition, as derived from modeling the shape of the emission band, is a mix of amorphous olivine and pyroxene, amorphous carbon (which controls the dust temperature), crystalline fosterite, and clino- and orthopyroxene (*13*, *14*). In particular, the resonance peak seen at 11.2 μm is indicative of Mg-rich crystalline olivine. Indeed, the degree of crystallinity in the dust grains was substantially higher in the impact ejecta relative to pre-impact measurements. Organic refractory

material was not needed to model the emission band. The shape of the post-impact silicate feature is strikingly similar to the spectra of active, long-period comets, especially Hale-Bopp. The silicate emission band persisted for about 20 to 26 hours after impact; after that time, the spectral features had disappeared and the comet had returned to its pre-impact mid-IR flux.

Space-based mid-IR observations were performed in phase with the rotation period to ensure that the comet was sampled at similar states of activity. Moreover, in the wavelength segments that are inaccessible from the ground (5 to 8 μm, 13 to 18 μm, and >25 μm), the space-based data filled in the gaps. Imaging at $\lambda = 16$ μm at the time of impact may have revealed thermal emission from the hot impact plume, albeit with a spatial resolution that was poorer than that of the ground-based telescopes by a factor of 5 to 10. Spectroscopic coverage of the entire 5- to 40-μm region after impact revealed compositional and grain temperature information similar to what was seen on the ground. The 9- to 37-μm region showed evidence of crystalline pyroxene in addition to the olivine seen from the ground. Spectral features due to H_2O, CO_2, and carbonaceous material were also seen (*15*).

Polarization of the dust coma was monitored by several groups. Before impact, polarization in visible wavelengths was measured to be 7.0 ± 0.5%. After impact, some variation of polarization with wavelength (0.65 to 0.9 μm) and also with distance from the nucleus was seen, suggesting a change in grain size, porosity, or composition.

Photometric behavior. The transient photometric behavior of the comet's inner coma in the first 15 to 30 min after impact was recorded by many groups. For a small aperture of radius ~1 arc sec, the comet brightened by about 2.3 mag in the visible wavelengths. Note that the nucleus had a magnitude of ~17 in standard Cousins *R* band at the time of impact.

Subtle changes in the light curve can be linked to post-impact phenomena on the comet's surface. A typical light curve with high temporal resolution is shown in Fig. 5. In the first few minutes, there were three distinct rates of brightening. From impact to ~1 min after, the comet brightened sharply. Then, for the next 6 min, the brightening rate was more gradual. However, at ~7 min after impact, the brightening rate increased again, although not as steeply as at first. This rate remained constant for the next 10 to 15 min, at which point the comet's flux began to level off. In the smallest apertures (radius ≈ 1 arc sec), the flux then began to decrease again ~45 min after impact.

This three-sloped light curve as seen in Fig. 5 could be directly linked to the formation of the impact crater, its evolution, and the evolution of the outgassing from it. The falloff in brightness by the first few hours after impact is related to a decrease in the level of activity from the new crater. However, the effect is also partly due to the ejecta moving beyond the edge of the photometric aperture; the peak of the light curve depends strongly on aperture size. Light curves from larger apertures displayed later times of peak brightness; moreover, the comet did not stay at its peak brightness for very long, regardless of aperture. This means that the outgassing from the crater, although much less fecund relative to its activity immediately after impact, had not completely ceased. If it had, light curves with large apertures would show a flat peak flux lasting for the length of time needed for the dust to move out of the aperture.

No group reported seeing an unambiguous, short-duration (<1 s) flash at the exact moment of impact, despite the impact site being visible from Earth. This is likely due to the low contrast of the flash versus the rest of the light from the inner coma as seen in most Earth-based telescopes.

Natural outbursts. The comet was observed to have a series of natural outbursts in addition to the one induced by Deep Impact. These outbursts were identifiable above the comet's normal, gradual brightening as it approached perihelion. The brightness of the comet's dust coma varied with heliocentric distance *r* as $r^{-6.7}$ until early May and dropped thereafter. The first identified outburst occurred on 23 and 24 February (*16*) as the comet brightened by ~40%.

Morphological analysis of an outburst was carried out from visible-wavelength images obtained on 14 June. The outburst showed an arc of material extending over position angles of 215° to 45°. At the peak of the outburst, the comet's brightness was higher than that in previous dates by ~50 to 60%. This outburst was also seen by the Deep Impact spacecraft itself. Observations by multiple telescopes allowed a projected velocity of the dust from the outburst to be calculated: ~200 m/s. Note that this is similar to the speed of the Deep Impact ejecta.

After this discovery, more intense photometric monitoring was initiated, and a series

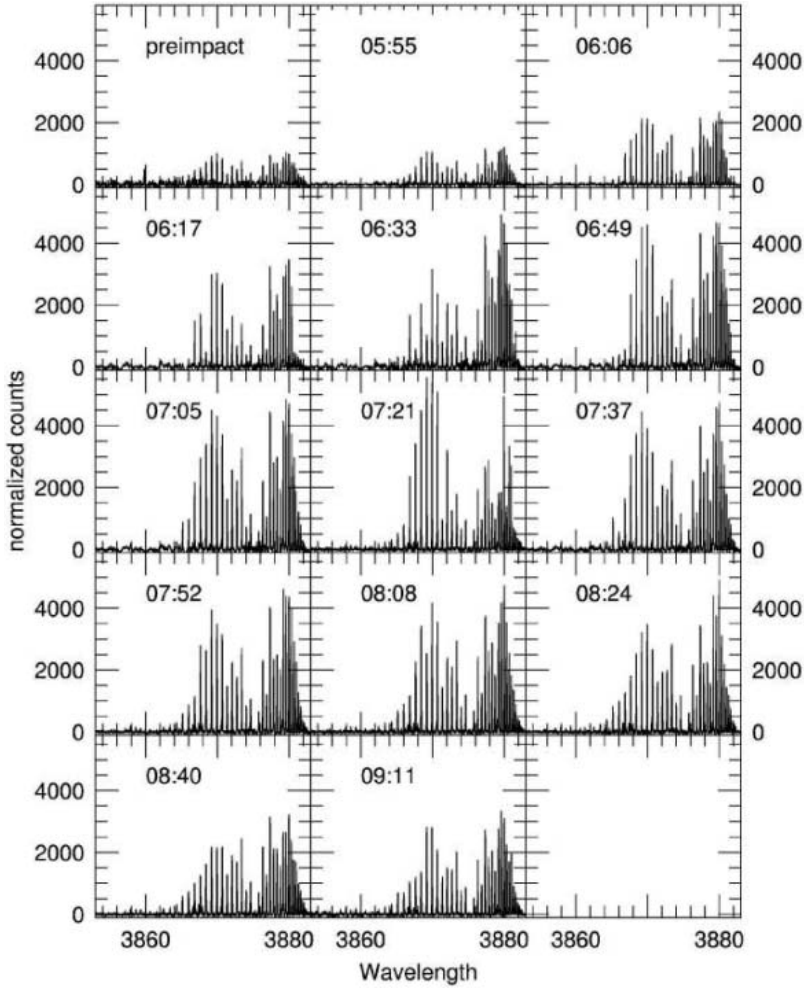

Fig. 3. Spectra (normalized to 1 air mass and 15 min exposure time) of the CN $\Delta v = 0$ emission band ($\delta v = 0$) on 4 July 2005. Data were obtained with the Keck I telescope. The plot shows that the intensity of the CN lines increased by more than a factor of 5 from the pre-impact level to the peak post-impact level (UT 07:21, ~1.5 hours after impact). The emission then begins to decrease; the ejecta must have filled the slit, and the decrease represents the dilution of the gas by expansion. This is consistent with a gas outflow velocity of ~1.1 km/s.

of outbursts occurred approximately every 8 days. On 22 June, there was another outburst and the dust coma morphology was similar to the one on 14 June. On 29 June, mid-IR and x-ray observations revealed another outburst.

On 2 July, another outburst was reported by the spacecraft and by several observers. This was the only event for which a submillimeter continuum detection was obtained; no such detection was reported for the impact event itself. An outburst that was seen by ground-based radio observations of OH occurred on 6 July. Further outbursts were reported on 8 July (in x-rays) and 9 July (in visible wavelengths).

This series of pre- and post-impact natural outbursts bears strong resemblance to the one induced by the impact itself. The projected expansion velocity of the dust cloud has been ~200 m/s for every outburst. The coma morphologies induced by both the natural outbursts and the impact-induced one have been very similar. Specifically, the shape of the ejecta cloud and the ejecta opening angles (~180°) behave similarly, expanding until the radiation pressure starts to dominate the structure.

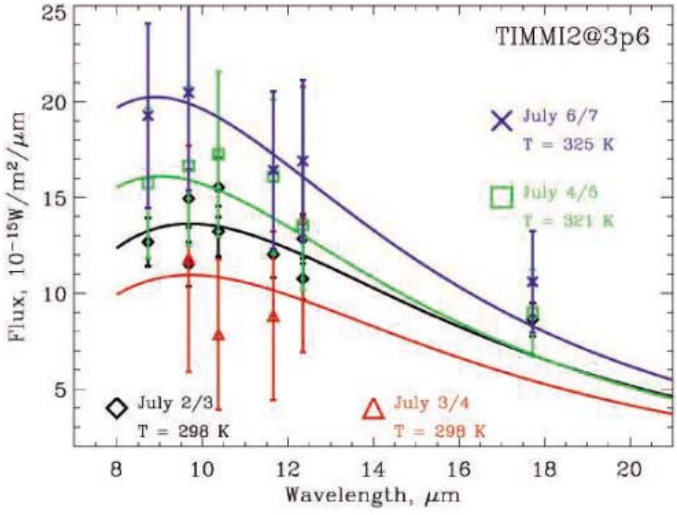

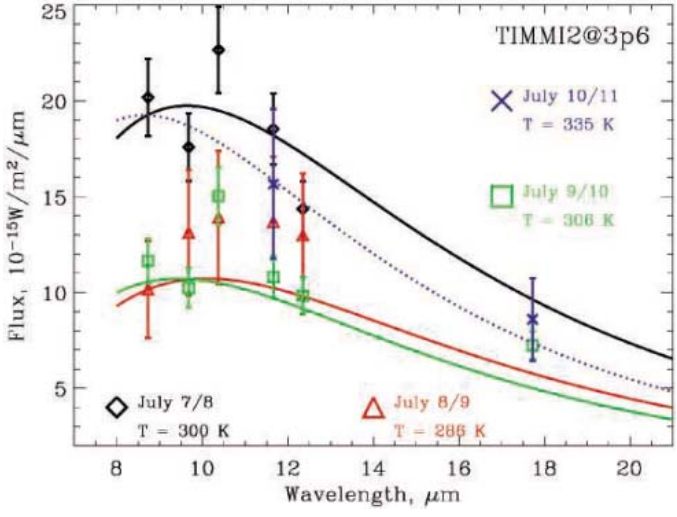

Fig. 4. Synoptic presentation of photometrically calibrated mid-IR fluxes as measured with the European Southern Observatory's 3.6-m telescope. Aperture size was 2500 km at the comet. Data were obtained from 2 days before impact to 7 days after impact. The scatter in the data is due to the "noise" introduced by the normal comet activity. This is consistent with observations done in February and March 2005 (*17*). Blackbody curves are drawn for each epoch to give an indication of the amount of "nonthermal" flux in the filters sensitive to solid-state features (at 9, 10, and 11 μm).

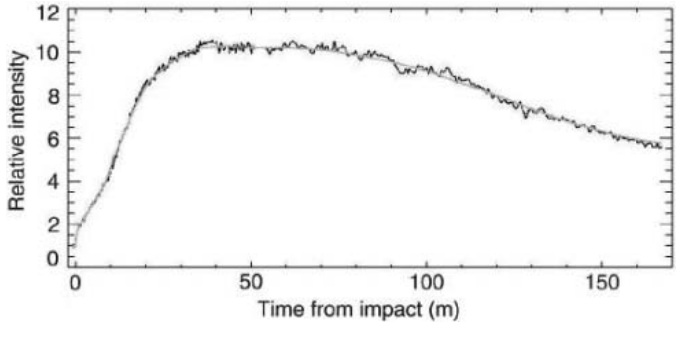

Fig. 5. Impact light curve taken from the charge-coupled device guide camera at United Kingdom Infrared Telescope, sampled at 20 Hz. The triple-slope phenomenon in the first few minutes after impact is clear. The data have been ratioed to the brightness at the time of impact.

Summary. The ground-based observing campaign brought together a collaboration of unprecedented size and scope for support of a spacecraft mission. We had worldwide international cooperation, which was critical for addressing fundamental questions revealed by the Deep Impact experiment. Data analysis continues, but several conclusions can be made.

We now have adequate observations to understand the detailed composition of dust in a Jupiter-family comet. Furthermore, this dust comes from deeper subsurface layers than normal, so it is less processed than the cometary dust we normally see. The dust to gas ratio in the ejecta was larger than what was measured before impact, which suggests that the volatile content of the nucleus's material is depleted even several meters below the surface.

The consensus from the observing campaign was that the impact was an impulsive event. A large amount of material was ejected into the coma in a very short time and took no more than 5 days to dissipate, but the amount of material emitted from the impact site was relatively small. Although we cannot conclusively state that the impact did not create a new source, we can conclude that any new source must be small when compared to the sources that already existed on the nucleus.

References and Notes

1. M. J. S. Belton *et al.*, *Space Sci. Rev.* **117**, 137 (2005).
2. K. J. Meech *et al.*, *Space Sci. Rev.* **117**, 297 (2005).
3. Note that for succinctness the term "Earth-based" is used to describe observations from ground-based telescopes, Earth-orbiting telescopes, and Sun-orbiting telescopes.
4. Z. Sekanina, H. Boehnhardt, *Earth Moon Planets* **78**, 313 (1999).
5. L. Lara *et al.*, in preparation.
6. D. G. Schleicher *et al.*, in preparation.
7. M. F. A'Hearn, R. L. Millis, D. G. Schleicher, D. J. Osip, P. V. Birch, *Icarus* **118**, 223 (1995).
8. M. J. Mumma *et al.*, *Science* **310**, 270 (2005).
9. D. Hutsemekers *et al.*, *Astron. Astrophys.*, in press (available at http://arXiv.org/abs/astro-ph/0508033).
10. C. M. Lisse, T. E. Cravens, K. Dennerl, in *Comets II*, M. C. Festou *et al.*, Eds. (Univ. of Arizona Press, Tucson, AZ, 2005), pp. 631–643.
11. C. M. Lisse *et al.*, *Space Sci. Rev.* **117**, 161 (2005).
12. M. F. A'Hearn *et al.*, *Science* **310**, 258 (2005); published online 8 September 2005 (10.1126/science.1118923).
13. S. Sugita *et al.*, *Science* **310**, 274 (2005).
14. D. E. Harker, C. E. Woodward, D. H. Wooden, *Science* **310**, 278 (2005).
15. C. Lisse *et al.*, *Intl. Astron. Union Circ. 8571* (2005).
16. Amateur Monitoring by the Observadores_Cometas Group (http://astrosurf.com/somyce/c_cometas/9P/9P.htm).
17. H. U. Käufl *et al.*, *Intl. Astron. Union Circ. 8593* (2005).

18. Supported by the University of Maryland and by University of Hawaii subcontract Z667702, which was awarded under prime contract NASW-00004 from NASA. We thank telescope allocation committees everywhere, too numerous to list, for their generous support of time.

17 August 2005; accepted 1 September 2005
Published online 8 September 2005;
10.1126/science.1118978
Include this information when citing this paper.

Parent Volatiles in Comet 9P/Tempel 1: Before and After Impact

Michael J. Mumma,[1*] Michael A. DiSanti,[1] Karen Magee-Sauer,[2] Boncho P. Bonev,[1,3] Geronimo L. Villanueva,[1] Hideyo Kawakita,[4] Neil Dello Russo,[5] Erika L. Gibb,[6] Geoffrey A. Blake,[7] James E. Lyke,[8] Randall D. Campbell,[8] Joel Aycock,[8] Al Conrad,[8] Grant M. Hill[8]

We quantified eight parent volatiles (H_2O, C_2H_6, HCN, CO, CH_3OH, H_2CO, C_2H_2, and CH_4) in the Jupiter-family comet Tempel 1 using high-dispersion infrared spectroscopy in the wavelength range 2.8 to 5.0 micrometers. The abundance ratio for ethane was significantly higher after impact, whereas those for methanol and hydrogen cyanide were unchanged. The abundance ratios in the ejecta are similar to those for most Oort cloud comets, but methanol and acetylene are lower in Tempel 1 by a factor of about 2. These results suggest that the volatile ices in Tempel 1 and in most Oort cloud comets originated in a common region of the protoplanetary disk.

Comets are the best-preserved material remaining from the earliest epoch of our planetary system, and they hold key evidence for testing their role in delivering water and prebiotic organic chemicals to the young Earth-Moon system (*1–3*). Today, comets reside in two principal reservoirs (the Oort cloud and Kuiper-Edgeworth belt) that have different properties. About 10 trillion comet nuclei are contained in the Oort cloud—a nearly spherical shell that spans distances ranging from 10,000 to 50,000 astronomical units (AU) from the Sun (*4*). The Kuiper-Edgeworth disk (KED) contains perhaps several billion comets centered on the ecliptic and orbiting at heliocentric distances ranging from ~40 to several hundred astronomical units (*5*, *6*). The scattered KED population is thought to be the principal source of the ecliptic comets such as Tempel 1 (*7*). Comet nuclei can be ejected from either reservoir by various gravitational effects; once within the terrestrial planets' region they can be activated by sunlight. If warmed sufficiently, their surface ices sublimate and escaping gases can entrain small dust particles, together forming the often spectacular "tails" of dust and ionized gas seen from Earth.

Astronomers have sought to classify comets based on the composition of their native ices and dust; these should be controlled by the locations at which precometary material formed in the protoplanetary disk (*8–10*). A gradation in composition is expected with distance from the proto-Sun, from one dominated by interstellar chemistry at the largest distances (>40 AU) to one dominated by thermochemistry at the smallest comet-forming distances (~6 AU). The picture is clouded by the expected radial migration of cometesimals within the protoplanetary disk and by the outward transport of processed grains and gases from the terrestrial planets' region (*11–13*). An individual comet nucleus might contain discrete cometesimals formed in distinct regions of the disk and thus its chemical composition may well be heterogeneous. Accumulation models suggest diameters near tens of meters for such cometesimals (*14*).

Once a comet evolves into a short-period orbit (<200-year period), its mean lifetime against removal (complete destruction or

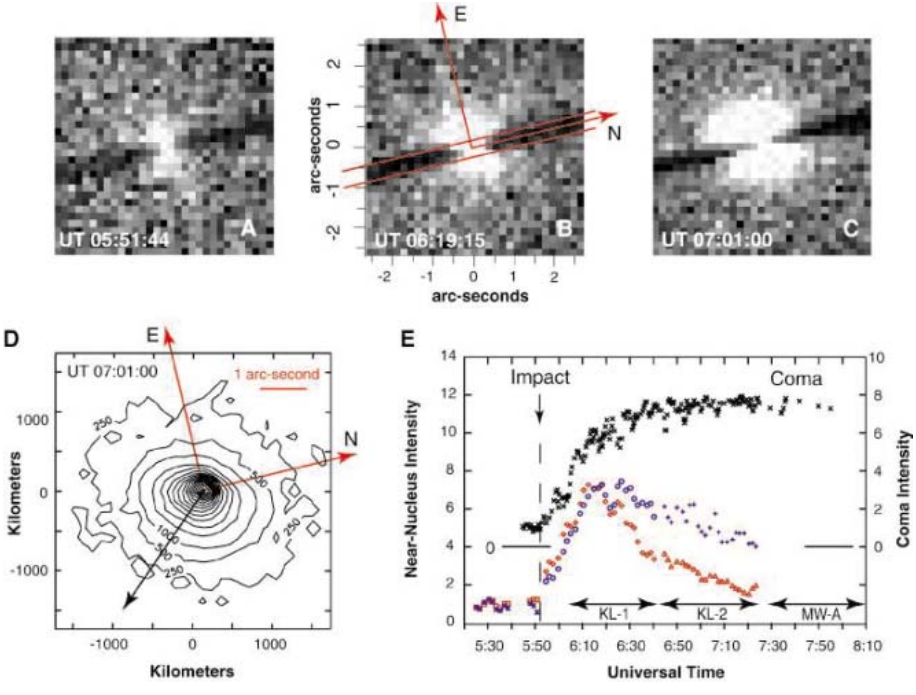

Fig. 1. The development of Tempel 1 on impact night, as observed with NIRSPEC at Keck-2. (**A** to **C**) Three images taken with the SCAM, in light reflected from the polished slit plate. The black band extending left to right in each panel locates the spectrometer entrance slit. (A) The appearance of Tempel 1 just before impact. (B) The comet 27 min after impact. The edges of the spectrometer entrance slit are shown along with the cardinal directions. (C) The comet 69 min after impact. (**D**) Contours of the coma obtained from a median-filtered image (created from 10 SCAM frames) centered 69 min after impact. The axis of symmetry of ejection is shown along with the cardinal directions. (**E**) Light curves obtained from the SCAM images (black) and from the spectral continuum (3.3 μm) in individual spectra. All light curves show a rapid rise of intensity after impact. After its maximum, the peak spectral intensity (red) falls rapidly to its preimpact value by UT 7:20. The total spectral intensity (blue) decays more slowly, and the coma intensity (black) plateaus. Time blocks (KL1, KL2, and MWA) are indicated for the mean spectral extracts shown in Fig. 2.

[1]Solar System Exploration Division, NASA Goddard Space Flight Center, Greenbelt, MD 20771, USA. [2]Department of Physics and Astronomy, Rowan University, Glassboro, NJ 08028–1701, USA. [3]Ritter Astrophysical Research Center, Department of Physics and Astronomy, University of Toledo, Toledo, OH 43606, USA. [4]Department of Physics, Kyoto Sangyo University, Motoyama, Kamigamo, Kita-ku, Kyoto 603-8555, Japan. [5]Space Department, Planetary Exploration Group, Applied Physics Laboratory/Johns Hopkins University, 11100 Johns Hopkins Road, Laurel, MD 20723–6099, USA. [6]Department of Physics and Astronomy, University of Missouri, St. Louis, MO 63121–4499, USA. [7]Division of Geological and Planetary Sciences, California Institute of Technology, Pasadena, CA 91125, USA. [8]W. M. Keck Observatory, 65-1120 Mamalahoa Highway, Kameula, HI 96743, USA.

*To whom correspondence should be addressed. E-mail: michael.j.mumma@nasa.gov

scattering out of the solar system) is only ~500,000 years (*15*, *16*). During this time, the comet nucleus may build up a surface layer of particles too large to be dragged away by the escaping gases, eventually causing sublimation to decrease markedly or even cease. Excess heating of the (inactive) surface layer could drive chemical fractionation of the layers below and might cause the released gases to differ from the pristine interior (*17*). A principal goal of Deep Impact was to test this hypothesis by excavating material from below the processed layer and measuring its chemical composition (*18*).

We measured organic volatiles and water in 9P/Tempel 1 using the high-dispersion near-infrared spectrometer (NIRSPEC) at the Keck-2 telescope on Mauna Kea, Hawaii, before, during, and after the Deep Impact event (*19*, *20*). Acquired spectra cover the wavelength range of 2.8 to 5.0 μm at a resolving power ($\lambda/\delta\lambda \sim 24{,}000$), sufficient to reveal individual spectral lines of parent volatiles.

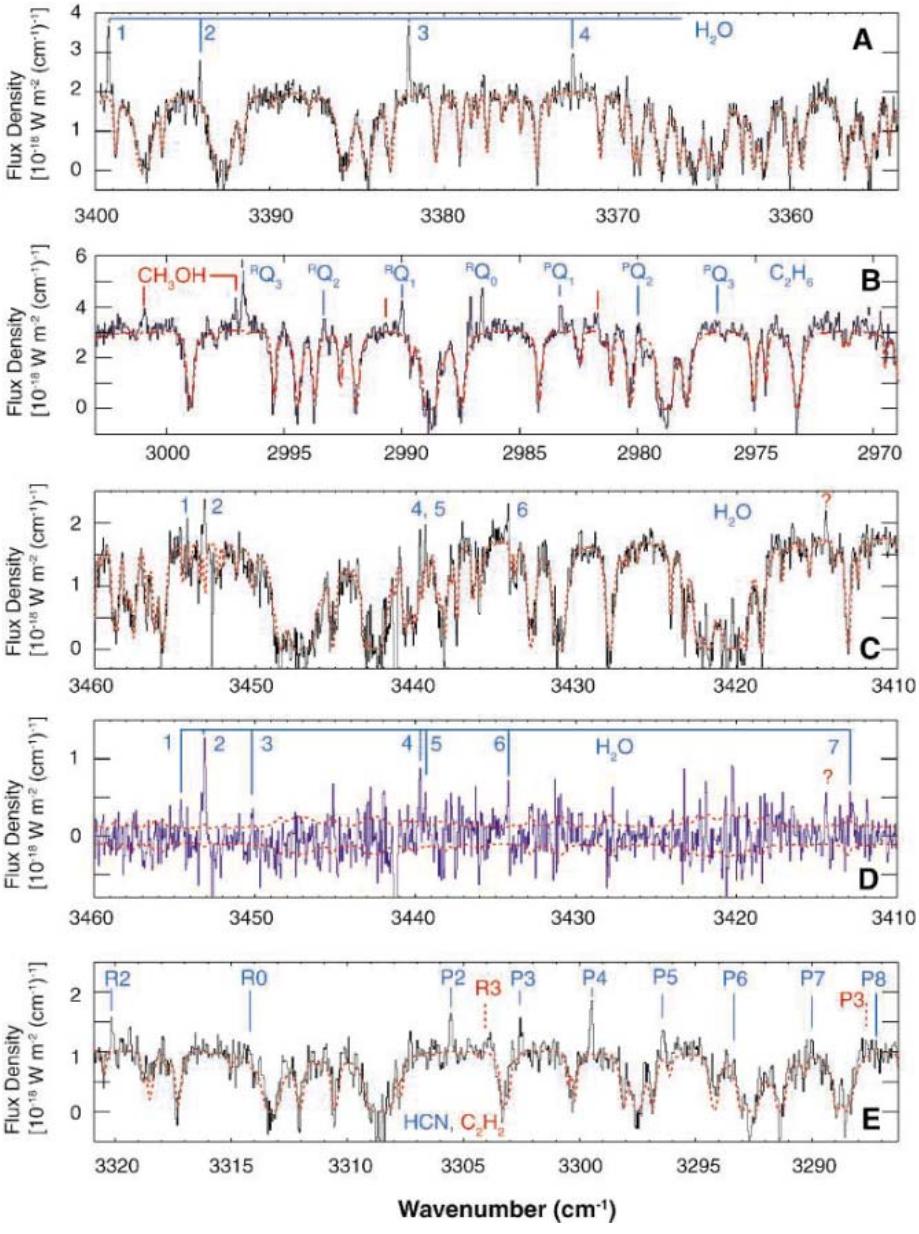

Fig. 2. Detection of parent volatiles and dust in comet Tempel 1 on UT 4 July, after the impact event. We averaged over the intervals shown in Fig. 1E. The dashed line in each panel represents the cometary continuum convolved with a synthetic transmittance spectrum of the terrestrial atmosphere. (**A** and **B**) Spectra extracted from setting KL1. (A) Four spectral lines of H_2O are shown. (B) Six Q-branches of C_2H_6 are detected along with features of CH_3OH. (**C** to **E**) Spectra extracted from setting KL2. (C) Five spectral lines of H_2O are marked. (D) Seven H_2O spectral lines are seen in the residuals of (C) after subtraction of the cometary continuum convolved with the atmospheric transmittance. (E) Eight spectral lines of HCN are detected, along with two lines of C_2H_2. Quantitative results are given in Table 1.

On universal time (UT) 4 July, spectral acquisition began at 5:22 UT (shortly after sunset) and continued until 8:10 UT. For guiding, we imaged a nearby field star (using the PXL guide camera) and kept the telescope centered on the comet during the observations with the use of nonsidereal guide rates. We documented the position of the slit on the comet and recorded development of the ejecta cloud at 10-s intervals with the slit-viewing camera (SCAM) [supporting online material (SOM) text S1]. The measured stellar point-spread function (PSF) from a full set of stacked images was consistently better than 0.35 arc sec full width at half maximum (FWHM) throughout the observing of Tempel 1.

A selected sample of SCAM images is shown in Fig. 1, A to C, along with a contour map of a median-filtered image taken near UT 7:01 (Fig. 1D). The black streak appearing in Fig. 1, A, B, and C, maps the location of the entrance slit of our spectrometer (SOM text S2). The SCAM images sample light scattered from coma material at slant distances outside our slit; the slit edges and the cardinal directions on the sky are indicated in Fig. 1B. These panels show a small patch of sky (31 × 31 pixels or 5.4 × 5.4 arc sec) centered on Tempel 1. The total coma intensity (background subtracted) was extracted from a box (27 × 27 pixels) centered on the comet, and its temporal evolution is shown in Fig. 1E (coma). The coma brightened noticeably in the first minute after impact, achieved its maximum brightness at ~6:37 UT, and maintained that brightness until our observations ceased at 8:10 UT (Fig. 1E).

We used three separate spectrometer settings (horizontal bars, Fig. 1E) (SOM text S3). The first setting (KL1, 28 min total time on source) revealed spectral lines of H_2O (four lines), C_2H_6 (six Q-branches), and CH_3OH (many lines). The second setting (KL2, 24 min on source) yielded lines of H_2O (seven lines), HCN (eight lines), CH_3OH (many lines), C_2H_2 (two lines, tentatively), and a tentative detection of CH_4. The third setting (MWA, 14 min on source) revealed H_2O and CO.

We also extracted the peak intensity of the dust spatial profile measured along the slit and the spatially integrated intensity (Gaussian-equivalent area) implied by the spatial profile (Fig. 1E) (SOM text S4). The peak intensity samples a region close to the nucleus (e.g., a PSF of 0.35 arc sec corresponds to half width at half maximum of ~113 km at the comet), and so it represents our best information on the ejection event and its evolution with time. The peak intensity grew rapidly for the first 15 min after impact but then stabilized and thereafter decreased to values similar to the quiescent state (Fig. 1E). The spatially integrated intensity also rose rapidly toward its maximum but then fell off more slowly than the peak intensity. The rapid growth of both spectral signatures requires an increase in the effective dust cross-section and possibly in its temperature. A full treatment must

Table 1. The parent volatile composition of comet 9P/Tempel 1. H_2O is measured in every instrument setting, and it provides the standard for abundance ratios of trace species (SOM text S8). We tabulate the effective line flux required to produce the derived column number and global production rates (SOM text S9). The temperature is the rotational temperature, determined from Boltzmann analysis of individual line intensities. If too few lines were available for independent rotational analyses, a representative value (40 K) was adopted. The reported errors in production rates (Q) and relative abundances are 1σ standard errors, which incorporate not only photon noise but also uncertainties in line-by-line evaluation of Q for the same species (SOM text S10). This approach is consistent with our previous work. In this case, 95% confidence intervals are typically 2σ to 3σ, after accounting for the limited number of lines detected. For most species, we have clear detections of more than three lines (Fig. 2). The exception is C_2H_2, which is based on only two sampled lines and thus has a much larger confidence interval. ph s^{-1} $molec^{-1}$, photons per second per molecule.

Species detected	Line flux 10^{-19} W m^{-2}	g_1 10^{-5} ph s^{-1} $molec^{-1}$	Temperature K	Total no. 10^{28} molecules (N)	Abundance (relative) (ratio of N's)	Q 10^{25} s^{-1}
UT 3 June 2005						
KL1 6:37:29 to 8:08:37 44 min						
H_2O	3.5 ± 0.27	0.0475	(40)	430 ± 33	100	1244 ± 95
C_2H_6	2.56 ± 0.50	20.2	(40)	0.84 ± 0.16	0.194 ± 0.041	2.42 ± 0.47
CH_3OH	1.38 ± 0.18	1.6	(40)	5.67 ± 0.73	1.32 ± 0.20	16.4 ± 2.1
KL2 8:35:15 to 9:54:44 40 min						
H_2O	2.90 ± 0.51	0.0405	(40)	409 ± 72	100	1184 ± 207
HCN	3.18 ± 0.92	25.9	33^{+8}_{-6}	0.73 ± 0.21	0.18 ± 0.061	2.11 ± 0.61
UT 4 July 2005						
Preimpact: KL1 5:22:12 to 5:52:13 16 min						
H_2O	2.79 ± 0.47	0.036	(40)	588 ± 99	100	1037 ± 174
C_2H_6	1.65 ± 0.70	8.95	(40)	1.59 ± 0.67	0.27 ± 0.12	2.8 ± 1.2
CH_3OH	1.16 ± 0.21	1.60	(40)	6.28 ± 1.13	1.07 ± 0.26	11.1 ± 2.0
Postimpact: KL1 6:07:35 to 6:41:47 20 min						
H_2O (ord 26)*	4.92 ± 0.69	0.036	(40)	1042 ± 145*	100*	1835 ± 256
H_2O (ord 27)*	22.8 ± 0.64	0.17	38 ± 3	984 ± 28*	100*	1734 ± 49
C_2H_6	8.16 ± 0.57	20.2	(40)	3.48 ± 0.24	0.353 ± 0.027*	6.13 ± 0.43
CH_3OH	1.80 ± 0.30	1.60	(40)	9.73 ± 1.64	0.99 ± 0.17*	17.2 ± 2.9
Postimpact: KL2 6:43:16 to 7:24:49 24 min						
H_2O	9.04 ± 1.02	0.079	38 ± 6	859 ± 97	100	1703 ± 192
HCN	6.54 ± 0.66	28.1	37 ± 3	1.81 ± 0.18	0.21 ± 0.032	3.61 ± 0.37
C_2H_2	0.57 ± 0.17	4.1	(40)	1.08 ± 0.32	0.13 ± 0.04	2.06 ± 0.61
CH_4	5.45 ± 2.96	9.97	(40)	4.64 ± 2.52	0.54 ± 0.30	9.22 ± 5.0
H_2CO	2.32 ± 0.41	2.98	43 ± 4	7.24 ± 1.28	0.84 ± 0.18	15.3 ± 2.7
Postimpact: MWA 7:38:30 to 8:10:23 14 min						
H_2O	6.14 ± 1.17	0.062	(40)	1192 ± 227	100	2100 ± 400
CO	59.1 ± 20.7	13.7	(40)	51.7 ± 18.1	4.3 ± 1.7	91.3 ± 32
UT 5 July 2005: MWA 5:55:20 to 7:06:40 32 min						
H_2O	5.85 ± 1.17	0.062	(40)	1135 ± 227	100	2000 ± 400
CO	45.4 ± 8.4	11.10	(40)	49.0 ± 9.1	4.3 ± 1.2	86.5 ± 16

*H_2O lines appeared in two spectral orders (ord 26 and ord 27) of KL1; the values retrieved for each order are given. We used the weighted mean column number ($986 \times 10^{28} \pm 27 \times 10^{28}$) when comparing abundance ratios for this setting.

consider dissolution of dust clusters as their icy "glue" sublimates, heating of dust grains as they are warmed by sunlight, reduction in optical depth as the ejecta cloud expands, and similar effects, which are beyond the scope of this Report.

The rapid falloff in peak intensity and the slower falloff in the spatially integrated spectral intensity likely represent continued expansion of the dust cloud along with cessation of ejection. The time required for material to traverse the radius of our pencil beam (~140 km) is about 5 min if the expansion velocity is 500 m/s. The integrated intensity samples dust over a larger spatial region (up to ~550 km projected distance), and so it falls more slowly as expansion continues. The SCAM images sample material over the largest spatial region (up to ~1600 km projected distance), and so they show the slowest temporal response. Inspection of the three light curves reveals this effect directly (Fig. 1E) (SOM text S4). Gas densities in the inner coma likely never reached spatial profiles representative of steady-source conditions.

Mean spectra were formed for intervals after impact when the intensities were most stable (horizontal bars, Fig. 1E), and examples of time-averaged flux-calibrated spectra for Tempel 1 are shown in Fig. 2 (SOM text S5). The spectral extracts (Fig. 2) are taken from a pencil beam centered on the comet nucleus (3×9 pixels, subtending 280×1109 km and centered on the comet), and they measure the column of material distributed along the line of sight. The water column numbers extracted from these postimpact mean spectra are in agreement (within their confidence limits), and they are larger than the preimpact column number for H_2O by about a factor of 2 (Table 1). Measurements of H_2O and trace species were simultaneous in each instrument setting, eliminating many sources of systematic error and enabling a meaningful comparison of their abundance ratios based on column numbers.

Intensities were measured for individual spectral lines of H_2O, HCN, and H_2CO in the mean spectra (averaged over the sampling intervals mentioned above) and rotational temperatures were obtained independently for each species with the use of a Boltzmann analysis. The measured rotational temperatures cluster near 40 K (Table 1); where a rotational temperature could not be obtained, 40 K was assumed for other parent species reported here. We calculated the total number of molecules for each species in the column (3×9 pixels) using the measured (or adopted) rotational temperature.

We derived effective global production rates from nucleus-centered flux measurements (3×9 pixels) by adopting a standard coma model (a spherically symmetric coma with uniform outflow and steady production over the lifetime of the parent volatile) and applying standard analytical procedures (SOM text S6) (Table 1). These conditions are likely valid for the quiescent production on 3 June and 4 July (before impact) and the production rates for those times are valid (Table 1). However, the impulsive impact event is far from steady, and it likely varies for some time after ejection as icy grains sublimate, for example.

Table 2. The organic volatile composition of Tempel 1 and other comets. Citations to original source papers on Oort cloud comets appear in (*10*). NMS, neutral mass spectrometer.

H_2O = 100	C_2H_6	HCN	CH_3OH	CO (native only)	CH_4	C_2H_2
9P/Tempel 1						
A. Preimpact (3 June)	0.194 ± 0.041	0.18 ± 0.06	1.32 ± 0.20			
B. Postimpact (total)	0.353 ± 0.027	0.21 ± 0.032	0.99 ± 0.17	4.3 ± 1.2	0.54 ± 0.30	0.13 ± 0.04
C. Ejecta	0.59 ± 0.18					
Oort cloud comets						
153P/Ikeya-Zhang	0.62 ± 0.13	0.18 ± 0.05	2.5 ± 0.5	4.7 ± 0.8	0.51 ± 0.06	0.18 ± 0.05
Lee	0.67 ± 0.07	0.29 ± 0.02	2.1 ± 0.5	1.8 ± 0.2	1.45 ± 0.18	0.27 ± 0.03
Hale-Bopp	0.56 ± 0.04	0.27 ± 0.04	2.1	12.4 ± 0.4	1.45 ± 0.16	0.31 ± 0.1
Hyakutake	0.62 ± 0.07	0.18 ± 0.04	1.7 – 2	14.9 ± 1.9	0.79 ± 0.08	0.16 ± 0.08
1P/Halley (Giotto NMS)	~0.4	~0.2	1.7 ± 0.4	3.5	<1	~0.3
C/1999 S4	0.11 ± 0.02	0.10 ± 0.03	<0.15	0.9 ± 0.3	0.18 ± 0.06	<0.12

After impact, the measured column number is the sum of material from the quiescent source(s) and the impulsive event. If the new source has reached steady production by 20 min after impact, we expect the effective production rate to be a fair estimate of the true value (the true rate is likely to be larger by a factor up to about 1.6, i.e., $\pi/2$) (SOM text S7). However, the rapid decrease in peak spectral intensity after UT 6:20 demonstrates that steady-state production was not achieved (red points, Fig. 1E). Therefore, these production rates should be interpreted solely as indicators of activity—the quantitative values are sensitive to model assumptions. However, the total column number measured for water during the three time intervals was the same, suggesting that transient corrections to the steady production approximation are not large.

In contrast to the global production rate, the derived total column abundance is less sensitive to model assumptions because the two key variables (line flux and rotational temperature) are taken directly from our spectral measurements. Moreover, common observational factors (such as atmospheric seeing and guiding errors) affect all species measured in a given setting in the same way, and so they cancel when the ratio of column abundances is taken (Table 1). For dates on which gas production can be assumed to be steady in time (e.g., UT 3 June), the chemistry of released material may be taken either from column number ratios or from ratios of production rates.

We extracted column abundances and quiescent production rates for H_2O, C_2H_6, CH_3OH, and HCN on UT 3 June and again (excepting HCN) on UT 4 July (before impact) (Table 1). The abundance ratios measured on UT 3 June are more accurate because the comet was brighter then and more time was available for measurement (we used 44 min on source for KL1 on 3 June versus only 16 min preimpact on 4 July).

After impact, the total column number represents the sum of two contributions: (i) material produced by steady release during the interval before impact, and (ii) the (partially filled) column of gas resulting from the ejection event (Table 1). The total column number measured for water during the three time intervals was the same, within errors. The abundance ratios (relative to water) for minor species are taken from the ratio of column numbers (Table 1). The ratio of effective global production rates is not a valid measure of composition because the two components do not fill the coma in the same way and the assumed coma model is not appropriate for the impact ejecta.

The total column of material measured after impact was enriched in ethane by a factor of 1.82 ± 0.40 relative to material released on UT 3 June (0.353 ± 0.027 versus 0.194 ± 0.041, Table 1), but methanol and hydrogen cyanide were unchanged within errors. However, we cannot be certain that the steady production seen on 3 June and 4 July (preimpact) exhibit the same chemistry. Although the heliocentric distance was virtually unchanged during this time, it is possible that chemically distinct regions were active on these two dates. This could cause chemical differences in the released material if the nucleus is heterogeneous in its composition. For this reason, we considered two possibilities for steady production on the two dates: (i) independent chemistries and (ii) a common chemistry. For the first case, we adopted the apparent column numbers derived from measured line intensities and compared them with H_2O (measured simultaneously) to obtain abundance ratios (A and B in Table 2). The abundance ratios before and after impact on 4 July agree within their confidence limits, however, this test is not very sensitive or revealing because the confidence limits before impact are large (Table 1) (*21*).

For the second case, we assumed that the composition of material released before impact on UT 4 July was the same as that on UT 3 June. We then combined the more accurate abundance ratios of 3 June with the preimpact H_2O column number on 4 July to estimate the column numbers for C_2H_6, CH_3OH, and HCN from the steady source on impact night. We assumed this steady contribution was not affected by the impact event and we subtracted it from the total column numbers measured after impact (Table 1). The net column content represents the ejecta. The ejecta is enriched in ethane by nearly a factor of 3 (3.0 ± 1.1) compared with the quiescent source on UT 3 June (A and C in Table 2). CH_3OH, and HCN show no difference, and other species (CH_4, C_2H_2, H_2CO, and CO) were measured only postimpact.

Chemical diversity among comets (and even within a given comet nucleus) is expected if chemical gradients existed in the giant planets' region of the protoplanetary disk. It is interesting to compare abundance ratios found for Tempel 1 with those of other comets (Table 2). The hypervolatiles CO and CH_4 vary strongly among comets (e.g., native CO varies by a factor of ~20 among comets, whereas CH_4 varies by a factor of ~7), and CO and CH_4 in Tempel 1 fall within these ranges. By contrast, ethane is notably constant. The dominant group of Oort cloud (OC) comets (8 of 10 OC comets) shows C_2H_6:H_2O = 0.6:100 (Table 2). The unusual OC comet C/1999 S4 was depleted in most forms of volatile carbon, including ethane, whereas only one OC comet was enriched in ethane (C/2001 A2, C_2H_6:H_2O = 1.6:100). Among comets of probable Kuiper-Edgeworth belt origin, the values for comet 2P/Encke [(0.3 to 0.4):100] and 21P/Giacobini-Zinner (C_2H_6:H_2O = 0.22 ± 0.13:100) agree with the total value for Tempel 1 after impact (B in Table 2). Methanol is somewhat lower in Tempel 1, both before and after impact.

Ethane depletion on 3 June could be the signature of thermal processing of surface material leading to preferential loss of hypervolatiles. Of the four species measured both pre- and postimpact, three are high-temperature volatiles (H_2O, CH_3OH, and HCN) that likely would not be affected by thermal processing of near-surface material. Of the hypervolatiles, only C_2H_6 was measured before impact and its abundance ratio then was significantly lower than after impact. The hypervolatiles were detected (CO) or constrained (CH_4) postimpact at abundance ratios that are within the range of those found for OC comets in our sample, but C_2H_2 was somewhat lower (Table 1). The observed chemical difference could instead be the signature of cosmogonic heterogeneity; radial migration in

the protoplanetary disk could cause cometesimals of diverse chemistry to be incorporated within the final nucleus. The impactor targeted a region between two circular features on the nucleus surface; these could be the exposed rims of primordial cometesimals, and if so, the impact ejecta might represent material from them.

If we assume independent chemistries for the steady production on these dates, then we cannot extract separate volatile abundances for the steady (preimpact) production and the ejecta on 4 July. If we assume a common chemistry for the steady production on 3 June and 4 July (preimpact), the abundance ratios (relative to water) for most species in the ejecta are within the range of those found for the dominant group of OC comets. Some differences are noted: Methanol is lower by a factor of about 2 in Tempel 1, as is acetylene.

These chemical similarities suggest that Tempel-1 and most OC comets originated in a common region of the protoplanetary disk; this is consistent with the view that the comet nuclei in the scattered KED [the proposed source reservoir for most ecliptic comets (*7*)] and OC comets both originated in the outer giant planets' region of the protoplanetary disk. The depleted ethane abundance on 3 June and its similarity to similar values found for 2P/Encke and 21P/Giacobini-Zinner then suggests that the surfaces of short-period comets have been processed thermally.

References and Notes

1. D. Bockelée-Morvan, J. Crovisier, M. J. Mumma, H. A. Weaver, in *Comets II* (Univ. of Arizona Press, Tucson, AZ 2005), pp. 391–423.
2. W. M. Irvine, F. P. Schloerb, J. Crovisier, B. Fegley, M. J. Mumma, in *Protostars and Planets IV* (Univ. of Arizona Press, Tucson, AZ, 2000), pp. 1159–1200.
3. M. J. Mumma, P. R. Weissman, S. A. Stern, in *Protostars and Planets III* (Univ. of Arizona Press, Tucson, AZ, 1993), pp. 1177–1252.
4. L. Dones *et al.*, in *Comets II* (Univ. of Arizona Press, Tucson, AZ, 2005), pp. 153–174.
5. B. Gladman, *Science* **307**, 71 (2005).
6. A. Morbidelli, M. E. Brown, in *Comets II* (Univ. of Arizona Press, Tucson, AZ, 2005), pp. 175–191.
7. G. Bernstein *et al.*, *Astron. J.* **128**, 1364 (2004).
8. M. F. A'Hearn *et al.*, *Icarus* **118**, 223 (1995).
9. N. D. Biver *et al.*, *Earth Moon Planets* **90**, 323 (2002).
10. M. J. Mumma *et al.*, *Adv. Space Res.* **31**, 2563 (2003).
11. Y. Aikawa, E. Herbst, *Astrophys. J.* **526**, 314 (1999).
12. D. Bockelee-Morvan *et al.*, *Astron. Astrophys.* **384**, 1107 (2002).
13. A. Delsemme, *Icarus* **146**, 313 (2000).
14. S. J. Weidenschilling, in *Comets II* (Univ. of Arizona Press, Tucson, AZ, 2005), pp. 97–104.
15. H. F. Levison, M. Duncan, *Icarus* **108**, 18 (1994).
16. H. F. Levison, in *Completing the Inventory of the Solar System* (Astronomical Society of the Pacific, San Francisco, 1996), pp. 173–191.
17. S. Espinasse *et al.*, *Planet. Space Sci.* **41**, 409 (1993).
18. M. F. A'Hearn *et al.*, *Space Sci. Rev.* **117**, 1 (2005).
19. I. S. McLean *et al.*, *Proc. SPIE* **3354**, 566 (1998).

20. We requested observing time on the two nights before impact to guard against this problem, but it was not awarded.

21. We thank J. W. Feuss and C. Makrides for assistance. This work was supported by NASA's Planetary Astronomy Program under RTOP 344-32-30-07 (M.J.M.) and RTOP 344-32-98 (M.A.D.); the NSF Research at Undergraduate Institutions program no. 0407052 (K.M.S.), the National Research Council (G.L.V., a resident research associate), and the NASA Origins of Solar Systems program (G.A.B.). Our data were obtained at the W. M. Keck Observatory, which is operated as a scientific partnership among the California Institute of Technology, the University of California, and NASA. The Observatory was made possible by the generous financial support of the W. M. Keck Foundation. 9P/Tempel 1 data obtained on 4 July are available via the Keck Observatory Archive (http://www2.keck.hawaii.edu/science/deepimpact/KeckDeepImpact.html).

Supporting Online Material
www.sciencemag.org/cgi/content/full/1119337/DC1
SOM Text
References

18 August 2005; accepted 9 September 2005
Published online 15 September 2005;
10.1126/science.1119337
Include this information when citing this paper.

REPORT

Subaru Telescope Observations of Deep Impact

S. Sugita,[1,4,5]* T. Ootsubo,[6] T. Kadono,[1,7] M. Honda,[4] S. Sako,[2] T. Miyata,[2] I. Sakon,[3] T. Yamashita,[8] H. Kawakita,[9] H. Fujiwara,[3] T. Fujiyoshi,[8] N. Takato,[8] T. Fuse,[8] J. Watanabe,[10] R. Furusho,[11] S. Hasegawa,[4] T. Kasuga,[10] T. Sekiguchi,[10] D. Kinoshita,[12] K. J. Meech,[13] D. H. Wooden,[14] W. H. Ip,[12] M. F. A'Hearn[15]

The impact cratering process on a comet is controversial but holds the key for interpreting observations of the Deep Impact collision with comet 9P/Tempel 1. Mid-infrared data from the Cooled Mid-Infrared Camera and Spectrometer (COMICS) of the Subaru Telescope indicate that the large-scale dust plume ejected by the impact contained a large mass (~10^6 kilograms) of dust and formed two wings approximately ±45° from the symmetric center, both consistent with gravity as the primary control on the impact and its immediate aftermath. The dust distribution in the inner part of the plume, however, is inconsistent with a pure gravity control and implies that evaporation and expansion of volatiles accelerated dust.

We conducted mid-infrared (mid-IR) observations of comet 9P/Tempel 1 before and after its collision with NASA's 370-kg Deep Impact (DI) probe (*1*). Because mid-IR light is sensitive to dust radiation but not influenced by gas emission, it is suitable for observing the dust excavated by the DI collision. Both imaging and spectroscopic measurements were performed with the Cooled Mid-Infrared Camera and Spectrometer (COMICS) mounted on the Subaru Telescope on Mauna Kea, Hawaii. This long wavelength range is not covered by the DI spacecraft's instruments (*2*), and the spatial resolution achieved by the large (8.2 m) aperture of the Subaru telescope surpasses that of space telescopes. Information on the impact physics of the DI collision is crucial to putting chemical and mineralogical data obtained by other observations (*3*, *4*) into context.

Both N-band (8-to-13 μm) spectroscopy data and spectral energy distribution (SED) data based on multiband imaging measurements on universal time (UT) 2 and 3 July 2005 show that the cometary coma was compact [only 1.3 times the point spreading function (~0.4″) of the Subaru/COMICS system at the 10.5-μm band] before the DI collision. The first image of comet 9P/Tempel 1 an hour after the impact showed a large fan-shaped plume with a symmetry line at 225° position angle (PA) from the comet nucleus (Fig. 1). This direction turned out to be close to the direction of the surface normal vector of the impact point of the comet (*3*).

The plume expanded at an approximately constant velocity (125 ± 10 m/s) (*5*) throughout the observed time on UT 4 July 2005. As the plume expanded, its surface brightness decreased monotonically. The relation between

[1]Department of Complexity Science and Engineering, University of Tokyo, Kashiwa, Chiba, Japan. [2]Institute of Astronomy, University of Tokyo, Miaka, Tokyo, Japan. [3]Department of Astronomy, University of Tokyo, Hongo, Tokyo, Japan. [4]Institute of Space and Astronautical Science, Japan Aerospace Exploration Agency, Sagamihara, Kanagawa, Japan. [5]Department of Geological Sciences, Brown University, Providence, RI, USA. [6]Division of Particle and Astrophysical Sciences, Nagoya University, Nagoya, Aichi, Japan. [7]Institute for Research on Earth Evolution, Japan Agency for Marine-Earth Science and Technology, Yokosuka, Kanagawa, Japan. [8]Subaru Telescope, National Astronomical Observatory of Japan, National Institutes of Natural Sciences, Hilo, HI, USA. [9]Department of Physics, Kyoto Sangyo University, Kamigamo, Kyodo, Japan. [10]National Astronomical Observatory of Japan, Mitaka, Tokyo, Japan. [11]Waseda University, Nishiwaseda, Tokyo, Japan. [12]Institute of Astronomy, National Central University, Chung-Li, Taiwan. [13]Institute for Astronomy, University of Hawaii, Honolulu, HI, USA. [14]Space Science Division, NASA Ames Research Center, Moffett Field, CA, USA. [15]Department of Astronomy, University of Maryland, College Park, MD, USA.

*To whom correspondence should be addressed. E-mail: sugita@k.u-tokyo.ac.jp

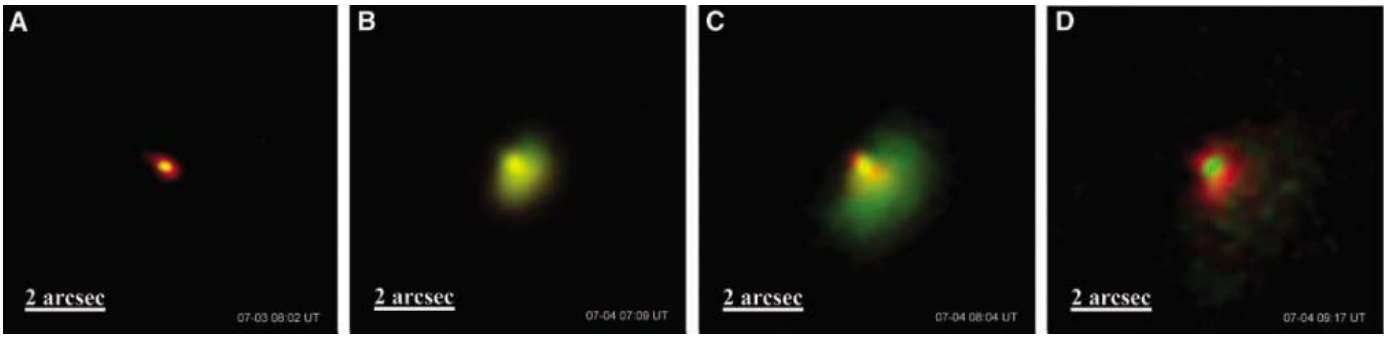

Fig. 1. (**A** to **D**) False-color images of comet 9P/Tempel 1 before and after the collision with the DI projectile. Red shows the continuum component of the spectra: $I_{cont} = (I_{8.8\mu m} + I_{12.4\mu m})/2$. Green shows the 10-μm silicate peak component: $I_{peak} = I_{10.5\mu m} - I_{cont}$. The peak component comes from fine-grain silicate dust, and the continuum component comes from carbon-rich dust and/or larger size silicate dust. The times when the images are obtained are shown in each panel. Each image is subtracted by the image taken 2 days before the impact (i.e., UT 2 July 2005). The image in (A) shows that the dust around the comet is dominated by the continuum component even after the small burst activity that occurred soon after our observation on UT 2 July 2005.

plume expansion and decay in surface brightness can be seen more quantitatively in light curve measurement (*5*) (Fig. 2). The light flux within each aperture size reached the maximum within the first hour after the impact. After the first hour, the light flux within small apertures [4-pixel and 8-pixel radii (*6*)] decreased rapidly. In contrast, the rate of decrease in the light flux within larger apertures was rather small in the first 3 hours and became larger subsequently. These photometric observations suggest that the decrease in light flux is simply attributed to the escape of dust from the observed apertures and does not require any special dust elimination process.

The monotonic decrease in the total light flux from the comet after the first hour also indicates that there was no sustained major supply of dust from the cometary surface, which would have increased the total light flux (*7*, *8*). Thus, most of the dust in the plume most likely represents the impact ejecta thrown out directly by the DI cratering event.

Another important aspect of the dust plume is its color change. The emission spectrum from the coma was dominated by the continuum component (Fig. 1A, red) with little sign of silicate feature at the wavelength of 10 μm (green), but the DI collision markedly increased the silicate feature within 1 hour (Fig. 1B). The strong 10-μm silicate emission feature continued throughout the rest of the observation time on UT 4 July 2005 (up to 3.5 hours after the impact). However, the 10-μm peak had disappeared by the beginning of our observation on UT 5 July 2005.

Such time evolution can be seen more quantitatively in the SED measurement. The SED before the impact showed almost no 10-μm feature and is relatively flat through the observed wavelength range (fig. S2). After the impact, however, a strong signal of 10-μm silicate feature appeared (Fig. 3). This indicates that small (submicrometer to micrometer) silicate grains were excavated from the comet interior (*9*, *10*). The continuum component of light throughout all observed wavelengths also increased. The increase at wavelengths of 17.7 and 18.8 μm in the Q band is consistent with the presence of small silicate grains in the dust plume (*9*, *10*). The light flux decreased rather rapidly across all wavelengths and returned almost to the pre-impact level after 1 day. However, the elevated Q-band light flux was still present (fig. S2).

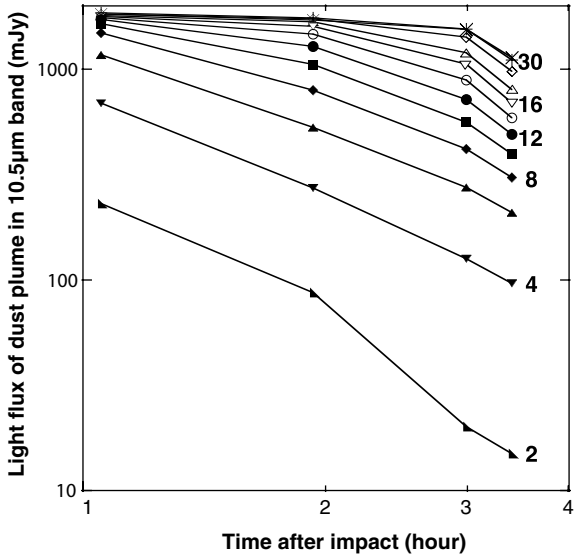

Fig. 2. Time evolution of the light flux of the impact-induced dust plume around comet 9P/Tempel 1 at 10.5 μm, as a function of time for different apertures. The light flux of the dust plume shown is calculated by subtracting the pre-impact light flux obtained on UT 3 July 2005 from the light flux observed after the impact. The time origin is taken to be the impact point. The radii of apertures are shown in pixels (i.e., 0.13 arc sec); the radii of the nine smallest apertures shown in the figure are from 2 to 18 pixels in increments of 2 pixels, and those of the three largest are from 22 to 30 pixels in increments of 4 pixels. mJy, millijansky.

A more detailed examination of SED data reveals that the 10-μm silicate feature decreased more rapidly than the N-band continuum in the close vicinity of the comet nucleus (fig. S2). This selective decrease in the 10-μm peak around the comet can also be seen in the multiband color images, in a reddish color near the center in Fig. 1D. This emergence of continuum-dominated light (i.e., carbon-rich or large dust grains) near the nucleus suggests that the ejection of fine silicate grains was short-lived and was replaced rather rapidly by a different type of dust, which is similar to that found around typical Jupiter-family comets.

Although the SED data unambiguously show the presence of fine-grained silicates in the dust plume, spectroscopic measurement and analysis are required to obtain more quantitative characteristics of the dust, such as mineralogical composition, porosity, crystallinity, and size distribution. We carried out model calculations with a variety of size distribution functions and a wide range of free parameters (*5*).

Model-fitting with a power-law size distribution, the Hanner size distribution (*11*), log-normal distribution, and constant number distribution between maximum and minimum sizes yielded similar estimates for mineralogical composition, crystallinity, and porosity of dust (*5*). The masses (in 10^5 kg) of crystalline olivine, amorphous olivine, crystalline pyroxene, amorphous pyroxene, and amorphous carbon grains in the dust plume estimated with the Hanner size distribution function are 1.59 ± 0.14, 4.05 ± 0.44, 0.18 ± 0.04, 1.65 ± 0.87, and 0.84 ± 0.16, respectively (*5*). The fractal dimension (*12*) of amorphous grains is estimated to be between 2.7 and 2.8. The high mass ratio of crystalline silicates to amorphous silicates shows that comet 9P/Tempel 1, a Jupiter-family comet, contains a large fraction of a high-temperature component of the solar nebula, similarly to Oort-cloud comets. A similar result was obtained from Gemini telescope observations (*13*).

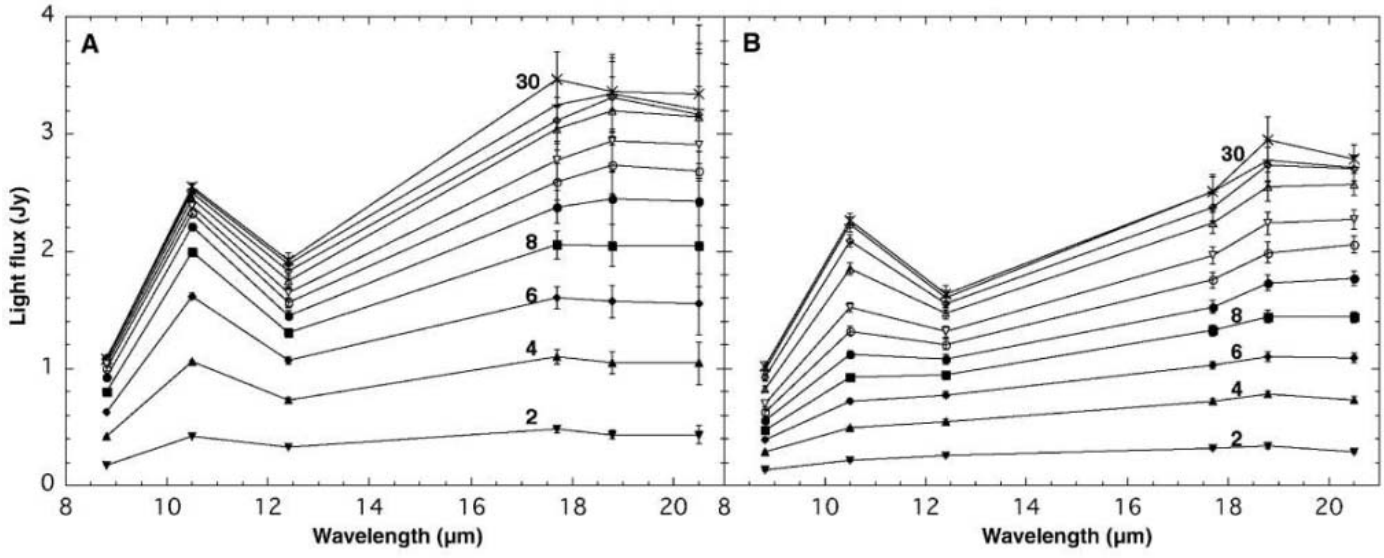

Fig. 3. The SED of comet 9P/Tempel 1 (**A**) 1 hour and (**B**) 3.5 hours after the DI impact. Light fluxes for different radii of apertures at each wavelength are shown. The radii of apertures are indicated in pixels. The radii of apertures are the same as in Fig. 2.

The observed high mass ratio (~0.3) of crystalline silicates to amorphous silicates observed for the interior of comet 9P/Tempel 1, a Jupiter-family comet, is much higher than that (~0.02) observed for another Jupiter-family comet, 78P Gehrels 2, and is the highest among any Jupiter-family comets observed so far (*14*). The high mass ratio is rather close to those for Oort-cloud comets, such as comets Hale-Bopp (~0.7) and C/2001 Q4 (NEAT) (~0.2), where the mass ratios for the two comets are calculated on the basis of the dust number ratios obtained by previous observations (*15*, *16*) and the dust size range used in this study. Jupiter-family comets have not been thought to have many high-temperature silicate grains, unlike Oort-cloud comets. The high abundance of crystalline silicates suggests that the interior of Jupiter-family comets may contain a substantial amount of material that went through high-temperature conditions in the early solar nebula.

The spectral analysis also provides information on grain size distribution. A χ^2 test indicates that four of the five distribution functions we tried provided similarly good fits to the data when similar parameter values were chosen (*5*). Regardless of the choice of a model function, the calculations show that the peak grain size was around 1 μm and that the dust ranged in size from <1 to ~10 μm across, and perhaps even larger (*17*).

The observed spectrum is best fit with a power-law in the large dust size range (>1 μm) with an exponent of between –3.5 and –3.6. These values are similar to those for Oort-cloud comets, such as comets Hale-Bopp and C/2001 Q4 (NEAT) (*15*, *16*). This similarity in size distribution again suggests that the DI collision excavated fresh cometary material from the interior of 9P/Tempel 1.

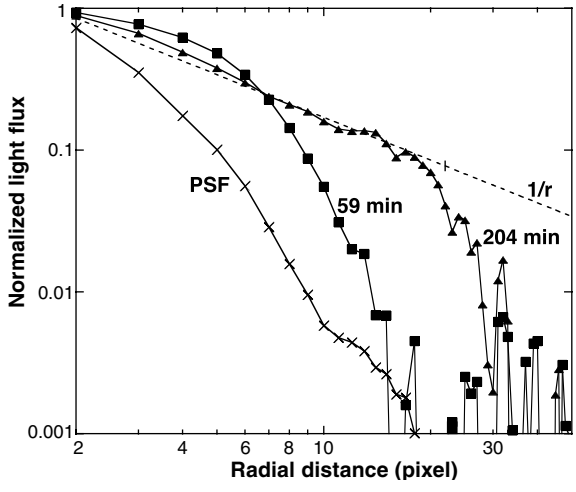

Fig. 4. Time evolution of the radial brightness profile around comet 9P/Tempel 1 at the 10.5-μm wavelength. The normalized radial profiles observed along the 225° PA line at 59 and 204 min after the impact are shown with point spreading function (PSF). The dotted straight line is r^{-1}, where r is the radial distance from the nucleus.

The observation that the interior of a Jupiter-family comet, 9P/Tempel 1, has a dust distribution and a crystalline-to-amorphous ratio of silicates similar to those of Oort-cloud comets such as Hale-Bopp and C/2001 Q4 (NEAT) suggests that these two families of comets with different dynamic characteristics may have a similar origin. Recent observations and dynamical simulations suggest that the most likely precursors of Jupiter-family comets are not classical Kuiper-belt bodies, which are thought to have formed farther from the Sun than Neptune, but scattered disk bodies in the Kuiper belt, which are thought to have formed in the giant planets region (*18*). The observed similarity in the dust properties between 9P/Tempel 1 and Oort-cloud comets, which are also thought to have formed in the giant planets region, supports this hypothesis.

The results of the analysis for the size distribution and composition allow us to estimate that, based on our SED measurement of the comet, 1.4×10^5 to 1.9×10^5 kg of crystalline dust particles were emitted by the impact (*19*). This is a lower estimate. Because the maximum size of dust is difficult to constrain using the spectroscopic data, we took a 1-m block as the maximum size. The total mass would then be 2.8×10^7 to 7.0×10^7 kg, which gives an upper estimate. Such large blocks of solid material would be expected to have been observed by the spacecraft, but no sign of such large blocks was reported (*3*). Thus, the total dust mass would be substantially smaller than the upper estimate. When the maximum dust size is taken to be 10 μm, based on the above N-band spectroscopic analysis, and the standard Hanner size distribution is used, the total mass is estimated to be 5.6×10^5 to 8.5×10^5 kg. This range is probably closest to the actual total dust mass in the plume (*5*).

The lower estimate for the crystalline silicate mass is 10 times the upper estimate for the mass that can be devitrified by impact

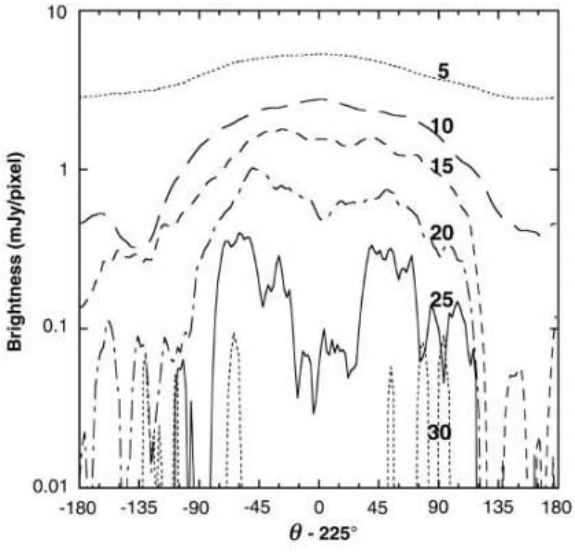

Fig. 5. Angular profile of brightness around 9P/Tempel 1 3 hours after the impact. The light flux per pixel (0.130″ × 0.130″) at different radial distances from the nucleus is shown as a function of θ – 225°, where θ and 225° are position angle and the symmetry direction of the plume, respectively. The radial distances in pixels from the nucleus are indicated.

shock heating due to the DI collision (*5*). Thus, most of the crystalline dust particles were not devitrified and likely represent the intrinsic composition of the cometary interior.

The observed dust mass in the plume can be used to constrain the cratering style. The observed dust mass should correspond to the mass of ejecta thrown from the impact site at velocities higher than the escape velocity of 9P/Tempel 1. If the crater growth was controlled by gravity, the mass of ejecta at velocities higher than the escape velocity is estimated to be $\sim 1.5 \times 10^6$ kg (*5*). Because this mass includes both dust and ice, the dust mass in the plume should be slightly smaller. The dust mass predicted for gravity-controlled cratering will then be close to the observed dust mass (5.6×10^5 to 8.5×10^5 kg). However, if compaction and/or target strength plays an important role in cratering, the ejecta mass will be reduced significantly (*20*, *21*) and become inconsistent with the observed dust mass. This suggests that the cratering process induced by the DI collision was controlled by gravity.

The high-resolution mid-IR images of 9P/Tempel 1 also reveal important aspects of the dust plume dynamics. Figure 4 shows the time progression of the radial profile of 10.5-μm brightness along the 225° PA from the comet nucleus. The radial profile exhibits a monotonic decrease as a function of distance from the nucleus. A classic ejecta curtain model predicts that the mass distribution will decrease monotonically as a function of ejection velocity (*22*). However, a quantitative comparison shows a discrepancy between the observation and a simple cratering model. A standard ejecta mass-velocity relation in the gravity regime predicts an $r^{-3.22}$ profile, where r is the distance from the nucleus (*5*), but the observed radial profile does not follow this trend. It is better fit with two power-law slopes: an inner r^{-1} profile and an outer r^{-5} profile (*23*).

An r^{-1} radial profile is commonly seen in typical cometary coma. This profile is maintained by a steady-state gas production on the nucleus surface and a constant radial expansion velocity (*24*). The observed constant expansion velocity of the dust plume is also consistent with such a steady-state gas production model. A major steady-state dust supply from the cometary surface, however, would contradict the observed monotonic decrease in the total light flux (Fig. 2).

It is likely that the r^{-1} profile requires an acceleration process for dust particles in addition to gravity-controlled excavation flow, such as volatile evaporation and expansion. One possible model for the observed radial brightness profile is that low-velocity ejecta with a large fraction of ice, which stays initially around the nucleus, is gradually vaporized by the solar radiation and expands radially. If the ejecta evaporation rate is regulated by the solar influx, an apparent constant gas production may be achieved. Vaporization of micrometer-sized ices, however, will take much less than a few hours. Much larger millimeter-sized ice grains are needed to account for such a long time scale, but it is uncertain at this point if there are such large ice grains in the plume.

The angular profile of the dust plume provides additional information on the DI cratering process and the subsequent plume dynamics. Figure 5 shows angular profiles of brightness of the dust plume at different radial distances from the nucleus. A relatively isotropic brightness distribution near the nucleus (e.g., a 5-pixel radius circle) gradually changed to a profile with a clear concentration centered at ~225° PA (e.g., a 20-pixel radius circle). Near the leading edge of the dust plume (a 25-pixel radius circle), the brightness was concentrated in two directions, about ±45° away from the symmetric center (~225° PA) of the plume (*5*). The maximum brightness of the two peaks is almost 10 times the average outside the peaks. Such peaks in the about ±45° directions (*5*) suggest the presence of a classic ejecta curtain (*25*, *26*), not consistent with compaction-controlled cratering, which typically forms a high-angle ejecta plume (*27*). However, such peaks at about ±45° are limited to the leading part of the plume. The inner part of the plume exhibits an oval or single-fan-shaped distribution without a central depression near 225° PA. The angular distribution pattern in the inner part of the dust plume is rather inconsistent with a simple crater ejecta curtain model. This may also reflect the effect of the outgassing process from ice-rich ejecta.

Thus, analyses of both radial and angular profiles show that the outer part of the dust plume is consistent with a gravity-controlled cratering model and that the inner part was influenced further by volatile evaporation and expansion. This is qualitatively consistent with crater excavation dynamics, because higher speed ejecta (i.e., the outer portion of the ejecta curtain) comes from near the surface and slower ejecta (i.e., the inner portion of the ejecta curtain) is biased toward material from deeper in the target (richer in volatiles in the DI case) (*28*). The inference that DI excavated a volatile-rich layer is further consistent with both the detection of gaseous molecules by other telescopes and the DI spacecraft (*3*, *4*) and with our observation of fine silicate grains with properties similar to those of active Oort-cloud comets, which are generally rich in volatiles.

The reason why a major jet did not occur after the excavation of a volatile-rich layer remains unanswered. It may be because the excavated fresh material inside comet 9P/Tempel 1 had been partially depleted in volatiles or because a jet cannot form by a simple exposure of volatile-rich material to the space.

References and Notes

1. Observation was conducted for four nights on UT 2 to 5 July 2005. In particular, observation on UT 4 July 2005 was conducted in coordination with the Gemini telescope in order to obtain data complementary to each other (*13*).
2. D. L. Hampton *et al.*, *Space Sci. Rev.* **117**, 43 (2005).
3. M. F. A'Hearn *et al.*, *Science* **310**, 258 (2005); published online 8 September 2005 (10.1126/science.1118923).
4. K. J. Meech *et al.*, *Science* **310**, 265 (2005); published online 8 September 2005 (10.1126/science.1118978).
5. Materials and methods are available as supporting material on *Science* Online.
6. The scale for the COMICS imaging mode is 0.130″ per pixel. This corresponds to 84.2 km/pixel on the surface of comet 9P/Tempel 1.
7. The cooling of impact-generated heat is not expected to contribute significantly to the decrease in light flux. The radiative cooling time scale for 10-μm size silicate particles from 1000 K to 200 K is on the order of a minute, much shorter than the observation time scale of this study.
8. The observed data do not rule out a minor dust supply from the surface, which has a total dust production much smaller than the total dust amount in the plume.
9. M. S. Hanner, D. K. Lynch, R. W. Russell, *Astrophys. J.* **425**, 274 (1994).
10. J. Crovisier *et al.*, *Science* **275**, 1904 (1997).
11. M. S. Hanner, *Comet. Explor.* **2**, 1 (1983).
12. The porosity of amorphous grains is given by fractal dimension D. The porosity increases as a function of size when $D < 3$. The porosity of crystalline grains is assumed to be zero (i.e., $D = 3$).

13. D. E. Harker, C. E. Woodward, D. H. Wooden, *Science* **310**, 278 (2005); published online 15 September 2005 (10.1126/science.1119143).
14. J. Watanabe *et al.*, *IAU Symp. Abstr. 229, Asteroids, Comets, Meteors*, Rio de Janeiro, Brazil, 7 to 12 August 2005, p. 47 (2005).
15. D. E. Harker, D. H. Wooden, C. E. Woodward, C. M. Lisse, *Astrophys. J.* **615**, 1081 (2004).
16. D. H. Wooden, C. E. Woodward, D. E. Harker, *Astrophys. J.* **612**, L77 (2004).
17. Because most of the light in the 10-μm emission peak comes from the smallest grains (sub-μm to μm), the smallest grains can account for the magnitude of the observed 10-μm peak light flux. The observed N-band spectral shape of the 10-μm peak, however, cannot be reproduced well with the smallest grains only and requires larger grains. The synthetic spectral shape improves gradually as the maximum grain size is increased to 10 μm. In contrast, when the maximum size is increased to significantly larger than 10 μm, the synthetic spectrum neither improves nor deteriorates. Thus, N-band spectroscopy cannot constrain the size distribution of dust larger than 10 μm. This is because these large grains do not contribute to the silicate feature around the 10-μm wavelength (*9*, *10*).
18. B. Gladman, *Science* **307**, 71 (2005).
19. We used the SED data obtained 1 hour after the impact for estimating the total dust mass in the plume. Because the total light flux of the plume was approximately constant in the first few hours in our observation (Fig. 2), the mass estimate does not change significantly during this time.
20. K. R. Housen, K. Holsapple, *Icarus* **163**, 102 (2003).
21. H. J. Melosh, *Impact Cratering: A Geologic Process* (Oxford Univ. Press, New York, 1989).
22. K. R. Housen, R. M. Schmidt, K. A. Holsapple, *Geophys. Res.* **88**, 2485 (1983).
23. Because the r^{-5} slope in the outer portion is similar to that of PSF, the exponent value of –5 may be artificial. Thus, the actual outer profile may be significantly steeper than r^{-5}. Results of impact experiments indicate that the power-law relation between mass and ejection velocity has a cut-off velocity above which ejecta mass is much smaller than that predicted by equation (fig. S5) (*29*, *30*). This will lead to a radial profile significantly steeper than $r^{-3.22}$. This may account for the observed steep profile in the outer portion of the dust plume.
24. K. S. Krishna Swamy, *Physics of Comets* (World Scientific, Singapore, 1997), ed. 2.
25. D. E. Gault, E. D. Heitowit, *Proc. Sixth Hypervelocity Impact Symp.* **2**, 419 (1963).
26. M. J. Cintala, L. Berthoud, F. Hörz, *Meteor. Planet. Sci.* **34**, 605 (1999).
27. P. H. Schultz, C. M. Ernst, J. L. B. Anderson, *Space Sci. Rev.* **117**, 207 (2005).
28. S. K. Croft, *Proc. Lunar Planet. Sci. Conf.* **11**, 2347 (1980).
29. W. K. Hartmann, *Icarus* **63**, 69 (1985).
30. S. Yamamoto, T. Kadono, S. Sugita, T. Matsui, *Icarus*, in press; published online 25 May 2005.
31. This report is based on data collected at the Subaru Telescope, which is operated by the National Astronomical Observatory of Japan (allocation nos. S05A-042 and S05A-OT11). This research is partially supported by a Grant in Aid from the Japan Society for the Promotion of Science.

Supporting Online Material
www.sciencemag.org/cgi/content/full/1119091/DC1
Materials and Methods
Figs. S1 to S5
References and Notes

19 August 2005; accepted 9 September 2005
Published online 15 September 2005;
10.1126/science.1119091
Include this information when citing this paper.

REPORT

The Dust Grains from 9P/Tempel 1 Before and After the Encounter with Deep Impact

David E. Harker,[1]* Charles E. Woodward,[2] Diane H. Wooden[3]

Gemini-N observed the properties of dust ejected from the nucleus of comet 9P/Tempel 1 before and after its encounter with Deep Impact. Marked changes were seen in the 7.8- to 13-micrometer spectral energy distribution and derived grain properties of the inner coma. A strong, broad silicate feature dominated by emission from amorphous pyroxene, amorphous olivine, and magnesium-rich crystalline olivine had developed by 1 hour after impact. The ejected dust mass is ≅10^4 to 10^6 kilograms on the basis of our models. Twenty-six hours later the silicate feature had faded, leaving a smooth featureless spectrum, similar to that observed before the impact, suggesting that the impact did not produce a new active region releasing small particles on the nucleus.

Comets are composed of ices, gases, and dust extant at the epoch of planet formation. Cometary dust properties can be determined using mineral resonance features observable through mid-infrared (IR) remote-sensing spectrophotometry. Many long-period Oort cloud (OC) comets (*1*–*4*) and a few Jupiter-family (JF) comets (*5*, *6*) contain crystalline silicates that formed in the early solar nebula at temperature $T > 1000$ K. The properties of cometary grains provide insight into the thermal processing and radial transport of dust during the epoch of planet formation (*7*). JF comet nuclei originated in the Kuiper Belt (*8*), a region populated by icy bodies, and completed their aggregation and inward radial migration in the trans-Neptune region (*9*, *10*), whereas OC comet nuclei were ejected from the trans-Jupiter region (*9*). The Deep Impact (DI) event (*11*) provided an opportunity to examine the mineral composition of material within the potentially pristine subsurface layers below the highly processed nuclear surface of the short-period JF comet, 9P/Tempel 1 (9P), at a heliocentric distance (r_h) of 1.51 astronomical units (AU), and to compare coma grain properties to the ostensibly more pristine dust that characterizes the coma of OC comets. Here we present mid-IR observations obtained with the MICHELLE imaging spectrograph on the 8-m Fredrick C. Gillette (Gemini-N) telescope on Mauna Kea, Hawaii, spanning a 30-hour period during DI (*12*).

Before impact (time $t = -0.08$ hours), we acquired narrowband 11.7-μm images of the nucleus to position the 0.6 arc sec wide MICHELLE-slit. The data show (Fig. 1) that the coma surface brightness was centrally condensed. The 7.8- to 13.0-μm spectral energy distribution [SED; derived using a 0.6 arc sec by 1.0 arc sec extraction aperture ("the beam") centered on the peak coma surface brightness] was featureless. We fit a 287 ± 10 K blackbody (BB) to the featureless emission at wavelengths $\lambda \leq 8.2$ μm and $\lambda \geq 12.4$ μm, outside of silicate resonance features (*13*); the silicate feature strength (defined as $F_{feature}/F_{continuum,BB}$ at 10.3 μm; $\Delta\lambda = 1.0$ μm) was about unity before the impact. After impact, the coma flux brightened and the shape of the SED changed. The silicate feature strength increased to 1.6 (on the basis of a 294 ±10 K blackbody continuum) and changed in shape to a broad silicate feature showing individual mineral resonances ($t = +1.0$ hours). The 11.7-μm surface brightness became extended, forming an asymmetric plume along a position angle of ≈225° from the comet nucleus, a feature evident from the deep mid-IR imagery obtained by the Subaru/COMICS team (*14*). About 1.8 hours after impact, the silicate feature strength began to decline (to ~1.4 with a 286 ± 10 K blackbody continuum), returning to the value of 1 within ≈26.4 hours.

The measured comet flux is a combination of the instrumental point spread function (PSF) due to the nucleus and an extended surface brightness (which generally varies as ρ^{-n}, where ρ is the projected distance from the nucleus and $n \sim 1$) (*15*) due to the surrounding dusty coma. We derived an estimate of the nuclear flux by comparing cumulative photometry measurements in synthetic apertures of increasing radii (*16*) applied to 10.3-μm images of comet 9P and the standard Kappa Virginis (representing the instrumental PSF) both obtained on 2 July 2005 UT

[1]Center for Astrophysics and Space Sciences, University of California, San Diego, 9500 Gilman Drive, Department 0424, La Jolla, CA 92093–0424, USA. [2]Department of Astronomy, University of Minnesota, 116 Church Street, SE, Minneapolis, MN 55455, USA. [3]NASA Ames Research Center, MS 245-3, Moffett Field, CA 94035–1000, USA.

*To whom correspondence should be addressed. E-mail: dharker@ucsd.edu

with an identical instrumental configuration. By this technique, the relative ratio of the nuclear flux to the total flux measured in our spectral beam at 10.3 μm was constrained to be ≅0.80 ± 0.02. The rotation period of the comet is slow enough such that the nucleus has a low thermal inertia, i.e., the nucleus is essentially isothermal (*11*, *17*). Although there are some variations in nuclear brightness as the comet rotates (*11*, *17*), we found that between 3 and 5 July 2005 UT, the 11.7-μm flux in our beam only varied between 0.40 and 0.43 ± 0.01 Jy, and on 2 July 2005 UT, the 11.2-μm flux was 0.38 ± 0.01 Jy. Therefore, in our model, we account for the nucleus flux by using the Asteroid Standard Thermal Model (STM) (*18*) with a nuclear effective radius of 3.3 km and geometric albedo of 0.04 (*17*), scaled to contribute 80% of the thermal flux at 10.3 μm at all epochs. The peak temperature of the nucleus of comet 9P calculated from the STM is 352 K.

We modeled the spectra (Fig. 1) using a thermal grain model developed for the analysis of OC comet C/1995 O1 (Hale-Bopp) (*1*, *2*) further refined to self-consistently calculate the temperature and thermal emission from crystalline silicates using laboratory optical constants (*19*). This model uses the Hanner grain size distribution (HGSD) (*2*, *20*, *21*) to calculate the emission from a population of grains varying in radii from 0.1 to 100 μm. The slope of the grain size distribution, N, is fixed at 3.7 to match the canonical fit from our thermal modeling of Hale-Bopp and the slope, M, is varied to modify the location of the peak (a_p) of the size distribution (*22*). The fractal porosity, D, of the grains is also a variable parameter (*23*, *24*). The high signal-to-noise (≅14) of the Gemini-N (+MICHELLE) spectra are well fit by our thermal models [reduced chi-squared (χ^2_ν) ~ 0.7], constraining the six free parameters in the model.

Before impact (t = −0.08 hours), the measured thermal emission from comet 9P was dominated by flux from the nucleus. The flatness of the spectrum indicates that submicrometer-sized silicate grains were not present in any appreciable amount in the coma. This is consistent with our best-fit χ^2-models composed of a population of fractal porous (D = 2.857; a 1-μm radii grain is 28% vacuum) preimpact grains, mineralogically dominated by amorphous olivine, with a HGSD that peaks with a_p = 0.9 μm. Adding other materials into the coma dust population did not produce a better fit. The best-fit model using only solid grains (D = 3.0) peaks at a_p = 0.8 μm, but does not provide as good a χ^2-fit as the D = 2.857 grain model.

Dust released by the impact was clearly detected. The spectrum at t = +1.0 hours indicates that the number of submicrometer-sized silicates increased, as did the number of amorphous carbon grains, which contribute to the featureless emission outside the silicate resonances ($\lambda \leq 8.2$ μm and $\lambda \geq 12.4$ μm), i.e., the "10 μm continuum" (Fig. 2). Also evident is a sharp peak at 11.2 μm due to emission from relatively transparent (i.e., poorly absorbing), Mg-rich crystalline olivine (*25*). Orthopyroxene signatures (~9.2 and 10.5 μm) were not clearly evident in the spectra of comet 9P, and addition of this material in our models did not improve the fit.

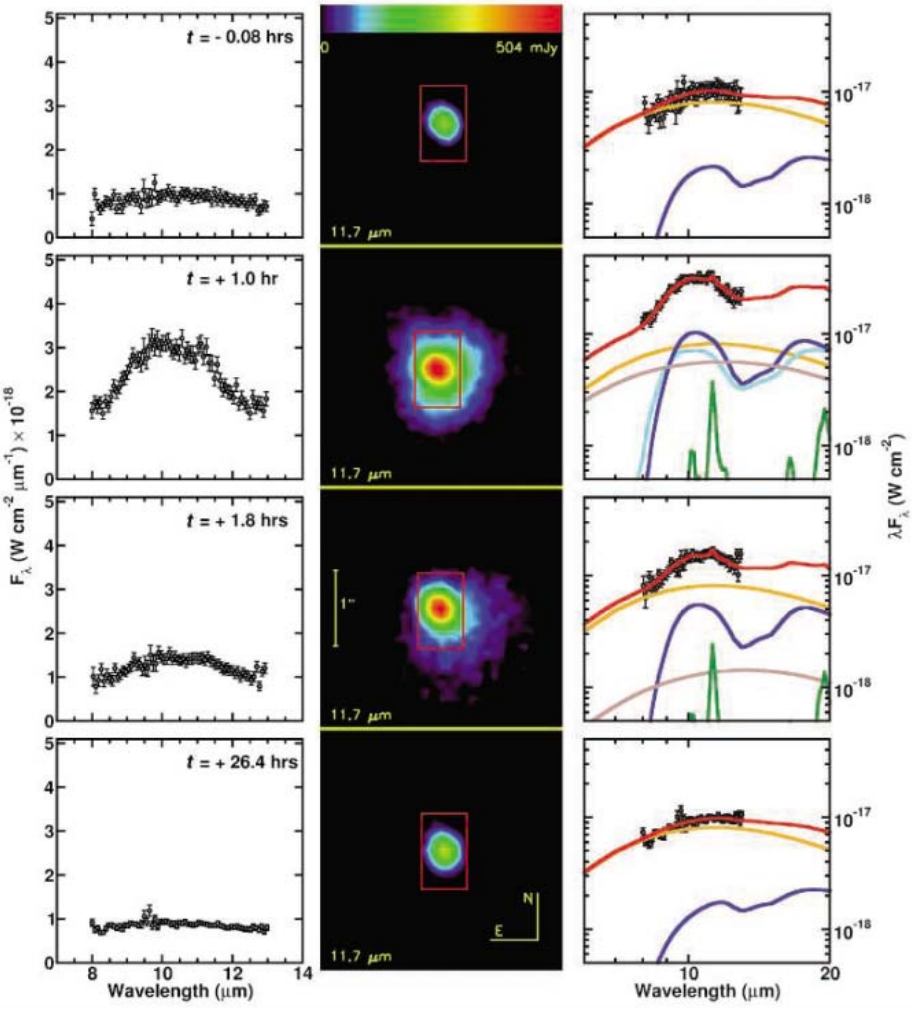

Fig. 1. Imaging and spectroscopy of four temporal epochs of comet 9P/Tempel 1 obtained before and after impact. For each epoch, the 10-μm spectrum [(left column, F_λ (W cm^{-2} μm^{-1})] and an 11.7-μm image (center column) is shown. The thermal model (right column, λF_λ (W cm^{-2})] for each epoch is plotted on top of the observed spectra. For epochs t = −0.08, +1.0, and +1.8 hours, the on-source integration time for each spectrum is 100.8 s. For the t = +26.4-hours epoch, the on-source integration time for the spectrum is 705.6 s. The size of the extraction aperture for all spectra is a 0.6 arc sec by 1.0 arc sec rectangle (392 km by 653 km) centered on the brightest part of the coma, and is indicated in red in each image. Plotted model components are the total model SED (red line); STM nucleus flux (orange line); amorphous olivine (blue line); amorphous pyroxene (cyan line); amorphous carbon (brown line); and crystalline olivine (green line).

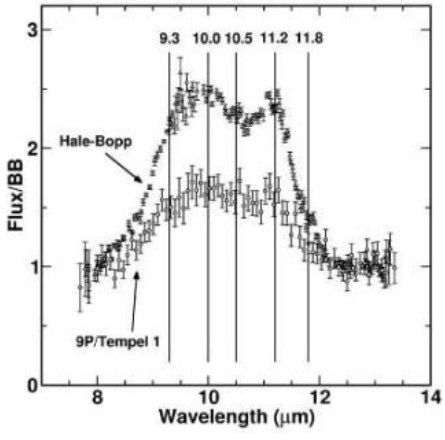

Fig. 2. Comparison of blackbody continuum normalized spectra of Jupiter Family comet 9P/Tempel 1 (open circles) at t = +1.0 hours after impact (287 K blackbody) to the Oort cloud comet C/1995 O1 (Hale-Bopp) obtained after perihelion on June 22 1997 UT (r_h = 1.7 AU; 283 K blackbody) (open triangles). The labeled vertical lines identify possible crystalline silicate features including Mg-rich crystalline olivine (10.0, 11.2, and 11.8 μm) and orthopyroxene (9.3 and 10.5 μm). The error bars denote 1σ error in the flux.

Table 1. Mass ratio of materials in the coma of comet 9P/Tempel 1 to total of submicrometer-sized grains for four temporal epochs relative to the impact time.

t (hours)	Amorphous pyroxene	Amorphous olivine	Amorphous carbon	Crystalline olivine	χ^2_ν	Silicate/ carbon	Crystalline silicate/ amorphous silicate
−0.08	0.	1.0	0.	0.	0.603	…	…
+1.0	0.411	0.273	0.212	0.104	0.734	3.7	0.15
+1.8	0.106	0.456	0.120	0.309	0.386	7.3	0.55
+26.4	0.	1.0	0.	0.	0.915	…	…

Thus, the dust ejected into the coma as a result of the impact in comet 9P was a mixture of grains with a composition of amorphous carbon, amorphous pyroxene, amorphous olivine, and Mg-rich crystalline olivine (HGSD peak a_p = 0.3 μm and M = 7.4). The amorphous grains are slightly porous (D = 2.857), whereas the crystalline grains remain solid (D = 3.0). The derived relative masses of the submicrometer-sized grains and the silicate-to-carbon and crystalline-to-amorphous silicate ratios show the changes in the composition of the dust ejecta at the observed epochs (Table 1). The total mass of dust seen in the beam is dependent on the cutoff of the grain-size distribution. At t = +1.0 hour, the total mass of dust within our beam (projected area 392 km by 653 km) calculated using the fit HGSD cutoff at 1- and 100-μm-radius grains is 7.3 × 10^4 and 1.5 × 10^6 kg, respectively.

At t = +1.8 hours after impact, the strength of the silicate feature is clearly less than at t = +1.0 hours. To drift entirely out of our beam over this temporal period, grains would have to have a minimum velocity projected onto the sky of 0.13 km/s. Therefore, our measured decrease in silicate feature strength at t = +1.8 hours after impact most likely is a consequence of the small silicate grains moving faster than 0.13 km/s traveling out of the beam.

Thermal modeling of the dust grains at t = +1.8 hours reveals that the feature is still composed of the same materials as at t = +1.0 hours, but that the peak of the HGSD (a_p) has increased to 0.5 μm. Again, this is indicative of the smaller grains having moved outside of our beam. The remaining (larger) amorphous grains are still slightly fractal porous with D = 2.857. The relative masses of amorphous pyroxene and amorphous carbon have dropped substantially compared with those of amorphous and crystalline olivine.

The shape of the feature at t = +26.4 hours is nearly identical to that of the preimpact spectrum at t = −0.08 hours. It is apparent from this spectrum that a new, persistent active dust-producing area was not created by the impact. The surface brightness morphology of the 11.7-μm images show that the coma emission from comet 9P returned to the same flux level as existed before the impact, and none of the fan of material seen in the mid-IR in the hours after impact is evident. The grain model fitted to this epoch is identical in mineralogy and fractal porosity to the preimpact model: amorphous olivine grains and fractal porosity for the amorphous grains of D = 2.857. However, the HGSD has shifted to larger grains, constrained by our χ^2-fit to peak in the range of 1.5 to 1.8 μm in radii and the relative masses of the mineral grains changes (Table 1). By the next night, all submicrometer grains released by the impact appeared to be cleared out of the inner coma region at ~26 hours.

Our modeling of the spectra implies that in the preimpact nominally active or quiescent coma, larger dust grains (≥0.9 μm) of predominately amorphous olivine composition are present, presumably originating from the highly processed nuclear surface of this JF comet. These larger olivine-type grains could be aggregates of submicrometer mineral subgrains that display substantially reduced spectral contrast resonant features due to their incorporation into aggregate grain structures (*26*, *27*). Anhydrous chondritic porous interplanetary dust particles (IDPs) with IR spectra (bulk aggregate) similar to that of amorphous olivine and lacking in crystalline resonances are 1- to 10-μm-sized porous aggregates dominated by submicrometer subgrains of amorphous silicates, which also contain abundant fine-grained amorphous carbon. IR spectra of microtomed thin sections of these IDPs show distinct resonances of embedded submicrometer crystals (*26*–*28*). However, the ubiquitous presence of fine-grained amorphous carbon coatings on the surfaces of siliceous subgrains may make their mid-IR resonances indistinct (*29*, *30*). The fragmentation of such aggregate porous particles could free their submicrometer constituents so as to make their mid-IR resonances distinguishable in contrast with the observable continuum. In the DI ejecta, the presence of abundant amorphous olivine and crystalline olivine, together with amorphous carbon and amorphous pyroxene, makes a fragmentation scenario plausible.

On the other hand, the impact may have ejected pristine subsurface submicrometer mineral grains similar to those pristine grains present in the comae of highly active (jet-dominated) OC comets Hale-Bopp and C/2001 Q4 (NEAT) (*1*, *2*, *31*). The submicrometer grains in the impact-induced ejecta of comet 9P have size distributions and mineralogies similar to those of dust produced by the highly active areas (jets) in the former OC comet comae. This suggests that, for a period, the new population of postimpact comet 9P coma grains were associated with, or were stimulated to fragment by their association with, volatiles released from a temporally transient active area triggered by the DI impact (*11*, *13*).

References and Notes

1. D. E. Harker, D. H. Wooden, C. E. Woodward, C. M. Lisse, *Astrophys. J.* **615**, 108 (2004).
2. D. E. Harker, D. H. Wooden, C. E. Woodward, C. M. Lisse, *Astrophys. J.* **580**, 579 (2002).
3. D. H. Wooden, *Earth Moon Planets* **89**, 247 (2002).
4. M. S. Hanner, J. P. Bradley, in *Comets II*, M. Festou *et al.*, Eds. (Univ. of Arizona Press, Tucson, AZ, 2005), p. 555–564.
5. W. Reach, paper presented at the 36th Annual Division of Planetary Sciences Meeting, Louisville, KY, 8 November 2004.
6. J. Crovisier *et al.*, *ASP Conf. Ser.* **196**, 109 (2000).
7. D. H. Wooden, D. E. Harker, A. J. Brearley, in *Chondrites and the Protoplanetary Disk* (Astronomical Society of the Pacific, Provo, UT, 2005).
8. S. A. Stern, *Nature* **424**, 639 (2003).
9. H. F. Levison, A. Morbidelli, *Nature* **426**, 419 (2003).
10. R. S. Gomes, *Icarus* **161**, 404 (2003).
11. M. F. A'Hearn *et al.*, *Science* **310**, 258 (2005); published online 8 September 2005 (10.1126/science.1118923).
12. Materials and methods are available as supporting material on *Science* Online.
13. M. S. Hanner, D. K. Lynch, R. W. Russell, *Astrophys. J.* **425**, 274 (1994).
14. S. Sugita *et al.*, *Science* **310**, 274 (2005); published online 15 September 2005 (10.1126/science.1119091).
15. D. Jewitt, in *Comets in the Post-Halley Era*, R. L. Newburn Jr. *et al.*, Eds. (Kluwer, Dordrecht, Netherlands, 1991), vol. 1, pp. 19–65.
16. D. H. Wooden, Y. R. Fernandez, M. F. Kassis, D. E. Harker, C. E. Woodward, IAU Symp. No. 229 (2005).
17. C. M. Lisse *et al.*, *Astrophys. J.* **625**, L139 (2005).
18. M. Delbo, A. W. Harris, *Meteorit. Planet. Sci.* **37**, 1929 (2002).
19. Laboratory Astrophysics Group of the AIU Jena, www.astro.uni-jena.de/Laboratory/OCDB/newsilicates.html
20. M. S. Hanner, in *Cometary Exploration*, T. I. Gombosi, Ed. (Hungaria Academy of Sciences, Budapest, 1983), vol. 2, pp. 1–22.
21. $n(a) = (1 - a°/a)^M\ (a°/a)^N$; $a° = 0.1$ μm.
22. $a_p = a°\ (M + N)/N$.
23. C. M. Lisse *et al.*, *Astrophys. J.* **496**, 971 (1998).
24. The filling factor of vacuum to be used in Maxell-Garnett mixing theory to produce a porous grain is $f = 1 - (a/a°)^{D-3}$.
25. C. Koike *et al.*, *Astron. Astrophys.* **399**, 1101 (2003).
26. J. P. Bradley *et al.*, *Science* **285**, 1716 (1999).
27. F. J. Molster *et al.*, *Lunar Planet. Sci. Conf.* **32**, 1391 (2001).
28. J. P. Bradley *et al.*, *Lunar Planet. Sci. Conf.* **29**, 1737 (1998).
29. L. P. Keller, S. Messenger, J. P. Bradley, *J. Geophys. Res.* **105**, 10397 (2000).
30. B. Wopenka, *Earth Planet. Sci. Lett.* **88**, 221 (1988).
31. D. H. Wooden, C. E. Woodward, D. E. Harker, *Astrophys. J.* **612**, L77 (2004).
32. D.E.H. and C.E.W. acknowledge support from the NSF (AST03-07466). D.E.H. and D.H.W. acknowledge support from the NASA Planetary Astronomy Program (RTOP 344-32-21-04). We thank S. Fisher, C. Trujillo, and G. Trancho for their support. Based on observations obtained at the Gemini Observatory (Gemini observing program GN-2005A-DD-9), which is operated by the Association of Universities for Research in Astronomy, Inc., under a cooperative agreement with the NSF on behalf of the Gemini partnership: the NSF (United States), the Particle Physics and Astronomy Research Council (UK), the National Research Council (Canada), CONICYT (Chile), the Australian Research Council (Australia), CNPq (Brazil), and CONICET (Argentina).

Supporting Online Material

www.sciencemag.org/cgi/content/full/1119143/DC1
SOM Text

22 August 2005; accepted 2 September 2005
Published online 15 September 2005;
10.1126/science.1119143
Include this information when citing this paper.

Deep Impact Observations by OSIRIS Onboard the Rosetta Spacecraft

Horst Uwe Keller,[1]* Laurent Jorda,[2] Michael Küppers,[1] Pedro J. Gutierrez,[3] Stubbe F. Hviid,[1] Jörg Knollenberg,[4] Luisa-Maria Lara,[3] Holger Sierks,[1] Cesare Barbieri,[5] Philippe Lamy,[2] Hans Rickman,[6] Rafael Rodrigo[3]

The OSIRIS cameras (optical, spectroscopic, and infrared remote imaging system) onboard the European Space Agency's Rosetta spacecraft observed comet 9P/Tempel 1 for 17 days continuously around the time of NASA's Deep Impact mission. The cyanide-to-water production ratio was slightly enhanced in the impact cloud, compared with that of normal comet activity. Dust particles were flowing outward in the coma at >160 meters per second, accelerated by the gas. The slope of the brightness increase showed a dip about 200 seconds after the impact. Dust Afρ values before and long after the impact confirm the slight decrease of cometary activity. The dust-to-water mass ratio was much larger than 1.

The European Space Agency activated the Rosetta spacecraft on its way to comet 67P/Churyumov-Gerasimenko for an observational campaign of comet 9P/Tempel 1 during Deep Impact. The distance of the Rosetta spacecraft from the comet was 7.95×10^7 km, and the phase angle (sun-comet-Rosetta) was 69°. The scientific camera ensemble OSIRIS was used to make observations for 17 days from 28 June (23:45 UTC) to 14 July 2005 (15:00 UTC) and at up to one image per minute around the time of impact. The wide angle camera (WAC) used narrow-band filters to observe the gas components OH (H_2O), CN, Na, and OI with a scale of 7800 km per pixel. The narrow angle camera (NAC) used broad-band filters to characterize the dust with a scale of 1500 km per pixel. Observations through the CN (387 ± 2.5 nm) and orange (648 ± 43 nm) filters are reported here. The impact produced 1.5×10^{32} water (H_2O) molecules, based on OSIRIS OH observations (*1*).

To improve the signal-to-noise ratio of the narrow band WAC images, clusters of 4 × 4 pixels (super pixels) were binned on the charge-coupled device (CCD), reducing the spatial resolution to 31,200 km per super pixel. Images taken with the ultraviolet (UV) 375-nm filter were scaled with the solar spectrum and subtracted from the CN images to correct for the dust continuum.

Initial observations determined the steady-state production of CN before the impact. We summed the median of the intensity of pre-impact images over artificial apertures, with radii between one and five super pixels. Intensities were converted to the number of molecules in each aperture using the fluorescence efficiencies from (*2*). Then the Haser model (*3*, *4*) for the radial outflow of the unknown parent molecule(s) and the radical (dissociation product) CN were used to determine the production rate. We assumed that the outflow velocities of the molecules was 0.7 km s^{-1} (*5*), and we fixed the dissociation lifetime of CN at 3.5×10^5 s [all lifetimes and scale lengths relate to 1 astronomical unit (AU)] to yield a scale length of 2.5×10^5 km (*6*). The lifetime of the parent molecule(s) of CN is uncertain (*6*). Several lifetimes for the parent molecule were therefore tried, and a short lifetime of 3×10^4 s agreed best with the data. The corresponding production rate of the CN parent before the impact is $(4.1 \pm 0.2) \times 10^{24}$ s^{-1} and $(5.4 \pm 0.5) \times 10^{24}$ s^{-1} for parent lifetimes of 3×10^4 s and 5.5×10^4 s, respectively.

The CN cloud was observed as it expanded from the vicinity of the nucleus by increasing virtual apertures centered on the nucleus. The data yield the total number of CN radicals produced by the impact (Fig. 1). This analysis is independent of the outflow velocity of the species but does depend on their lifetimes. The data are in better agreement with a longer lifetime of the parent of CN ($>4 \times 10^4$ s) than determined for the production before and, later, after the impact. HCN, with a lifetime of approximately 7×10^4 s (*7*, *8*), has been suggested as the parent molecule of CN. If the lifetime of the CN parent in the impact-created cloud is indeed larger than it was before the impact, HCN is more important relative to other CN parents in the impact cloud than in the normal production.

A lifetime of the CN parent of 5.5×10^4 s is marginally consistent with both the pre-impact production of CN and the CN in the gas cloud created by the impact. In this case, $(5 \pm 1) \times 10^{29}$ molecules have been emitted due to the impact. Comparison with the impact-produced water [$(1.5 \pm 0.5) \times 10^{32}$ molecules (*1*)] yields a CN-to-H_2O ratio of $(3.3 \pm 1.1) \times 10^{-3}$ for the impact cloud. This is somewhat higher than before or after the impact [$(1.6 \pm 0.3) \times 10^{-3}$ for a preimpact water production rate of 3.4×10^{27} s^{-1} (*1*)]. Should the lifetime of the CN parent in the impact-created cloud be larger than during normal activity, the CN-to-H_2O ratio in the impact cloud would be higher (approximately 4×10^{-3} for 7×10^4 s).

The data suggest an enhanced abundance of the CN precursors in the impact cloud relative

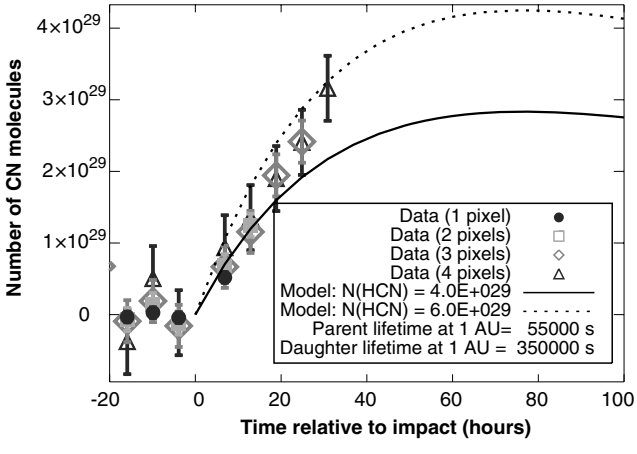

Fig. 1. Number of impact-created CN molecules as a function of time. The data for apertures of different radii (1 pixel = 31,200 km) are compared with models showing approximate lower (4×10^{29}) and upper limits (6×10^{29}) for the number of parent molecules created at the time of the impact.

[1]Max-Planck Institut für Sonnensystemforschung, Max-Planck-Strasse 2, 37191 Katlenburg-Lindau, Germany. [2]Laboratoire d'Astrophysique de Marseille, Boite Postal 8, 13376 Marseille Cedex, France. [3]Instituto de Astrofísica de Andalucía–Consejo Superior de Investigaciones Científicas, C/ Camino Bajo de Huétor, 50, 18008 Granada, Spain. [4]Deutsches Zentrum für Luft- und Raumfahrt, Institut für Planetenforschung, Rutherfordstrasse 2, 12489 Berlin, Germany. [5]Dipartimento di Astronomia e Centro Interdipartimentale Studi ed Attività Spaziali "G. Colombo," Università di Padova, Vicolo dell'Osservatorio 5, 35100 Padova, Italy. [6]Uppsala Astronomical Observatory, Box 515, 75120 Uppsala, Sweden.

*To whom correspondence should be addressed. E-mail: keller@mps.mpg.de

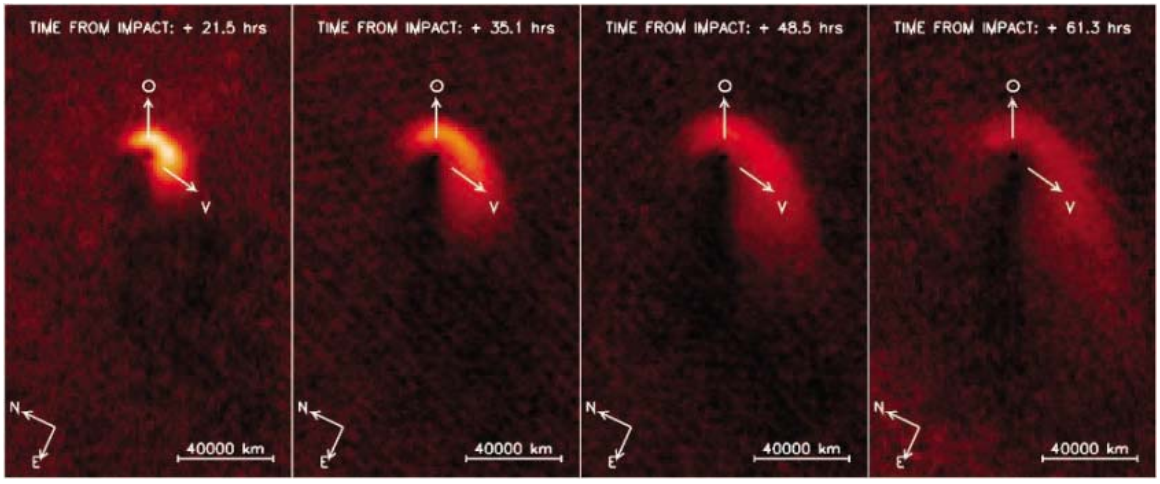

Fig. 2. Appearance of the impact-generated dust cloud at different times after the impact. The preimpact coma has been subtracted from the images by centering on the brightness maximum at the nucleus. The resolution is about 3000 km.

to normal activity and, by inference, in the cometary nucleus relative to its surface. However, the OSIRIS observations do not show a substantially stronger fraction of the CN precursor(s) in the interior of the nucleus of 9P/Tempel 1 than observed in the coma of other comets.

The dust production of 9P/Tempel 1 was observed using the following NAC broad-band filters: clear, 640 (orange), 744, 882, and 990 nm. The dust production before the impact, expressed as Afρ = 102 ± 4 cm (*9*) within an aperture of 7500 km radius (5 pixels), is slightly higher than 94 ± 2 cm at the end of our observation campaign. The total brightness of the dust observed through the orange filter corresponds to a surface of 33 ± 3 km^2, assuming a scattering albedo of 1 (*1*). In the outer coma, the motion of the dust particles is influenced by solar radiation.

The dynamics of the dust cloud caused by the impact are revealed by analyzing its brightness distribution proportional to the geometric cross section of the particles (Fig. 2). We assumed that the cloud was ejected into a 90° cone directed toward right ascension (RA) = 86° and declination = –25° (*10*), and OSIRIS looked at the plume from the side. At 21.5 hours after impact, the dust was detached from the nucleus and formed an arc pointing into the westerly direction and extending over a hemisphere. The dust maximum shifted to the side south of the solar direction. With time, the dust arc extended even more in the anti-solar direction and moved away from the nucleus while becoming fainter. Three days after impact, the dust reached a distance of about 150,000 km from the nucleus. Traces of the dust could be found up to 7 days after impact.

The acceleration of the particles (with radius a) relative to the nucleus is determined by β, the ratio of solar radiation pressure force ($\propto a^2$) to gravity force ($\propto a^3$). This acceleration varies inversely to a. The position of a dust particle at a certain time after the impact is hence determined by its outflow velocity and its

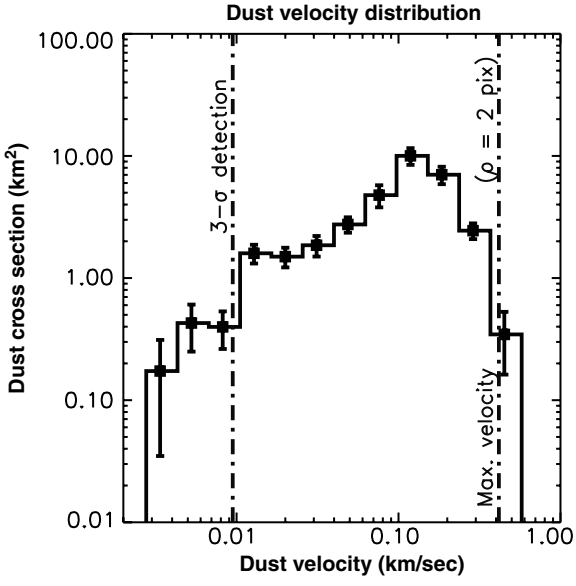

Fig. 3. Dust cross section as a function of outflow velocity for an albedo of 1 assuming isotropic scattering. Values need to be divided by the dust albedo (~0.1) at phase angle of 69° for the actual geometric dust cross section. The vertical lines indicate the 3σ detection limit of dust and the maximum detectable velocity in the minimum virtual aperture radius.

β value. The analysis shows that the fastest particles moved with velocities >400 m s^{-1}. However, slow particles moving at speeds comparable to the escape velocity from the nucleus (*11*) also contribute to the observed brightness (Fig. 3). The analysis of the brightness shows that most of the dust left the inner coma at >160 m s^{-1}. This velocity is much higher than what is expected from an impact in the gravity regime. In this case, by applying scaling laws (*12*), it is clear that at best, a few percent of the dust mass will reach velocities of more than 50 m s^{-1}. Speeds of several hundred meters per second are commonly observed for small grains in the normal coma. The grains are dragged away from the surface of the nucleus and then are rapidly accelerated by outward-streaming gas in the vicinity of the nucleus. Most of the energy of the impactor (2×10^{10} J) is used to excavate the nucleus material and to accelerate it into the plume. The impact energy is not sufficient to sublime the observed amount of 1.5×10^{32} water molecules for which 1.2×10^{13} J (2.5×10^6 J kg^{-1} at 200 K) are required. Therefore the excavated material will have retained most of its original (water) ice content. The plume is optically thick at first, and most of its dust particles are not visible. Cometary dust is well known to fragment easily (*13–15*). The dust particles are rapidly heated once the sunlight can penetrate into the plume. The liberated dust particles are accelerated by the hot (200 K) water molecules and the surrounding coma. This process takes about 40 min; after that time, when the brightness increase leveled off, only large "wet" dust particles were left to fragment. The low-speed dust plume traveled about 10 nuclear radii before it dispersed (with a bulk outflow of 10 m s^{-1}, a distance of 24 km is reached). This is well within the collisional regime of the coma (*16*). The assumption that the dust grains were radially accelerated from the nucleus area at the time of impact is therefore justified for our analysis. The observed dust distribution (Fig. 2) is similar to that of a time-limited (<90 min) outburst from an active area. Connecting the

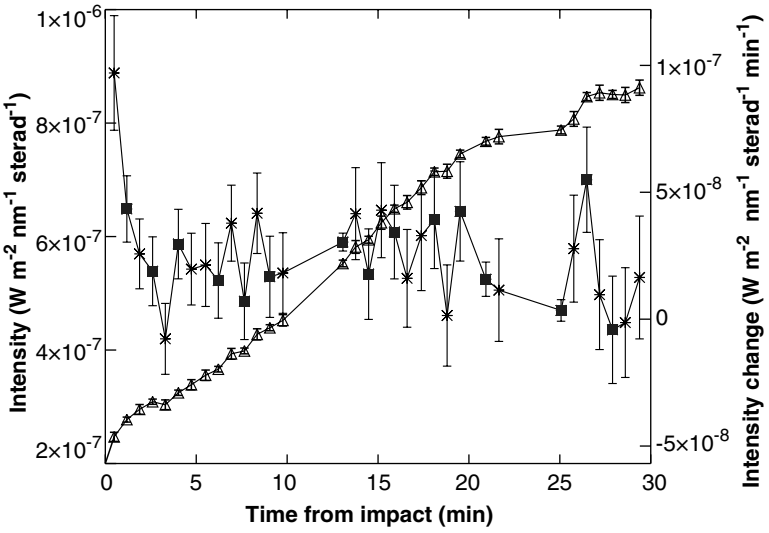

Fig. 4. Intensity within an aperture of 3000-km radius with the orange and the clear filter. Intensity (triangles) and intensity change (asterisk and squares for the orange and clear filter, respectively) are shown as a function of time.

particle size to the outflow velocity via β (that varies over several orders of magnitude) suggests that large particles have a smaller outflow velocity than do small ones and yields the particle size distribution. The integrated mass of the dust particles is much bigger than is the mass of the liberated water (dust-to-ice ratio >1).

To further characterize the brightness increase immediately after impact, we plot its derivative, the change in brightness per time interval (Fig. 4). We also include the exposures through the clear filter. The first exposure begins 10 s after the impact (integration time is 45 s, followed by a clear exposure of 35 s, repetition time 80 s), when the brightness of the nascent expanding ejecta cloud is increasing rapidly, the high temperature flash of the impact has just decayed. The brightness increased further (second exposure after impact) but the slope (brightness change per time) decreased rapidly and dropped to near zero for the fifth exposure around 200 s. The slope increased again after ~230 s reaching a steady value for 20 min before dropping again for 5 min. After about 40 min, the brightness increase leveled off; after 90 min, further increases in brightness were not evident.

What is the explanation for the dip in brightness increase about 200 s after impact? In the case of a gravity-controlled impact, a large amount of the ejecta, the curtain, leaves the crater with low outflow (on the order of meters per second), and most of the ejecta is deposited near the crater (*17*). This redeposition (loss) of dust is reflected in the slow increase of overall brightness of the plume and seems to be finished when the constant slope is reached after about 230 s. The observed time scale is in agreement with the prediction of the crater formation on 9P/Tempel 1 (*17*) and could possibly be used to constrain the crater size.

References and Notes

1. M. Küppers *et al.*, *Nature,* in press.
2. M. C. Festou, J.-M. Zucconi, *Astron. Astrophys.* **134**, L4 (1984).
3. L. Haser, *Bull. Acad. R. Sci. Liege* **43**, 740 (1957).
4. K. S. Krishna Swamy, *Physics of Comets* (World Scientific Series in Astronomy and Astrophysics, Singapore, ed. 2, 1997), vol. 2.
5. M. R. Combi, W. M. Harris, W. H. Smyth, in *Comets II*, M. C. Festou, H. U. Keller, H. A. Weaver, Eds. (The Univ. of Arizona Press, Tucson, AZ, 2005), pp. 523–552.
6. H. Rauer *et al.*, *Astron. Astrophys.* **397**, 1109 (2003).
7. J. Crovisier, *J. Geophys. Res.* **99**, 3777 (1994).
8. W. F. Huebner, J. J. Keady, S. P. Lyon, *Astrophys. Space Sci.* **195**, 7 (1992).
9. M. A. A'Hearn, *Astron. J.* **89**, 579 (1984).
10. T. Farnham (Deep Impact Team), private communication.
11. M. J. S. Belton *et al.*, *Space Sci. Rev.* **117**, 137 (2005).
12. K. R. Housen, R. M. Schmidt, K. A. Holsapple, *J. Geophys. Res.* **88**, 2485 (1983).
13. H. U. Keller, M. L. Marconi, N. Thomas, *Astron. Astrophys.* **227**, L1 (1990).
14. I. Konno, W. F. Huebner, D. C. Boice, *Icarus* **101**, 84 (1993).
15. M. R. Combi, *Astron. J.* **108**, 304 (1994).
16. C. M. Lisse *et al.*, *Space Sci. Rev.* **117**, 161 (2005).
17. P. H. Schultz, C. M. Ernst, J. L. B. Anderson, *Space Sci. Rev.* **117**, 207 (2005).

18. OSIRIS was built by a European consortium and is part of the Rosetta spacecraft, provided by the European Space Agency. Without the outstanding contributions of the OSIRIS coinvestigators M. F. A'Hearn, F. Angrilli, M. E. Bailey, P. Barthol, M. A. Barucci, J.-L. Bertaux, J. A. Burns, G. Cremonese, W. Curdt, M. DeCecco, S. Debei, M. Fulle, F. Gliem, W.-H. Ip, D. Koschny, R. Kramm, E. Kührt, A. Llebaria, J. J. Lopez Moreno, F. Marzari, G. Naletto, L. Sabau, A. Sanz Andrés, J. P. Sivan, N. Thomas, G. Tondello, and K.-P. Wenzel, these results would not have materialized. We acknowledge the funding of the national space agencies Agenzie Spaziale Italiana, Centre National d'Etudes Spatiales, Deutsches Zentrum für Luft- und Raumfahrt (contract number 50 QP 9703/8), Swedish National Space Board, by the Spanish Space Program (Ministerio de Educación y Ciencia), and the European Space Agency.

18 August 2005; accepted 2 September 2005
Published online 8 September 2005;
10.1126/science.1119020
Include this information when citing this paper.

NORTHWESTERN UNIVERSITY

CALL FOR NOMINATIONS

NEMMERS PRIZES

$150,000

Northwestern University invites nominations for the Erwin Plein Nemmers Prize in Economics and the Frederic Esser Nemmers Prize in Mathematics to be awarded during the 2005-06 academic year. Each award includes payment to the recipient of $150,000. Made possible by a generous gift to Northwestern by the late Erwin Esser Nemmers and the late Frederic Esser Nemmers, the awards are given every other year.

Candidacy for the Nemmers Prizes is open to those with careers of outstanding achievement in their disciplines as demonstrated by major contributions to new knowledge or the development of significant new modes of analysis. Individuals of all nationalities and institutional affiliations are eligible except current or recent members of the Northwestern University faculty and recipients of the Nobel Prize.

The 2006 recipient of either Nemmers Prize will deliver a public lecture and participate in other scholarly activities at Northwestern University for 10 weeks during the 2006-07 academic year.

Nominations for both prizes will be accepted until December 1, 2005. Nominating letters of no more than three pages should describe the nominee's professional experience, accomplishments, and qualifications for the award. A brief *curriculum vitae* of the nominee is helpful but not required. Nominations from experts in the field are preferred to institutional nominations; direct applications will not be accepted.

Nominations may be sent to:
nemmers@northwestern.edu

The Nemmers Prizes/Office of the Provost/
Northwestern University/Evanston, IL 60208

www.northwestern.edu/provost/awards/nemmers

Northwestern University is an equal opportunity, affirmative action educator and employer.

RECIPIENTS OF THE ERWIN PLEIN NEMMERS PRIZE IN ECONOMICS

ROBERT J. AUMANN
PETER A. DIAMOND
DANIEL L. MCFADDEN
EDWARD C. PRESCOTT
ARIEL RUBINSTEIN
THOMAS J. SARGENT

RECIPIENTS OF THE FREDERIC ESSER NEMMERS PRIZE IN MATHEMATICS

JOHN H. CONWAY
MIKHAEL L. GROMOV
JOSEPH B. KELLER
YURI I. MANIN
YAKOV G. SINAI
EDWARD WITTEN

State of New Jersey Commission on Spinal Cord Research

RESEARCH GRANT AWARDS

Five-Year named Chairs for Senior and Junior Faculty, maximum of $1,100,000 over a five-year period.

One-Time Start-Up Cost Grant, maximum of $1,000,000.

Individual Grants, maximum of $200,000 per year, research grants for basic or clinical research on spinal cord injury and disease.

Postdoctoral & Graduate Student Fellowship Awards

Applicants must be associated with a New Jersey Institution and may collaborate with researchers out-of-state and country.

Application form and details at:
www.state.nj.us/health/spinalcord/

Application form and details from:
New Jersey Commission on Spinal Cord Research
PO Box 360
Market and Warren Streets
Trenton, New Jersey 08625-0360
Tel: 609-292-4055
E-mail: njcscr@doh.state.nj.us

Closing Date for Grant Applications:
December 8, 2005

A Secondary Symbiosis in Progress?

Noriko Okamoto and Isao Inouye*

Endosymbiosis is a major driving force in the evolution and diversification of plants and algae. Plastids originated from a cyanobacterial symbiont harbored in the first eukaryotic algae, of which three "primary algae" are direct descendants: Glaucophyta and Rhodophyta (the red algae) and Viridiplantae (the green algae and land plants). After this primary endosymbiosis, successive secondary endosymbioses occurred in which a primary alga was engulfed and integrated as a plastid. Four algal divisions (Dinophyta, Cryptophyta, Heterokontophyta, and Haptophyta) plus one parasitic phylum (Apicomplexa) acquired red algal plastids, and two algal divisions (Chlorarachniophyta and Euglenophyta) acquired green algal plastids (*1*).

Endosymbiosis unites different cells into one organism. Requisite steps include a lateral gene transfer from the symbiont to the host nucleus and the establishment of protein transport machinery back into the symbiont, resulting in loss of the symbiont's autonomy (*2*). Synchronization of host-symbiont cell cycles and cosegregation is another critical step in permanent fusion of the two partners. However, how the synchronization occurs and how the integrated organism responds to external conditions are unknown.

Here we describe a flagellate (Fig. 1A) that appears to be in the formative stages of an ongoing endosymbiosis. The flagellate, which we tentatively refer to as Hatena ("enigmatic" in Japanese), will be formally described as a member of a recently elected division Katablepharidophyta (*3*). Hatena is currently uncultivable, so cells from natural populations were used for investigations. Nearly all the cells had a green "plastid" with an eyespot at the cell apex. However, this plastid was inherited by only one daughter cell (Fig. 1B), indicating the structure is a symbiont.

We determined the identity of the endosymbiont by sequencing of the plastid 16S ribosomal DNA (rDNA) and by phylogenetic analysis. The symbiont belongs to the genus *Nephroselmis* (Prasinophyceae, Viridiplantae) (fig. S1), which is abundant in the habitat.

The symbiont cell retains its nucleus, mitochondria(on), plastid, and occasionally a vestigial Golgi body, but the flagella, cytoskeleton, and endomembrane system are lost. Free-living *Nephroselmis* cells are flat-kidney-shaped, are ~10 μm in length, and possess a single plastid with a single pyrenoid (*4*). In contrast, the symbiont's plastid is more than 10 times as large (Fig. 1A) and contains multiple pyrenoids.

Ultrastructure also indicates remarkably close interaction between the host-symbiont partnership. An eyespot (located in the endosymbiont's plastid) is always situated at the host's apex (Fig. 1A, arrowhead), where four membranes (the inner and outer plastid membranes, the symbiont-enveloping membrane, and the host's plasma membrane) are tightly apposed (Fig. 1C). The eyespot is part of a photosensor that enables phototaxis (*5*). Intimate morphological association between the endosymbiont and the host indicates endosymbiont-guided host phototaxis.

The corresponding region in the colorless, symbiont-lacking cells is occupied by a complex feeding apparatus. Thus, the uptake of the symbiont also induces drastic changes to the host cell. We tested the specificity of the host-symbiont interaction by feeding symbiont-free hosts with a different *Nephroselmis* strain (one with 31 out of 335 base pairs different, according to partial 16S rDNA sequencing). Although the prey was engulfed and remained undigested, it did not undergo the modifications described above, suggesting a highly strain-specific interaction.

The Hatena life cycle thus alternates from a predator phase to an autotrophic host phase (Fig. 1D). First, a green cell (step a) divides (b) into one green (c) and one colorless (d) cell. The colorless cell develops a feeding apparatus de novo (d to e) and engulfs a *Nephroselmis* (e to g). The symbiont plastid develops and the feeding apparatus degenerates (g to a). As we never observed any dividing cell without a symbiont (d) or with an "immature" plastid (h), symbiont acquisition and modification apparently occur within one generation. How many generations the symbiont persists is an open question.

Hatena represents an early stage in the development of an ongoing secondary endosymbiosis. Some dinoflagellates are also known to be in the process of acquiring symbionts (*6*). However, past research has been focused only on symbiont changes. Hatena demonstrates changes in both host and symbiont. It now remains to be determined whether there has been lateral gene transfer between Hatena and its *Nephroselmis* symbiont, as such genetic amalgamation was a key step in the evolution of modern plants and algae.

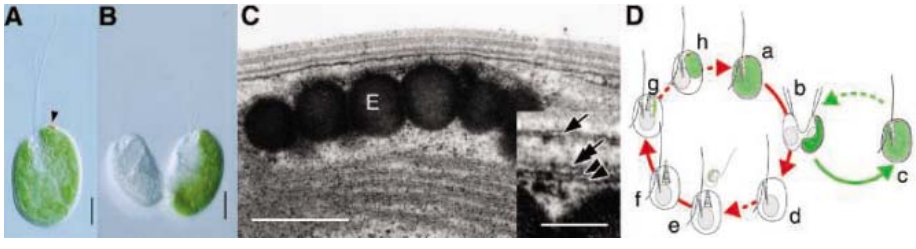

Fig. 1. (**A**) Hatena (ventral view). All green, symbiont-possessing cells have an eyespot at the cell apex (arrowhead). Scale bar, 10 μm. (**B**) A dividing cell (ventral view). The symbiont is always inherited by only one of the daughter cells. Scale bar, 10 μm. (**C**) The ultrastructure of eyespot integration (longitudinal view). E, eyespot granules. Scale bar, 400 nm. Inset: A magnified view of the membranes. The inner and outer plastid membranes (arrowheads), the single symbiont-enveloping membrane (double arrow), and the host plasma membrane (arrow) are tightly layered. Scale bar, 50 nm. (**D**) The life cycle of Hatena, based on observations of natural populations. Hatena alternates between a host phase that harbors a green endosymbiont and a predator phase that acquires the endosymbiont after division. Solid line, observed steps in the process; broken line, hypothetical steps.

References and Notes

1. D. Bhattacharya, H. S. Yoon, J. D. Hackett, *Bioessays* **26**, 50 (2004).
2. P. R. Gilson, G. I. McFadden, *Genetica* **115**, 13 (2002).
3. N. Okamoto, I. Inouye, *Protist* **156**, 163 (2005).
4. I. Inouye, R. N. Pienaar, *Nord. J. Bot.* **4**, 409 (1984).
5. K. W. Foster, R. D. Smyth, *Microbiol. Rev.* **44**, 572 (1980).
6. J. D. Hackett, D. M. Anderson, D. L. Erdner, D. Bhattacharya, *Am. J. Bot.* **91**, 1523 (2004).
7. Supported by Japan Society for the Promotion of Sciences (JSPS) grant nos. RFTF00L0162 (I.I.) and 1612007 (N.O.) and by a JSPS Research Fellowship for Young Scientists (N.O.).

Supporting Online Material
www.sciencemag.org/cgi/content/full/310/5746/287/DC1
Materials and Methods
Fig. S1
References and Notes

14 June 2005; accepted 14 September 2005
10.1126/science.1116125

Graduate School of Life and Environmental Sciences, University of Tsukuba, 1-1-1 Tennodai, Tsukuba, Ibaraki 305-8572, Japan.

*To whom correspondence should be addressed. E-mail: iinouye@sakura.cc.tsukuba.ac.jp

Wings for Life - SCI research - Call for Proposal

The Wings for Life Spinal Cord Research Foundation is a grant giving charity based in Austria with the sole purpose of funding research **aimed at resolving spinal cord injury–induced impairments**. We invite applications for project grants in basic sciences, applied basic sciences, and clinical sciences (incl. neurorehabilitation) that build on established knowledge in the field of spinal cord injury repair. Proposals should have a view to translation from the laboratory to the clinical setting and have the likelihood of providing real benefits to human patients. Preference will be given to applications that involve studies in the adult mammalian spinal cord, or that provide explicit justification for the use of other systems and how the results could be verified and translated. All planned lesion models and assessment methodologies must be appropriate. Proposals will undergo peer review and will be evaluated for novelty, originality and potential. Information for applicants is available on our website www.wingsforlife.com

The last date for proposal submission is ***December, 1st 2005***.

Wings for Life Spinal Cord Research Foundation
Fürstenallee 4, 5020 Salzburg, Austria
email: office@wingsforlife.com

Metal-Insulator Transition in Disordered Two-Dimensional Electron Systems

Alexander Punnoose[1]* and Alexander M. Finkel'stein[2]

We present a theory of the metal-insulator transition in a disordered two-dimensional electron gas. A quantum critical point, separating the metallic phase, which is stabilized by electronic interactions, from the insulating phase, where disorder prevails over the electronic interactions, has been identified. The existence of the quantum critical point leads to a divergence in the density of states of the underlying collective modes at the transition, causing the thermodynamic properties to behave critically as the transition is approached. We show that the interplay of electron-electron interactions and disorder can explain the observed transport properties and the anomalous enhancement of the spin susceptibility near the metal-insulator transition.

Measurements in high-mobility two-dimensional (2D) semiconductors have made it possible to study the properties of the 2D electron gas at low carrier densities. In a clean system at very low carrier densities, the electrons are expected to solidify into a Wigner crystal. In a wide range of low electron concentrations, before the Wigner crystal phase, the electron system exists as a strongly interacting liquid (*1*). Understanding the properties of this strongly interacting system in the presence of disorder has proven to be an extremely challenging theoretical problem. The discovery of a metal-insulator transition (MIT) in 2D electron gas (*2*), when none was expected for more than a decade (*3*), generated renewed interest in this field (*4*).

The MIT, observed initially in high-mobility silicon metal-oxide-semiconductor field-effect transistors (Si-MOSFETs) and subsequently in a host of other 2D systems such as gallium arsenide (*p*-GaAs) heterostructures, occurs when the resistance R is of the order of the quantum resistance h/e^2, emphasizing the importance of quantum effects. In the metallic phase, the resistance drops noticeably as the temperature is lowered. This drop is suppressed when an in-plane magnetic field is applied (*4*). Additionally, Si-MOSFET samples show a strong enhancement of the spin susceptibility as the MIT is approached (*5*, *6*). There are indications that the spin susceptibility in samples of different mobilities behaves critically near the transition. The sensitivity to in-plane magnetic fields, together with the anomalous behavior of the spin susceptibility, highlights the importance of electron-electron (*e*-*e*) interactions in this phenomenon.

In the presence of impurities, perturbations of the charge and spin densities (if spin is conserved) relax diffusively at low frequencies and large distances. Formally, this relaxation occurs via the propagation of particle-hole pair modes. In a system that obeys time-reversal symmetry, the modes in the particle-particle channel (the Cooper channel) also have a diffusive form, leading to the celebrated weak-localization corrections to the conductivity. These two mode families are, in conventional terminology, referred to as Diffusons and Cooperons, respectively. Taken together, they describe the low-energy dynamics of a disordered electron liquid (*7*). The modes have the diffusive form $D(q,\omega) = 1/(Dq^2 - iz\omega)$, where D is the diffusion coefficient and the parameter z determines the relative scaling of the frequency (that is, energy) with respect to the length scale (*8*, *9*); $z = 1$ for free electrons. The addition of *e*-*e* interactions results in the scattering of these diffusion modes. Both D and z therefore acquire corrections in the presence of the interactions. Conversely, diffusing electrons dwell long in each other's vicinity, becoming more correlated at low enough energies. As a result, the *e*-*e* scattering amplitudes γ_2 and γ_c characterizing the scattering of the Diffuson and Cooperon modes, respectively, acquire corrections as a function of the disorder. All these corrections, because of the diffusive form of the propagator $D(q,\omega)$, are logarithmically divergent in temperature in two dimensions (*10*). They signal the breakdown of perturbation theory and the need for a re-summation of the divergent terms.

A consistent handling of these mutually coupled corrections to D and z on the one hand, and of γ_2 and γ_c on the other, requires the use of a renormalization group (RG) that effectively sums the logarithmic series (*8*, *11*, *12*), allowing one to approach the strong-coupling region of the MIT (*9*, *13*). We show that an internally consistent solution of the MIT can be obtained within a suitably defined large-N model involving N flavors of electrons. Bearing in mind that the conduction band in semiconductors often has almost degenerate regions called valleys (*14*), the electrons carry both spin and valley indices. Taking the number of valleys $n_v \to \infty$, we derive the relevant RG equations to two-loop order and show that a quantum critical point (QCP) that describes the MIT exists in the 2D interacting disordered electron liquid.

Because the intervalley scattering requires a large change of the momentum, we assume that the interactions couple electrons in different valleys but do not mix them. This implies that, intervalley scattering processes, including those due to the disorder, are neglected. This assumption is appropriate for samples with high mobility. In this limit, the RG equations describing the evolution of the resistance and the scattering amplitude γ_2 in two dimensions are known to have the form (*15*)

$$\frac{d\ln\rho}{d\xi} = \rho\left[n_v + 1 - (4n_v^2 - 1)\left(\frac{1+\gamma_2}{\gamma_2}\ln(1+\gamma_2) - 1\right)\right] \quad (1)$$

$$\frac{d\gamma_2}{d\xi} = \rho\frac{(1+\gamma_2)^2}{2} \quad (2)$$

where $\xi = -\ln(1/T\tau)$ with $T\tau \ll 1$ (diffusive regime), τ is the elastic scattering time, and the dimensionless resistance parameter $\rho = (e^2/\pi h)R$ is related to D as $\rho = 1/[(2\pi)^2 n_v \nu D]$, with ν being the density of states of a single spin and valley species. (For repulsive interactions, the scattering amplitude in the Cooper channel, γ_c, scales to zero when n_v is finite and is, therefore, neglected for now; the situation in the large-n_v limit is different and is discussed later.) Though the initial values of ρ and z, determined at some initial temperature, depend on the system and are therefore not universal, the flow of ρ can be described for each n_v by a universal function $R(\eta)$ (*8*)

$$\rho = \rho_{max} R(\eta) \text{ and } \eta = \rho_{max}\ln(T_{max}/T) \quad (3)$$

where $R(\eta)$ is a nonmonotonic function with a maximum at a temperature T_{max} corresponding to the point where $d\rho/d\xi$ in Eq. 1 changes

[1]Bell Laboratories, Lucent Technologies, Murray Hill, NJ 07974, USA. [2]Department of Condensed Matter Physics, Weizmann Institute of Science, Rehovot 76100, Israel.

*To whom correspondence should be addressed. E-mail: punnoose@lucent.com

sign. It follows that the full temperature dependence of the resistance ρ is completely controlled by its value ρ_{max} at the maximum; there are no other free (or fitting) parameters. The antilocalization effect of the *e-e* interactions fundamentally alters the commonly accepted point of view (*3*) that in two dimensions, all states are "eventually" (that is, at $T = 0$) localized.

This solution has obvious limitations, however. Because the RG equations were derived in the lowest order in ρ, the single curve solution $R(\eta)$ in Eq. 3 cannot be applied in the critical region of the MIT where $\rho \sim 1$. [In fact, for $n_v = 2$, $R(\eta)$ describes quantitatively the temperature dependence of the resistance of high-mobility Si-MOSFETs in the region of ρ up to $\rho \sim 0.5$ (*15*), which is not so far from the critical region.] Therefore, to approach the MIT, the disorder has to be treated beyond the lowest order in ρ, while adequately retaining the effects of the interaction. This also touches on the delicate issue of the internal consistency and nature of the theory as $T \to 0$. The problematic feature of the scaling described by Eqs. 1 and 2 is that the amplitude γ_2 diverges at a finite temperature T^* and thereafter the RG theory becomes uncontrolled (*11*, *12*). Fortunately, the scale T^* decreases very rapidly with n_v as $\ln\ln(1/\tau T^*) \sim (2n_v)^2$, making the problem of the divergence of γ_2 for all practical purposes irrelevant even for $n_v = 2$. Still, to get an internally consistent solution up to $T = 0$, it is useful to study the limit $n_v \to \infty$, for which $T^* \to 0$.

The valley degrees of freedom are akin to flavors in standard field-theoretic models. Generally, closed loops play a special role in the diagrammatic RG analysis in the limit when the number of flavors N is taken to be very large (*16*). This is because each closed loop involves a sum over all the flavors, generating a large factor N per loop. It is then typical to send a coupling constant λ to zero in the limit $N \to \infty$, keeping λN finite. For interacting spin-1/2 electrons in the presence of n_v valleys ($N = 2n_v$), enhancing the screening makes the bare values of the electronic interaction amplitudes γ_2 and γ_c scale as $1/2n_v$. Furthermore, the increase in the number of conducting channels makes the resistance ρ scale as $1/n_v$. It is therefore natural to introduce the amplitudes $\theta_2 = 2n_v\gamma_2$ and $\theta_c = 2n_v\gamma_c$, together with the resistance parameter $t = n_v\rho$, which remain finite in the large-n_v limit. The parameter t is the resistance per valley, $t = 1/(2\pi)^2 \nu D$, and it reveals itself in the theory via the momentum integration involving the diffusion propagators $D(q,\omega)$. In terms of these variables, a contribution of a closed loop connected to the rest of the diagram by one interaction amplitude, γ_2 (or γ_c), after integrating over the momentum flowing through the loop and summing over the spin and valley degrees of freedom, is proportional to $2n_v t\gamma_2 = t\theta_2$ (or $t\theta_c$). Although such a contribution remains finite at large n_v, those diagrams with more than one interaction for every closed loop are negligible. This one-to-one correspondence between the number of loops in a given diagram and the number of interaction amplitudes limits the maximum number of interaction vertices for a given power of t. This is the crucial simplification on taking the large-n_v limit.

For repulsive interactions at finite n_v, rescattering in the Cooper channel leads to the vanishing of the effective amplitude γ_c at low energies. The amplitude θ_c is, however, relevant in the large-n_v limit because the rescattering is not accompanied by factors of n_v. We introduce the parameter $\alpha = 1$ to mark the contributions arising from the Cooper channel. The violation of time-reversal symmetry (for example, by a magnetic field) suppresses the Cooperon modes (*7*). Setting $\alpha = 0$ switches the Cooper channel off. Following the large-n_v approximation scheme detailed above, the RG equations to order t^2 are derived for $\alpha = 0$ and 1

$$\frac{d\ln t}{d\xi} = t(\alpha - \Theta) + t^2(1 - \alpha - \alpha\Theta + c_t\Theta^2) \tag{4}$$

$$\frac{d\Theta}{d\xi} = t(1 + \alpha + \alpha\Theta) - 4t^2\left[(1 + \alpha)\Theta + \frac{\alpha}{2}\Theta^2 + c_\theta\Theta^3\right] \tag{5}$$

The constants here are $c_t = (5 - \pi^2/3)/2 \approx 0.8$ and $c_\theta = (1 - \pi^2/12)/2 \approx 0.08$. It turns out that in the large-n_v limit, the amplitudes θ_2 and θ_c appear together in the combination $\Theta = \theta_2 + \alpha\theta_c$. The fact that they come together as a single parameter Θ is unique to the large-n_v limit. Equation 4 reproduces the known result to order t^2 when the electronic interactions are absent (*17*). Although the maximum power of Θ is limited by the order of t, the opposite is not true; it is the number of momentum integrations of the diffusion propagators that determines the power of t.

Equations 4 and 5 describe the competition between the electronic interactions and disorder in two dimensions. The flow of $t(\xi)$ and $\Theta(\xi)$ is plotted in Fig. 1 for the case $\alpha = 1$ (the flow diagram is qualitatively the same for $\alpha = 0$). The arrows indicate the direction of the flow as the temperature is lowered. The QCP, corresponding to the fixed point of Eqs. 4 and 5, is marked by the circle. The attractive ("horizontal") separatrices separate the metallic phase, where $t \to 0$, from the insulating phase, where $t \to \infty$. Crossing one of these separatrices (*18*) by changing the initial values of t and Θ (for example, by changing the carrier density) leads to the MIT. Near the fixed point, these separatrices are almost insensitive to temperature, which is in agreement with the experiments in Si-MOSFETs (*19*, *20*). The accidental (but fortunate) smallness of the fixed point parameters $t_c \approx 0.3$ and $t_c\Theta_c \approx 0.27$ permits us to believe that the two-loop equations derived in the large-n_v limit capture accurately enough the main features of the transition.

We now discuss the renormalization of the parameter z due to the *e-e* interactions. The RG equation for z is described by an independent equation, which quite generally (*11*) takes the form $d\ln z/d\xi = \beta_z(t,\gamma_2,\gamma_c; n_v)$. Observe that β_z, as well as Eqs. 4 and 5 for t and Θ, are all independent of z. Consequently, z in the vicinity of the MIT is critical: $z \sim 1/T^\zeta$ with a critical exponent ζ equal to the value of the function β_z at the critical point (*9*, *13*). The parameter z, being related to the

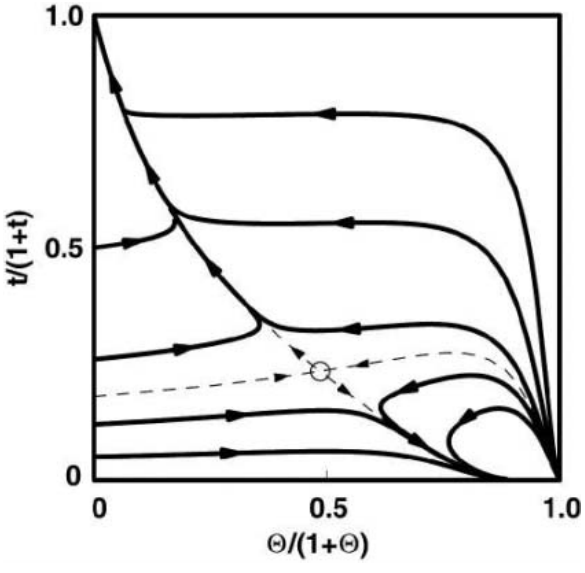

Fig. 1. The disorder-interaction (t=Θ) flow diagram of the 2D electron gas obtained by solving Eqs. 4 and 5 with the Cooper channel included ($\alpha = 1$). Arrows indicate the direction of the flow as the temperature is lowered. The circle denotes the QCP of the MIT, and the dashed lines show the separatrices.

frequency renormalization, can be interpreted as the density of states of the diffusion modes and therefore controls the contribution of the diffusion modes to the specific heat $C_V \sim (zv)T$ (*21*, *22*). Hence, in the critical regime $C_V \sim T^{1-\zeta}$. (The fact that C_V must vanish as $T \rightarrow 0$ constraints the exponent $\zeta < 1$.) Furthermore, the Pauli spin susceptibility χ in the disordered electron liquid has the general form $\chi \sim (zv)(1 + \gamma_2)$ (*11*, *12*). Apart from the Stoner-like enhancement of the g factor, $(1 + \gamma_2)$, it is proportional to the renormalized density of states z. The enhancement of z near the QCP implies that the spin susceptibility diverges as $\chi \sim 1/T^{\zeta}$, whereas the spin diffusion coefficient $D_s = D/z(1 + \gamma_2)$ scales to zero. At the fixed point, the g factor remains finite, and therefore the divergence of the spin susceptibility is a priori not related to any magnetic instability. In the large-n_v limit, we find that no terms of the order t^2 are generated in the equation for z

$$d\ln z/d\xi = t\Theta \qquad (6)$$

Therefore, we get for the critical exponent $\zeta \approx 0.27$, which is noticeably smaller than 1.

We propose that the existence of the QCP explains the anomalous enhancement of the spin susceptibility that has been observed near the MIT in Si-MOSFETs with different critical densities (*5*, *6*). Additionally, an important consequence of this theory is that the compressibility $\partial n/\partial\mu$ is regular across the transition, in agreement with the experiments in p-GaAs (*23*, *24*).

In the insulating phase, the parameter t diverges at a finite scale ξ_c, indicating the onset of strong localization. Because the t^2 term in Eq. 5 is negative, it forces the interaction amplitude Θ to vanish in the insulating phase. It can be shown that the parameter z is finite at the scale ξ_c. The vanishing of the interaction amplitude Θ and a finite value of z make the insulating phase similar to the Anderson insulator.

On the metallic side, a state with decreasing resistance $t \rightarrow 0$ and enhanced amplitude $\Theta \rightarrow \infty$ is stabilized by the electronic interactions as $T \rightarrow 0$ in the large-n_v limit. It can be shown within this solution that $z \sim 1/t$, implying that the quasi-particle diffusion coefficient defined as $D_{qp} = D/z$ (*22*) behaves regularly in the metallic phase. Deep in the metallic phase, the enhancement in χ will be observed only at exponentially small temperatures. This holds even in the case of finite n_v, because the scale T^* at which the RG Eqs. 1 and 2 become uncontrolled is immeasurably small even for $n_v = 2$. The question of the existence of the QCP at finite n_v is distinct from the problem of the divergence of the parameter γ_2 at $T = T^*$, because the two phenomena occur in different parts of the phase diagram.

A description of the MIT is obtained within the two-loop approximation in the limit of a large number of degenerate valleys. Although the properties of the thermodynamic quantities in the critical region are obtained in the large-n_v limit, it captures the generic features of the MIT for any n_v. Our solution gives a physical picture that is in qualitative agreement with the experimental situation. In particular, it is shown that the point of the MIT is accompanied by a divergence in the spin susceptibility, whose origin is not related to any magnetic instability.

References and Notes

1. B. Tanatar, D. M. Ceperely, *Phys. Rev. B* **39**, 5005 (1989).
2. S. V. Kravchenko, G. V. Kravchenko, J. E. Furneaux, V. M. Pudalov, M. D'Iorio, *Phys. Rev. B* **50**, 8039 (1994).
3. E. Abrahams, P. W. Anderson, D. C. Licciardello, T. V. Ramakrishnan, *Phys. Rev. Lett.* **42**, 673 (1979).
4. S. V. Kravchenko, M. P. Sarachik, *Rep. Prog. Phys.* **67**, 1 (2004).
5. O. Prus, Y. Yaish, M. Reznikov, U. Sivan, V. M. Pudalov, *Phys. Rev. B* **67**, 205407 (2003).
6. A. A. Shashkin *et al.*, http://xxx.lanl.gov/abs/cond-mat/0409100.
7. B. L. Altshuler, A. G. Aronov, *Modern Problems in Condensed Matter Physics* (Elsevier, North Holland, 1985), chap. X, p. 1.
8. A. M. Finkel'stein, *Sov. Phys. J. Exp. Theor. Phys.* **57**, 97 (1983).
9. A. M. Finkel'stein, *J. Exp. Theor. Phys. Lett.* **37**, 517 (1983).
10. B. L. Altshuler, A. G. Aronov, P. A. Lee, *Phys. Rev. Lett.* **44**, 1288 (1980).
11. A. M. Finkel'stein, *Z. Phys. B* **56**, 189 (1984).
12. C. Castellani *et al.*, *Phys. Rev. B* **30**, 1596 (1984).
13. M. A. Baranov, I. S. Burmistrov, A. M. M. Pruisken, *Phys. Rev. B* **66**, 075317 (2002).
14. For example, the electron band in the (001) plane in Si-MOSFET has two valleys.
15. A. Punnoose, A. M. Finkel'stein, *Phys. Rev. Lett.* **88**, 016802 (2002).
16. K. G. Wilson, *Phys. Rev. D* **7**, 2911 (1973).
17. K. B. Efetov, *Sov. Phys. J. Exp. Theor. Phys.* **55**, 514 (1982).
18. The important question of which of the attractive separatrices are crossed at the transition can be resolved by magnetoresistance measurements in a weak in-plane magnetic field.
19. S. V. Kravchenko, T. M. Klapwijk, *Phys. Rev. Lett.* **84**, 2909 (2000).
20. See figure 3 in (*4*).
21. C. Castellani, C. D. Castro, *Phys. Rev. B* **34**, 5935 (1986).
22. C. Castellani, G. Kotliar, P. A. Lee, *Phys. Rev. Lett.* **59**, 323 (1987).
23. S. C. Dultz, H. W. Jiang, *Phys. Rev. Lett.* **84**, 4689 (2000).
24. S. Ilani, A. Yacoby, D. Mahalu, H. Shtrikman, *Science* **292**, 1354 (2001).

25. A.P. benefited from discussions with R. Whitney. A.F. was supported by the MINERVA Foundation.

Supporting Online Material

www.sciencemag.org/cgi/content/full/310/5746/289/DC1
SOM Text
References

2 June 2005; accepted 15 September 2005
10.1126/science.1115660

The Promotional Effect of Gold in Catalysis by Palladium-Gold

Mingshu Chen, Dheeraj Kumar, Cheol-Woo Yi, D. Wayne Goodman*

Acetoxylation of ethylene to vinyl acetate (VA) was used to investigate the mechanism of the promotional effect of gold (Au) in a palladium (Pd)-Au alloy catalyst. The enhanced rates of VA formation for low Pd coverages relative to high Pd coverages on Au single-crystal surfaces demonstrate that the critical reaction site for VA synthesis consists of two noncontiguous, suitably spaced, Pd monomers. The role of Au is to isolate single Pd sites that facilitate the coupling of critical surface species to product, while inhibiting the formation of undesirable reaction by-products.

Mixtures of Pd and Au are used as catalysts for a number of applications (*1*–*4*), including hydrogen fuel cells (*5*) and pollution control (*6*). The addition of Au to Pd can greatly enhance Pd's overall catalytic activity, selectivity, and stability; however, the promotional role of Au has not been elucidated. Here, acetoxylation of ethylene to vinyl acetate (VA) was selected as a probe reaction of Pd-Au bimetallic surfaces. Acetoxylation of ethylene on Pd-Au bimetallic silica-supported catalysts promoted with potassium acetate (KOAc) is a well-established commercial route for the synthesis of VA (*1*, *3*, *7*–*12*), given by the following reaction

$$CH_3COOH + C_2H_4 + 0.5\ O_2 \rightarrow CH_3COOCHCH_2 + H_2O$$

The nature of the key reaction intermediates, the mechanism, and the active ensemble are still unresolved. A critical ensemble consisting of several Pd atoms has been suggested as the reactive site for VA synthesis (*13*). Here we present evidence that the rate of VA formation is significantly enhanced on Pd/Au(100) compared with Pd/Au(111), implying that the critical reaction site for VA synthesis consists of two noncontiguous, suitably spaced Pd monomers. This structure-activity relation provides insights into the elementary steps in-

Department of Chemistry, Texas A&M University, College Station, TX 77842–3012, USA.

*To whom correspondence should be addressed. E-mail: goodman@mail.chem.tamu.edu.

volved in the oxidative coupling of ethylene and acetic acid to form VA and shows that the promotional role of Au is to isolate Pd monomer sites, thereby preventing undesirable pathways to CO, CO_2, and surface carbon. This discovery should aid in the optimization of existing VA synthesis catalysts and motivate the synthesis of single-phase Pd-Au alloy catalysts with specific surface morphologies.

VA synthesis was carried out on Pd/Au(100) and Pd/Au(111) at 453 K (*14*). Pd atoms were evaporated onto clean Au surfaces from a filament source and then annealed at 550 K for 10 min. The rate of VA formation is expressed as a turnover frequency (TOF) or as the number of VA molecules produced per surface active site per second. Because the VA formation rate on an Au-only surface is negligible compared with the rate on a Pd/Au surface (fig. S1) (*14*), the catalytic active site is assumed to consist of surface Pd atoms. The VA formation rate is computed based on the initial Pd coverage and estimated using the Auger electron spectroscopy breakpoint method (*14*). Plots of the VA formation rate of Pd/Au surfaces as a function of the Pd coverage are shown in Fig. 1. The rate (TOF) on the Au(100) surface increases significantly with a decrease in the Pd coverage until a maximum is reached at a Pd coverage of ~0.07 monolayers (ML, defined as one Pd atom per substrate Au atom). The corresponding VA formation rates for Pd on Au(111) rise steadily as the Pd coverage is decreased; whereas at all Pd coverages, the rates on Au(111) are significantly lower compared with the rate for the corresponding Pd coverage on Au(100). The higher VA formation rates observed at relatively low Pd coverages (Fig. 1 and fig. S1) are consistent with isolated Pd sites, that is, Pd monomers (Fig. 1, schematic inset), being more active for VA synthesis, compared with surface ensembles containing contiguous Pd atoms (figs. S2 and S3).

The formation of surface Pd monomers for Pd/Au(100) and Pd/Au(111) was confirmed by measuring the adsorption of carbon monoxide (CO) accompanied by infrared reflection absorption spectroscopy (IRAS). Intense CO vibrational features between 1900 and 2000 cm^{-1}, corresponding to CO adsorption on twofold bridging and/or threefold hollow sites (*15*–*17*), were observed for multilayer Pd on Au(100) and Au(111) deposited at or below room temperature (Fig. 2 and fig. S4). These data are evidence for the formation of Pd overlayers on Au(111) or Au(100), in agreement with previous studies (*18*, *19*). Upon annealing Pd/Au(100) or Pd/Au(111) at 600 K, the CO features in the IRAS data corresponding to bridging and/or threefold hollow sites disappear, and the intensity of the features corresponding to atop sites between 2080 and 2125 cm^{-1} increases significantly. These data demonstrate that contiguous surface Pd ensembles are eliminated upon annealing, leaving exclusively isolated Pd sites or monomers, i.e., Au_4Pd on Au(100) and Au_6Pd on Au(111) (Fig. 1, schematic). The formation of surface Pd monomers on Au(111) has been observed by scanning tunneling microscopy (*20*). Furthermore, after heating to 500 K, a significant decrease in the surface Pd coverage on Au(111) was observed by low-energy ion scattering spectroscopy (LEISS) (*18*). A maximum in the density of Pd monomers should occur at 0.5 ML Pd on Au(100) and at 0.33 ML Pd on Au(111), coverages which correspond to the Au(100)-c(2 × 2)-Pd and Au(111)-($\sqrt{3}$ × $\sqrt{3}$)R30°-Pd structures, respectively (fig. S1, inset). However, no such well-ordered surface structures were observed, likely because Pd and Au are completely miscible over the entire range of compositions; i.e., bulk diffusion of Pd occurs. The much lower surface energy of Au also favors surface enrichment by Au (*21*). A Pd-Au film composed of an equimolar mixture of Pd and Au was shown to have a surface Pd coverage of 0.2 ML and to exhibit exclusively monomeric Pd sites as determined by LEISS and IRAS after annealing to 700 K (*22*).

The surface coverage of Pd on Au(100) or Au(111) after annealing increases continuously with Pd deposited, as seen by the concomitant increase in the ratio of Pd relative to Au by Auger electron spectroscopy (AES) and LEISS (*21*, *23*). If each surface Pd atom can serve as an active site for VA synthesis, then the VA formation rate (TOF) per Pd should increase steadily with an increase in the Pd coverage up to 1 ML. However, the data in Fig. 1 show a maximum rate (TOF) at ~0.07 ML, followed by a marked decrease with increasing Pd coverage from 0.07 to 1 ML for Pd/Au(100) and a continuous decrease over the entire coverage range for Pd/Au(111). For both surfaces, there is an increase in the reaction rate (fig. S1), with an increase in the Pd coverage from 0 to 0.1 ML followed by a gradual decline in the rate from 0.1 to 1.0 ML, eventually approaching the rate observed for Pd(100) at 1.0 ML. These results strongly implicate isolated Pd sites, i.e. monomers, as catalytically active sites on Au(100) and Au(111) for VA synthesis (figs. S2 and S3).

For Pd/Au(111), the monotonic increase in the TOFs for VA formation in Fig. 1 with decreasing Pd coverage is consistent with iso-

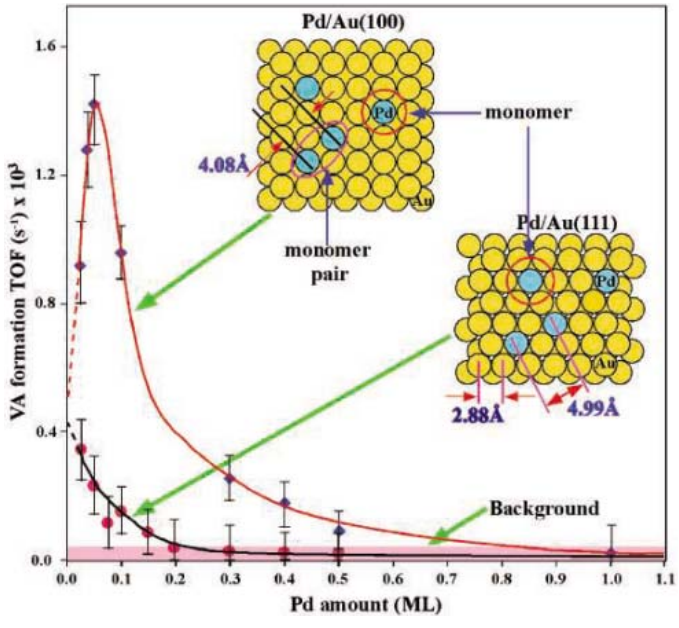

Fig. 1. Vinyl acetate (VA) formation rates (TOFs) as a function of Pd coverage on Au(100) and Au(111). The VA synthesis was carried out at 453 K, with acetic acid, ethylene, and O_2 pressures of 4, 8, and 2 torr, respectively. The total reaction time was 3 hours. The error bars are SD, based on background rate data. The two insets show Pd monomers and monomer pairs on the Au(100) and Au(111) surfaces.

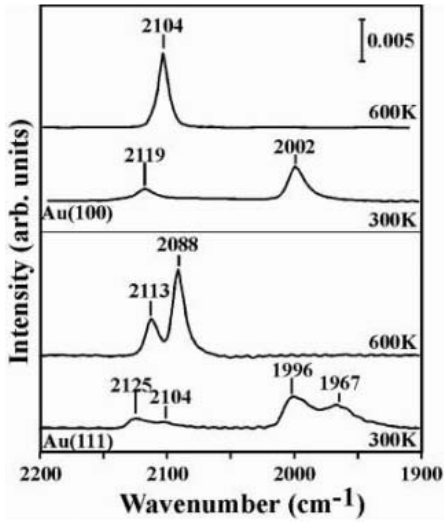

Fig. 2. IRAS spectra for CO adsorption on Pd/Au(100) and Pd/Au(111) surfaces at 100 K showing the presence (300 K anneal) and absence (600 K anneal) of contiguous Pd sites. The Pd/Au(100) and Pd/Au(111) surfaces were prepared by depositing 4 ML of Pd at 100 K, then annealing to 300 and 600 K, respectively, for 10 min. The annealing temperatures are indicated on each spectrum.

lated Pd atoms being active catalytic sites. However, the sharp maximum in the data for Pd/Au(100) in Fig. 1 at a Pd coverage of ~0.07 ML suggests that a pair of noncontiguous Pd sites, i.e., a pair of Pd monomers (as indicated in the inset of Fig. 1), is much more effective for VA formation than is a single isolated Pd site (fig. S5). The differences in VA synthesis activities between Pd/Au(100) and Pd/Au(111) then merit discussion. The reaction mechanism for VA synthesis remains uncertain; however, two pathways have been proposed: (i) adsorption and subsequent activation of ethylene to form a vinyl species that then couples with a coadsorbed acetate species to form VA (*7*), and (ii) adsorbed ethylene reacts with an adsorbed acetate nucleophile to form an ethyl acetate–like intermediate, which then undergoes a β-H elimination to form VA (*8*). Scavenging of the hydrogen with oxygen occurs to complete the reaction.

Both mechanisms assume that the coupling of a surface ethylenic species and acetate to form VA is the rate-limiting step (*7*, *8*, *13*). An illustration of a possible coupling reaction between a surface ethylenic and acetate species using a pair of Pd sites is shown in Fig. 3. Support for the insertion of ethylene into an adsorbed acetate species followed by β-H elimination as the rate-limiting step for VA formation is found in recent experimental results of Tysoe *et al*. (*24*). The presence of a π-bonded ethylenic and a bidentate acetate species on Pd monomers is supported by ancillary high-resolution electron energy loss (HREEL) data (figs. S6 and S7). On the basis of bond lengths of the parent molecular species, the optimum spacing between two active sites for coupling the reacting species is estimated to be ~3.3 Å. On the Au(100) surface, the spacing between two neighboring Pd monomers is 4.08 Å (Fig. 1, inset), which is acceptably close for coupling of the adsorbed surface species. However, on the Au(111) surface, the nearest distance between two noncontiguous Pd monomers is 4.99 Å (Fig. 1, inset), which is much larger than the ideal 3.3 Å, yielding as a consequence a much lower rate of VA formation compared with Pd/Au(100). The maximum VA synthesis rate on a pair of Pd monomers on Pd/Au(100), calculated by assuming that the ratio of Pd monomer pairs to the total Pd coverage is 6% (fig. S5), is almost two orders higher than that for an isolated Pd site. Much larger Pd ensembles have been predicted as a prerequisite for carrying out VA synthesis (*13*). The data presented here show that larger Pd ensembles are not required and that larger ensembles containing contiguous Pd atoms are much less efficient than a properly spaced pair of Pd monomers.

The significantly higher VA formation rate at Pd monomer sites could be explained by alloying (electronic), strain, and/or ensemble effects. With respect to an electronic effect, the chemisorptive properties of a metal overlayer on a dissimilar metal can differ dramatically from those of the parent bulk overlayer metal (*25*). For example, the adsorption energies and dissociative reaction barriers of small molecules such as CO have been correlated with changes in the electronic properties of certain alloy overlayers (*26*). However, for a Pd-Au alloy, the lattice strain is minimal with only a 4% lattice mismatch between a relaxed Pd overlayer and an Au(100) or Au(111) surface. Furthermore, the work functions for Au and Pd are very similar (5.3 versus 5.6 eV, respectively) and the electronegativities are identical (1.4). X-ray photoelectron spectroscopy core-level data imply very limited charge transfer between Pd and Au in Pd-Au alloys (*18*). Altogether, these data, the similar CO chemisorptive properties (*27*), and the identical activities for acetylene cyclotrimerization to benzene (*19*) of a monolayer of Pd on Au(111) compared with Pd(111) are consistent with minimal electronic and strain effects in a Pd-Au alloy.

The most plausible explanation for the unusually high activity of a Pd monomer for VA formation is an ensemble effect; i.e., the formation of Pd monomers inhibits the formation of undesirable by-products, CO, CO_2, and surface carbon (figs. S8 and S9). Ancillary adsorption experiments show that ethylene binds less strongly to a Pd monomer compared with contiguous Pd atoms (fig. S10), whereas VA bonds weakly to Pd monomers and contiguous Pd sites. Furthermore, the addition of Au to Pd significantly suppresses carbon deposition via reactant and product decomposition (*28*, *29*).

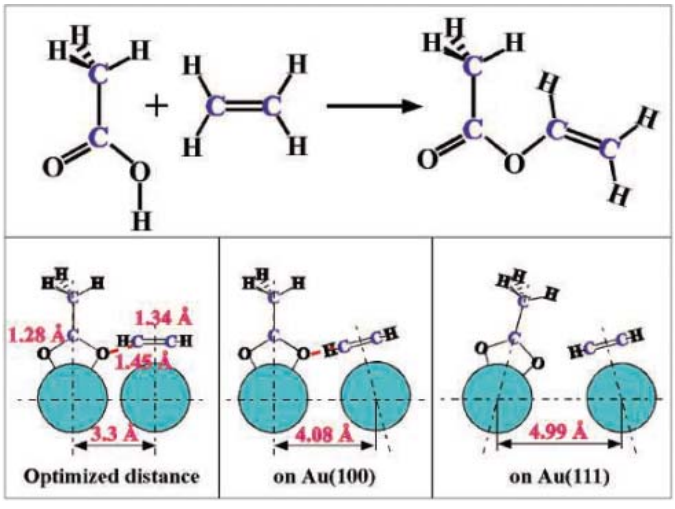

Fig. 3. Schematic for VA synthesis from acetic acid and ethylene. The optimized distance between the two active centers for the coupling of surface ethylenic and acetate species to form VA is estimated to be 3.3 Å. With lateral displacement, coupling of an ethylenic and acetate species on a Pd monomer pair is possible on Au(100) but implausible on Au(111).

References and Notes

1. E. G. Allison, G. C. Bond, *Catal. Rev.* **7**, 233 (1972).
2. P. N. Rylander, *Catalytic Hydrogenation in Organic Synthesis* (Academic Press, London, 1979).
3. R. Abel, P. Collins, K. Eichler, I. Nicolau, D. Peters, in *Handbook of Heterogeneous Catalysis*, G. Ertl, H. Knözinger, J. Weitkamp, Eds. (Wiley VCH, Weinheim, Germany, 1997), vol. 5, pp. 2298–2301.
4. A. M. Venezia, V. La Parola, V. Nicoli, G. Deganello, *J. Catal.* **212**, 56 (2002).
5. D. L. Trimm, Z. I. Onsan, *Catal. Rev.* **43**, 31 (2001).
6. M. Bonarowska, A. Malinowski, W. Juszczyk, Z. Karpinski, *Appl. Catal. B* **30**, 187 (2001).
7. S. Nakamura, T. Yasui, *J. Catal.* **17**, 366 (1970).
8. B. Samanos, P. Boutry, *J. Catal.* **23**, 19 (1971).
9. W. D. Provine, P. L. Mills, J. J. Lerou, *Stud. Surf. Sci. Catal.* **101**, 191 (1996).
10. N. Macleod, J. M. Keel, R. M. Lambert, *Appl. Catal. A* **261**, 37 (2004).
11. Y. F. Han, D. Kumar, D. W. Goodman, *J. Catal.* **230**, 353 (2005).
12. D. Stacchiola, F. Calaza, L. Burkholder, W. T. Tysoe, *J. Am. Chem. Soc.* **126**, 15384 (2004).
13. M. Neurock, *J. Catal.* **216**, 73 (2003).
14. Materials and methods are available as supporting material on *Science* Online.
15. W. K. Kuhn, J. Szanyi, D. W. Goodman, *Surf. Sci.* **274**, L611 (1992).
16. C. T. Campbell, *Curr. Opin. Solid State Mater. Sci.* **3**, 439 (1998).
17. K. Wolter *et al.*, *Surf. Sci.* **402-404**, 428 (1998).
18. B. E. Koel, A. Sellidj, M. T. Paffett, *Phys. Rev. B* **46**, 7846 (1992).
19. C. J. Baddeley *et al.*, *Surf. Sci.* **314**, 1 (1994).
20. F. Maroun, F. Ozanam, O. M. Magnussen, R. J. Behm, *Science* **293**, 1811 (2001).
21. A. Jablonski, S. H. Overbury, G. A. Somorjai, *Surf. Sci.* **65**, 578 (1977).
22. C.-W. Yi, K. Luo, T. Wei, D. W. Goodman, *J. Phys. Chem. B*, in press.
23. D. G. Swartzfager, S. B. Ziemecki, M. J. Kelley, *J. Vac. Sci. Technol.* **19**, 185 (1981).
24. D. Stacchiola *et al.*, *Angew. Chem. Int. Ed. Engl.* **44**, 4572 (2005).
25. J. A. Rodriguez, D. W. Goodman, *Science* **257**, 897 (1992).
26. B. Hammer, Y. Morikawa, J. K. Norskov, *Phys. Rev. Lett.* **76**, 2141 (1996).
27. A. Sellidj, B. E. Koel, *Phys. Rev. B* **49**, 8367 (1994).
28. Y. F. Han, D. Kumar, C. Sivadinarayana, A. Clearfield, D. W. Goodman, *Catal. Lett.* **94**, 131 (2004).
29. M. Bowker, C. Morgan, *Catal. Lett.* **98**, 67 (2004).

30. We acknowledge support by the Department of Energy, Office of Basic Energy Sciences, Division of Chemical Sciences, and the Robert A Welch Foundation. We gratefully thank Z. Dohnalek (Pacific Northwest National Laboratories) for valuable contributions and K. Luo, W. Tao, Z. Yan, W. T. Wallace, and S. Lee for helpful discussions and comments and for making available the supporting data displayed online.

Supporting Online Materials

www.sciencemag.org/cgi/content/full/310/5746/291/DC1
Materials and Methods
Figs. S1 to S10

7 June 2005; accepted 20 September 2005
10.1126/science.1115800

Shocks in Ion Sputtering Sharpen Steep Surface Features

H. Henry Chen,[1]* Omar A. Urquidez,[2] Stefan Ichim,[2]
L. Humberto Rodriquez,[2] Michael P. Brenner,[2] Michael J. Aziz[2]†

We report a regime of ion beam sputtering that occurs for sufficiently steep slopes. High slopes propagate over large distances without dissipating the steepest features. Both the propagation velocity and the dynamically selected slope are universal, independent of the details of the initial shape of the surface. The resulting behavior can be understood as the propagation of a shock front that self-selects a stable slope, as has been previously observed in thin-film fluid flows. Experiments confirm predictions of the theory. An important implication of the propagative behavior at high surface slopes is that a pattern can be fabricated at a large length scale and, through uniform ion irradiation, reduced to a smaller length scale while preserving, or even sharpening, the sharpest features.

Methods of micro- and nanofabrication of three-dimensional (3D) structures are of increasing interest owing to their importance for the creation of compact 3D devices and their assembly into functional 3D systems. Examples include microelectromechanical systems, 3D integration of electronic microprocessors, 3D information storage, and photonic band gap waveguides. Ion beam irradiation of steeply sloping surfaces has been used for micromachining tall, steep features (*1*, *2*); fabricating semiconductor quantum dots through a self-organization process (*3*, *4*); templating for guided self-organization of sputter patterns (*5*); and ion beam sculpting of nanopore single-biomolecule detectors (*6*, *7*). Because ion irradiation is currently used for doping control in the mass production of semiconductor devices, there may be little impediment to its rapid uptake for morphology control if the predictability is improved.

The theory of ion sputtering (*8*, *9*) has been applied to nearly flat surfaces and has received a great deal of attention in the context of pattern-forming morphological instabilities (*3*, *4*, *10*–*19*). However, current theories expand the sputtering behavior in powers of surface slope and are restricted to small slopes, and thus comparisons of theory and experiment have focused on small-slope evolution. Through theory, experiments, and computer simulations, we have discovered a new regime of ion beam sputtering that occurs for sufficiently steep slopes. High slopes propagate over large distances without dissipating the steepest features. Both the propagation velocity and the dynamically selected slope are universal, independent of the details of the initial shape of the surface.

Our theoretical results make use of the classical theory of sputtering (*8*, *9*) and develop a small-curvature approximation that is valid for any slope. The resulting behavior can be understood as the propagation of a shock front that self-selects a stable slope; the mathematical structure of the solutions is the same as that previously observed in thin-film fluid flows (*20*, *21*). An important implication of the propagative behavior at high surface slopes is that a pattern can be fabricated at a large length scale and, through uniform ion irradiation, reduced to a smaller length scale while preserving, or even sharpening, the sharpest features.

Our experiments use a focused ion beam (FIB) of 30-keV gallium to sputter a silicon target. The FIB is rastered over a rectangular region containing prefabricated pits of various depths and lateral dimensions. Surprisingly, the pits are not smeared out by the sputtering, but rather expand at fixed rates while maintaining steep walls throughout the expansion (Fig. 1). Crystallographic anisotropy is not a possible origin of this effect, because the surface becomes amorphous during the initial stage of ion implantation.

What is the mechanism for maintaining the sharp fronts? The simplest possibility is that it arises from the standard picture of sputtering due to Sigmund (*8*, *9*), which posits that as an average ion penetrates the surface a distance a parallel to its initial flight trajectory, its kinetic energy is distributed via collisions in a Gaussian ellipsoid with longitudinal and lateral widths σ and μ, respectively. The probability that a surface atom is ejected is proportional to the total energy that reaches it from all ion bombardments. Redeposition of surface atoms is assumed to be negligible.

To test this hypothesis, we solve numerically a model combining Sigmund's mechanism with surface diffusion. Because the radius of the pit in the experiments is much larger than the scale over which the surface slope varies, we consider the edge of the pit as straight and track the evolution of its cross-sectional profile, described by the height function $z = h(x,t)$. We orient the z axis along the ion beam, with the ions impinging in the downward direction. The dynamics can then be written as an integral-differential equation for the rate at which the surface retracts in the locally normal direction

$$-\frac{\partial h/\partial t}{\sqrt{1+h_x^2}} = pJ\epsilon \int dx' E(x;x') - B\nabla^2\kappa \quad (1)$$

The first term on the right represents sputtering, where J is the ion flux, p is the sputtering rate per unit power density, ε is the energy released per ion, and $E(x;x')$ is the normalized distribution of energy on the surface at x due to an ion bombardment at x'. The second term on the right describes surface diffusion (*22*) for a surface with mean curvature κ (reckoned positive for concave surfaces), with B a phenomenological constant; the classical equilibrium microscopic description of B (*22*) might be modified during sputtering. The collision parameters (a,σ,μ) can be obtained either through atomistic simulations (*23*) or through fits of sputter yield as a function of angle for a flat surface [SOM Text, Sect. 1.1 (*24*)].

Numerical solutions ("simulations") of Eq. 1 show two different regimes, depending on the initial maximum slope of the pit. When the inclination angle of the initial pit wall is above the critical value of ≈68°, the leading edge of the profile evolves to a constant slope region (inclination ≈76°) moving with a constant speed,

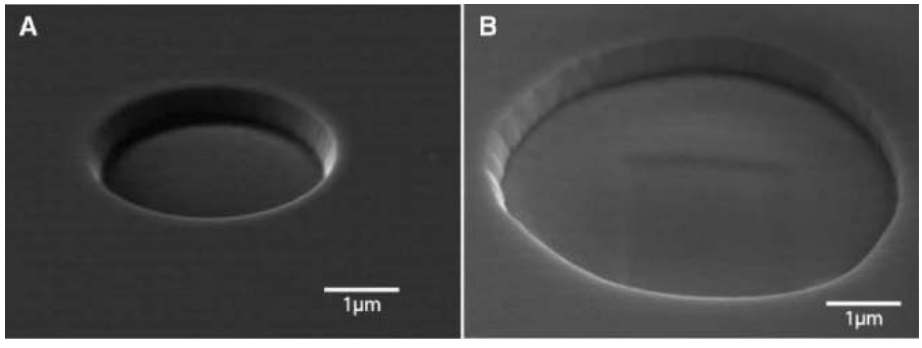

Fig. 1. (**A**) An SEM image of an initial circular pit in silicon with 3-μm diameter and 0.5-μm depth. (**B**) The wall of the enlarged pit is still sharp after uniform ion exposure to a fluence of ~1.5 × 10^{19} ions/cm^2.

[1]Department of Physics, [2]Division of Engineering and Applied Sciences, Harvard University, Cambridge, MA 02138, USA.

*Present address: Lawrence Livermore National Laboratory, Livermore, CA 94550, USA.
†To whom correspondence should be addressed. E-mail: maziz@harvard.edu

in units of distance per unit fluence (Fig. 2A). Behind the leading edge there is a "snail's foot," which grows with time and gradually invades the constant slope region. Notably, both the velocity and the slope at the leading edge are universal, independent of the initial shape of the pit. Different initial conditions lead to quantitatively identical behaviors (compare Fig. 2, A and B). In contrast, if the initial maximum inclination is below the critical value, both the slope and the velocity continuously decrease: The steep edge dissipates.

We seek to understand why these regimes exist, by reducing Eq. 1 to a nonlinear partial differential equation that is more amenable to analysis. Previous reductions [e.g., (*19*)] have focused on surface modulations that are small relative to the ion penetration depth and hence are not suited for the evolution of tall and steep morphological features such as step edges. Instead, we note that although the slopes occurring in the solutions depicted in Fig. 1 are high, the length scale l over which the slope changes is in fact large compared to the penetration depth a. This motivated us to carry out an expansion for the Sigmund integral in Eq. 1 in terms of the ratio a/l [SOM Text, Sect. 1.2 (*24*)], leading to

$$\frac{\partial h}{\partial t} = -Y(b) + D(b)\frac{\partial^2 h}{\partial x^2} + B\frac{\partial^2 \kappa}{\partial s^2} \quad (2)$$

where $b \equiv \partial h/\partial x$. This expansion shows that the Sigmund mechanism reduces to two simple (nonlinear) physical effects. $Y(b)$ represents the erosion rate of a surface of constant slope b: Steeper surfaces erode faster than shallow ones because energy is deposited closer to the surface. The curvature coefficient $D(b)$ is the origin of the celebrated Bradley-Harper instability (*10*): At small b, $D(b) < 0$, causing concave regions to erode faster than convex regions. The instability is opposed by surface diffusion, as characterized by the final term in Eq. 2 and described in the SOM Text, Sect. 1.3 (*24*). Note the differentiation with respect to the arclength s.

Numerical comparison of solutions to both the reduced dynamics (Eq. 2) and the full Sigmund model (Eq. 1) shows that Eq. 2 quantitatively reproduces the full simulations [SOM Text, Sect. 1.4 (*24*)]. The terms in Eq. 2 that are most important for the traveling step are the erosion rate $Y(b)$ and surface diffusion: The curvature effect $D(b)$ is small and can be neglected without significant error. To make further progress, it is particularly illuminating to drop the curvature term and differentiate Eq. 2:

$$\frac{\partial b}{\partial t} + C\frac{\partial b}{\partial x} = B\frac{\partial}{\partial x}\frac{\partial^2 \kappa}{\partial s^2} \quad (3)$$

The left-hand side of the equation now has the canonical mathematical structure of a nonlinear conservation law (*25*), with $C(b) \equiv (\partial/\partial b)Y(b)$ playing the role of a local advection velocity. Equations of this form arise in many physical contexts and typically result in nonlinear waves, such as shocks or rarefaction waves. The nonlinear dependence of the advection velocity on surface slope can lead to sharpening, which is counteracted by surface diffusion.

To understand when steps can propagate without dissipation, we seek solutions of Eq. 3 of the form $b(x,t) = S(x - Ut)$, where U is the propagation velocity. The numerical simulations indicate the solutions have zero slope on the right [$b(x\to\infty)\to 0$] and fixed positive slope on the left [$b(x\to-\infty)\to b\_$]. Equation 3 then implies [SOM Text, Sect. 1.5 (*24*)]

$$U = \frac{Y(b\_) - Y(0)}{b\_} \quad (4)$$

In shock dynamics, Eq. 4 is referred to as the Rankine-Hugoniot condition. For classical shocks, the shock velocity U satisfies the Lax condition $C(b\_) > U > C(0) = 0$: The advection velocity of the rear (front) of the shock is faster (slower) than the shock speed, and the profile is "compressed" from both sides. Figure 2D shows both the shock velocity and the advection velocity. For slopes below $b\_ = 2.5$ or inclination angles below 68°, the Lax condition holds; hence, there is a continuous family of steady shock solutions over this range. However, for $b\_ > 2.53$, the trailing edge of a putative shock is slower than the shock speed, which suggests that the shock would continuously spread in time.

Nonetheless, when the Lax condition is violated, steady shocks can still exist, as long as the dominant mechanism of smoothing is fourth-order diffusion (in this case, surface diffusion). However, such undercompressive shocks (*26*, *27*) exist only if $b\_$ is chosen to be a particular value. This result can be derived [SOM Text, Sect. 1.5 (*24*)] by determining the conditions under which solutions to the ordinary differential equation for the shock profile $S(x-Ut) = S(\eta)$ are compatible with the boundary conditions.

Motivated by this argument, we conducted a numerical search for the selected velocity of the undercompressive shock and found that such a solution exists for $b\_ = 3.9$ ($\theta = 76°$) and $U = 0.085(pJ\varepsilon/\sigma)$. Figure 2C shows that this solution agrees with numerical simulations of Eq. 1. The ratio of the shock velocity to the downward velocity of the sputtered surface at normal incidence is a fixed constant: $U_{shock}/U_{sputter} = 1.7$. This dimensionless number depends only on the shape of $Y(b)$ through the parameters a/σ and μ/σ. The surface diffusion parameter B does not affect the selected slope and velocity: B affects only the scale $\sim B^{1/3}$ over which the slope changes from $b\_$ to 0. Hence, the essential slope-steepening mechanism is independent of the surface diffusivity, as long as the dominant diffusive fluxes are fourth order.

To test this theory, we fabricated and then observed the subsequent evolution of pits in Si(001) at room temperature using a FEI DualBeam DB235 FIB–scanning electron microscope (SEM). We used a beam of Ga^+ at 30 keV and 3 nA to machine rectangular pits (the "original fabrication pit" in Fig. 3) with lateral dimensions 25 μm by 12 μm. To minimize the effects of deposition of material sputtered from one pit edge onto another edge during subsequent evolution experiments, the pits straddled the cleaved edge of the Si wafer, so there was no opposite edge facing the "experimental edge" parallel to the cleaved boundary (Fig. 3). We milled rectangular pits with vertical side walls ~1.7 μm deep. For subsequent evolution, we irradiated the experimental edge with a rastered (20 μm by 20 μm) rectangle (the "evolution pit") shorter than the edge length and extending farther from the cleavage edge than the original fabrication pit (Fig. 3). Irradiation was carried out in a vacuum of $\approx 3 \times 10^{-6}$ mbar. The beam current was 3 nA and the spot size was nominally 60 nm. During rastering the beam dwells at each discrete location for 1 μs and then moves rapidly to an adjacent location. The separation between adjacent locations was set to nominally 50% overlap, which in

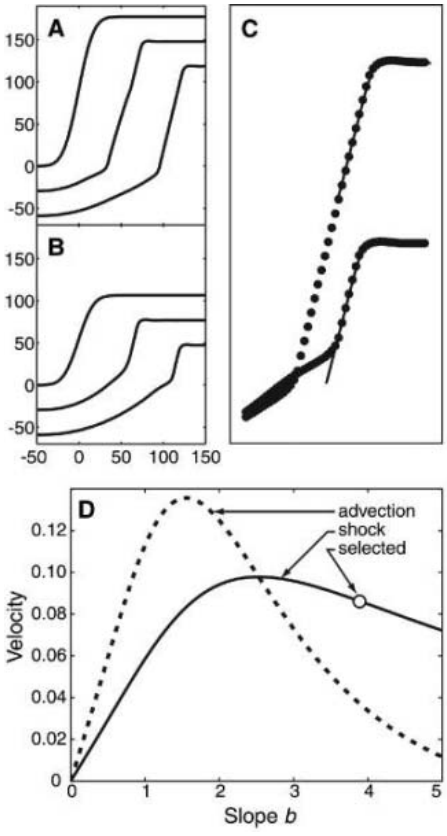

Fig. 2. Predicted profile evolution. (**A** and **B**) Time sequences showing evolution of $h(x)$ starting from two different initial conditions. The maximum initial slope in (A) is 5.0 and in (B) is 3.0; the final slope for each is 3.9. (**C**) Each final profile agrees with the same similarity solution (solid line). (**D**) Comparison of the shock velocity U and the advection velocity C as functions of slope. An undercompressive shock solution exists at $b = 3.9$, indicated by the circle. Distances are normalized by σ and velocities are normalized by $pJ\varepsilon/\sigma$.

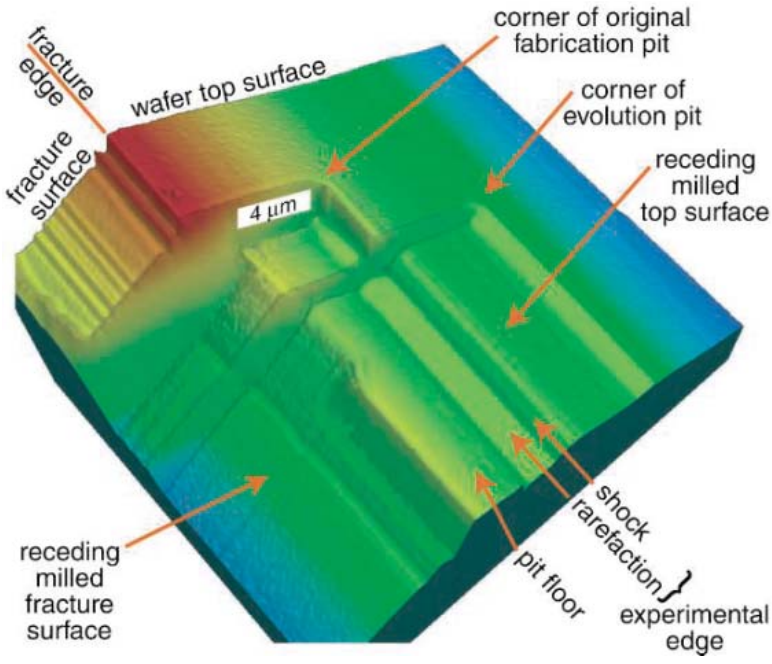

Fig. 3. Perspective view of pit milled by focused ion beam. The original fabrication pit had vertical side walls and straddles the fracture edge. Subsequently, the evolution pit was centered on the "experimental edge" of the original fabrication pit, causing edge morphology evolution. The original edge can be seen near corner of the original fabrication pit. As the evolution pit was milled, the original edge broke up into a steep side wall ("shock") and shallower snail's foot ("rarefaction"), as predicted. Note also the formation of another steep shock on the upper edge of the milled fracture surface, adjacent to the pit floor.

this case meant a 30-nm center-to-center spacing. The current profile within the beam is believed to be roughly Gaussian. We rastered various samples for varying durations.

The morphology evolution of the experimental edge was characterized using a Nanoscale OP 200M confocal optical profilometer (Hyphenated Systems, LLC, Burlingame, California). Relevant cross sections of the 3D images obtained are seen in the foreground of Fig. 4. These images provide compelling qualitative confirmation of the theory. In Fig. 4, the features of the profile of the experimental edge are, from right to left, the horizontal upper surface of the wafer that was milled vertically by rastering; a series of undulations that grew as the experimental edge was approached; a very steep edge corresponding to the undercompressive shock; a lower-slope rarefaction wave connecting the steep wall with the pit floor; a trough and ridge where the rarefaction wave intersects the pit floor; and a horizontal pit floor. As predicted (Fig. 2, A and B), with increasing fluence the height of the shock front gradually decreased, the size of the rarefaction wave gradually increased, and the steep slope did not dissipate. The undulations ahead of the shock front are related to surface diffusion and can be used to evaluate the diffusion parameter B. The valley and ridge at the intersection of the rarefaction wave and the pit floor are not predicted by the Sigmund mechanism; we expect that secondary collisions between scattered ions or recoiled atoms and the surface are important here. Note, however, the shock that developed accidentally on the fracture surface, adjacent to the pit floor in Fig. 3. Whereas the shock on the "experimental edge" developed from a more steeply sloped feature, the shock on the fracture surface developed from a less steeply sloped feature, thereby confirming another prediction of the theory of a regime of feature "antidissipation".

The ability to propagate sharp features without dissipation leads to the intriguing possibility of prepatterning a surface (by lithography or some other means) and then uniformly irradiating it to develop predetermined structures on an even smaller length scale (*28*). Directing two fronts toward each other might be exploited as a method of sublithographic patterning and may lead to new phenomena as well [e.g., (*29*)].

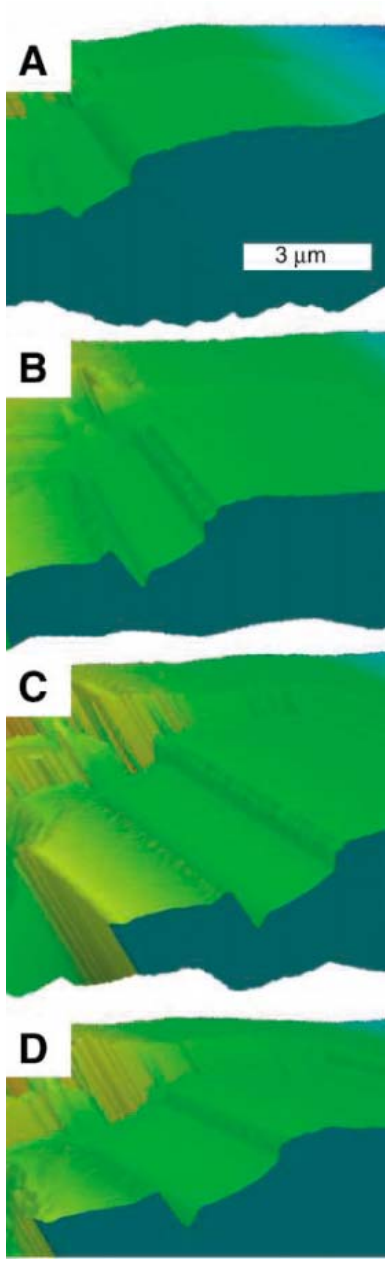

Fig. 4. Advancing pit as seen in experiment after (**A**)128, (**B**) 256, (**C**) 384, and (**D**) 512 s, corresponding to fluences of 0.6×10^{18}, 1.2×10^{18}, 1.8×10^{18}, and 2.4×10^{18} Ga^+ ions/cm^2. For ease of imaging, each sample was tilted arbitrarily before imaging; for comparison, the resulting images were rotated, so the sputtered top surface appears horizontal.

References and Notes

1. M. J. Vasile, Z. Niu, R. Nassar, W. Zhang, S. Liu, *J. Vac. Sci. Technol. B* **15**, 2350 (1997).
2. D. Adams, M. Vasile, T. Mayer, V. Hodges, *J. Vac. Sci. Technol. B* **21**, 2334 (2003).
3. S. Facsko *et al.*, *Science* **285**, 1551 (1999).
4. F. Frost, A. Schindler, F. Bigl, *Phys. Rev. Lett.* **85**, 4116 (2000).
5. A. Cuenat, H. B. George, K. C. Chang, J. Blakeley, M. J. Aziz, *Adv. Mater.*, in press.
6. J. Li *et al.*, *Nature* **412**, 166 (2001).
7. D. Stein, J. Li, J. A. Golovchenko, *Phys. Rev. Lett.* **89**, 2761606 (2002).
8. P. Sigmund, *Phys. Rev.* **184**, 383 (1969).
9. P. Sigmund, *J. Mater. Sci.* **8**, 1545 (1973).
10. R. M. Bradley, J. M. E. Harper, *J. Vac. Sci. Technol. A* **6**, 2390 (1988).
11. R. Cuerno, A. L. Barabasi, *Phys. Rev. Lett.* **74**, 4746 (1995).
12. G. Carter, V. Vishnyakov, *Phys. Rev. B* **54**, 17647 (1996).
13. S. Park, B. Kahng, H. Jeong, A. L. Barabasi, *Phys. Rev. Lett.* **83**, 3486 (1999).
14. J. Erlebacher, M. Aziz, E. Chason, M. Sinclair, J. Floro, *Phys. Rev. Lett.* **82**, 2330 (1999).
15. J. Erlebacher, M. J. Aziz, E. Chason, M. B. Sinclair, J. A. Floro, *J. Vac. Sci. Technol. A* **18**, 115 (2000).
16. S. Habenicht, *Phys. Rev. B* **63**, 125419 (2001).
17. C. C. Umbach, R. L. Headrick, K. C. Chang, *Phys. Rev. Lett.* **87**, 246104 (2001).
18. U. Valbusa, C. Boragno, F. B. de Mongeot, *J. Phys. Condens. Matter* **14**, 8153 (2002).

19. M. A. Makeev, R. Cuerno, A. L. Barabasi, *Nucl. Instrum. Methods Phys. Res. B* **197**, 185 (2002).
20. A. L. Bertozzi, A. Munch, X. Fanton, A. M. Cazabat, *Phys. Rev. Lett.* **81**, 5169 (1998).
21. J. Sur, A. L. Bertozzi, R. Behringer, *Phys. Rev. Lett.* **90**, 126105 (2003).
22. W. W. Mullins, *J. Appl. Phys.* **28**, 333 (1957).
23. J. F. Ziegler, J. P. Biersack, U. Littmark, *The Stopping and Range of Ions in Solids* (Pergamon, New York, 1985).
24. Details of the analysis are available as supporting material on *Science* Online.
25. G. B. Whitham, *Linear and Nonlinear Waves* (Wiley, New York, 1974).
26. A. L. Bertozzi, A. Munch, M. Shearer, *Physica D* **134**, 431 (1999).
27. A. L. Bertozzi, M. Shearer, *SIAM J. Math. Anal.* **32**, 194 (2000).
28. For a given lateral propagation distance, one would need to pattern features of a predictable minimum height.
29. M. Castro, R. Cuerno, L. Vazquez, R. Gago, *Phys. Rev. Lett.* **94**, 016102 (2005).
30. We are grateful to H. Bola George and W. MoberlyChan for technical assistance. This research was supported by Harvard Materials Research Science and Engineering Centers (MRSEC) grant NSF-DMR-0213805, U.S. Department of Energy grant DE-FG02-01ER45947 (O.A.U.), and NSF grants NSF-DMR-0306997 (M.J.A.) and NSF-DMS-0296056 (M.P.B.). S.I. was partially supported by the Harvard College Research Fund. L.H.R. and S.I. were supported by the Research Experience for Undergraduates program (DMR-0353937) of the Harvard MRSEC.

Supporting Online Material
www.sciencemag.org/cgi/content/full/310/5746/294/DC1
SOM Text
Figs. S1 and S2
References

11 July 2005; accepted 29 August 2005
10.1126/science.1117219

Structure and Freezing of $MgSiO_3$ Liquid in Earth's Lower Mantle

Lars Stixrude[1]*† and Bijaya Karki[2]

First-principles molecular-dynamics simulations show that over the pressure regime of Earth's mantle the mean silicon-oxygen coordination number of magnesium metasilicate liquid changes nearly linearly from 4 to 6. The density contrast between liquid and crystal decreases by a factor of nearly 5 over the mantle pressure regime and is 4% at the core-mantle boundary. The ab initio melting curve, obtained by integration of the Clausius-Clapeyron equation, yields a melting temperature at the core-mantle boundary of 5400 ± 600 kelvins.

The structure of silicate liquids over most of the mantle pressure regime is unknown. There is experimental evidence that silicate liquid structure changes substantially on compression and that these changes include an increase in Si-O coordination number from 4 toward 6 (*1*), although there are no experimental observations within the liquid stability field at lower mantle pressure.

Most simulations of silicate liquids have been based on atomistic models, which permit much faster computation but have the disadvantage of being based on empirical force fields, the forms of which are uncertain (*2*, *3*). First-principles molecular-dynamics (FPMD) simulations are considerably more costly because the electronic structure must be computed at each time step, but they are also more robust because they make no assumptions about the type of bonding or the shape of the charge density.

Here, we present FPMD simulations of $MgSiO_3$ liquid over the pressure-temperature range of Earth's mantle, based on density functional theory in the local density approximation and the plane-wave pseudopotential method (*4*). The simulations are performed in the canonical ensemble with periodic boundary conditions and a Nosé thermostat (*5*). The primary cell is cubic, with 80 atoms (16 formula units). The initial condition is a pyroxene structure homogeneously strained to a cubic cell shape and the desired volume. The simulated strained crystal is melted at 6000 K and then cooled isochorically to 4000 K and 3000 K. Melting was confirmed by inspection of the radial distribution function and the mean square displacement. Total run durations are 3 ps, with the last 2.4 ps used for computing equilibrium averages. To ensure that the results are not sensitive to initial conditions, we performed simulations with twice the number of atoms (160 atoms initiated with a cubic majorite structure), twice the duration (6 ps), and different initial configurations (80-atom perovskite supercell homogeneously strained to a cubic cell shape) and found that the computed properties of the liquid were unchanged within statistical uncertainties. We explore a range of volumes $V = V_X$ to $V = V_X/2$, where V_X = 38.9 cm^3 mol^{-1} is the experimental value for the liquid at the ambient-pressure melting point (1830 K) (*6*).

To explore freezing, we also performed simulations of orthorhombic $MgSiO_3$ perovskite, following the same procedures as the liquid simulations except that at each volume the shape of the unit cell was taken to be that found by structural relaxation at static conditions. We found that the unstrained perovskite structure persisted (meta) stably at all volumes $V < 0.7V_X$. We are thus able to compare directly the simulated properties of liquid and perovskite over the entire lower mantle pressure-temperature regime.

Inspection of the equilibrated liquid structure shows that compression has a large influence on the atomic arrangement (Fig. 1). At the experimental zero-pressure volume, the liquid shows four-fold Si-O coordination, as does the stable crystalline phase at this volume, but without the elements of longer ranged order exhibited by the crystal, such as the infinitely long linear chains of tetrahedra that characterize pyroxenes. The liquid also shows a few non-four-fold-coordinated silicon atoms. At high pressure, the liquid structure is much more densely packed.

In the simulations, the average Si-O coordination number increased smoothly and nearly linearly with compression, with no discernible influence of temperature, reaching a value of 6 at a pressure corresponding to the base of Earth's mantle (Fig. 1). The coordination change does not take place over a narrow pressure interval, as has been suggested (*7*). Such a rapid structural change would be expected to cause changes in the compressibility of the liquid (*7*) and in the slope of the melting curve (*8*) over a correspondingly narrow pressure interval, anomalies for which we find no evidence in our simulations.

The liquid equation of state can be accurately described by the Mie-Grüneisen form

$$P(V,T) = P_c(V,T_0) + \frac{\gamma}{V} C_V (T - T_0) \quad (1)$$

where P_c is the reference isotherm, taken to be at T_0 = 3000 K, γ is the Grüneisen parameter, and C_V is the isochoric heat capacity. The latter quantities are computed from the simulations by noting that the internal energy E and pressure P vary linearly with temperature along isochores to within our uncertainty. The value of γ is then calculated at each volume from

$$\gamma = \frac{V}{C_V}\left(\frac{\partial P}{\partial T}\right)_V \quad (2)$$

and $C_V = (\partial E / \partial T)_V$. We find that C_V decreases by about 10% from 4.12 ± 0.11 Nk at $V = V_X$ [the experimental value is 4.17 ± 0.18 Nk (*9*)] to 3.54 ± 0.11 Nk at $V = V_X/2$, where N is the number of atoms and k is the Boltzmann constant. γ increases by a factor of three over the same range of volume, reflecting the increase in thermal pressure. All known mantle crystalline phases show the opposite behavior: γ decreases on compression (*10*).

The unusual behavior of γ in the liquid can be understood on the basis of the pressure-

[1]Department of Earth and Planetary Science, University of California, Berkeley, CA 94720, USA. [2]Department of Computer Science, Louisiana State University, Baton Rouge, LA 70803, USA.

*On leave from Department of Geological Sciences, University of Michigan, Ann Arbor, MI 48109, USA.
†To whom correspondence should be addressed. E-mail: stixrude@umich.edu

induced change in liquid structure (Fig. 2). Experimental data on crystalline $MgSiO_3$ phases show that, although compression reduces the value of γ in each individual phase, polymorphic phase transformations have an even larger and opposing effect, with the higher coordinated phase showing the larger value of γ. As the coordination number of the liquid increases on compression, the liquid adopts values of γ characteristic of the more highly coordinated state. The behavior of the liquid is consistent with theoretical analyses of the influence of pressure-induced coordination changes on γ (*11*). Previous theoretical and experimental studies have also found that γ increases on isothermal compression in liquids (*12*–*14*).

The volume of the liquid closely approaches, but does not fall below, that of perovskite over the mantle pressure regime (Fig. 3). The volume difference is 4% at 6000 K and 140 GPa, as compared with 18% at the ambient-pressure melting point (*6*). Studies based on dynamic compression also find that the volume of fusion is markedly reduced at deep lower mantle conditions (*15*). The enthalpy difference between liquid and perovskite increases nearly linearly with increasing temperature and changes little with compression over the pressure regime of perovskite stability ($25 < P < 140$ GPa) (Fig. 3). The quantity $\Delta H/T$ varies little throughout this regime and has a value near 1.5 *Nk*, significantly greater than the value *Nk* ln2 often assumed for the entropy of fusion in high-pressure melting studies, and based primarily on one-component, close-packed materials. The larger value in our simulations can be understood on the basis of liquid structure: Throughout the lower mantle pressure regime, the liquid shows a wide range of different coordination environments, which adds a configurational component to the entropy that is absent in structurally simpler liquids (*16*). A recent FPMD study of MgO also found values of the entropy of melting ~1.5 *Nk* at high pressure (*17*).

We used our simulations to predict the melting curve of $MgSiO_3$ by integrating the Clausius-Clapeyron equation (*18*)

$$\frac{\partial T_M}{\partial P} = \frac{\Delta V}{\Delta H/T} \qquad (3)$$

The quantities on the right-hand side are computed from our simulations over the entire lower mantle regime. The integration constant is set by assuming a single fixed point along the melting curve. We choose this point as 25 GPa, 2900 K near the low-pressure limit of perovskite melting, where many different experiments are mutually consistent.

Our predicted melting curve lies between previous experimental determinations, which diverge widely at pressures above 30 GPa (Fig. 4). The differences between theory and experiment can be understood in detail. Because we find $\Delta V > 0$, our melting slope and melting temperature must be greater than experimental results with a vanishingly small melting slope, which requires $\Delta V = 0$ (*19*, *20*). Zerr and Boehler (*21*) argued that their much higher melting slope is consistent with the Lindemann law, a simple scaling argument that is valid if neither solid nor liquid undergo considerable structural change on compression (*22*). This picture of melting is incompatible with the large structural changes that we find in $MgSiO_3$ liquid. Moreover, because the structural changes we see lead to more efficient packing, and therefore to reduced liquid-solid volume contrast, our melting slope and melting temperature should be correspondingly reduced. Some of the discrepancy among experiments may be due to differences in composition—Fe-free (*21*) versus ~10% Fe (*8*, *19*, *20*)—but the wide divergence among diamond-anvil cell studies more likely reflects difficulties in detecting melt at high pressure (*23*). In this context, we note that a recent determination based on dynamic compression (*15*) agrees well with our predicted melting curve.

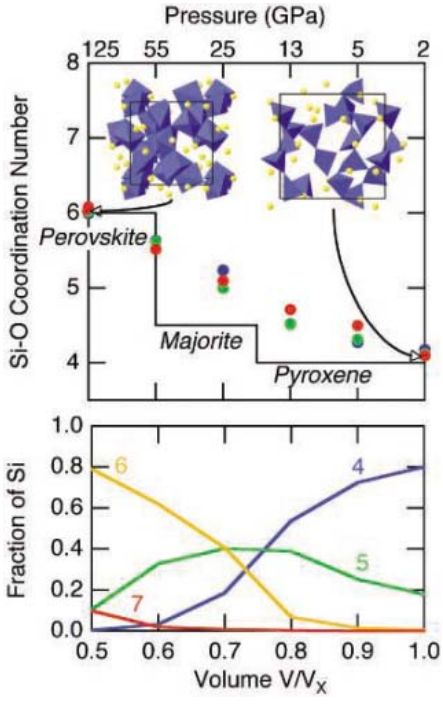

Fig. 1. (**Top**) Mean Si-O coordination number at 3000 K (blue), 4000 K (green), and 6000 K (red) compared with that of the crystalline solidus phases plotted over their approximate range of stability. (**Bottom**) Distribution of Si-O coordination environments in $MgSiO_3$ liquid at 3000 K. Pressures are those found in our FPMD simulations along the 3000 K isotherm for the liquid. Also shown are snapshots from the equilibrated portion of the simulations at 3000 K and $V = V_X$ (right) and $V = V_X/2$ (left). In blue are the Si-O coordination polyhedra and in yellow the Mg ions. The primary simulation cell, which contains 80 atoms, is indicated by the black line.

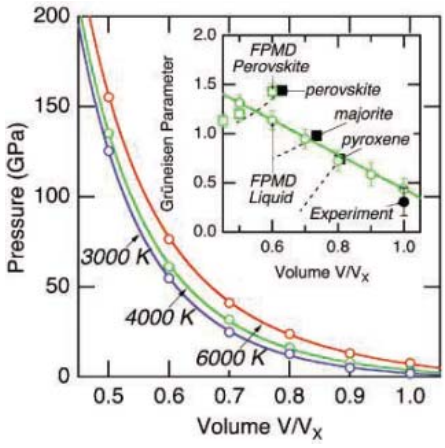

Fig. 2. Equation of state of $MgSiO_3$ liquid. FPMD results (open symbols) and Mie-Grüneisen equation of state (lines) fit to the FPMD results at 6000 K (red), 4000 K (green), and 3000 K (blue). Uncertainties in pressure, estimated on the basis of the appropriate statistics (*35*), are 1 to 2 GPa and are smaller than the size of the symbols on this scale. (**Inset**) Grüneisen parameter of liquid (open circles) and perovskite (open squares) from FPMD simulations, and experimental value (filled circle) for the liquid near its ambient melting point, calculated from the identity $\gamma = \alpha K_T V/C_V$. Also shown are the Grüneisen parameter of $MgSiO_3$ solidus crystalline phases at ambient conditions (filled squares) and under compression (dashed lines) (*10*). Experimental values of the thermal expansivity α, isothermal bulk modulus K_T, and volume *V* are from (*6*), and isochoric heat capacity C_V is from (*9*). The Mie-Grüneisen equation of state of the liquid is given by Eq. 1, with a third-order Eulerian finite strain expression for P_c and $T_0 = 3000$ K, $V_0 = 1.13V_X$, $K_0 = 10.1$ GPa, $K_0' = 7.6$, $C_V = 3.7Nk$, and $\gamma = 0.21 - 1.75(V-V_0)/V_X$.

The marked decrease in the volume of fusion of $MgSiO_3$ that we find means that liquids are likely to be denser than coexisting solids in the deep mantle. In a multicomponent system, the density contrast between liquid and coexisting solid is a function of the volume contrast and the difference in chemical composition. In the shallow mantle, the volume contrast dominates, and liquids are less dense despite being enriched in heavy major elements such as Fe and Ca. In the deep mantle, where the volume contrast is small, the difference in composition is likely to be the determining factor. Experiments show that Fe and Ca continue to be preferentially incorporated in the liquid phase at least up to 25 GPa (*24*). For example, an apparent Fe-Mg partition coefficient between solid and liquid $K = [(X_{Fe}^{sol} X_{Mg}^{liq})/(X_{Fe}^{liq} X_{Mg}^{sol})] \approx 0.4$, where X_A^{α} is the mole fraction of element *A* in phase or phase assemblage α, would be sufficient to overcome the volume difference between $MgSiO_3$ liquid and perovskite and make the liquid denser.

The mantle solidus has been estimated to lie 800 to 1300 K below that of pure $MgSiO_3$ (*25*).

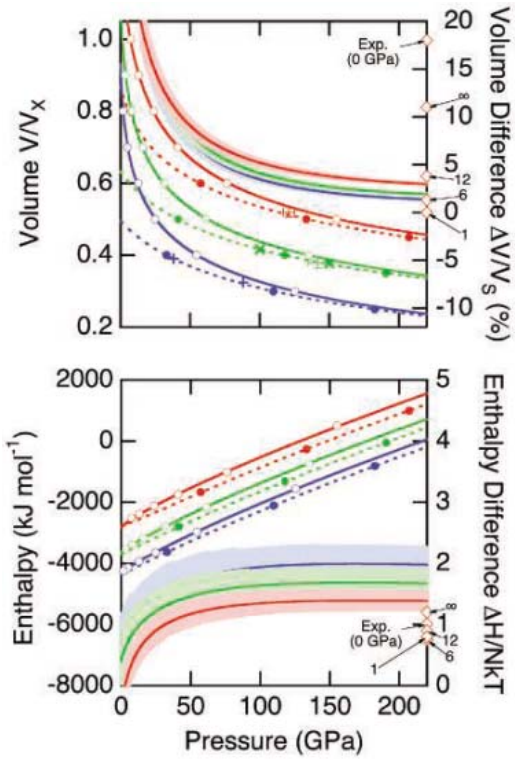

Fig. 3. (**Top**) Volume and (**Bottom**) enthalpy of liquid (open circles and solid lines) and perovskite (filled circles and dashed lines) at 3000 K (blue), 4000 K (green), and 6000 K (red). For clarity, values at 3000 K and 4000 K are shifted downward in volume by 0.1 and 0.2, and in enthalpy by 500 and 1000 kJ mol^{-1}, respectively. Statistical uncertainties are smaller than the size of the symbols. Lines with shading indicating estimated uncertainties are referred to the right-hand axes and show the liquid-perovskite volume and enthalpy differences. The volume difference is divided by the volume of the solid, and the enthalpy difference is divided by *NkT*. Lines are computed from the Mie-Grüneisen equation of state previously described (Fig. 2) and with $H(P = 0,T_0) = -3295$ kJ mol^{-1} for the liquid. Parameters for the solid equation of state are $T_0 = 3000$ K, $V_0 = 0.696V_X$, $K_0 = 162$ GPa, $K_0' = 4.3$, $C_V = 3.1Nk$, $\gamma = 1.62 + 2.00(V-V_0)/V_X$, and $H(P = 0,T_0) = -3372$ kJ mol^{-1}. Previous results for perovskite are shown as plusses (*32*), crosses (*33*), and error bars (*36*). Open symbols show the volume and entropy of melting according to experiments at the ambient-pressure melting point (*6*, *9*) and monatomic model liquids interacting through inverse power law repulsive pair potentials with the power indicated (*37*).

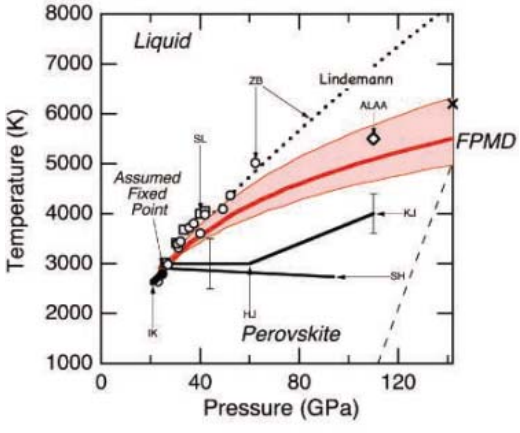

Fig. 4. FPMD melting curve of $MgSiO_3$ perovskite (red line with shading indicating uncertainties) compared with experimental determinations: HJ (*19*), KJ (*8*), IK (*38*), SH (*20*), ZB (*21*), SL (*39*), and ALAA (*15*). The fixed point assumed for the Clausius-Clapeyron integration is indicated. The dashed curve is the extrapolation by Zerr and Boehler (*21*) of their experimental results according to the Lindemann law. Thin long-dashed line shows the perovskite (pv) to post-perovskite (ppv) phase transformation (*40*). The cross is the pv-ppv-melt triple point computed using a classical pair-potential model "corrected" by comparing the location of lattice instabilities in quantum and classical molecular dynamics simulations (*3*).

Combining this estimate with our ab initio value of the melting point at 136 GPa of 5400 ± 600 K yields a mantle solidus temperature of 3500 to 5200 K, which overlaps a range of previous estimates of the temperature at the core-mantle boundary (*26*, *27*). Melting of normal mantle at its base cannot be ruled out and appears to be plausible.

The presence of neutrally or negatively buoyant melt in the deep mantle would have fundamental implications for our understanding of the Hadean Earth (*28*) and of the structure and chemical evolution of the core-mantle boundary. If melting extended to the base of the mantle during accretion, perovskite may have floated in coexisting liquid as it crystallized out of the magma ocean, providing a possible means of large-scale chemical differentiation. In the present-day Earth, dense melt may provide a natural explanation for the ultralow velocity zone at the base of the mantle (*29*).

References and Notes

1. Q. Williams, R. Jeanloz, *Science* **239**, 902 (1988).
2. M. Matsui, *Geophys. Res. Lett.* **23**, 395 (1996).
3. A. B. Belonoshko *et al.*, *Phys. Rev. Lett.* **94**, 195701 (2005).
4. We use ultrasoft pseudopotentials (*30*) and the Vienna ab initio simulation package code, which is efficient and widely tested on silicates and oxides (*31*). We compute the electronic structure at the Brillouin zone center and use an energy cutoff of 400 eV: Pulay (finite basis set) corrections to the pressure are found to vary linearly with V from 2 GPa at $V = V_X$ to 5 GPa at $V = V_X/2$. To account for the error inherent in the approximation to the exchange-correlation functional, we follow previous work (*32*, *33*) by adding a uniform correction of 2 GPa to the pressure in addition to the Pulay correction. The simulations are confined to the Born-Oppenheimer surface and include the influence of finite temperature on the electronic structure through the Mermin functional (*34*).
5. S. Nose, *J. Chem. Phys.* **81**, 511 (1984).
6. R. A. Lange, I. S. E. Carmichael, *Geochim. Cosmochim. Acta* **51**, 2931 (1987).
7. S. M. Rigden, T. J. Ahrens, E. M. Stolper, *J. Geophys. Res.* **93**, 367 (1988).
8. E. Knittle, R. Jeanloz, *Geophys. Res. Lett.* **16**, 421 (1989).
9. J. F. Stebbins, I. S. E. Carmichael, L. K. Moret, *Contrib. Mineral. Petrol.* **86**, 131 (1984).
10. L. Stixrude, C. Lithgow-Bertelloni, *Geophys. J. Int.* **162**, 610 (2005).
11. R. Jeanloz, M. Roufosse, *J. Geophys. Res.* **87**, 763 (1982).
12. R. Boehler, G. C. Kennedy, *J. Appl. Phys.* **48**, 4183 (1977).
13. E. Wasserman, D. A. Yuen, J. R. Rustad, *Phys. Earth Planet. Inter.* **77**, 189 (1993).
14. L. Vocadlo, D. Alfe, M. J. Gillan, G. D. Price, *Phys. Earth Planet. Inter.* **140**, 101 (2003).
15. J. A. Akins, S. N. Luo, P. D. Asimow, T. J. Ahrens, *Geophys. Res. Lett.* **31**, L14612 (2004).
16. R. Jeanloz, in *Proceedings of the Gibbs Symposium*, G. D. Mostow, D. G. Caldi, Eds. (American Mathematical Society, Providence, RI, 1990), pp. 211–226.
17. D. Alfe, *Phys. Rev. Lett.* **94**, 235701 (2005).
18. R. Boehler, M. Ross, D. B. Boercker, *Phys. Rev. B* **53**, 556 (1996).
19. D. L. Heinz, R. Jeanloz, *J. Geophys. Res.* **92**, 11437 (1987).
20. J. S. Sweeney, D. L. Heinz, *Geophys. Res. Lett.* **20**, 855 (1993).
21. A. Zerr, R. Boehler, *Science* **262**, 553 (1993).
22. M. Ross, F. J. Rogers, *Phys. Rev. B* **31**, 1463 (1985).
23. R. Jeanloz, A. Kavner, *Philos. Trans. R. Soc. London Ser. A* **354**, 1279 (1996).
24. R. G. Tronnes, D. J. Frost, *Earth Planet. Sci. Lett.* **197**, 117 (2002).
25. Y. H. Zhou, G. H. Miller, *Geochim. Cosmochim. Acta* **61**, 2957 (1997).
26. R. Jeanloz, S. Morris, *Annu. Rev. Earth Planet. Sci.* **14**, 377 (1986).
27. R. Boehler, *Annu. Rev. Earth Planet. Sci.* **24**, 15 (1996).
28. G. H. Miller, E. M. Stolper, T. J. Ahrens, *J. Geophys. Res. Solid Earth Planets* **96**, 11831 (1991).
29. Q. Williams, E. J. Garnero, *Science* **273**, 1528 (1996).
30. G. Kresse, J. Hafner, R. J. Needs, *J. Phys. Condens. Matter* **4**, 7451 (1992).
31. G. Kresse, J. Furthmuller, *Comput. Mater. Sci.* **6**, 15 (1996).
32. A. R. Oganov, J. P. Brodholt, G. D. Price, *Nature* **411**, 934 (2001).
33. R. M. Wentzcovitch, B. B. Karki, M. Cococcioni, S. de Gironcoli, *Phys. Rev. Lett.* **92**, 018501 (2004).
34. N. D. Mermin, *Phys. Rev.* **137**, A1441 (1965).
35. H. Flyvbjerg, H. G. Petersen, *J. Chem. Phys.* **91**, 461 (1989).
36. S. N. Luo, J. A. Akins, T. J. Ahrens, P. D. Asimow, *J. Geophy. Res. Solid Earth* **109** (2004).
37. D. A. Young, *Phase Diagrams of the Elements* (Univ. California Press, Berkeley, 1991).
38. E. Ito, T. Katsura, in *High-Pressure Research: Application to Earth and Planetary Sciences*, Y. Syono, M. H. Manghnani, Eds. (American Geophysical Union, Washington, DC, 1992), pp. 315–322.
39. G. Y. Shen, P. Lazor, *J. Geophys. Res. Solid Earth* **100**, 17699 (1995).
40. T. Tsuchiya, J. Tsuchiya, K. Umemoto, R. A. Wentzcovitch, *Earth Planet. Sci. Lett.* **224**, 241 (2004).

41. We thank R. Jeanloz, M. Bukowinski, and D. Depaolo for stimulating discussions and comments on the manuscript. This work was supported by the National Science Foundation under grant EAR-0409121 and the Miller Institute for Basic Research in Science.

5 July 2005; accepted 8 September 2005
10.1126/science.1116952

Basal Anthropoids from Egypt and the Antiquity of Africa's Higher Primate Radiation

Erik R. Seiffert,[1]* Elwyn L. Simons,[2] William C. Clyde,[3] James B. Rossie,[4] Yousry Attia,[5] Thomas M. Bown,[6] Prithijit Chatrath,[2] Mark E. Mathison[7]

Early anthropoid evolution in Afro-Arabia is poorly documented, with only a few isolated teeth known from before ~35 million years ago. Here we describe craniodental remains of the primitive anthropoid *Biretia* from ~37-million-year-old rocks in Egypt. *Biretia* is unique among early anthropoids in exhibiting evidence for nocturnality, but derived dental features shared with younger parapithecids draw this genus, and possibly >45-million-year-old *Algeripithecus*, into a morphologically and behaviorally diverse parapithecoid clade of great antiquity.

The early or early middle Eocene Algerian primate *Algeripithecus* establishes that higher primates have been evolving on the Afro-Arabian land mass for at least 45 million years (*1*–*3*), but that genus is only known from a few isolated teeth that have precluded meaningful inferences about its adaptations and phylogenetic affinities. Late middle and early late Eocene anthropoid evolution in Afro-Arabia is documented by only a single lower molar of the Algerian anthropoid *Biretia piveteaui* (*4*). The much-better-documented oligopithecids, parapithecids, and proteopithecids first appear around 35 million years ago (Ma) in the Jebel Qatrani Formation of northern Egypt (*5*, *6*).

Recent paleontological work in Egypt's Fayum Depression has resulted in the discovery of a diverse primate fauna at a site called Birket Qarun Locality 2 (BQ-2) (*7*). Here we describe two new species of *Biretia* from that locality—*B. fayumensis* (*8*) and *B. megalopsis* (*9*)—and provide magnetostratigraphic evidence that supports an earliest late Eocene (earliest Priabonian, ~37 Ma) age for these taxa. The character complexes exhibited by the new species support the inclusion of *Biretia* in an expanded parapithecoid clade and reveal new evidence for behavioral diversity and morphological homoplasy among early African anthropoids.

Locality BQ-2 is situated 229 m below Quarry L-41, the next-oldest primate-bearing

[1]Department of Earth Sciences, University of Oxford, and Oxford University Museum of Natural History, Parks Road, Oxford, OX1 3PW, UK. [2]Department of Biological Anthropology and Anatomy, Duke University, and Division of Fossil Primates, Duke Primate Center, 1013 Broad Street, Durham, NC 27705, USA. [3]Department of Earth Sciences, University of New Hampshire, 56 College Road, Durham, NH 03824, USA. [4]Department of Anthropology, Stony Brook University, Stony Brook, NY 11794, USA. [5]Egyptian Geological Museum, Misr el Kadima, Ethar el Nabi, Cairo, Egypt. [6]Erathem-Vanir Geological, 2300 Arapahoe Avenue, no. 236, Boulder, CO 80302, USA. [7]Department of Geological and Atmospheric Sciences, Iowa State University, Ames, IA 50011, USA.

*To whom correspondence should be addressed. E-mail: erik.seiffert@earth.ox.ac.uk

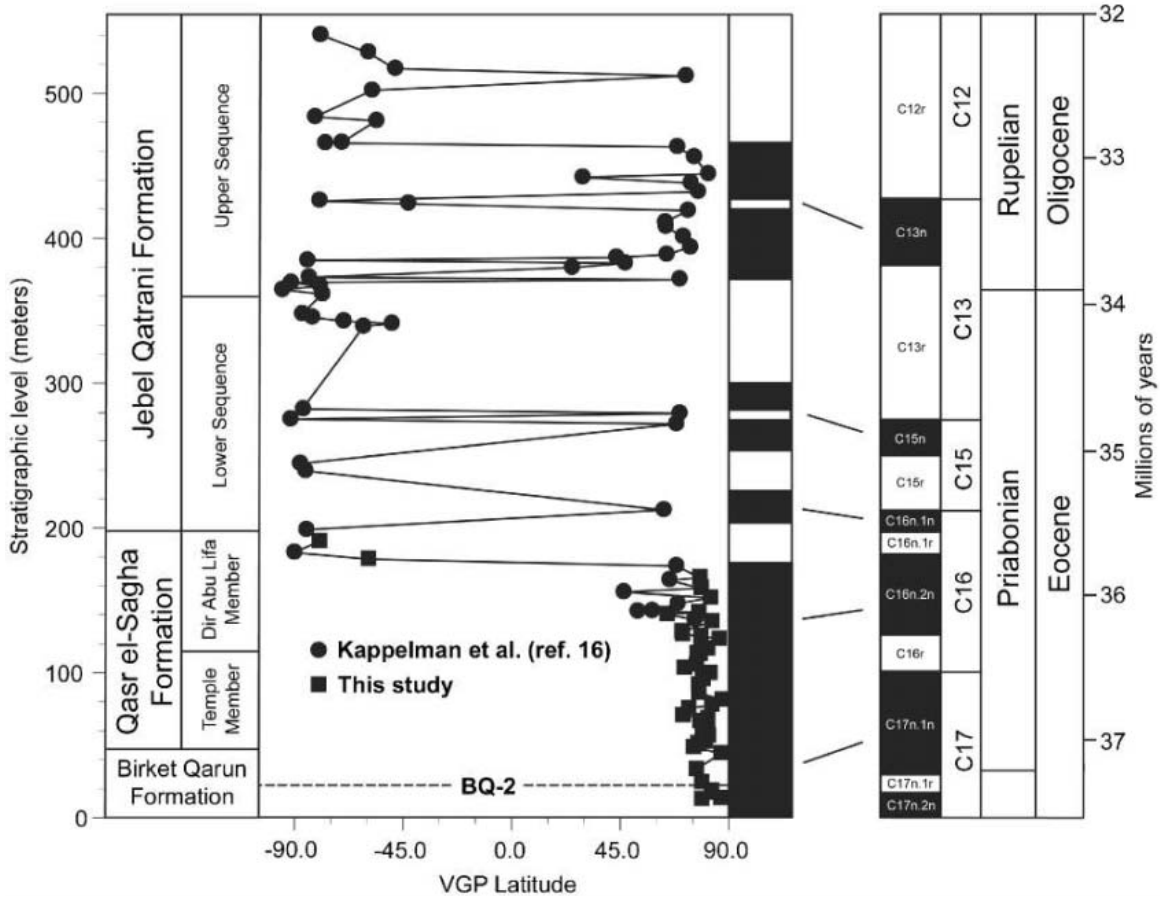

Fig. 1. Fayum magnetostratigraphy and preferred correlation with the GPTS. Paleomagnetic data are from this study (squares) and Kappelman *et al.* (*16*) (circles). The time scale is from Ogg and Smith (*18*). VGP, virtual geomagnetic pole. Three or more oriented samples from 53 sites were demagnetized progressively, using a combination of alternating field and thermal demagnetization (figs. S1 and S2 and methods in the supporting online material). The long normal-polarity zone at the base of the section likely correlates to Chron C16n and part of C17n. Chron C16r may be missing due to an erosional unconformity at the Temple/Dir Abu Lifa contact. The upper part of the section matches Kappelman *et al.*'s (*16*) preferred correlation (their correlation 1), but other correlations are possible. BQ-2 correlates to C17n.1n (early Priabonian, ~37 Ma) in our preferred correlation.

locality in Egypt, and has also produced remains of strepsirrhine primates (*7*), proboscideans, hyracoids, herodotiines, ptolemaiids, creodonts, anomaluroid and hystricognathous rodents, chiropterans, and insectivores. The primary fossiliferous horizons at BQ-2 occur in intraclastic ironstone pebble and cobble conglomerate beds that are about 5 to 15 cm thick; the new anthropoid specimens were collected either by quarrying or dry-screening these sediments. Sedimentary structures preserved at BQ-2 provide strong evidence for a fluvial origin of these deposits. This horizon was originally placed in the Birket Qarun Formation by Beadnell (*10*) but was more recently assigned to a new (Umm Rigl) Member of the Qasr el-Sagha Formation by Gingerich (*11*). We include the Umm Rigl Member in the top of the Birket Qarun Formation, because the lithology of this unit does not correspond with that of the estuarine and lagoonal facies preserved in the overlying Temple and Dir Abu Lifa Members of the Qasr el-Sagha Formation (*12*). Retaining these sediments in the Birket Qarun Formation is also consistent with the suggestion that that unit preserves the oldest known Cenozoic coastal deposits in Egypt (*11*, *12*).

BQ-2 is younger than the underlying Gehannam Formation, which preserves late middle Eocene [Bartonian, Zone P14 (*13*)] planktic foraminifera (*14*, *15*). The exact placement of the Eocene-Oligocene boundary in the Fayum area has been a matter of debate (*5*, *11*, *16*), but the Qasr el-Sagha and Birket Qarun Formations are Eocene under all interpretations. Magnetostratigraphic sampling of the Qasr el-Sagha Formation and upper Birket Qarun Formation reveals that these sediments are almost entirely of normal polarity, although a polarity reversal recorded at the top of the Qasr el-Sagha Formation coincides precisely with a reversal recorded at the base of the section that was previously sampled by Kappelman *et al*. (*16*) (Fig. 1 and fig. S3). There are several potential correlations of the Fayum magnetostratigraphy with the geomagnetic polarity time scale (GPTS) (*16*); however, the long normal-polarity zone at the base of the section is likely to include part of Chron C16n under any correlation. Significant erosional unconformities mark the contacts of the Qasr el-Sagha and Jebel Qatrani Formations and the Temple and Dir Abu Lifa Members of the Qasr el-Sagha Formation (*11*, *12*), and may cut out more than 95 m of sediment, suggesting that the lower part of the long normal-polarity zone at the base of the section encompassing BQ-2 represents Chron C17n.1n (*17*). These constraints indicate that BQ-2 is likely to be earliest Priabonian in age or ~37 million years old on the most recent time scale (*18*). Thus, the new species of *Biretia* are probably ~3.5 million years older than the derived parapithecids and propliopithecids from the early Oligocene Fayum Quarries I and M, ~2 million years older than late Eocene anthropoids such as *Catopithecus* and *Proteopithecus* from Quarry L-41 (*5*), and roughly the same age as *Bahinia*, *Myanmarpithecus*, *Amphipithecus*, and *Pondaungia* from the Pondaung Formation in Myanmar, which have also been tied to Chron C17n.1n (*19*).

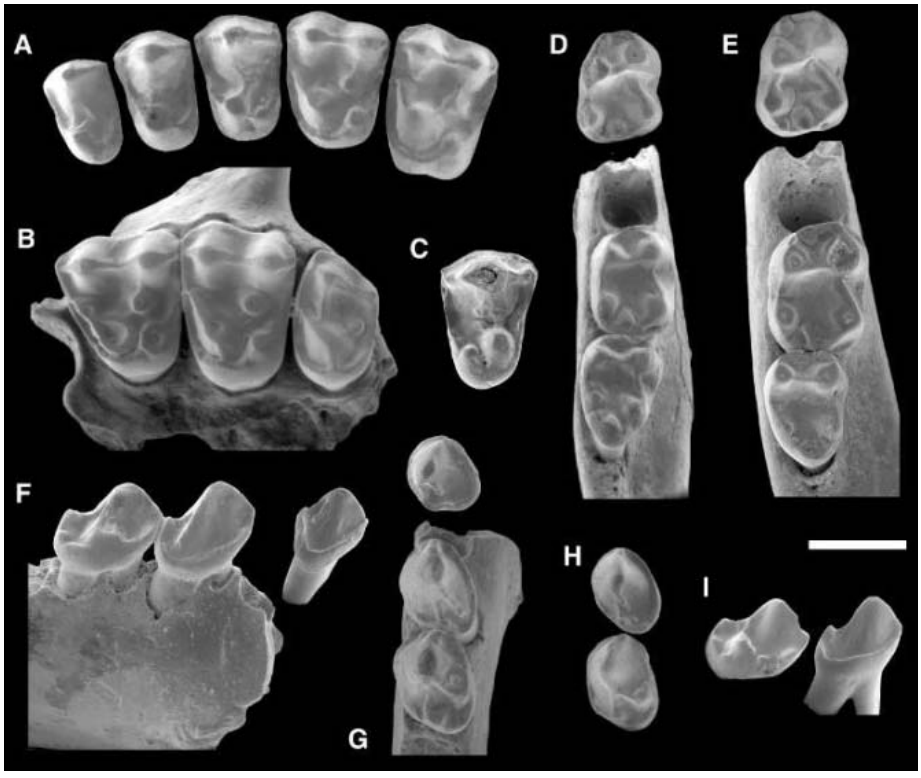

Fig. 2. (**A**) *B. fayumensis*, new species, composite of isolated P2 (DPC 21759C), P3 (DPC 21249E), P4 (DPC 21371A), M1 (DPC 21250D), and M2 (DPC 21539E, reversed). (**B**) *B. megalopsis*, new species, maxilla with M1 through M3 (DPC 21358F). (**C**) *B. megalopsis*, P4 (DPC 22279D). (**D**) *B. fayumensis*, isolated m1 (DPC 21220A) and holotype mandible with m2 and m3 (CGM 83658). (**E**) *B. megalopsis*, isolated m1 (DPC 22442G) and holotype mandible with m2 and m3 (CGM 83661). (**F** and **G**) *B. megalopsis*, mandible with p3 and p4 and alveoli for c and p2 (DPC 21539B) and isolated p2 (DPC 21757E, reversed) in lingual (F) and occlusal (G) views. (**H** and **I**) *B. fayumensis*, isolated p3 (DPC 21296D, reversed) and p4 (DPC 21757D) in occlusal (H) and lingual (I) views. Scale bar, 2 mm.

B. fayumensis is one of the smallest known Fayum anthropoids, with mean body mass estimates of 273 and 160 g, based on extant anthropoid and all primate regressions, respectively, of body mass on m1 area (m, lower molar; M, upper molar) (*20*). The new material provides additional support for the hypothesis that *Biretia* is more closely related to younger parapithecoids (here defined as a clade containing *Arsinoea* and the parapithecids *Abuqatrania*, *Qatrania*, *Apidium*, and *Parapithecus*) than it is to other Paleogene African anthropoids (*4*, *21*). In addition to the centrally placed molar hypoconulids, distolingual foveae, and generalized bunodonty already observable on the type specimen of *B. piveteaui*, *B. fayumensis* shares with the early Oligocene parapithecids *Apidium* and *Parapithecus* a three-rooted and bicuspid P2 (p, lower premolar; P, upper premolar), a distinct paraconule on M1, and well-developed metaconules on M1-2 (Fig. 2). *B. fayumensis* shares other features of the upper dentition exclusively with *Apidium*, such as hypocones on P3 and P4 and a pericone on M2, but lacks the apomorphic lower dental features that unite later parapithecoids, such as an absence of lower molar protocristids (fig. S4). *B. fayumensis* also lacks the well-developed upper premolar paraconules observable in *Apidium* and *Parapithecus*, but does have a trenchant crest coursing labially from the P4 protocone that terminates in a tiny cuspule. A similar crest is observable in the amphipithecids *Myanmarpithecus* (*22*) and *Pondaungia* (*23*) as well as in some Oligocene propliopithecids, but in neither group is there any development of a cuspule at the crest's terminus. Despite the numerous apomorphic characters aligning *B. fayumensis* with younger parapithecoids, this species nevertheless retains a few apparent plesiomorphies, such as a premetacristid on m1, a relatively long and narrow p4, and a distally oriented p3 protocristid, that are not observable in any of the late Eocene parapithecoid or proteopithecid species rep-

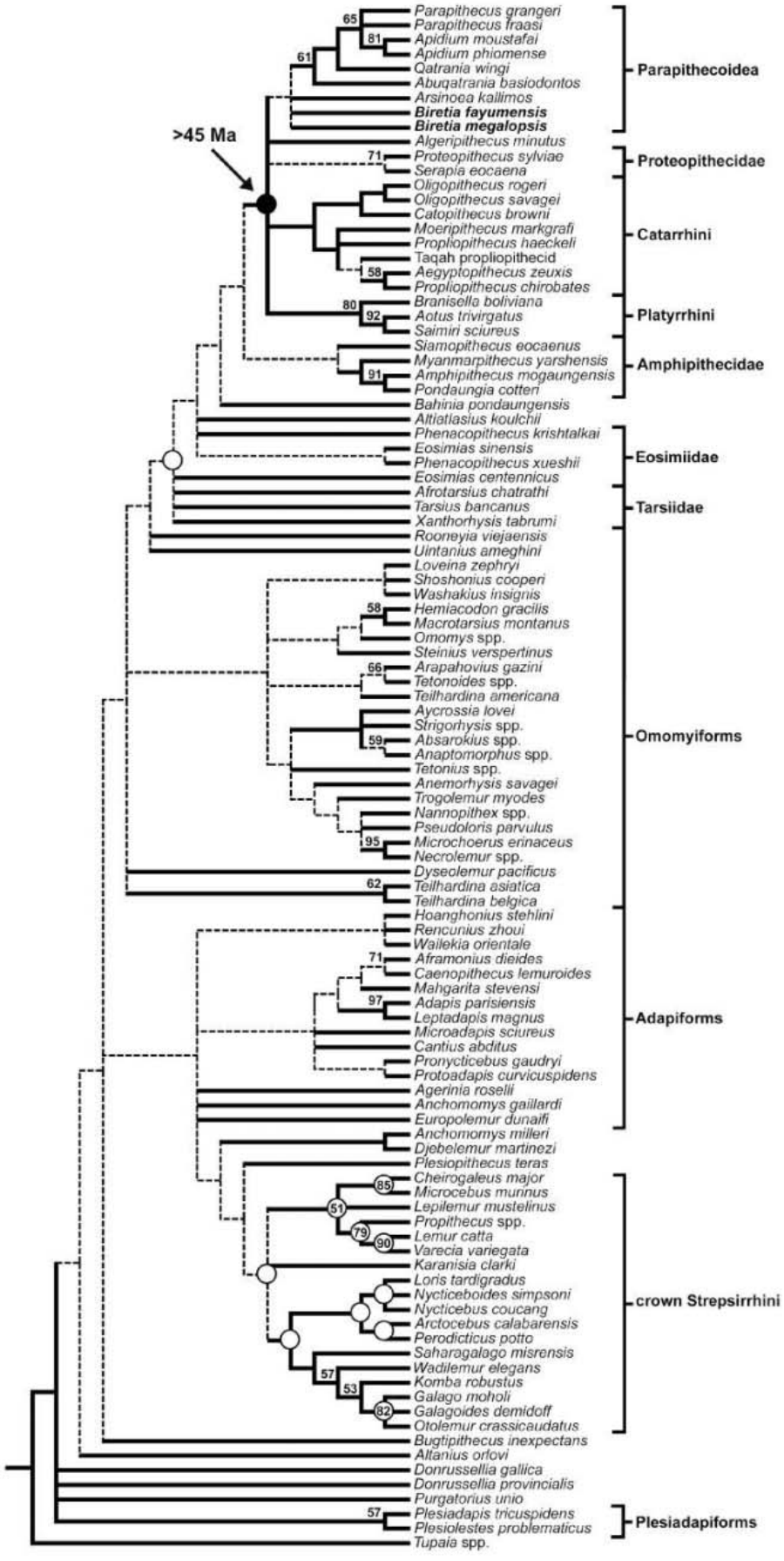

Fig. 3. Strict/Adams consensus tree summarizing all 9992 trees recovered from two parsimony analyses of 360 morphological characters, one in which some multistate characters were ordered and scaled [22 equally parsimonious trees (EPTs), tree length (TL) = 2104.398, consistency index (CI) = 0.2044, retention index (RI) = 0.5890, rescaled consistency index (RCI) = 0.1219] and one in which all characters were unordered (9970 EPTs, TL = 3814, CI = 0.2485, RI = 0.5369, RCI = 0.1346). Solid lines in the cladogram indicate which clades are present in the strict consensus of all 9992 trees; dotted lines indicate which clades are present in the Adams consensus tree, which relocates those taxa that are placed in conflicting positions in the tree, either within or across analyses, to the node held in common by all such conflicting positions. Open circles denote constrained clades supported by Alu SINEs (short interspersed nuclear elements; see supporting online material). Bootstrap support values greater than 50 (derived from analysis of the "ordered/unordered" data set only) are shown above branches. Character support for Parapithecoidea is available in the supporting online material.

resented at L-41 but are present in much more primitive primates such as eosimiids. Regardless of where *Biretia* is placed relative to other Paleogene anthropoids, a considerable amount of dental homoplasy is implied, but parsimony analysis (*24*) consistently aligns the genus with parapithecoids (Fig. 3 and figs. S5 and S6).

B. megalopsis shares with Oligocene parapithecids the same suite of apomorphic upper molar features observable in *B. fayumensis* but is slightly larger than its contemporary, is more bunodont, exhibits variable presence of the m1 premetacristid (a crest that is absent in late Eocene *Arsinoea*, *Abuqatrania*, and *Qatrania*), and shares larger conules and reduced or absent postprotocristae on P4-M3 with *Apidium* and *Parapithecus*. As in *B. fayumensis*, the p4 of *B. megalopsis* is also relatively long, and both taxa have more complex p4 talonids (with tall hypoconids, small entoconids, and trenchant oblique cristids and protocristids) than younger parapithecoids. The presence of these features in primitive parapithecoids suggests that this morphology might have been present in the last common ancestor of catarrhines, platyrrhines, proteopithecids, and parapithecoids and was subsequently secondarily simplified in younger parapithecids. The phylogenetic placement of the new *Biretia* species within Parapithecoidea is sensitive to assumptions about ordering and scaling of multistate characters; parsimony analysis with some multistate characters ordered and scaled recovers a *Biretia* clade to the exclusion of parapithecids (fig. S5), whereas the Adams consensus tree derived from an analysis with all characters unordered renders *Biretia* paraphyletic with respect to Parapithecidae (fig. S6).

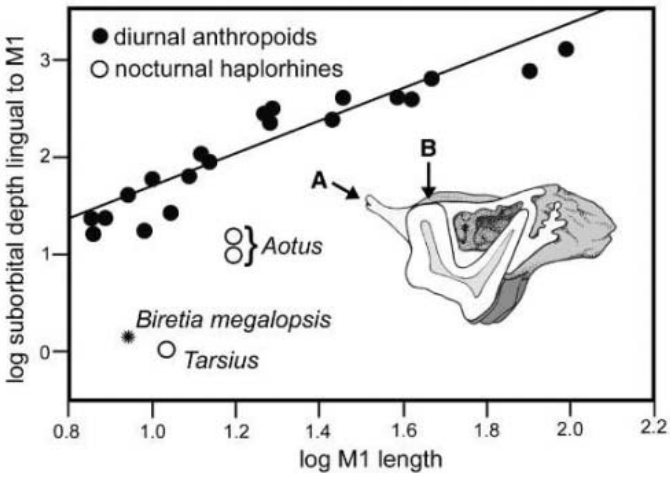

Fig. 4. Bivariate plot of log suborbital depth lingual to M1 versus log M1 length, and least-squares regression line ($Y = 1.633x + 0.049$, $R^2 = 0.882$) for diurnal anthropoids (black circles), compared with extant nocturnal haplorhines (*Tarsius* and *Aotus*) and *B. megalopsis*. All measurements derive from high-resolution computed tomographic (micro-CT) coronal scans taken through the lingual roots of M1. *B. megalopsis* scales in a manner most similar to the nocturnal taxa. The inset line drawing is a mesial view of the *B. megalopsis* maxilla at the level of the M1 lingual root, based on a reconstruction from high-resolution micro-CT scans, to illustrate the lack of a maxillary sinus as well as (A) complete fusion of the bony laminae making up the floor of the orbit and hard palate, and (B) exposure of the lingual root of M1 in the orbit floor.

B. megalopsis is unlike other early anthropoids in having an extremely compressed suborbital region, with lingual tooth roots of M1 and M2 exposed in the floor of the orbit (fig. S7), no development of a maxillary sinus lingual to the molars, and complete fusion of the bony laminae forming the floor of the orbit and hard palate medial to M1 and M2. These characteristics are likely related to orbital hypertrophy, because the only other living or extinct haplorhine known to exhibit all of these features in combination is nocturnal *Tarsius* (fig. S8), whose relative orbit size is greater than that of any other living or extinct primate. A plot of suborbital depth (*23*) relative to the length of the first upper molar (Fig. 4) demonstrates that *B. megalopsis* falls far from the regression line for diurnal anthropoids and deviates in a manner most similar to *Tarsius* and *Aotus*, the only extant nocturnal anthropoid. The possibility that *B. megalopsis*'s morphology is due to its small size therefore appears unlikely, because the suborbital depth of like-sized diurnal callitrichid platyrrhines scales in a manner similar to that of other diurnal anthropoids (Fig. 4). Orbital hypertrophy might also account for the fact that there is no evidence for postorbital closure in *B. megalopsis*, because in *Aotus* the jugal and alisphenoid components of the postorbital septum are separated from the maxilla by an enlarged inferior orbital fissure. In the absence of other evidence, we conclude that *B. megalopsis* probably had hypertrophied orbits on a scale equal to or greater than *Aotus* and was, by analogy, presumably nocturnal. Despite *B. megalopsis*'s great antiquity, however, we suspect that identification of this species as a probable nocturnal form is unlikely to be relevant to the origin of anthropoid activity patterns, because the last common ancestor of the clade containing *Bahinia*, parapithecoids, proteopithecids, catarrhines, and platyrrhines would still be reconstructed as having been primitively diurnal (*25*).

The upper molar morphology of >45-million-year-old *Algeripithecus* is remarkably similar to that of *B. fayumensis*, and our phylogenetic analyses consistently nest the former genus deep within the Afro-Arabian anthropoid radiation as either a basal parapithecoid or as a proteopithecid. Either placement would require that a number of key morphological features that parapithecoids and proteopithecids share with platyrrhines and catarrhines [such as full postorbital closure, diurnality, and high-acuity vision (*25*, *26*)] had already appeared by the early Eocene, and probably at small body size (probably 150 to 250 g), because *Algeripithecus* was even smaller than tiny *B. fayumensis*. Although parapithecoids and proteopithecids are generally considered to be stem anthropoids (*27*), our analyses provide no support for that hypothesis (Fig. 3). The lack of phylogenetic resolution among the parapithecoid, proteopithecid, platyrrhine, and catarrhine clades—one of which likely includes >45-million-year-old *Algeripithecus*—leaves open the possibility that crown anthropoid origins may also extend back to the early part of the middle Eocene, as suggested by a recent molecular estimate (*28*).

Finally, our phylogenetic analysis supports the hypothesis that the oldest known crown primate, the African late Paleocene genus *Altiatlasius*, is a primitive stem anthropoid (*27*, *29*). Given the likelihood that crown primates are of Asian (or at least Laurasian) origin (*27*, *29*), *Altiatlasius*'s basal position in anthropoid phylogeny would appear to imply either (i) an immigration into Afro-Arabia independent of the clade that later gave rise to parapithecoids, proteopithecids, platyrrhines, and catarrhines; or (ii) the presence of ancient parallel radiations of anthropoids in Asia and Afro-Arabia (*29*) whose reciprocal monophyly cannot currently be recovered by parsimony analysis because of missing data and rampant morphological convergence. These competing hypotheses appear to us to be equally viable on the basis of available evidence and can be tested with the recovery of additional basal anthropoid taxa from BQ-2 and other, more ancient, horizons in Afro-Arabia.

References and Notes

1. M. Godinot, M. Mahboubi, *Nature* **357**, 324 (1992).
2. M. Godinot, M. Mahboubi, *C. R. Acad. Sci. Paris Ser. II* **319**, 357 (1994).
3. F. Mebrouk, M. Mahboubi, M. Bessedik, M. Feist, *Geobios* **30**, 171 (1997).
4. L. de Bonis, J.-J. Jaeger, B. Coiffait, P.-É. Coiffait, *C. R. Acad. Sci. Paris Ser. II* **306**, 929 (1988).
5. E. L. Simons, D. T. Rasmussen, T. M. Bown, P. Chatrath, in *Anthropoid Origins*, J. G. Fleagle, R. F. Kay, Eds. (Plenum, New York, 1994), pp. 179–202.
6. E. L. Simons, E. R. Seiffert, P. S. Chatrath, Y. Attia, *Folia Primatol. (Basel)* **72**, 316 (2001).
7. E. R. Seiffert, E. L. Simons, Y. Attia, *Nature* **422**, 421 (2003).
8. Systematic paleontology: Primates Linnaeus 1758, Anthropoidea Mivart 1864, Parapithecoidea Schlosser 1911, Genus *Biretia* de Bonis *et al*. 1988 (*4*). *Biretia fayumensis*, new species. **Diagnosis.** Differs from other Paleogene anthropoids in combining the following features: small size (mean estimate of 273 g based on m1 area), bunodont molar morphology, p3 protocristid oriented toward cristid obliqua, small metaconid and absence of paraconid on p4, small paraconid and buccally placed cristid obliqua terminus on m1, distolingual foveae on m1 and m2, centrally placed hypoconulids on m1 through m3, three-rooted P2 with small protocone, hypocones on P3 through M2, small paraconule on M1, small metaconules on M1 and M2, poorly developed postprotocristae on M1 and M2, and pericone on M2. Differs from *B. piveteaui* in its smaller size. **Holotype.** CGM 83658, mandible with m2 and m3. **Etymology.** Named for the Fayum area in which the species is found. **Locality.** BQ-2, Umm Rigl Member of Birket Qarun Formation, Fayum Depression, northern Egypt. **Description.** See supporting online material.
9. Systematic paleontology: Primates Linnaeus 1758, Anthropoidea Mivart 1864, Parapithecoidea Schlosser 1911, Genus *Biretia* de Bonis *et al*. 1988 (*4*). *Biretia megalopsis*, new species. **Diagnosis.** Differs from Paleogene anthropoids other than *B. fayumensis* in the following combination of features: bunodont molar morphology, small metaconid and absence of paraconid on p4, distolingual foveae on m1 and m2, centrally placed hypoconulids on m1 through m3, hypocones on M1 and M2, well-developed paraconule on M1 and metaconules on M1 through M3, and pericone on M2. Differs from *B. fayumensis* in its larger size (mean estimate of 376 g based on m1 area); in having a distolingually oriented p3 protocristid and a more lingually placed cristid obliqua terminus on m1; in lacking both a postprotocristid on p4 and, variably, a premetacristid on m1; in having larger paraconules and metaconules on M1 and M2; and in exhibiting the variable presence of postprotocristae on M1 and M2. **Holotype.** CGM 83661, partial mandible with m2 and m3. **Etymology.** Combination of *megal-*, Greek for large, and *ops*, Greek for eye. **Locality.** BQ-2, Umm Rigl Member of Birket Qarun Formation, Fayum Depression, Egypt. **Description.** See supporting online material.
10. H. J. L. Beadnell, *The Topography and Geology of the Fayum Province of Egypt* (Survey Department of Egypt, Cairo, 1905).
11. P. D. Gingerich, *Univ. Mich. Pap. Paleontol.* **30**, 1 (1992).

12. T. M. Bown, M. J. Kraus, *U.S. Geol. Surv. Prof. Paper* **1452**, 1 (1988).
13. M. Toumarkine, H. P. Luterbacher, in *Plankton Stratigraphy*, H. M. Bolli, J. B. Saunders, K. Perch-Nielsen, Eds. (Cambridge Univ. Press, Cambridge, 1985), pp. 88–153.
14. A. Strougo, M. A. Y. Haggag, *N. Jb. Geol. Paläontol. Monat.* **1**, 46 (1984).
15. M. A. Y. Haggag, *Rev. Esp. Micropaleontol.* **17**, 27 (1985).
16. J. Kappelman, E. L. Simons, C. C. Swisher III, *J. Geol.* **100**, 647 (1992).
17. Typical sediment accumulation rates through the upper part of the section would place the base of Chron C16n.2n near the Temple Member–Dir Abu Lifa Member unconformity, where Chron C16r may have been lost to erosion. The fluvial sediments preserved at BQ-2, which are bounded above and below by nearshore marine beds, can also be explained by the major sea-level lowstand that occurred near the Bartonian-Priabonian boundary.
18. J. G. Ogg, A. G. Smith, in *A Geological Time Scale 2004*, A. G. Smith, Ed. (Cambridge Univ. Press, Cambridge, 2004), pp. 63–86.
19. M. Benammi *et al.*, *J. Geol.* **110**, 748 (2002).
20. G. C. Conroy, *Int. J. Primatol.* **8**, 115 (1987).
21. K. C. Beard, in *The Primate Fossil Record*, W. C. Hartwig, Ed. (Cambridge Univ. Press, Cambridge, 2002), pp. 133–149.
22. M. Takai *et al.*, *J. Hum. Evol.* **40**, 393 (2001).
23. N. Shigehara *et al.*, *J. Hum. Evol.* **43**, 143 (2002).
24. Materials and methods are available as supporting material on *Science* Online.
25. C. P. Heesy, C. F. Ross, in *Anthropoid Origins: New Visions*, R. F. Kay, Ed. (Kluwer/Plenum, New York, 2004), pp. 665–698.
26. E. C. Kirk, R. F. Kay, in *Anthropoid Origins: New Visions*, R. F. Kay, Ed. (Kluwer/Plenum, New York, 2004), pp. 539–602.
27. E. R. Seiffert, E. L. Simons, C. V. M. Simons, in *Anthropoid Origins: New Visions*, C. F. Ross, R. F. Kay, Eds. (Kluwer/Plenum, New York, 2004), pp. 157–181.
28. E. Eizirik, W. J. Murphy, M. S. Springer, S. J. O'Brien, in *Anthropoid Origins: New Visions*, C. F. Ross, R. F. Kay, Eds. (Kluwer/Plenum, New York, 2004), pp. 45–64.
29. K. C. Beard, *The Hunt for the Dawn Monkey: Unearthing the Origins of Monkeys, Apes, and Humans* (Univ. of California Press, Berkeley, 2004).
30. A. Abd el-Raouf, Z. el-Alfy, F. Imbabi, and the staff of the Egyptian Mineral Resources Authority and Egyptian Geological Museum facilitated work in the Fayum area. We thank F. Ankel-Simons, J. Fleagle, B. Hanson, R. Kay, C. Seiffert, and two anonymous reviewers for commenting on or editing the manuscript; T. Ryan and A. Walker for providing the micro-CT scans of the *B. megalopsis* maxilla; C. Heesy, R. Kay, and C. Ross for commenting on that specimen; C. Beard, M. Godinot, and L. Marivaux for access to fossils and casts; L. Gannon for helping to process the paleomagnetic samples; the Fayum field crews of 2001–2003 for their work at BQ-2; and the team of local workers from Kom Aushim led by M. Hassen Taha. This research was supported by NSF grants to E.L.S, E.R.S., and J.B.R., and by Leakey Foundation grants to E.R.S. This is Duke Primate Center publication no. 800.

Supporting Online Material
www.sciencemag.org/cgi/content/full/310/5746/300/DC1
Materials and Methods
SOM Text
Figs. S1 to S8
Tables S1 to S3
References
Movies S1 and S2

24 June 2005; accepted 30 August 2005
10.1126/science.1116569

Selection on Heritable Phenotypic Plasticity in a Wild Bird Population

Daniel H. Nussey,[1,2]* Erik Postma,[1] Phillip Gienapp,[1] Marcel E. Visser[1]

Theoretical and laboratory research suggests that phenotypic plasticity can evolve under selection. However, evidence for its evolutionary potential from the wild is lacking. We present evidence from a Dutch population of great tits (*Parus major*) for variation in individual plasticity in the timing of reproduction, and we show that this variation is heritable. Selection favoring highly plastic individuals has intensified over a 32-year period. This temporal trend is concurrent with climate change causing a mismatch between the breeding times of the birds and their caterpillar prey. Continued selection on plasticity can act to alleviate this mismatch.

Phenotypic plasticity—defined as the ability of a single genotype to alter its phenotype in response to environmental conditions—is an important mechanism by which populations can respond rapidly to changes in ecological conditions (*1–3*). Plasticity in life history traits is ubiquitous in animal populations (*1*), with traits often varying within the lifetimes of individuals depending on the conditions they experience (*4*, *5*). It is typically conceptualized and measured using reaction norms: linear functions describing the change in a trait across an environmental gradient (*3*, *6*). Laboratory research has shown that genetic variation for plasticity exists (*7*, *8*) and that heritable plasticity can respond to artificial selection (*2*, *9*).

Given that many species are currently experiencing long-term anthropogenically driven environmental change (*10*, *11*), a better understanding of how natural selection acts on plasticity under altered levels of environmental variation in the wild is imperative. Detailed analyses of within-population variation in life history plasticity are rarely undertaken in naturally occurring populations, because such analyses require data from large numbers of individuals breeding repeatedly across their lifetimes. Recent research using mixed-effects linear models has shown that individuals in two wild vertebrate populations vary in their levels of life history plasticity (*4*, *12*). At present, little is known about the consequences of environmental change for the action of natural selection on plasticity and, ultimately, the ability of populations to continue to respond adaptively to environmental variation. Here we present data from a wild bird population showing temporal trends in natural selection on heritable phenotypic plasticity in the timing of reproduction, which are concurrent with changes in climate and the timing of food availability.

After a warm spring, female passerines often breed earlier than they do after a cold spring (*13*, *14*). This is a result of phenotypic plasticity (*14*, *15*), an individual-level response to temperature. Such a response is considered adaptive because it synchronizes the birds' phenology with the temperature-dependent hatching times and growth rates of the caterpillars they rely on to feed their nestlings (*16*, *17*).

A long-term study of great tits (*Parus major*) in the Hoge Veluwe, one of the Netherlands' largest national parks, has revealed that after recent warming of spring temperatures in

Table 1. Linear mixed-effects model of 2195 laying date observations from 833 female great tits that bred in more than 1 year during the period 1973 to 2004. Estimated covariance (female, female × spring temperature) = 1.16 ± 0.31 (SE).

	Random effects		
Term	Variance	SE	LRT
Year of breeding	9.54	2.55	558.33***
Female	8.05	0.76	226.73***
Female × spring temperature	1.05	0.31	27.07***
Residual	14.97	0.64	
	Fixed effects		
Term	Wald statistic	df	Wald/df
Spring temperature	45.47	1	45.47***
Age	116.91	1	116.91***
Age × spring temperature	7.26	1	7.26**

**$P < 0.01$. ***$P < 0.001$.

[1]Netherlands Institute of Ecology (NIOO-KNAW), Post Office Box 40, 6666 ZG Heteren, Netherlands. [2]Institute of Evolutionary Biology, University of Edinburgh, Edinburgh EH9 3JT, UK.

*To whom correspondence should be addressed. E-mail: d.h.nussey@sms.ed.ac.uk

the region, the timing of growth of their caterpillar prey has advanced while the phenology of the birds has not (*17*). As a result, over the past three decades, the laying dates of female great tits have moved closer to the peak in the caterpillar biomass, so that the peak in demand for food for their offspring no longer coincides with the peak in prey availability (*14*, *17*). Selection on the heritable component of great tits' plastic responses to spring temperatures could act to reduce this phenological mismatch (*14*).

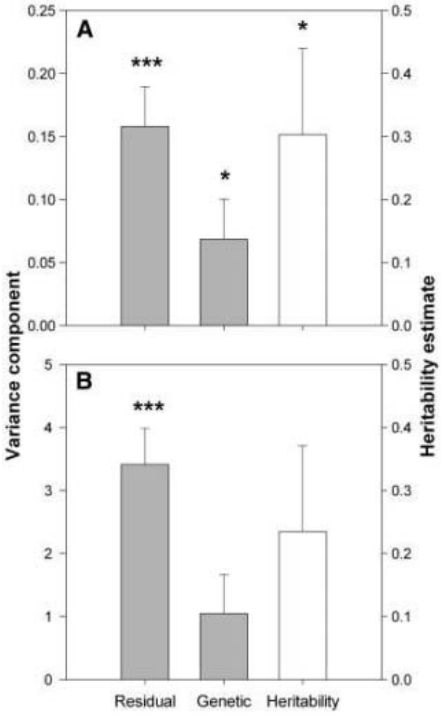

Fig. 1. Significant genetic variation exists for laying date plasticity. The bar plots show "animal model" estimates of residual and additive genetic variance (gray) and heritability (white) with SE bars for (**A**) laying date–spring temperature slope and (**B**) laying date elevation. The left *y* axis shows variance component values for the gray bars; the right *y* axis shows predicted heritabilities for the white bars. Asterisks above bars indicate an estimate that is significantly greater than 0 (*$P < 0.05$, ***$P < 0.001$).

We used information on laying dates for 833 females breeding in more than 1 year between 1973 and 2004 to examine variation among females in their laying date reaction norms. A random-coefficients model of laying dates (*18*) showed that after a warm spring, on average, females began laying earlier than they did after a cold spring (Table 1). We found significant variation between females in both their estimated laying date at the average spring temperature [likelihood ratio test (LRT) = 226.73, df = 1, $P < 0.001$] and the magnitude of their response to spring temperature (LRT = 27.07, df = 2, $P < 0.001$). Females in this population lay early after a warm spring, but the magnitude of this plastic response varies between females (*19*). There was a significant, positive correlation between elevation and slope ($r = 0.40$, LRT = 15.41, df = 1, $P < 0.001$): Females that lay early in the average environment are also the most plastic females.

Significant genetic variation in a trait must exist for there to be any response to selection (*20*). We generated predictors for the two components of each female's reaction norm: her laying date in the average environment (elevation), and her change in laying date in response to temperature (plasticity or slope) (*3*). We used an "animal model" (*21*) to estimate the genetic component of phenotypic variance in predictors of female elevation and slope (*18*). We found that significant genetic variation for laying date plasticity exists in the Hoge Veluwe great tit population and that laying date plasticity was significantly heritable [$h^2 = 0.30 \pm 0.14$ (SE), $z_{(<>0)} = 2.21$, $P < 0.05$ (Fig. 1A)]. Genetic variation and heritability estimates for laying date elevation were relatively high but were not significantly greater than 0 [$h^2 = 0.24 \pm 0.14$, $z_{(<>0)} = 1.73$, $P > 0.05$ (Fig. 1B)]. However, the genetic correlation between slope and elevation was highly positive and not significantly different from 1 ($r_A = 0.77 \pm 0.18$, $z_{(<1)} = 1.28$, $P > 0.05$).

To investigate selection on laying date plasticity across the study period, we measured the relationship between a female's lifetime reproductive success (LRS) and predictors of her laying date elevation and slope (*18*). There was evidence for directional selection on both reaction norm components, and there was no evidence of stabilizing or correlated selection (table S1). Females that laid earlier in the average environment (low elevation) and responded more strongly to temperature (more negative slope) had significantly more of their offspring recruit into the population as breeding adults (standardized selection gradients for elevation and slope: –0.094 ± 0.039 and –0.085 ± 0.039, respectively).

Over the study period, selection favoring females that advance their laying dates strongly in response to warm spring temperatures increased (Fig. 2; slope × cohort interaction: $F_{1,804} = 7.22$, $P < 0.01$). It is clear from both the fitted interaction (Fig. 2A) and the data themselves (Fig. 2, B to D) that selection has been strongest in the last two decades of the study, during which time the phenological mismatch with the peak in caterpillar biomass first emerged and then increased (*14*). The same pattern of changing selection over time is observed on estimates of females' laying date elevation (table S2) (*18*).

It appears that the strong correlation between females' elevation and slope renders these two components of their reaction norms indistinguishable. Selection favored those highly plastic females that also lay early on average. How can we explain the correlation between elevation and slope? Both plasticity

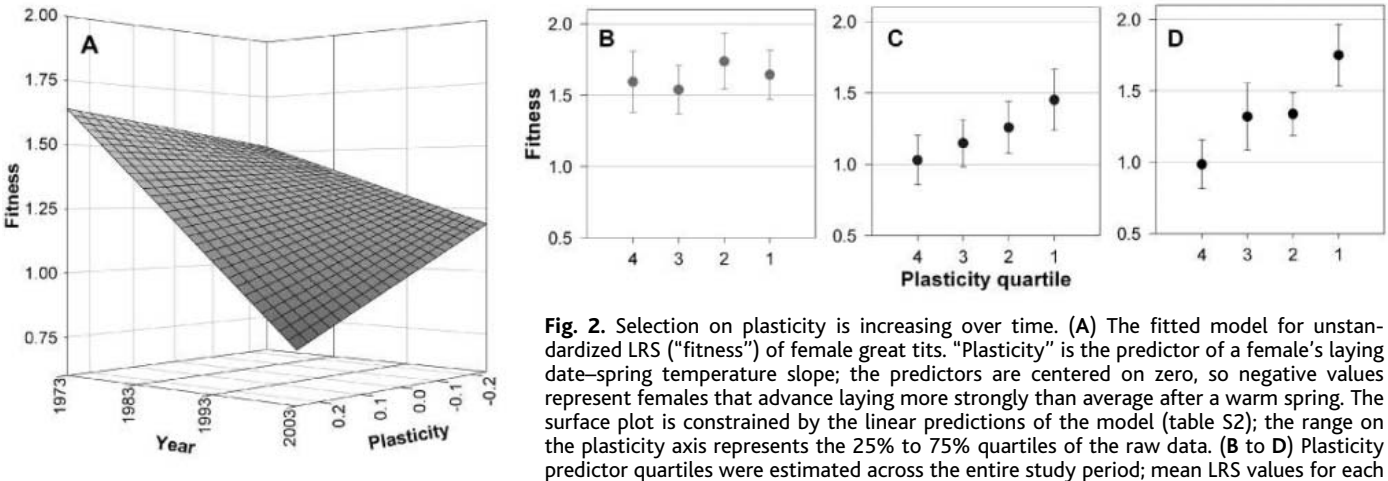

Fig. 2. Selection on plasticity is increasing over time. (**A**) The fitted model for unstandardized LRS ("fitness") of female great tits. "Plasticity" is the predictor of a female's laying date–spring temperature slope; the predictors are centered on zero, so negative values represent females that advance laying more strongly than average after a warm spring. The surface plot is constrained by the linear predictions of the model (table S2); the range on the plasticity axis represents the 25% to 75% quartiles of the raw data. (**B** to **D**) Plasticity predictor quartiles were estimated across the entire study period; mean LRS values for each quartile (with SE bars) are shown for females first breeding during the periods 1973 to 1982 (B), 1983 to 1992 (C), and 1993 to 2002 (D). Quartile 1 contains the most plastic females.

and elevation in laying date may be correlated to some unmeasured aspect of individual quality or condition (*4*, *12*, *22*). If birds differ in their ability to lay early in the year because of variation in some aspect of individual quality—for example, because of differences in their ability to gather resources—high-quality birds will lay early in warm years and later in cold years and will have steeper slopes and lower elevations, whereas poor-quality birds will usually lay later regardless of temperature and will therefore have shallower slopes. The early/plastic birds would be expected to match their reproductive timing better with the peak in caterpillar biomass, especially as spring temperatures become increasingly warm.

To substantiate the relationship between the great tits' reaction norms and the mismatch with the peak in food availability, we estimated each female's "lifetime synchrony" (*18*). Improved lifetime synchrony was associated with increased laying date plasticity ($F_{1,806} = 189.4$, $P < 0.001$) and earlier breeding in the average environment ($F_{1,806} = 582.4$, $P < 0.001$). Furthermore, the synchrony of highly plastic females increased over time relative to less plastic individuals (slope × cohort interaction: $F_{1,804} = 55.8$, $P < 0.001$). The observed changes in selection on plasticity, as the phenological mismatch has increased over time, appear to be driven by the fact that highly plastic females breed in closer synchrony with the peak in food availability and hence have more resources available for provisioning their young.

Female LRS has decreased across the study period (Fig. 2; cohort main effect: $F_{1,804} = 9.92$, $P < 0.01$). If such a decline persists alongside increased mismatching of phenologies between birds and caterpillars, the population's viability may ultimately be threatened. A phenotypic response to recent selection on laying date reaction norms cannot yet be demonstrated in this population (*23*), although the presence of additive genetic variance for plasticity means that a response to selection is predicted (*20*, *21*). However, a microevolutionary response to selection on the laying date reaction norms toward lower elevations and stronger plasticity would be expected to result in closer synchrony between the great tits' laying dates and the peak in food availability, and ultimately could alleviate the trophic mismatch.

We have shown that selection affects life history plasticity and that it can change with prevailing ecological conditions to potentially alter reaction norms in a wild population. This finding has wider implications because climate change has the potential to induce mismatches in the timing of breeding between trophic levels across a wide variety of ecosystems (*17*, *24*, *25*). The capacity for evolutionary change in phenological reaction norms shown here represents a potential means for natural selection to alleviate such mismatches and their ultimately negative consequences for population viability and ecosystem function (*11*, *26*). However, it remains to be seen whether microevolutionary change in reaction norm shape can occur fast enough to keep up with the rapid rate of change in ecological conditions.

References and Notes

1. M. Pigliucci, *Phenotypic Plasticity* (Johns Hopkins University Press, Baltimore, 2001).
2. S. M. Scheiner, *Annu. Rev. Ecol. Syst.* **24**, 35 (1993).
3. S. Via *et al.*, *Trends Ecol. Evol.* **10**, 212 (1995).
4. D. H. Nussey, T. H. Clutton-Brock, D. A. Elston, S. D. Albon, L. E. B. Kruuk, *J. Anim. Ecol.* **74**, 387 (2005).
5. D. Réale, A. G. McAdam, S. Boutin, D. Berteaux, *Proc. R. Soc. London Ser. B* **270**, 591 (2003).
6. A. E. Weis, W. L. Gorman, *Evolution* **44**, 820 (1990).
7. R. A. Newman, *Evolution* **48**, 1773 (1994).
8. J. R. Stinchcombe, L. A. Dorn, J. Schmitt, *J. Evol. Biol.* **17**, 197 (2004).
9. S. M. Scheiner, *J. Evol. Biol.* **15**, 889 (2002).
10. N. C. Stenseth *et al.*, *Science* **297**, 1292 (2002).
11. G. R. Walther *et al.*, *Nature* **416**, 389 (2002).
12. J. E. Brommer, J. Merila, B. C. Sheldon, L. Gustafsson, *Evolution* **59**, 1362 (2005).
13. R. H. McCleery, C. M. Perrins, *Nature* **391**, 30 (1998).
14. M. E. Visser, C. Both, M. M. Lambrechts, *Adv. Ecol. Res.* **35**, 89 (2004).
15. C. Both *et al.*, *Proc. R. Soc. London Ser. B* **271**, 1657 (2004).
16. M. E. Visser, L. J. M. Holleman, *Proc. R. Soc. London Ser. B* **268**, 289 (2001).
17. M. E. Visser, A. J. van Noordwijk, J. M. Tinbergen, C. M. Lessells, *Proc. R. Soc. London Ser. B* **265**, 1867 (1998).
18. See supporting data on *Science* Online.
19. Between-year variation in laying date was controlled for by adding an additional random effect for year of breeding (as a factor) to the random-coefficients model.
20. M. Lynch, B. Walsh, *Genetics and Analysis of Quantitative Traits* (Sinauer, Sunderland, MA, 1998).
21. L. E. B. Kruuk, *Philos. Trans. R. Soc. London Ser. B* **359**, 873 (2004).
22. D. H. Nussey, T. H. Clutton-Brock, S. D. Albon, J. Pemberton, L. E. B. Kruuk, *Biol. Lett.*, in press.
23. The absence of phenotypic trends in laying date reaction norm components is evidenced by non-significant fixed-effects terms for year (as a covariate) and its interaction with spring temperature, respectively, in the random-coefficients model.
24. J. M. Durant, T. Anker-Nilssen, N. C. Stenseth, *Proc. R. Soc. London Ser. B* **270**, 1461 (2003).
25. M. Edwards, A. J. Richardson, *Nature* **430**, 881 (2004).
26. N. C. Stenseth, A. Mysterud, *Proc. Natl. Acad. Sci. U.S.A.* **99**, 13379 (2002).

27. We thank J. H. van Balen and J. Visser for managing the long-term study for many years, the board of De Hoge Veluwe for kindly allowing us to work on their property, and L. Kruuk, J. Bommer, K. Lessells, and four anonymous referees for comments on earlier drafts of the manuscript. Supported by British Ecological Society small ecological project grant 2429 (D.H.N.).

Supporting Online Material

www.sciencemag.org/cgi/content/full/310/5746/304/DC1
Materials and Methods
SOM Text
Tables S1 to S3
References

6 July 2005; accepted 7 September 2005
10.1126/science.1117004

Akt-Mediated Phosphorylation of EZH2 Suppresses Methylation of Lysine 27 in Histone H3

Tai-Lung Cha,[1,2]* Binhua P. Zhou,[1]† Weiya Xia,[1] Yadi Wu,[1] Cheng-Chieh Yang,[1,2] Chun-Te Chen,[1] Bo Ping,[1] Arie P. Otte,[3] Mien-Chie Hung[1,2]‡

Enhancer of Zeste homolog 2 (EZH2) is a methyltransferase that plays an important role in many biological processes through its ability to trimethylate lysine 27 in histone H3. Here, we show that Akt phosphorylates EZH2 at serine 21 and suppresses its methyltransferase activity by impeding EZH2 binding to histone H3, which results in a decrease of lysine 27 trimethylation and derepression of silenced genes. Our results imply that Akt regulates the methylation activity, through phosphorylation of EZH2, which may contribute to oncogenesis.

Posttranslational modification of histones plays a central role in the regulation of many biological functions (*1*). Histone methylation, in particular, is linked to the regulation of gene expression and chromatin conformation (*2*–*4*). This process, which used to be considered a permanent modification, has recently been shown to be reversible, and the enzymes responsible for demethylation have been identified (*5*–*8*). Perturbation of this epigenetic balance has important links to carcinogenesis (*9*). For instance, overexpression of EZH2, a central member of Polycomb repressive complexes (PRCs) that has intrinsic histone methyltransferase (HMTase) activity (*10*, *11*), has been implicated in cancer progression and metastases in multiple cancer types (*12*–*14*).

The phosphoinositide 3-kinase–Akt (PI3K-Akt) signaling pathway is involved in processes such as survival, proliferation, growth, and motility (*15*, *16*). In an attempt to identify potential upstream regulators for HMTase of EZH2, we unexpectedly found that cells with high levels of activated, and therefore phosphorylated, Akt generally have lower levels of histone 3 (H3) lysine 27 (K27) trimethylation

($P < 0.05$; fig. S1). This inverse correlation prompted us to test whether alteration of Akt activity may change H3 K27 trimethylation. Indeed, insulin-like growth factor (IGF)–induced activation of Akt by phosphorylation reduced H3 K27 trimethylation, which could be blocked by the PI3K-Akt inhibitor, LY294002 (Fig. 1, A and B; fig. S2). Similarly, expression of dominant-negative Akt (DN-Akt) (*17*) (Fig. 1C) or knocking down Akt expression with small interfering RNA (siRNA) (Fig. 1D; fig. S3) also enhanced H3 K27 trimethylation. The H3 K27 trimethylation was further shown to be inversely correlated with Akt activity over time (fig. S4).

To address whether EZH2 might be a target of Akt, we performed coimmunoprecipitation experiments and detected an association between Myc-tagged EZH2 and hemmagglutinin (HA)-tagged Akt (Fig. 2A). Both wild-type (WT)- and ΔSET-EZH2 (without the SET domain) associate more strongly with constitutively activated Akt (CA-Akt) than with DN-Akt. We also found an association between endogenous Akt and EZH2, and this association was reduced in cells treated with LY294002 (Fig. 2B; fig. S5), which indicates that these two molecules interact in vivo.

We noticed that there was one potential Akt phosphorylation site, serine 21, in the EZH2 protein and that this site was highly conserved across species (Fig. 2C). To examine whether Akt can phosphorylate EZH2, we immunoprecipitated EZH2 and probed it with an antibody that recognizes the phosphorylated form of Akt substrates. EZH2 was phosphorylated in CA-Akt–expressing cells three times as much as in DN-Akt (Fig. 2D). An in vitro kinase assay also demonstrated that Akt phosphorylated wild-type EZH2 but not variants of EZH2 in which Ser^{21} was replaced by Ala or Asp (S21A and S21D, respectively) and glutathione *S*-transferase (GST) (Fig. 2E). To further confirm that Akt can indeed phosphorylate EZH2 at Ser^{21} in vivo, we generated a polyclonal antibody that specifically recognized an EZH2 peptide harboring phosphorylated Ser^{21} but failed to detect an unphosphorylated EZH2 peptide or an unrelated peptide (fig. S6). This antibody was used to show that Ser^{21} phosphorylation of EZH2 is correlated with the presence of activated, phosphorylated Akt in multiple cell lines (fig. S7). To further test whether EZH2 phosphorylation is regulated by Akt, endogenous EZH2 from MDA-MB453 cells with or without LY294002 treatment or from DN-Akt/MDA453 cells was immunoprecipitated and probed with the phospho-EZH2 antibody. The phosphorylation of EZH2 was detected in wild-type MDA-MB453 cells but not in cells treated with LY294002 or in DN-Akt/MDA453 cells (Fig. 2F). When the same lysates were subjected to immunoprecipitation with phospho-EZH2 antibody followed by Western blotting with EZH2-specific antibody, blocking Akt activity decreased the intracellular level of phosphorylated EZH2 (Fig. 2G). A similar result was obtained in human embryonic kidney (HEK) 293T cells transiently transfected with wild-type or mutant EZH2 (Fig. 2H). Together, these results indicate that Akt physically interacts with EZH2 and phosphorylates it at Ser^{21} in vivo.

Next, we examined whether Akt-mediated phosphorylation of EZH2 inhibits K27 trimethylation of histone H3. We observed that DN-Akt enhanced H3 K27 trimethylation and CA-Akt suppressed it (Fig. 3A). Also, H3 K27 trimethylation level was indeed 3 to 5 times that in cells transfected with S21A-EZH2 (mimicking the unphosphorylated state), than cells transfected with WT-EZH2 and S21D-EZH2 (mimicking the phosphorylated state) (Fig. 3B). Moreover, knock-down of EZH2 by siRNA rendered DN-Akt unable to enhance H3 K27 trimethylation (Fig. 3C). Similar results were also obtained by immunofluorescence analysis of K27 trimethylation on transfected 293T cell lines (fig. S8). Thus, phosphoryl-

[1]Department of Molecular and Cellular Oncology, the University of Texas M. D. Anderson Cancer Center, Houston, TX 77030, USA. [2]Graduate School of Biomedical Sciences, the University of Texas Health Science Center at Houston, Houston, TX 77030, USA. [3]Swammerdam Institute for Life Sciences, University of Amsterdam, Kruislaan 406, 1098 SM Amsterdam, the Netherlands.

*Present address: Division of Urology, Department of Surgery, Tri-Service General Hospital, National Defense Medical Center, National Defense University, Taipei, 104, Taiwan.

†Present address: Sealy Center for Cancer Cell Biology, the University of Texas Medical Branch, Galveston, TX 77555–1048, USA.

‡To whom correspondence should be addressed. E-mail: mhung@mdanderson.org

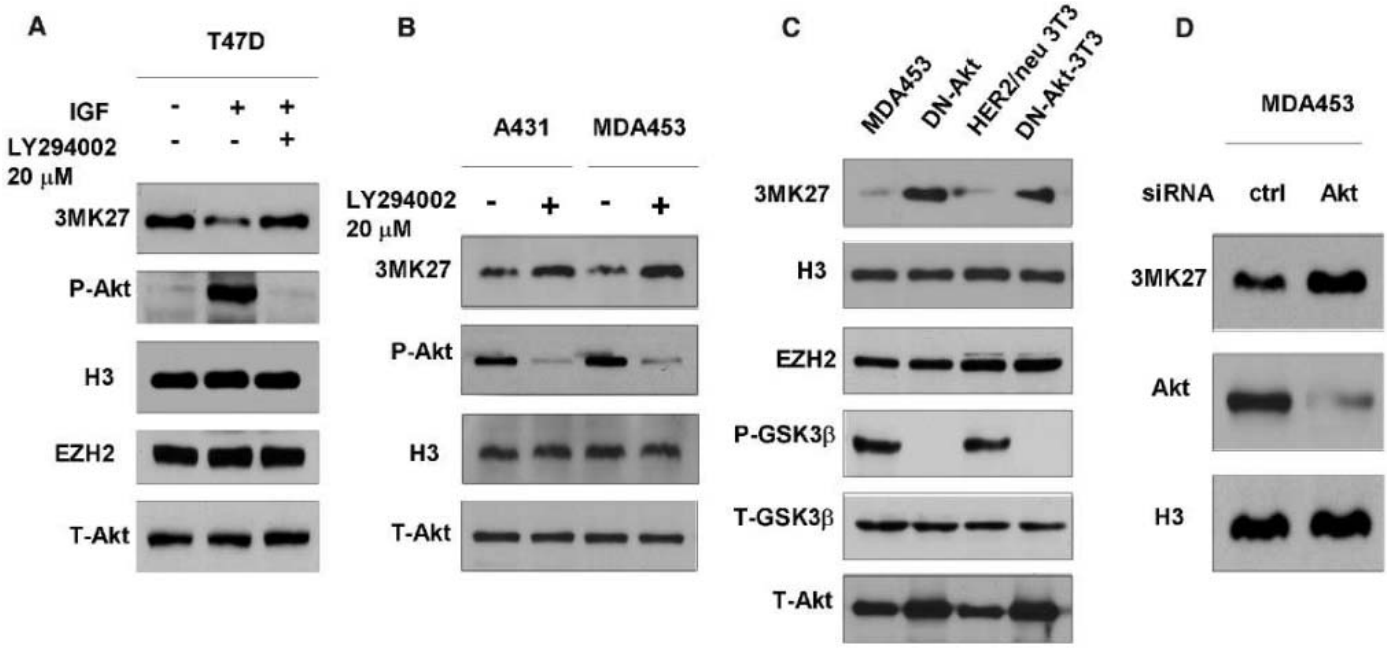

Fig. 1. Akt negatively regulates H3 K27 trimethylation. Cell lysates from cell lines as marked on the top of each panel were analyzed by Western blotting by using antibodies indicated to the left of each panel. (**A**) T47D cells were pretreated with IGF (20 ng/ml) for 30 min before LY294002 (20 μM) treatment for 24 hours. (**B**) Cells were treated with or without 20 μM LY294002. (**C**) Two pairs of wild-type and stable DN-Akt transfectants (MDA-MB453/DN-Akt, HER2-neu-3T3/DN-Akt-3T3) were examined for the level of H3 K27 trimethylation. (**D**) Immunoblot analysis of H3 K27 trimethylation in MDA-MB453 cells transfected with control (ctrl) or Akt siRNA for 48 hours. Detailed experimental conditions are in (*19*).

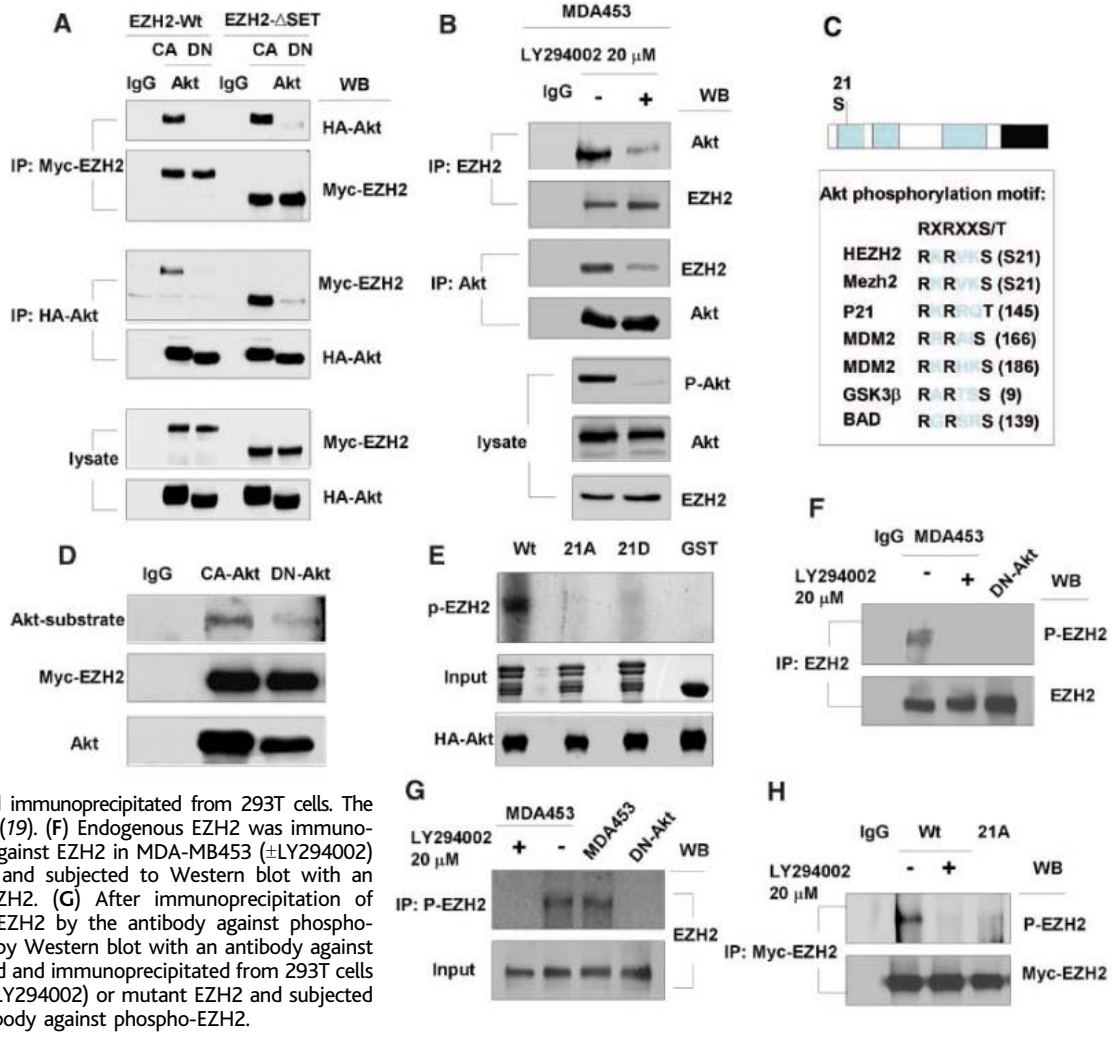

Fig. 2. Akt interacts with and phosphorylates EZH2 on Ser[21]. (**A**) Coimmunoprecipitation assay of EZH2 and Akt. Lysates from 293T cells transfected with the indicated plasmids were immunoprecipitated with antibodies against HA or Myc. Whole-cell lysate (lysate) was also subjected to Western blot analysis to examine the expression of EZH2 and Akt. (**B**) Examination of the interaction between endogenous EZH2 and Akt by immunoprecipitation and Western blotting with antibodies against either EZH2 or Akt in MDA-MB453 cells (±LY294002). (**C**) Comparison of the amino acid sequences of the Akt-phosphorylaton motifs of EZH2 and other known Akt substrates. (**D**) EZH2 was immunoprecipitated from 293T cells cotransfected with Myc-tagged WT-EZH2 and either CA-Akt or DN-Akt, and then subjected to Western blot analysis with an Akt substrate antibody. (**E**) HA-tagged Akt was expressed and immunoprecipitated from 293T cells. The kinase reaction is described in (*19*). (**F**) Endogenous EZH2 was immunoprecipitated by an antibody against EZH2 in MDA-MB453 (±LY294002) or in DN-Akt/MDA453 cells and subjected to Western blot with an antibody against phospho-EZH2. (**G**) After immunoprecipitation of phosphorylated endogenous EZH2 by the antibody against phospho-EZH2, lysates were analyzed by Western blot with an antibody against EZH2. (**H**) EZH2 was expressed and immunoprecipitated from 293T cells transfected with wild-type (±LY294002) or mutant EZH2 and subjected to Western blot with an antibody against phospho-EZH2.

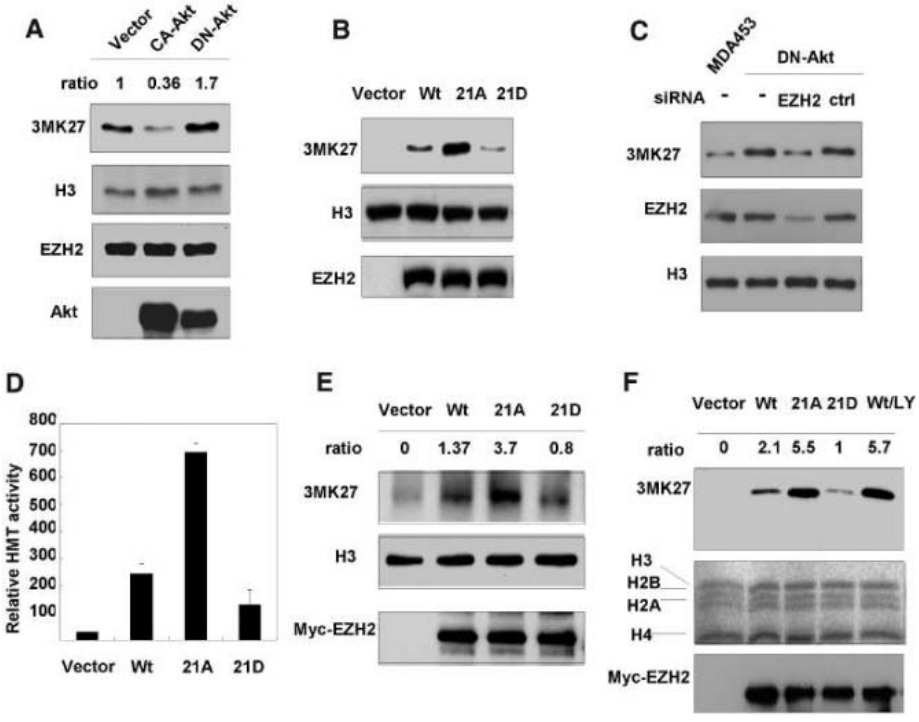

Fig. 3. Akt suppresses EZH2 HMTase activity. Detection of various proteins was measured by Western blotting with antibodies shown to the left of each panel. (**A**) 293T cells were cotransfected with EZH2 and CA-Akt or DN-Akt. (**B**) Wild-type or mutant EZH2 (S21A, S21D) was transfected into 293T cells. (**C**) DN-Akt/MDA453 cells were transfected with control (ctrl) or EZH2 siRNA. (**D**) In vitro HMTase assays were performed with immunoprecipitated wild-type or mutant Myc-tagged EZH2 incubated with recombinant histone H3 and ^{3}H-labeled *S*-adenosylmethionine (SAM). The quantification of enzyme activity with error bars from three independent experiments is shown. (**E**) Immunoprecipitated wild-type or mutant Myc-tagged EZH2 or vector was incubated with histone H3 in the presence of cold SAM; H3 K27 trimethylation was detected by Western blotting analysis. (**F**) Wild-type or mutant EZH2 immunoprecipitates isolated from 293T cells (±LY294002) were subjected to an in vitro methyltransferase assay by using native nucleosome as substrate (upper panel). The amount of protein in the methyltransferase reactions was controlled by Coomassie blue staining (lower panel). Expression of transfected Myc-tagged EZH2 was measured by Western blotting using an antibody against Myc.

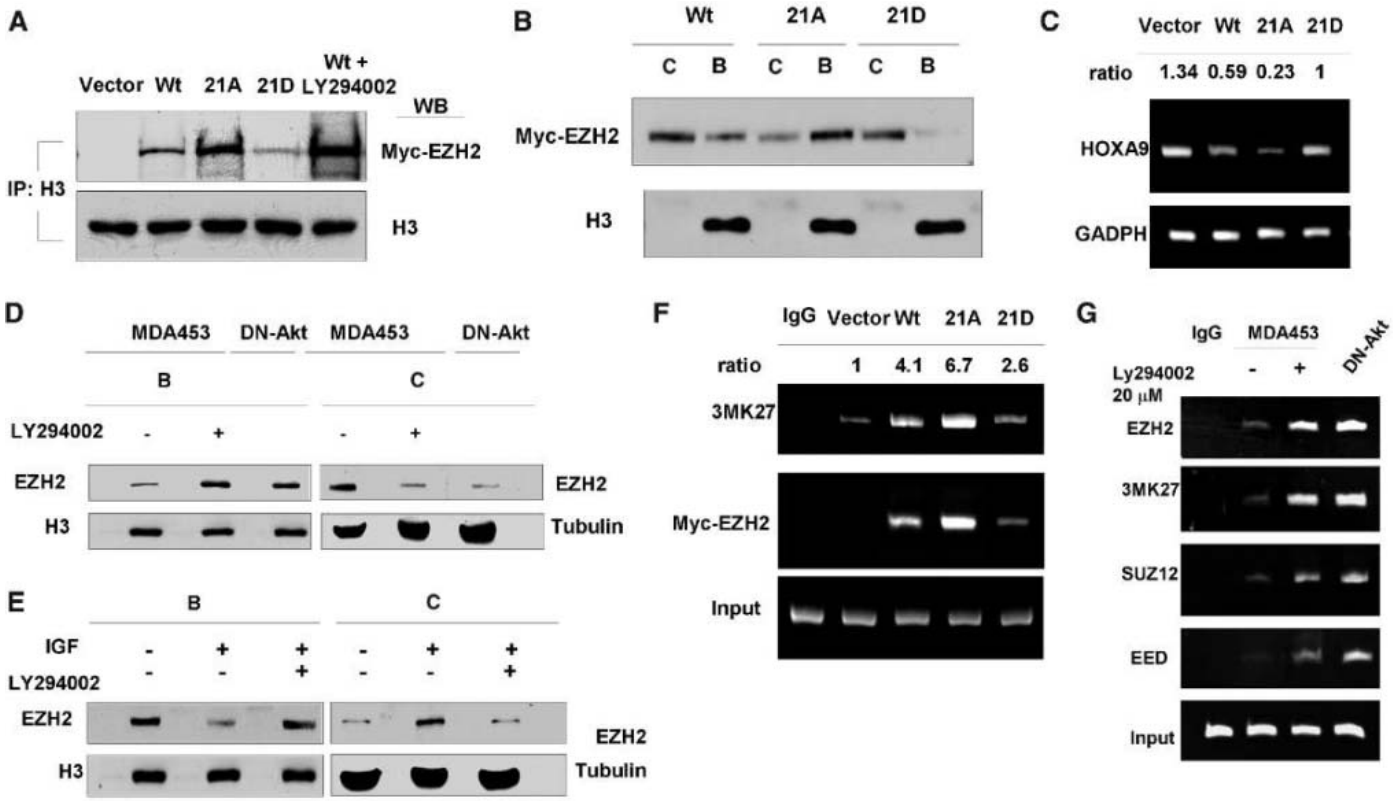

Fig. 4. Akt-mediated phosphorylation of EZH2 changes substrate affinity. (**A**) Coimmunoprecipitation between endogenous histone H3 and transfected wild-type or mutant EZH2 in 293T cells. (**B**) Western blot analysis of soluble (C) and chromatin-bound (B) fractions from cells in response to exogenous expression of wild-type or mutant EZH2. (**C**) Expression of HOXA9 in response to exogenous expression of wild-type or mutant EZH2 in 293T cells. (**D** and **E**) Western blot analysis of endogenous EZH2 in soluble (C) and chromatin-bound (B) fractions from MDA-MB453 (±LY294002) and DN-Akt/MDA453 cells (D) or from T47D cells (E) treated with IGF (20 ng/ml) or the combination of IGF and LY294002. The loading protein amounts were 150 μg (total ~2000 μg) for soluble and 40 μg (total ~150 μg) for chromatin-bound fraction, respectively. (**F** and **G**) Chromatin immunoprecipitation analysis on HOXA9 promoter by using antibodies as indicated to the left of the panel were performed in HeLa cells transfected with wild-type or mutant EZH2, (F) in MDA453 cells (±LY294002) and (G) in DN-Akt stable transfectants. The primers used for PCR are described in (*19*).

ation of EZH2 at Ser^{21} by Akt decreases H3 K27 trimethylation.

To further investigate whether this phenomenon is due to alteration of HMTase activity after EZH2 is phosphorylated by Akt, we performed in vitro HMTase activity assays. S21A-EZH2 exhibited 3 to 5 times the HMTase activity of WT-EZH2 and S21D-EZH2 when we used either recombinant histone H3 (Fig. 3, D and E) or oligonucleosomes (Fig. 3F) as substrates. In addition, inhibition of Akt activity by LY294002 also enhanced EZH2 HMTase activity 5.7 times in vitro (Fig. 3F).

Akt-mediated EZH2 phosphorylation did not change its subcellular localization or its interaction with Polycomb group (PcG) proteins Suz12 and Eed (fig. S9, supporting online text), rather, phosphorylation altered the affinity of EZH2 for its substrate, histone H3. Immunoprecipitation experiments showed that S21A-EZH2 has greater association with H3 than WT-EZH2 or S21D-EZH2 had by a factor of 2 to 4; and treatment with LY294002 enhanced the association between H3 and WT-EZH2 (Fig. 4A). In addition, we isolated soluble and insoluble (chromatin-bound) nuclear fractions from 293T cells that were transfected with wild-type or mutant EZH2. S21A-EZH2 predominantly existed in an insoluble nuclear fraction, which suggested that it strongly associated with chromatin (Fig. 4B). We further investigated the chromatin association of endogenous EZH2 in cells in which Akt activity was either induced or blocked. Blockage of Akt consistently increased the chromatin-bound EZH2, whereas activation of Akt had the opposite effect (Fig. 4, D and E; fig. S10).

To determine whether EZH2 phosphorylation mediated by Akt is functionally important, we tested whether it affects gene expression. Reverse transcription polymerase chain reaction (RT-PCR) showed that expression of *HOXA9*, a known EZH2-targeted gene (*18*), was suppressed by S21A-EZH2 (Fig. 4C), and this result was consistent with the high H3 K27 trimethylation on the HOXA9 promoter (Fig. 4F). This phenomenon was also observed in MDA453 cells treated with LY294002 or in DN-Akt stable transfectants (Fig. 4G). Similar results were observed when other PcG proteins such as Suz12 and Eed were examined by chromatin immunoprecipitation (ChIP) assay (Fig. 4G). Thus, phosphorylation of EZH2 on Ser^{21} by Akt does not seem to change the composition of the PRC, but it does reduce the affinity of EZH2 toward histone H3, which results in a decrease in H3 K27 trimethylation and derepression of genes normally silenced by EZH2.

Our study demonstrates that the HMTase activity of EZH2 responsible for H3 K27 trimethylation is regulated by the Akt signaling pathway through phosphorylation of EZH2. Phosphorylation of EZH2 suppresses H3 K27 trimethylation and disrupts gene silencing and thus may contribute to oncogenesis. Furthermore, S21D-EZH2 enhanced cell growth in culture and tumor development in animals, and phosphorylated EZH2 also correlated with Ki67, a proliferative marker in primary tumor tissues (figs. S11 and S12, tables S1 and S2, supporting online text) (*19*). Although Akt-mediated phosphorylation of EZH2 reduces its affinity toward histone H3, it did not compromise PRC composition, which is known to be responsible for its methyltransferase activity: The phosphorylated-EZH2 complex, instead, may target nonhistone substrates that are important for tumorigenicity. In this scenario, the dynamic changes in EZH2 substrate affinity induced by Akt may provide an explanation for why EZH2, which is overex-

pressed in cancers, has less HMTase activity toward histone H3.

References and Notes

1. T. Jenuwein, C. D. Allis, *Science* **293**, 1074 (2001).
2. Y. Zhang, D. Reinberg, *Genes Dev.* **15**, 2343 (2001).
3. A. J. Bannister, R. Schneider, T. Kouzarides, *Cell* **109**, 801 (2002).
4. R. J. Sims 3rd, K. Nishioka, D. Reinberg, *Trends Genet.* **19**, 629 (2003).
5. Y. Wang *et al.*, *Science* **306**, 279 (2004).
6. Y. Shi *et al.*, *Cell* **119**, 941 (2004).
7. Y. Zhang, *Nature* **431**, 637 (2004).
8. S. Kubicek, T. Jenuwein, *Cell* **119**, 903 (2004).
9. A. P. Feinberg, B. Tycko, *Nat. Rev. Cancer* **4**, 143 (2004).
10. R. Cao, Y. Zhang, *Curr. Opin. Genet. Dev.* **14**, 155 (2004).
11. A. Kuzmichev, T. Jenuwein, P. Tempst, D. Reinberg, *Mol. Cell* **14**, 183 (2004).
12. F. M. Raaphorst, A. P. Otte, C. J. Meijer, *Trends Immunol.* **22**, 682 (2001).
13. S. Varambally *et al.*, *Nature* **419**, 624 (2002).
14. C. G. Kleer *et al.*, *Proc. Natl. Acad. Sci. U.S.A.* **100**, 11606 (2003).
15. I. Vivanco, C. L. Sawyers, *Nat. Rev. Cancer* **2**, 489 (2002).
16. M. L. Sulis, R. Parsons, *Trends Cell Biol.* **13**, 478 (2003).
17. B. P. Zhou *et al.*, *Nat. Cell Biol.* **3**, 973 (2001).
18. R. Cao, Y. Zhang, *Mol. Cell* **15**, 57 (2004).
19. Materials and Methods and supporting text are available as supporting material on *Science* Online.

20. This study was supported by the NIH R01 109311 and P01 099031 (to M.-C.H.) and T.-L.C. was partially supported by the Tri-Service General Hospital, Taiwan. We greatly appreciate A. M. Chinnaiyan, D. Reinberg, and Y. Zhang for providing the pCDNA3-Myc-EZH2 plasmid, anti-Eed antibodies, and purified oligonucleosome, respectively. We also thank R. B. Arlinghaus, S. Roth Dent, D. Yu, P. D. McCrea, and M. W. Van Dyke for critically reading this manuscript and J. C. Cheng for editing the manuscript.

Supporting Online Material

www.sciencemag.org/cgi/content/full/310/5746/306/DC1
Materials and Methods
SOM Text
Figs. S1 to S12
Tables S1 and S2
References and Notes

16 August 2005; accepted 21 September 2005
10.1126/science.1118947

Counting Cytokinesis Proteins Globally and Locally in Fission Yeast

Jian-Qiu Wu[1] and Thomas D. Pollard[1,2]*

We used fluorescence microscopy to measure global and local concentrations of 28 cytoskeletal and signaling proteins fused to yellow fluorescent protein (YFP) in the fission yeast *Schizosaccharomyces pombe*. Native promoters controlled the expression of these functional YFP fusion proteins. Fluorescence measured by microscopy or flow cytometry was directly proportional to protein concentration measured by quantitative immunoblotting. Global cytoplasmic concentrations ranged from 0.04 (formin Cdc12p) to 63 micromolar (actin). Proteins concentrated up to 100 times in contractile rings and 7500 times in spindle pole bodies at certain times in the cell cycle. This approach can be used to measure the global and local concentrations of any fusion protein.

To understand any complicated cellular process, one must know the global and local concentrations of the participating proteins. Concentrations reveal stoichiometries and are prerequisites for mathematical modeling of biological systems. Unfortunately, concentration measurements are rarely available. In the case of cytokinesis, only one estimate of the concentration of myosin-II in the cleavage furrow is available (*1*). Antibodies can be used to estimate the cellular abundance of a few native proteins (*2*) or thousands of proteins carrying molecular tags (*3*) but not their local concentrations. Light microscopy of cells expressing proteins with a fluorescent tag is an attractive approach, but previous calibration methods depended on assumptions that are difficult to verify, such as the assumption that the quantum yield and detection efficiency are the same inside and outside cells (*4*–*6*). Even with careful microscopy, absolute concentration may be unknown, because a fluorescent fusion protein was expressed from a plasmid along with endogenous native protein. Tests to verify the functionality of the fusion protein are often lacking.

Here we show that the fluorescence of functional fluorescent fusion proteins expressed from native promoters is directly proportional to the number of molecules in live cells. This calibration allowed us to measure the global and local concentrations of 28 different cytoskeletal and signaling proteins as the fission yeast *Schizosaccharomyces pombe* goes through the cell cycle. This approach is applicable to a medium-scale analysis of proteins participating in any cellular process, even without genomic integration of the fusion protein.

We integrated the coding sequence for monomeric yellow fluorescent protein (mYFP) or YFP into the genome of *S. pombe* at the N or C termini of 27 different proteins, so the fusion proteins were expressed from their endogenous promoters (*7*, *8*). We varied the position of mYFP and the size of linker to find functional constructs. We ruled out partial loss of function by observing normal colony formation and cellular morphology under both standard and stressful conditions and by observing the lack of synthetic phenotypes when crossed to strains with other mutations (*9*). The abilities of these tagged constructs to function normally suggest that their expression levels are not substantially different from those of the native proteins. We confirmed this by immunoblotting Arp3p and by microscopy of Myo2p, IQGAP Rng2p, and pombe Cdc15 homology (PCH) protein Cdc15p (fig. S1) (*9*).

We combined two measurements to determine the fluorescence per fusion-protein molecule. First, we collected stacks of confocal sections through whole cells to measure the total and local fluorescence from each strain (Fig. 1A and fig. S2). For most tagged proteins, the mean fluorescence intensity was constant from cell to cell, with standard deviations from the mean intensity of only 8 to 37% (Table 1). Second, we measured the average number of mYFP fusion molecules per cell by quantitative immunoblotting (Fig. 1B). After background subtraction, the mean fluorescence per cell measured microscopically was directly proportional (R = 0.99) to the average number of molecules per cell for seven fusion proteins (Fig. 1C). Flow cytometry confirmed the linear relationship between fluorescence and concentration for all 27 proteins (Fig. 1C and fig. S3). The variance was smaller by microscopy, especially for global concentrations <0.5 μM. The total fluorescence of Fim1p–mYFP was the same whether concentrated in patches or dispersed by treating cells with Latrunculin A (fig. S4), so quenching was not an issue even when proteins were crowded together in the cell. Similarly, the fluorescence of formin Cdc12p and the Unc45/Crolp/She4p–related (UCS) protein Rng3p with triple YFP tags was three times that of single YFP tags. Because of photobleaching and low signal-to-noise ratios, the measured concentrations of low abundance proteins are less accurate than those of abundant proteins (fig. S3).

Knowing the fluorescence per molecule in live cells, we measured the global concentrations of 20 other proteins tagged with YFP or mYFP from the integrated fluorescence intensity of asynchronous cells (Table 1). Point counting stereology of electron micrographs established that cytoplasm is 29% of the total

[1]Department of Molecular, Cellular, and Developmental Biology and [2]Departments of Cell Biology and Molecular Biophysics and Biochemistry, Yale University, New Haven, CT 06520–8103, USA.

*To whom correspondence should be addressed. E-mail: thomas.pollard@yale.edu

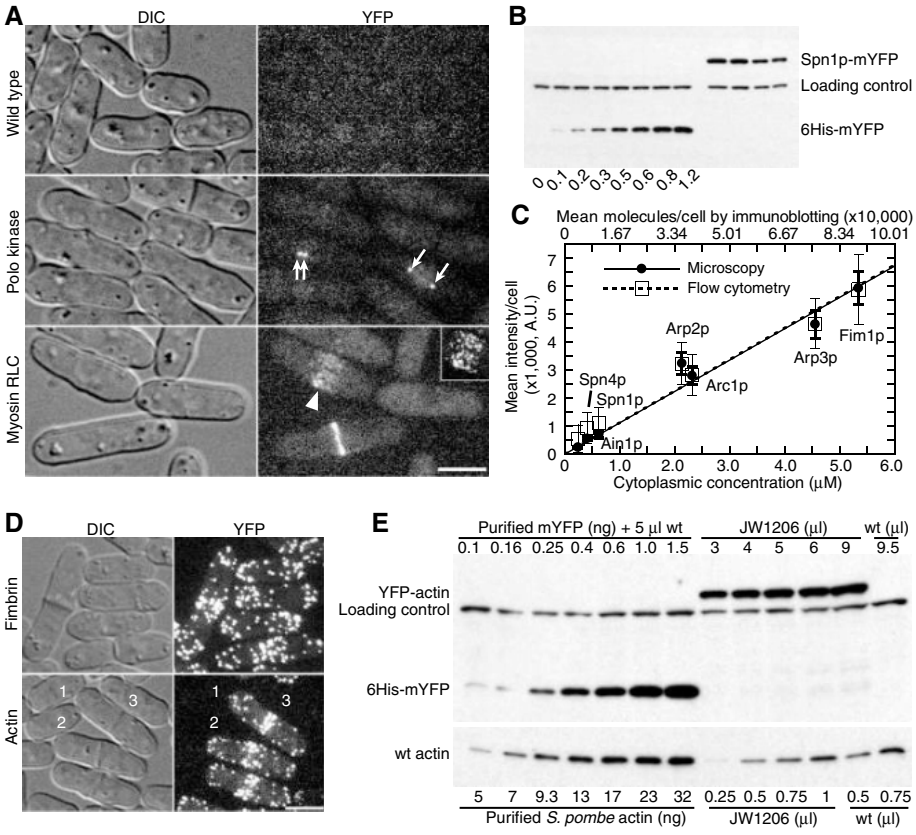

Fig. 1. Measurement of protein concentrations by fluorescence microscopy, flow cytometry, and quantitative immunoblotting. (**A** and **D**) Differential-interference contrast and fluorescence micrographs of living wild-type (wt) cells and cells expressing integrated polo kinase Plo1p-mYFP (SPBs marked by arrows), myosin regulatory light chain Rlc1p-mYFP, and fimbrin Fim1p-mYFP at endogenous levels, or YFP-actin from a plasmid (strain JW1206). Fluorescence micrographs of 12 z-sections spaced at 0.6-μm intervals were projected into a two-dimensional image using (A) a sum intensity projection or [(D) and (A, inset)] maximum intensity projection. The inset in (A) shows the broad band marked by the arrowhead. Numbered cells in (D) expressed YFP-actin at low levels but were included in measurements. (**B**) Quantitation of septin Spn1p-mYFP by immunoblotting with antibody to YFP. In lanes 1 to 8, a standard curve was generated with 0 to 1.2 ng of purified 6His-mYFP mixed with 5 μl of wt cell extract. Lanes 9 to 12 have duplicate samples of 5.0 and 2.5 μl of cell extract, giving Spn1p-mYFP signal in the linear range of standard curve. A nonspecific band from cell extract provided a convenient loading control. (**C**) The correlation of average fluorescent molecules per cell from immunoblots (upper *x* axis) and cytoplasmic concentration (lower *x* axis) with cell-size–corrected integrated mYFP fluorescence intensity per cell from microscopy (mean ± 1 SD; solid circles and darker error bars; $y = 0.0676x$, $R = 0.99$) and fluorescence intensity from flow cytometry (mean ± 1 SD; open squares and lighter error bars; $y = 0.0676x$, $R = 0.99$) for strains expressing integrated mYFP fusion proteins. (**E**) Measurements of actin concentration by immunoblotting using antibodies to YFP (upper blot) and antibodies to actin (lower blot). Dilutions of cell extract of a strain with YFP-actin plasmid (JW1206) or wt JW729 grown in minimal medium for 36 hours and then in rich medium for 4 hours, and standards of purified 6His-mYFP (upper blot) and *S. pombe* actin (lower blot) with or without cell extract from wt cells were separated by SDS-polyacrylamide gel elecrophoresis. Scale bars, 5 μm.

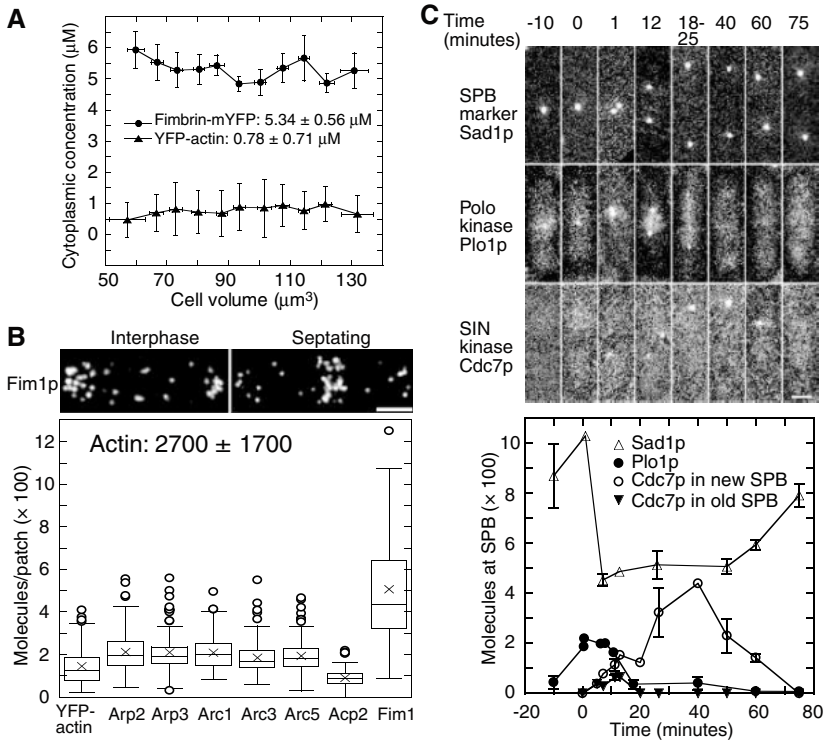

Fig. 2. Measurement of protein concentrations by fluorescence microscopy. (**A**) Cytoplasmic concentration of fimbrin (solid circles) and YFP-actin (solid triangles) as a function of cell volume. Mean concentrations and cell volumes ± 1 SD are shown. (**B**) Local accumulation of proteins in actin patches. Top: Fluorescence micrographs (maximum intensity projection) of interphase and septating cells expressing Fim1p-mYFP. Bottom: Box plots of molecules of YFP or mYFP fusion proteins per patch in 70 to 200 patches in 2 to 6 cells for each protein. Box plots display mean (marked with ×), median (line inside the box), and outliers (cicles). The box represents the middle 50% data and the bars represent the top and bottom 25% data. (**C**) Local accumulation of proteins in SPBs during cytokinesis. SPB separation defines time zero. The cell-cycle time was calculated from the separation of the SPBs and septum diameter. Top: Micrographs (sum intensity projection) of cells expressing mYFP (YFP for Cdc7p) fusion proteins. Bottom: Time course of the mean accumulation ± 1 SD of three fusion proteins in SPBs. Scale bars, 2.5 μm.

cellular volume. We used this number to calculate cytoplasmic concentrations from the total fluorescence.

None of the several different YFP-actin constructs could replace the native actin gene, so we expressed N-terminally tagged YFP-actin at low levels from a plasmid, under the control of attenuated *81nmt1* promoter. Cells tolerated YFP-actin and incorporated it into actin patches with capping protein (*10*) but not into the contractile ring, likely because formin Cdc12p cannot handle YFP-actin (Fig. 1D). The fluorescence intensity of YFP-actin expressed from the plasmid varied widely from cell to cell, with the standard deviation (0.71 μM) equal to the mean 0.78 μM (Figs. 1D and 2A). Quantitative immunoblots gave cytoplasmic actin concentrations of 31.3 ± 1.3 μM in minimal medium (Fig. 1E) and 63.2 μM in rich medium (fig. S5). Cell size differed by less than 5% under these conditions. Immunoblots with YFP antibody showed that an average of 1.8% of the actin was tagged with YFP in cells grown on minimal medium (Fig. 1E). To estimate the number of actin molecules in individual cells, we determined the ratio of that cell's volume to the average volume of all the cells in the population.

Global cytoplasmic concentrations of cytokinesis proteins (Table 1) range from 0.04 μM formin Cdc12p (600 molecules per cell) to 63.2 μM actin (1.43 million molecules per cell). The concentration of myosin-II light chain Cdc4p (4.8 μM) is 10-fold higher than that of Myo2p (0.45 μM), which is in keeping with evidence for functions beyond its partnership with myosins (*11*–*14*). Most of the proteins studied are more abundant in *S. pombe* than in haploid strains of *S. cerevisiae* (table S2), in part because of the 1.7-fold higher protein content per cell of *S. pombe* (*15*, *16*).

Most protein concentrations were constant with cell volume, an estimate of position in the cell cycle (Fig. 2A and fig. S6). This confirms with better resolution previous immunoblotting measurements on bulk samples of synchronized cells for formin Cdc12p (*17*), both types of myosin-II heavy chain (*18*), and polo kinase Plo1p (*19*). One exception is the anillin-like protein, Mid2p, which is only detected during septation and cell separation (fig. S6E), as reported (*20*). The concentrations of anillin-like protein Mid1p and PCH protein Cdc15p are constant across the cell cycle, in spite of fluctuations in mRNA levels (*19*, *21*–*23*), so the ratios of these mRNAs to their proteins vary over time.

The biochemical reactions depend on local concentrations, so we used fluorescence and our standard curve (Fig. 1C) to measure local concentrations. Actin patches concentrate at cell poles and at the cell-division site where the cell wall grows (Fig. 2B). The molecular composition of each patch varies over its 20-s lifetime (*24*) as it forms, matures, and dissociates (*24*, *25*), so measurements on patches with random ages vary considerably (Fig. 2B and Table 1; standard deviations 38 to 62% of means). Assuming that the ratio of YFP-actin to native actin is at least as high in patches as the cell as a whole and assuming that patches are spheres 250 nm in diameter (*26*), an average patch has at least 2700 actin molecules (minimal local concen-

Table 1. Global cytoplasmic concentrations, mean molecules per cell, and local accumulation in actin patches, spindle pole bodies, or the division site for 28 proteins measured by fluorescence microscopy and immunoblotting.

Protein (number of cells analyzed for global concentration; local concentration; number of patches)	Exposure time/slice (ms)	Global cytoplasmic concentration (μM)	Mean polypeptides per average cell with a volume of 92 μm³	Local accumulation %* [mean (maximum observed)]	Local concentration [mean polypeptides (mean concentration, μM)]
Actin patch proteins					
YFP-actin Act1p† (302; 2; 89)	69	0.78 ± 0.71	17,600 ± 16,000	13 (16)	145 ± 89 (29)
Actin Act1p† (118 × 10⁶)	Imm/blot	63.2 ± 10.5‡	(1.43 ± 0.24) × 10⁶‡	>13	2,700 ± 1,700 (530)
Arp2 (Arp2p) (104; 6; 168)	69	2.88 ± 0.35	46,600 ± 5,700	10 (11)	212 ± 94 (42)
Arp3 (Arp3p) (86; 6; 158)	69	4.12 ± 0.45	66,700 ± 7,300	7 (8)	210 ± 87 (42)
ARPC1 (Arc1p/Sop2p) (85; 6; 199)	69	2.49 ± 0.29	40,300 ± 4,700	15 (17)	208 ± 79 (41)
ARPC3 (Arc3p/Arc21p) (85; 6; 165)	69	2.39 ± 0.22	38,700 ± 3,600	12 (14)	185 ± 73 (37)
ARPC5 (Arc5p/Arc16p) (94; 6; 165)	69	1.88 ± 0.14	30,500 ± 2,300	12 (13)	193 ± 76 (38)
Capping protein Acp2p (42; 2; 69)	99	1.19 ± 0.16	19,200 ± 2,600	17 (19)	90 ± 48 (18)
Fimbrin Fim1p (121; 4; 121)	69	5.34 ± 0.56	86,500 ± 9,100	15 (21)	507 ± 290 (100)
Spindle pole body proteins					
SPB protein Sad1p† (58; 58)	198	0.15 ± 0.05	3,300 ± 1,100	31 (52)	450–1,030 (900–1,120)
Polo kinase Plo1p† (65; 38)	399	0.29 ± 0.06	6,600 ± 1,400	1 (6)	30–220 (33–440)
SIN kinase Cdc7p (103; 22)	399	0.24 ± 0.08	4,000 ± 1,300	5 (13)	0–440 (0–480)
Cytokinesis proteins					
					Mature contractile ring
Anillin-like Mid1p† (94; 23)	300	0.09 ± 0.02	2,100 ± 500	40 (68)	700 ± 200 (4)
Myosin-II Myo2p *kan*ʳ§ (53; 13)	300	0.45 ± 0.08	7,300 ± 1,400	27 (50)	2,900 ± 400 (20)
Myosin-II ELC Cdc4p (54; 15)	78	4.75 ± 0.67	77,000 ± 10,800	22 (31)	24,900 (165)
Myosin-II RLC Rlc1p (45; 10)	399	0.60 ± 0.09	9,600 ± 1,500	18 (28)	3,200 ± 600 (28)
IQGAP Rng2p *kan*ʳ§ (112; 17)	300	0.17 ± 0.04	2,700 ± 600	35 (62)	1,300 ± 100 (10)
mYFP-Cdc15p *kan*ˢ§ (102; 16)	198	2.13 ± 0.33	35,600 ± 5,400	21 (34)	16,100 ± 2,300 (94)
Formin Cdc12p‖ (98; 9)	600	0.04 ± 0.01	600 ± 200	11 (26)	300 ± 50 (3)
Actin Act1p† (118 × 10⁶)	Imm/blot	63.2 ± 10.5‡	(1.43 ± 0.24) × 10⁶‡	4	~76,000 (460)
UCS protein Rng3p‖ (72; 12)	600	0.12 ± 0.03	1,900 ± 400	3 (8)	60 ± 20 (0.5)
Rng3p in *myo2-E1*‖ (42; 13)	198	0.32 ± 0.11	6,800 ± 2,400	30 (50)	4,200 ± 1,600 (28)
Alpha-actinin Ain1p (101; 10)	300	0.22 ± 0.03	3,600 ± 500	8 (12)	500 ± 100 (4)
Myosin-II Myp2p (89; 14)	399	0.38 ± 0.07	6,100 ± 1,100	21 (28)	2,000 (15)
Septin Spn1p (159; 24)	198	0.63 ± 0.10	10,300 ± 1,600	35 (50)	7,000 ± 800 (21)
Septin Spn4p (131; 28)	198	0.50 ± 0.07	8,100 ± 1,200	34 (50)	6,100 ± 1,200 (18)
Anillin-like Mid2p (116)	198	0.11 ± 0.19	1,800 ± 3,100	NA	NA
Protein kinase C Pck2p (102; 19)	399	0.27 ± 0.04	4,300 ± 600	13 (24)	800 ± 100 (6)
Rho GEF Rgf1p (89; 9)	300	0.27 ± 0.05	4,300 ± 700	5 (8)	200 ± 30 (1)
Rho GEF Rgf3p (44; 6)	999	0.20 ± 0.08	3,200 ± 1,300	4 (13)	200 ± 40 (1)
Chitin synthase Chs2p (97; 9)	600	0.13 ± 0.07	2,100 ± 1,100	3 (8)	100 ± 30 (0.5)

*Percent of total molecules localized to actin patches, SPB(s), or the cell-division site (excluding medial patches). †Actin, Sad1p, Plo1p, and Mid1p were not excluded from the nucleus (*40*–*44*). We assumed equal concentrations of these proteins in the cytoplasm and nucleus. ‡The average of the two methods using *S. pombe* actin as standard as shown in fig. S5. §Strain analyzed with (*kan*ʳ) or without (*kan*ˢ), the *kanMX6* selectable marker. ‖Triple YFP tag gave three times the signal of single YFP and less variance in the measurements.

tration 530 μM). Patches also contain 202 Arp2/3 complexes (40 μM; with 1:1:1:1:1 stoichiometry of 5 subunits), 90 capping proteins Acp2p (18 μM), and a remarkable number, 507, of the actin filament crosslinker fimbrin Fim1p (100 μM). The fractions of each protein in patches range from 6 to 21% (Table 1). Assuming that each Arp2/3 complex nucleates an actin filament as a branch on an older filament, the filaments in patches consist of at least 13 subunits (≥30-nm-long) and half are capped. This minimum length is similar to that of filaments of 20 subunits in patches isolated from *S. cerevisiae* (*27*, *28*).

Spindle pole bodies (SPBs) have both stable and transient components (Table 1 and Fig. 2C) that organize microtubules for mitosis and regulate cytokinesis (*29*, *30*). These plaque-like oblate ellipsoids are 0.18 μm in diameter and 0.09 μm thick (0.05 μm early in mitosis) (*31*). Throughout the cell cycle, about 30% of Sad1p (an SPB marker protein) concentrates up to 7500-fold in SPBs relative to the global cytoplasmic concentration. When mature SPBs separate early in mitosis, the ~1000 molecules of Sad1p divide equally between the two daughter SPBs, which then recruit ~5 molecules of Sad1p each minute as the cell cycle progresses (Fig. 2C). Early in mitosis, 6% of polo kinase Plo1p (220 molecules per SPB) concentrates transiently on both SPBs and, to a lesser extent, in the mitotic spindle to trigger the septation initiation network (SIN) (*30*). About 10 min later, the SIN pathway kinase Cdc7p starts to accumulate at ~10 molecules per minute in the new SPB (*32*), peaks at ~440 molecules late in anaphase, and then drops to undetectable levels (Fig. 2C). Thus, the signal from Plo1p is only amplified by a factor of two in terms of accumulation of Cdc7p, the first kinase downstream from the guanosine triphosphatase Spg1p in the SIN pathway, and most of both Plo1p and Cdc7p are free to function throughout the cytoplasm. Fluorescence recovery after photobleaching (FRAP) experiments also show dynamic association of other SIN pathway components, Spg1p and Sid2p kinase, with SPBs (*33*).

Fission yeast begin cytokinesis when anillin-like Mid1p exits from the nucleus and initiates assembly of at least seven proteins in a broad band of 50 to 120 dots at the cleavage site (Fig. 3A) (*34*). Given ~75 dots, each would have about 21 molecules of Mid1p, 43 myosin-II heavy chains Myo2p, 35 myosin regulatory light chains Rlc1p, a vast excess of 289 myosin light chains Cdc4p, 23 IQGAP Rng2p, 22 Cdc15p proteins, and only 2 Cdc12p formin dimers. Thus the stoichiometry of Mid1p to dimeric myosin-II molecules to IQGAP to Cdc15 is close to 1:1:1:1. Formin homodimers nucleate and remain attached to the barbed end of elongating actin filaments (*35*). Thus each dot could grow about 2 actin filaments anchored by Cdc12p, sufficient for myosin-II to pull the dots together into a continuous contractile ring early in mitosis. The numbers of both Cdc4p and Cdc15p in dots exceed their known binding partners included in this study [myosin-II heavy chain Myo2p and IQGAP Rng2p (*13*, *14*), and Cdc12p (*36*)] by a factor of 10, consistent with evidence for other binding partners (myosins-V and -I) and functions.

Our measurements provide the first quantitative inventory of contractile ring proteins. Given a circumference of 10.3 μm and about 20 actin filaments in a cross section estimated from published electron micrographs (*37*), an uncontracted actin ring has ~206 μm of filaments consisting of ~76,000 subunits (given 370 actin subunits per micrometer of filament), which implies a local actin concentration of ~460 μM. If each of the 150 Cdc12p dimers in a mature contractile ring nucleates an actin filament, an average filament is ~1.4 μm long. A mature contractile ring includes ~2900 molecules of Myo2p (Fig. 3, A and B), enough for 14 myosin heavy chains (~one myosin-II mini-filament) per micrometer of actin filament. When activated by the UCS protein Rng3p, myosin-II moves actin filaments at 0.5 μm/s (*14*). If the actin filaments are about 1 μm long, a minimum of 3 or 4 sarcomere-like contractile units would encircle the equator and constrict the circumference of an unloaded contractile ring at ~3 to 4 μm/s, which is ~10^3 times faster than observed. More likely, the number of contractile units in series is >4, increasing the maximum rate of contraction. If all the myosin-II heads in such a contractile unit were active, they would produce ~1500 pN of force. Thus, either the load is consid-

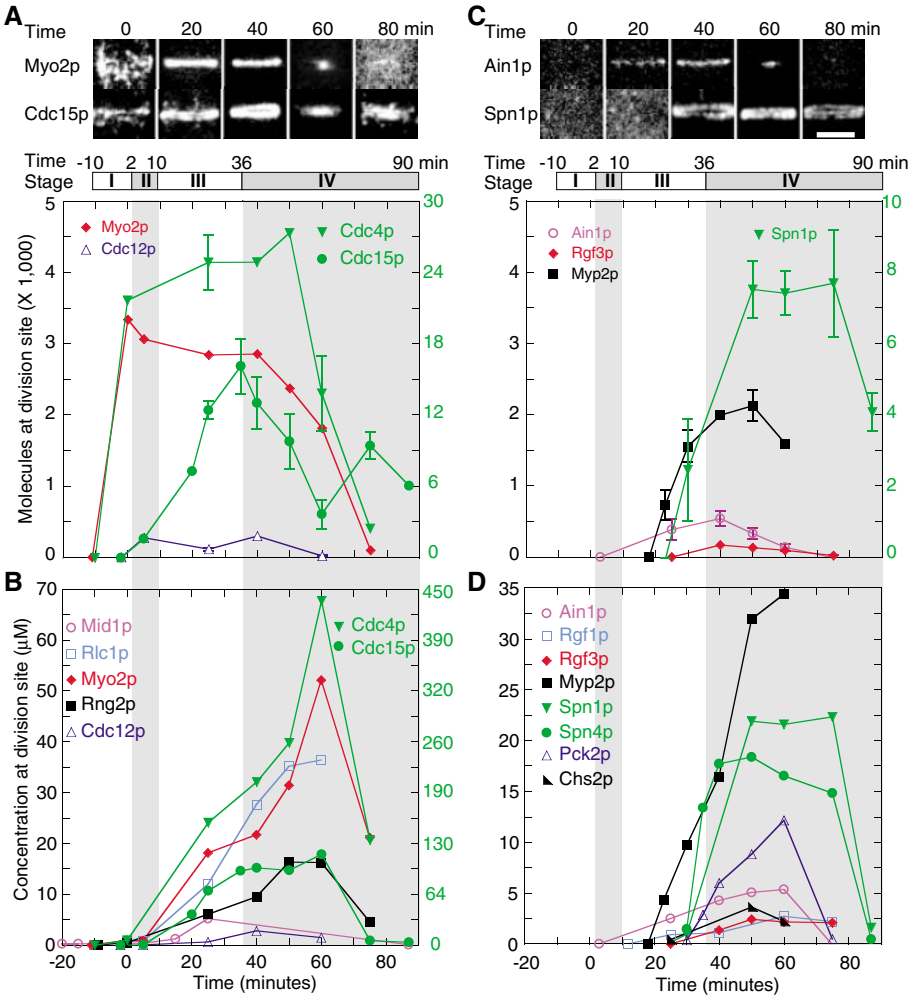

Fig. 3. Local accumulation and concentrations of mYFP fusion proteins at the cell-division site measured by fluorescence microscopy. SPB separation defines time zero. The cell-cycle time and stage (*8*) of each cell were estimated from the morphology and diameters of the contractile ring and septum. (**A** and **C**) Fluorescence micrographs (maximum intensity projection) of cells at various stages expressing mYFP fusions of myosin-II Myo2p (JW1110), PCH protein Cdc15p (JW1063), α-actinin Ain1p, and septin Spn1p. The brightness and contrast of images were linearly adjusted to show the contracted ring. Graphs plot the local accumulation [(A) and (C)] (mean ± 1 SD) and local concentrations (**B** and **D**) of molecules in contractile rings and entire broad band including spaces between the dots. The data for Cdc15p after 60 min show the protein in the septum region after ring contraction. In (A) to (C), the green symbols and lines use scale on the right. All others use scale on the left. Scale bar, 2.5 μm.

erable or few myosin heads are active. The ratio of one Rng3p per 50 myosin-II heads in the contractile ring (Table 1 and fig. S7) supports the latter hypothesis. In the temperature-sensitive *myo2-E1* mutant, the concentration of Rng3p is higher by threefold globally and ~60-fold in the contractile ring, perhaps to compensate for the minimal motor activity of this mutant (*14*). Large pools of most contractile-ring proteins remain in the cytoplasm during cytokinesis (Table 1) available for exchange with assembled rings, as observed in FRAP experiments (*38*, *39*).

The number of conventional myosin-II (Myo2p, Cdc4p, and Rlc1p) molecules in contractile rings is roughly constant from the time that a ring condenses through constriction (Fig. 3), so the local myosin concentration and force-producing capacity increase dramatically as the diameter of the ring declines. Cdc15p not only participates in ring assembly, but its number of molecules increases ~10-fold as rings mature during anaphase in preparations for septum formation. As rings constrict, the local concentrations of actin-binding proteins IQGAP Rng2p, Cdc15p, formin Cdc12p, and alpha-actinin Ain1p are nearly constant, so all are lost in proportion to the decline in the volume of ring. Septins Spn1p and Spn4p arrive late at the division site, forming rings with 15 to 22 μM septin that do not constrict as the septum forms (Fig. 3, C and D).

If used with caution, microscopy with fluorescent fusion proteins provides a precision measuring tool for quantitative biology. Our calibration method can be used to determine the concentration of any protein in yeast or other organisms with homologous recombination. Episomal expression of a YFP-fusion protein with measurement of the ratio of tagged and untagged proteins can be used where homologous gene replacement is impossible.

References and Notes

1. D. N. Robinson, G. Cavet, H. M. Warrick, J. A. Spudich, *BMC Cell Biol.* **3**, 4 (2002).
2. H. N. Higgs, T. P. Pollard, *J. Cell Biol.* **150**, 1311 (2000).
3. S. Ghaemmaghami *et al.*, *Nature* **425**, 737 (2003).
4. D. W. Piston, G. H. Patterson, S. M. Knobel, *Methods Cell Biol.* **58**, 31 (1999).
5. K. Hirschberg, R. D. Phair, J. Lippincott-Schwartz, *Methods Enzymol.* **327**, 69 (2000).
6. M. Dundr, J. G. McNally, J. Cohen, T. Misteli, *J. Struct. Biol.* **140**, 92 (2002).
7. J. Bähler *et al.*, *Yeast* **14**, 943 (1998).
8. J.-Q. Wu, J. R. Kuhn, D. R. Kovar, T. D. Pollard, *Dev. Cell* **5**, 723 (2003).
9. Materials and methods are available as supporting material on *Science* Online.
10. D. R. Kovar, J.-Q. Wu, T. D. Pollard, *Mol. Biol. Cell* **16**, 2313 (2005).
11. P. Nurse, P. Thuriaux, K. Nasmyth, *Mol. Gen. Genet.* **146**, 167 (1976).
12. M. Desautels, J. P. Den Haese, C. M. Slupsky, L. P. McIntosh, S. M. Hemmingsen, *J. Biol. Chem.* **276**, 5932 (2001).
13. V. M. D'Souza, N. I. Naqvi, H. Wang, M. K. Balasubramanian, *Cell Struct. Funct.* **26**, 555 (2001).
14. M. Lord, T. D. Pollard, *J. Cell Biol.* **167**, 315 (2004).
15. See the fission yeast handbook (available at www.sanger.ac.uk/PostGenomics/S_pombe/docs/nurse_lab_manual.pdf).
16. F. Sherman, *Methods Enzymol.* **350**, 3 (2002).
17. F. Chang, D. Drubin, P. Nurse, *J. Cell Biol.* **137**, 169 (1997).
18. M. Bezanilla, T. D. Pollard, *Mol. Biol. Cell* **11**, 79 (2000).
19. M. Anderson *et al.*, *EMBO J.* **21**, 5745 (2002).
20. J. J. Tasto, J. L. Morrell, K. L. Gould, *J. Cell Biol.* **160**, 1093 (2003).
21. C. Fankhauser *et al.*, *Cell* **82**, 435 (1995).
22. X. Peng *et al.*, *Mol. Biol. Cell* **16**, 1026 (2005).
23. G. Rustici *et al.*, *Nat. Genet.* **36**, 809 (2004).
24. V. Sirotkin, C. C. Beltzner, J.-B. Marchand, T. D. Pollard, *J. Cell Biol.* **170**, 637 (2005).
25. M. Kaksonen, Y. Sun, D. G. Drubin, *Cell* **115**, 475 (2003).
26. T. Takagi, S. A. Ishijima, H. Ochi, M. Osumi, *J. Electron Microsc.* **52**, 161 (2003).
27. M. E. Young, J. A. Cooper, P. C. Bridgman, *J. Cell Biol.* **166**, 629 (2004).
28. A. A. Rodal, L. Kozubowski, B. L. Goode, D. G. Drubin, J. H. Hartwig, *Mol. Biol. Cell* **16**, 372 (2005).
29. M. K. Balasubramanian, E. Bi, M. Glotzer, *Curr. Biol.* **14**, R806 (2004).
30. B. A. Wolfe, K. L. Gould, *Trends Cell Biol.* **15**, 10 (2005).
31. R. Ding, R. R. West, D. M. Morphew, B. R. Oakley, J. R. McIntosh, *Mol. Biol. Cell* **8**, 1461 (1997).
32. A. Grallert, A. Krapp, S. Bagley, V. Simanis, I. M. Hagan, *Genes Dev.* **18**, 1007 (2004).
33. J. L. Morrell *et al.*, *Curr. Biol.* **14**, 579 (2004).
34. J.-Q. Wu, T. D. Pollard, data not shown.
35. D. R. Kovar, T. D. Pollard, *Proc. Natl. Acad. Sci. U.S.A.* **101**, 14725 (2004).
36. R. H. Carnahan, K. L. Gould, *J. Cell Biol.* **162**, 851 (2003).
37. T. Kanbe, I. Kobayashi, K. Tanaka, *J. Cell Sci.* **94**, 647 (1989).
38. R. J. Pelham, F. Chang, *Nature* **419**, 82 (2002).
39. K. C. Y. Wong *et al.*, *Curr. Biol.* **12**, 724 (2002).
40. K. Nabeshima *et al.*, *Mol. Biol. Cell* **9**, 3211 (1998).
41. J. Bähler *et al.*, *J. Cell Biol.* **143**, 1603 (1998).
42. A. Paoletti, F. Chang, *Mol. Biol. Cell* **11**, 2757 (2000).
43. M. Sohrmann, C. Fankhauser, C. Brodbeck, V. Simanis, *Genes Dev.* **10**, 2707 (1996).
44. C. A. Blessing, G. T. Ugrinova, H. V. Goodson, *Trends Cell Biol.* **14**, 435 (2004).

45. We are grateful to M. Morphew and J. R. McIntosh for the generous gift of electron micrographs; K. L. Gould for Arp3p antibodies; J. Lessard for actin antibody; G. Law for help with the spinning disk confocal microscope; and M. Li, X.-Y. Wang, and T. Taylor for help with flow cytometry. We thank M. Manix and L. Zhao for some data analysis; C. Beltzner, D. Kovar, and M. Lord for yeast strains; D. Kovar and V. Sirotkin for actin plasmids; A. Downs for purified *S. pombe* actin; J. Kuhn, R. Mahaffy, and R. de Rooij for suggestions on microscopy and data analysis; and P. Forscher, P. Dalhaimer, D. Kovar, M. Lord, R. Mahaffy, and V. Sirotkin for comments on the manuscript. We are also grateful to other members of the Pollard laboratory for helpful suggestions. This work was supported by NIH Grant GM-26231 to T.D.P. and an Anna Fuller Fund Fellowship to J.-Q.W.

Supporting Online Material

www.sciencemag.org/cgi/content/full/310/5746/310/DC1
Materials and Methods
Figs. S1 to S7
Tables S1 and S2
References and Notes

6 April 2005; accepted 15 September 2005
10.1126/science.1113230

Calorie Restriction Promotes Mitochondrial Biogenesis by Inducing the Expression of eNOS

Enzo Nisoli,[1,2]* Cristina Tonello,[1] Annalisa Cardile,[1] Valeria Cozzi,[1] Renata Bracale,[1] Laura Tedesco,[1] Sestina Falcone,[1,3] Alessandra Valerio,[1] Orazio Cantoni,[4] Emilio Clementi,[1,3,5] Salvador Moncada,[6] Michele O. Carruba[1,2]

Calorie restriction extends life span in organisms ranging from yeast to mammals. Here, we report that calorie restriction for either 3 or 12 months induced endothelial nitric oxide synthase (eNOS) expression and 3′,5′-cyclic guanosine monophosphate formation in various tissues of male mice. This was accompanied by mitochondrial biogenesis, with increased oxygen consumption and adenosine triphosphate production, and an enhanced expression of sirtuin 1. These effects were strongly attenuated in eNOS null-mutant mice. Thus, nitric oxide plays a fundamental role in the processes induced by calorie restriction and may be involved in the extension of life span in mammals.

Calorie restriction (CR) extends life span in numerous organisms from yeast (*1*) to rodents and possibly primates (*2*). In mammals, CR delays the onset of age-associated diseases including cancer, atherosclerosis, and diabetes (*3*). A decrease in oxidative damage has been proposed as a mechanism (*4*); however, a lack of correlation between reactive oxygen species (ROS) production and life span was recently reported in *Drosophila* (*5*). Furthermore, increasing evidence suggests that SIRT1, the mammalian ortholog of the *SIR2* gene that mediates the life-extending effect of CR in yeast (*1*, *6*), is a key regulator of cell defenses and survival in mammals in response to stress (*7*).

Eight-week-old male wild-type mice were fed either ad libitum (AL) or with a CR diet (food provided on alternate days) for 3 or 12

[1]Integrated Laboratories Network, Department of Preclinical Sciences, Luigi Sacco Hospital, Milan University, 20157 Milan, Italy. [2]Istituto Auxologico Italiano, 20149 Milan, Italy. [3]Eugenio Medea Scientific Institute, 23842 Bosisio Parini, Italy. [4]Istituto di Farmacologia e Farmacognosia, University of Urbino "Carlo Bo," 61029 Urbino, Italy. [5]Stem Cell Research Institute, Dipartimento di Biotecnologie, Ospedale San Raffaele, 20132 Milan, Italy. [6]Wolfson Institute for Biomedical Research, University College London, London WC1E 6BT, UK.

*To whom correspondence should be addressed. E-mail: enzo.nisoli@unimi.it

months (*8*). Mice maintained on a CR feeding schedule consume 30 to 40% fewer calories over time compared with animals fed AL, have a lower body weight (fig. S1), and are known to have an extended life span (*9*). At 3 months of treatment, the amounts of mitochondrial DNA (mtDNA, a marker of mitochondrial content), the expression of peroxisome proliferator-activated receptor–γ coactivator 1α (PGC-1α), nuclear respiratory factor–1 (NRF-1), and mitochondrial transcription factor A (Tfam) [master regulators of mitochondrial biogenesis (*10*)], and expression of cytochrome c oxidase (COX-IV) and cytochrome c (Cyt c) (two mitochondrial proteins involved in cell respiration) were higher in white adipose tissue (WAT) and many other tissues of CR mice when compared with AL mice (Figs. 1A and 2A). This was consistent with increased mitochondrial biogenesis and mitochondrial gene expression (*11*–*13*).

To confirm that CR increases mitochondrial function, we measured oxygen consumption and expression of mitofusin (Mfn) 1 and 2 [the mitochondrial transmembrane guanosine triphosphatases crucial to the mitochondrial fusion process and metabolism (*14*, *15*)]. These parameters were higher in several tissues, particularly in WAT, of CR than in AL animals (Figs. 1, A and B, and 2). This suggests that CR induces mitochondrial biogenesis with increased respiration and expression of genes crucial for the dynamic fusion processes required for oxidative function. We then investigated whether the increase in respiration was associated with an increase in adenosine triphosphate (ATP) synthesis and found that CR increased ATP concentrations in WAT (0.025 ± 0.001 nmol/mg tissue in CR mice compared with 0.018 ± 0.002 nmol/mg tissue in AL mice, $P < 0.001$, $n = 4$ animals) and in other tissues (table S1). Similar results were obtained in mice treated for 12 months. Thus, the molecular changes induced by CR occur early and are long-lasting, consistent with the early onset and persistent effect of CR on life span (*9*).

Nitric oxide (NO) generated by eNOS increases mitochondrial biogenesis and enhances respiration and ATP content in various mammalian cells by acting through its second messenger, 3′,5′-cyclic guanosine monophosphate (cGMP) (*11*, *16*). We investigated whether eNOS and cGMP play a role in the mitochondrial biogenesis induced by CR. The expression of eNOS, unlike neuronal and inducible NOS, was higher in CR than in AL mice (Figs. 1A and 2) and was accompanied by higher concentrations of cGMP (Figs. 1C and 2) in WAT and in several other tissues. The increased serum concentrations of nitrite and nitrate (an index of NO production) and plasma cGMP in obese subjects exposed to CR in controlled weight loss trials (*17*, *18*) are consistent with our findings.

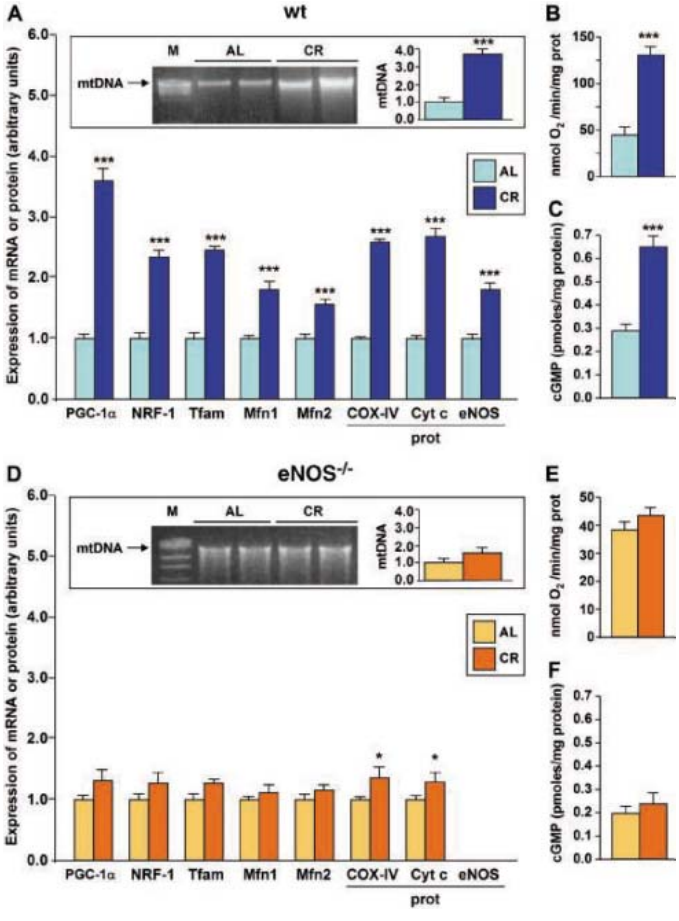

Fig. 1. CR induces mitochondrial biogenesis in WAT of wild-type (wt) but not eNOS$^{-/-}$ mice through eNOS expression and cGMP formation. (**A** and **D**) PGC-1α, NRF-1, Tfam, Mfn1, and Mfn2 mRNA were analyzed by means of quantitative reverse transcription polymerase chain reaction (RT-PCR); COX IV, Cyt c, and eNOS proteins were detected by immunoblot analysis. (Insets) WAT mtDNA (gel shows a representative experiment with two mice per group). The relative values were obtained by densitometric analysis, with those measured in the AL mice taken as 1.0. (**B** and **E**) O_2 consumption and (**C** and **F**) cGMP concentrations in WAT. Each experiment ($n = 10$) was repeated at least three times. Triple asterisks indicate $P < 0.001$, and single asterisk, $P < 0.05$, compared with AL-fed mice. Error bars indicate SEM.

To verify the role of eNOS in the mitochondrial biogenesis induced by CR, we fed 8-week-old male eNOS null-mutant (eNOS$^{-/-}$) mice either an AL or a CR diet for 3 months (Fig. 1, D to F, and fig. S2, A to C). In particular, mtDNA content and PGC-1α, NRF-1, Tfam, Mfn1, and Mfn2 mRNA amounts, although different from those in wild-type animals, were not significantly greater in CR eNOS$^{-/-}$ mice compared to in AL eNOS$^{-/-}$ animals. Moreover, COX IV and Cyt c expression did not increase significantly in CR animals except in WAT and brain, where these parameters increased to a much lesser extent than those in wild-type animals (Fig. 1D and fig. S2A). Thus, CR was unable to induce significant mitochondrial biogenesis in a number of tissues of eNOS$^{-/-}$ mice, including WAT. To confirm this, we measured oxygen consumption (Fig. 1E and fig. S2B) and cGMP (Fig. 1F and fig. S2C) and ATP concentrations (table S1) in WAT and other tissues (table S1) of both CR and AL eNOS$^{-/-}$ animals. These parameters also did not increase significantly as a result of CR in knock-out compared to in wild-type mice. AL eNOS$^{-/-}$ mice displayed greater feed efficiency (body weight gain per food intake) than their wild-type counterparts (*11*), suggesting that both energy expenditure and oxidative metabolism are partly NO-dependent. The CR wild-type mice showed lower feed efficiency values than AL wild-type animals (0.295 ± 0.023 compared with 0.488 ± 0.028, respectively; $P < 0.001$, $n = 10$ animals), whereas there was no difference between CR eNOS$^{-/-}$ mice and AL eNOS$^{-/-}$ animals (0.67 ± 0.025 and 0.654 ± 0.019, respectively; $n = 10$ animals). Thus, the CR-induced increase in oxidative metabolism appears to be blunted in the absence of eNOS expression in mammals.

Given the role of yeast SIR2 protein in life span extension by CR (*1*, *6*), we studied the expression of SIRT1 and found it to be higher in many tissues (fig. S3) of CR wild-type animals than of AL wild-type mice, including WAT (Fig. 3A) (*19*), where SIRT1 triggers lipolysis and loss of fat (*20*). SIRT1 mRNA and protein were ~threefold higher in cultured white adipocytes exposed either to NO donors, such as (Z)-1-[2-(2-aminoethyl)-N-(2-ammonioethyl)amino] diazen-1-ium-1,2 diolate (DETA-NO) and S-nitrosoacetyl penicillamine (SNAP), or to a cGMP analog (8 Br-cGMP) than in untreated cells (Fig. 3B) and ~80% lower in WAT of eNOS$^{-/-}$ mice when compared with wild-type animals (Fig. 3, C and D). Thus, the expression of SIRT1 in WAT during CR might be partly mediated by NO acting via cGMP.

To investigate whether the CR-induced SIRT1 expression was dependent on eNOS-derived NO, we performed immunoblot analysis in WAT of eNOS$^{-/-}$ mice fed either an AL or a CR diet. In eNOS$^{-/-}$ mice fed a CR diet, SIRT1 expression was also increased (~30%) in WAT compared with that of eNOS$^{-/-}$ mice

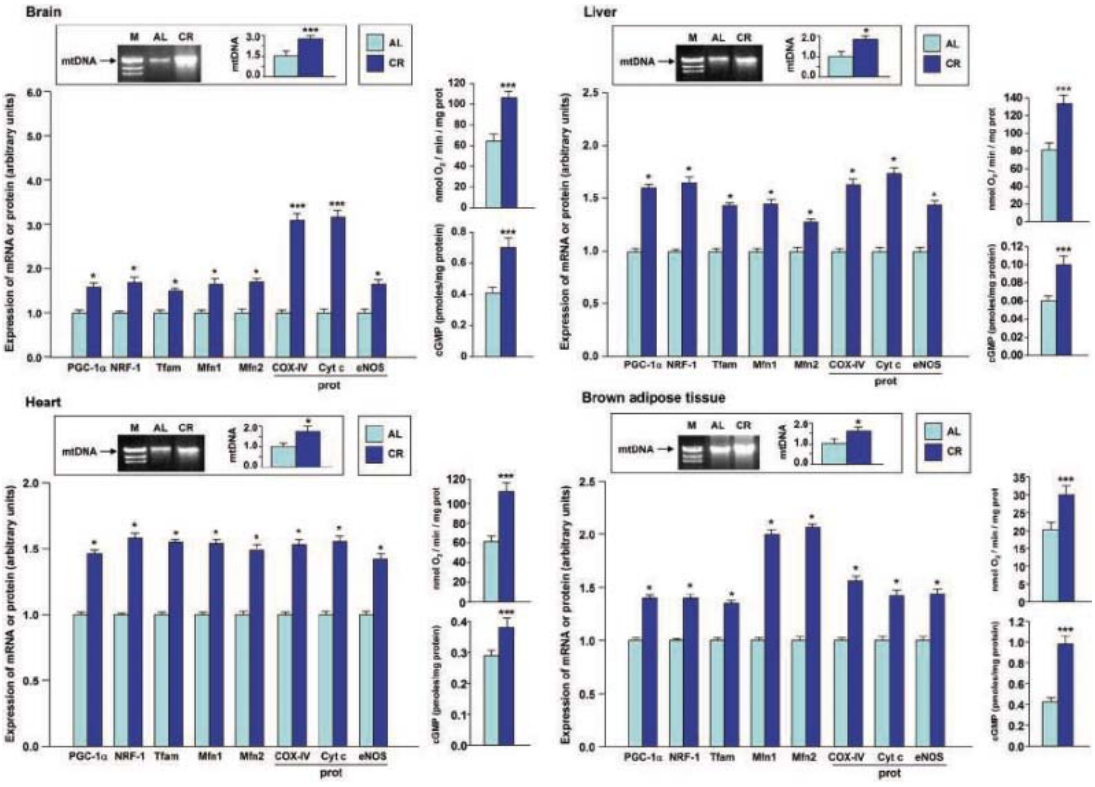

Fig. 2. CR induces mitochondrial biogenesis in different tissues of wt mice through eNOS expression and cGMP formation. (Large bar graphs) PGC-1α, NRF-1, Tfam, Mfn1, and Mfn2 mRNA were analyzed by means of quantitative RT-PCR with gene-specific oligonucleotide probes. COX IV, Cyt c, and eNOS proteins were detected by immunoblot analysis. (Top images) MtDNA (gel shows one representative experiment from one mouse per group). The relative values were obtained by densitometric analysis, with those measured in the AL mice taken as 1.0. (Top small bar graphs) O_2 consumption and (bottom small bar graphs) cGMP concentrations. Each experiment (n = 10 animals) was repeated at least three times. Triple asterisks, $P < 0.001$, and single asterisk, $P < 0.05$, compared with AL-fed mice. Error bars indicate SEM.

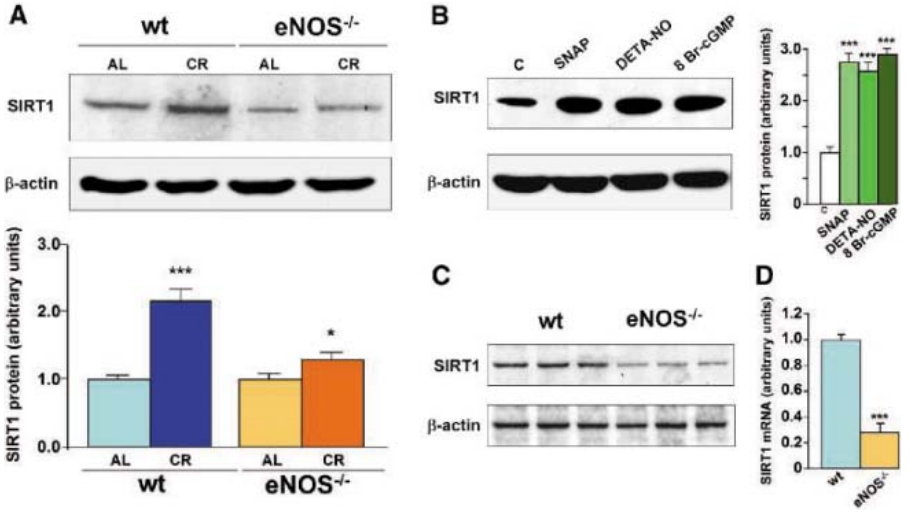

Fig. 3. SIRT1 expression is regulated by NO in WAT and white adipocytes. (**A**) SIRT1 protein levels in WAT of either AL or CR wt and eNOS$^{-/-}$ mice. A representative experiment is shown, with means ± SEM of densitometric measurements performed in 10 animals per group. The histogram values were obtained by densitometric analysis, with values measured in the AL mice taken as 1.0. (**B**) SIRT1 protein concentrations in white adipocytes cultured for 3 days with or without SNAP (100 μM), DETA-NO (50 μM), and 8 Br-cGMP (3 mM). A representative experiment is shown, with means ± SEM of densitometric measurements performed in five separate experiments. The protein concentrations were obtained by densitometric analysis, with values measured in the untreated cells (c) taken as 1.0. (**C** and **D**) SIRT1 protein and mRNA expression, respectively, in WAT of male eNOS$^{-/-}$ mice compared with wt mice. Each experiment (n = 10 animals) was repeated at least three times. The relative values of mRNA were obtained by densitometric analysis, with values measured in wt mice taken as 1.0. Triple asterisks, $P < 0.001$ and single asterisk, $P < 0.05$ compared with AL-fed wild-type mice or untreated cells.

fed an AL diet (Fig. 3A), although the change was much smaller than that in wild-type animals (~120%, $P < 0.001$). Similar results were obtained in the other tissues tested (fig. S3).

Thus, CR induces an increase in eNOS expression, which in turn is involved in both mitochondrial biogenesis and SIRT1 expression in a variety of tissues. The enhanced expression of SIRT1 by CR is consistent with a potential increase in life span. This transcription factor may be an evolutionarily ancient biological stress response that slows aging, promoting the mobilization of fat into the blood from WAT stores (*20*), the down-regulation of adipogenesis (*20*), and the long-term survival of irreplaceable cells (*7*, *19*). The increase in mitochondrial activity, i.e., in oxidative metabolism, that we see in CR animals is intriguing in view of the widely accepted hypothesis that CR increases longevity by slowing metabolism and reducing mitochondrial ROS and accompanying cellular damage (*4*). In fact, metabolic rate normalized to body weight does not decline in CR mice, and the lifetime metabolic output of these animals is therefore larger than that of their AL cohorts (*21*). Respiration actually increases during CR in yeast (*22*) and the nematode worm *Caenorhabditis elegans* (*23*). The effects of CR on life span may be independent of excessive ROS production.

The effects of CR in mammals are complex, affecting many organs and physiological pathways. Nevertheless, the significantly reduced effects observed in eNOS$^{-/-}$ animals point to a role for NO in the response to CR. eNOS$^{-/-}$ mice are characterized by a reduced life span (*24*) due to age-related diseases (*25*). One possibility is that in wild-type CR animals NO, acting via mitochondrial biogenesis and expression of SIRT1, increases β-oxidation and lipolysis. This would result in a reduction in the accumulation of fat, which is known to have an impact on life span (*26*, *27*).

References and Notes

1. S.-J. Lin, P.-A. Defossez, L. Guarente, *Science* **289**, 2126 (2000).
2. D. K. Ingram *et al.*, *Ann. N.Y. Acad. Sci.* **1019**, 412 (2004).
3. E. J. Masoro, *Exp. Gerontol.* **35**, 299 (2000).
4. R. S. Sohal, R. Weindruch, *Science* **273**, 59 (1996).
5. S. Miwa, K. Riyahi, L. Partridge, M. D. Brand, *Ann. N.Y. Acad. Sci.* **1019**, 388 (2004).
6. R. M. Anderson, K. J. Bitterman, J. G. Wood, O. Medvedik, D. A. Sinclair, *Nature* **423**, 181 (2003).
7. J. Luo *et al.*, *Cell* **107**, 137 (2001).
8. Materials and methods are available as supporting material on *Science* Online.
9. C. L. Goodrick, D. K. Ingram, M. A. Reynolds, J. R. Freeman, N. Cider, *Mech. Ageing Dev.* **55**, 69 (1990).
10. D. P. Kelly, R. C. Scarpulla, *Genes Dev.* **18**, 357 (2004).
11. E. Nisoli *et al.*, *Science* **299**, 896 (2003).
12. D. Larrouy, H. Vidal, F. Andreelli, M. Laville, D. Langin, *Int. J. Obes. Relat. Metab. Disord.* **23**, 1327 (1999).
13. Y. Higami *et al.*, *FASEB J.* **18**, 415 (2004).
14. T. Koshiba *et al.*, *Science* **305**, 858 (2004).
15. D. Bach *et al.*, *J. Biol. Chem.* **278**, 17190 (2003).
16. E. Nisoli *et al.*, *Proc. Natl. Acad. Sci. U.S.A.* **101**, 16507 (2004).
17. C. P. Fenster *et al.*, *Free Radic. Biol. Med.* **37**, 695 (2004).
18. P. Dessi-Fulgheri *et al.*, *Hypertension* **33**, 658 (1999).
19. H. Y. Cohen *et al.*, *Science* **305**, 390 (2004); published online 17 June 2004 (10.1126/science.1099196).
20. F. Picard *et al.*, *Nature* **429**, 771 (2004).
21. E. J. Masoro, B. P. Yu, H. A. Bertrand, *Proc. Natl. Acad. Sci. U.S.A.* **79**, 4239 (1982).
22. S. J. Lin *et al.*, *Nature* **418**, 344 (2002).
23. K. Houthoofd *et al.*, *Exp. Gerontol.* **37**, 1359 (2002).
24. E. Dere *et al.*, *Genes Brain Behav.* **1**, 204 (2002).
25. S. Cook *et al.*, *Swiss Med. Wkly.* **133**, 360 (2003).
26. M. Bluher, B. B. Kahn, C. R. Kahn, *Science* **299**, 572 (2003).
27. C. H. Chiu, W. D. Lin, S. Y. Huang, Y. H. Lee, *Genes Dev.* **18**, 1970 (2004).

28. We thank A. Higgs for help with the preparation of the manuscript, A. Marino for the early experiments of this research, and A. Mejetta for technical assistance. This work was supported by grants from the Ministero dell'Istruzione, dell'Università e della Ricerca cofinanziamento 2003, the Italian Ministry of Health, and the Italian Association of Cancer Research (AIRC).

Supporting Online Material

www.sciencemag.org/cgi/content/full/310/5746/314/DC1
Materials and Methods
Figs. S1 to S3
Table S1
References

21 July 2005; accepted 6 September 2005
10.1126/science.1117728

Sequence Variants in *SLITRK1* Are Associated with Tourette's Syndrome

Jesse F. Abelson,[1,2]* Kenneth Y. Kwan,[3,4]* Brian J. O'Roak,[2]* Danielle Y. Baek,[1,2] Althea A. Stillman,[2] Thomas M. Morgan,[2] Carol A. Mathews,[8] David L. Pauls,[9] Mladen-Roko Rašin,[3] Murat Gunel,[5] Nicole R. Davis,[1,2] A. Gulhan Ercan-Sencicek,[1,2] Danielle H. Guez,[2] John A. Spertus,[10] James F. Leckman,[1] Leon S. Dure IV,[11] Roger Kurlan,[12] Harvey S. Singer,[13] Donald L. Gilbert,[14] Anita Farhi,[7] Angeliki Louvi,[5] Richard P. Lifton,[2,6,7] Nenad Šestan,[3,4] Matthew W. State[1,2,4,6]†

Tourette's syndrome (TS) is a genetically influenced developmental neuropsychiatric disorder characterized by chronic vocal and motor tics. We studied *Slit and Trk-like 1* (*SLITRK1*) as a candidate gene on chromosome 13q31.1 because of its proximity to a de novo chromosomal inversion in a child with TS. Among 174 unrelated probands, we identified a frameshift mutation and two independent occurrences of the identical variant in the binding site for microRNA hsa-miR-189. These variants were absent from 3600 control chromosomes. *SLITRK1* mRNA and hsa-miR-189 showed an overlapping expression pattern in brain regions previously implicated in TS. Wild-type SLITRK1, but not the frameshift mutant, enhanced dendritic growth in primary neuronal cultures. Collectively, these findings support the association of rare *SLITRK1* sequence variants with TS.

TS is a potentially debilitating developmental neuropsychiatric disorder, characterized by the combination of persistent vocal and motor tics, that affects as many as 1 in 100 individuals (*1*, *2*). A substantial portion of clinically referred TS patients also suffer from obsessive-compulsive disorder (OCD), attention deficit hyperactivity disorder (ADHD), or depression (*3*). A TS spectrum of disorders that includes chronic vocal or motor tics as well as tic-related OCD and ADHD is widely recognized. Phenomenological and neurobiological evidence also supports the inclusion of some habit disorders, including trichotillomania (TTM), in this phenotypic spectrum (*4*, *5*).

Several decades of investigation have confirmed a substantial genetic contribution to TS (*6*). Early segregation analyses suggested that the disorder was inherited as a rare, autosomal dominant trait (*7*). However, more recent studies have supported poly- or oligogenic inheritance (*8*). Genome-wide analysis of linkage has implicated intervals on chromosomes 4, 5, 8, 11, and 17 (*9*–*12*), but to date no disease-related mutations have been identified. These investigations have been complicated by a phenotype that typically decreases in severity with age, a high population prevalence of transient tics, and symptoms that overlap with common disorders such as ADHD and OCD (*13*). In addition, marked locus heterogeneity, gene-environment interactions, and the further confounding of assortative mating (*14*, *15*) have all likely hindered gene-mapping efforts.

We focused on a rare subset of TS patients with chromosomal anomalies to circumvent some of these obstacles and identify candidate genes for intensive mutational screening. Such a strategy provides the opportunity to characterize functional sequence variants largely irrespective of their mode of inheritance. We identified a patient presenting with TS and ADHD and carrying a de novo chromosome 13 inversion, inv(13)(q31.1;q33.1) (*16*). There was no family history of tics, TS, OCD, TTM, or ADHD (Fig. 1). Genotyping with multiple short tandem repeat (STR) markers confirmed paternity (*16*) (table S1). The co-occurrence of a de novo chromosomal abnormality with the only known case of TS in the pedigree led us to fine map the rearrangement with the use of fluorescence in situ hybridization (FISH). We found that bacterial artificial chromosomes (BACs) RP11-375K12 and RP11-255P5 span the 13q31.1 and 13q33.1 breakpoints, respectively (Fig. 1, C to F, and table S2).

Three genes map within 500 kilobases (kb) of these two breakpoints (Fig. 1, E and F). Of these, *Slit and Trk-like family member 1* (*SLITRK1*), encoding a single-pass transmembrane protein with two leucine-rich repeat (LRR) motifs in its extracellular domain, was considered the strongest candidate for further study because of its

[1]Child Study Center, [2]Department of Genetics, [3]Department of Neurobiology, [4]Interdepartmental Neuroscience Program, [5]Department of Neurosurgery, [6]Center for Human Genetics and Genomics, [7]Howard Hughes Medical Institute, Yale University School of Medicine, New Haven, CT 06520, USA. [8]Department of Psychiatry, University of California–San Diego, San Diego, CA 92093, USA. [9]Psychiatric and Neurodevelopmental Genetics Unit, Massachusetts General Hospital, Harvard Medical School, Boston, MA 02114, USA. [10]Department of Medicine, University of Missouri–Kansas City, Kansas City, MO 64111, USA. [11]Division of Pediatric Neurology, Department of Pediatrics, University of Alabama at Birmingham, Birmingham, AL 35233, USA. [12]Department of Neurology, University of Rochester School of Medicine, Rochester, NY 14642, USA. [13]Departments of Neurology and Pediatrics, Johns Hopkins University School of Medicine, Baltimore, MD 21287, USA. [14]Division of Neurology, Cincinnati Children's Hospital Medical Center, Cincinnati, OH 45229, USA.

*These authors contributed equally to this work.
†To whom correspondence should be addressed. E-mail: matthew.state@yale.edu

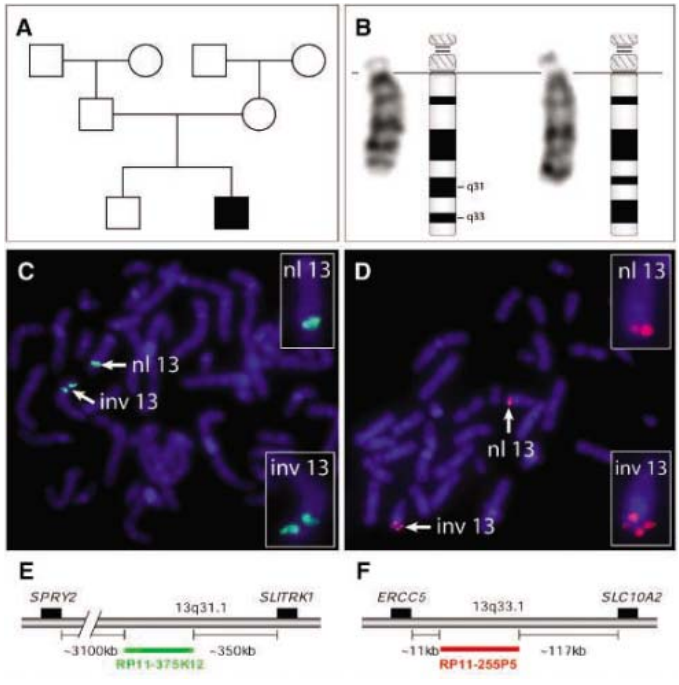

Fig. 1. Mapping of a de novo chromosome 13 paracentric inversion in a child with TS. (**A**) Pedigree of Family 1, with a single affected male child with TS and ADHD (*16*). The parents, grandparents, and younger sibling are not affected with TS, tics, ADHD, TTM, or OCD. Four maternal siblings, not presented on the pedigree, are all unaffected. (**B**) G-banded metaphase chromosomes 13. The ideogram for the normal (left) and inverted (right) chromosomes are presented. (**C** and **D**) FISH mapping of BAC RP11-375K12 (C) and BAC RP11-255P5 (D). The experimental probe is visualized at the expected positions on the normal (nl) chromosomes 13q31.1 and 13q33.1, respectively. Two fluorescence signals are visible on the inverted (inv) chromosomes, indicating that the probes span the breakpoint. Photographs were taken with a 100× objective lens. (**E**) Diagram of the interval surrounding the spanning BAC RP11-375K12 at 13q31.1. *SLITRK1* (National Center for Biotechnology Information accession code NM_052910) maps approximately 350 kb telomeric, and *SPRY2* (NM_005842) maps more than 3 million base pairs centromeric, to the breakpoint. (**F**) Diagram of the interval surrounding the spanning BAC RP11-255P5 at 13q33.1. The gene *ERCC5* (NM_000123.2), mutated in xeroderma pigmentosum group G, maps 11 kb from the spanning BAC clone. The gene *SLC10A2* (NM_000452.1), implicated in primary bile acid malabsorption, maps approximately 100 kb from the spanning BAC clone.

high relative expression in brain regions previously implicated in TS and its suggested role in neurite outgrowth (*17*, *18*). *ERCC5* and *SLC10A2*, mapping immediately centromeric and telomeric, respectively, to the 13q33.1 breakpoint, were not excluded as candidates but were considered less likely alternatives because both have been shown to lead to disorders with no known relationship to TS (*19*, *20*) (Fig. 1F).

The 13q31.1 chromosomal breakpoint mapped well outside the coding region of *SLITRK1*, and direct sequencing of the transcript in the affected individual showed no abnormalities (*16*). Consequently, we hypothesized that the expression of the gene might be altered by a position effect (*21*). However, the genomic organization of the transcript in a single coding exon, in conjunction with its low levels of expression in peripheral lymphocytes, precluded our direct quantitative assessment of *SLITRK1* mRNA in the patient versus controls.

We reasoned, however, that if altered SLITRK1 function contributed to the risk for TS in the patient carrying the inversion, we would expect a subset of TS patients to have mutations in this gene. Accordingly, we screened *SLITRK1* in 174 affected individuals (*16*). We identified one proband, diagnosed with TS and ADHD, who possessed a single-base deletion in the coding region leading to a frameshift, predicted to result in a truncated protein lacking a substantial portion of the second LRR as well as its transmembrane and intracellular domains (Fig. 2).

Four additional family members were ascertained and genotyped (*16*). The mutation

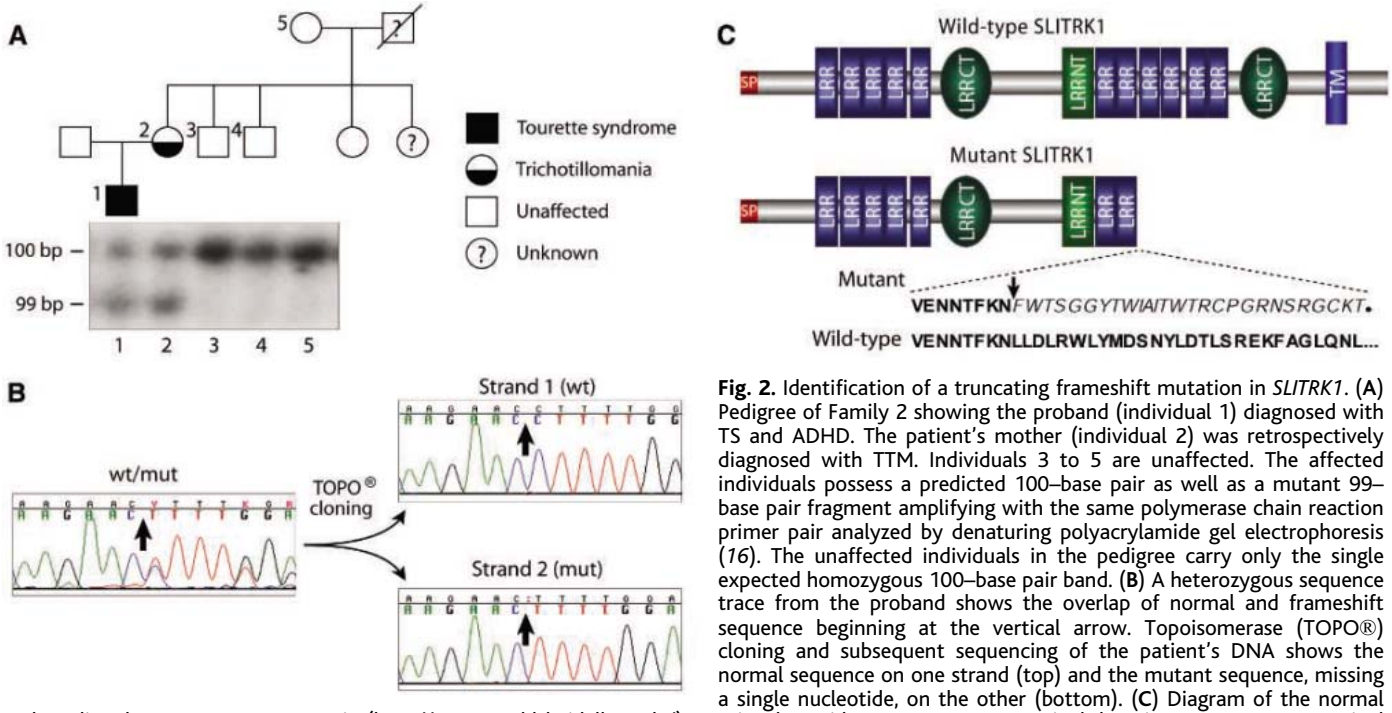

Fig. 2. Identification of a truncating frameshift mutation in *SLITRK1*. (**A**) Pedigree of Family 2 showing the proband (individual 1) diagnosed with TS and ADHD. The patient's mother (individual 2) was retrospectively diagnosed with TTM. Individuals 3 to 5 are unaffected. The affected individuals possess a predicted 100–base pair as well as a mutant 99–base pair fragment amplifying with the same polymerase chain reaction primer pair analyzed by denaturing polyacrylamide gel electrophoresis (*16*). The unaffected individuals in the pedigree carry only the single expected homozygous 100–base pair band. (**B**) A heterozygous sequence trace from the proband shows the overlap of normal and frameshift sequence beginning at the vertical arrow. Topoisomerase (TOPO®) cloning and subsequent sequencing of the patient's DNA shows the normal sequence on one strand (top) and the mutant sequence, missing a single nucleotide, on the other (bottom). (**C**) Diagram of the normal and predicted mutant SLITRK1 protein (http://smart.embl-heidelberg.de/). SP, signal peptide; LRRNT, LRR N-terminal domain; LRRCT, LRR C-terminal domain; TM, transmembrane domain. The predicted amino acid sequence of the mutant protein, showing 27 nonsynonymous substitutions followed by a premature stop codon (•), is presented under the truncated protein diagram and is compared with the wild-type sequence.

was found in the patient's mother, affected with TTM, but not in the two at-risk maternal uncles or in the maternal grandmother, all of whom were unaffected (Fig. 2A). Moreover, the mutation was not present in 3600 control chromosomes (*16*). Finally, no truncating mutations or apparently deleterious variants were identified upon comprehensive mutation screening of the *SLITRK1* coding region in 253 controls (*16*) (table S4).

In addition to this frameshift mutation, the identical noncoding sequence variant (var321) was identified in two apparently unrelated individuals with TS and obsessive-compulsive (OC) symptoms. The single-base change maps to the 3′ untranslated region (UTR) of the transcript and corresponds to a highly conserved nucleotide within the predicted binding site for the human microRNA (miRNA) hsa-miR-189, one of two mature miRNAs derived from the hsa-miR-24 precursor (*22*, *23*) (Fig. 3, A to D, and table S6). This variant was absent from 4296 control chromosomes, demonstrating a statistically significant association with TS ($P = 0.0056$; Fisher's exact test) and raising the question of whether the two occurrences might represent independent genetic events. To evaluate this, we genotyped STRs and single-nucleotide polymorphisms in close proximity to var321. In each case, the variant was found to reside on a distinct haplotype, with distinguishing polymorphisms 83.5 kb centromeric and 3.8 kb telomeric to the variant (table S7), providing strong evidence that the two occurrences arose independently. With a conservative estimate of the mutation frequency at this base ($\sim 10^{-7}$), the likelihood of identifying an independent recurrence of the variant by chance among 346 chromosomes is remote ($P = 0.000056$) (*16*).

DNA samples from the families of both probands carrying var321 were sought. Samples were unavailable from family 3, in which both the mother and father were affected; the mother had a history of chronic motor tics and the father suffered chronic vocal and motor tics, OC symptoms, and hair pulling. In family 4, only the proband carried a formal diagnosis; however, her mother, sister, a maternal grandfather, and a paternal uncle all had a history of tics, subclinical OC symptoms, or both (*16*). DNA was obtained from the immediate family, and its analysis showed that the proband and her mother carried the variant (*16*).

The var321 replaces a G:U wobble base pair with an A:U Watson-Crick pairing at position 9 in the miRNA binding domain. The extent of conservation of this G:U pairing, in both *SLITRK1* 3′UTR and miR-189 (Fig. 3, B and C), as well as evidence that G:U wobble base pairs inhibit miRNA-mediated protein repression to a greater degree than would be expected on the basis of their thermodynamic properties alone (*24*), suggested that var321 might affect SLITRK1 expression. To test this hypothesis, we inserted the full-length *SLITRK1* 3′UTR downstream of a luciferase reporter gene and transfected the construct into Neuro2a (N2a) cells. In the presence of miR-189, the expression of luciferase was significantly reduced (Fig. 3, B to D, and table S8), confirming the functional potential of the mRNA-miRNA duplex. We next inserted the 3′UTR containing var321 and found that the sequence variant resulted in a modest but statistically significant and dose-dependent further repression of luciferase expression compared with that of the wild type (Fig. 3G and table S8).

On the basis of the hypothesis that an altered interaction of *SLITRK1* mRNA with miR-189 contributed to TS in the patients carrying var321, we reasoned that *SLITRK1* and miR-189 expression should overlap in the developing brain. In situ hybridization in postnatal mouse demonstrated that *Slitrk1* mRNA is expressed in the neocortex, hippocampus, thalamic and subthalamic nuclei, striatum, globus pallidus, and cerebellum, in agreement with earlier findings (Fig. 4, A and B) (*17*). We observed mmu-miR-189 expression in the developing neocortex, hippocampus, thalamus, basal ganglia, and cerebellum, overlapping

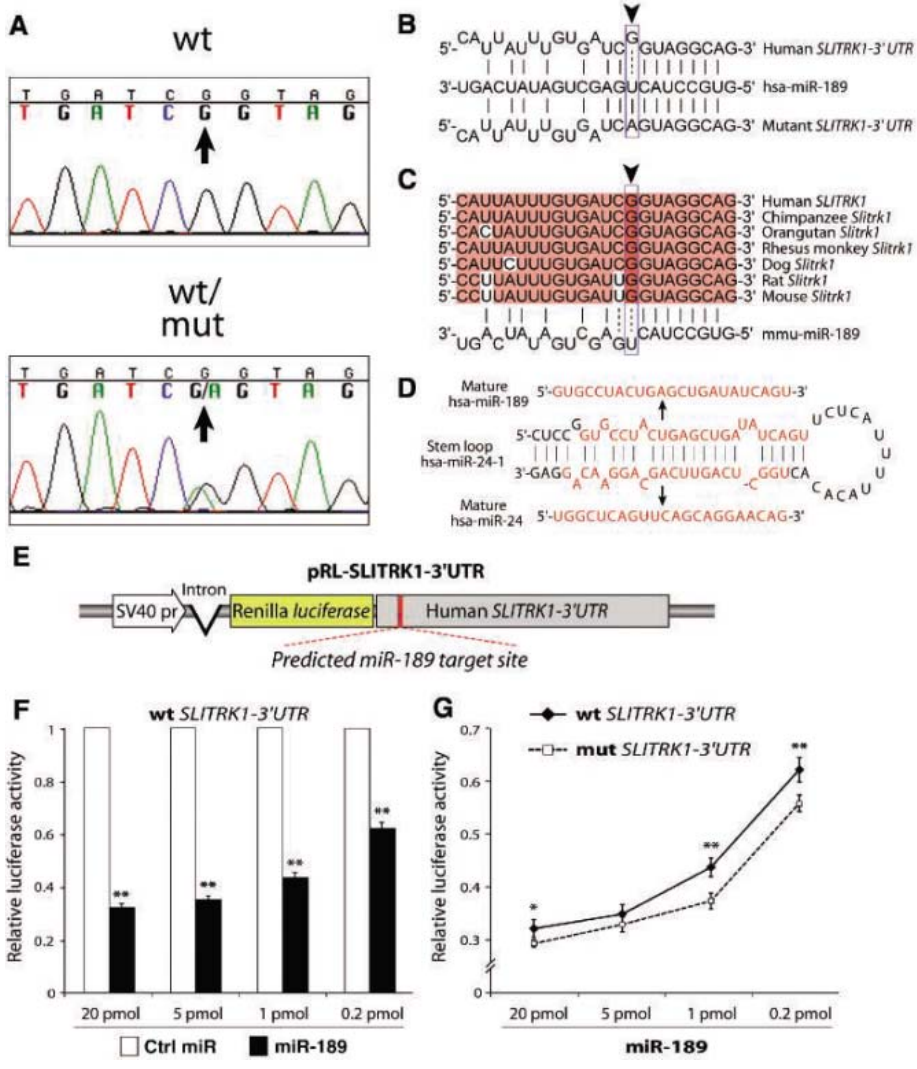

Fig. 3. Characterization and functional analysis of the *SLITRK1* 3′UTR. (**A**) The sequence of the normal 3′UTR and the substitution of G to A found in two probands. (**B**) The substitution maps within a predicted miRNA binding site for miR-189. Base pairing is indicated by a solid (Watson-Crick) or a dashed (wobble) vertical line. (**C**) Conserved bases in the binding domain are shown in red. (**D**) The precursor molecule hsa-miR-24-1 gives rise to hsa-miR-189 and hsa-miR-24. (**E**) pRL-*SLITRK1*-3′UTR contains an SV40 promoter, the *Renilla luciferase* gene, and the full-length 3′UTR of human *SLITRK1*. (**F**) miR-189 and pRL-wt *SLITRK1*-3′UTR, containing the native human sequence, were cotransfected into N2a cells. Relative luciferase activity (*y* axis) versus a random 23–base pair control miRNA. Each experiment was repeated six times for each of four different quantities of miRNA. **, $P = 0.002$ (Mann-Whitney U test). Error bars show maximum values. (**G**) Relative luciferase activity in the presence of miR-189 is shown for the wild-type (wt) *SLITRK1* 3′UTR (solid line) and mutant (mut) *SLITRK1* 3′UTR, containing the substitution of G to A (dashed line). *, $P = 0.009$; **, $P = 0.002$ (Mann-Whitney U test). Error bars show maximum and minimum values.

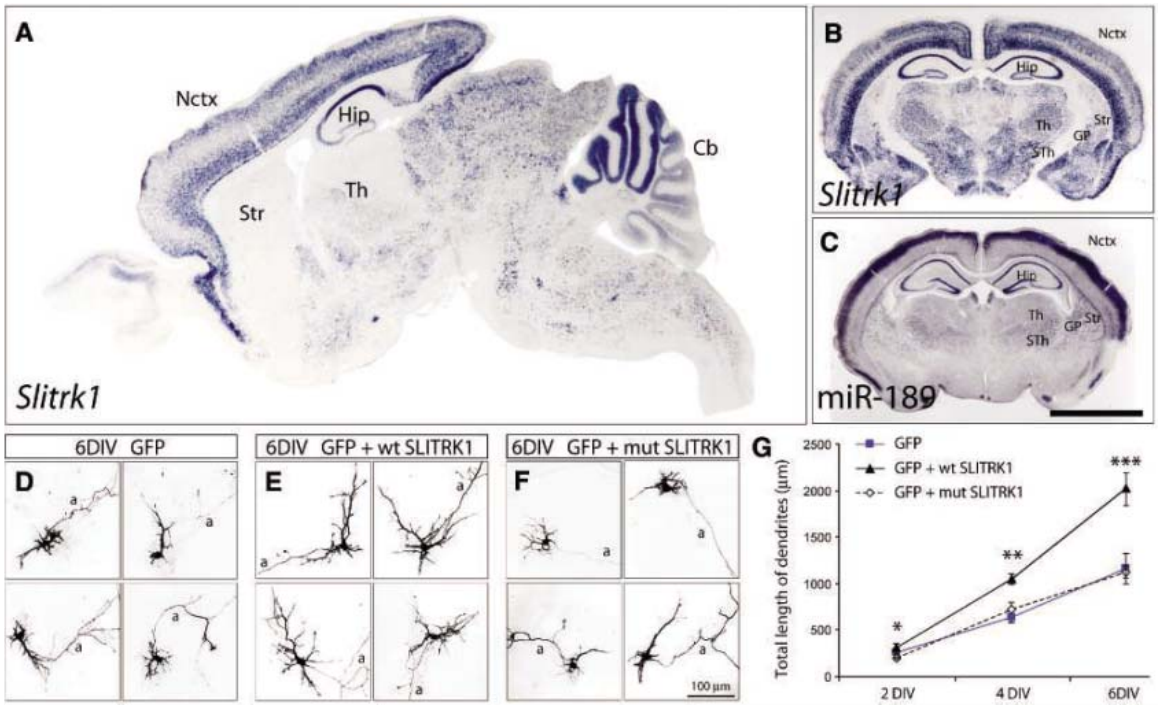

Fig. 4. Overlapping expression of *Slitrk1* mRNA and miRNA-189. (**A** and **B**) *Slitrk1* mRNA is detected in the neocortex (Nctx), hippocampus (Hip), striatum (Str), globus pallidus (GP), thalamus (Th), subthalamus (STh), and cerebellum (Cb) of postnatal day 14 (P14) mouse. (**C**) miR-189 expression is detected in neocortex, hippocampus, and cerebellum at P14. At P9, miR-189 expression is also detected in the striatum, thalamus, and subthalamus (fig. S1). Scale bar, 2 mm. (**D** to **G**) SLITRK1 overexpression enhances dendritic growth in cortical neurons. Images of cell bodies and dendrites, as well as proximal axonal segments (a), of representative GFP-immunopositive cortical neurons cultured for 6 DIV [(D) to (F)]. Primary cultures were prepared from embryonic day 15.5 (E15.5) embryos that were electroporated in utero at E14.5 with control *GFP* plasmid (GFP), *GFP* and wild-type human *SLITRK1* (GFP + wt SLITRK1), or *GFP* and human *SLITRK1* carrying the frameshift mutation (GFP + mut SLITRK1). (G) The total length of dendrites of GFP-immunopositive neurons was measured with the Neurolucida system (*16*) at 2, 4, and 6 DIV. *, $P = 0.002$; **, $P = 0.001$; ***, $P = 0.0007$ (Student's t test for wild-type SLITRK1 versus mutant SLITRK1). Error bars show mean ± SEM.

substantially with *SLITRK1* (Fig. 4C and fig. S1). In fetal human brain at 20 weeks of gestation, we detected *SLITRK1* mRNA in multiple regions, including the developing neocortical plate, subplate zone, striatum, globus pallidus, thalamus, and subthalamus (fig. S2). hsa-miR-189 was highly expressed in the cortical plate and intermediate zone (fig. S2), but not in the basal ganglia or thalamus. Overall, our results demonstrate a developmentally regulated and overlapping pattern of expression of *SLITRK1* mRNA and miR-189 in the neuroanatomical circuits most commonly implicated in TS, OCD, and habit formation (*25*).

Among the six known members of the *SLIT* and *TRK*-like gene family, SLITRK1 is unique in that it lacks tyrosine phosphorylation sites in its short intracellular domain. In this respect, it resembles the SLIT proteins, multifunctional secreted molecules with roles in axon repulsion (*26*) as well as dendritic patterning in the cerebral cortex (*27*). Given the high levels of cortical expression of *SLITRK1*, we investigated its effects on dendritic growth and morphology. Cortical pyramidal neurons were placed in culture after in utero electroporation of mouse embryos with wild-type human *SLITRK1* or the frameshift mutant, along with green fluorescent protein (GFP) (Fig. 4, D to F). At 2 days in vitro (DIV), dendrites expressing wild-type SLITRK1 were significantly longer than those expressing the frameshift ($P = 0.002$; Student's t test). By 4 and 6 DIV, dendrites expressing wild-type SLITRK1 were significantly longer than either comparison group, control or frameshift (Fig. 4G and table S9). These findings resemble, in part, the phenotype elicited by the exposure of cortical neurons to SLIT1 (*27*) and suggest both that SLITRK1 may promote dendritic growth and that the frameshift mutation likely results in a loss of function.

For many complex disorders, the discovery of rare mutations in small subsets of patients has had a major impact in the identification of fundamental pathways that underlie disease pathogenesis. Further study of this new candidate gene, *SLITRK1*, may serve a similar role in the effort to better understand TS at the molecular and cellular level.

References and Notes

1. H. Hornse, S. Banerjee, H. Zeitlin, M. Robertson, *J. Child Psychol. Psychiatry* **42**, 1035 (2001).
2. M. M. Robertson, *J. Psychosom. Res.* **55**, 3 (2003).
3. R. Kurlan *et al.*, *Neurology* **59**, 414 (2002).
4. R. L. O'Sullivan *et al.*, *Biol. Psychiatry* **42**, 39 (1997).
5. J. F. Leckman, *Lancet* **360**, 1577 (2002).
6. D. L. Pauls, *J. Psychosom. Res.* **55**, 7 (2003).
7. D. L. Pauls, J. F. Leckman, *N. Engl. J. Med.* **315**, 993 (1986).
8. J. T. Walkup *et al.*, *Am. J. Hum. Genet.* **59**, 684 (1996).
9. C. Merette *et al.*, *Am. J. Hum. Genet.* **67**, 1008 (2000).
10. P. Paschou *et al.*, *Am. J. Hum. Genet.* **75**, 545 (2004).
11. H. Zhang *et al.*, *Am. J. Hum. Genet.* **70**, 896 (2002).
12. The Tourette Syndrome Association International Consortium for Genetics, *Am. J. Hum. Genet.* **65**, 1428 (1999).
13. H. S. Singer, *Lancet Neurol.* **4**, 149 (2005).
14. R. Kurlan, V. Eapen, J. Stern, M. P. McDermott, M. M. Robertson, *Neurology* **44**, 2336 (1994).
15. P. A. Hanna, F. N. Janjua, C. F. Contant, J. Jankovic, *Neurology* **53**, 813 (1999).
16. Materials and methods are available as supporting material on *Science* Online.
17. J. Aruga, K. Mikoshiba, *Mol. Cell. Neurosci.* **24**, 117 (2003).
18. J. Aruga, N. Yokota, K. Mikoshiba, *Gene* **315**, 87 (2003).
19. P. Oelkers, L. C. Kirby, J. E. Heubi, P. A. Dawson, *J. Clin. Invest.* **99**, 1880 (1997).
20. T. Nouspikel, S. G. Clarkson, *Hum. Mol. Genet.* **3**, 963 (1994).
21. D. A. Kleinjan, V. van Heyningen, *Am. J. Hum. Genet.* **76**, 8 (2005).
22. E. A. Miska *et al.*, *Genome Biol.* **5**, R68 (2004).
23. M. Lagos-Quintana, R. Rauhut, J. Meyer, A. Borkhardt, T. Tuschl, *RNA* **9**, 175 (2003).
24. J. G. Doench, P. A. Sharp, *Genes Dev.* **18**, 504 (2004).
25. H. S. Singer, K. Minzer, *Brain Dev.* **25** (suppl. 1), S70 (2003).
26. K. Brose *et al.*, *Cell* **96**, 795 (1999).
27. K. L. Whitford *et al.*, *Neuron* **33**, 47 (2002).

28. Funded by NIH grants NINDS-R01 NS43520, NCRR-K23 RR16118 and an institutional grant from the Howard Hughes Medical Institute (M.W.S.), NINDS-R01 NS054273 (N.S.), awards from the Shepherd Foundation and the Lawrence Family (M.W.S.), and a Natural Sciences and Engineering Research Council postgraduate scholarship (K.Y.K.). We thank the additional members of the Yale Tourette Syndrome Pediatric Autoimmune Neuropsychiatric Disorders Associated with Streptococcal Infections (PANDAS) Consortium: R.A. King, B. Coffey, P. J. Lombroso, E. Kaplan, and P. Como; S. Hannigen, H. Grantz, L. Katsovich, D. Pendley, C. Drazinic, C. Nelson-Williams, J. J. Miller, J. Garoza, N. Lifton, B. Levy, M. Pappy, and L. Golovyan for their assistance; S. Levi Pearl of the Tourette Syndrome Association and the Tourette Syndrome Association International Consortium for Genetics; and the participating patients and families, without whom this work would not have been possible.

Supporting Online Material

www.sciencemag.org/cgi/content/full/310/5746/317/DC1
Materials and Methods
SOM Text
Figs. S1 and S2
Tables S1 to S9
References

23 June 2005; accepted 20 September 2005
10.1126/science.1116502

A Fine-Scale Map of Recombination Rates and Hotspots Across the Human Genome

Simon Myers, Leonardo Bottolo, Colin Freeman, Gil McVean,* Peter Donnelly*†

Genetic maps, which document the way in which recombination rates vary over a genome, are an essential tool for many genetic analyses. We present a high-resolution genetic map of the human genome, based on statistical analyses of genetic variation data, and identify more than 25,000 recombination hotspots, together with motifs and sequence contexts that play a role in hotspot activity. Differences between the behavior of recombination rates over large (megabase) and small (kilobase) scales lead us to suggest a two-stage model for recombination in which hotspots are stochastic features, within a framework in which large-scale rates are constrained.

Several recent studies (*1*, *2*) have shown that fine-scale recombination rates can be successfully estimated from genetic variation data by coalescent-based methods, but to date these have only been applied to small fractions of the human genome. Here we studied recombination rates across the entire genome by applying one such method, LDhat (*1*), to a previously published genome-wide survey of genetic variation in which ~1.6 million single-nucleotide polymorphisms (SNPs) were genotyped in three samples: 24 European Americans, 23 African Americans, and 24 Han Chinese from Los Angeles (*3*). Informally, the method fits a statistical model based on the coalescent to patterns of linkage disequilibrium, the nonrandom association between nearby SNPs, and then estimates recombination rates within this model in a Bayesian framework in which the prior distribution encourages smoothness and reduces overfitting in estimated rates. Recombination rates were estimated separately for each population sample and averaged to give a single estimate (*4*). As a further validation of the approach used here, scatterplots of our estimated recombination rates against known rates from pedigree studies (*5*, *6*) show extremely good agreement over the megabase scales for which the pedigree rates have good resolution (fig. S1, genome-wide $R^2 = 0.96$). At the fine scale, we find strong concordance between genetic variation–based and sperm-typing estimates of recombination rates and the location of hotspots across 3.3 Mb of the human major histocompatibility region (*4*, *7*) (fig. S2).

The fine-scale genetic map for each of the 22 autosomes and the X chromosome is shown in fig. S3 (*8*); Fig. 1 shows an example for chromosome 12. Compared to existing genetic maps, recombination rates show much greater variation at fine scales (Figs. 1 and 2A), and pedigree-based rate estimators are poor predictors of rates over smaller physical distances (Fig. 2B). For example, across the genome, the rank correlation between the rate over each 5-cM region and that for the 50-kb interval centered within it is 0.35, and the rank correlation between the rate over each 5-cM region and that for the 5-kb interval centered within it is 0.24. In large part this is because the fine-scale recombination landscape is dominated by recombination hotspots: Rate estimates show sharp, narrow peaks, with the bulk of the recombination occurring in a small proportion of the sequence. Typically, 80% of the recombination occurs in 10 to 20% of the sequence (Fig. 2C). An interesting exception to this pattern is chromosome 19, which has a much lower density and intensity of hotspots in addition to having the highest gene density (*9*) and proportion of open chromatin (*10*).

Earlier analyses of pedigree-based maps reported the presence of recombination deserts (*6*, *11*)—large (megabase-sized) regions where there is very little or no recombination. We also identified such regions (the left-hand tail of the 5-Mb histogram in Fig. 2A), but closer inspection revealed that in all such deserts there are recombination hotspots—although they are relatively scarce and have low intensities. An additional nonparametric analysis (*12*), which allows for plausible levels of genotyping error (*13*), shows that apart from the centromeres, there are no regions of the genome larger than 200 kb that are completely devoid of recombination.

To date, fewer than 20 human hotspots have been identified by direct analyses, typically through sperm typing in males. Previous coalescent analyses of population data have identified rather more (*1*, *2*). The approach we have applied here and elsewhere (*1*, *14*) ("LDhot") has recently been shown empirically to have reasonable power and, crucially, a low false positive rate (*15*). Using it, we identified more than 25,000 recombination hotspots (*4*), all but a few hundred of which had not previously been characterized. Of the hotspots detected in other studies where full

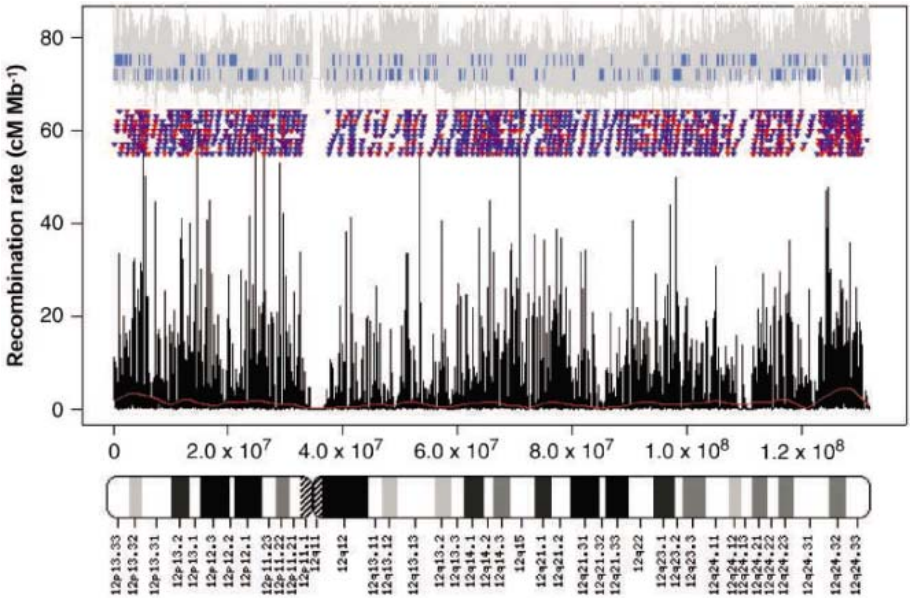

Fig. 1. Recombination rate variation along chromosome 12. Shown are estimated recombination rate (black), locations of statistically significant recombination hotspots [triangles; colors indicate relative amount of recombination from low (blue) to high (red)], and estimated recombination rates from the deCODE (*6*) genetic map (red curve near bottom). Also shown are the location of ENSEMBL genes on the two strands (blue segments), fluctuations in local GC content (gray lines; averages over 1000-bp windows shown on an arbitrary scale), and an ideogram of chromosome banding.

Department of Statistics, University of Oxford, 1 South Parks Road, Oxford OX1 3TG, UK.

*These authors jointly directed the project.
†To whom correspondence should be addressed. E-mail: donnelly@stats.ox.ac.uk

resequencing and very dense genotyping were used, we identified 50 to 60% (*4*), which suggests an average hotspot density across the genome of approximately one every 50 kb.

The figure of 25,000 to 50,000 recombination hotspots is comparable to estimates of the number of genes in the human genome (*16*) and therefore suggestive of the alpha-hotspot model in yeast (*17*), where recombination machinery is recruited to sites bound by transcription factors. To address the relationship between genes and recombination, we have plotted recombination rate as a function of distance from the start codon (Fig. 3). In contrast to the alpha-hotspot model, we find that recombination rates are on average lower within genes and increase with distance from the gene symmetrically in either direction for ~30 kb before decreasing again. In short, recombination hotspots in humans seem to preferentially occur near (within 50 kb of) genes, but are preferentially located outside the transcribed domain.

To investigate whether other factors—particularly repeat sequences and simple sequence motifs—are associated with hotspots, we matched detected hotspot regions with regions of the same size and SNP density that showed no evidence for being a hotspot (we call these matched regions "coldspots"). We found interesting differences in the frequency of certain sequence features between hotspots and coldspots (*4*). For example, the long terminal repeats of two retrovirus-like retrotransposons, THE1A [frequency in hotspot/frequency in coldspot (RR) = 2.3] and THE1B (RR = 1.7), are strongly overrepresented in hotspots, as are CT-rich repeats (RR = 1.4) and GA-rich repeats (RR = 1.4). By contrast, $(TA)_n$ repeats (RR = 0.7), GC-rich repeats (RR = 0.3), and certain L1 long interspersed nuclear elements (LINEs) (RR = 0.4) are strongly underrepresented in hotspots (in terms of both presence and length).

Comparison of THE1A/B elements in hotspots with those outside of hotspots revealed several marked sequence differences. The strongest signal is for the 7-nucleotide oligomer CCTCCCT, which aligns to positions 261 to 267 in the THE1B consensus (*18*). This motif is more frequent in hotspot THE1Bs than in THE1Bs elsewhere in the genome by a factor of 5.9 ($P < 10^{-33}$, Fisher's exact test); similarly, it is more frequent in hotspot THE1As than in THE1As elsewhere in the genome by a factor of 5.1 ($P < 10^{-5}$, Fisher's exact test). In each case, the consensus sequence for the repeat has a C in the seventh position. Two separate lines of evidence also point to the motif CCTCCCT, or possibly a larger motif containing it, playing an important role in hotspot determination. After masking repeat elements, we compared hotspot and coldspot regions for differences in the frequency of all motifs of length 5 to 9; the motif CCTCCCT showed the greatest enrichment in hotspots of any of the 8192 7-nucleotide oligomers. Further independent evidence comes from sperm typing studies. These have previously shown directly that the recombination rate at hotspot DNA2 is polymorphic in men, with a specific polymorphism suppressing hotspot activity (*19*). We examined the DNA sequence immediately surrounding this polymorphism. Strikingly, chromosomes active for the hotspot contain the motif CCTCCCT, with the "suppressor" mutation being a change from T to C in its third position. The THE1A/B context seems to be strongly influential in the function of this motif (although, as in the case of DNA2, not essential). We estimate that within this THE1A/B background, the motif will result in a hotspot 60% of the time, but outside of repeats this reduces to as little as 2 to 3%. Overall, the motif could explain about 11% of the 25,000 hotspots we studied, with occurrences outside THE1A/B elements contributing most of this total because of their far greater frequency in the genome (*4*). The CCTCCCT motif does not appear to match any sequences previously linked to recombination activity.

Our analysis also reveals how sequence-context effects in determining recombination hotspots can be both complex and extensive. First, we have identified additional motifs that are enriched among the THE1A/B elements within hotspots and that are both independent of and at some distance [up to 132 base pairs (bp)]

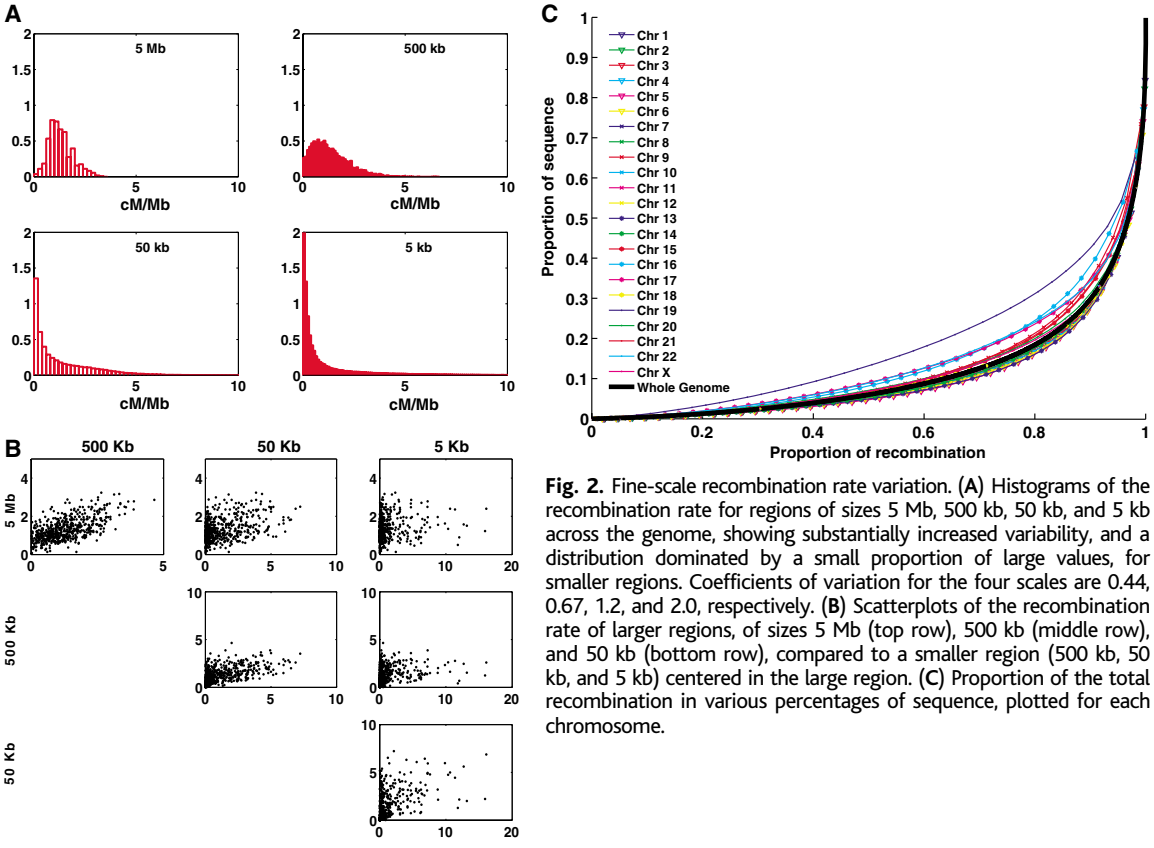

Fig. 2. Fine-scale recombination rate variation. (**A**) Histograms of the recombination rate for regions of sizes 5 Mb, 500 kb, 50 kb, and 5 kb across the genome, showing substantially increased variability, and a distribution dominated by a small proportion of large values, for smaller regions. Coefficients of variation for the four scales are 0.44, 0.67, 1.2, and 2.0, respectively. (**B**) Scatterplots of the recombination rate of larger regions, of sizes 5 Mb (top row), 500 kb (middle row), and 50 kb (bottom row), compared to a smaller region (500 kb, 50 kb, and 5 kb) centered in the large region. (**C**) Proportion of the total recombination in various percentages of sequence, plotted for each chromosome.

from the 7-nucleotide oligomer described above (*4*). Second, we find that L1 elements are strongly underrepresented in hotspots, and the effect is stronger the nearer the elements are to their full length of 6 to 7 kb. In *Drosophila*, transposons are biased toward regions of low recombination (*20*, *21*), which has been interpreted as evidence for selection against genome instability caused by ectopic recombination (either direct selection against elements that transpose to hotspots and subsequently cause genome rearrangement, or a chromatin-silencing mechanism of the genome that restricts germline transposition and consequently recombination). However, the sequence contexts found in repeat elements, rather than their transposon ancestry, may well be the primary determinant of their relationship with recombination in humans, given our findings that repeat elements can be enriched, suppressed, or unaffected by recombination hotspots; that specific motifs within these hotspots can have additional influences on recombination activity; and that other motifs (such as the 9-nucleotide oligomer CCCCACCCC) can play a role in promoting hotspot recombination outside repeat elements (*4*).

The extent to which differences in recombination rates over larger scales are due to differences in the numbers of hotspots, and/or to differences in the intensities of the hotspots in different regions, is an open question (*22*). We find that both are important determinants of large-scale recombination rate variation.

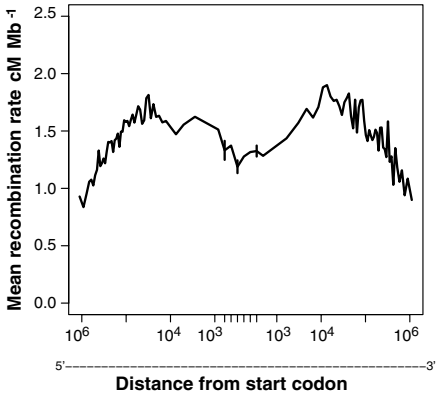

Fig. 3. Recombination rate as a function of distance from the nearest gene. The average recombination rate for SNP intervals is shown as a function of the physical distance between the midpoint of the SNP interval and the nearest gene (both 5′ and 3′). The left and right vertical tick marks respectively refer to the average rate in the first and last exons, and the central tick mark is the average over all intervals in internal exons; intervening points represent rates in first, internal, and last introns, respectively. Some caution may be needed in interpreting the results for the largest distances from genes. These relate to data points in gene deserts, which have atypical sequence features, and the decreased rate may be due to these other features rather than directly to the distance from the gene.

For example, it is well known that over large scales, recombination rates tend to be higher in telomeric, as compared to centromeric, chromosomal regions. In telomeric regions, the mean detected hotspot spacing is 90 kb and the mean intensity (total rate across the hotspot) per hotspot is 0.115 cM, whereas for centromeric regions the mean spacing is 123 kb and the mean intensity is 0.070 cM.

Population data only allow estimation of sex-averaged historical recombination rates (*23*). Notwithstanding this, some information can be gleaned about sex-specific differences in the recombination process. We do this in two ways. The first is to compare recombination on the X chromosome (which is necessarily female-specific) with that on the autosomes (where our estimates are sex-averaged). The second is by comparing autosomal regions in which pedigree estimates show large differences between male and female rates. Although the smaller sample size and SNP density on the X chromosome reduces power to detect hotspots, these are definitely present and hence definitively a feature of the human female recombination process. To enable direct X-autosome comparisons, we created a new autosomal data set matched to the X chromosome for sample size, SNP density, and the allele frequency spectrum by randomly deleting individuals and SNPs from the original data. We then reestimated recombination rates and hotspots from this matched autosomal data set. Having done so, the overall recombination landscape, and the extent to which it is dominated by hotspots, looks similar between the X chromosome and the autosomes (*4*) (fig. S4).

We also identified 66 paired regions of 2 Mb each, matched for sex-averaged recombination rate, where one region had a strong skew toward male recombination and the other had a strong skew toward female recombination [as estimated from the deCODE (*6*) map; see (*4*)]. Regardless of whether the region had much higher male rates than female rates or the opposite, the local recombination landscapes looked similar with regard to hotspot density, hotspot intensity (except for a slight deficit of very hot hotspots in regions where female rates are much higher than male rates), and the proportion of recombination in different proportions of sequence (fig. S4). Previous studies (*1*, *15*) have argued that there are no female-specific hotspots in two small regions, each about 200 kb. Our analyses show that there are definitely hotspots in female recombination, and suggest that the overall density and (except in the right-hand tail) intensity of hotspots, and their role in determining overall rates, is similar in male and female meioses.

Several studies (*14*, *24*–*26*) have shown substantial differences between recombination hotspots in humans and chimpanzees, establishing that hotspots have evolved very quickly relative to sequence differences. More recently, two lines of evidence—namely hotspots characterized by sperm typing that are present in some men but not in others (*19*, *27*) and differences between contemporary intensities and historical rates in hotspots—suggest that hotspots may even be evolving over the time scales of human polymorphism (*15*). This leads to a striking paradox. As noted above (Fig. 2C) and elsewhere (*1*, *14*), it is the pattern of hotspots and hotspot intensities that is largely responsible for recombination rate variation over centimorgan scales. The hotspots themselves are evolving very rapidly. So over centimorgan scales, contemporary sex-averaged rates estimated from pedigrees should differ from historical rates estimated from population data. But this is not the case. In contrast to the picture at individual hotspots (*15*), contemporary rates and historical rates are effectively identical over 5-Mb regions (fig. S1). Furthermore, over these large scales, recombination rates are reasonably well predicted by a few sequence and genomic features (*6*, *22*). But by combining multiple fine-scale genomic features, we can, at best, explain little more than 4% of the variation in recombination rate at the 5-kb scale (corresponding to the scale of recombination hotspots) (*4*). Finally, although there are documented differences in the presence (or absence) of hotspots and their intensities in men, no significant differences have been detected in male genome-wide recombination rates (*5*, *6*).

This suggests a two-stage process for recombination. A possible model is that recombination rates are constrained over large scales, plausibly by physical stresses acting on the DNA and/or by access to the recombination machinery, and that these constraints are slowly evolving and can be reasonably well predicted by sequence and genomic features. Within this big picture, the fine-scale landscape of hotspots is much less constrained and is rapidly evolving. Several lines of evidence support meiotic drive as a mechanism by which hotspots will in effect extinguish themselves (*15*, *19*), but the so-called "hotspot paradox" asks where new hotspots come from. If recombination rates over large scales are tightly constrained, then it might be the relative, rather than the absolute, propensity toward formation of double-strand breaks (DSBs) that matters. Over time, when one hotspot dies out, the relative recombination rates of others may increase, and/or new hotspots may arise in the locations that are next in an evolving queue of relative likelihood for DSB formation. This is consistent with observations in yeast of local competition between hotspots: A high frequency of DSBs at one site suppresses DSBs at nearby sites (*28*–*32*).

There are several testable predictions of this model. One is that large-scale recombination rates are likely to be correlated between humans and chimpanzees, in contrast to fine-scale rates. Although there is evidence for weak correlation of human and chimpanzee rates over intermedi-

ate (50-kb) scales (*24*), comparisons over larger scales will require either a chimpanzee genetic map or coalescent analyses of much larger chimpanzee polymorphism surveys than are currently available. Another prediction relates to hotspots detected by sperm typing that are polymorphic among men. In a set of men who do not have a particular hotspot, the model would predict increased activity in other hotspots and a similar total amount of recombination over large regions containing the polymorphic hotspot.

References and Notes

1. G. A. McVean *et al.*, *Science* **304**, 581 (2004).
2. D. C. Crawford *et al.*, *Nat. Genet.* **36**, 700 (2004).
3. D. A. Hinds *et al.*, *Science* **307**, 1072 (2005).
4. See supporting data on *Science* Online.
5. K. W. Broman, J. C. Murray, V. C. Sheffield, R. L. White, J. L. Weber, *Am. J. Hum. Genet.* **63**, 861 (1998).
6. A. Kong *et al.*, *Nat. Genet.* **31**, 241 (2002).
7. M. Cullen, S. P. Perfetto, W. Klitz, G. Nelson, M. Carrington, *Am. J. Hum. Genet.* **71**, 759 (2002).
8. Full details of the map and the location of recombination hotspots are available from the Mathematical Genetics and Bioinformatics groups, University of Oxford (www.stats.ox.ac.uk/mathgen/Recombination.html).
9. International Human Genome Sequencing Consortium, *Nature* **409**, 860 (2001).
10. N. Gilbert *et al.*, *Cell* **118**, 555 (2004).
11. A. Yu *et al.*, *Nature* **409**, 951 (2001).
12. R. R. Hudson, N. L. Kaplan, *Genetics* **111**, 147 (1985).
13. From genotype data, the presence of at least two copies of each of the four possible SNP haplotypes had to be unambiguously detected.
14. W. Winckler *et al.*, *Science* **308**, 107 (2005); published online 10 February 2005 (10.1126/science.1105322).
15. A. J. Jeffreys, R. Neumann, M. Panayi, S. Myers, P. Donnelly, *Nat. Genet.* **37**, 601 (2005).
16. International Human Genome Sequencing Consortium, *Nature* **431**, 931 (2004).
17. T. D. Petes, *Nat. Rev. Genet.* **2**, 360 (2001).
18. J. Jurka *et al.*, *Cytogenet. Genome Res.* **110**, 462 (2005).
19. A. J. Jeffreys, R. Neumann, *Nat. Genet.* **31**, 267 (2002).
20. E. Montgomery, B. Charlesworth, C. H. Langley, *Genet. Res.* **49**, 31 (1987).
21. C. H. Langley, E. Montgomery, R. Hudson, N. Kaplan, B. Charlesworth, *Genet. Res.* **52**, 223 (1988).
22. M. I. Jensen-Seaman *et al.*, *Genome Res.* **14**, 528 (2004).
23. Historical rates represent time averages of the recombination rate over the time scales during which the polymorphism has evolved. In the case of humans, this is likely to be on the order of 500,000 to 1 million years.
24. S. E. Ptak *et al.*, *Nat. Genet.* **37**, 429 (2005).
25. J. D. Wall, L. A. Frisse, R. R. Hudson, A. Di Rienzo, *Am. J. Hum. Genet.* **73**, 1330 (2003).
26. S. E. Ptak *et al.*, *PLoS Biol.* **2**, e155 (2004).
27. A. J. Jeffreys, R. Neumann, *Hum. Mol. Genet.* **14**, 2277 (2005).
28. J. Stamberg, *Heredity* **24**, 361 (1969).
29. Q. Fan, F. Xu, T. D. Petes, *Mol. Cell. Biol.* **15**, 1679 (1995).
30. T. C. Wu, M. Lichten, *Genetics* **140**, 55 (1995).
31. L. Xu, N. Kleckner, *EMBO J.* **14**, 5115 (1995).
32. Q. Q. Fan, F. Xu, M. A. White, T. D. Petes, *Genetics* **145**, 661 (1997).

33. We thank D. Cox and colleagues at Perlegen, and C. Spencer. Supported by NIH grant U54 HG2750 and the SNP Consortium (G.M.) and by NIH grant U54 HG2750, the Nuffield Trust, the SNP Consortium, the Wellcome Trust, and the Wolfson Foundation (P.D.).

Supporting Online Material

www.sciencemag.org/cgi/content/full/310/5746/321/DC1
Materials and Methods
Tables S1 to S11
Figs. S1 to S4
References

11 July 2005; accepted 9 September 2005
10.1126/science.1117196

Coincident Scrapie Infection and Nephritis Lead to Urinary Prion Excretion

Harald Seeger,[1]* Mathias Heikenwalder,[1]* Nicolas Zeller,[1] Jan Kranich,[1] Petra Schwarz,[1] Ariana Gaspert,[2] Burkhardt Seifert,[3] Gino Miele,[1] Adriano Aguzzi[1]†

Prion infectivity is typically restricted to the central nervous and lymphatic systems of infected hosts, but chronic inflammation can expand the distribution of prions. We tested whether chronic inflammatory kidney disorders would trigger excretion of prion infectivity into urine. Urinary proteins from scrapie-infected mice with lymphocytic nephritis induced scrapie upon inoculation into noninfected indicator mice. Prionuria was found in presymptomatic scrapie-infected and in sick mice, whereas neither prionuria nor urinary PrP^{Sc} was detectable in prion-infected wild-type or PrP^{C}-overexpressing mice, or in nephritic mice inoculated with noninfectious brain. Thus, urine may provide a vector for horizontal prion transmission, and inflammation of excretory organs may influence prion spread.

The prion, the infectious agent of transmissible spongiform encephalopathies (TSEs), is detectable at extraneural sites long before clinical symptoms appear (*1*). PrP^{Sc}, a protease-resistant isoform of the host protein PrP^{C}, accumulates mostly in central nervous system and lymphoid organs of infected organisms and may represent the infectious principle (*2*, *3*). In addition to PrP^{C} (*4*), splenic prion replication requires follicular dendritic cells (FDCs), the maintenance of which depends on B cells expressing lymphotoxins (LT) α and β (*5*). By activating local LTα/β signaling, which induces lymphoneogenesis, chronic inflammation enables ectopic prion replication (*6*). Inflammatory kidney conditions induced by bacteria, viruses, or autoimmunity are frequent in animals and humans, and urosepsis can occur in terminally demented patients (*7*). We therefore wondered whether renal inflammatory conditions might lead to urinary prion excretion.

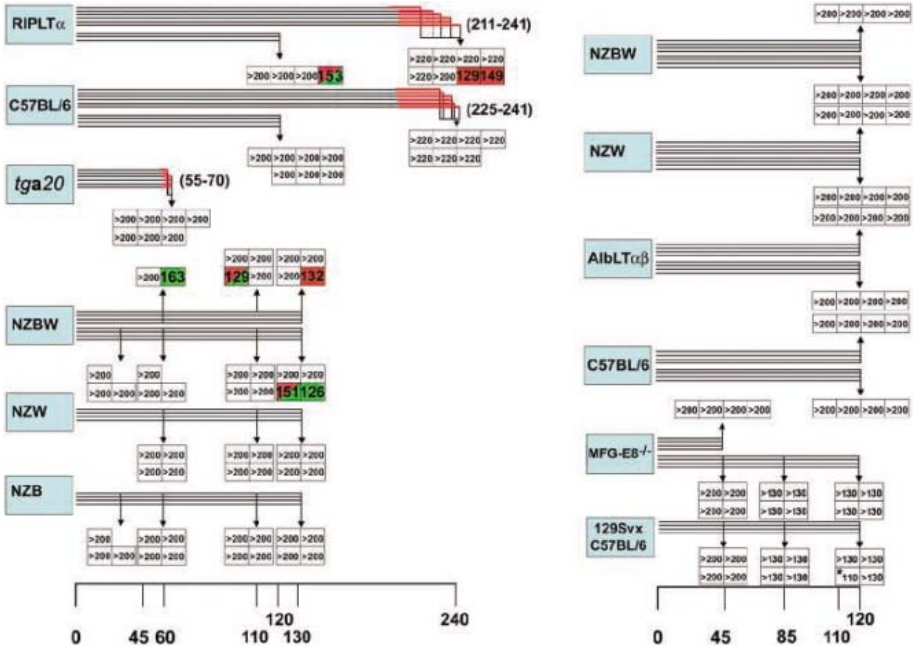

Fig. 1. Transmission of prions through urine. Urine samples were collected from individual donors (horizontal lines) at time points after inoculation, denoted by vertical lines, and pooled (intersections between lines, arrows). Squares represent individual *tga20* mice inoculated i.c. with urinary proteins. White squares: no scrapie symptoms; red squares: histopathologically confirmed scrapie; green squares: positive PrP^{Sc} immunoblot. Numbers within squares: days to terminal disease. Clinical disease: red line. Prion incubation time is expressed in days. Asterisk: intercurrent death without clinical scrapie signs.

To probe this possibility, we administered prions to RIPLTα and NZB × NZW F_1 mice (henceforth termed NZBW) suffering from lymphocytic nephritis (figs. S1 and S2 and table S1), as well as NZW mice and milk fat globule–epidermal growth factor 8 (MFG-E8)–deficient mice, which develop glomerulonephritis but lack lymphofollicular inflammation (fig. S1).

After intraperitoneal (i.p.) prion inoculation [3 and 5 $\log LD_{50}$ (50% lethal dose) units of the Rocky Mountain Laboratory (RML) scrapie strain (passage 5, henceforth called RML5) (*8*)], brains and spleens of RIPLTα, NZBW, MFG-E8$^{-/-}$, and control mice displayed similar prion and PrP^{Sc} loads (fig. S3, A to C). Whereas RIPLTα and NZBW kidneys progressively accumulated PrP^{Sc} and prion infectivity at 60 to 90 days postinoculation (dpi), presymptomatic (66 dpi) and terminally sick MFG-E8$^{-/-}$ mice lacked renal PrP^{Sc} (fig. S3D). Histoblot and immunohistochemical analysis identified PrP^{Sc} in renal lymphofollicular infiltrates of RIPLTα and NZBW mice (*6*).

RIPLTα, AlbLTαβ, C57BL/6 (4 to 6 months old), NZW, NZB, NZBW, MFG-E8$^{-/-}$, *tga20*, and 129Sv × C57BL/6 mice (8 to 16 weeks old) were inoculated i.p. with 3 or 5 $\log LD_{50}$ scrapie prions. We dialyzed and purified urinary proteins from pools of three to six mice of each genotype at 30, 45, 60, 85, 110, 120, and 130 dpi (all presymptomatic) and from terminally scrapie-sick mice (Fig. 1). Each urine donor was confirmed to contain brain or spleen PrP^{Sc} and/or infectivity upon necropsy (fig. S3, A to C).

Next, we quantified the recovery of spiked PrP^{Sc} and infectivity from urinary proteins (fig. S4). Scrapie cell endpoint assay (*9*) revealed a higher prion titer in dialyzed samples (fig. S4, C and D), possibly because dialysis removed biocontaminants inhibiting infection of PK1 cells.

Urinary proteins were purified by ultrafiltration followed by dialysis (~600 μg pooled from groups of three to six mice), or by dialysis followed by ultracentrifugation, and inoculated intracerebrally (i.c.) into groups of three to eight *tga20* mice that overexpress PrP^{C} (*10*). We found prion infectivity within pools of presymptomatic (120 dpi, $n = 3$) and scrapie-sick RIPLTα ($n = 6$) and NZBW mice ($n = 16$). However, we did not find infectivity in C57BL/6 ($n = 18$), MFG-E8$^{-/-}$ ($n = 8$), 129Sv × C57BL/6 ($n = 4$), NZW ($n = 12$), or NZB ($n = 4$) urine at any time point after prion inoculation (Fig. 1). Urine from terminally scrapie-sick NZBW, NZW, and NZB mice could not be collected because the incubation

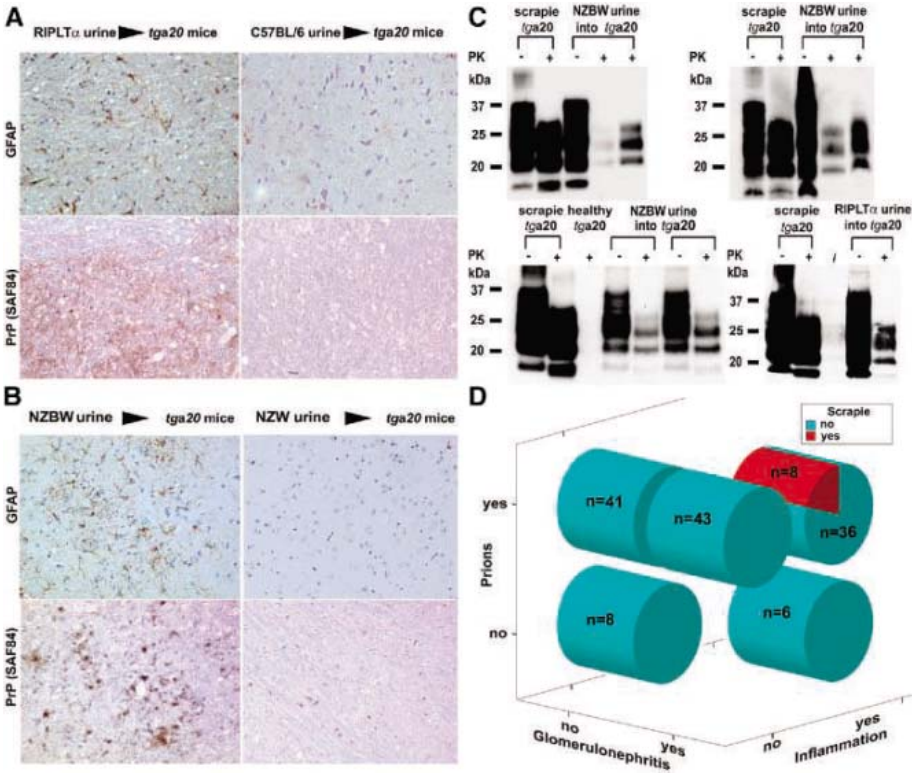

Fig. 2. Scrapie pathology in mice exposed to urine of nephritic mice. (**A** and **B**) Brain sections of *tga20* mice that succumbed to scrapie after i.c. inoculation with urinary proteins from RIPLTα (terminal) (**A**) or NZBW mice (130 dpi) (**B**), showing gliosis (GFAP, glial fibrillary acidic protein) and PrP deposition (SAF84). *Tga20* brains inoculated with urine from terminally sick C57BL/6 or presymptomatic NZW mice showed little or no astrogliosis and no PrP deposition. (**C**) (Upper panels) PrP^{Sc} in brains of *tga20* mice inoculated i.c. with NZBW urinary proteins (130 dpi). Ten micrograms (left) or 20 μg (right) of *tga20* brain were digested with proteinase K and immunoblotted. (Lower left panel) PrP^{Sc} in brains of *tga20* mice inoculated i.c. with NZBW or RIPLTα urinary proteins. Lanes 4 to 7: Inoculation with NZBW urinary proteins at 60 dpi (lanes 4 and 5) and 110 dpi (lanes 6 and 7). Positive controls: scrapie-sick *tga20* brain homogenate (left two lanes of each blot). Negative control: brain homogenate of a healthy *tga20* mouse. (Lower right panel) Inoculation with RIPLTα urinary proteins at 120 dpi. (**D**) Prions were detected in *tga20* mice exposed to urine from mice with lymphocytic nephritis (18.2%), but not in mice without kidney pathology or with isolated glomerulonephritis.

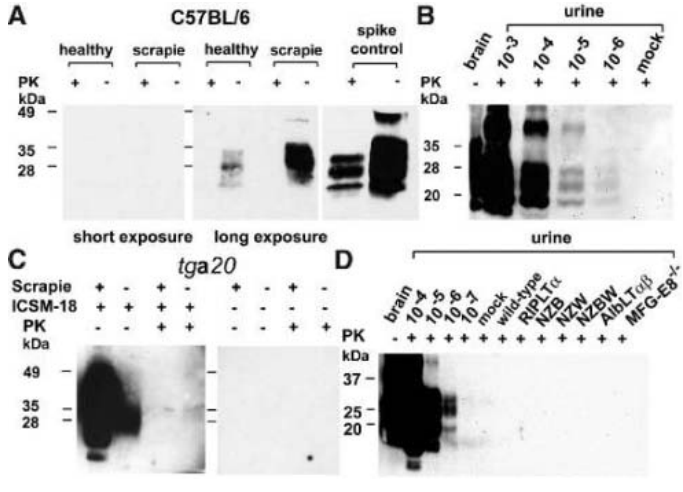

Fig. 3. Failure to detect urinary PrP^{Sc}. (**A**) Immunoblot analysis of urinary proteins from terminally scrapie-sick C57BL/6 mice. No PrP^{Sc} was found after ultracentrifugation. For control, *Prnp*$^{o/o}$ urine was spiked with scrapie brain homogenate. (**B**) Threshold of PrP^{Sc} detection in urinary proteins purified by dialysis and ultracentrifugation. C57BL/6 urine was spiked with serial dilutions of brain homogenate. Assay sensitivity: ≥100 ng of terminal brain homogenate per milliliter of urine (≅10^3 ID_{50} units/ml). (**C**) Immunoblot analysis of urinary proteins after ultracentrifugation. Scrapie-sick *tga20* mice lacked $UPrP^{Sc}$. PK, proteinase K digestion; ICSM-18, primary antibody to PrP. Omission of primary antibody (right) abolished all signals. (**D**) Immunoblot analysis of urinary proteins from presymptomatic [NZB, NZW, and NZBW (100 dpi)] and terminally scrapie-sick mice. No PrP^{Sc} was detected after ultracentrifugation (long exposure). Controls: scrapie brain homogenate used for spiking (lane 1); urine spiked with brain homogenate from scrapie-sick (lanes 2 to 5) or healthy mice (lane 6).

[1]Institute of Neuropathology, [2]Institute of Clinical Pathology, University Hospital of Zürich, Schmelzbergstrasse 12, CH-8091 Zürich, Switzerland. [3]Institute of Biostatistics, University of Zürich, Sumatrastrasse 30, CH-8006 Zürich, Switzerland.

*These authors contributed equally to this work.
†To whom correspondence should be addressed. E-mail: adriano@pathol.unizh.ch

time of scrapie exceeded the natural life span of these mice.

All clinically unaffected *tga20* indicator mice were killed at ≥200 dpi. Histopathological and immunoblot analyses confirmed scrapie in all clinically diagnosed *tga20* mice and excluded it from all others (Fig. 2, A to C, and fig. S5C). Phosphotungstate-mediated concentration of PrP^{Sc} from 1000 μg of protein did not reveal PrP^{Sc} in brains of clinically healthy urine-inoculated *tga20* mice (fig. S5B). Thus, two pathogenetically distinct chronic inflammatory conditions of the kidney, in concert with prion infection, result in prionuria well before the onset of clinically overt prion disease.

Whereas RIPLTα and NZBW mice suffer from combined interstitial lymphofollicular inflammation and glomerulonephritis, MFG-$E8^{-/-}$, NZW, and NZB mice display glomerulonephritis but lack lymphofollicular foci (figs. S1 and S2). Hence, prionuria necessitates intrarenal organized inflammatory foci (*6*) and is not elicited by isolated glomerulonephritis (Fisher's exact test, $P = 0.031$). Urinary proteins from presymptomatic and terminal RIPLTα mice induced similar attack rates, suggesting similar urinary prion infectivity titers in presymptomatic and scrapie-sick mice. The consistent lack of infectivity in urine from noninoculated mice and prion-sick wild-type mice makes it unlikely that infectivity found in urine of nephritic mice represents a contaminant.

Scrapie-infected hamsters and Creutzfeldt-Jakob disease (CJD) patients were reported to excrete urinary PrP^{Sc} ($UPrP^{Sc}$) (*11*). However, these findings were not reproduced (*12*) and were deemed artifactual (*13*, *14*). We attempted to detect $UPrP^{Sc}$ in presymptomatic and terminally sick RIPLTα, MFG-$E8^{-/-}$, *tga20*, C57BL/6, and 129Sv × C57BL/6 mice, as well as in presymptomatic NZW, NZB, and NZBW mice. Overnight dialysis did not affect the quantitative recovery of spiked PrP^{Sc} from urine (fig. S4, A and B); the detection threshold was ≥100 ng of terminal brain homogenate per milliliter of urine (Fig. 3, B and D), equivalent to 10^3 median infectious dose (ID_{50}) units/ml. Under these conditions, we failed to reveal any $UPrP^{Sc}$, even in prionuric mice (Fig. 3 A, C, and D). These negative findings are not unexpected, because urinary infectivity titers were typically ≤1 ID_{50} units per 2 ml of pooled urine (Fig. 1), which is below the detectability of PrP^{Sc} (Fig. 3B).

We then tested whether inflammation of nonexcretory organs leads to prionuria. We administered prions to AlbLTαβ mice, which lack nephritis but develop hepatitis (*6*). Urine from AlbLTαβ and appropriate wild-type control mice (four pools of $n = 4$ mice, 120 dpi) lacked prion infectivity and $UPrP^{Sc}$ (Figs. 1 and 3D; fig. S5, B and C). Thus, extrarenal inflammation, though enabling prion accumulation at the site of inflammation, does not induce prionuria.

Because PrP^{C} is necessary for prion replication (*4*), its expression may be rate-limiting for urinary prion excretion. We assessed prionuria in *tga20* mice, whose renal PrP^{C} content is six to eight times that of wild-type mice (fig. S3F). Pooled urinary proteins (600 μg each) from six terminally scrapie-sick *tga20* mice were inoculated i.c. into *tga20* mice (Fig. 1). None of the recipient *tga20* mice developed scrapie. Upon necropsy (>200 dpi), no scrapie histopathology was detected (fig. S5C). Thus, PrP^{C} overexpression does not induce prionuria. The PrP^{C} content of RIPLTα, NZBW, and MFG-$E8^{-/-}$ kidneys was similar to those of wild-type controls (fig. S3, G and H). RIPLTα and NZBW kidneys contain FDC-$M1^{+}$ cells with high, focal levels of PrP^{C} (*6*), which may facilitate local prion replication (*5*). Inoculation of urinary protein from noninfected mice did not elicit any abnormality in *tga20* mice (fig. S5C).

How do prions enter the urine? Upon extrarenal replication, blood-borne prions may be excreted by a defective filtration apparatus. Alternatively, prions may be produced locally and excreted during leukocyturia. Although prionemia occurs in many paradigms of peripheral prion pathogenesis (*15*, *16*), the latter hypothesis appears more likely, because prionuria was invariably associated with local prion replication within kidneys.

Urine from one CJD patient was reported to elicit prion disease in mice (*17*, *18*), but not in primates (*19*). Perhaps unrecognized nephritic conditions may underlie these discrepant observations. Inflammation-associated prionuria may also contribute to horizontal transmission among sheep, deer, and elk, whose high efficiency of lateral transmission is not understood.

References and Notes

1. H. Fraser, A. G. Dickinson, *Nature* **226**, 462 (1970).
2. J. Castilla, P. Saa, C. Hetz, C. Soto, *Cell* **121**, 195 (2005).
3. S. B. Prusiner, *Science* **216**, 136 (1982).
4. H. Büeler *et al.*, *Cell* **73**, 1339 (1993).
5. A. Aguzzi, M. Heikenwalder, *Immunity* **22**, 145 (2005).
6. M. Heikenwalder *et al.*, *Science* **307**, 1107 (2005).
7. S. R. Jones, *Am. J. Med.* **88**, S30 (1990).
8. Materials and methods are available as supporting material on *Science* Online.
9. P. C. Klohn, L. Stoltze, E. Flechsig, M. Enari, C. Weissmann, *Proc. Natl. Acad. Sci. U.S.A.* **100**, 11666 (2003).
10. M. Fischer *et al.*, *EMBO J.* **15**, 1255 (1996).
11. G. M. Shaked *et al.*, *J. Biol. Chem.* **276**, 31479 (2001).
12. M. W. Head, E. Kouverianou, L. Taylor, A. Green, R. Knight, *Neurology* **64**, 1794 (2005).
13. A. Serban, G. Legname, K. Hansen, N. Kovaleva, S. B. Prusiner, *J. Biol. Chem.* **279**, 48817 (2004).
14. H. Furukawa *et al.*, *J. Biol. Chem.* **279**, 23661 (2004).
15. C. A. Llewelyn *et al.*, *Lancet* **363**, 417 (2004).
16. F. Houston, J. D. Foster, A. Chong, N. Hunter, C. J. Bostock, *Lancet* **356**, 999 (2000).
17. Y. Shibayama *et al.*, *Acta Pathol. Jpn.* **32**, 695 (1982).
18. J. Tateishi, Y. Sato, M. Koga, H. Doi, M. Ohta, *Acta Neuropathol. (Berlin)* **51**, 127 (1980).
19. D. C. Gajdusek, C. J. Gibbs Jr., M. Alpers, *Science* **155**, 212 (1967).

20. We thank H. Moch, C. Sigurdson, M. Kurrer, P. Klöhn, M. Prinz, R. Moos, A. Marcel, J. Collinge, and B. Odermatt for technical help. N. Ruddle provided RIPLTα mice, and S. Nagata provided MFG-$E8^{-/-}$ mice. Supported by grants from the Bundesamt für Bildung und Wissenschaft, the Swiss National Foundation, and the National Center of Competence in Research on neural plasticity and repair (to A.A.). M.H. is supported by a Career Development Award of the University of Zürich.

Supporting Online Material

www.sciencemag.org/cgi/content/full/310/5746/324/DC1
Materials and Methods
Figs. S1 to S5
Table S1
References

15 August 2005; accepted 18 September 2005
10.1126/science.1118829

Wolbachia Establishment and Invasion in an *Aedes aegypti* Laboratory Population

Zhiyong Xi,* Cynthia C. H. Khoo, Stephen L. Dobson†

A proposed strategy to aid in controlling the growing burden of vector-borne disease is population replacement, in which a natural vector population is replaced by a population with a reduced capacity for disease transmission. An important component of such a strategy is the drive system, which serves to spread a desired genotype into the targeted field population. Endosymbiotic *Wolbachia* bacteria are potential transgene drivers, but infections do not naturally occur in some important mosquito vectors, notably *Aedes aegypti*. In this work, stable infections of *w*AlbB *Wolbachia* were established in *A. aegypti* and caused high rates of cytoplasmic incompatibility (that is, elimination of egg hatch). Laboratory cage tests demonstrated the ability of *w*AlbB to spread into an *A. aegypti* population after seeding of an uninfected population with infected females, reaching infection fixation within seven generations.

Aedes aegypti (yellow fever mosquito) is the principle vector of dengue viruses throughout the tropical world. Without a registered vaccine or other prophylactic measures, efforts to reduce cases of dengue fever and dengue hemorrhagic fever are limited to vector con-

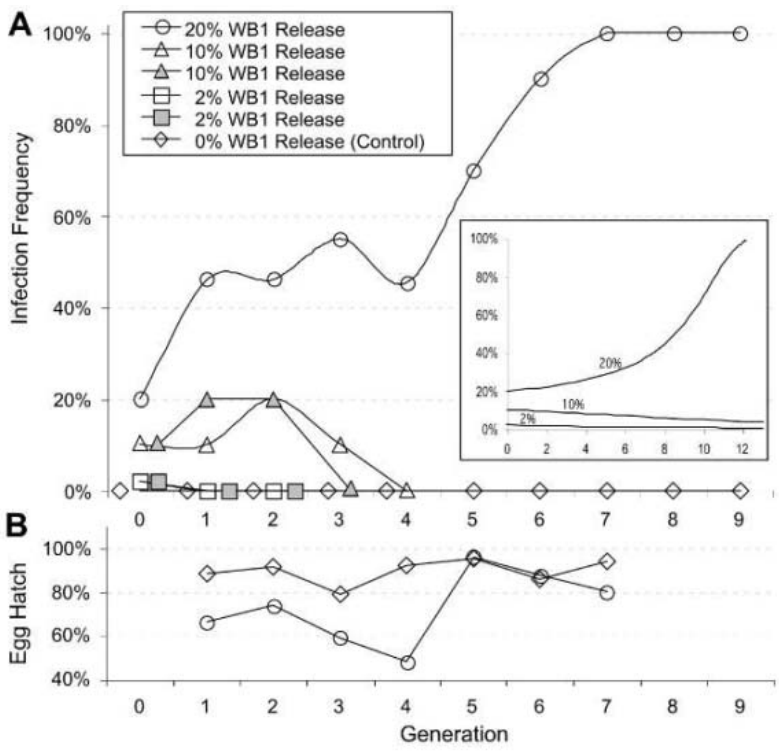

Fig. 1. (**Left**) Oocytes of uninfected Waco and *w*AlbB-infected WB1 stained with a *Wolbachia*-specific FISH probe. FISH staining methods were as previously described (*7*). **Fig. 2.** (**Right**) *Wolbachia* infection frequency (**A**) and egg hatch rates (**B**) after a single release of WB1 females into Waco populations. (Inset) Graph displays model predictions (*8*) of *Wolbachia* infection dynamics assuming complete CI, 100% maternal transmission, and a 15% fecundity cost associated with *Wolbachia* infection.

trol. Unfortunately, traditional mosquito control measures are not succeeding. With an estimated 100 million human cases of dengue fever every year (*1*), substantial effort is being devoted to the development of new strategies to complement existing vector control methods. One such method is population replacement, in which natural *A. aegypti* populations would be replaced with modified populations that are refractory to dengue transmission. Recent advances toward the production of refractory *A. aegypti* strains include the development of methods for stable genetic transformation of *A. aegypti*, RNA interference technology, and genomic sequencing efforts (*2*–*4*). In contrast, there has been relatively little progress toward the development of a vehicle that will serve to drive the refractory genotype into the field population.

Department of Entomology, University of Kentucky, Lexington, KY 40546, USA.

*Present address: Department of Microbiology and Immunology, Bloomberg School of Public Health, Johns Hopkins University, Baltimore, MD 21205, USA.
†To whom correspondence should be addressed. E-mail: sdobson@uky.edu

A gene-drive vehicle is an important component of vector population replacement strategies, providing a mechanism for the autonomous spread of desired transgenes into the targeted population. Compared with strategies that rely on inundative releases and Mendelian inheritance, gene-drive strategies would require relatively small "seedings" of transgenic individuals into a field population. Perhaps more important than increased cost efficacy, gene-drive strategies can facilitate population replacement with transgenic individuals that have a lower fitness relative to the natural population.

Cytoplasmic incompatibility (CI), induced by naturally occurring intracellular *Wolbachia* bacteria, has attracted scientific attention as a potential vehicle for gene drive. CI occurs when a *Wolbachia*-infected male mates with an uninfected female, resulting in karyogamy failure and early developmental arrest of the mosquito embryo (*5*). Although CI and other forms of reproductive parasitism have made *Wolbachia* an evolutionary success, with an estimate that infections occur in ~20% of insect species (*6*), *Wolbachia* infections do not naturally occur in *A. aegypti*, raising the question of whether *A. aegypti* can support a *Wolbachia* infection. Although *Wolbachia* infections have been introduced into *Drosophila* and other insects (*7*), *Wolbachia* infection may not cause CI in *A. aegypti* and may not invade an uninfected population. Key parameters in *Wolbachia* infection dynamics include the intensity of CI (number of hatching eggs resulting from an incompatible cross), the maternal inheritance rates (number of uninfected progeny produced by an infected female), and mosquito fitness

Table 1. CI pattern resulting from crosses of the naturally uninfected Waco and the *w*AlbB-transfected WB1 *A. aegypti* strains. Percent egg hatch ± standard deviation and number of cross replicates are shown for each of the four cross types. Crosses were conducted as previously described (*7*).

	Male Waco	Male WB1
Female Waco	92.5 ± 3.7% (n = 9)	0.0 ± 0.0% (n = 15)
Female WB1	69.1 ± 11.7% (n = 9)	50.6 ± 12.9% (n = 15)

costs associated with the infection (*8*). These parameters also determine the infection frequency after a population replacement event, an important consideration because the goal of population replacement is for the entire mosquito population to carry the desired genotype.

A. aegypti were infected by embryonic microinjection with the *w*AlbB *Wolbachia* infection from *A. albopictus* (*7*). In brief, cytoplasm from *A. albopictus* eggs (Hou strain superinfected with *w*AlbA and *w*AlbB) was injected into *A. aegypti* eggs (Waco strain). *Wolbachia* were detected by polymerase chain reaction (PCR) as previously described (*9*) in each of the five females (G_0) that survived from injection to adult. Only three females successfully produced progeny (G_1). PCR tests of G_1 individuals demonstrated the offspring of one female to be uninfected. The lines established from the remaining two females were only infected with the *w*AlbB, and one line (designated WB1) was selected for additional tests. In previous work on *A. albopictus*, *w*AlbB infections were obtained and not *w*AlbA (*7*). This may reflect the lower infection rate of *w*AlbA relative to *w*AlbB (*10*).

PCR assays of WB1 individuals in subsequent generations ($\leq G_{12}$) consistently identified *Wolbachia* infection. As a specific test of the maternal inheritance rate, progeny were collected from isolated WB1 females (G_{12}). After PCR confirmation of *Wolbachia* infection in 10 G_{12} females, the progeny (10 daughters and 10 sons for each G_{12} female) were assayed with PCR. All of the G_{13} progeny ($n = 200$) were infected by *Wolbachia* (95% binomial confidence interval between 0.9851 and 1.0). Fluorescence in situ hybridization (FISH) confirms high *Wolbachia* infection rates in WB1 oocytes (Fig. 1). The infection appears highest in the anterior, posterior, and cortical regions of oocytes, similar to the pattern observed in naturally infected *A. albopictus* (*7*).

Crosses were conducted to determine whether CI occurs as a result of the *Wolbachia* infection in the WB1 strain. The design of the cross experiment was as previously described (*9*). As shown in Table 1, the pattern of egg hatch resulting from crosses is consistent with strong CI, similar to that observed in *A. albopictus*, from which the *w*AlbB infection was derived (*7*). No egg hatch resulted from >3800 eggs examined from crosses of uninfected Waco females and infected WB1 males.

Among the compatible crosses, egg hatches resulting from WB1 crosses [51% and 69% (Table 1)] were significantly lower [Kruskal-Wallis, df (degrees of freedom) = 1, $P < 0.01$] than the egg hatch observed in compatible crosses of Waco individuals (92%). Because the progeny of the WB1 G_0 female were sibling-mated during production of the WB1 isofemale line, the low egg hatch may reflect an inbreeding effect. Therefore, virgin WB1 females (G_3) were mated with uninfected Waco males. After the repeat of this introgression for six generations, the egg hatch increased to an average of 89% (G_9).

Strong CI and high maternal transmission rates suggest that *w*AlbB infection will invade an uninfected population. To test this prediction, we released WB1 females at different ratios into replicate Waco laboratory populations (Fig. 2A). The population cage experimental design was as previously described (*9*). In the 20% initial release cage, the *w*AlbB infection frequency was observed to increase to 100% infection frequency within seven generations. Additional sampling in the eighth and ninth generations demonstrated that the infection frequency remained fixed at 100% (Fig. 2A). Consistent with model predictions (*11*), a transient drop in egg hatch was observed during the cytotype replacement (circa generation four) (Fig. 2B). The latter is expected owing to the frequent occurrence of CI crosses; however, once the infection becomes fixed within the population, CI crosses no longer occur, and the egg hatch rates recover.

In cages established with an initial infection frequency of ≤10%, the infection was detected for up to four generations before its disappearance from the population (Fig. 2A). Infection could not be detected in populations in cages initially infected at a rate of 2% release of WB1 females. Hence, the loss of *Wolbachia* infection from a population is predicted if the initial infection frequency is below a required threshold determined by CI level, fidelity of maternal transmission, and fitness costs associated with *Wolbachia* infection (*8*). Complete CI and no evidence of maternal transmission failure were observed in this study. If no fitness costs were associated with the infection, we would predict *Wolbachia* invasion in all cages in which WB1 females were released. However, we estimated a threshold infection frequency of ~20%, suggesting there is a substantial fitness cost associated with *w*AlbB infection in *A. aegypti*. By using a previously developed model (*8*), we predicted an approximate 15% fecundity cost to be associated with the *w*AlbB infection on the basis of the observed population replacement events (Fig. 2A inset).

An analysis of fecundity costs associated with the *w*AlbB infection neither revealed any differences in egg number ($P > 0.3$, *t* test) in comparisons of WB1 females (57.8 ± 17.6 eggs per female, $n = 12$) with Waco females (52.4 ± 8.5 eggs per female, $n = 14$) nor revealed any differences in egg hatch rate between Waco and WB1 strains (χ^2 test, df = 1, $P > 0.05$). Thus, future experiments need to investigate additional types of fitness costs (e.g., reduced mating competitiveness or immature survivorship). Furthermore, the laboratory population cage tests conducted here represent an initial proof of principle, but future field cage tests will provide a more accurate prediction of infection dynamics in natural populations (*12*).

Nevertheless, important obstacles currently prevent implementation of genetic modification strategies using *Wolbachia* as a vehicle to drive transgenes into *A. aegypti* populations. Notably absent is a method for linking transgenes to *Wolbachia*. However, the ability to artificially infect *A. aegypti* with *w*AlbB into a major disease vector is an important step toward proposed population replacement strategies. The observed high CI rates, high maternal inheritance, and ability of *w*AlbB to invade an uninfected laboratory population to infection fixation represent desired characteristics for population replacement strategies. Additional study is needed to define the fitness of *w*AlbB-infected *A. aegypti* relative to uninfected individuals, and population replacement experiments need to be performed under conditions that resemble the natural environment. Transfection success with *A. aegypti* suggests that the transfection approach may be successful with other medically important disease vectors, including *Anopheles* species.

References and Notes

1. T. P. Monath, *Proc. Natl. Acad. Sci. U.S.A.* **91**, 2395 (1994).
2. Z. N. Adelman, N. Jasinskiene, A. A. James, *Mol. Biochem. Parasitol.* **121**, 1 (2002).
3. P. W. Atkinson, K. Michel, *Genesis* **32**, 42 (2002).
4. F. Gould, P. Schliekelman, *Annu. Rev. Entomol.* **49**, 193 (2004).
5. U. Tram, W. Sullivan, *Science* **296**, 1124 (2002).
6. J. H. Werren, D. M. Windsor, *Proc. R. Soc. London Ser. B* **267**, 1277 (2000).
7. Z. Xi, J. L. Dean, C. Khoo, S. L. Dobson, *Insect Biochem. Mol. Biol.* **35**, 903 (2005).
8. A. A. Hoffmann, M. Turelli, L. G. Harshman, *Genetics* **126**, 933 (1990).
9. S. L. Dobson, E. J. Marsland, W. Rattanadechakul, *Genetics* **160**, 1087 (2002).
10. T. J. Dutton, S. P. Sinkins, *Insect Mol. Biol.* **13**, 317 (2004).
11. S. L. Dobson, C. W. Fox, F. M. Jiggins, *Proc. R. Soc. London Ser. B* **269**, 437 (2002).
12. T. W. Scott, W. Takken, B. G. J. Knols, C. Boete, *Science* **298**, 117 (2002).

13. The authors thank J. Dean and L. Ng for their assistance with experiments and J. Rasgon for comments on a draft manuscript. This work was supported by NIH grant (NIH-AI-51533). This is publication 05-08-083 of the University of Kentucky Agricultural Experiment Station.

Supporting Online Material

www.sciencemag.org/cgi/content/full/310/5746/326/DC1
Materials and Methods
Fig. S1
Tables S1 and S2
References and Notes

19 July 2005; accepted 14 September 2005
10.1126/science.1117607

Identification and Functional Characterization of Brainstem Cannabinoid CB_2 Receptors

Marja D. Van Sickle,[1]* Marnie Duncan,[1]* Philip J. Kingsley,[2] Abdeslam Mouihate,[1] Paolo Urbani,[3] Ken Mackie,[4] Nephi Stella,[5] Alexandros Makriyannis,[6] Daniele Piomelli,[7] Joseph S. Davison,[1] Lawrence J. Marnett,[2] Vincenzo Di Marzo,[3] Quentin J. Pittman,[1] Kamala D. Patel,[1] Keith A. Sharkey[1]†

The presence and function of CB_2 receptors in central nervous system (CNS) neurons are controversial. We report the expression of CB_2 receptor messenger RNA and protein localization on brainstem neurons. These functional CB_2 receptors in the brainstem were activated by a CB_2 receptor agonist, 2-arachidonoylglycerol, and by elevated endogenous levels of endocannabinoids, which also act at CB_1 receptors. CB_2 receptors represent an alternative site of action of endocannabinoids that opens the possibility of nonpsychotropic therapeutic interventions using enhanced endocannabinoid levels in localized brain areas.

Endocannabinoids, anandamide, and 2-arachidonoylglycerol (2-AG) are lipid mediators that act at CB_1 and CB_2 receptors (*1*, *2*). Their actions are terminated through cellular uptake facilitated by a putative endocannabinoid transporter, followed by intracellular enzymatic hydrolysis. Two degradative enzymes for endocannabinoid metabolism are known; fatty acid amide hydrolase (FAAH) preferentially degrades anandamide, and monoacylglycerol lipase preferentially degrades 2-AG (*1*, *3*, *4*). The CB_1 receptor is highly expressed in the CNS, where cannabinoids act at presynaptic CB_1 receptors to elicit changes in the synaptic efficacy of neuronal circuits (*5*). The CB_2 receptor has been found outside the CNS and is particularly associated with immune tissues, such as the spleen and thymus, as well as in various circulating immune cell populations (*6*). In the CNS, CB_2 receptor mRNA has been reported in cerebellar granule cells (*7*), and CB_2 receptors have been described on perivascular microglial cells and in cultured cerebrovascular endothelium (*8*, *9*). CB_2 receptor expression is enhanced on glia in neuritic plaques and on immune cells in simian immunodeficiency virus encephalitis (*10*, *11*). To date, however, the CB_2 receptor protein has not been localized on central neurons, and the effects of endocannabinoids in the brain have always been attributed to an action at CB_1 receptors.

We found CB_2 receptor mRNA expression in the brain (cerebellum, cortex, and brainstem) and spleen of the rat using reverse transcription polymerase chain reaction (RT-PCR) (Fig. 1). Sequencing of the 472–base pair PCR product showed that the products amplified from the spleen, cortex, and brainstem were identical to the rat CB_2 receptor sequence (*12*, *13*). Using quantitative real-time RT-PCR, we determined that the brainstem contained $1.5 \pm 0.9\%$ of the CB_2 receptor mRNA found in the spleen (fig. S1) (*14*). Amplification of CB_2 receptor from the brainstem was not due to genomic contamination of our sample, because amplification of RNA that was not reverse-transcribed did not lead to the generation of a product. Furthermore, our real-time PCR primers spanned intron-exon borders, which ensured that the only product that could be amplified was the spliced mRNA.

We next investigated whether CB_2 receptor protein could be detected by Western blotting and/or immunohistochemistry (*14*). Western blotting for the CB_2 receptor in the brainstem and cerebellum revealed three bands at about 45, 55, and 60 kD (Fig. 1), similar to previous reports in spleen (*15*). In the brainstem, CB_2 receptor immunoreactivity was found in neurons within the dorsal motor nucleus of the vagus (DMNX), the nucleus ambiguous, and the spinal trigeminal nucleus; glial cells and blood vessels did not express detectable CB_2 receptor immunoreactivity (*16*). Preincubation with the cognate peptide of the CB_2 receptor antibody completely abolished cellular staining. These results are in contrast to the conclusions drawn by Derbenev *et al.* (*17*), who reported no CB_2 mRNA or receptor protein in similar regions of the rat brainstem. However, evaluation of their figures reveals a faint band of immunoreactivity in Western blots, consistent with our observations, and their RT-PCR primers were directed against different regions of the CB_2 receptor mRNA. The differences in the conclusions drawn likely reflect the low abundance of CB_2 receptor in the brain relative to the spleen and the choice of RT-PCR primers.

We next pursued the functional significance of this observation. The major psychoactive cannabinoid, Δ^9-tetrahydrocannabinol (THC), is effective in the treatment of nausea and vomiting (emesis) (*18*). THC acts on neurons in the dorsal vagal complex of the brainstem, the site of integration of emetic reflexes that includes the nucleus of the solitary tract (NTS), the area postrema, and DMNX (*18*, *19*), where we found CB_2 receptor expression. These well-characterized actions of CBs have been demonstrated in the ferret. Because of the inability of rodents to vomit, we verified our observations of the receptor distribution in this species (Fig. 1). Indeed, as in the rat, we observed major bands of immunoreactivity in Western blots at about the same relative molecular weights and a similar distribution of CB_2 receptor expression in neurons of the DMNX.

These results led us to investigate whether endocannabinoids could act at the CB_2 receptor in the brainstem to inhibit emesis. Using morphine-6-glucuronide (M6G) as an emetic stimulus, we found that both anandamide and 2-AG dose-dependently reduced emesis in the ferret (Fig. 2) (*14*). Using selective CB receptor antagonists, we attempted to reverse the actions of these endocannabinoids. The antiemetic effect of anandamide was almost completely reversed by the selective CB_1 receptor antagonist AM251 but was not significantly altered by the CB_2 antagonist AM630, which is consistent with the fact that the anandamide is not very efficacious at CB_2 receptors (*2*) and indicates that the dose of AM630 used does not antagonize CB_1 receptors. In contrast, the antiemetic effects of 2-AG were reversed by both AM251 and AM630 (Fig. 2). Thus, the CB_2 receptor may be functionally expressed in the ferret brainstem and could be targeted by an endocannabinoid. As we observed the ferrets during our studies, we noted that 2-AG administration was far less sedating than anandamide (Fig. 2). This action is consistent with a preferential effect at a CB_2 receptor, because CB_1 receptor activation *in vivo* is associated with sedation (*2*).

[1]Institute of Infection, Immunity, and Inflammation and Hotchkiss Brain Institute, Department of Physiology and Biophysics, University of Calgary, Calgary, AB, Canada T2N 4N1. [2]Department of Biochemistry, Vanderbilt Institute of Chemical Biology, Center in Molecular Toxicology, Vanderbilt-Ingram Cancer Center, Vanderbilt University School of Medicine, Nashville, TN 37232–0146, USA. [3]Endocannabinoid Research Group, Institute of Biomolecular Chemistry, Consiglio Nazionale delle Ricerche, Pozzuoli, Naples, Italy. [4]Department of Anesthesiology and Department of Physiology and Biophysics, University of Washington, Seattle, WA 98195–6540, USA. [5]Department of Pharmacology, Psychiatry, and Behavioral Sciences, University of Washington, Seattle, WA 98195–7280, USA. [6]Center for Drug Discovery, Department of Pharmaceutical Sciences, Northeastern University, Boston, MA 02115, USA. [7]Department of Pharmacology, Gillespie Neuroscience Facility, University of California, Irvine, CA 92697–6180, USA.

*These authors contributed equally to this work.
†To whom correspondence should be addressed. E-mail: ksharkey@ucalgary.ca

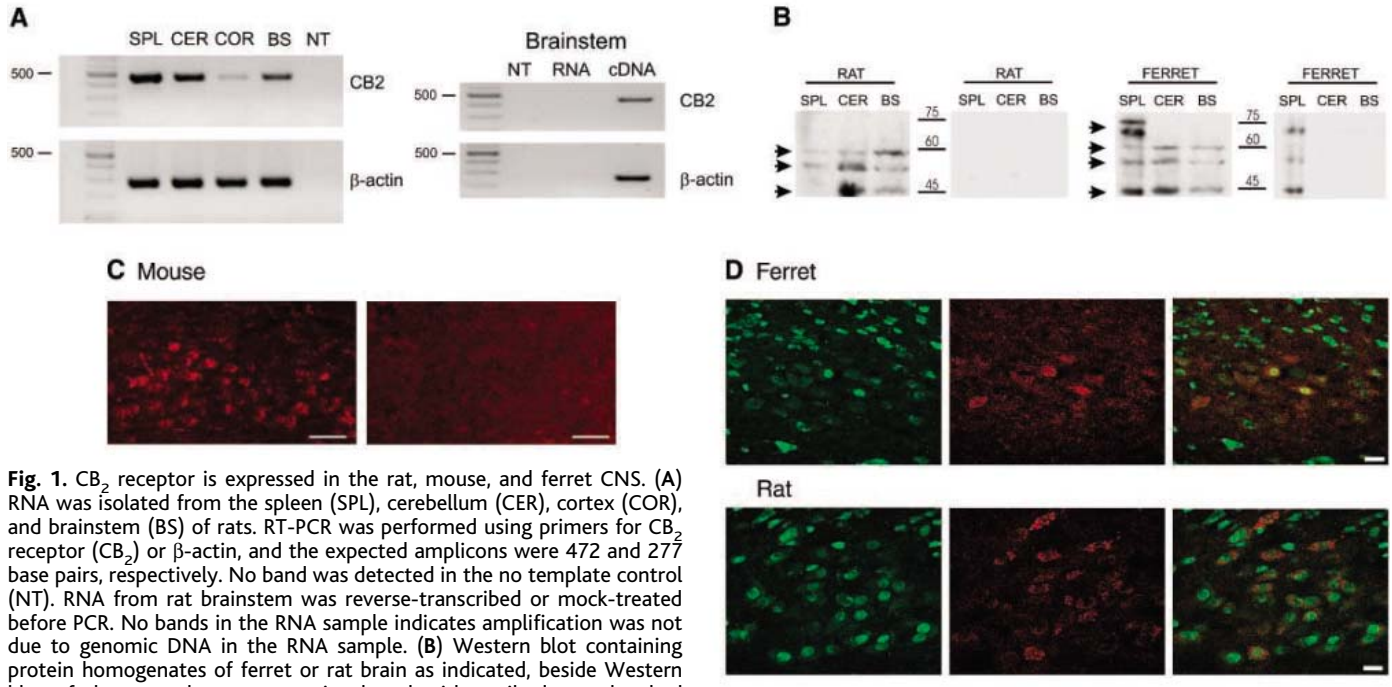

Fig. 1. CB_2 receptor is expressed in the rat, mouse, and ferret CNS. (**A**) RNA was isolated from the spleen (SPL), cerebellum (CER), cortex (COR), and brainstem (BS) of rats. RT-PCR was performed using primers for CB_2 receptor (CB_2) or β-actin, and the expected amplicons were 472 and 277 base pairs, respectively. No band was detected in the no template control (NT). RNA from rat brainstem was reverse-transcribed or mock-treated before PCR. No bands in the RNA sample indicates amplification was not due to genomic DNA in the RNA sample. (**B**) Western blot containing protein homogenates of ferret or rat brain as indicated, beside Western blot of the same homogenates incubated with antibody preabsorbed with control peptide. Major bands were observed at about 45, 55, and 60 kD in rat and ferret brainstem (arrows; $n = 6$). In the ferret spleen, higher molecular weight bands were also observed (arrow). In the rat brain and spleen and ferret brain, we completely preabsorbed all the immunoreactive bands. However, in the ferret spleen, bands were substantially reduced, but not completely preabsorbed, with the concentration of peptide used. (**C**) CB_2 receptor immunoreactivity in the dorsal motor nucleus of the vagus of wild-type (left) and $CB_2^{-/-}$ (right) mice (*30*). Note the lack of immunoreactive cell bodies in the knockout mouse ($n = 3$ per group). Scale bar, 50 μm. (**D**) Immunoreactivity for the neuronal nuclear marker NeuN (left, green) and CB_2 receptor immunoreactivity (center, red) in neurons of the dorsal motor nucleus of the vagus of the ferret and rat, as indicated. Overlay (right) of NeuN and CB_2 receptor illustrates that CB_2 receptor immunoreactivity is present in neurons of both the ferret and rat ($n = 4$), where it is localized on the cell membrane and in the cytoplasm of the neurons. Scale bars, 20 μm.

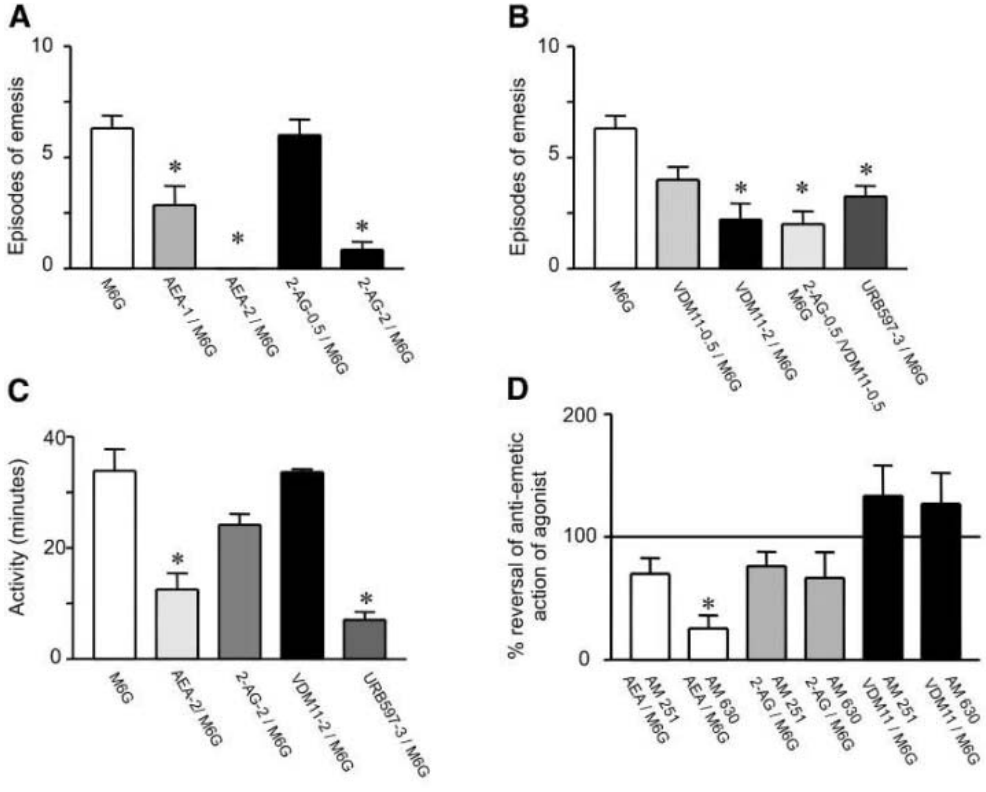

Fig. 2. Endocannabinoids reduce emesis induced by M6G. (**A**) Episodes of emesis after treatments of emetic agent alone, M6G (0.05 mg/kg, subcutaneously; $n = 10$) or the following treatments ($n = 3$ to 7) preceding M6G; anandamide (AEA-1, 1 mg/kg; and AEA-2, 2 mg/kg); and 2-arachidonoyl glycerol (2-AG-0.5, 0.5 mg/kg; and 2-AG-2, 2 mg/kg). AEA and 2-AG had no emetic actions when given alone. (**B**) Episodes of emesis after M6G alone; or with the transport inhibitor (VDM11-0.5, 0.5 mg/kg; and VDM11-2, 2 mg/kg); paired ineffective doses of VDM11 and 2-AG (0.5 mg/kg); an FAAH inhibitor URB 597 (3 mg/kg). (**C**) Activity during the 60-min observation after the treatments indicated. (**D**) CB_1 antagonist AM251 (5 mg/kg) reversed the effects of anandamide (AEA, 2 mg/kg), 2-AG (2 mg/kg), and VDM11 (2 mg/kg). In contrast, the CB_2 antagonist AM630 (5 mg/kg) did not reverse the effect of AEA (2 mg/kg), but effectively reversed the action of 2-AG (2 mg/kg) and VDM11 (2 mg/kg). In the presence of AM630 (5 mg/kg), there were 3.4 ± 0.7 emetic episodes ($n = 5$) in animals given a lower dose of AEA (1 mg/kg), which is not significantly different from the 2.8 ± 1.3 emetic episodes ($n = 5$) in the absence of AM630. AM251 and AM630 had no emetic actions when given alone. AM630 did not potentiate the effects of M6G, whereas AM251 enhanced emesis as previously described (*17*). Results are expressed as percentage of number of episodes of emesis induced by M6G. *Significant differences compared with M6G alone, $P < 0.05$. Bars represent mean ± SEM.

Although these data were strongly indicative of the actions of 2-AG at CB_2 receptors, it was important to evaluate whether endogenously released endocannabinoids reduce emesis through an action at CB_2 receptors. We used two approaches that would raise endocannabinoid levels in the brain. First, we tested whether the selective endocannabinoid reuptake inhibitor VDM11 (*20*) inhibited emesis. Second, we tested whether an FAAH inhibitor (URB 597) (*21*) reduced emesis. In both cases, we blocked or reduced the extent of emesis induced by M6G (Fig. 2). We extended these studies to find whether VDM11 would potentiate the effects of 2-AG. We used doses of VDM11 and 2-AG that alone did not significantly reduce emesis. When VDM11 was given together with 2-AG, we found a significant attenuation in the number of emetic episodes (Fig. 2). URB 597 strongly sedated animals, which suggested that this compound may selectively enhance anandamide levels. Conversely, VDM11 had no sedative effects, and the antiemetic effects were reversed by both AM251 and AM630, which suggested that VDM11 may preferentially affect 2-AG levels.

If the arguments made above were correct and if endocannabinoids undergo increased turnover in response to an emetic stimulus, treatment with VDM11 or URB 597 would be expected to increase the levels of endocannabinoids in the brainstem. We investigated this using a model of emesis under anesthetized conditions, so that the brains could be rapidly removed and frozen in order to limit the inherent instability of endocannabinoids in tissue samples (*14*). Ferrets were given hypertonic saline as an emetic stimulus because M6G is an inconsistent emetic in anesthetized animals. Levels of anandamide and total arachidonoyl glycerol [which reflect tissue 2-AG levels (*14*)] were measured in the brainstem and, for comparison, the cerebellum. Levels of endocannabinoids in the ferret under basal conditions or after emesis were comparable to levels previously found in rodents (Fig. 3). As expected from the pharmacological experiments described above, VDM11 specifically increased levels of total arachidonoyl glycerol in the brainstem and cerebellum, whereas pretreatment with URB 597 only increased the levels of anandamide in the brainstem.

These results led us to investigate whether selective CB_2 receptor agonists reduced emesis. We observed no statistically significant reductions in emesis in animals given the CB_2 receptor agonists AM1241 (1 or 2 mg/kg) or JWH 133 (1 or 5 mg/kg) before M6G (*22*). This finding was not completely surprising, as inhibitors of endocannabinoid inactivation can be more efficacious than "direct" agonists (*23*–*25*). Furthermore, these data suggest that CB_2 receptor activation alone is not sufficient to inhibit emesis and that, under appropriate conditions, for example, those produced by inhibiting endocannabinoid inactivation, the CB_2 receptor can be activated in local brain regions together with CB_1 receptors and can inhibit emesis. This hypothesis was supported by a significant reduction in episodes of emesis (7.1 ± 0.5 to 5.0 ± 0.7; $n = 6$ to 10; $P < 0.05$) when anandamide (0.5 mg/kg) and AM1241 (1 mg/kg) were administrated together at doses that were not antiemetic when either compound was given alone with M6G.

The behavioral evidence cited above is not a direct measure of neuronal activation and does not directly show functionally active CB_2 receptors in the brainstem. To determine whether CB_2 receptor agonists can activate neurons of the DMNX, we investigated the expression of phosphorylated extracellular signal–regulated kinase 1/2 (pERK) in rat DMNX neurons by immunohistochemistry (*14*), because phosphorylation of this enzyme is enhanced by cannabinoid agonists in other regions of the brain and in cell lines (*26*, *27*). Administration of the CB_2 receptor agonist AM1241 increased pERK in DMNX neurons when compared with vehicle-treated controls (Fig. 4).

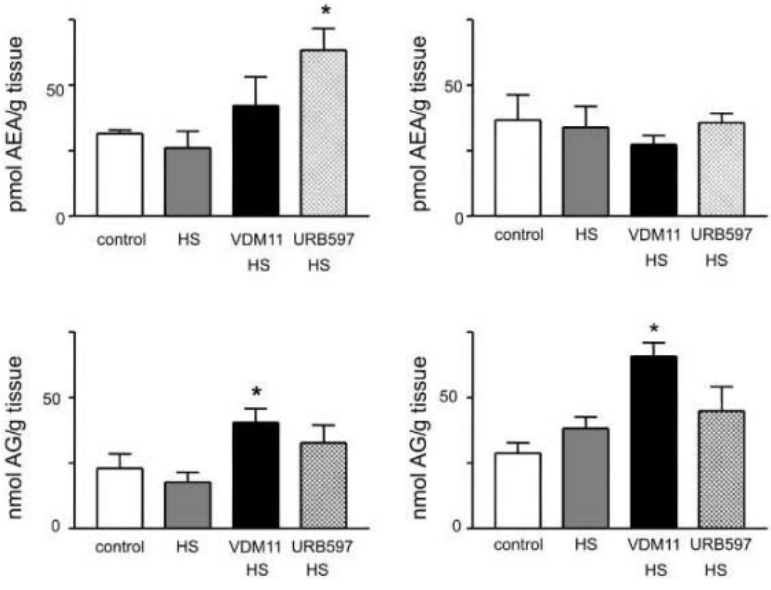

Fig. 3. Endocannabinoid levels in the ferret brainstem (**left**) and cerebellum (**right**). Control ferrets received intragastric normal saline ($n = 4$ to 7). After the emetic stimulus intragastric hypertonic saline (HS), levels were not significantly increased. URB597 (5 mg/kg) increased anandamide (AEA) levels in the brainstem but not in the cerebellum. VDM11 (3 mg/kg) increased total arachidonoyl glycerol (1-AG and 2-AG, 1AG accounts for about 20% and 2-AG about 80% of total) in both the brainstem and cerebellum when compared with the HS group ($P < 0.05$).

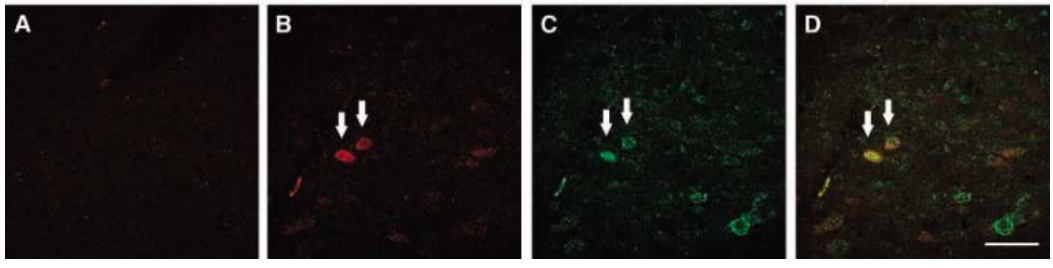

Fig. 4. A CB_2 receptor agonist activates neurons in the dorsal motor nucleus of the vagus (DMNX) of the rat. Immunoreactivity for pERK in rats treated with vehicle (**A**) ($n = 3$) and (**B**) the selective CB_2 receptor agonist, AM1241 (1 mg/kg; $n = 7$). AM1241 stimulated the expression of 5.6 ± 1.2 pERK immunoreactive cells per section in the DMNX compared with 1.2 ± 0.2 pERK immunoreactive cells in vehicle-treated animals. pERK immunoreactive cells were also observed in the nucleus of the solitary tract (not shown on figure). pERK immunoreactivity (red) was observed in nuclei and cytoplasm of activated cells. (**C**) CB_2 receptor immunoreactivity (green) was observed on the cell membrane and in the cytoplasm of DMNX neurons. (**D**) Overlay of pERK and CB_2 receptor illustrate the presence of pERK in neurons that express the CB_2 receptor (arrows). pERK immunoreactivity was observed in about 15 to 20% of the CB_2 immunoreactive neurons. Scale bar, 50 μm.

We have shown that CB_2 receptors are present in the brainstem and also in the cortex and cerebellum. As inferred by the use of a selective CB_2 antagonist, the brainstem receptors are functionally coupled to inhibition of emesis when costimulated with CB_1 receptors by an endogenous cannabinoid capable of activating both receptors. The extent of participation of CB_2 receptors in this effect is sufficient to reduce the widespread behavioral actions associated with the administration of CB_1 agonists. However, generalized activation of CB_2 receptors leads to immunosuppression (*28*) and is potentially deleterious if used as a therapy. Others have suggested that modulating the endocannabinoid system in the CNS represents a promising strategy for therapies for CNS disorders (*29*). Our observations suggest that targeting specific local populations of cannabinoid receptors (both CB_1 and CB_2) by enhancing endocannabinoid levels where they are released represents a therapeutic strategy that may be useful in disorders where either CB_1 or CB_2 receptor activation alone would not be desirable. This approach would circumvent the psychotropic and immunosuppressive side effects of exogenously administered cannabinoids and would provide an alternative approach for the therapeutic utilization of this unique neuroregulatory system.

References and Notes

1. V. Di Marzo, M. Bifulco, L. De Petrocellis, *Nat. Rev. Drug Discov.* **3**, 771 (2004).
2. A. C. Howlett *et al.*, *Pharmacol. Rev.* **54**, 161 (2002).
3. L. De Petrocellis, M. G. Cascio, V. Di Marzo, *Br. J. Pharmacol.* **141**, 765 (2004).
4. T. P. Dinh *et al.*, *Proc. Natl. Acad. Sci. U.S.A.* **99**, 10819 (2002).
5. T. F. Freund, I. Katona, D. Piomelli, *Physiol. Rev.* **83**, 1017 (2003).
6. T. W. Klein *et al.*, *J. Leukoc. Biol.* **74**, 486 (2003).
7. S. D. Skaper *et al.*, *Proc. Natl. Acad. Sci. U.S.A.* **93**, 3984 (1996).
8. E. Nunez *et al.*, *Synapse* **53**, 208 (2004).
9. S. A. Golech *et al.*, *Brain Res. Mol. Brain Res.* **132**, 87 (2004).
10. C. Benito *et al.*, *J. Neurosci.* **25**, 2530 (2005).
11. C. Benito *et al.*, *J. Neurosci.* **23**, 11136 (2003).
12. G. Griffin, Q. Tao, M. E. Abood, *J. Pharmacol. Exp. Ther.* **292**, 886 (2000).
13. S. M. Brown, J. Wager-Miller, K. Mackie, *Biochim. Biophys. Acta* **1576**, 255 (2002).
14. Materials and methods are available as supporting material on *Science* Online.
15. I. Matias *et al.*, *Eur. J. Biochem.* **269**, 3771 (2002).
16. M. D. Van Sickle, Q. J. Pittman, K. A. Sharkey, unpublished observations.
17. A. V. Derbenev, T. C. Stuart, B. N. Smith, *J. Physiol.* **559**, 923 (2004).
18. M. D. Van Sickle *et al.*, *Gastroenterology* **121**, 767 (2001).
19. P. J. Hornby, *Am. J. Med.* **111** (suppl. 8A), 106S (2001).
20. L. De Petrocellis, T. Bisogno, J. B. Davis, R. G. Pertwee, V. Di Marzo, *FEBS Lett.* **483**, 52 (2000).
21. D. Fegley *et al.*, *J. Pharmacol. Exp. Ther.* **313**, 352 (2005).
22. M. D. Van Sickle, J. S. Davison, K. A. Sharkey, unpublished observations.
23. G. Marsicano *et al.*, *Science* **302**, 84 (2003).
24. S. Gaetani, V. Cuomo, D. Piomelli, *Trends Mol. Med.* **9**, 474 (2003).
25. J. P. Chhatwal, M. Davis, K. A. Maguschak, K. J. Ressler, *Neuropsychopharmacology* **30**, 516 (2005).
26. E. Valjent *et al.*, *Proc. Natl. Acad. Sci. U.S.A.* **102**, 491 (2005).
27. M. Bouaboula *et al.*, *Eur. J. Biochem.* **237**, 704 (1996).
28. T. W. Klein *et al.*, *J. Leukoc. Biol.* **74**, 486 (2003).
29. B. F. Cravatt, A. H. Lichtman, *Curr. Opin. Chem. Biol.* **7**, 469 (2003).
30. N. E. Buckley *et al.*, *Eur. J. Pharmacol.* **396**, 141 (2000).

31. We thank L. Oland, W. Ho, and N. Shariat for excellent technical support and animal care. Q.J.P., J.S.D., and K.A.S. were supported by the Canadian Institutes of Health Research (CIHR); K.D.P. by a CIHR group grant in leukocyte trafficking; L.J.M. by GM15431; and K.M., N.S., A.M., and D.P. by U.S. National Institutes of Health. M.D.V.S. is an Alberta Heritage Foundation for Medical Research (AHFMR) graduate student; M.D. is an AHFMR and Canadian Association of Gastroenterology/CIHR/Janssen-Ortho postdoctoral fellow; K.D.P. holds a Canada research chair and is an AHFMR senior scholar; and Q.J.P. and K.A.S. are AHFMR medical scientists.

Supporting Online Material
www.sciencemag.org/cgi/content/full/310/5746/329/DC1
Materials and Methods
Fig. S1
References

6 June 2005; accepted 9 September 2005
10.1126/science.1115740

Observing Others: Multiple Action Representation in the Frontal Lobe

Koen Nelissen,[1] Giuseppe Luppino,[2] Wim Vanduffel,[1,3] Giacomo Rizzolatti,[2] Guy A Orban[1]*

Observation of actions performed by others activates monkey ventral premotor cortex, where action meaning, but not object identity, is coded. In a functional MRI (fMRI) study, we investigated whether other monkey frontal areas respond to actions performed by others. Observation of a hand grasping objects activated four frontal areas: rostral F5 and areas 45B, 45A, and 46. Observation of an individual grasping an object also activated caudal F5, which indicates different degrees of action abstraction in F5. Observation of shapes activated area 45, but not premotor F5. Convergence of object and action information in area 45 may be important for full comprehension of actions.

Understanding actions performed by others is a fundamental social ability. There is now wide consensus that the activation of the motor system is a necessary requisite for this ability. A mere visual representation, without involvement of the motor system, provides a description of the visible aspects of the movements of the agent, but does not give information critical for understanding action semantics, i.e., what the action is about, what its goal is, and how it is related to other actions (*1*, *2*). Action information, however, without knowledge about the identity of the object acted upon, is not sufficient to provide a full understanding of the observed action. Only when information about the object identity is added to the semantic information about the action can the actions of other individuals be completely understood (*3*).

The functional properties of a set of neurons in monkey ventral premotor cortex (area F5) provide evidence for the involvement of the motor system in action understanding. These "mirror" neurons discharge both when the individual performs an action and when the individual observes another person performing the same action (*4*, *5*). They therefore match the observed action with its internal motor representation. F5 neurons responding to the observation of grasping respond equally well when a piece of food or a solid object of similar size and shape is being grasped. The object's identity appears to be ignored in F5 (*4*, *5*).

We used fMRI in five awake monkeys (M1, M3 to M6) (*6*–*9*) to test how actions performed by others are represented in the monkey frontal lobe. In experiment 1, we intended to localize the frontal lobe regions involved in action observation. Monkeys saw video clips showing a full view of a person grasping an object ("acting person"), or an isolated hand grasping objects ("hand action") and static single frames or scrambled videos as controls. The acting person movies approximate the visual stimulation used in F5 single-cell studies (*4*, *5*) and provide context information that is lacking in the hand action movies, which has been used in most human

[1]Laboratorium voor Neuro-en Psychofysiologie, Katholieke Universiteit Leuven Medical School, Leuven, Belgium. [2]Dipartimento di Neuroscienze, Università di Parma, via Volturno 39, 43100 Parma, Italy. [3]Massachusetts General Hospital, Massachusetts Institute of Technology, Harvard Medical School, Athinoula A. Martino's Center for Biomedical Imaging, Charlestown, MA 02129, USA.

*To whom correspondence should be addressed. E-mail: guy.orban@med.kuleuven.ac.be

imaging studies of action observation (*10*). The aim of experiment 2 was to identify areas combining shape sensitivity with sensitivity for action observation and to demonstrate selectivity for action observation as opposed to mere sensitivity for motion. The main stimuli in this experiment consisted of shapes, hand actions, and stationary and moving objects. In experiment 3, we examined whether the activation by action observation requires human effectors and the presence of an object. Monkeys viewed videos showing human and robot hands grasping and human hands performing a grasp with (goal-directed actions) and without an object (mimicked actions), as well as their static controls in two by two factorial designs (*11*).

Both a constrained analysis using anatomically defined regions of interest (ROIs) and the unconstrained statistical parametric mapping (SPM) analysis revealed multiple frontal regions involved in action observation. The unconstrained analysis (Fig. 1; fig. S1) revealed three local maxima in the frontal lobe for the contrast observation of hand actions versus static and scrambled controls. One local maximum (arrow 1, Fig. 1A) appears to include both banks of the arcuate sulcus (inferior branch), and two maxima are located on the cortical convexity. The most medial (arrow 2 in Fig. 1A) of these two activation sites most likely corresponds to area 46, and the lateral one (arrow 3 in Fig. 1A) to area 45A (*12*, *13*).

The spatially constrained ROI analysis concentrated on the arcuate region, which we characterized architectonically (Fig. 2; fig. S2). The following architectonic fields were distinguished (*14*): area F5 convexity (F5c), F5 "posterior sector of posterior bank" (F5p), F5 "anterior sector of posterior bank" (F5a), and area 45B (*13*, *14*). This parcellation provided the anatomical basis for defining four ROIs (Fig. 1C) used for statistical analysis.

In experiment 1, observation of hand action, compared with static or scrambled controls, produced significant magnetic resonance (MR) signal increases in F5p, F5a, and 45B, both in the group and single subjects (Fig. 3 left; figs. S3 and S4, table S1). Observation of an acting person (Fig. 3, right; fig. S1) revealed significant signal increases in the same regions. In addition, the latter stimuli activated area F5c, the F5 sector where mirror neurons have been described (*4*). The interaction between type of action (hand or person) and conditions (action, scramble, or static) was significant in F5c (table S1).

In experiment 2, we compared sensitivity for action observation with that for shape and motion. The observation of hand actions replicated the findings of experiment 1 (Fig. 4, left column; table S2). Viewing static intact shapes (*8*, *15*) versus scrambled shapes activated area 45B, but none of the subdivisions of area F5 (Fig. 4, middle column; table S2). The interaction between ROIs and conditions (intact and scrambled shapes) was significant (*14*), indicating that, indeed, 45B differed from all three premotor ROIs with respect to shape sensitivity. These static shapes also activated putative area 45A on the cortical convexity (Fig. 1B). Similar results were obtained in the control test with the static and

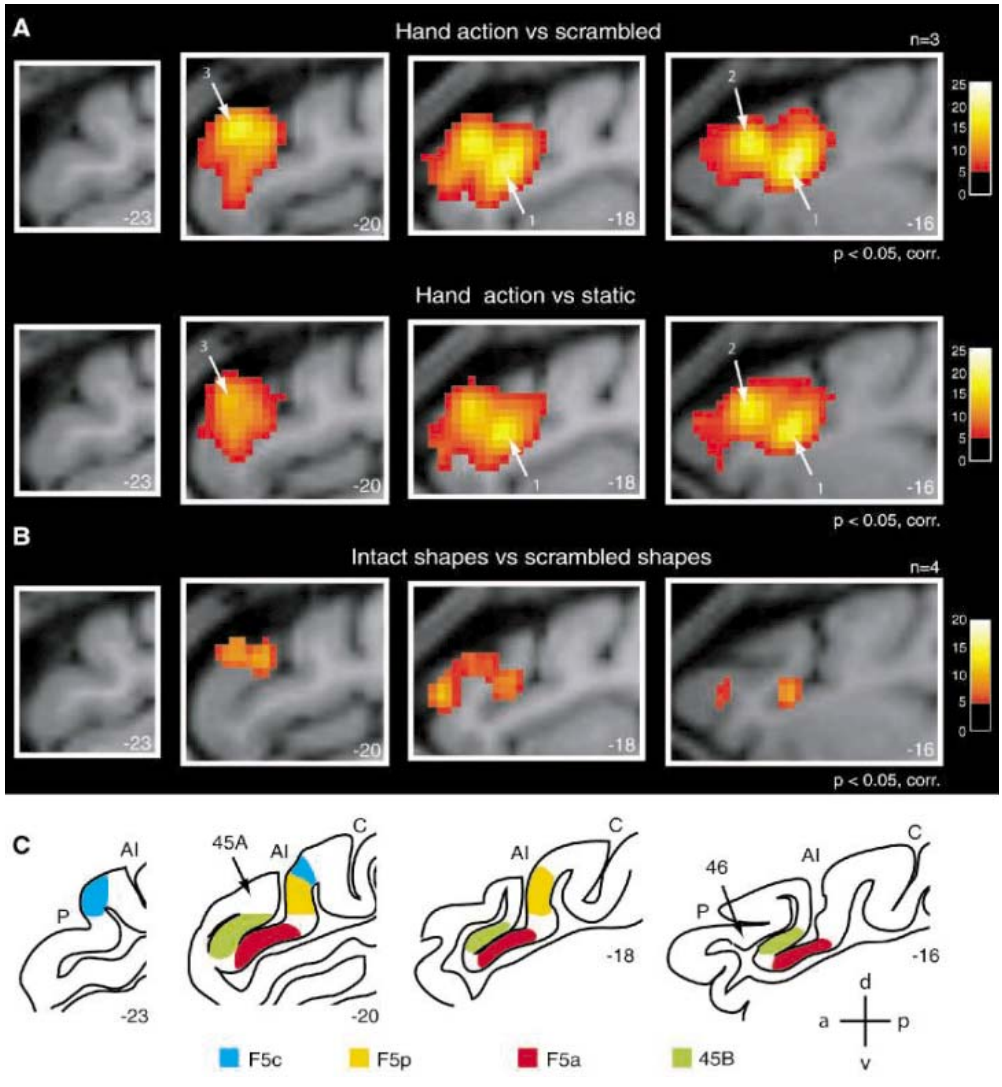

Fig. 1. (**A**) SPMs plotting voxels (colored red to yellow), which were significantly ($P < 0.05$, corrected for multiple comparisons) more active when monkeys viewed actions of the isolated hand compared with viewing their scrambled counterpart (upper row) or their static control (lower row) in the group of three monkeys (M1, M3, M5) superimposed on sagittal sections through the left hemisphere of M3, at levels ranging from –23 to –16. (**B**) SPMs plotting voxels (colored red to yellow), which were significantly ($P < 0.05$ corrected) more active when monkeys (group: M1, M3, M4, M5) viewed intact compared with scrambled images of objects, superimposed on sagittal sections through the left hemisphere of M3, at same levels as in (A). (**C**) Schematic representation of the four ROIs on four sagittal sections through M3's brain at same levels as in (A) and (B). P, principal sulcus; AI, arcuate sulcus inferior ramus; C, central sulcus; d, dorsal; v, ventral; a, anterior; and p, posterior. In (A), arrows point to local maxima in the arcuate sulcus (arrow 1), area 46 (arrow 2); and 45A (arrow 3).

moving shapes (*14*). Comparison of hand actions and motion of the grasped object with their static counterparts (Fig. 4, right column) (*14*) revealed a significantly larger difference in activation in both F5a and area 45B for observation of actions than for viewing of moving objects, relative to their respective static controls. Finally, a further control test for motion sensitivity in general showed that F5a and 45B hardly respond to optic flow stimuli, which are known to drive area MT/V5 and its satellites in the superior temporal sulcus (*14*).

In experiment 3, we attempted to clarify the nature of the action observation signals in the four ROIs. Observation of grasping performed by the robot hand activated both F5a and 45B (fig. S5, left column). The interaction between human and robot actions was significant in F5a, with stronger activation for human than for robot actions compared with their controls. No interaction was found in 45B (fig. S5, left column). Observation of mimicked human actions also activated both F5a and 45B (fig. S5, right column). The interaction between mimicked and goal-directed actions was significant in 45B, but not in F5a. In 45B, the signal was significantly stronger, compared with static controls, during goal-directed action than during mimicked action (fig. S5, right column).

Single-neuron studies (*4*, *5*) have shown that the observation of others' actions activates neurons in F5c. In the present study, the fMRI technique provided a more complete description of the frontal areas activated by action observation. They include premotor area F5, which appears to house at least two distinct representations (F5c and F5a), and prefrontal areas 45B, 45A, and 46 [(*12*), for taxonomy (*14*)]. Also, human fMRI studies have shown that action observation evokes widespread frontal activation, including that of premotor area 6 and of prefrontal areas 44 and 45 (*10*).

The two premotor representations differ in their properties. F5c is active only when the observer sees an action that includes a view of its agent. The observation of a grasping hand alone is insufficient. Note that the mirror neurons were discovered and subsequently studied by testing them with the experimenter in full view (*4*, *5*, *16*). The second F5 action representation (F5a), located in the depth of the arcuate sulcus, appears to code actions in a less context-dependent way. The observation of an isolated arm action is already an effective stimulus for this representation. Similarly, the observation of a mimicked action, which is not effective in activating F5c (*4*), is as effective in F5a as is the observation of a goal-directed action. Finally, the observation of a grasping action performed by a robot hand, although less effective than the observation of a similar action performed by a human hand, also evokes a significant signal increase in F5a. Thus, the basic essence of grasping appears to be coded here, regardless of three facts: (i) that the coded action is without object, (ii) that there is no view of the action's agent, and even, (iii) that the grasping is done by an artificial device.

There are no single-neuron data available on the motor properties of F5a. Yet, considering its architectonic organization and the general properties of premotor areas, it is likely that F5a neurons have motor properties (*17*). Thus, the F5a action representation could be considered part of the mirror neuron system (*18*), like the F5c representation, but with more abstract, less context-related or less detailed properties.

Area 45B was among the frontal regions activated by action observation. Unlike all subdivisions of F5, it is activated not only by observation of an action, but also by observation of images of objects. Neurons, named canonical neurons, have previously been described in F5 that respond to real, graspable 3-D objects (*19*). These neurons are known to play an important role in the visuomotor transformation for grasping, but they do not appear to have any role in objects' identification. This view is consistent with our finding that none of the subdivisions of F5 was activated by the shape stimuli used in the present study (Fig. 4, middle column), with the exception of images of small graspable objects in Fig. 4 (right column, top panel). The small object activation in F5c might represent the signal of the canonical neurons and may indicate how to perform an action with the object. The difference between 45B and F5 in response to object images is consistent with their connection pattern with the posterior cortical areas. Area F5 receives its main visual input from the anterior intraparietal (AIP) area and PF-PFG areas in the inferior parietal lobule (*20*, *21*), where objects are described for pragmatic purposes (*22*, *23*), whereas area 45B is strongly connected with the inferotemporal cortex (*24*), where objects are described for the purpose of identification or recognition (*25*). Furthermore,

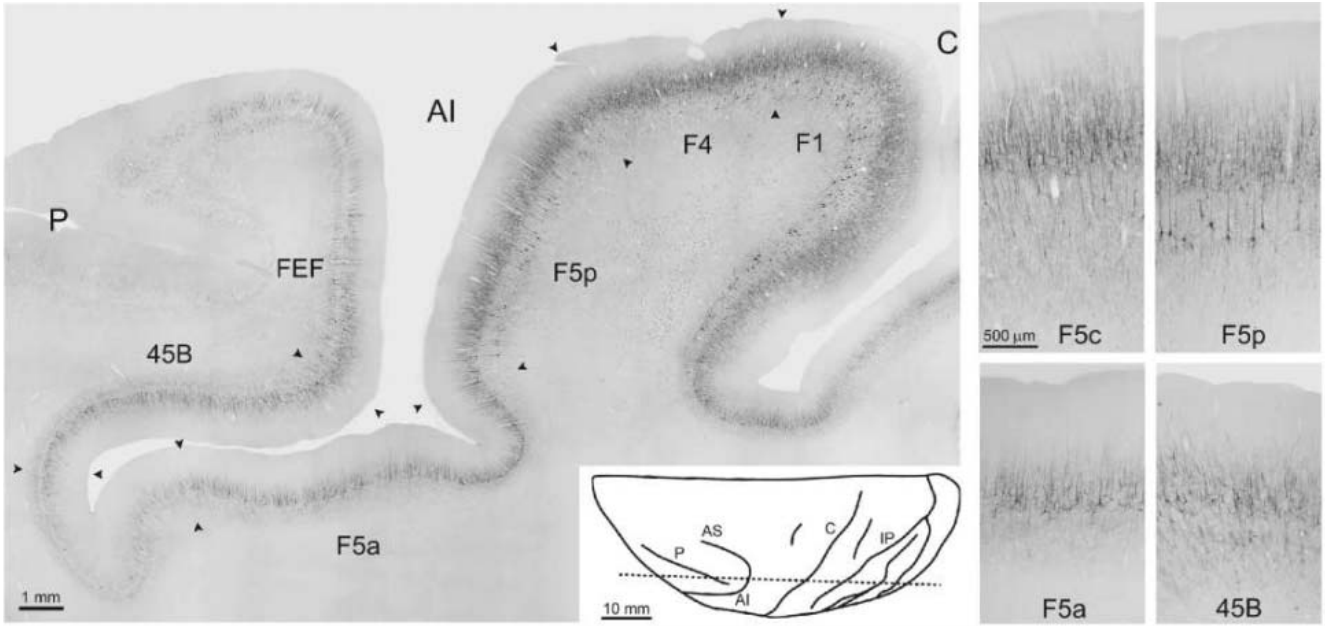

Fig. 2. Architectonic subdivisions of ventral premotor and prearcuate cortices. (**Left**) Low-power microphotograph of a sagittal section of M4 cortex stained for SMI-32 immunoreactivity showing areas F1, F4, F5p, F5a, 45B, and frontal eye field (FEF). The level of the section is indicated by the dashed line on the brain drawing shown in the inset. P, principal sulcus; AI, arcuate sulcus inferior ramus; AS, arcuate sulcus superior ramus; C, central sulcus; and IP, intraparietal sulcus. (**Right**) Higher magnification views of areas F5c, F5p, F5a, and 45B. F5c is taken from a more lateral section shown in fig. S2.

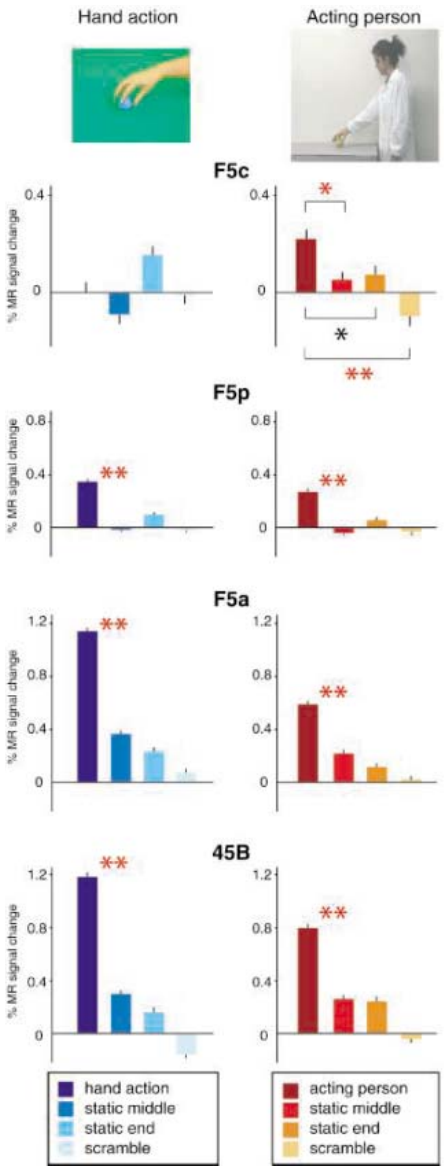

Fig. 3. Activity profiles of the four anatomically defined ROIs in experiment 1. The MR signal change (as a percentage) compared with fixation baseline (group data, $n = 2$) is plotted for the observation of the action and the observation of the three control stimuli: static hand selected from the middle of the action sequence (static middle), static hand at the end of sequence (static end), and scrambled video (scramble), for hand action videos in the left column and acting person videos in the right column (indicated by frame inset). Vertical bars indicate standard errors of the mean (SEMs) across functional volumes. Double red asterisks indicate that the action condition differed at the $P < 0.001$ corrected level from all three control conditions in both temporal and spatial statistics (see methods). In F5c, the acting person condition differed significantly from its three control conditions, but at different levels: $P < 0.001$ corrected from scrambled, $P < 0.05$ corrected from static middle, and $P < 0.05$ uncorrected from static end in the temporal statistic and $P < 0.001$ corrected for all three controls in the spatial statistics.

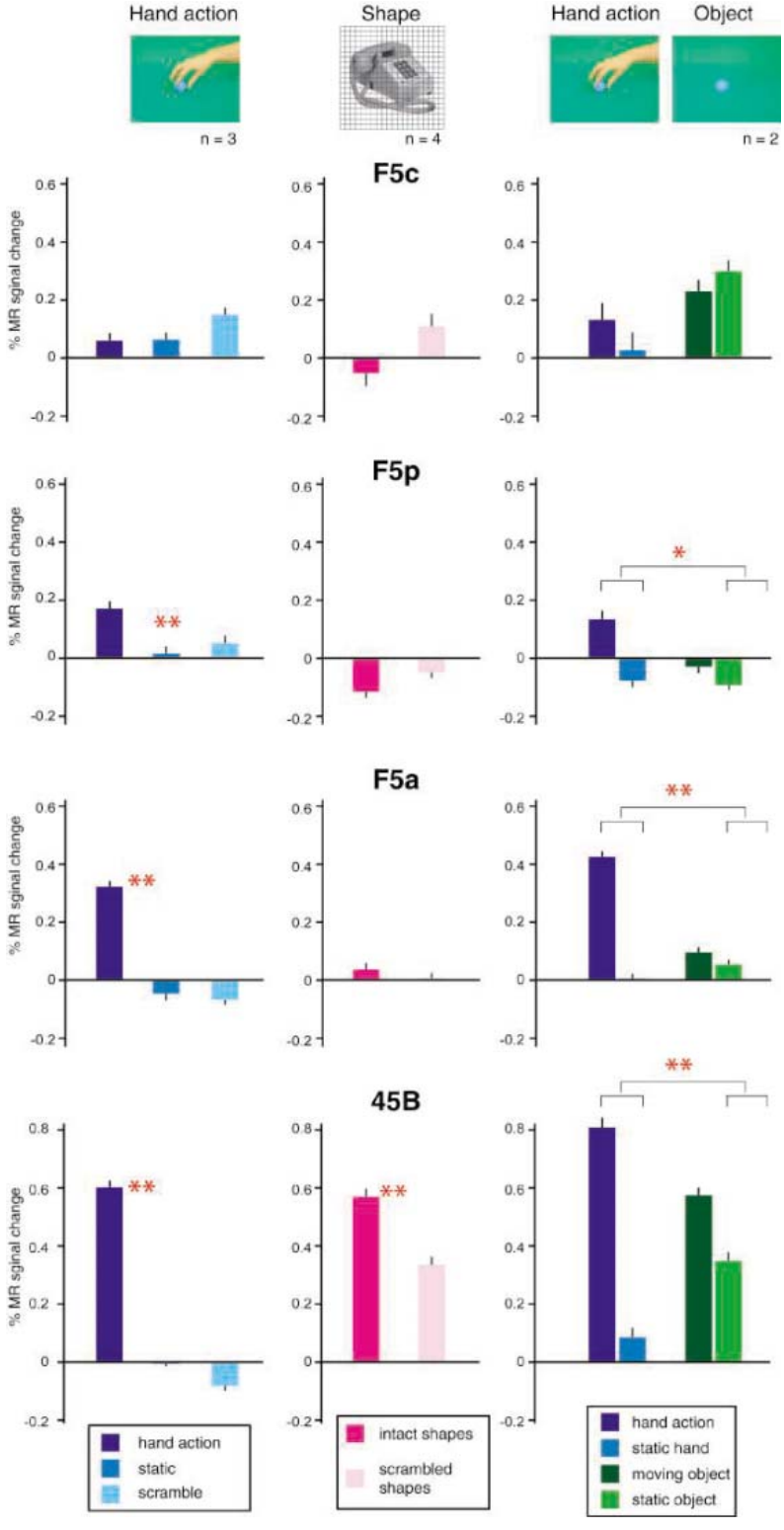

Fig. 4. Activity profiles of the four ROIs in experiment 2. (**Left**) The percent MR signal change compared with fixation baseline is plotted for the observation of the hand action and the observation of static hands selected from the middle of the action sequences and scrambled video. (**Middle**) The percent change in MR activity compared with fixation baseline is plotted for observation of intact and scrambled images of objects (average of gray scale images and drawings). (**Right**) The MR activity change compared with fixation baseline is plotted for the action observation, observation of graspable object motion, and their static controls. Same conventions as in Fig. 3; n indicates number of monkeys in the different tests (group analysis). Double and single red asterisks, respectively, indicate significance at $P < 0.001$ corrected (both statistics) and at $P < 0.05$ corrected (both statistics). It is worth noting that the activation by the static object was significantly larger than that by the static hand in area 45B ($P < 0.001$ corrected for temporal and $P < 0.05$ corrected for spatial statistics).

shapes such as those used in the present study were shown to strongly activate inferotemporal cortex, with little or no activation in AIP or PF-PFG (*8*).

In conclusion, the frontal lobe of the monkey hosts multiple representations of others' actions. The representation located in the caudal part of F5 (*14*) is context dependent and is activated only when the agent is seen, whereas the representations located in rostral F5 and in the prefrontal lobe code the action as such. Furthermore, the activation of 45B is little influenced by which agent (human hand or robot hand) performs the action, whereas in rostral F5, the observation of human hand action is more effective. Finally, vision of shapes in general, whether images of graspable or not graspable objects, activated 45B, but not area F5.

In humans, areas 44 and 45, the areas considered the homologs of F5a and 45, respectively (*13*, *14*, *26*), play a fundamental role in speech. Language typically describes actions in abstract terms. For example, the sentence "a hand grasping an apple" does not specify any characteristics of the hand, of the apple, nor of the movements bringing the hand to the object. In contrast, all these aspects are inherent to the visual and visuomotor representations of the same action. Thus, it is plausible that the transition, in the monkey frontal lobe, from context-dependent descriptions in F5c to more abstract descriptions in F5a and 45B represents the ancient prelinguistic basis from which the abstract description of an action, necessary for language, evolved. In turn, the action plus the shape description found in area 45B, could be seen as the prelinguistic link between the verb and the object. As Lieberman (*27*) wrote: "it is there (where action is represented), not in the remote recesses of cognitive machinery, that the specifically linguistic constituents make their first appearance." Our findings support this contention.

References and Notes

1. G. Rizzolatti, L. Fogassi, V. Gallese, *Nat. Rev. Neurosci.* **2**, 661 (2001).
2. M. Jeannerod, *Int. J. Sport Exerc. Psychol.* **2**, 376 (2004).
3. R. Saxe, S. Carey, N. Kanwisher, *Annu. Rev. Psychol.* **55**, 87 (2004).
4. V. Gallese, L. Fadiga, L. Fogassi, G. Rizzolatti, *Brain* **119**, 593 (1996).
5. G. Rizzolatti, L. Fadiga, V. Gallese, L. Fogassi, *Brain Res. Cogn. Brain Res.* **3**, 131 (1996).
6. The state of wakefulness is a condition indispensable for obtaining activations in parieto-frontal circuits.
7. W. Vanduffel *et al.*, *Neuron* **32**, 565 (2001).
8. K. Denys *et al.*, *J. Neurosci.* **24**, 2551 (2004).
9. M. Koyama *et al.*, *Neuron* **41**, 795 (2004).
10. G. Rizzolatti, L. Craighero, *Annu. Rev. Neurosci.* **27**, 169 (2004).
11. The human hand actions (as opposed to robot) and the goal-directed hand actions (as opposed to mimicked actions) in experiment 3 were identical to the hand actions in experiment 2.
12. The attribution of the two sites on the frontal convexity to area 46 and 45A is only tentative. For this reason, the description of more detailed properties will be limited to those areas for which we defined anatomical ROIs.
13. M. Petrides, D. N. Pandya, *Eur. J. Neurosci.* **16**, 291 (2002).
14. Material and Methods and SOM text are available as supporting material on *Science* Online.
15. Z. Kourtzi, N. Kanwisher, *J. Neurosci.* **20**, 3310 (2000).
16. E. Kohler *et al.*, *Science* **297**, 846 (2002).
17. M. Petrides, G. Cadoret, S. Mackey, *Nature* **435**, 1235 (2005).
18. S. J. Blakemore, C. Frith, *Neuropsychologia* **43**, 260 (2005).
19. A. Murata *et al.*, *J. Neurophysiol.* **78**, 2226 (1997).
20. G. Luppino, A. Murata, P. Govoni, M. Matelli, *Exp. Brain Res.* **128**, 181 (1999).
21. M. Petrides, D. N. Pandya, *J. Comp. Neurol.* **228**, 105 (1984).
22. H. Sakata, M. Taira, *Curr. Opin. Neurobiol.* **4**, 847 (1994).
23. M. Jeannerod, M. A. Arbib, G. Rizzolatti, H. Sakata, *Trends Neurosci.* **18**, 314 (1995).
24. J. D. Schall, A. Morel, D. J. King, J. Bullier, *J. Neurosci.* **15**, 4464 (1995).
25. Y. Miyashita, *Annu. Rev. Neurosci.* **16**, 245 (1993).
26. G. Rizzolatti, M. A. Arbib, *Trends Neurosci.* **21**, 188 (1998).
27. A. M. Lieberman, *Haskins Lab. Status Rep. Speech Res.* **113**, 1 (1993).

28. We thank G. Buccino, Y. Celis, A. Coeman, M. De Paep, W. Depuydt, C. Fransen, P. Kayenbergh, and G. Meulemans for technical support and J. Durand, H. Sawamura, and C. Wardak for help with the scan sessions. We are grateful to L. Fogassi, S. Grafton, P. Janssen, S. Raiguel, and R. Vogels for invaluable comments on the manuscript. This study is supported by grants GOA 2005/18, IUAP 5/04, FWO G 0151.04, EU projects QLGR-CT-2002-00746 and IST-FET-001917 (Neurobotics). The Laboratoire Guerbet (Roissy, France) provided the contrast agent (Sinerem).

Supporting Online Material

www.sciencemag.org/cgi/content/full/310/5746/332/DC1
Materials and Methods
SOM Text
Figs. S1 to S7
Tables S1 and S2
Movies S1 to S8
References and Notes

1 June 2005; accepted 5 September 2005
10.1126/science.1115593

Career advice, insight and tools.

Turn to the experts for the big picture.
Visit www.ScienceCareers.org

Your career is too important to leave to chance. So to find the right job or get career advice, turn to the experts. At ScienceCareers.org we know science. And we are committed to helping take your career forward. Our knowledge is firmly founded on the expertise of *Science*, the premier scientific journal, and the long experience of AAAS in advancing science around the world. Put yourself in the picture with the experts in science. Visit www.ScienceCareers.org.

ScienceCareers.org
We know science AAAS

Gordon Research Conferences

2006 Winter and Spring Meetings

VISIT THE *frontiers of science* GO TO A GORDON CONFERENCE

GRC is a non-profit organization managed by and for the benefit of the scientific community. The 2006 Winter and Spring Gordon Research Conferences will be held in Ventura and Buellton, California in the United States and Il Ciocco in Barga, Italy.

FEES: WINTER / SPRING 2006

	Conferee			Adult Guest		
	Single	Double	Off-Site	Single	Double	Off-Site
California	$895	$800	$675	$720	$625	$500
Graduate Seminar (Bioinorganic Chemistry) *	$470	$410	$325	$470	$410	$325
Graduate Seminar (Protein Folding Dynamics)	$360	$320	$260	$360	$320	$260
Graduate Seminar (Bioanalytical Sensors)	$360	$320	$260	$360	$320	$260
Il Ciocco, Italy	$1100	$940	$730	$925	$765	$555

Conferees attending both **Metals in Biology** and the 3-day **Graduate Research Seminar on Bioinorganic Chemistry** should add $370 to the 5-day single room rate or $330 to the 5-day double room rate.

The Gordon Research Conferences web site at **http://www.grc.org/** contains the most up-to-date information we have for any given Conference. Be sure to take a look at the scientific program or any other information that has been posted. Applications to any Conference can be submitted via our web site at **http://www.grc.org/application/**. A printed form may be obtained from our web site or requested from:

Visit us on the Web at:

www.grc.org

E-mail: **grc@grc.org**
FAX: 401-783-7644
Phone: 401-783-4011, ext. 100

List of meetings with confirmed sessions/themes and speakers as of September 2005:

(discussion leaders are italicized)

AGING, BIOLOGY OF
VENTURA BEACH MARRIOTT
VENTURA, CA
JAN 29-FEB 3, 2006
MONICA DRISCOLL &
ROGER MCCARTER, CO-CHAIRS
HOLLY BROWN-BORG, ALEXANDER BUERKLE,
& LA DORA THOMPSON, CO-VICE CHAIRS

- **Keynote Lecture**
  (Tom Kirkwood)
- **The Impact of Insulin/IGF Signaling on Healthspan**
  (*Nadia Rosenthal* / Gary Ruvkun / Cynthia Kenyon / Lee Sweeney / Leonard Guarente)
- **Fat and Dietary Restriction**
  (*Steve Helfand* / Kaveh Ashrafi / Su-Ju Lin / Pere Puigserver / David Sinclair)
- **Mitochondria and Oxidative Stress**
  (*David Nicholls* / Sigfried Hekimi / Holly Van Remmen / Victor Darley-Usmar)
- **Extracellular Matrix in Aging**
  (*Pidder Janssen-Durr* / Robert Baxter / Hassy Cohen / Olivier Toussaint / William Hornebeck)
- **The Impact of Innate Immunity on the Ability to Live Long and Healthy**
  (*Marc Tatar* / Danielle Garsin / Scott Pletcher / Janet Lord)
- **Systems Networks in Aging**
  (*Daniel Promislow* / Greg Gibson / Andreas Wagner / Marie-Anne Felix / Simon Melov)
- **Vascular Function in Aging**
  (*William Sonntag* / May Reed / Sue Duckles / Gabor Kaley / Muhammad Ashraf)
- **Maintenance of MacroMolecular Integrity**
  (*Holly Brown-Borg* / *Alexander Buerkle* / *LaDora Thompson* / Jacob Moskovitz / Alfred Goldberg / Vilheim Bohr / Grace Pavlath)

BASEMENT MEMBRANES
IL CIOCCO
BARGA, ITALY
JUN 18-23, 2006
REINHARD FAESSLER, CHAIR
JEFFREY MINER, VICE CHAIR

- **Keynote Lecture**
  (Matthias Mann)
- **Structure/Biophysics of Matrix Proteins and Receptors**
  (*Martin Humphries* / Clair Baldock / Iain Campbell / Mark Yeager)
- **Genetics of BM and BM Receptors I**
  (*Lynn Sakai* / Nick Brown / Ralf Adams)
- **Proteoglycans and Signaling**
  (*Renato Iozzo* / Scott Selleck / Sumana Datta / Bjorn Olsen)
- **BM Receptors and Signaling**
  (*Elisabeth Georges-Labouesse* / Bill Wadsworth / Mary Beckerle / Cord Brakebusch)
- **Protease Activities in Matrix and Tissue Function**
  (*Mina Bissell* / Pepper Jo Schedin / John Muschler)
- **Genetics of BM and BM Receptors II**
  (*Jeff Miner* / Olivier Lefebvre / Brigid Hogan / Kevin Campbell / Roy Zent)
- **BMs in Disease**
  (*Monique Aumailley* / Paul Khavari / Lydia Sorokin)
- **BMs in Neural Development and Function**
  (*Peter Yurchenco* / Bruce Patton / Holly Colognato / Markus Ruegg)

BIOANALYTICAL SENSORS
HOLIDAY INN
VENTURA, CA
FEB 26-MAR 3, 2006
ADRIAN MICHAEL &
ZEEV ROSENZWEIG, CO-CHAIRS
CHRIS TAITT, VICE CHAIR

- **Plenary Session**
  (*Zeev Rosenzweig* / Roger Tsien / Paul Alivisatos)
- **Nucleic Acid Probes**
  (*Steven Soper* / Larry Gold / Weihong Tan / Ulf Landegren)
- **Single-Cell Analysis**
  (*Raoul Kopelman* / Norman Dovichi / Edgar Arriaga / Tuan Vo-Dinh)
- **Nanoparticles in Diagnostics I**
  (*Richard Van Duyne* / Charles Lieber / Raoul Kopelman / Naomi Halas)
- **Nanoparticles in Diagnostics II**
  (*Richard Van Duyne* / Shimon Weiss / Sandy Simon)
- **Biosensing Arrays**
  (*Thomas Joos* / Michael Heller / Shana Kelley / Joanna Albala)

- **Young Investigators**
  (*Chris Taitt* / Gavin Macbeath / Facundo Fernandez / Lin He / Stephane Petoud)
- **Biosensors for Pathogen Detection**
  Richard Durst / Jiri Homola / Antje Baeumner / Joany Jackman / Ruqin Yu)
- **Biosensors for Cancer Detection**
  Adrian Michael / Steven Soper / James Baker)

CHROMATIN STRUCTURE & FUNCTION
IL CIOCCO
BARGA, ITALY
MAY 21-26, 2006
SHARON DENT, CHAIR
PETER BECKER, VICE CHAIR

- **Chromatin Structure: The Nucleosome and Beyond**
  (*Karolin Luger* / Johnathan Widom / Tim Richmond / Daniela Rhodes / Jeff Hansen)
- **Histone Variants, Chromatin Assembly, and Repair**
  (*Mary Ann Osley* / Karolin Luger / Genevieve Almouzni / David Tremethick / Mitch Smith / Xuetong Shen / Craig Peterson)
- **Dynamic Chromatin**
  (*Ali Shilatifard* / Carl Wu / Brad Cairns / Robert Kingston / Toshio Tsukiyama)
- **Histone Modifications and Signaling**
  (*Jane Mellor* / David Allis / Shelley Berger / Tony Kouzarides / Jerry Workman / Mary Ann Osley / Michael Grunstein / Yang Shi)
- **Transcribed Chromatin**
  (*Sally Elgin* / Ali Shilatifard / Jane Mellor / Brain Strahl / Igrid Grummt)
- **Silent Chromatin**
  Susan Gasser / Robin Allshire / Shiv Grewal / Sally Elgin / Vince Pirotta / Renato Paro / Thomas Jenuwein / Danesh Moazed)
- **Chromosome Organization**
  Genevieve Almouzni / Gary Felsenfeld / Ann Dean / Bryan Turner / Uli Laemmli)
- **Nuclear Organization**
  Brian Strahl / Susan Gasser / Andy Belmont / Wendy Bickmore / Peter Fraser / Shelley Barton / Danny Reinberg / Yi Zhang)
- **Chromatin Programming in Development and Disease**
  Shelley Barton / Wolf Reik / Jill Schumacher / Patrick Grant / Bob Roeder)

COLLOIDAL, MACROMOLECULAR & POLYELECTROLYTE SOLUTIONS
FOUR POINTS SHERATON: HARBORTOWN
VENTURA, CA
FEB 5-10, 2006
ERIC KALER, CHAIR
RALPH COLBY &
ESIN GULARI, CO-VICE CHAIRS

- **Arrested Colloids**
  (Kenneth Dawson / Peter Schurtenberger)
- **Colloid Assembly and Phase Transitions**
  (*Matt Lynch* / David Pine / Hartmut Loewen / Ken Schweizer)
- **Directed Colloidal Assembly**
  David Marr / Orlin Velev / Alfons van Blaaderen)
- **Polyelectrolytes**
  Eric Furst / Tom Waigh / Matthias Ballauff / Paula Hammond)
- **Polymers in Two Dimensions**
  Shenda Baker / Maria Santore / Gerry Fuller)
- **Polymers**
  (*Seth Fraden* / Robert Prud'homme / Chi Wu / Juan de Pablo)
- **Networks and Gels**
  (*Lee Magid* / Zhen-Gang Wang / Annelise Barron)
- **Surfactants of All Sizes**
  (*Pat Spicer* / Lynn Walker / Michael Gradzielski / Dan Hammer)
- **Historical Reflections**
  (Jacob Israelachvili)

COMPOSITES
HOLIDAY INN
VENTURA, CA
JAN 15-20, 2006
ALAN LESSER, CHAIR
TON PEIJS, VICE CHAIR

- **Fracture Behavior of Composites**
  (A.J. Kinloch / Raymond Pearson / John Nairn)
- **Experimental & Theoretical Mechanics**
  (Sindee Simon / Frank R. Jones / Harry Hilton)
- **New Applications**
  (Patrick Mather / Kenneth Reifsnider / Richard Lyon)
- **Bio-Composites**
  (Peter Fratzl / Joanna Aizenberg / H. Daniel Wagner)
- **Self-Healing Composites**
  (Scott White / Anna Balazs / Jeff Moore / Fred Wudl)
- **Nanocomposite Processing**
  (Sadhan Jana)
- **Optical and Electrical Phenomena**
  (Todd Emrick / Richard Vaia / Robert J. Young)
- **Diffusion of Nanocomposites**
  (Benny Freeman)

CRANIOFACIAL MORPHOGENESIS & TISSUE REGENERATION
FOUR POINTS SHERATON: HARBORTOWN
VENTURA, CA
JAN 22-27, 2006
YANG CHAI, CHAIR
IRMA THESLEFF, VICE CHAIR

- **Evolution**
  (Ken Weiss / Jukka Jernvall / Benedikt Hallgrimsson / Daniel Lieberman)
- **Fate Determination of Neural Crest**
  (Nicole Le Douarin / Marianne Bronner-Fraser / David Raible / Paul Trainor)
- **Organogenesis**
  (Elaine Fuchs / Heiko Peters / Ken Yamada)
- **Craniofacial Patterning**
  (Anne Calof / Jill Helms / Chuck Kimmel / Marja Mikkola)
- **Craniofacial Bones**
  (Andrew Wilkie / Rob Maxson / David Rice)
- **Signaling Interactions and Morphogenesis**
  (Paul Sharpe / Phil Soriano / Jim Martin / David Ornitz)
- **Human Genetics and Dysmorphology**
  (Mary Marazita / Jeff Murray / David Fitzpatrick / Max Muenke)
- **Tissue Engineering**
  (Michael Longaker / YiPing Chen / Songtao Shi)
- **Keynote Speaker**
  (Gail Martin)

DNA DAMAGE, MUTATION & CANCER
HOLIDAY INN
VENTURA, CA
MAR 5-10, 2006
ROBERT P FUCHS, CHAIR
JOHN HAYS, VICE CHAIR

- **Keynote Lecture**
  (Alain Sarasin)
- **Spontaneous Lesions: From Structure to Biology**
  (Serge Boiteux / John Essigman / Cindy Burrows)
- **How Specialyzed DNA Polymerases Function in Lesion Bypass?**
  (Edward Loechler / Roger Woodgate)
- **Trading Places Between Replicative and Specialized DNA Polymerases**
  (Thomas Kunkel / Ellen Fanning)
- **Regulation of DNA Polymerases Switching: Ubiquitination and Other Modifications**
  (Helle Ulrich / Alan Lehmann / G. McGregor)
- **Lesion Recognition by Repair Processes**
  (Nora Goosen / John Hays / Joyce Reardon)
- **Isolation and Cellular Localization of Large Repair / Replication Complexes**
  (Akira Yasui / Leon Mullenders / Kiyoji Tanaka / Wim Vermeulen)
- **Damage Avoidance Strategies by Recombination Related Mechanisms**
- **Damage Induced Cellular Responses or Mismatch Repair Responses to DNA Lesions**

ELECTROCHEMISTRY
SANTA YNEZ VALLEY MARRIOTT
BUELLTON, CA
FEB 12-17, 2006
HECTOR ABRUNA, CHAIR
CAROL KORZENIEWSKI, VICE CHAIR

- **Inaugural Session**
  (Allen J. Bard / Royce W. Murray)
- **Molecular Electronics**
  (HongKun Park / Paul McEuen / Vladimiro Mújica)
- **Supramolecular Electrochemistry**
  (Fraser Stoddart / Josef Michl)
- **Electrocatalysis**
  (Harry Gray / Dan Nocera / Katrina Krishner)
- **Maracas and Biology**
  (Luis Echegoyen / Christian Amatore)
- **Young Punks**
  (Stefan Bernhard / Yu-Ye Tong / Sang-Bok Lee / Jeff Long)
- **Open Session**
- **Fuel Cells**
  (Helmut Baltruschat / Karen Swider-Lyons / Enrique Herrero)
- **Conducting Polymers**
  (Tobin Marks / John Reynolds)

ENVIRONMENTAL ENDOCRINE DISRUPTORS
IL CIOCCO
BARGA, ITALY
JUN 4-9, 2006
REX HESS & PAOLO MOCARELLI, CO-CHAIRS
SHANNA SWAN, VICE CHAIR

- **Keynote - Dioxin: 30 Years After Seveso** (*Rex Hess* / Linda Birnbaum / Paolo Mocarelli)
- **Transgenerational Endocrine Disruption I: Epigenetics** (*John McCarrey* / Jacquetta Trasler / Wolf Reik / Paolo Sassone-Corsi)
- **Transgenerational Endocrine Disruption II: DNA Modification and Mechanisms** *Paolo Sassone-Corsi* / Michael K. Skinner / Gail Prins / Felix Althaus)
- **Endocrine Disruption of Cell Signaling Pathways I: Cross Talk** *Richard Peterson* / Chiharu Tohyama / Michael S. Denison / Shigeaki Kato / Michael Mancini)
- **Endocrine Disruption of Cell Signaling Pathways II: Receptor Mediated** (Jan-Ake Gustafsson / Maria Luisa Brandi / Peter Thomas)
- **Experimental and Human Observations: Similarities and Differences** *Niels Skakkebaek* / Richard Sharpe / Youko Tuomisto / Vincent Markowski / Andrea Gore)
- **Metabolic Syndrome and Endocrine Disruption** *Jerry Heindel* / Angel Nadal / Retha Newbold / Alex Odermatt)
- **Non-Monotonic Dose-Response Curves and Low-Dose Effects** *Frederick S. vom Saal* / Wade Welshons / Andreas Kortenkamp / Ana Soto)
- **Stem Cells and Endocrine Disruptor Toxicology** *John McLachlan* / Angelo Vescovi / Paul De Sousa / Louis J. Guillette, Jr.)

FIBROBLAST GROWTH FACTORS IN DEVELOPMENT & DISEASE
FOUR POINTS SHERATON: HARBORTOWN
VENTURA, CA
MAR 12-17, 2006
BRADLEY OLWIN & DAVID ORNITZ, CO-CHAIRS
DAVE FERNIG, VICE CHAIR

- **Keynote Lectures** (*David Ornitz* / *Bradley Olwin* / Gail Martin / Joseph Schlessinger)
- **Carbohydrate Regulation of FGF Function** (*Alan Rapraeger* / David Fernig / Moosa Mohammadi)
- **Developmental Events Regulated by FGFs** (*Gail Martin* / Saverio Bellusci / Walace McKeehan / Kory Lavine)
- **Cellular Physiology and FGFs** (*Nobu Itoh* / Andrew Wilkie / Sabine Werner)
- **Skeletal Development** (*Gillian Morriss-Kay* / Marja Hurley / Kai Yu)
- **Diversity of FGF Signaling Pathways** (*Sabine Werner* / Enrique Amaya / Dina Ron)
- **FGF Function in the Central Nervous System** (*Juha Partanen* / Alex Joyner)
- **Patterning and FGFs** (*Claudio Basilico* / Nobu Itoh / Matthew Hoffman / Gary Schoenwolf)
- **Novel Mechanisms for FGF Function in Development and Disease** (*William Horton* / Lena Claesson-Welsh / Olivier Pourquie)

GENES & BEHAVIOR
FOUR POINTS SHERATON: HARBORTOWN
VENTURA, CA
FEB 12-17, 2006
ROBERT HITZEMANN, CHAIR
MARLA SOKOLOWSKI, VICE CHAIR

- **Introduction to Genes and Behavior** (Robert Hitzemann / *Trudy Mackay* / *Robert Gerlai* / Steve Arnold / Jonathan Flint / Andy Sih)
- **Behavioural Genetics of Social Interactions** (*Mike Ritchie* / *Felix Breden* / Michelle Arbeitman / David Clayton / Mark Blows / Chris Thompson / Elizabeth Hammock)
- **Learning and Memory** (*Martin Heisenberg* / *Brian Smith* / Frederick Mery / Ikue Mori / Abraham Palmer / Christina Alberini)
- **Personality and Temperament** (*Doug Wahlsten* / *Bill Iacono* / Judy Cameron / Andrew Holmes / Samuel Gosling / Alison Bell / HIll Goldsmith)
- **Experience, Development, and Gene Expression** (*Bill Greenough* / *Mike Meaney* / Cathy Rankin / Alison Fleming / Joel Levine / Adele Diamond)
- **Gene Networks and Behavior** (*Eric Shadt* / *Tamara Phillips* / Ralph Greenspan / Jason Wolf / Elissa Chesler / Mario de Bono / Rob Williams)
- **Data Blitz** (*Robert Anholt* / *John Crabbe*)
- **Alternative Strategies: Genetic Polymorphisms and Phenotypic Plasticity** (*Hans Hoffman* / *John Ewer* / Doug Emlen / Scott Douglas / Greg Velicer / Annelie Persson)
- **Common Threads** (*Gene Robinson* / Allen Moore / Ken Kendler)

GLYCOLIPID & SPHINGOLIPID BIOLOGY
HOLIDAY INN
VENTURA, CA
JAN 8-13, 2006
TONY FUTERMAN, CHAIR
GERRIT VAN MEER, VICE CHAIR

- **Sphingolipid Biophysics** (*Toshi Kobayashi* / *Ken Hanada* / Alicia Alonso / Rhoderick Brown)
- **Sphingolipid Biosynthesis** *Howard Riezman* / *Bob Dickson* / Yoshio Hirabayashi / Scott Summers / Yasu Igarashi / Charles Chalfant)
- **Defects in Sphingolipid Degradation** *Ed Schuchman* / *Jim Shayman* / Rick Proia / Steve Walkley)
- **Translational Aspects (I): Cancer** *Lina Obeid* / *Sandro Sonnino* / Rich Kolesnick / Besim Ogretmen / Barry Maurer / Christoph Geilen)
- **Cell Biology** (*Konrad Sandhoff* / *Thierry Levade* / Richard Pagano / Jean Greenberg)
- **Translational Aspects (II): Pathology** (*Ron Schnaar* / *Mark Kester* / Irina Petrache / Erich Gulbins / Hugh Willison / Mariana Nikolova-Karakashian)
- **Translational Aspects (III): Infectivity and Immunity** (*Maurizio Del Poeta* / *Fran Platt* / Albert Bendelac / Steven Beverley)
- **Hot Topics** (*Sarah Spiegel*)
- **Poster Talks** (*Walt Holleran* / *Steve Pfeiffer* / *Pam Fredman*)
- **Sphingolipidomics and Emerging Technologies** (*Al Merrill* / *Yusuf Hannun* / Eberhard Voit / May Wang)

GRADUATE RESEARCH SEMINAR: BIOANALYTICAL SENSORS
HOLIDAY INN
VENTURA, CA
FEB 24-26, 2006
AMANDA HAES &
BRIDGET MAHON WILLOUGHBY, CO-CHAIRS
ANDRE ADAMS, VICE CHAIR

- **Career Paths and Career Planning in the Bioanalytical Sensors Field** (*Amanda Haes* / Joanna S. Albala / Michael J. Natan / Raoul Kopelman)
- **Micro/Nano Materials** (*Bridget Mahon Willoughby*
- **Biosensor Development** (*Andre Adams*)
- **Biosensor Applications** (*Amanda Haes*)

All talks will be selected from submitted abstracts.

GRADUATE RESEARCH SEMINAR: BIOINORGANIC CHEMISTRY
FOUR POINTS SHERATON: HARBORTOWN
VENTURA, CA
FEB 2-5, 2006
ANNE REYNOLDS, CHAIR
TROY STICH, VICE CHAIR

- **Metalloprotein Folding & Structure**
- **Synthetic Models of Protein Active Sites**
- **Physical & Computational Methods**
- **Metalloenzyme Kinetics & Mechanism**
- **Metalloregulatory Proteins & Environmental Bioinorganic Chemistry**

GRADUATE RESEARCH SEMINAR: PROTEIN FOLDING DYNAMICS
FOUR POINTS SHERATON: HARBORTOWN
VENTURA, CA
JAN 6-8, 2006
CHARLES BROOKS & JANE CLARKE, CO-CHAIRS

- **Basic Principles of Experimental Studies of Protein Folding** (Jane Clarke)
- **Basic Principles of Theoretical Studies of Protein Folding** (Charles Brooks)
- **Current Topics and Controversies in Experimental Studies of Protein Folding** (Sheena Radford)
- **Current Topics and Controversies in Theoretical Studies of Protein Folding** (Joan Shea)
- **Graduate and Post Doc Talks** (to be selected from submitted abstracts)

ISOTOPES IN BIOLOGICAL & CHEMICAL SCIENCES
HOLIDAY INN
VENTURA, CA
FEB 12-17, 2006
CHARLES PERRIN, CHAIR
DANIEL QUINN, VICE CHAIR

- **Isotopic Analysis**
  (*Alexander Van Hook* /
  Marilyn L. Fogel / David M. Perrin)
- **Organic Reactions**
  (*Daniel A. Singleton* / Miguel Garcia-Garibay /
  John E. Baldwin / Weston Thatcher Borden)
- **Hydrogen Bonding**
  (*Hans Limbach* / Andy C. LiWang /
  Janez Mavri)
- **Organometallic Chemistry**
  (*Klaus Theopold* / Ged Parkin /
  Charles P. Casey / Guy Lloyd-Jones)
- **Enzyme Mechanisms**
  (*David N. Silverman* / Vernon Anderson /
  Paul F. Cook)
- **Proton Transfer**
  (*Piotr Paneth* / Thomas J. Meyer /
  Jose M. Lluch / J.T. Hynes)
- **Structure and Function Of Biomolecules**
  (*Amnon Kohen* / William Bachovchin /
  Dean A. Myles)
- **Gas-Phase Chemistry**
  Rudolph A. Marcus / Steven Kass /
  Helmut Schwarz / Mark H. Thiemans)
- **Protein Folding and Dynamics**
  John P. Richard / S. Walter Englander /
  Tobin R. Sosnick)

LIGAND RECOGNITION & MOLECULAR GATING
IL CIOCCO
BARGA, ITALY
JUN 11-16, 2006
BENJAMIN KAUPP, CHAIR
SUSAN BUCHANAN, VICE CHAIR

- **Cl- Channels and Cl- Carriers**
  (T.Y. Chen / C. Miller / M. Pusch)
- **Bacterial Carriers**
  (C. Hunte)
- **Structure of Cyclic Nucleotide-Sensitive Channels**
  (J.H. Morais-Cabral / R. Seifert /
  S.A. Siegelbaum / W.N. Zagotta)
- **Voltage-Sensing Ion Channels**
  (Rod MacKinnon / F. Bezanilla /
  D.E. Clapham)
- **Recognition in G-Protein Coupled Receptors**
  (J.L. Baneres / W.A. Hendrickson /
  M.J. Lohse)
- **Rhodopsin and Rhodopsin-Like Molecules**
  (U. Alexiev / P. Hegemann / G.F. Schertler)
- **Novel Fluorescence Techniques**
- **Unusual Signaling Pathways**
  (C. Steegborn)

MAMMARY GLAND BIOLOGY
IL CIOCCO
BARGA, ITALY
MAY 28-JUN 2, 2006
ROBERT CLARKE, CHAIR
STEVEN ANDERSON, VICE CHAIR

- **Opening Address**
  (Edison Liu)
- **Models of Mouse Development and Cancer**
  (*Paul Edwards* / Bill Muller /
  Jos Jonkers / Nicolas Kenney)
- **Breast Cancer Susceptibility and Prevention**
  (*Julian Peto* / Thea TIsty / Tony Howell)
- **Adult Mammary Gland Development**
  (*Dan Medina* / Bernt Groner /
  Jane Visvader / John Stingl)
- **Hormone and Growth Factor Signaling Pathways**
  (*Barbara Vonderhaar* /
  Steffi Osterreich / Paraic Kenney)
- **Developmental Signaling Pathways**
  (*Bob Callahan* / Cathrin Brisken /
  Caroline Alexander / Keith Brennan /
  Salvatore Pece)
- **Lactation**
  (*Steve Anderson* / Chris Ormandy /
  Peggy Neville)
- **Models of Human Development and Cancer**
  (*Christine Clarke* / Joan Brugge /
  Ole-William Petersen /
  Charlotte Kuperwasser)
- **Keynote Address**
  (Gil Smith)

MARINE NATURAL PRODUCTS
VENTURA BEACH MARRIOTT
VENTURA, CA
FEB 26-MAR 3, 2006
NOBUHIRO FUSETANI, CHAIR
PHILLIP CREWS, VICE CHAIR

- **New Methodology**
  (*William Gerwick* / Tadeusz Molinski /
  Jerzy Jaroszewski / John Blunt)
- **MNP Discovery: New Sources and New Structures**
  (*John Cardellina* / Paul Jensen /
  Kirk Gustafson / Guy Carter)
- **Drug Discovery**
  (*Valerie Bernan* / Ernesto Fattorusso)
- **Molecular Basis for Intra- and Inter-Specific Interactions**
  (*Valerie Paul* / Werner Müller /
  Georg Pohnert / Pei Yuan Qian)
- **Synthesis of Marine Natural Products**
  (*Tadeusz Molinski* / Amos Smith /
  Masaaki Miyashita / Thomas Lindel)
- **Fresh off the Bench**
  (*Yuzuru Shimizu*)
- **Biosynthesis: Enzymatic Pathways and Symbiosis**
  (*Alison Butler* / Christopher Walsh /
  Eric Schmidt / Marcel Jaspars / Russell Kerr)
- **Drug Development: Modes of Action and Supply**
  (*David Newman* / Richard Lewis /
  José Jimeno)
- **The Paul J. Scheuer Award in Marine Natural Products**

METALS IN BIOLOGY
FOUR POINTS SHERATON: HARBORTOWN
VENTURA, CA
JAN 29-FEB 3, 2006
DAVID DOOLEY, CHAIR
ROBERT SCOTT, VICE CHAIR

- **Keynote Lecture**
  (Ed Stiefel)
- **Inorganic Metabolism**
  (Peter Kroneck / Chris Rensing /
  David Richardson / Caroline Kisker)
- **Inorganic Sensing & Signaling**
  (Chuan He / Judith Burstyn / David Benson)
- **Mechanistic Bioinorganic Chemistry**
  (Marty Bollinger / Rick Finke /
  Bill Tolman / Justine Roth)
- **Metal Ions in Imaging and Therapeutics**
  (*Tom Meade* / Jonathan Sessler /
  Ralph Weissleder)
- **Applications of Theoretical & Computational Methods**
  (Tom Brunold / Eric Oldfield /
  Sharon Hammes-Schiffer / Ulf Ryde)
- **Metalloproteomics/Metallogenomics: Developing Technologies**
  (*Bob Scott* / Michael Crowder /
  Patrick Grant / Deborah Zamble)
- **Molybdenum in Biology**
  (Martin Kirk / Ralf Mendel /
  Markus Ribbe / Russ Hille)
- **Joint Session with Graduate Research Seminar**
  (*Dave Dooley* / Amy Rosenzweig

MOLECULAR & IONIC CLUSTERS
HOLIDAY INN
VENTURA, CA
FEB 19-24, 2006
MICHAEL DUNCAN &
SOTIRIS XANTHEAS, CO-CHAIRS
JEREMY HUTSON &
DAN NEUMARK, CO-VICE CHAIRS

- **Astrophysical Clusters**
  (*Bill Klemperer* / Michael McCarthy /
  John Maier)
- **Reactions and Radicals**
  (*Dan Neumark* / Marsha Lester /
  Joe Francisco / Anna Krylov)
- **Helium Droplets**
  (*Roger Miller* / Birgitta Whaley /
  Martina Havenith)
- **Metal Clusters and Complexes**
  (*Will Castleman* / Martin Jarrold /
  Atsushi Nakajima / Lai-Sheng Wang)
- **Ionic Clusters**
  (*Jim Lisy* / Masaaki Fuji / Kit Bowen)
- **Hydrogen-Bonded Networks**
  (*Ken Jordan* / Mark Johnson /
  Anne McCoy / Martin Suhm)
- **Dynamics in Clusters**
  (*Carl Lineberger* / David Nesbitt /
  Takayuki Ebata)
- **Clusters Containing Biological Molecules**
  (*Mattanjah de Vries* / Tim Zwier /
  Bernd Brutschy / Klaus Mueller-Dethlefs)
- **Intermolecular Potentials**
  (*Jeremy Hutson* / Wolfgang Domcke /
  Joel Bowman)

MOLECULAR EVOLUTION
HOLIDAY INN
VENTURA, CA
FEB 5-10, 2006
CHARLES AQUADRO, CHAIR
BILLIE SWALLA, VICE CHAIR

- **Ancestral Protein Reconstruction**
  (*Eric Gaucher* / Belinda Chang /
  Joe Thornton)
- **Computational Evolutionary Genomics**
  (*Bret Larget* / Lior Pachter /
  Pavel Pevzner / Lindell Bromham)

- **Microbial Diversity and Evolution**
  (*Peg Riley* / Lin Chao / John M. Logsdon)
- **Evolution of Body Plans**
  (*Billie Swalla* / Antonia Monteiro / Ken Halanych / Elena Kramer)
- **Sex Chromosome Evolution**
  (Bernardo Carvalho / Jennifer Marshall Graves)
- **Adaptive Evolution**
  (*David Rand* / Brian Lazzaro / Stephen Wright / Michael Nachman)
- **Evolution of Novelty and Gene Regulation**
  (*Kevin White* / Douglas L. Crawford)
- **Molecular Evolution of Interspecific Hybrids**
  (*Chung-I Wu* / Daniel Barbash / Rudy Raff / Toby Bradshaw)
- **Evolution of the Germ Line**
  (*Eric Haag* / Mark Martindale / Cassandra Extavour)

MYELIN
VENTURA BEACH MARRIOTT
VENTURA, CA
FEB 12-17, 2006
ROBERT MILLER, CHAIR
PETER BROPHY, VICE CHAIR

- **Keynote Lecture**
  (John Griffin)
- **Pathologies of Myelin and Myelin-Forming Cells: CNS and PNS**
  (*Bruce Trapp* / Jim Salzer)
- **Axonal-Glial Interchanges: Generation and Regeneration**
  (*Marie Filbin* / *Ben Barres* / Sha Mi / Mitch Goldfarb)
- **Transcriptional Regulation of Oligodendrocyte Development**
  (*Vittorio Gallo* / David Rowitch / Regina Armstrong / Patrizia Casaccia-Bonnefil / Gabriel Corfas)
- **Model Systems: Invertebrate and Vertebrate Myelin Formation**
  (*David Colman* / Petra Lenz / Dan Hartline)
- **Origin and Dispersal of Myelinating Cells**
  (*Bill Richardson* / *Boris Zalc* / Richard Lu / Mensheng Qui / Nikki Kessaris)
- **Oligodendrocyte Signaling**
  (*Chuck Stiles* / *Steve Pfeiffer* / Charles ffrench-Constant / Klaus-Armin Nave / Tim Vartanian / Elior Peles)
- **MS Pathology, Trials and Immunology**
  (*Rick Rudick* / *Peter Calabresi* / Steve Miller)
- **Genes: Dreams and Reality in Myelin**
  (*Tony Campagnoni* / Wendy Macklin)

NEW ANTIBACTERIAL DISCOVERY & DEVELOPMENT
VENTURA BEACH MARRIOTT
VENTURA, CA
MAR 5-10, 2006
TREVOR TRUST, CHAIR
ROBERT HANCOCK, VICE CHAIR

- **The Picture Today and Tomorrow**
  (*John Bartlett* / Christopher Walsh / John Rex)
- **Targets and Target Selection**
  (*David J. Payne* / Philip J. Hajduk / Stewart Fisher / Joyce Sutcliffe / Eefjan Breukink)
- **Screening Strategies and Hit Generation**
  (*Lynn Silver* / Colin Edge / Richard Baltz / Mick Gwynn / Alita Miller)
- **Hit to Lead and Lead Optimization Strategies**
  (*Michael Barbachyn* / John Hodgson / Kathryn Bracken / Steven Brickner / Stefan Pelzer)
- **Physical Properties, DMPK and Safety Considerations for Antibacterials**
  (*Karen Bush* / John Primeau / Mark Macielag)
- **Bacterial Topoisomerase Inhibition**
  (*Ann Eakin* / Anthony Maxwell / Edmund Ellsworth / Trudy Grossman / Glenn Dale)
- **Overcoming Resistance**
  (*John Barrett* / Robert Hancock / Ronald N. Jones / Olga Lomovskaya / Karl Drlica)
- **Selected Topics and Late Breakers**
  (*Robert Hancock*)
- **Recent Experience with Clinical Trials**
  (*David Krause* / Evan Loh / Barry Eisenstein)
- **Towards More Efficient Antibacterial Development**
  (*Steven Projan* / Mair Powell / John Powers / George Drusano)

ORGANIC STRUCTURES & PROPERTIES
SANTA YNEZ VALLEY MARRIOTT
BUELLTON, CA
JAN 8-13, 2006
STEVEN ZIMMERMAN, CHAIR
JOANNA AIZENBERG &
MIREILLE BLANCHARD-DESCE, VICE CHAIRS

- **Molecular and Supramolecular Chirality**
  (*Michael Ward* / Ronald Breslow / Takuzo Aida)
- **Molecular Recognition System**
  (*Steven Zimmerman* / Marcey Waters / Eric Anslyn / Jeremy Sanders / Heather Maynard)
- **Nanoscale Recognition. Polymers and (Bio)Materials 1**
  (*Joanna Aizenberg* / Deborah Leckband / Milan Mrksich / Shu Yang)
- **Nanoscale Recognition. Polymers and (Bio)Materials 2**
  (*Nathaniel Finney* / Samuel Stupp / Karen Wooley / Rainer Haag / Christine Keating / Theresa Reineke)
- **Self-Assembling Systems**
  (*Jay Siegel* / Peter Stang / Nobuo Kimizuka / Makoto Fujita)
- **Nanoscale Structures, Properties, and Recognition**
  (*Ilya Zharov* / Vincent Rotello / Craig Hawker / Bradley Smith / Todd Emrick)
- **Cyclodextrin and Cucurbiturils - Nanoscale Building Blocks**
  (*Zhibin Guan* / Akira Harada / Kimoon Kim / Nobuhiko Yui)
- **Molecular and Supramolecular Photoactive Systems**
  (*Dmitry Rudkevich* / Mireille Blanchard-Desce / Harry Anderson / Luisa DeCola / Zoe Prikramenou)
- **Bio-Inspired and Biomimetic Systems**
  (*Craig Hawker* / Annelise Barron / Virgil Percec)

OXYGEN RADICALS
VENTURA BEACH MARRIOTT
VENTURA, CA
FEB 5-10, 2006
HENRY JAY FORMAN &
RAFAEL RADI, CO-CHAIRS
STANLEY HAZEN &
KEVIN MOORE, CO-VICE CHAIRS

- **Keynote Lecture**
  (Christine Winterbourn)
- **Chemistry of Redox Signaling**
  (*Garry Buettner*/ Jon Fukuto / Tak Yee Aw)
- **Iron Homeostasis and Nitric Oxide Metabolism & Emerging Technologies and Biomarkers in Free Radical Biology**
  (*Balaraman Kalyanaraman* / Jean Claude Drapier / Ronald Mason / Ohara Augusto)
- **NADPH Oxidases in Signaling**
  (*John Eaton* / David Lambeth / Tom Leto)
- **Thiol Oxidation in Signaling**
  (*Art Cederbaum* / Matilde Maiorino / Aron Fisher / P. Boon Chock)
- **Lipid Derived Radicals and Nitric Oxide**
  (*Bruce Freeman* / Homero Rubbo / Paul Baker)
- **Oxidants-Antioxidants in Infection and Inflammation**
  (*Etsuo Niki* / Madia Trujillo / Paolo Di Mascio / Augustine Choi)
- **Sources of Reactive Species**
  (*Kelvin Davies* / Edgar Pick / Paul Brookes)
- **Redox and Electrophilic Signaling**
  (*Lester Packer* / Masayuki Yamamoto / Michel Toledano / Aimee Landar)
- **Panel Discussion: What Have We Learned in Twenty Five Years of Oxygen Radical Gordon Conferences and What Do We Still Need to Learn?**
  (*Angelo Azzi* / Kelvin Davies / Bruce Freeman / Balaraman Kalyanaraman / John Eaton / Etsuo Niki / Art Cederbaum / Garry Buettner / Norman Krinsky / Lester Packer)
- **Young Investigator Talks**
  (to be selected from submitted abstracts)

PEPTIDES, CHEMISTRY & BIOLOGY OF
VENTURA BEACH MARRIOTT
VENTURA, CA
FEB 19-24, 2006
ROBERT HODGES & DALE MIERKE, CO-CHAIRS
CARRIE HASKELL-LUEVANO &
KIT LAM, CO-VICE CHAIRS

- **Keynote Addresses**
  (Roger M. Freidinger / Luis Moroder)
- **G-Protein Coupled Receptors**
  (*Dale Mierke* / Roland Riek / Alessandro Bisello / Sam R.J. Hoare / Indraneel Ghosh)
- **Peptides in Cancer Biology**
  (*Kit Lam* / Terry Moody / Ziwei Huang)
- **Design/Synthesis Peptidomimetics**
  (*Armin Geyer* / Christian Schafmeister / William Lubell / Mark Spaller / Marcey Waters)
- **Peptides: Microbiology/Immunology**
  (*Pravin T.P. Kaumaya* / Esteban Celis / Vincenzo Cerundolo)
- **Drug Delivery**
  (*John Mayer* / Tom Strack / Alessio Fasano / Eric Dadey / Edward Maggio)
- **Peptides to Proteins**
  (*William Lubell* / Armin Geyer / Annelise Barron / Floyd Roemsberg)

- **Peptides Metabolism**
  (*Carrie Haskell-Luevano* / John Mayer

PERIODONTAL DISEASES
IL CIOCCO
BARGA, ITALY
JUN 4-9, 2006
MICHAEL CURTIS, CHAIR
DENIS KINANE, VICE CHAIR

- **Microbial Genomics**
  (*Mogens Kilian* / Julian Parkhill / Margaret Duncan)
- **Microbial Virulence**
  (*Anne Progulske Fox* / Andreas Peschel / Koji Nakayama / Donald Demuth)
- **Complex Community Lifestyles**
  Paul Kolenbrander / Ned Ruby / Philip Marsh)
- **Host Microbe Recognition**
  Mike Curtis / Richard Darveau / Denis Kinane)
- **AG Presentation / Specific Immune Response**
  Jeff Ebersole / Per Brandtzaeg / George Hajishengallis / Suzanne Barbour)
- **Controlling Inflammation**
  Salaman Amar / Tom MacDonald / Tom Van Dyke / Lior Shapira)
- **Invited Oral Presentations**
  Denis Kinane
- **Mechanisms of Wound Healing**
  (Mark Ferguson / Dana Graves / Martha Somerman)
- **Stem Cell and Tissue Transplantation**
  (Maurizio Tonetti / Paul Sharpe)

PHOTOIONS, PHOTOIONIZATION & PHOTODETACHMENT
SANTA YNEZ VALLEY MARRIOTT
BUELLTON, CA
JAN 29-FEB 3, 2006
ROBERT CONTINETTI, CHAIR
KLAUS MULLER-DETHLEFS, VICE CHAIR

- **Photodetachment**
  (*Mark Johnson* / W. Carl Lineberger / Kit Bowen)
- **Time-Resolved Phenomena**
  (*Peter Weber* / Toshinori Suzuki / Albert Stolow / David Villeneuve / Andrei Sanov)
- **Photoionization**
  (*Cheuk-Yiu Ng* / Tom Baer / Steve Pratt)
- **Exotic Anions**
  (*Caroline Dessent* / Lai-Sheng Wang / Jack Simons / Lars Andersen / J. Matthias Weber)
- **Inner-Shell Phenomena**
  (*Nora Berrah* / John Eland / Erwin Poliakoff)
- **Vector Correlations**
  (*Kiyoshi Ueda* / Ivan Powis / Uwe Becker / Katharine Reid / Joachim Ullrich)
- **Ionization Probes of Reactions and Aerosols**
  (*John Hepburn* / Steve Leone / Arthur Suits)
- **Ions and Ionization-Theory**
  (*Robert Lucchese* / Thomas Sommerfeld / Chris Greene)
- **Hot Topics**
  (*Klaus-Mueller Dethlefs* / Yuxiang Mo / Paul Wenthold)
- **ZEKE Probes of Molecules and Clusters**
  (*Wei Kong* / Fredric Merkt / Dong-Sheng Yang)

PHOTOSENSORY RECEPTORS & SIGNAL TRANSDUCTION
IL CIOCCO
BARGA, ITALY
APR 30-MAY 5, 2006
ROBERTO BOGOMOLNI, CHAIR
KLAAS HELLINGWERF, VICE CHAIR

- **Overview of Photoreceptor Structure and Activation Mechanism**
  (*John Spudich*)
- **Receptor Structure and Activation Mechanisms I: Rhodopsins and Bacterial Rhodopsins**
  (*Hartmut Luecke* / *Janos Lanyi*
- **Receptor Structure and Activation Mechanisms II: Bacterial and Lower Eukaryote Photoreceptors**
  (*Klaas Hellingwerf*)
- **Receptor Structure and Activation Mechanisms III: Phototropins and Other LOV-Domain Photoreceptors**
  (*Winslow Briggs*)
- **Receptor Structure and Activation Mechanisms IV: Phytochromes and Cryptochromes**
  (*Clark Lagarias* / *J. Chory*)
- **Mechanisms of Signal Relay and Signal Transduction I: Rhodopsins and Bacterial Rhodopsins**
  (*Wayne Hubbell* / *Martin Engelhard*)
- **Mechanisms of Signal Relay and Signal Transduction II: Phytochromes and Cryptocromes**
  (*E. Schaefer* / *Chentao Lin*)
- **Biological Clocks and Circadian Rhythms**
  J. Woodland Hastings)
- **Novel Photoreceptor Systems and General Discussion on the Future of Sensory Phototransduction**
  Francesco Lenci / *Masamitsu Wada* / Winslow Briggs / Janos Lanyi / John Spudich)

PINEAL CELL BIOLOGY
SANTA YNEZ VALLEY MARRIOTT
BUELLTON, CA
JAN 15-20, 2006
GREGORY CAHILL, CHAIR
JORG STEHLE, VICE CHAIR

- **The Central Themes**
  (*Steve Reppert* / Michael Menaker / Walter Gehring)
- **Circdadian Clock Mechanisms**
  (*Marty Zatz* / Steve Reppert / Carla Green / Joe Takahashi)
- **Melatonin Effects**
  (*David Weaver* / Vinnie Cassone / Mireille Masson-Pevet / Margarita Dubocovich)
- **Regulation of AANAT**
  (*David C. Klein* / Jose Aranjo / Tae-Don Kim / Tony Ho)
- **Retinal Melatonin and Rhythms**
  (*Pierre Voisin* / Mike Iuvone / Jola Zawilska / Jack Falcon / Stu Dryer)
- **Development**
  (Masauke Araki / Steven W. Wilson / Don Zack)
- **Photodetection by the Circadian System**
  (David Whitmore / David Berson)
- **Photoperiodism**
  (*Andrew Loudon* / Gerald Lincoln / David Hazelrigg / Michael Gorman / Peter Morgan)
- **Human Biology**
  (*Jo Arendt* / Al Lewy / Ann Smith / Hirotoshi Okamura)

PLASMINOGEN ACTIVATION & EXTRACELLULAR PROTEOLYSIS
FOUR POINTS SHERATON: HARBORTOWN
VENTURA, CA
FEB 19-24, 2006
STEVEN GONIAS &
FRANCESCO BLASI, CO-CHAIRS
TONI ANTALIS, VICE CHAIR

- **Fibrinolysis Protein Structural Biology**
  (*Francis Castellino* / Michael Ploug / Cynthia Peterson)
- **Fibrinolysis Receptors and Associated Plasma Membrane Proteins**
  (*Niels Behrendt* / Nicolai Sidenius / Vincent Ellis / Sharon Stack)
- **The LRP Family - Regulators of Proteolysis**
  (*Joachim Herz*)
- **Intravascular Fibrinolysis and Thrombolysis**
  (*Katherine Hajjar* / Paul Bock / Daniel Lawrence / Douglas Vaughan)
- **Transmembrane Proteases / Extracellular Proteolysis**
  (*Thomas Bugge* / Toni Antalis / Stephen Weiss)
- **Fibrinolysis Proteins in Neurologic Disease**
  (*Dudley Strickland* / Katerina Akassoglou / Sidney Strickland)
- **Hot Topics**
  (*Toni Antalis* / *Francesco Blasi*)
- **Fibrinolysis Proteins in Inflammation and the Immune Response**
  (*David Ginsburg* / Massimo Alfano / Steven Idell)
- **Stem Cells and the Fibrinolysis System**
  (Pia Ragno / Marc Tjwa)

PROLACTIN FAMILY
HOLIDAY INN
VENTURA, CA
JAN 29-FEB 3, 2006
ARTHUR GUTIERREZ-HARTMANN, CHAIR
HALLGEIR RUI, VICE CHAIR

- **Historical Highlights of 25 Years of PRL Family GRC Meetings**
  (*Arthur Gutierrez-Hartmann* / Frank Talamantes / Paul Kelly)
- **PRL & GH Receptors**
  (*Vincent Goffin* / Michael Waters / John Kopchick / Anthony Kossiakoff / Chuck Clevenger)
- **PRL & GH Intracellular Signaling**
  (*Li Yu-Lee* / Jorge Martin-Perez / Stuart Frank / Barbara Vonderhar)
- **PRL/GH-Induced Gene Regulation**
  (*Shlomo Melmed* / Lothar Hennighausen / Gunnar Norstedt / Iain Robinson / David Waxman)
- **PRL Family Gene Transcription**
  (*Nancy Cooke* / Richard Day / Cheryl Watson / Michael Soares)
- **PRL/GH Target Organs**
  (*Nira Ben-Jonathan* / Kay-Uwe Wagner / Linda Schuler / Geula Gibori / Betty Diamond)
- **PRL & GH Ligands**
  (*Marc Freeman* / Ameae Walker / Carmen Clapp / Chris Ormandy)

- **Pituitary Development & Tumorigenesis** (*Michael Thorner* / Shareen Ezzat / Eduardo Arzt / Patrice Mollard / Robert Osamura)
- **Keynote Lecture** (*Hallgeir Rui* / Sally Camper)

PROTEIN DERIVED COFACTORS, RADICALS AND QUINONES
HOLIDAY INN
VENTURA, CA
JAN 22-27, 2006
VICTOR DAVIDSON, CHAIR
JOAN BRODERICK, VICE CHAIR

- **Radical SAM Enzymes** (*Squire Booker* / Perry Frey / Joan Broderick)
- **Novel Biosynthetic Mechanisms** (*James Whittaker* / Wilfred van der Donk / Joseph Jarrett / Carrie Wilmot)
- **Protein-Derived Cofactors** (*Katsuyuki Tanizawa* / Judith Klinman / Michael McPherson)
- **Amine Oxidases and Dehydrogenases** (*Lawrence Sayre* / Nigel Scrutton / Tiina Salminen / Dale Edmondson)
- **Oxygenases** (*Jonathan Hosler* / Martin Bollinger / Ah-Lim Tsai)
- **Protein-Bound Quinones and Radicals** (*Kurt Warncke* / Marilyn Gunner / Fraser MacMillan / Melvin Okamura)
- **Protein-Mediated Electron Transfer** (*Victor Davidson* / Harry Gray / William Cramer)
- **Complex Redox Proteins** *Stephen Ragsdale* / Steven Chapman / Bridgette Barry / Fahmi Himo)
- **Ribonucleotide Reductase** *David Britt* / JoAnne Stubbe / Britt-Marie Sjoberg)

PROTEIN FOLDING DYNAMICS
FOUR POINTS SHERATON: HARBORTOWN
VENTURA, CA
JAN 8-13, 2006
JANE CLARKE, CHAIR
CHARLES BROOKS, VICE CHAIR

- **Keynote Talks** (Chris Dobson / Alan Fersht / Jeff Kelly / Peter Wolynes)
- **Fast and Early Events in Folding** (Bill Eaton / Steve Hagen / Vijay Pande / Bill Swope / *Tobin Sosnick*)
- **Misfolding and Aggregation** (Valerie Daggett / Yuji Goto / Carol Hall / *Sheena Radford*)
- **Exploring the Folding Landscape** (Phil Dawson / Mikael Oliveberg / José Onuchic / Dan Raleigh / *Angel Garcia*)
- **Folding in the Cell** (Silvia Cavagnero / Art Horwich / *Anmon Horovitz*)
- **Single Molecules / Complex Folding Problems** (Gilad Haran / Susan Marqusee / *Kevin Plaxco*)
- **Evolution and Protein Folding** (Cyrus Chothia / Eugene Shakhnovich / Sarah Teichmann / *Teresa Head-Gordon*)
- **Investigating Species on Folding Pathways** (Michele Vendruscolo / Peter Wright / *Joan Shea*)

PROTONS & MEMBRANE REACTIONS
FOUR POINTS SHERATON: HARBORTOWN
VENTURA, CA
FEB 26-MAR 3, 2006
SHELAGH FERGUSON-MILLER, CHAIR
PETER BRZEZINSKI, VICE CHAIR

- **Protein Interactions with Membranes** (*Werner Mantele* / Stephen White / Carola Hunte)
- **Membrane Channels: Model Systems** (*Cecilia Tommos* / Tim Cross / Kathleen Howard)
- **Protons at Interfaces** (*Norbert Dencher* / Menachem Gutman / Wolfgang Junge)
- **Proton Pumps and Pathways** (*Peter Rich* / Klaus Gerwert / Marten Wikstrom / Jonathan Hosler / Deborah Hanson)
- **Water in Membrane Proteins: Computational Approaches** (*Greg Voth* / Arieh Warshel / Y.S. Lee / Don Bashford / Alexei Stuchebrukhov)
- **ATP Synthase/ATPase: Proton and Sodium Channels** (*Robert Fillingame* / John Walker / Peter Dimroth / Aleksei Aksimentiev / George Oster)
- **Ion Transporters/Other Systems** (*Colin Wraight* / Thomas Walz / Ron Kaback / Poul Nissen / Regis Pomes)
- **Advances in Studying Membrane Proteins** (*Bob Gennis* / Richard Armstrong / Nicholeta Bondar / Martin Caffrey)
- **Physiological Significance of Proton Transport** (*Jan Rydstrom* / Tom DeCoursey / Etana Padan / Larry Pinto / Michael Pusch)
- **Grotthuss 200th Anniversary** (*Peter Nicholls* / Sam Cukierman)

QUANTUM INFORMATION SCIENCE
IL CIOCCO
BARGA, ITALY
MAY 7-12, 2006
IGNACIO CIRAC & PETER ZOLLER, CO-CHAIRS
MICHEL DEVORET &
ROBERT SCHOELKOPF, CO-VICE CHAIRS

- **Advances in Quantum Computing** (*Martin Wilkens* / David Wineland / Steve Girvin)
- **Atomic Systems I** (*Jeff Kimble* / Eugene Polzik / Gerhard Rempe / Maciej Lewenstein)
- **Atomic Systems II** (*Rainer Blatt* / Immanuel Bloch / Philippe Grangier)
- **Solid State Systems** (*Daniel Loss* / Leo Kouwenhoven / Jake Taylor / Rob Schoelkopf)
- **Other Systems** (*Gerhard Milburn*
- **Quantum Information Theory** (*Charles Bennett* / Andreas Winter / Wolfgang Dür / Frank Verstraete)
- **Quantum Computing** (*Richard Jozsa* / Barbara Terhal / Daniel Gottesman)
- **Quantum Algorithms** (John Waltrous / Andrew Childs / Harry Buhrman)
- **Quantum Cryptography** (*Hoi-Kwong Lo* / Barbara Kraus)

REVERSIBLE ASSOCIATIONS IN STRUCTURAL & MOLECULAR BIOLOGY
FOUR POINTS SHERATON: HARBORTOWN
VENTURA, CA
JAN 15-20, 2006
GARY ACKERS &
GEOFFREY HOWLETT, CO-CHAIRS
MICHELLE ARKIN &
COLIN KLEANTHOUS, CO-VICE CHAIRS

- **Protein Design in Evolution & Recognition** (*Gideon Schreiber* / Tanja Kortemme / Homme Helinga)
- **Emerging Technologies** (*Carol Robinson* / Tony Mittermaier)
- **Ligand/Macromolecule Complexes & Drug Design** (*Jim Wells* / Jeffrey Huth / Jack Taunton)
- **Single Molecule Mechanics** (*Ignacio Tinoco* / Carlos Bustamante / Julio Fernandez / Koen Visscher)
- **Protein/Lipid Recognition** (*Steve White* / Karen Fleming / Lukas Tamm / Jim Bowie)
- **Protein Switches & Networks** (*Rob Russell*)
- **Advances in Classic Methods** (*Peter Schuck* / Mattia Rocco / Alexandre Bonvin)
- **Functional Transitions in Protein-Nucleic Acid Assemblies** (*Dorothy Beckett* / Jonathan Widom / Leemor Joshua-Tor / Andrew Feig)
- **Closing Address** (Tom Laue)

SENSORY TRANSDUCTION IN MICROORGANISMS
VENTURA BEACH MARRIOTT
VENTURA, CA
JAN 22-27, 2006
KATHERINE BORKOVICH, CHAIR
ANN STOCK, VICE CHAIR

- **Motors and Signaling Output** (*Shin-Ichi Aizawa* / Birgit Scharf / Keiichi Namba / Elizabeth Smith / Peter Satir / Margaret Titus)
- **Receptors and Associated Proteins** (*John S. Parkinson* / Dennis Thomas / Janine Maddock / John Spudich / Mark Johnson / David Stone / Gerald Hazelbauer / Sriram Subramaniam)
- **Intracellular Signaling I** (*Michael Eisenbach* / Urs Jenal / Mark Gomelsky / Elaine Elion / Victor Sourjik / Frederick Dahlquist)
- **Intracellular Signaling II** (*Philip Matsumura* / Brian Crane / Ann West / Wenyuan Shi / Judith van Houten / Peter Devreotes / Robert Weis / Ady Vaknin)
- **Type III Secretion Systems and Surface Motility** (*Zhaomin Yang* / Ariel Blocker / John Kirby / David Zusman / Guenther Gerisch / Patricia Hartzell)
- **Intercellular Communication, Development and Pathogenesis** (*Heidi Kaplan* / Peter Greenberg / Richard Novick / Elizabeth Sockett / Richard Firtel / Michael Surette / Hao Chen)
- **Signaling, the Cytoskeleton and Cell Division** (*William Loomis* / Christine Jacobs-Wagner / William Margolin / Peter Graumann / Michelle Momany / Louise Glass)

- **Environmental Diversity and Bioenergetics**
(*Caroline Harwood* / Judith Armitage / Samuel Kaplan / Linda McCarter / Bianca Brahamsha / Gladys Alexandre / Frances Arnold / Benjamin Horwitz)
- **Modeling and Systems Biology Approaches to Signaling**
George Oster / Michael Laub / Adam Arkin / Yuhai Tu / Karen Lipkow / Igor Zhulin)

SPIROCHETES, BIOLOGY OF
IL CIOCCO
BARGA, ITALY
APR 23-28, 2006
DAVID HAAKE, CHAIR
SVEN BERGSTROM, VICE CHAIR

- **The Role of the Host Immune Response in Bacterial Persistence**
(*Erol Fikrig* / Lalita Ramakrishnan / Janis Weis / Richard Flavell)
- **Host-Pathogen Interactions in Bacterial Pathogenesis**
(*Sheila Lukehart* / Staffan Normark / Linden Hu / Magnus Höök / Jon Skare)
- **Spirochete Genetics and Genetic Manipulation**
(*Patti Rosa* / Matthieu Picardeau / Chris Fenno / Phillip Stewart)
- **Spirochetes: The Genomic Perspective**
(*Isabelle Saint Girons* / Petra Brandt / Richard Zuerner / Jared Leadbetter / Wolfram Zückert)
- **Invasive Strategies of Spirochetal Pathogens**
(*Rich Ellen* / Jenifer Coburn / Jarlath Nally / Annette Moter
- **Spirochete Biology and Diversity**
Tom Schwan / Nyles Charon / Steve Norris / Jonas Bunikis / Darren Trott)
- **Evasion of Host Defense Mechanisms by Spirochetal Pathogens**
Marina Cinco / Arturo Centurion-Lara / Sakari Jokiranta / Peter Kraiczy)
- **Regulation of Gene Expression**
Ira Schwartz / Brian Stevenson / Alan Barbour / Frank Yang / Ben Adler)
- **Late Breaking Session**
Caroline Cameron / James Matsunaga)

SUPERCONDUCTIVITY
SANTA YNEZ VALLEY MARRIOTT
BUELLTON, CA
JAN 22-27, 2006
J.C. SEAMUS DAVIS, CHAIR
NICOLE BONTEMPS, VICE CHAIR

- **Excitations of Underdoped Cuprates**
(*J. Orenstein* / D. Bonn / C. Panagopolous / M. Sutherland / Y. Kohsaka)
- **New Superconductors: Actinide**
(*J. Sarrao* / P.M. Openeer / D. Aoki / N. Curro)
- **Cuprate Nano-Disorder & Transport**
(*P. Hirschfeld* / T. Nunner/ A. Kapitulnik / F. Rullier-Albenque / K. McElroy)
- **New Superconductors: Cobaltates**
(*H. Alloul* / H. Ding / K. Ishida / M. Ogata)
- **Late Developments**
- **Cuprate Spectral Weight Shifts**
(*M. Norman* / A.B. Kuzmenko / C. Bernhard / A. Santander-Syro)
- **Theoretical Advances in Correlated Superconductivity**
- **Superconducting Quantum Coherent Devices**
(*M. Devoret* / R.W. Simmonds / I. Siddiqui / A. Walraff / N. Boulant)
- **Spin/Charge/Lattice Interactions in Cuprates**
(*A. Lanzara* / H. Takagi / T. Cuk / S.V. Borisenko / L. Pintschovius)

THREE DIMENSIONAL ELECTRON MICROSCOPY
IL CIOCCO
BARGA, ITALY
JUN 25-30, 2006
HELEN SAIBIL, CHAIR
WERNER KUEHLBRANDT &
PHOEBE STEWART, CO-VICE CHAIRS

- **Keynote Lectures**
(*Helen Saibil* / Jacques Dubochet / Helen Berman)
- **Ordered and Icosahedral Assemblies**
(*David Stokes* / Sarah Butcher)
- **Evaluating and Improving Reconstruction Methods, Dealing with Heterogeneity**
(*Joachim Frank* / Elena Orlova)
- **Single Particles**
(*Jose Carrascosa* / Trevor Sewell)
- **Poster Presentations 1**
(*Phoebe Stewart*)
- **Tomography and Cell Biology**
(*Wolfgang Baumeister* / Keith Gull / Kay Grunewald)
- **Instrumentation**
(*Richard Henderson*)
- **Hybrid Structures and Databases**
(*Wah Chiu* / Florence Tama / Maya Topf / Kim Henrick)
- **Poster Presentations 2**
(*Werner Kuhlbrandt*

ULTRAFAST PHENOMENA IN COOPERATIVE SYSTEMS
SANTA YNEZ VALLEY MARRIOTT
BUELLTON, CA
FEB 5-10, 2006
JURE DEMSAR &
PAUL VAN LOOSDRECHT, CO-CHAIRS
ANTOINETTE TAYLOR, VICE CHAIR

- **Photoinduced Phase Transitions I**
(*Keith Nelson* / Andrea Cavalleri / Klaus Sokolowski-Tinten / Keiichiro Nasu)
- **Quasiparticle Dynamics in Correlated Solids I**
(*Tony Heinz* / Dragan Mihailovic / Richard Averitt / Jay Kikkawa)
- **Photoinduced Phase Transitions II**
(*Herve Cailleau* / Marylise Buron / Manfred Fiebig / Jim Cao)
- **Quasiparticle Dynamics in Correlated Solids II**
(*Jure Demsar* / Robert Kaindl / Viktor Kabanov / Joseph Orenstein)
- **Photoinduced Metal-Insulator Transitions**
(*Zackary Fisk* / Shin-ya Koshihara / Hiroshi Okamoto / Munira Khalil)
- **Coherent Dynamics**
(*Oleg Misochko* / Muneaki Hase / Roberto Merlin / Thomas Dekorsy)
- **Ultrafast Magnetism**
(*Antoinette Taylor* / Paul Crowell / Bert Koopmans / Alexei Kimel)
- **Spin Manipulation**
(*David Awschalom* / Scott Crooker / Bernd Beschoten / Roberto Myers)
- **Exciton Dynamics**
(*Paul van Loosdrecht* / Audrius Pugzlys / Makoto Kuwata-Gonokami / Leonid Butov / Victor Klimov)

VIRAL VECTORS FOR GENE THERAPY, THE SCIENCE OF
HOLIDAY INN
VENTURA, CA
MAR 12-17, 2006
JOSEPH C. GLORIOSO, CHAIR
PAUL D. ROBBINS, VICE CHAIR

- **Gene Therapy: What are the Challenges?**
(*Savio Woo* / A. Dusty Miller / Don Kohn / Jean Bennett)
- **Determinants of Virus Attachment and Entry: Prospects for Retargeting**
(*David T. Curiel* / Nick Muzcyzka / Guoying Zhou / Steve Russell / James Wilson / Paul McCray)
- **Mechanism of Vector Trafficking and Packaging**
(*John Engelhardt* / Gabrielle Campedelli-Fiume / Xiao Xiao / Mark Kay / Philip Leopold)
- **Mechanisms of Vector Persistence**
(*Luigi Naldini* / Frederic Bushman / Christopher Baum / Adrian Thrasher / Christof vonKalle)
- **Vector Genome Structure and Transgene Expression**
(*Bernard Roizman* / R. Jude Samulski / Steve Triesenberg / Michel Sadelain)
- **Immune Response to Vectors**
(*Pedro Lowenstein* / Patrick Moore / Katherine High / Maria Grazia Roncarolo / Hildegund Ertl)
- **Overcoming Innate Host Defenses**
(*Matthew Weitzman* / Mark O'Connor / Clodagh O'Shea / Robert Kalejta / Didier Trono)
- **Oncolytic Vector Biology and Design**
(*Steve Russell* / Karen Mossman / Andre Leiber / John Bell / Roberto Cattaneo / Matthias Gromeier)
- **Vector Promising Technology and Applications**
(*Mark Kay* / Katherine High / Inder Verma / John Rossi / David Russell / R. Jude Samulski / David Fink / Jeffrey Chamberlain)

VISUAL SYSTEM DEVELOPMENT
IL CIOCCO
BARGA, ITALY
MAY 14-19, 2006
PAMELA RAYMOND, CHAIR
ROSS CAGAN, VICE CHAIR

- **Seymour Benzer Symposium**
(*Pamela Raymond* / *Ross Cagan* / *Francesca Pignoni* / Kevin Moses)
- **Eye Determination**
(*Graeme Mardon* / Justin Kumar / Maria Dominguez / Paola Bovolenta / Peter Mathers / Ruth Ashery-Padan)
- **Interacting Signaling Pathways**
(*Monica Vetter* / Ichiro Masai / William Harris / Anne Calof / Y. Henry Sun)

- **Evolution and Organization of Photoreceptors**
  (*Tanya Wolff* / Claude Desplan / Chi-Hon Lee / Otto Baumann / Jarema Malicki / Shoji Kawamura / Ruben Adler)
- **Complex or Novel Regulatory Mechanisms**
  (*Jessica Treisman* / Muriel Perron / Thomas Glaser / Rachael Pearson / Ilaria Rebay)
- **Ocular Growth and Polarity**
  (*Marek Mlodzik* / Jochen Wittbrodt / Andrew Fischer / Richard Carthew / Helen McNeill / Michael Simon)
- **Cell Cycle Regulation**
  (*Thomas Reh* / Nicholas Baker / Matthew Freeman / Brian Link / Edward Levine)
- **Retinal Degeneration and Regeneration**
  (*Nansi Colley* / Baruch Minke / Joseph O'Tousa / Amir Rattner / Peter Hitchcock / Katia Del Rio-Tsonis)
- **Axon Guidance and Plasticity**
  (*Nadean Brown* / Christine Holt / Stephen Smith / Ian Meinertzhagen / Yasushi Hiromi)

75 years at the frontiers of science

In 2006, the Gordon Research Conferences will be celebrating its 75th Anniversary.

Over the past year, GRC has been developing a commemorative publication and web site chronicling our long and exciting history at the frontiers of science.

We are looking forward to sharing these with our attendees in 2006!

The Gordon Research Conferences & The Kenan Institute for Engineering, Technology & Science are pleased to announce the Gordon-Kenan Graduate Research Seminars for 2006

The Gordon-Kenan Graduate Research Seminars are highly successful and unique opportunities for young researchers to share in the GRC experience. Attendees come together to discuss their current research while building informal networks with their peers that may lead to a lifetime of collaboration and scientific achievement. These two to four day seminars are organized by and for graduate students and post docs, with the support from the leading scientists from the related Gordon Research Conference in that topic. Young investigators in the following fields are encouraged to experience the excitement of a Gordon-Kenan Graduate Research Seminar in 2006!

GRADUATE RESEARCH SEMINAR:
PROTEIN FOLDING DYNAMICS
January 6-8, 2006
Four Points Sheraton: Harbortown, Ventura, CA
http://www.grc.org/programs/2006/gradprot.htm

GRADUATE RESEARCH SEMINAR:
BIOANALYTICAL SENSORS
February 24-26, 2006
Holiday Inn, Ventura, CA
http://www.grc.org/programs/2006/gradsens.htm

GRADUATE RESEARCH SEMINAR:
BIOINORGANIC CHEMISTRY
February 2-5, 2006
Four Points Sheraton: Harbortown, Ventura, CA
http://www.grc.org/programs/2006/gradbio.htm

GRADUATE RESEARCH SEMINAR:
ORIGIN OF LIFE
July 21-23, 2006
Bates College, Lewiston, ME
http://www.grc.org/programs/2006/gradorig.htm

GORDON RESEARCH CONFERENCES

KENAN INSTITUTE
ENGINEERING, TECHNOLOGY & SCIENCE

Celebrating our 75th Anniversary on the Frontiers of Science (1931-2006)

When Smart Becomes Simple:
Brilliant Imaging At Your Fingertip!

The innovative Leica DMI 6000 B offers optimal solutions:

- Contrast Manager – The correct contrast settings a fingertip away
- Internal Fast Filter Wheel IFW – Change in milliseconds between different excitations
- Camera Ports – Choose from more than 200 possible configurations the setup which is just right for you
- Fluorescence Intensity Manager FIM – Adjust the excitation light and protect your specimens effectively

@ www.leica-microsystems.com/microscopes

Leica
MICROSYSTEMS

» advances in:

Genomics

Transfecting the Cell Basic research on cell biology and development of gene therapy require scientists to introduce genes and proteins into cells. To do so, they have a choice among several emerging technologies. BY PETER GWYNNE AND GARY HEEBNER

In this issue:

- DNA and RNA transfection
- Electroporation
- Microinjection
- Biolistic devices
- Carrier molecules
- Lipid-based transfection agents
- PNA complexes
- Viral-based transfection systems
- Protein delivery

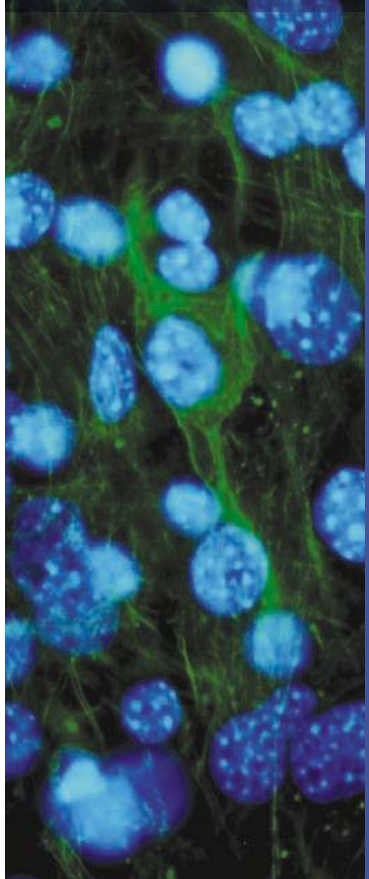

To explore the inner workings of cells, biomedical researchers must find effective ways of overcoming the cells' natural resistance to the insertion of genes and other probes. Clinicians who want to influence the behavior of cells through gene therapy have an added criterion: Their methods must ensure the safety of the organisms whose cells they transfect by avoiding immune responses and other deleterious outcomes.

Researchers don't expect to reach those goals overnight. "Transfection is still not a mature science," says John Archdeacon, director of R&D at **Active Motif**. "A lot of work needs to be done – for example, to deliver cells in vivo and to expand the number of cell types that can be transfected."

Five Years of Progress

Nevertheless, scientists and suppliers have made progress during the past half decade. "We're seeing increased use in screening and process environments and the emergence of new applications such as RNA interference," says Steve Kulisch, marketing manager for gene transfer at **Bio-Rad Laboratories**. "New reagents are coming out for particular cell lines, and we're seeing a lot of niche products," adds Jeff Emch, product manager for **Roche Applied Science**. Beyond that, says Rainer Christine, CEO of **Amaxa GmbH**, "It's become easier to work with primary cells."

Certainly the biomedical community has no one-size-fits-all approach to transfecting cells. Nor does it want one, because the demands on transfection methods differ considerably with the type of study. "When you do basic research, you don't have to worry about too many safety issues," explains Nicolas Hoffmann, product manager of viral vectors and gene expression for **Qbiogene**, a subsidiary of MP Biomedicals. "But for clinical cases you have to comply with very stringent protocols mandated by the **U.S. Food and Drug Administration** [FDA] and in some cases the Recombinant DNA Advisory Committee at the **National Institutes of Health**."

That mandate stems in large measure from the 1999 death of Jesse Gelsinger, a patient undergoing gene therapy for a liver disease at the University of Pennsylvania. "It put a damper on gene therapy and everybody has become gun-shy," says David Roth, vice president of research and development at **Gene Therapy Systems**. "There are no therapy products approved yet by the FDA. But as soon as one is registered, there will be a lot of gene therapy–related therapeutics and vaccines." That, of course, will stimulate further work on safe methods of transfection. Beyond the United States, the Chinese FDA has approved Gendicine, a gene therapy medicine produced by **Shenzhen SiBiono GeneTech Co., Ltd.**, for treatment of head and neck squamous cell carcinomas. MORE ›››

Inclusion of companies in this article does not indicate endorsement by either AAAS or Science, *nor is it meant to imply that their products or services are superior to those of other companies.*

This is the final special supplement this year on Advances in Genomics. The first three appeared in the 11 February, 10 June, and 29 July issues of Science.

» advances in: Genomics

Means of inserting DNA and RNA into living cells fall naturally into three categories: physical procedures that introduce material directly into cells; chemical techniques that rely on carrier molecules; and biological approaches in which the material piggybacks into the cell aboard viruses. All three methods have advantages and disadvantages in specific types of experiment.

Physical Methods

"With physical systems, inert substances come into contact with the cells, so there's relatively little toxic response," Emch says. "And physical methods can penetrate the cell wall and ensure localized delivery." However, Roth cautions, "The problem is that physical methods such as electroporation kill about 50 percent of the cells." As a result, they require samples containing large numbers of cells – and conclusions are made on a population of surviving, and presumably, rehabilitating cells.

Emch outlines the advantages of chemical carriers in introducing genes into cells. "They have ease of use, rapidity of repetition, low cost, and a relatively high success rate," he says. But they have their own drawbacks. "The primary disadvantage of some chemical methods is the toxicity introduced into the cells," Kulisch says. "There's no reagent that has no toxic impact on a cell."

Viruses offer one key benefit. "They have unmatched efficiency," Kulisch explains. "After all, they've had a several million year head start over other methods." However, Christine adds, "They need to be tailored and fine-tuned to the specific cell; that means a lot of preparation. Viral vectors also have the drawback of unwanted influences on cells." In addition, Hoffman says, "There are limits on the sizes of DNA they can insert."

Physical methods of transfection also group into three varieties. Electroporation systems use electrical pulses to open up the membranes of mammalian cells for the passage of genes. Microinjection and biolistic devices insert samples of DNA or RNA more directly.

Amaxa has developed an electroporation technology that it calls Nucleofector to introduce DNA into the nuclei of mammalian cells. "The technology has broad applicability to signal transduction, apoptosis, and cell-cell interactions," Christine says. "It is also used for RNA interference. We see a shift away from short interfering RNA [siRNA] to short hairpin RNA, which is plasmid based and needs to be delivered to the nucleus. This is what the Nucleofector does." Other companies that offer electroporation systems include Bio-Rad, **BTX**, and **Inovio Biomedical**, which is conducting clinical trials using electroporation.

Microinjection and Light

When researchers have too few cells for electroporation, they can turn to microinjection, coupled with light microscopy to visualize the delivery. Vendors of microinjection systems include Bio-Rad and **Narishige**.

Bio-Rad also offers two biolistic instruments that use helium pulses to shoot subcellular-sized tungsten or gold microprojectiles coated with DNA into cells over a range of speeds and target distances. "The PDS-1000 is a benchtop instrument and the Helios 'gene gun' system is a handheld device," Kulisch says.

The most popular chemical methods rely on lipid-DNA complexes created by combining DNA with cationic lipids. The complexes fuse with the cell membrane and are then transported into the cell. Much of the DNA transfected into a cell by lipids remains in endosomes; that reduces the rate of transfection. However, vendors have mitigated that situation by developing better formulations. Several companies, among them Bio-Rad, **EMD Biosciences**, **Invitrogen**, **Mirus Bio**, **Promega**, **Polyplus**, and Roche Applied Science, have developed new liposomal and nonliposomal based chemical agents and other improved transfection reagents and systems.

"When we entered chemical transfection, we launched DOTAP and DOSPER, both liposomal agents able to transfect DNA, RNA, oligonucleotides, and proteins," says Roche Applied Science's Emch. "Both are reasonably effective over a large number of cell lines, but can have cytotoxic effects. We then moved onto our premier reagent for plasmid DNA transfection – the synthetic, nonliposomal based FuGene 6 transfection reagent. It has now been shown to work with over 700 cell lines for which we have communications and references demonstrating its broad applicability and acceptance.

"But it may not perform at a satisfactory level on all cell lines," Emch continues. "So we introduced our X-tremeGENE Q2 transfection reagent as a complementary product specific for Jurkat and K-562 cell lines. And because FuGene 6 has a relatively low efficiency introducing siRNA into cells, we developed the X-tremeGENE siRNA transfection reagent." Later this year the company plans to introduce the FuGene HD transfection reagent for analytical protein expression in eukaryotic adherent and suspension adapted cell lines.

Targeted Transfection with PNAs

Gene Therapy Systems has developed a method of targeting transfection based on peptide nucleic acid (PNA) complexes that recognize specific DNA sequences. PNAs are DNA mimics that are not degraded by nucleases, are more stable in solution, and can be modified with additional functional groups when needed. "Our 'Gene Grip' PNA technology does

Automation in the Lab

LabAutomation2006, the annual meeting of the **Association for Laboratory Automation** (ALA), will take place in Palm Springs, California, from January 21 to January 25. The event will focus on advances in laboratory technologies, tools, and informatics. Featured sectors will include detection and separation, micro- and nanotechnologies, high throughput technologies, informatics, and frontiers beyond biopharma.

» http://www.labautomation.org/LA/LA06

» advances in: Genomics

gene tracking using a variety of reporter genes," Roth explains. "We have a number of different vectors and a whole line of products in easy-to-use kits."

The appeal of viral based transfection systems lies in their ability to achieve almost 100 percent transfection. But working with infectious or potentially infectious particles, coupled with the possibility of undesirable immune response from an organism, counterbalances the high transfection rates, especially for research in the clinic.

Those concerns apply particularly to retroviruses, which insert their genetic material into the genomes of actively dividing host cells. Another type of vector – the adenovirus – avoids those problems. "Adenoviruses have very high efficiency and very low risk of insertional mutagenesis," says Qbiogene's Hoffmann. "Another advantage is that, as a human virus, adenovirus stays in the human system. It doesn't need a helper virus, it can be used in suspension culture, and you can express several genes on the same virus." Qbiogene provides an Adenovator Kit for a large number of vectors to generate viruses and a repressor based system that allows scientists to turn off gene expression. "We also have ready-to-use reporter gene–expressing viruses that we call AdenoExpress viruses," Hoffmann says. "And we offer services from A to Z for generation of a virus."

Other companies that offer virus based transfection systems include **Retrogen**, and **Stratagene**. Retrogen offers retroviral vectors based on the Moloney Murine leukemia virus. This minimized retroviral vector allows the insertion of larger complementary DNAs of interest.

Why Not Proteins?

If scientists can insert genes into cells, why not take the next step and transfect proteins, to study their effects on cellular function? "A gene needs to go to the nucleus to be expressed," Active Motif's Archdeacon points out. "If you have an expressed protein, you can deliver it into the cell and have an immediate effect."

Unfortunately, mammalian cell membranes create strong barriers to most proteins and peptides. Until recently, scientists had to use microinjection or electroporation to introduce those entities into cells. But several other products that facilitate the delivery of proteins to cells' nuclei and cytoplasm have come to market from companies such as Active Motif, Gene Therapy Systems, and Stratagene.

"Our Chariot reagent, introduced in 2001, was the first noncovalent method of delivery," Archdeacon says. "Now we are working on systems that bring cargoes into cells in vivo and deliver siRNAs. We have developed versions of peptides that deliver siRNAs and other entities."

Gene Therapy Systems has started to develop its own methods of transfecting proteins into cells for research on gene therapy. "Using our BioPORTER, a cationic lipid reagent, we can get small and mid-sized proteins into various cell lines and primary cell cultures – in cases where it's too hard to get the genes themselves into the cell or nucleus or to get the genes expressed," Roth says. How will this affect patients? "If you can take out their target cells and transfect in your protein, DNA, or RNA of interest, that will alter the cells in a positive way; then it might be of use to patients," Roth explains. "Systemic and organ- or tissue-specific transfection and expression by any molecules have been daunting problems in the 20-year history of gene therapy. It's all about delivery, and the intellectual property that surrounds the transgenes and their delivery to the target cells."

Animal Models

A group at France's **Pasteur Institute** is using the technology to develop a method of delivering a malaria antigen into mice, and a team at **Duke University** has expressed interest in applying it to developing technologies for research on animal models. Gene Therapy Systems is also using microparticles from brewers' yeast to develop ImmunoPORTER, a technology that allows scientists to transfect macrophages and dendritic cells that are vital for manipulation and regulation of the immune system.

Progress continues in mammalian cell transfection. Researchers can buy effective, user-friendly reagents to insert interesting genes and even proteins into mammalian cells. As manufacturers continue to refine these products, they reduce cell toxicity and improve the efficiency of transfection.

Peter Gwynne (pgwynne767@aol.com) is a freelance science writer based on Cape Cod, Massachusetts, U.S.A. Gary Heebner (gheebner@cell-associates.com) is a marketing consultant with Cell Associates in St. Louis, Missouri, U.S.A.

ScienceCareers.org

Classified Advertising

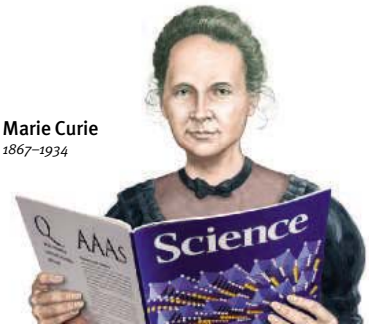

Marie Curie
1867–1934

For full advertising details, go to **www.sciencecareers.org** and click on **How to Advertise,** or call one of our representatives.

United States & Canada

E-mail: advertise@sciencecareers.org
Fax: 202-289-6742

JILL DOWNING
(CT, DE, DC, FL, GA, MD, ME, MA, NH, NJ, NY, NC, PA, RI, SC, VT, VA)
Phone: 631-580-2445

KRISTINE VON ZEDLITZ
(AK, AZ, CA, CO, HI, ID, IA, KS, MT, NE, NV, NM, ND, OR, SD, TX, UT, WA, WY)
Phone: 415-956-2531

KATHLEEN CLARK
Employment: AR, IL, LA, MN, MO, OK, WI, Canada; Graduate Programs; Meetings & Announcements (U.S., Canada, Caribbean, Central and South America)
Phone: 510-271-8349

EMNET TESFAYE
(Display Ads: AL, IN, KY, MI, MS, OH, TN, WV; Line Ads)
Phone: 202-326-6740

GABRIELLE BOGUSLAWSKI
(U.S. Recruitment Advertising Sales Director)
Phone: 718-491-1607

Europe & International

E-mail: ads@science-int.co.uk
Fax: +44 (0) 1223-326-532

TRACY HOLMES
Phone: +44 (0) 1223-326-525

HELEN MORONEY
Phone: +44 (0) 1223-326-528

CHRISTINA HARRISON
Phone: +44 (0) 1223-326-510

SVITLANA BARNES
Phone: +44 (0) 1223-326-527

JASON HANNAFORD
Phone: +81 (0) 52-789-1860

To subscribe to *Science*:
In U.S./Canada call 202-326-6417 or 1-800-731-4939
In the rest of the world call +44 (0) 1223-326-515

Science makes every effort to screen its ads for offensive and/or discriminatory language in accordance with U.S. and non-U.S. law. Since we are an international journal, you may see ads from non-U.S. countries that request applications from specific demographic groups. Since U.S. law does not apply to other countries we try to accommodate recruiting practices of other countries. However, we encourage our readers to alert us to any ads that they feel are discriminatory or offensive.

ScienceCareers.org
We know science AAAS

POSITIONS OPEN

University of Central Florida

NEURODEGENERATIVE DISEASES

University of Central Florida is building a major Biomedical Research and Education Program. We seek outstanding **SCIENTISTS** in neuroscience with an emphasis on neurodegenerative diseases. Faculty at any rank will be considered. The Department of Molecular Biology and Microbiology and the Biomolecular Science Center in the new Burnett College of Biomedical Sciences (**website: http://www.biomed.ucf.edu**) are in the process of hiring 34 tenure-track/tenured faculty members over a five year period. Successful applicants will be expected to establish a well-funded research program, contribute to teaching at the undergraduate/graduate level, and participate in the Biomolecular Science Ph.D. program. Exceptional candidates can be considered for Provost's Research Excellence Professorships.

Competitive salaries, startup funds, new laboratories, transgenic animal facilities and access to shared core instrumentation facilities will be provided. The new 150,000 square-feet Burnett Biomedical Science building will house state-of-the-art laboratories.

The University of Central Florida has over 45,000 students and an outstanding technology-based infrastructure including CREOL (**website: http://www.creol.ucf.edu**) in the College of Optics and Photonics and the Nanoscience Technology Center (http://nanotech.research.ucf.edu). It is located in Orlando, a dynamic and progressive metropolitan region, a major player in high-tech industry, and adjacent to a top-ranked research park including the "National Technology Incubator of the Year" and a great place to live and work.

Review of candidates will begin on November 15, 2005. Please send a curriculum vitae, a two-page summary of research plans, and the names and contact information of three or more references to: **Chair, Neuro Search (e-mail: biomed@mail.ucf.edu) 4000 Central Florida Boulevard, HPAII, 335, University of Central Florida, Orlando, FL 32816-2360.**

As a member of the Florida State University System, all application materials and selection procedures are available for public review. *The University of Central Florida is an Affirmative Action/Equal Opportunity Employer.*

TENURED OR TENURE-TRACK POSITIONS
High Resolution Electron Microscopy

Brandeis University in Waltham, MA is seeking to hire two qualified individuals to fill tenured or tenure-track positions in high resolution electron microscopy, to begin on or after July 1, 2006. Candidates have established, or plan to establish, a vigorous externally funded research program and will be enthusiastic teachers at the undergraduate and graduate levels. Brandeis has a highly interactive faculty and encourages interdisciplinary approaches to research. Ideally, the candidate's research program will interface in one or more areas of existing strength including, but not limited to, structural biology, neuroscience, cell and molecular biology, chemistry, and physics. The University has a state-of-the-art electron microscope facility including a 300 kV field emission cryo EM with energy filter and a 4k CCD camera, and substantial image processing capabilities. Curriculum vitae and three letters of recommendation should be sent to: **EM Search Committee, Provost's Office M.S. 134, Brandeis University, 415 South Street, Waltham, MA 02454.** Consideration of completed applications will begin on November 15, 2005. *Brandeis University is an Equal Opportunity Employer, committed to building a culturally diverse intellectual community, and strongly encourages applications from women and minorities.*

POSITIONS OPEN

CELL AND MOLECULAR BIOLOGY TENURE-TRACK FACULTY POSITION
Biology Department
Williams College

The Biology Department at Williams College invites applications for a tenure-track position at the level of Assistant Professor to begin July 2006. We are seeking a broadly trained Cell or Molecular Biologist who could teach upper-level courses in their area of specialty, contribute to introductory courses in cellular and molecular biology, and participate in interdisciplinary programs in biochemistry, molecular biology, and/or bioinformatics. The successful candidate is expected to establish a research program that involves talented Williams College undergraduates and attracts extramural funding. Applications from outstanding candidates with expertise in any cell or molecular biology discipline will be considered; areas of particular interest that would complement existing strengths in the Department are immunology, microbiology, functional genomics, or signal transduction. Ph.D., postdoctoral experience, and a strong research record are required. Appointment is normally at the beginning Assistant Professor level, although a more senior appointment is possible under special circumstances.

Williams College is a premier liberal arts college with a longstanding tradition of excellence in the sciences. Startup funds and internal funding for research are available. Institutional support for faculty research includes core facilities for tissue culture, confocal and electron microscopy, and automated DNA sequencing. Faculty members typically teach one course and two laboratories, or the equivalent, each semester.

Applicants should submit curriculum vitae, brief statements of teaching and research interests, and arrange for three letters of recommendation to be sent to: **Marsha Altschuler, Chair, Department of Biology, Williams College, Williamstown, MA 01267.** To be assured of full consideration, all materials should be received by November 11, 2005. **Website: http://www.williams.edu/Biology.**

An Equal Opportunity/Affirmative Action Employer, Williams College especially welcomes applications from women and minority candidates.

THREE TENURE-TRACK FACULTY POSITIONS IN ECOLOGY

Purdue University seeks to complement existing strengths in ecology and climate change by filling three tenure-track, academic-year positions at the rank of Assistant Professor in the areas of Aquatic Community Ecology (ACE), Ecological Impacts of Climate Change (EICC), and Quantitative Wildlife Ecology (QWE). Abundant opportunities for collaborative and interdisciplinary activities exist within a vibrant academic atmosphere facilitated by the Purdue Climate Change Research Center, the Purdue Interdisciplinary Center for Ecological Sustainability, and the newly created Discovery Park Center for the Environment.

The successful candidates will be expected to teach and develop dynamic, externally funded research programs within the following focal areas: (1) ACE – quantitative approaches in understanding the structure, function, and dynamics of aquatic communities in freshwater ecosystems; (2) EICC – impacts of climate change on the ecology of terrestrial and/or aquatic populations or communities at landscape to global scales; (3) QWE – development and/or application of quantitative methods and analytical tools to study behavioral, population or community processes of wild vertebrates. Qualifications: A Ph.D. and evidence of significant research accomplishments. Screening of applications will begin on November 15, 2005, and continue until the positions are filled. Details on application procedures and complete descriptions of the positions are available at: **http://www.agriculture.purdue.edu/fnr/**. Please direct questions or inquiries to: **mbrown4@purdue.edu.** *Purdue University is an Equal Access/Equal Opportunity /Affirmative Action Employer. Women and minorities are encouraged to apply.*

Mainline Activity

Genetics and Genomics

IN A FEW SHORT YEARS, GENOMICS HAS BECOME A STAPLE OF R&D IN SUCH FIELDS AS MEDICAL DIAGNOSIS AND THERAPY AND AGRICULTURE. SCIENTISTS QUALIFIED IN THE FIELD CAN CHOOSE AMONG A WIDE VARIETY OF CAREER OPPORTUNITIES. BY PETER GWYNNE

Sequencing the genomes of humans and other organisms has revolutionized life science. Its impact has already extended beyond molecular biology, into such fields as medical diagnostics, medical therapy, and agriculture. "The sequencing of DNA and all the related genomics activity is mainline activity now," declares Ronald Phillips, director of the Center for Microbial and Plant Genomics and search committee chair in the University of Minnesota's Department of Agronomy and Plant Genetics. "From my perspective it ties together biology, agriculture, and medicine."

Certainly genomics has had a huge impact on academic research. "It has just expanded the possibilities of information analysis in all kinds of directions, and has challenged a lot of ingrained theories, which is a good thing," says Kevin Becker, head of the Gene Expression and Genomics Unit at the National Institute on Aging. "It has rolled the dice and reset a lot of programs."

Deepak Srivastava, professor and director of the Gladstone Institute of Cardiovascular Disease at the University of California, San Francisco, agrees. "It's had an enormous impact in our recognition of the significance of parts of the genome that previously weren't fully understood. For example, the comparative sequencing of multiple organisms has made it clear that many previously unrecognized areas of the genome are equally important, including areas that regulate genes. And the recent discovery of genes that encode microRNAs will play a critical role in every process in the organisms."

- **Beckman Coulter GenomeLab Development**
  http://www.beckmancoulter.com
- **Department of Agronomy and Plant Genetics, University of Minnesota**
  http://agronomy.coafes.umn.edu
- **Gene Expression and Genomics Unit, National Institute on Aging**
  http://www.grc.nia.nih.gov
- **Gladstone Institute of Cardiovascular Disease, University of California, San Francisco**
  http://www.gladstone.ucsf.edu

KEVIN BECKER

Influence on Business

Genomics has also influenced life science business, even though the impact has taken longer to mature. "It was a great boon for us," says Scott Boyer, group manager of GenomeLab Development at Beckman Coulter. "We always want to see if we can move products from the research side of the business to the diagnostic side. However, it can be a slow process, due to governmental regulations and requirements. For example, we released out first genetic analysis instrument into the basic research market in 1998 and just this year got our first molecular diagnostic product released into the clinical market."

The impact of genomics can only increase. "At the time of the sequencing of the human genome, there was a lot of hype about tailored medicine," Srivastava recalls. "For the most part that hasn't happened yet; it's been limited by the need for tools to analyze the genome in high throughput fashion at a reasonable cost. But in the five or so years since the genome was sequenced, the development of such tools has been exponential. We're right on the cusp of finally having the tools at the right price to do population studies relevant to disease states and reasonable therapeutics."

Researchers have made significant progress in applying genomics to the understanding of medical ailments. "It's had a lot of effect on rare diseases and has cleared up a lot of information about specific diseases," Becker explains. "For common diseases on which I work, gene sequencing has provided a lot of information for academics that is now brewing and stewing and will come to fruition over the next few years."

Agricultural scientists also look forward to major advances from the application of genomics. "It's being used to transfer genes from one variety of crop to another, by tagging genes with genetic markers," Phillips notes. "At present more than 200 million acres of fields are planted with transferred genes for insect resistance."

Research on Diseases

Becker's group at the National Institute on Aging concentrates on general aging research and specific applications in schizophrenia and inflammatory disorders. "We also have projects in CONTINUED »

Purpose built for you

Genomics Core Facility Scientific Manager
c£42,000 • Cambridge Cancer Research Institute

Our new Institute in Cambridge, is due to open its doors early next year.

With substantial levels of funding behind it, the Centre will represent the single most exciting development in UK cancer research for 25 years. On its completion, 350 specialists will be working with state-of-the-art technology in over 30 different research groups. At the same time, strong links will be forged with oncologists at Addenbrooke's hospital and Cambridge University as we rapidly build a global reputation for excellence.

Now comes your chance to play a pivotal role in our success. As well as setting up the Genomics core facility, this challenging brief will see you deliver a high quality technical service to scientists - including comprehensive data storage support.

To be considered, you should be a senior scientist who combines a PhD qualification with at least five years' background of working with the development of leading edge genomics technologies.

On the personal front, you must be a strong communicator, team player and problem solver with some management experience behind you.

Seldom does an opportunity of this calibre arise. To capitalise on it, in the first instance please email two copies of both your covering letter and CV to recruitment@cancer.org.uk or alternatively please post them to: Cancer Research UK, PO Box 123, Lincoln's Inn Fields, London WC2A 3PX.

Please quote reference number 3688 in all correspondence.

Further details and to apply online please go to https://jobs.cancerresearchuk.org/

Closing date: 28th October 2005.

For further information about the institute visit http://science.cancerresearchuk.org/cri/

CANCER RESEARCH UK

scios

Focusing Science to ADVANCE MEDICINE



Scios Inc., headquartered in Fremont, California, a member of the Johnson & Johnson family of companies, is changing the way heart failure is treated. We are developing new and exciting therapeutics for cardiovascular disease, inflammatory disease and cancer. Our winning combination of integrated research, clinical experience, and passionate commitment to patients with unmet medical needs is making a difference in the management of disease. Innovation, collaboration and education are the cornerstones of Scios' culture.

We provide mentoring and career development opportunities throughout our organization. Our ability to grow as a company depends on finding and nurturing individuals with entrepreneurial spirit and passion to change the way patients are treated.

To support our continued growth, we seek candidates in the following areas:

CLINICAL RESEARCH

- Clinical Data Coder
- Clinical Research Associates
- Directors
- Lead - Clinical Data Mangement
- Manager, Supervisor - Clinical Supplies
- Managers
- Scientist

RESEARCH

- Associate Director, Bioanalytics
- Post Doc - Cell Biology
- Managers - Bioanalytics
- Medical Writers
- Research Associates, Formulations, HTS, Analytical Chemistry
- Scientists - Genomics, Informatics Toxicology, Analytical Chemistry, Pharmacokinetics

MEDICAL AFFAIRS

- Associate Director
- Directors
- Managers
- Medical Education
- Medical Writer
- Manager, Medical Education
- Senior Biostatistician, Lead, Associate Director - Biostatistics

REGULATORY AFFAIRS

- Associates
- Directors
- Managers

QUALITY CONTROL/ QUALITY ASSURANCE

- Analysts
- Specialist

For more information about us, to view a complete job description, and to apply online, please visit us at:

www.sciosinc.com

Equal Opportunity Employer

Johnson & Johnson

Genetics and Genomics


SCOTT BOYER

bioinformatics, including one that deals with polymorphisms in human diseases," he says. "Much of this comes from relatively new genomic data."

The Gladstone Institute also studies disease states. "One of the areas we have decided to focus on is cardiovascular genetics, with the idea that the methods will be robust within three to four years to understand common diseases," Srivastava says. "We want to position ourselves to capitalize on those tools and discoveries as they come online so that we can ask, for example, if certain polymorphisms predispose to disease and whether we can identify people with those polymorphisms and tailor treatments to their genetic profile. That's where the future of medicine lies. We are using the current tools right now to understand genetic predisposition to heart disease – both congenital and acquired."

Minnesota's Department of Agronomy and Plant Genetics seeks to fill a recently endowed chair with a multidisciplinary mission. "We will ask the person to try to tie in genomics and agriculture with medicine, with the idea that most of our major human diseases are diet related," Phillips says. "The question is: How can we modify our foods to make that diet better?" Phillips's own center devotes half its space to scientists involved in genomics and its applications.

Beckman Coulter's nucleic acid testing business concentrates on genomic tools. "My group is focused on two different platforms," Boyer says. "One is capillary electrophoresis – the Swiss army knife of genomic tools that does sequencing, genotyping, a wide variety of genetic testing, and other tasks. It fits well in university labs and it's the basic platform for clinical environments. The other is what we call our SNPStream Genetic Analysis System that does SNP scoring; it's a high throughput system for the detection of mutations and polymorphisms."

Demonstrated Skills

What types of scientist do genomic groups hope to recruit? "We're looking to hire new faculty – principal investigators who have completed an M.D., Ph.D., or both, and have had a successful postdoctoral fellowship in which they have demonstrated that they excel in their skills," Srivastava says. "For our faculty positions, we clearly like to identify those who have substance. We feel that we have the environment here to help young investigators flourish by mentoring and with financial and tangible research support."

Becker seeks a specific specialty. "More and more we focus on bioinformatics," he says. "We're sitting on piles and piles of numbers and data." His unit expects to hire at the Bachelor's and postdoctoral levels. "We have open positions for people in web development and database development," he says. "Almost always, our hires are people with backgrounds in life science who have picked up some computer skills."

Phillips echoes that sentiment. "Any exposure to bioinformatics is useful," he says. "So is understanding of molecular biology." His department also seeks scientists with strong backgrounds in genetics or developmental biology. "Exposure to agriculture is even better," he says. The department expects to hire at the Ph.D. and postdoctoral levels and offers technical positions to scientists with Bachelor's degrees.

Boyer himself has more limited requirements. "I usually recruit molecular biologists for the wet chemistry," he says. "I'm looking for scientists who, in the best case, are molecular biologists with experience in the work we're doing." Beyond Boyer's team, Beckman Coulter has a wide variety of positions available. "We need engineers, scientists, writers, sales people, marketing people, and others," he continues. Boyer's team consists of roughly two-thirds Ph.D.s, with the remainder holding Master's and Bachelor's degrees. "We hire people with Bachelor's degrees right out of college or have them come in as interns while they are still undergraduates," Boyer says. "We'll also bring people into industrial postdoctoral positions, with the possibility that we'll hire them as full time staff scientists if they fit our needs."


DEEPAK SRIVASTAVA

Communications and Collegiality

Scientific skills are necessary but not sufficient for top-notch work in genomics. "I consider communication skills and collegiality extremely important," Srivastava says. "The communication skills are critical for those individuals who will lead their field; they will lead through their science and by having the personality and communication skills that will guide their field in certain directions. And collegiality is important for dealing with your neighbors in scientific teams. It's important to have people in a group who will provide a great deal of synergy."

"Collegiality is absolutely critical for our organization," Boyer agrees. "We always work in a team environment, with up to a hundred people working on any project at one time. They have to handle all things. We also support products when they get to customers, so we need people with very strong communication skills."

Phillips regards two other basic criteria as essential for success in the genomics world. "You have to have honesty and openness, not only in terms of sharing credit but also in terms of your hypothesis and willingness to go in different directions if the readings show it," he points out. "Collegiality is also important because a lot of this work is in teams and is multi-institutional."

Srivastava also looks for intangible qualities when he interviews applicants. "Enthusiasm is very important; people must be excited about their mission. That's contagious and can influence the group," he says. "I also look for evidence that people have a sense of urgency about their work. That's not only a reflection of their personality, but it also reflects their enthusiasm and burning desire to answer the questions they face."

A former science editor of Newsweek, *Peter Gwynne (pgwynne767@aol.com) covers science and technology from his base on Cape Cod, Massachusetts, U.S.A.*

The Gerstner Sloan-Kettering Graduate School of Biomedical Sciences offers the next generation of basic scientists a program to study the biological sciences through the lens of cancer — while giving students the tools they will need to put them in the vanguard of research that can be applied in any area of human disease.

PhD Program in Cancer Biology

An Internationally Recognized Research Faculty in:

- Cancer genetics
- Genomic integrity
- Cell signaling and regulation
- Structural biology
- Immunology
- Chemical biology
- Developmental biology
- Computational biology
- Experimental therapeutics
- Experimental pathology
- Imaging and radiation sciences
- Oncology
- Genomics
- Animal models of disease

An Innovative, Integrated Curriculum Provides a Fundamental Understanding of:

- The nature of genes and gene expression
- Cellular organization
- Tissue and organ formation
- Cell-cell interactions
- Cellular response to the environment
- Enzyme activity

All Matriculated Students Receive a Full Fellowship Package for the Duration of Study.

Gerstner Sloan-Kettering
Graduate School of Biomedical Sciences

New York City

Please visit our Web site to learn how to apply, for application deadlines, and for more information about our PhD program.

www.sloankettering.edu

gradstudies@sloankettering.edu | 646.888.6639

---

science-driven

With the industry-leading invest-ments in R&D that we make each year, Amgen's pipeline continues to grow — a pipeline from which significant break through treatments for anemia and inflammation have recently emerged. But investment alone is insufficient, for it's the people of Amgen who must deliver results. Devoted to science and open to new ideas, this diverse, accomplished team of professionals gives meaning to our values and our mission to serve patients throughout the world. • To apply and learn more, visit: www.amgen.com/careers. As an EEO/AA employer, Amgen values a diverse combination of perspectives and culture M/F/D/V.

AMGEN CURRENTLY HAS THE FOLLOWING OPPORTUNITIES IN ITS SOUTH SAN FRANCISCO, CA LOCATION:

SCIENTIST, CANCER (Job Id# amge-00013567)
Will identify novel cancer drug targets using RNAi-based genetic screens, characterize and validate their mechanisms of action, and lead pre-clinical drug discovery efforts to inhibit their function.

SCIENTIST/SENIOR SCIENTIST, METABOLIC DISEASE (Job Id# amge-00012015)
Will participate in the discovery of novel therapeutics to treat metabolic diseases using molecular, cellular and systems approaches to study the target-mediated biology of these new drugs; expertise in pancreatic islet biology is highly desirable.

SCIENTIST/SENIOR SCIENTIST, METABOLIC DISEASE, DIABETES (Job Id# amge-00014394)
Will investigate aspects of type II diabetes and disorders of lipid metabolism towards the development of novel therapeutics, focusing on target discovery and validation; experience with in vitro and in vivo RNAi based technologies for studying target biology is highly desirable.

SCIENTIST/SENIOR SCIENTIST, GPCR (Job Id# amge-00014395)
Will carry out research to discover novel targets and lead molecules in the area of G-protein coupled receptors, drawing on your expertise in molecular pharmacology to discover novel drugs to treat diseases in multiple therapeutic areas, including metabolic diseases, neuroscience, cancer and inflammation.

To learn more about these positions, as well as other opportunities at Amgen locations throughout the country, please visit our website or email scobin@amgen.com.

www.amgen.com/careers

AMGEN
Dramatically Improving People's Lives

Images: Portion of a SensiparTM (cinacalcet HCl) molecule

BRIGHAM AND WOMEN'S HOSPITAL

Brigham and Women's Hospital (BWH), a major teaching affiliate of Harvard Medical School (HMS), is seeking exceptional candidates with research interests in genetics and genomics to join the faculty of the Harvard Medical School - Partners HealthCare Center for Genetics and Genomics (HPCGG). We are particularly interested in individuals at the early stage of their career and expect that most appointments will be made at the level of tenure-track Assistant Professor.

The mission of HPCGG is to broadly promote genetics and genomics in research and clinical medicine. Under the leadership of Raju S. Kucherlapati, Ph.D., Scientific Director, the Center offers outstanding scholarly and scientific resources and the opportunity to teach graduate students, medical students, residents and fellows. The successful candidate will bring a creative and rigorous investigative program and interact with the exceptional research and clinical communities at BWH and HMS.

To promote the Center's mission, the following are targeted as major research areas:

Bioinformatics
Genetic Epidemiology
Genetic Models of Human Diseases
Genetics of Common Traits and Disorders
Population Genetics
Statistical Genetics
Translational Genetics

Applicants should submit a curriculum vitae, a brief (500 word) statement of research / clinical interest and three letters of reference. Electronic submission of materials is encouraged. Please send materials to: **Christine Seidman, M.D., Associate Director, HPCGG, c/o Andrea Wald, 77 Avenue Louis Pasteur, NRB 250, Boston, MA 02115**. Email to **awald@partners.org**. The application deadline is **November 25, 2005**.

Women and minority candidates are encouraged to apply. Harvard Medical School and Partners HealthCare System are Equal Opportunity/ Affirmative Action Employers.

ccri

CANCER SCIENTISTS

The **Children's Cancer Research Institute** (**CCRI**) of *The University of Texas Health Science Center at San Antonio* (UTHSCSA) is seeking outstanding candidates (Ph.D., M.D./Ph.D. or M.D.) for research or tenure-track positions at Assistant/Associate/Full Professor levels for its programs in molecular oncogenesis, hematologic malignancies, cancer genetics, and experimental cancer therapeutics. Applicants must have high quality peer-reviewed publications, evidence of independent research and competitive funding potential. The positions offer significant scientific resources and an attractive start-up support package.

The **CCRI** is a unique specialized cancer center, is housed in a new 100,000 sq. foot research facility on the North Campus of UTHSCSA and supported by a $200 million endowment from the tobacco settlement from the State of Texas [refer to http://ccri.uthscsa.edu]. Successful applicants will join a multidisciplinary team of researchers at the **CCRI**. The **CCRI** is a component of the UTHSCSA [refer to www.uthscsa.edu] which is located at the edge of the beautiful Texas Hill Country. San Antonio is the nation's eighth largest city and offers a rich, multi-cultural community with a thriving bioscience industry.

Review is ongoing and continues until positions are filled. Applicants should send current curriculum vitae, a description of research plans, and three letters of reference to:

Sharon B. Murphy, M.D.
Professor & Director

Children's Cancer Research Institute
The University of Texas Health Science Center at San Antonio

MC 7784
7703 Floyd Curl Drive
San Antonio, TX 78229-3900
[210] 562-9003 or murphysb@uthscsa.edu

All faculty appointments are designated as security sensitive positions.
UTHSCSA is an Equal Employment Opportunity/Affirmative Action Employer.

UIC

University of Illinois at Chicago
Biochemistry and Molecular Genetics
Faculty Positions

As part of a continuing major expansion, the Department of Biochemistry and Molecular Genetics in the College of Medicine at UIC seeks to add further strength in the following areas, **Membrane Biochemistry (M), Chromatin Function and Gene Expression (G)** and **Basic Mechanisms in Cancer Biology (C)**. Applications are invited from outstanding investigators for Assistant, Associate and Full Professor appointments. We are interested in scientists who apply modern biochemical and molecular approaches to these areas that complement current scientific interests within the department. Investigators utilizing **proteomics** in these areas will be of particular interest. We offer an intellectually stimulating environment in one of the great cities of North America. Visit our website at **http://www.uic.edu/com/bcmg**. Applicants for Assistant Professor appointments should have a doctoral degree and several years of postdoctoral training. Applicants for senior level appointments should have established research programs. Faculty members are generally expected to teach Graduate Students in their area of expertise and assist in some Medical School teaching. Applications should be received on or before **November 16, 2005** for full consideration.

Applicants should send a letter of interest, identifying their area, together with a curriculum vitae, copies of significant publications, a description of current and future research directions and names and contact information for three references to:

Jack H. Kaplan PhD, F.R.S.
Benjamin Goldberg Professor and Head
Faculty Search (M, C or G)
Department of Biochemistry & Molecular Genetics (M/C 669)
University of Illinois at Chicago
Room 2074 MBRB.
900 S. Ashland Ave.
Chicago, IL 60607

UIC is an AA/EOE

FACULTY POSITION
Genome Center of Wisconsin
Department of Biostatistics and Medical Informatics
University of Wisconsin-Madison

The Genome Center of Wisconsin (**http://www.biotech.wisc.edu/gcow**) and the Department of Biostatistics and Medical Informatics (**http://www.biostat.wisc.edu/**) at the University of Wisconsin-Madison are seeking outstanding applicants for a tenure-track position at the **Assistant Professor** or **Associate Professor** level. Candidates with a PhD in statistics, biostatistics, computer science, or related field and who are addressing questions in genomics, proteomics, or systems biology are invited to apply. The successful candidate is expected to establish a strong independent and extramurally funded research program, interact with members of Genome Center and Department of Biostatistics and Medical Informatics, and participate in undergraduate and graduate teaching.

This position is part of a broader mission at both the Genome Center of Wisconsin and the Department of Biostatistics and Medical Informatics to promote highly collaborative and cross-disciplinary genomic and medical research. Faculty in the Genome Center bridge multiple, diverse departments across campus, including departments in biological, chemical, computer, and engineering sciences. As part of both groups, the successful candidate is expected to actively interact and collaborate with members of the Genome Center and Department of Biostatistics and Medical Informatics, as well as with the broader campus community.

Application review will begin **January 17, 2006** and will continue until the position is filled. Applicants should send curriculum vitae, statement of research objectives, and representative publications as PDF files to: **hunter@biotech.wisc.edu**. Arrange to have three letters of recommendation sent to:

GCW Search Committee
c/o Mr. Hunter Johnson
Biotechnology Center
University of Wisconsin-Madison
425 Henry Mall
Madison, WI 53706-1580

GRADUATE PROGRAMS

Graduate School of GENOME SCIENCE & TECHNOLOGY

The University of Tennessee (UT) & Oak Ridge National Laboratory (ORNL)

http://gst.ornl.gov/

Seeking Outstanding Students

- Full tuition waiver and Health Benefits
- Stipend of $18,000
- Accepting applicants with biological, physical, or computational backgrounds

Interdisciplinary Program

- UT and ORNL facilities/expertise
- Seventy-five faculty
- Academic environment and team approaches

Areas of Study

- Genetics/Genomics
- Structural Biology/Proteomics
- Computational Biology/ Bioinformatics
- Bioanalytical Technologies

To apply visit the website: http://gst.ornl.gov
Or Write: Dr. Cynthia B. Peterson, Director
UT/ORNL Graduate School of Genome Science & Technology
1060 Commerce Park
Oak Ridge, TN 37830-8026
cbpeters@utk.edu

MGH 1811 — CHGR — Penn

Assistant Professor
Massachusetts General Hospital
Center for Human Genetic Research

The Center for Human Genetic Research is a new cross-departmental thematic center created to foster multidisciplinary basic, clinical and translational research into genetic mechanisms in human disease. We are seeking to recruit a number of outstanding faculty members at the Assistant Professor level, with research interests in human genetics, including identification and characterization of susceptibility and modifier loci in human disease or in animal models, utilization of genetic approaches to dissect mechanisms of pathogenesis in human disease, bioinformatics or functional approaches to exploiting genome biology, or translation of genetic findings to therapeutic development or patient care. Candidates should have a doctoral degree (PhD and/or MD) in a relevant discipline, postdoctoral or other professional experience, and evidence of outstanding research potential, and publication record. The successful applicants will be appointed in an appropriate department at the Massachusetts General Hospital and at Harvard Medical School.

Applicants should submit curriculum vitae, a brief description of research interest and three letters of reference. Applications by mail or email will be considered until all positions are filled. Please send materials to: **Dr. James F. Gusella, Chair, CHGR Search Committee, Massachusetts General Hospital, Richard B. Simches Research Center, 185 Cambridge Street, Boston MA 02114** or by email to **gusella@helix.mgh.harvard.edu**.

Massachusetts General Hospital and Harvard Medical School are Equal Opportunity/Affirmative Action Employers with institutional commitments to diversity in their faculty.

DNA*®

Bioinformatics Specialists and Product Managers

DNASTAR is a leading developer of software for molecular biologists. Established in 1982, our software products are used by pharmaceutical, biotechnology and academic researchers in 65 countries.

We are expanding our marketing and research and development staffs with the creation of several new positions, including one or more Bioinformatics Specialists and one or more Product Managers in several product areas, including sequence analysis software, supporting the Lasergene product line, and microarray gene expression analysis software, supporting our new ArrayStar product offering.

Product Managers are responsible for DNASTAR software products from design through commercialization, requiring demonstrated expertise in genomic research with suitable experience as an Application Scientist or Product Manager to support the scientific marketing of DNASTAR software products. Areas of focus may include sequence analysis, genotyping and SNP analysis, nuclear RNA analysis, proteomics, and gene expression analysis using microarrays. You will support the informational and technical needs of the internal sales staff and distributors for designated product areas and develop relationships within the research community to support the development of new product marketing requirements.

Bioinformatics Specialists are responsible for understanding current and future product and market directions in specified areas of focus. You will be expected to be hands-on in using competitor products and in developing new product idea prototypes for our software engineers. You need a solid grasp of the market as well as ideas for where we can best focus for greatest future commercial success.

Requirements for these positions include an advanced degree in Molecular Biology or related field (Ph. D. preferred), 5 years applicable industry experience, strong communication skills and solid computer capabilities. The Bioinformatics Specialists should also have strong programming capability in languages suitable for prototyping and simple development.

We offer competitive health, dental and 401k benefits. All positions will be located in Madison, WI, USA. Some travel may be required.

To apply, send resume to **resume@dnastar.com** or mail it to: **General Manager, DNASTAR, Inc., 3801 Regent St., Madison, WI 53705**. No calls please.

DNASTAR is an Equal Opportunity Employer.

CAREERS IN GENETICS & GENOMICS

St. Jude Children's Research Hospital
ALSAC • Danny Thomas, Founder

Finding cures. Saving children.

Our diverse research at St. Jude Children's Research Hospital, located in Memphis, TN, ranges from discovery-focused basic laboratory science to clinical trials of specific agents, regimens, and therapeutic interventions. Current opportunities include:

LABORATORY SUPERVISOR (Microscopy/Imaging)

Immunology (Job Number: 09245)

Focuses on the overall management of scientific endeavors and oversees a developing interdisciplinary, multi-user microscopy/imaging laboratory. Assists with advanced microscopy techniques and new methodologies, including intravital microscopy and live cell imaging, as well as routine maintenance of the instrumentation infrastructure.

FLOW CYTOMETRY SPECIALIST

Genetics (Job Number: 10122)

Operates the facility's cell sorters and analyzers according to demand, with primary responsibility for the operation of one cell sorter and performs daily setup, maintenance and quality control for these instruments.

Other opportunities are also available for research staff at the **BS, MS or PhD levels**. Research focus areas include:

Biochemistry • Developmental Neurobiology
Hartwell Center for Bioinformatics and Biotechnology
Hematology/Oncology • Structural Biology

To learn about these and other current opportunities, and to apply online, visit:
www.stjude.org/jobs

www.stjude.org
An Equal Opportunity Employer

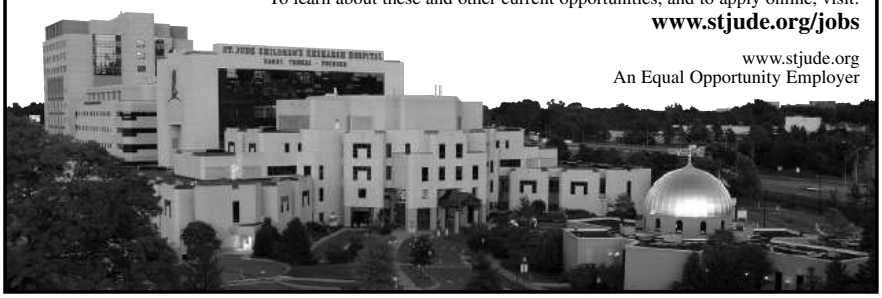

CAREERS IN GENETICS & GENOMICS

TRINITY COLLEGE
The University of Dublin

RECRUITMENT

Smurfit Institute of Genetics
Lectureships (3) in Genetics

Salary Range: €33,332 - €67,268 / €67,077 - €76,404 per annum

The Smurfit Institute of Genetics invites applications for three newly established permanent lectureships to be filled in early 2006.

The staff of the Smurfit Institute have a wide and sustained commitment to high quality teaching and research. The new lecturers will be expected to immediately develop their own research groups through competitive funding, for example from Science Foundation Ireland, The Wellcome Trust, etc.

Applications will be welcomed from people working in any field of Genetics, including those primarily involving mathematical and computational methods.

Further information may be obtained from:
Professor David McConnell, Vice-Dean,
Smurfit Institute of Genetics, Trinity College,
Dublin 2, Ireland. david.mcconnell@tcd.ie

www.tcd.ie/staff_office

Applications together with a research outline and the names of three referees, should be sent to the Recruitment Executive (margaret.kelly@tcd.ie), Staff Office, Trinity College, Dublin 2 before 12 noon on Thursday 10th November, 2005.

Trinity College is an Equal Opportunities Employer

POSITIONS OPEN

Okinawa Institute of Science and Technology Postdoctoral Fellows & Investigators

The Okinawa Institute of Science and Technology, a new International Graduate University in Okinawa, has established a Research Initiative with a number of Research Groups. We are seeking postdoctoral fellows in the areas of Molecular Cell Biology, Molecular Cellular Neuroscience, Computational and Experimental Neurobiology to join the following groups:

- Neural Computation: Dr. K. Doya
- Experimental studies of Learning and Memory: Dr. S. Endo
- G0-cell: Yeast Cell Cycle: Dr. M. Yanagida
- Molecular Neuroscience: Dr. S. Brenner, Dr. I. Maruyama, Dr. T. Naito

In addition, we have several openings for investigators with independent research projects in these areas.

Applicants for Postdoctoral fellowships should send their CVs, a description of their area of research interest, and the names of two references.

Applicants for Investigator positions should, in addition, provide a brief outline (1000 words) of the research that they would like to carry out and the resources required for it. Successful candidates will be invited to present more detailed proposals.

The research groups are at present housed in well-equipped temporary laboratories and a major construction program for the new University is underway.

Postdoctoral fellows will be appointed for two years in the first instance with the possibility of renewal. Investigators will receive renewable 5-year appointment as well as the resources required for their research.

Further details about the Institute can be viewed on our website (**www.oist.jp**) which also has the last research report. Interested, qualified candidates: Please send your resumes to **Human Resources Department, Okinawa Institute of Science and Technology, 12-22 Suzaki, Uruma-shi, Okinawa 904-2234, Japan.**

Or resumes may be **faxed to: 81-(0)98-934-8448**, or **emailed to: careers@irp.oist.jp**

Deadline: December 17, 2005

BROWN

Faculty Position in Genomics and Proteomics Assistant, Associate or Full Professor Division of Biology and Medicine

The Division of Biology and Medicine at Brown University announces the opening of a tenure-track faculty position, with the start date of July 1, 2006. Qualifications include a Ph.D. or M.D. degree and a track record of excellence in research. Applicants will be expected to pursue independent, externally-funded research programs that emphasize genomic and proteomic approaches to contemporary biological problems. Applications from physician-scientists are welcome. The applicants will be expected to engage in graduate, undergraduate and/or medical school teaching, and will have the opportunity to participate in several NIH-funded training programs.

Research space will be provided in a new, state-of-the-art facility. The faculty position is part of an ongoing interdepartmental strategic initiative whose objective is to spearhead contemporary biomedical research and to coordinate multidisciplinary approaches in basic science with clinical programs at affiliated hospitals. Researchers in the fields of cancer biology, biology of aging, and those using mouse models to study mechanisms of disease are especially encouraged to apply.

Applications for Associate or Full Professor rank will be treated with confidentiality and need not include letters of recommendation; a list of references may be requested later. Applications at the Assistant Professor level should include at least three reference letters. Review of applications, which should include a curriculum vitae and a description of research interests, will commence on **November 1, 2005**, and will continue until the position is filled. Specific qualifications for appointment at the different faculty ranks can be requested in writing. Contact address: **Dr. John M. Sedivy, c/o Ms. Tammy Glass, Box G-E438, 70 Ship Street, Brown University, Providence, RI 02912**. Please submit one copy of application materials to the above address, and an electronic version (in PDF format) to **tammy_glass@brown.edu**.

Brown University is an EEO/AA Employer and welcomes applications from women and minorities.

UNIVERSITY OF MICHIGAN

CENTER FOR STEM CELL BIOLOGY

The Life Sciences Institute and the University of Michigan Medical School invite applications for tenure track **ASSISTANT PROFESSOR** positions. We are seeking outstanding scholars, with Ph.D., M.D. or equivalent degrees and relevant postdoctoral experience, who show exceptional potential to develop an independent research program that will address fundamental issues in any aspect of stem cell biology. Applicants who have already established successful independent research programs will be considered for tenured **ASSOCIATE PROFESSOR** or **PROFESSOR** positions.

Applicants should send a curriculum vitae, copies of up to three reprints, a one- to two-page summary of research plans, and arrange to have three letters of reference sent directly by **November 15, 2005** to:

Stem Cell Search Committee
c/o Erin Stephens
Life Sciences Institute
University of Michigan
210 Washtenaw Avenue
Ann Arbor, Michigan, 48109-2216

The University of Michigan is an Affirmative Action/ Equal Opportunity Employer.

life sciences institute

New York University

FACULTY POSITIONS

Department of Biology

CENTER FOR COMPARATIVE FUNCTIONAL GENOMICS

NEW YORK UNIVERSITY CENTER FOR COMPARATIVE FUNCTIONAL GENOMICS

As part of a multi-year hiring plan, **New York University's Center for Comparative Functional Genomics** in the Department of Biology invites applications for multiple faculty positions (rank open) to begin September 1, 2006, or as negotiated, pending budgetary and administrative approval. **Candidates using high throughput approaches and/or computational methods to investigate biological regulatory mechanisms and their evolution at the level of systems and networks are especially encouraged to apply**.

Candidates will be expected to have or develop active, externally funded research programs and to participate in the department's teaching activities at both the undergraduate and graduate levels. The Center and the Department (http://www.nyu.edu/fas/dept/biology) offer an outstanding and collegial research environment and opportunities for active collaborations with other related divisions within the university including the NYU Courant Institute's Departments of Mathematical and Computer Science and with genomic consortia formed with other New York institutions.

Applications should include cover letter, research statement, curriculum vitae, and three letters of reference and sent to **Chair of the Search Committee, New York University, Center for Comparative Functional Genomics, Department of Biology, New York University, 1009 Silver Center, 100 Washington Square East, New York, N.Y. 10003**. Electronic applications as PDF files may be sent to **biology.recruitment@nyu.edu**. *Selection of initial candidates will begin on **November 15, 2005**, and proceed on a rolling basis thereafter.*

NYU is an Equal Opportunity/Affirmative Action Employer.

UNIVERSITY OF MARYLAND

Faculty Position in Genomics, Bioinformatics, and Genome Technologies University of Maryland, College Park

The **University of Maryland** invites applications for a faculty position held jointly in the **Department of Cell Biology and Molecular Genetics (www.chemlife.umd.edu/CBMG/)** and the **Center for Bioinformatics and Computational Biology (cbcb.umd.edu)** at the rank of **assistant professor, associate professor or professor**. A doctorate in a relevant field and appropriate experience are required. The primary responsibility of the new hire will be to lead a nationally visible research program in the area of genomics, bioinformatics and genome technologies. The new hire will have access to significant high-end computing infrastructure, and the new Bioscience Research Building, with wet lab research space, is scheduled for completion in the summer of 2006. The University of Maryland is located near the nation's capital and provides abundant opportunities for collaboration with nearby institutions such as the NIH, Smithsonian, USDA-ARS, UMBI and TIGR.

We are accepting, and prefer, paperless applications. **To apply**, send a letter of application, curriculum vitae, statement of research plans, and three letters of recommendation to: **CBMG-CBCBjob@umiacs.umd.edu**. For best consideration, applications should be received by **November 8, 2005**, but applications may be accepted until the position is filled.

For further information, please contact **Steve Mount** by email at **smount@umd.edu**.

The University of Maryland is an Affirmative Action, Equal Opportunity Employer. Women and minorities are strongly encouraged to apply.

Positions @ NIH
THE NATIONAL INSTITUTES OF HEALTH

Chief, Laboratory of Neuropsychology
Intramural Research Program
National Institute of Mental Health

The Laboratory of Neuropsychology (LN) of the NIMH seeks a highly accomplished senior investigator conducting cognitive neuroscience research in nonhuman primates to head an active, ongoing program in this area. The position comes with complementary budget and staff. The strong scientific environment and outstanding resources at NIMH for carrying out such a program make this a unique opportunity for a high-achieving cognitive neuroscientist. The position also offers unparalleled opportunities for interdisciplinary collaboration with scientists throughout the NIH. The successful candidate will be expected to strengthen the current program.

Applicants should have: a Ph.D. and/or M.D. degree; broad experience as an independent investigator applying the techniques of neuropsychology, functional neuroanatomy, behavioral neuroimaging, behavioral electrophysiology, and/or neuropsychopharmacology to research with nonhuman primates; international recognition for studies in one or more of these disciplines; and experience in administering a neuroscience research program.

Salary is commensurate with experience and accomplishments, and a full Civil Service package of benefits (including retirement, health, life, and long-term care insurance, as well as a Thrift Savings Plan, etc.) is available. NIMH is a major research component of the National Institutes of Health and the Department of Health and Human Services, which have nationwide responsibility for improving the health and well being of all Americans. Interested applicants should send curriculum vitae, bibliography, statement of research interests, accomplishments, and goals, together with six letters of reference to: **Leslie Ungerleider, Chair, Search Committee for Chief of LN, Bldg. 10, Rm. 4C104, NIH, Bethesda, MD 20892-1366; or email to ungerlel@mail.nih.gov. Application deadline: November 20, 2005.**

Post Doctoral Position Open Now

A Postdoctoral Fellowship is open in the Eosinophil Biology Section, LAD/NIAID/NIH to study cellular and molecular biology of mammalian eosinophilic leukocytes and their role in host defense. Studies will focus on the roles of eosinophils in respiratory disease and in helminth infection, and the evolution of unique eosinophil secretory mediators. Approaches include molecular and cell biology, high throughput screening methods, and transgenic and gene-deleted mouse models. The preferred candidate will have an M.D. or Ph.D. degree in biological sciences and a recent peer-reviewed publication record. Interested individuals should e-mail or send a cover letter, curriculum vitae, and names and contact details (e-mail preferred) of three referees to:

H. F. Rosenberg, M.D., Ph.D.
EBS/LAD/NIAID/NIH
Bldg. 10, Rm. 11N104
9000 Rockville Pike
Bethesda, MD 20892
USA
Email: hrosenberg@niaid.nih.gov
web page: http://www.niaid.nih.gov/dir/labs/lad/rosenberg.htm

POSTDOCTORAL FELLOWSHIP IN VIRAL IMMUNOLOGY
Laboratory of Respiratory Biology
Research Triangle Park, North Carolina

Human health and human disease result from three interactive elements: environmental factors, individual susceptibility and age. The mission of the National Institute of Environmental Health Sciences (NIEHS) is to reduce the burden of human illness and dysfunction from environmental causes by understanding each of these elements and how they interrelate. The NIEHS achieves its mission through multidisciplinary biomedical research programs. A postdoctoral position is available in the laboratory of Viral Immunology, Laboratory of Respiratory Biology, to study the mechanism of viral regulation of respiratory inflammation and immune regulation. The prospective candidate will use molecular biology, biochemistry and immunology techniques for these studies. Applicants must have a strong work ethic and must possess superior communication skills in English, and a demonstrated record of accomplishment. Background in Immunology is highly recommended.

Applicants must have a Ph.D., M.D. or equivalent and less than five years of postdoctoral experience. For additional information contact **Dr. Farhad Imani at imani@niehs.nih.gov** To apply submit a cover letter, curriculum vitae, bibliography and the names of three references to:

Farhad Imani, Ph.D.
Laboratory of Respiratory Biology, DIR, NIEHS, NIH
P.O. Box 12233, Maildrop D2-01
111 Alexander Drive, Room E238 (For Express Mail)
Research Triangle Park, NC 27709
email: imani@niehs.nih.gov

Tenure Track and Senior Investigators
National Institute of Dental and Craniofacial Research

The Division of Intramural Research in the National Institute of Dental and Craniofacial Research, National institutes of Health, invites applications for Tenure Track and Senior Investigators who will develop and participate in an expanded program in salivary gland research at the Bethesda campus. This program will build on and bridge existing basic and translational research in the division (e.g. stem cell biology, extracellular matrix structure and function, salivary gland morphogenesis, secretory physiology and gene therapy). The program will encompass the major aspects of salivary gland cellular origins, development, function and dysfunction in humans and animal models. The common goals of this overall effort will be to advance the study of salivary glands as a model secretory organ and to pursue remediation of salivary hypofunction (dry mouth) through novel therapeutic approaches such as gene therapy, cell transplantation, regeneration, and the development of a salivary gland de novo from component cells and matrix.

Applicants for these positions who are interested in working on any aspect of this broad range of salivary gland biology will be considered. The individuals should have a Ph.D., D.M.D., D.D.S., M.D. or combined degrees. Applications should include the following: a letter describing research interests and their relationship to the program, a 3-5 page research proposal including salivary gland research, a current curriculum vitae and complete bibliography, and three letters of reference. Senior investigators (Associate or Full Professor rank, or equivalent) should include only the names and contact information for three referees. Send application to: **Cynthia Williams, 30 Center Drive, MSC 4326, Building 30 Room 5A503, Bethesda, MD 20892-4326, USA or email: cwilliams@mail.nih.gov.** Review of complete applications will begin one month after the advertisement date, but the NIDCR will continue to accept applications received after that date until the positions are filled.

WWW.NIH.GOV

Health Research in a Changing World

Fighting Diseases and Improving Lives

Tenure-Track Investigator Position in Immunology and Related Fields
National Institute of Allergy and Infectious Diseases
National Institutes of Health (NIH)

The National Institute of Allergy and Infectious Diseases (NIAID), Division of Intramural Research (DIR) is recruiting for a Tenure-Track Investigator in the Laboratory of Cellular and Molecular Immunology (LCMI). The NIAID is a major research component of the NIH and the Department of Health and Human Services (DHHS).

The Laboratory of Cellular and Molecular Immunology (LCMI) is seeking an M.D., Ph.D., D.V.M., or an equivalent degree for a tenure track position. Candidates with a strong record of creative, scientific accomplishments, and those with a novel, progressive approach to the discipline are particularly encouraged to apply.

The successful candidate will have a unique opportunity to establish an independent research program at the NIH main campus in Bethesda, Maryland. This facility houses one of the largest immunological research communities in the world, with access to flow cytometry, confocal microscopy, mass spectrometry and microarray production. This position will have committed resources for space, a technician and two postdoctoral fellows, as well as an allocated budget to cover service, supplies, animals and salaries.

Salary will be commensurate with research experience and accomplishments. A full Civil Service package of benefits is available, including retirement, health, life, long term insurance care and Thrift Savings Plan.

Address any questions about this position to Dr. Ron Schwartz at rs34r@nih.gov. To apply, candidates must submit: curriculum vitae and bibliography, and a 2-3 page description of a proposed research program and selected publications, preferably via email to Ms. Felicia Braunstein at braunsteinf@niaid.nih.gov. In addition, three letters of recommendation must be sent to Ms. Felicia Braunstein, Committee Manager, NIAID, NIH; Bldg. 10, Rm.4A30, MSC-1349; Bethesda, MD 20892-1349. All applications must be received by December 1, 2005. All applicants will be notified by e-mail or phone when their applications are received and then complete.

We invite you to explore our Institute and other job opportunities at http://healthresearch.niaid.nih.gov/science.

Please reference "Science" on your resume.

NIDDK

POSTDOCTORAL POSITIONS
CELL BIOLOGY
National Institute of Diabetes and Digestive and Kidney Diseases

Two postdoctoral positions are available to study nuclear transport and glycobiology. Current projects include characterizing a novel calmodulin-dependent nuclear transport pathway and a glycan-signaling pathway involved in insulin resistance, diabetes mellitus and neurodegeneration. Cell culture, mouse transgenics and C. elegans serve as model systems. Candidates must have a strong background in cell biology or glycobiology. Please send a C.V. and the names of three references to: **John A. Hanover, Chief, Laboratory of Cell Biochemistry and Biology, NIH/NIDDK, Building 8, Room 402, 8 Center Dr., Bethesda, MD, 20892; fax (301) 496-9431; jah@helix.nih.gov.**

NIDDK

TENURE-TRACK POSITION IN DEVELOPMENTAL BIOLOGY
LABORATORY OF CELLULAR AND DEVELOPMENTAL BIOLOGY

We seek an outstanding scientist to direct a vigorous, innovative research program in molecular mechanisms of development. Applicants must be highly motivated and have a demonstrated track record through publications that address significant biological problems. The successful candidate is expected to develop an independent, world-class research program complementary to current investigations within the Laboratory. The position comes with generous start up funds and on-going support (including salaries for research group) will be provided from intramural research funds.

The Laboratory of Cellular and Developmental Biology, NIDDK is located on the main NIH campus in Bethesda, Maryland, a suburb of Washington, DC. The Laboratory represents interests similar in range to those of an academic department. There are strong interactions among the independent research groups, and the position offers unparalleled opportunities for interdisciplinary collaboration within NIDDK and throughout NIH. Salary and benefits are commensurate with the experience of the applicant. Interested applicants should submit a curriculum vitae, bibliography, copies of three major publications, a summary of research accomplishments, a brief statement of future research goals, and arrange for three letters of reference to be sent to:

Lanette West-Johnson, Office Manager
Laboratory of Cellular and Developmental Biology, NIDDK
50 South Drive, MSC 8028, Building 50, Room 3133
National Institutes of Health, Bethesda, MD 20092-8028

Website: **http://www.niddk.nih.gov/intram/branchlb/lcdb.htm**
Application dateline: **October 28, 2005**

Department of Health and Human Services (DHHS)
National Institutes of Health (NIH)
National Cancer Institute (NCI)
Coordinating Center for Clinical Trials

Announcement Numbers: NCI-05-95178
Position: Director, Coordinating Center for Clinical Trials

We are searching for an M.D. and/or Ph.D. physician/scientist of national stature to serve as the Director of the Coordinating Center for Clinical Trials (CCCT), with overall responsibility for implementing, managing, and evaluating all functions of the CCCT. The Director will serve as an authoritative source of scientific expertise on the development and administration of a national clinical trials enterprise, to include solutions to a myriad of regulatory issues. The CCCT has been charged with implementing the recommendations of the National Cancer Advisory Board's chartered Clinical Trials Working Group (CTWG) on the development, conduct, infrastructure, and support necessary for the optimal coordination and future progress of the entire range of intramural and extramural clinical research trials supported by the NCI, including diagnosis, treatment, and prevention studies.

The CCCT will implement four critical initiatives in order to design a restructured national clinical trials enterprise that is not only more efficient and coordinated but founded on the best science. The first initiative is to improve coordination and cooperation among the functionally diverse components of the current system, including industry and Federal regulatory agencies. The second initiative is to improve prioritization and scientific quality by developing an open and transparent process for the design and prioritization of clinical trials that are science-driven and meet the needs of patient care. Additional initiatives that the CCCT will implement include improving standardization of tools and procedures for trial design, data capture, data sharing, and administrative functions to minimize duplication of effort, and to facilitate development of a shared infrastructure to support an integrated national cancer clinical trials network. Another major initiative includes improving operational efficiency by increasing the rate of patient accrual and reducing operational barriers so that trials can be initiated and executed in a timely, cost-effective manner. More information regarding these initiatives can be found in the final report of the CTWG at: **http://integratedtrials.nci.nih.gov/ict/.**

Total annual compensation will be commensurate with education and experience. Various incentives may apply in individual circumstances based on experience and expertise to increase total compensation to $200,000. A recruitment incentive and relocation expenses may also be available to the selectee. Full Federal benefits including health and life insurance options, retirement, paid holidays, vacation and sick leave will be provided.

To obtain the application requirements and other necessary information, please visit: **http://jobsearch.usajobs.opm.gov/a9nih.asp and search for Vacancy Announcement (VA) NCI-05-95178**. For more information regarding application procedures, please contact **Ms. Mary Lou Weathers at (301) 402-5059.**

Please send, at a minimum, your C.V., Bibliography and Response to the Selective Factor to:

Ms. Mary Lou Weathers
Human Resources Specialist
NIH, OHR, CSD, NCI HR Operations Branch
6120 Executive Boulevard, Room 550
Rockville, MD 20892

Responses to the selection criteria are encouraged. **Application materials may also be faxed to (301) 402-9333 or emailed to weatherm@mail.nih.gov.**

APPLICATIONS MUST BE RECEIVED BY NOVEMBER 14, 2005

Looking to the Future?

The future is now at UVA

Biomedical Sciences

Graduate Programs

Cell & Developmental Biology
Biomedical Engineering
Molecular Medicine
Microbiology, Immunology & Infectious Diseases
Biochemistry, Molecular Biology & Genetics
Neuroscience
Structural, Computational Biology & Biophysics

www.med.virginia.edu/bims
bims@virginia.edu

Many Training Programs Peer-Reviewed and Funded by NIH

UNIVERSITY of VIRGINIA

University of Virginia is an equal opportunity, affirmative action employer.

UCL

UCL Institute of Ophthalmology

Director of Institute of Ophthalmology

The Institute of Ophthalmology and Moorfields Eye Hospital NHS Foundation Trust form the largest single site for eye care and eye research in the world. Over the past 10 years, under the direction of Professor Adam Sillito, the Institute has seen a major expansion, almost tripling in size in both real estate and research staff. In both the last two UK Research Assessment Exercises (1996 and 2001), the Institute gained the highest grade of 5*A. Our 41 academic leaders and their teams are making outstanding research contributions in areas as diverse as disease pathogenesis, eye imaging, cell signalling, wound healing, ocular infection and immunology, ageing and the eye, development and the eye, neuroprotection and neurobiology, gene mapping and therapy, epidemiology and colour vision.

UCL invites applications for the post of Director of the Institute, in succession to Professor Sillito. Candidates should have an outstanding record of academic research and publication, and substantial academic management experience. Although a background in vision science or clinical ophthalmology is particularly desirable, we will be interested to receive applications from internationally excellent researchers in any area of science. A prime task of the Director is to ensure that the research endeavours of the Institute mesh with those of Moorfields Eye Hospital to optimise the translation of expanding scientific knowledge into improvements in patient care. The person appointed to the post of Director will also be appointed to a professorial position within UCL.

The appointment is available from May 2006. Salary is negotiable.

Preliminary enquiries about the post may be made to Professor John Greenwood, Institute of Ophthalmology (email: j.greenwood@ucl.ac.uk) and Professor Roger Hitchings, Director of Research and Development at the Moorfields Eye Hospital NHS Foundation Trust (email: roger.hitchings@moorfields.nhs.uk). Further particulars are available at http://www.ucl.ac.uk/ioo/jobs/research.htm or on request to UCL's Director of Academic Services (email: tim.perry@ucl.ac.uk).

Applications for the post should include a letter of application, a curriculum vitae, the names and addresses of three referees (including at least one referee based outside the candidate's country of residence) and details of current salary. It would be appreciated if candidates would submit both a hard copy (including a signed covering letter) and an electronic copy of their application, addressed to the President and Provost of UCL and sent to the Director of Academic Services, University College London, 5 Gower Street, London WC1E 6BT (email: tim.perry@ucl.ac.uk).

Closing date: 21 November 2005.

We particularly welcome female applicants and those from an ethnic minority, as they are currently under-represented within UCL at this level. This is in line with section 48 of the Sex Discrimination Act and section 38 of the Race Relations Act.

The **Department of Anthropology and the College of Medicine** at the **University of Illinois at Urbana-Champaign** seek to hire a biological anthropologist for a full-time (nine-month) tenured-track open rank position beginning August 16, 2006. We are interested in candidates with an established research program in functional or developmental morphology, human or primate paleontology, medical anthropology or human biology. Consideration also will be given to all candidates with research experience in other areas of biological anthropology that complement existing strengths in the Department of Anthropology. Candidates must be willing to assume responsibility for administration and instruction in human gross anatomy in the College of Medicine, and have demonstrated excellence as a human gross anatomy instructor. Scholarly excellence is our primary criterion. A Ph.D. degree in a relevant biological, anthropological or medical discipline is required, and applications from medical scholars (MD/PhD) are strongly encouraged. Salary will be commensurate with experience.

Please send a letter of application, vitae, samples of publications, a statement detailing research interests and plans, teaching experience and the names and addresses of three referees to: **Paul A. Garber, Head, Department of Anthropology, 109 Davenport Hall, 607 S. Mathews Avenue, Urbana, Illinois 61801; 217-333-3616**. Full consideration will be given to applications received by **November 21, 2005**. Position **#10134**.

The University of Illinois is an Affirmative Action/Equal Opportunity Employer.

UNMC EPPLEY Cancer Center

Postdoctoral Positions in Cancer Research

UNMC Eppley Cancer Center

University of Nebraska Medical Center

Biochemistry • Cellular, Molecular and Structural Biology • Chemical Biology Genetics • Genomics • Immunology

Postdoctoral positions funded by an NCI Training Grant are available for **US citizens** or **permanent residents**. Applicants must directly contact a member of the training faculty prior to submitting an application, which will include a letter of interest, cv, and long-term research goals.

For information on trainers see: **www.unmc.edu/Eppley/crgpfaculty.htm** or contact:

Diane Petersen
Eppley Institute for Research in Cancer and Allied Diseases
University of Nebraska Medical Center
Omaha, NE 68198-6805

After contacting a member of the training faculty you may apply to position **#0587** at **https://jobs.unmc.edu/applicants**.

Director, Interdisciplinary Center for Biotechnology Research
University of Florida
Gainesville, Florida

Salary: Commensurate with Qualifications and Experience

Closing Date: Formal review of applications will begin on November 15, 2005 and will continue until the position is filled.

Duties and Responsibilities: The mission of the Interdisciplinary Center for Biotechnology Research (ICBR) is to support the growth of the life science research program of the University of Florida and that of researchers throughout the state, by making widely available the needed facilities, technologies, training, and competent personnel. ICBR is a service-oriented organization. The Director will have a full-time position reporting to the University of Florida Vice President for Research with an initial appointment for a specified and negotiable period.

Qualifications: Candidates must possess an earned doctorate. The Director must have demonstrated successful leadership and administrative abilities; recognized excellence in research, teaching, outreach, and related scholarly activities; an exemplary funding record, and proven ability to foster cooperative relations within a university and among stakeholders at the state, national, and international levels. Appointment will be made at a tenure or non-tenure accruing track.

For additional position information, please visit our web site: **www.hr.ufl.edu/job**. The reference number for this vacancy is **034323**.

The University of Florida is an Equal Opportunity Institution.

College of Engineering
University of California, Davis
Faculty Positions in Biomedical Engineering

The College of Engineering at UC Davis invites applications from qualified candidates for two tenured or tenure-track faculty positions in the area of biomedical engineering. The Department of Biomedical Engineering has been a recipient of a Leadership-Development Award from the Whitaker Foundation that is responsible for our adding two new faculty members. Senior candidates should have an outstanding international research reputation in biomedical engineering and a track record of interdisciplinary collaboration. Junior candidates should have outstanding research potential. A Ph.D. degree in biomedical engineering or a related discipline is required. Particular areas of interest include bio-nanotechnology, stem cell related bioengineering and the development of new therapeutics. BME is located in an attractive new building with the Genome Center and Research Laboratories for Molecular Medicine. Therefore, candidates whose research emphasizes cellular or molecular scale aspects of biomedical engineering are particularly encouraged to apply. Applicants must be able to teach core undergraduate and graduate courses and be willing to help establish an innovative multidisciplinary curriculum in the field of biomedical engineering.

UC Davis is 14th among US universities in research funding and is ranked among the top ten public engineering colleges in the nation. Davis is a pleasant, family-oriented community in a college-town setting with excellent public schools and a mild climate. Davis is ideally located for many recreational, cultural and professional activities. It is just 15 miles from California's capital city of Sacramento and is within easy driving distance of the Sierra Nevada Mountains, San Francisco, Berkeley, Silicon Valley, wine country and the Pacific Coastal areas.

Interested candidates should submit all materials via the web-based online submission system (**http://jobs.bme.ucdavis.edu**). Required materials include a statement of research and teaching interests (this should include information about previous activities mentoring women, minorities, students with disabilities or other under-represented groups), a curriculum vitae, three to five representative publications and the names and contact information of at least 5 referees who have agreed to write letters of reference. Inquiries can be directed to the chair of the search committee at: **biomedicalengineering@ucdavis.edu**.

The review of applicants will begin on **December 1, 2005**. However, the positions will remain open until filled. The UC Davis College of Engineering is committed to building a diverse faculty, staff and student body as it responds to the changing population and educational needs of California and the nation. **http://www.bme.ucdavis.edu**.

The University of California is an Affirmative Action/Equal Opportunity Employer.

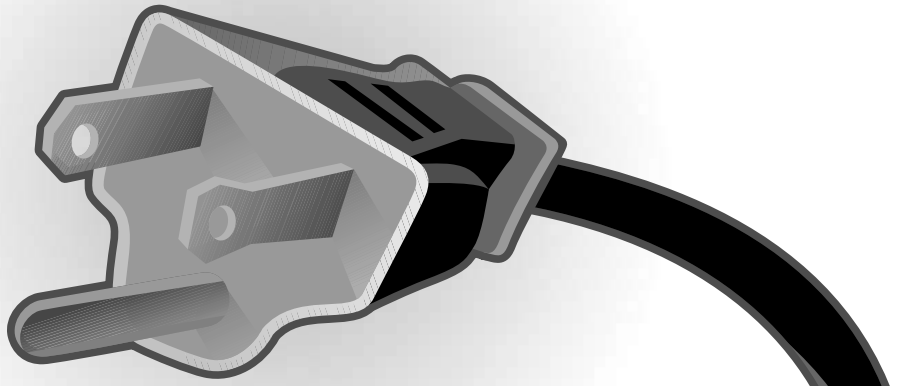

WANT TO PLUG THE POWER OF SCIENCE INTO PUBLIC POLICY?

Become a AAAS Science & Technology Policy Fellow.

What better way to connect your scientific expertise to serve society? Yearlong fellowships offer career-advancing opportunities to work with Congress or a federal agency in one of six thematic areas: Congressional • Diplomacy • National & Global Security • Health, Education, & Human Services • Energy, Environment, & Natural Resources • Revelle Global Stewardship. Stipends begin at $64,000.

Work in Dynamic Washington D.C.
What better place to apply your expertise to the decision-making process that affects people everywhere? You can focus your experience on your interests in national or international issues while you add valuable new perspective to your scientific training.

Join a Network of 1,700 Fellows.
Applicants must have a PhD or equivalent doctoral-level degree from any physical, biological, medical, or social science, or any engineering discipline. Individuals with a master's degree in engineering and at least three years of post-degree professional experience also may apply. U.S. citizenship is required and federal employees are not eligible. Since 1973, AAAS Fellows have benefited from a growing and diverse network of colleagues.

Apply for 2006–07 Fellowships by 10 January 2006.
Fellowships are awarded in the spring and begin 1 September with a two-week orientation. To apply, contact AAAS:

Phone 202-326-6700
E-mail fellowships@aaas.org
Website www.fellowships.aaas.org

Eureka! You've found the perfect connection between science and policy.

Enhancing Public Policy, Advancing Science Careers

www.fellowships.aaas.org

AAAS
ADVANCING SCIENCE, SERVING SOCIETY

POSITIONS OPEN

CARDIOVASCULAR SCIENCE

University of Central Florida is building a major Biomedical Research and Education Program. We seek outstanding **SCIENTISTS** working on molecular, cellular, physiological, biochemical, or pharmacological approaches to study important problems in cardiovascular diseases. Faculty at any rank will be considered. The Department of Molecular Biology and Microbiology and the Biomolecular Science Center in the new Burnett College of Biomedical Sciences (**website: http://www.biomed.ucf.edu**) are in the process of hiring 34 tenure-track/tenured faculty members over a five year period. Successful applicants will be expected to establish a well-funded research program, contribute to teaching at the undergraduate/graduate level, and participate in the Biomolecular Science Ph.D. program. Exceptional candidates can be considered for Provost's Research Excellence Professorships.

Competitive salaries, startup funds, new laboratories, transgenic animal facilities and access to shared core instrumentation facilities will be provided. The new 150,000 square-feet Burnett Biomedical Science building will house state-of-the-art laboratories.

The University of Central Florida has over 45,000 students and an outstanding technology-based infrastructure. It is located in Orlando, a dynamic and progressive metropolitan region, a major player in high-tech industry, and adjacent to a top ranked research park including the "National Technology Incubator of the Year" and a great place to live and work.

Review of candidates will begin on November 15, 2005. Please send a curriculum vitae, a two page summary of research plans, and the names and contact information of three or more references references to: **Chair, Cardio Search (biomed@mail.ucf.edu) 4000 Central Florida Boulevard, HPAII, 335, University of Central Florida, Orlando, FL 32816-2360.**

As a member of the Florida State University System, all application materials and selection procedures are available for public review. *The University of Central Florida is an Affirmative Action/Equal Opportunity Employer.*

CELL/MOLECULAR/DEVELOPMENTAL BIOLOGIST

The Department of Biological Sciences at Marquette University has a tenure-track **ASSISTANT PROFESSOR** position available August 16, 2006, for a biologist to join a faculty with broad research interests (**website: http://biology.marquette.edu**). Applicants must have a Ph.D. with postdoctoral experience. The successful candidate is expected to develop an extramurally funded research program. Teaching responsibilities include an annual undergraduate lecture course in animal development in the spring semester and a graduate lecture or seminar course in the candidate's area of expertise in the fall semester. Send curriculum vitae, statement of research interests, and three letters of reference by November 15, 2005, to: **Dr. Robert Fitts, Chair, Department of Biological Sciences, WLS 112, P.O. Box 1881, Milwaukee, WI 53201-1881.**

ASSISTANT PROFESSORS
Geneticist/Physiologist/Ecologist

The University of Mary Washington seeks three assistant professors for tenure-track appointments. Expertise in field, a Ph.D., and commitment to excellence in teaching required. Details and application materials required available at: **website: http://www.umw.edu/hr/employment/.** *In a continuing effort to enrich its academic environment and provide equal educational and employment opportunities, the University of Mary Washington actively encourages women and minorities to apply.*

FACULTY POSITION
Ecological Systems Modeling #0896

The Departments of Botany and Statistics at the University of Wyoming are seeking to fill a joint tenure-track position at the Assistant or Associate Professor level. Rank will be determined based on evidence of successful research and teaching. We seek an interactive colleague who uses inductive and simulation-based approaches to modeling ecological phenomena. A strong foundation in the application of statistical processes in model building is required. We are especially interested in individuals committed to the rapidly emerging area of spatially distributed modeling, linking time-dynamic process models over heterogeneous environmental domains. All qualified candidates will be considered, however. This position is the second of five to be hired into a new, NSF funded interdisciplinary Program in Ecology (**website: http://uwadmnweb.uwyo.edu/botany/Ecology/**). Candidates must hold a Ph.D. in an appropriate field and have had postdoctoral experience. Evidence of accomplishments in both research and teaching will be essential. The successful candidate will be expected to establish an independently funded research program and participate in both the undergraduate and graduate teaching programs. In the first two years, the new faculty member would be expected to teach a systems modeling course for one semester and a course in computationally intensive statistical programming in the other semester. After two years, the faculty member will be expected to also contribute to the teaching of the undergraduate general ecology course. The Departments are presently composed of 20 faculty members with diverse research interests supported by numerous grants. Salary and startup package will be competitive. The University enrolls 12,000 students including approximately 2,500 graduate students. Laramie is located in southeastern Wyoming about 120 miles from Denver, Colorado. For additional information about the University and departments, see **website: http://www.uwyo.edu/Botany/** and **website: http://uwadmnweb.uwyo.edu/Stats/.** Any questions can be directed to **e-mail: gkbrown@uwyo.edu.** Candidates should submit by e-mail a curriculum vitae, description of research experience and plans, a statement of teaching philosophy. Applicants must also arrange to have three letters of recommendation sent by e-mail to **bjm@uwyo.edu**. PDF formatting is preferred for these documents. Screening of completed applications will begin on October 30, 2005. *The University of Wyoming is an Affirmative Action/Equal Opportunity employer.*

The Biology Department at the University of Nevada, Reno (UNR), seeks a **CELL BIOLOGIST** for a tenure-track assistant professorship to start July 2006. The successful candidate will be provided with a competitive start-up package and will be expected to establish a nationally recognized, extramurally funded research program. The Biology Department has targeted developmental biology as a strategic area for growth and seeks a cell biologist whose research complements our current group of four developmental biologists. Teaching responsibilities will include an undergraduate lecture course in Cell Biology and mentoring graduate students. The Department has approximately 600 majors, 23 state-funded faculty, and averaged $4.7 million of extramural awards annually over the last two years. UNR has outstanding core facilities for genomic, proteomic, and bioinformatics research. Applicants should send curriculum vitae, statements of research plans and teaching philosophy electronically to: **website: http://www.unrsearch.com**, and three letters of recommendation to:

Dr. Grant Mastick
Cell Biologist Search
Department of Biology/314
University of Nevada
Reno, NV 89557

For complete position announcement, requirements, and to apply, visit **website: http:// www.unrsearch.com**. Applications received by November 21, 2005 will receive full consideration.

MOLECULAR BIOLOGY

University of Central Florida is building a major Biomedical Research and Education Program. We seek outstanding **SCIENTISTS** in molecular microbiology relevant to human diseases. Faculty at any rank will be considered. The Department of Molecular Biology and Microbiology and the Biomoecular Science Center in the new Burnett College of Biomedical Sciences (**website: http://www.biomed.ucf.edu**) are hiring 34 tenure-track/tenured faculty members over a five year period. Successful applicants will be expected to establish a well-funded research program, contribute to teaching at the undergraduate/graduate level, and participate in the Biomolecular Science Ph.D. program. Exceptional candidates can be considered for Provost's Research Excellence Professorships.

Competitive salaries, startup funds, new laboratories, access to shared core instrumentation facilities, and transgenic facilities will be provided. The new 150,000 square-feet Burnett Biomedical Science building will house state-of-the-art laboratories.

The University of Central Florida has over 45,000 students and an outstanding technology-based infrastructure. It is located in Orlando, a dynamic and progressive metropolitan region, a major player in high-tech industry, and adjacent to a top-ranked research park including the "National Technology Incubator of the Year" and a great place to live and work.

Review of candidates will begin on November 15, 2005. Please send curriculum vitae, a two-page summary of research plans, and the names and contact information of three or more references to: **Chair, Micro Search, (e-mail: biomed@mail.ucf.edu) 4000 Central Florida Boulevard, HPAII, 335, University of Central Florida, Orlando, FL 32816-2360.**

As a member of the Florida State University System, all application materials and selection procedures are available for public review. *The University of Central Florida is an Affirmative Action/Equal Opportunity Employer.*

Department of Psychology/Psychobiology, Centre College (**website: http://www.centre.edu/**), invites applications for two tenure-track **ASSISTANT PROFESSOR** positions beginning fall 2006.

Applicants for both positions should have a Ph.D. and show clear evidence of excellence in teaching. Collaborative research with undergraduates is expected and supported. Successful applicants for both positions will teach introductory psychology and one position is slated to teach an integrated science course for nonmajors. The two positions will complement each other in order to collectively cover courses in experimental psychobiology, physiological psychology, animal behavior, and sensation and perception. Other courses may include psychopharmacology and emotion, as well as an upper level course in one's specialty. The normal teaching load is 18 hours during the academic year, which can be fulfilled by four courses that include both lecture and laboratory.

Review of applications will begin October 31, 2005, and will continue until the positions are filled. Send letter of application indicating which of the specified courses you have previously taught or have a background to teach, along with curriculum vitae, transcripts, statement of teaching philosophy, statement of research interests, three letters of recommendation, and available teaching evaluations to:

Dean John C. Ward
Vice President for Academic Affairs
Centre College
600 W. Walnut Street
Danville, KY 40422
E-mail: wardj@centre.edu

EOE. Women and minorities are strongly encouraged to apply.

Department Chairman
Department of Health Sciences
Boston University

The Department of Health Sciences at Boston University Sargent College of Health and Rehabilitation Sciences is searching for a Department Chairman at the Professor level. The department has undergraduate and Master of Science programs in human anatomy and physiology, health science, nutrition, and exercise science as well as a Ph.D. program in human anatomy and physiology. Faculty members have diverse backgrounds including muscle biology, neuroscience, nutrition, and exercise science. The area of expertise of the successful candidate is broadly defined within the above disciplines. Applicants should have an earned doctorate, a strong scholarly record and funding from extramural sources, as well as a commitment to further development of undergraduate programs in human physiology, nutrition and health science.

Review of applications will commence upon receipt, and will continue until the position is filled. Applicants should submit a letter of application, curriculum vitae and three letters of reference to: **Chair, Health Sciences Search Committee, Boston University, 635 Commonwealth Avenue, 4th Floor, Boston, MA 02215**.

Boston University is an Equal Opportunity/ Affirmative Action Employer.

The University of Texas at San Antonio
Assistant Professor- Computational Biology

The Department of Biology at the University of Texas San Antonio invites applications for two tenure-track positions at the rank of Assistant Professor pending budget approval.

Required Qualifications: Candidates must have a M.D., or Ph.D. or the equivalent in biology or a related discipline, and at least 2 years of postdoctoral experience. Applicant's research interests should include experimental and computational techniques but can apply to any area of biological research. Preference will be given to candidates with a record of accomplishment in both experimental and model-based studies within the field of Neuroscience. We are seeking faculty with interests in sub cellular (e.g. channels, cell signaling, etc), neuronal (e.g. synaptic integration, or intrinsic electrical properties), systems level research or a combination of all three.

Responsibilities: The successful applicant is expected to establish and maintain an extramurally funded research program, and contribute to undergraduate and graduate teaching in courses offered either at the UTSA Downtown Campus or the 1604 campus, and occasionally at night. The successful candidate will join an interactive group of researchers in Neuroscience at UTSA and the nearby UT Health Science Center. For more information on this faculty group and the department, please visit bio.utsa.edu. Attractive startup packages, including new laboratory space and access to a variety of shared facilities are available pending budget approval.

Candidates please forward via email (**biofacultyad@utsa.edu**) or U.S. Post (**Ion Channel Search Committee, Department of Biology, UTSA, 6900 N. Loop 1604 W., San Antonio, TX 78249-0662**) a current curriculum vita, two or three representative publications, and a brief summary of future research interests and teaching philosophy. Include contact information (including email addresses) of three references. Applications will not be reviewed until all materials have arrived. Applicants who are not U. S. citizens must state their current visa and residency status.

For full consideration, applications should be received by **December 15, 2005**, but will be accepted until the position is filled. For further information contact the search committee at **biofacultyad@utsa.edu**.

UTSA is an Affirmative Action/Equal Opportunity Employer. Women, minorities, veterans, and individuals with disabilities are encouraged to apply. This position is security-sensitive as defined by the Texas Education Code ß51.215(c) and Texas Government Codeß411.094(a)(2).

ST. MARY'S UNIVERSITY

ASSISTANT PROFESSOR - PROTEIN BIOCHEMIST

St. Mary's University of San Antonio, a private, Catholic university, invites applications for a full-time tenure track faculty position in the department of Biological Sciences beginning August 2006. The primary responsibilities of this position will be teaching two courses with associated laboratory per semester. These courses will include biochemistry and introductory biology as well as a course in the candidate's area of specialty, such as protein biochemistry, bioinformatics, or proteomics, that will be developed by the candidate. While teaching is the primary function of the position, research, especially involving undergraduates, is expected of the successful candidate. The presence of an active biomedical research community in the San Antonio area provides the opportunity to establish collaborative research projects in many fields. A Ph.D. in biology or a related discipline is required and postdoctoral experience is preferred.

Founded in 1852 and operated by the Catholic order of the Society of Mary, St. Mary's University is a Hispanic Serving Institution with a proven history of preparing undergraduate science students for careers in health professions and research. For more information, visit the university Web site at www.stmarytx.edu or contact the chair at cnolan@stmarytx.edu or 210-436-3241. Salary is commensurate with experience and is accompanied by a strong benefits package. All qualified applicants are welcome; minorities and women are encouraged to apply.

Applicants should submit a letter of application detailing interest in the position and a description of teaching and professional development goals, a curriculum vitae, copies of transcripts, the e-mail addresses and telephone numbers of references, and have three letters of recommendation sent to: Dr. Colleen J. Nolan, Chair, Department of Biological Sciences, St. Mary's University, One Camino Santa Maria, San Antonio, TX, 78228-8511 no later than October 28, 2005. Review of applications will begin October 31, 2005 and will continue until a suitable candidate is identified.

St. Mary's is an Equal Opportunity Employer.

CSIRO Corporate, Food Futures Flagship

CSIRO

Theme Leaders - Advanced Genetics Innovative Processing

Attractive Remuneration Package
Ref: 2005/1125

CSIRO's National Research Flagship (NRF) program is one of the largest scientific initiatives ever mounted in Australia. An outstanding opportunity currently exists within the Food Futures Flagship for two experienced and motivated individuals to fill the roles of Theme Leader - Advanced Genetics which is concerned with creating novel high value products in cereals and oilseeds and Theme Leader - Innovative Processing which is concerned with creating new ingredients for healthy food and with processing technology.

You will have direct responsibility to the Flagship Director for successful execution and management of the Theme recommending strategic direction and overseeing the integration and delivery of the science. The Theme Leaders will need to be strongly client and outcome focused, with a demonstrated ability to lead strategic science projects, be innovative and a self starter who excels in complex environments. You will have experience interacting with people from a wide range of disciplines across all levels, proven ability of building partnerships and have excellent communication, organisational and coordination skills. You will have demonstrated senior level expertise in a science environment and have a reputation for achieving results.

The position will be located at one of the divisions involved in the Theme.

U53193

For selection documentation and details on how to apply visit

www.csiro.au/careers

Alternatively contact 1300 301 509

Australian Science, Australia's Future

POSITIONS OPEN

DEAN
College Of Natural Sciences
University Of Northern Iowa

The University of Northern Iowa (UNI) is soliciting applications and nominations for the position of the Dean of the College of Natural Sciences. UNI is a dynamic institution that ranks second in the U.S. News & World Report's "Midwestern Universities–Master's" category for public universities while the Princeton Review named UNI a 2006 Best College in Midwestern Region. UNI has approximately 12,500 students, with a full time faculty of about 675 (**website: http:// www.uni.edu**).

The deans of each of the six colleges report to the Vice President/Provost of the University. The Dean provides administrative leadership and support for undergraduate and graduate programs in seven academic departments (Biology, Chemistry, Earth Science, Industrial Technology, Mathematics, Computer Science, and Physics), two interdisciplinary programs (Environmental Science and Science Education) and three centers (Center for Energy and Environmental Education, Metal Casting Center, and Recycling and Reuse Technology Transfer Center). Master's degrees are offered through most departments and interdisciplinary programs and a doctorate (D.I.T.) is offered in Industrial Technology. The University is committed to the infrastructure of the College of Natural Sciences (**website: http://www.cns.uni.edu**) as seen by a recent $16.9 million addition to McCollum Science Hall, in-progress expansions of Computer Science and Industrial Technology facilities and a complete renovation of the Physics Building that will be started in 2006.

The University of Northern Iowa is located in a metropolitan area with a population of 125,000. Further information about the community can be found on **websites: http://www.cedarfallstourism.org** and **http://waterloochampber.orgcommunityinfo.htm.**

Starting date: Preference is July 1, 2006, but not later than August 1, 2006.

Qualifications: Applicants must (1) hold an earned doctorate in a discipline represented in the College; (2) have successful academic administrative experience; (3) have exceptional oral, written, analytical, and interpersonal skills; (4) have a distinguished record in teaching, research, publication and extramural funding commensurate with a tenured appointment as a full professor within a college department; (5) be committed to a participatory management style; and (6) exhibit a strong commitment to a diverse and international academic community.

Salary/benefits: The salary is competitive and is commensurate with experience. There are excellent fringe benefits, including TIAA/CREF.

Application deadline: Applications received by December 15, 2005 will receive full consideration. Include a letter of application, a curriculum vitae, a statement of administrative philosophy, and names, addresses, e-mail addresses and telephone numbers of four references. Applications will be held in confidence, and references will not be contacted until candidates have been consulted. Send applications to:

Dr. Kavita R. Dhanwada, Chair
Search Committee for Dean of CNS
c/o Department of Biology
University of Northern Iowa
Cedar Falls, IA 50614-0421

Electronic submission (PDF or M.S. WORD format) to **e-mail: cns-dean-search@uni.edu** is encouraged. For additional information, call **319-273-5976**.

The College encourages applications from minority persons, women, persons with disabilities and Vietnam era veterans. The University of Northern Iowa is an Equal Opportunity Educator and Employer with a comprehensive plan for affirmative action.

Engineering and Public Policy at Carnegie Mellon seeks **DOCTORAL STUDENTS** with technical backgrounds to address policy issues with important technical content. See **website: http://www.epp.cmu.edu.** Or contact **Victoria Finney, EPP, Carnegie Mellon, Pittsburgh, PA 15213, U.S.A.**

POSITIONS OPEN

UIC University of Illinois at Chicago

ASSISTANT, ASSOCIATE OR FULL PROFESSOR
Bacterial or Viral Research

The Center for Pharmaceutical Biotechnology and the Department of Microbiology and Immunology invite tenure-track faculty applications in areas relevant to mechanisms of pathogenesis and drug discovery. Systems and structural biology approaches are of strong interest. Ph.D. and postdoctoral experience required. Responsibilities include developing a strong, externally funded research program, and teaching in graduate and professional programs. Candidates at the Associate or Full Professor level must have a strong record of extramural funding. Successful candidate will have joint appointments within the Center and the Department of Microbiology and Immunology, with extensive collaborative opportunities in a major health sciences center. Forward curriculum vitae, description of research interests, and three reference letters to: **Dr. M. Johnson, Director, Center for Pharmaceutical Biotechnology, College of Pharmacy, University of Illinois at Chicago, 900 So. Ashland - m/c 870, Chicago, IL 60607-7173.** *Affirmative Action/Equal Opportunity Employer.*

BIOLOGY TENURE-TRACK POSITION

Berry College has an opening starting August 2006 for an ASSISTANT PROFESSOR of biology. Priority will be given to broadly trained and energetic, plant biologists who can teach our introductory sequence, as well as upper-level courses in their specialty. Successful candidates will be expected to develop a strong undergraduate research program. Those candidates who can use our vast outdoor campus are particularly encouraged to apply. Send cover letter, curriculum vitae, statement of teaching and research interests, and three letters of reference to: **Biology Search, School of Mathematical and Natural Sciences, Berry College, Mount Berry, GA 30149-5036.** Application deadline 15 November 2005. Please visit our **website: http://www2.berry.edu/academics/science/**. Berry College, located on 28,000 acres near Rome, Georgia, is an independent coeducational college with approximately 2,000 undergraduate and graduate students. The college's mission stresses academic excellence, practical work experience, and an interdenominational religion-in-life program. *Equal Opportunity Employer.*

CHAIR, DEPARTMENT OF PHARMACOLOGY AND TOXICOLOGY. Full-time, nine-month academic appointment. Candidates must have a Ph.D., and/or M.D., or equivalent in pharmacology or toxicology or a closely related scientific discipline and be eligible for appointment at the professor level. Candidates must have an established and outstanding record in education, research and service in the pharmacological or toxicological sciences, and the ability to attract and secure funding of research programs from federal, private, and/or industrial sources. Full announcement at **website: http:\\jobs.ku.edu.** Review of candidates begins December 1, 2005, and will continue until the position is filled. Completed applications will include current curriculum vitae, a concise summary of research interests and future goals, and three letters of reference. Questions and materials should be addressed to: **Dr. Christian Schöneich, Chair P&Tx Chair Search Committee, School of Pharmacy, The University of Kansas, 1251 Wescoe Hall Drive, Lawrence, KS 66045. Telephone: 785-864-4820, fax: 785-864-5736, e-mail: schoneic@ku.edu.** Paid for by KU. *Equal Opportunity/Affirmative Action Employer.*

POSITIONS OPEN

FACULTY POSITIONS
Microbiology

The Department of Biological Sciences at Clemson University invites applications for two tenure-track positions in the areas of microbial pathogenesis and microbial genetics at the Assistant Professor level to begin August 2006. Exceptional candidates of higher rank will be considered and postdoctoral experience is required. One position is expected to be filled by an individual whose research is on the ecology or pathogenesis of bacterial pathogens associated with plants or animals. The second position is to be filled by an individual whose research focus is based on microbial molecular genetics in the areas of industrial microbiology, food microbiology, biomedicine, or microbial ecology. The successful candidates will be expected to interact with faculty having diverse interests including cell and molecular biology, organismal biology, and ecology and evolution and to support the University emphasis areas of Sustainable Environment and Biotechnology and Biomedicine. Successful candidates will be expected to establish creative, externally funded research programs of national distinction using modern molecular techniques and to be inspiring teachers. Primary teaching responsibilities will be an undergraduate course for majors and graduate course(s) in one's specialty. Applications should include a curriculum vitae, up to three reprints, a statement of current and planned research, a statement of teaching philosophy and interests, and three letters of recommendation sent directly by the applicant's references to the search committee. Review of applications will begin on November 30, 2005, and will continue until the positions are filled. Hard copies of applications and letters of recommendation should be sent to: **Ms. Amy Wilson, Search Committee, Department of Biological Sciences, Clemson University, Clemson, SC 29643-0314.** (Letters & envelopes should clearly indicate the position sought, e.g., "pathogenic microbiology.") Further information concerning the positions, departmental resources, programs, and faculty research interests are available at: **website: http://www.clemson.edu/biosci.**

Clemson University is an Affirmative Action/Equal Opportunity Employer. Clemson University does not discriminate against any person or group on the basis of age, color, disability, gender, national origin, race, religion, sexual orientation, or veteran's status.

BIOCHEMISTRY AND MOLECULAR BIOLOGY
University of California, Los Angeles (UCLA)

The Biochemistry Division of the Department of Chemistry and Biochemistry invites applications for a tenure-track faculty position at the **ASSISTANT PROFESSOR** level. Appointments at other levels are possible in exceptional cases. We are seeking a candidate who will contribute to our Graduate Program in Biochemistry and Molecular Biology through the establishment of a vigorous and innovative research program. We invite outstanding candidates in any area of biochemistry, but have particular interests in systems biochemistry, chemical genomics, biological imaging or the biochemistry of epigenetics. Teaching responsibilities will include undergraduate biochemistry and participation in graduate courses appropriate to the appointee's interests. Applications should include a curriculum vitae, a statement of research accomplishments and future research plans, and two to three reprints of representative publications. Applicants should also arrange for three letters of recommendation to be mailed to the address below. To assure consideration, all application materials and letters should be received by November 15, 2005. Submit to:

Chair
Biochemistry Search Committee
Department of Chemistry and Biochemistry
UCLA, P.O. Box 951569
Los Angeles, CA 90095-1569
Fax: (310) 206-8010

The University of California is an Equal Opportunity/Affirmative Action Employer. Women and minorities are encouraged to apply.

Director of Research with Endowed Chair

The Department of Surgery at The Ohio State University Medical Center is seeking a tenured full-time faculty member at the level of Professor to direct research in the Division of Cardiothoracic Surgery. The successful candidate is an MD and/or PhD with substantial record of active extramural research funding and publications in tissue repair and remodeling. The position is supported by an endowed chair. The successful candidate will function in the rich environment of the Davis Heart and Lung Research Institute. Candidates with proven expertise in the fields of stem or progenitor cell biology, imaging or tissue engineering applied to heart failure and related problems are desirable. This position holds a co-appointment in the Biomedical Engineering program.

Applicants should send a resume and a statement of current research/funding activities to the **Chair of the Search Committee, Professor Chandan K. Sen, Vice Chairman of Research, Department of Surgery, sen-1@medctr.osu.edu. Ph: 614-247-7786, Fax 614-247-7818.**

The Ohio State University is an Equal Opportunity Affirmative Action Employer; women, minorities, and individuals with disabilities are encouraged to apply.

FELLOWSHIPS

Office of the Science and Technology Adviser to the Secretary of State

Jefferson Science Fellowships

The National Academies is pleased to announce a call for nominations and applications for the 2006 Jefferson Science Fellows program. This program establishes a new model for engaging the American academic science, technology and engineering communities in the formulation and implementation of U.S. foreign policy. Jefferson Science Fellows will spend one year at the U.S. Department of State in Washington, D.C. and may periodically travel to U.S. foreign embassies and/or missions. Following the fellowship year, the Jefferson Science Fellow will return to his/her academic career, but will remain available to the U.S. Department of State for short-term projects over the following five years.

Jefferson Science Fellow awards are open to tenured academic scientists, technologists and engineers from U.S. institutions of higher learning. Nominees/applicants must be U.S. citizens and will be required to obtain a security clearance.

Detailed information on the Jefferson Science Fellows program is available on the Web: **www.national-academies.org/jsf**. The deadline for nominations and applications for the 2006 program year is December 1, 2005.

The Jefferson Science Fellows program is sponsored by the MacArthur Foundation and the Carnegie Corporation. Women and minorities are especially encouraged to apply.

THE NATIONAL ACADEMIES
Advisers to the Nation on Science, Engineering, and Medicine

Faculty Positions

The MIT Nuclear Science and Engineering Department anticipates having tenure track faculty openings in the coming academic year. The department has research interests across the spectrum of nuclear science applications, but plays a special national role through its research, facilities, and collaborations in nuclear energy: fission and fusion. Applications from candidates with interests related to nuclear energy are therefore particularly encouraged. Expertise in a relevant technical specialty such as radiation and particle transport (including reactor and neutron science), nuclear chemical engineering, plasma physics, or fusion technology is essential.

To apply, submit a curriculum vitae, description of research interests, and the names of three references via e-mail to nedfacultysearch@mit.edu; or by mail to MIT, Nuclear Science and Engineering Dept, Faculty Search, Room 24-124, 77 Massachusetts Avenue, Cambridge MA 02139-4307.

MIT is an Equal Opportunity/Affirmative Action employer. Applications from women and underrepresented minority candidates are encouraged. MIT is a nonsmoking environment.

Massachusetts Institute of Technology

web.mit.edu/nse

SCOTT & WHITE

College of Medicine
The Texas A&M University System Health Science Center

Pediatric Hematology-Oncologist

The Section of Pediatric Hematology/Oncology at **Scott and White Clinic** and the **Texas A&M University System Health Science Center College of Medicine** (TAMUS HSC-COM) are seeking a clinician scientist with current research grants for a faculty position in a rapidly growing program. The candidate should be BE/BC in pediatric oncology and committed to an academic career. The successful candidates will join and enhance ongoing efforts in basic and translational research, with an institutional commitment to building a world-class experimental therapeutics program. An outstanding start-up package includes high quality laboratory space, excellent benefits and competitive salaries commensurate with academic qualifications. The position guarantees 75% protected time for research activities.

Scott & White Clinic is a 500+ physician directed multi-specialty group practice that is the leading provider of cancer care in Central Texas. Scott and White Clinic and the 486 bed tertiary Scott & White Memorial Hospital is the main clinical teaching facility for TAMUS HSC-COM. Outstanding clinical practice and laboratory facilities on campus that perform state of the art molecular and cellular biology research, flow cytometry, genomics and biostatistics are in place to support the research effort.

Please contact: **Don Wilson, M.D. Professor and Chairman, Department of Pediatrics, Scott & White, 2401 S. 31st, Temple, TX 76508. (800)725-3627 dwilson@swmail.sw.org Fax (254) 724-4974.**

For more information about Scott & White, please visit www.sw.org For Texas A&M www.tamhsc.edu. Scott & White is an equal opportunity employer.

POSITIONS OPEN

ANATOMY/PHYSIOLOGY FACULTY
Messiah College

The Department of Biological Sciences at Messiah College is seeking to fill a full-time, term-tenure-track faculty position in Anatomy/Physiology beginning fall 2006. Primary teaching responsibilities are in human anatomy and physiology (at entry, advanced and general education levels). The successful candidate will be expected to mentor undergraduate research projects, develop personal scholarship and contribute to institutional service. Ph.D., or comparable degree, in Anatomy, Physiology or related disciplines is required. Demonstrated excellence in college teaching, mentoring of student research, and scholarship is preferred. Must be committed to best educational practices as applied to undergraduate science education and the integration of Christian faith and learning. Nominations and applications are welcome. Applicants should submit a letter of interest and application (downloadable from **website: http://www.messiah.edu/offices/hr/forms/Faculty_Empl_Appl.pdf**). Also include two copies of each of the following: a current curriculum vitae, the names and contact information of three professional references, a signed statement of faith, signed permission for a criminal background check, and four personal statement essays (see faculty application for three essay topics. The fourth essay should describe candidates' research interests and how they would adapt these interests to provide collaborative research projects for undergraduate students). Please address all inquires, applications and nominations to:

Sheri Boyce, Ph.D.
Chair of the Search Committee
P.O. Box 3030
Messiah College
Grantham, PA 17027

Women and minorities are strongly encouraged to apply. For additional information about this position, please see the college website at **website: http://www.messiah.edu/offices/hr/job_opportunities/faculty.html.** *Messiah College, a Christian college of the liberal and applied arts and sciences, does not discriminate on the basis of age, color, ethnic/national origin, disability, race or gender in its education programs, admissions or employment policies.*

MEDICINAL CHEMISTRY/ DRUG DISCOVERY
Department of Pharmaceutical and Biomedical Sciences
College of Pharmacy
The University of Georgia, Athens

The Department of Pharmaceutical and Biomedical Sciences at the University of Georgia, Athens invites applications for a full-time, tenure-track faculty position at the Assistant Professor level. Applicants should possess a Ph.D. or a Pharm.D./ Ph.D. or equivalent degree, have demonstrated research skills, and be able to teach at both the Pharm.D. and Ph.D. levels. The successful applicant will also be expected to develop a dynamic, extramurally-funded research program in medicinal chemistry with an emphasis on drug discovery. Focus of the research program should be in one of the areas pertaining to drug discovery such as rational drug design and synthesis, mechanism of action or cellular studies that are applicable to new molecular species that have antiviral, antimicrobial, anticancer or other therapeutic activity. To be assured of full consideration, applications should be received by December 1, 2005. Interested qualified candidates should submit a letter of application, a curriculum vitae, a research plan, and three confidential letters of recommendation to**: Chair, Medicinal Chemistry Search Committee, Department of Pharmaceutical and Biomedical Sciences, R. C. Wilson Pharmacy Building, University of Georgia, Athens, GA 30602-2352.** Applicants may also apply on-line to **website: hhtp://pbssearch@rx.uga.edu**. *The University of Georgia is an Equal Employment Opportunity/ Affirmative Action Employer. Applications from qualified women and minority candidates are encouraged.*

PHYSICAL CHEMISTRY FACULTY
University of California, Los Angeles (UCLA)

The Department of Chemistry and Biochemistry of the University of California, Los Angeles, intends to make a tenure-track Faculty appointment in Physical Chemistry (either experimental or theoretical). Candidates at all ranks will be considered. Candidates must give evidence of exceptional promise (for a junior appointment) or great distinction (for a senior appointment) in research and teaching. Applications should include a curriculum vitae, a statement of research accomplishments and description of proposed research (not exceeding four pages), reprints of representative publications, and a list of professional references. Junior faculty applicants should arrange to have three letters of recommendation sent at the time of application. To assure consideration, all application materials should be received by November 15, 2005, and directed to:

Chair
Physical Chemistry Search Committee
Department of Chemistry and Biochemistry
P.O. Box 951569
University of California, Los Angeles,
CA 90095-1569
Fax: (310) 206-8010

UCLA is an equal opportunity/affirmative action employer. Women and minorities are encouraged to apply.

UNIVERSITY OF ARKANSAS FOR MEDICAL SCIENCES
College of Pharmacy

The Department of Pharmaceutical Sciences invites applications for a tenure-track **FACULTY POSITION**. Rank and salary are negotiable. The successful candidate will be expected to have an earned doctorate in pharmaceutical sciences or related discipline and to have a proven record of peer-reviewed research with on-going federally-funded grant support in an area complementary to college and/or campus research. Responsibilities include maintaining a funded research program and participating in graduate and professional education. Numerous opportunities exist for collaborations within the campus.

Application review will begin November 15, 2005. Interested candidates should forward a letter of interest, curriculum vitae, and contact information for at least three references to: **Russell B. Melchert, Ph.D., UAMS College of Pharmacy, Department of Pharmaceutical Sciences, 4301 W. Markham, #522-3, Little Rock, AR 72205. Telephone: 501-686-6495; fax: 501-686-6057; e-mail: melchertrussellb@uams.edu.** *The University of Arkansas for Medical Sciences is an Equal Opportunity/ Affirmative Action Employer.*

FACULTY POSITION

MIT's Department of Brain and Cognitive Sciences anticipates making a tenure-track appointment at the Assistant Professor level in cognitive science or cognitive neuroscience. Applicants should be conducting research with humans in the areas of perception, learning, memory, attention, motor control, language, knowledge representation, reasoning, decision-making, social cognition, development, or computational modeling of cognition.

It is important for applicants to identify the area or areas for which they are applying. Please enclose curriculum vitae, statement of teaching interests, statement of research interests, and representative reprints. Please arrange to have three letters of recommendation sent to the search committee. Review of applications will begin November 1, 2005, and continue until the position is filled.

Send applications to: **Cognitive Search Committee, 46-2005A, MIT, 77 Massachusetts Avenue, Cambridge, MA 02139-4307.** Information about the department can be found at **website: http://web.mit.edu/bcs/.** *Qualified women and minority candidates are especially encouraged to apply. MIT is an Affirmative Action/Equal Opportunity employer.*

FACULTY POSITION
Vertebrate Development

The Department of Genetics, Cell Biology & Development (GCD), in collaboration with the Developmental Biology Center (DBC) at the University of Minnesota is conducting a search for an Assistant, Associate, or Full Professor studying fundamental mechanisms of vertebrate development. The DBC (**website: http://www.med.umn.edu/dbc/**) is an interdepartmental group of more than 30 faculty, housed in two adjacent buildings. The Department of GCD (**website: http://www.gcd.med.umn.edu**) will provide a competitive salary and startup package, plus excellent laboratory space, with access to state-of-the-art core facilities. The candidate must have a Ph.D. or M.D. and at least two years of postdoctoral experience. Investigators using any vertebrate system will be considered, with originality directed at critical questions serving as the most important criterion for selection. Emphasis will also be placed on the potential for interaction with existing research programs in GCD and the DBC, as well as other centers and institutes such as the Stem Cell Institute, the Institute for Human Genetics and the Cancer Center. The person selected will be expected to develop or expand upon an independent, externally-funded research program and participate in the teaching mission of the department. Applications will be reviewed, beginning Dec 1, 2005, and will be accepted until the position is filled.

Please send a curriculum vitae, a brief statement of current and future research, and three letters of reference to: **GCD Vertebrate Development Faculty Search, c/o Mary Muwahid, University of Minnesota, Department of Genetics, Cell Biology and Development, 6-160 Jackson Hall, 321 Church Street SE, Minneapolis, MN 55455**. Contact **Mary Muwahid (email: muwah001@umn.edu**) with questions.

The University of Minnesota is an equal opportunity educator and employer.

TENURE-TRACK FACULTY POSITION
Genetics

Washburn University's Biology Department invites applications for tenure-track genetics position beginning August 2006. Qualifications: Ph.D. with broad background in genetics; commitment to quality undergraduate education; preference given to candidates with demonstrated teaching excellence. Responsibilities: Teach majors' courses (e.g., general genetics, human genetics) and introductory biology courses; supervise undergraduate research. Rank/salary commensurate with experience; $42,000 minimum. Application review begins November 1, 2005, and continues until suitable candidate identified. Send curriculum vitae, statements of teaching & research philosophies, transcripts, three letters of reference to: **Dr. John Mullican, Biology Department, Washburn University, Topeka, KS 66621. Website: http://www.washburn.edu.** *Washburn University is EOE.*

ASSISTANT PROFESSOR OF BIOLOGY
Anatomy and Physiology

St. Vincent College invites applications for a tenure-track position beginning fall 2006. Requirements include Ph.D., commitment to undergraduate education, and training in human anatomy and physiology. Postdoctoral or teaching experience preferred. Teaching responsibilities include anatomy, physiology, and pathophysiology for nurse anesthesia students; general biology for undergraduate biology majors; a course for nonscience majors; and supervision of senior research projects. Send letter of application, curriculum vitae, three letters of reference, graduate and undergraduate transcripts, statements of teaching philosophy and research interests by December 16, 2005, to: **Director of HR, St. Vincent College, 300 Fraser Purchase Road, Latrobe, PA 15650.** For more information, go to **website: http://www.stvincent.edu/hr2.** *Equal Opportunity Employer.*

UNC
N.C. CANCER HOSPITAL
LINEBERGER COMPREHENSIVE CANCER CENTER

Faculty Positions in Immunology

The UNC Lineberger Comprehensive Cancer Center and the Department of Microbiology and Immunology are searching for individuals with promising or established research programs in the broad areas of immunology. Candidates should have a Ph.D. and/or M.D. with a strong record of recent accomplishments as a postdoctoral fellow or sustained productivity as an established faculty member. Candidates chosen will be placed in tenure-track positions at The University of North Carolina at Chapel Hill. The search will be coordinated by Jenny Ting, Ph.D., Alumni Distinguished Professor and Immunology Program Leader, Lineberger Comprehensive Cancer Center.

Areas of interest include but are not limited to: Cancer immunology, immunity and infection, inflammation and cancer, innate immunity, macrophage and dendritic cell biology, immune signaling, and molecular immunology. Applicants should send a curriculum vitae, a description of research plans, and three letters of reference to:

Melissa Stroud Mack
UNC Lineberger Comprehensive Cancer Center, CB# 7295
University of North Carolina at Chapel Hill
Chapel Hill, NC 27599-7295

The committee will begin reviewing applications **December 15, 2005**.

The University of North Carolina at Chapel Hill is an Equal Opportunity/ADA Employer. Women and minorities are encouraged to apply.

Laboratory for Drug Discovery in Neurodegeneration Harvard Center for Neurodegeneration & Repair

HCNR

Research Fellowships in Drug Discovery Request for Applications

The Laboratory for Drug Discovery in Neurodegeneration (LDDN) is a core program of the Harvard Center for Neurodegeneration & Repair and has a mission to identify chemical agents that can be used as lead structures for the development of therapeutics. To discover these compounds, LDDN screens their large collection of drug-like molecules for the ability of these compounds to modulate the biological activity of molecular and cellular processes that are thought to play causative roles in neurodegenerative diseases. Optimization of these compounds is achieved by focused programs of medicinal chemistry. To facilitate these activities, the LDDN has a permanent staff of a dozen scientists with industrial experience in assay design, high-throughput screening, informatics, and medicinal chemistry.

The LDDN was recently awarded a grant from the NINDS Cooperative Program in Translational Research that allows us to establish a Fellowship Program in Drug Discovery Research. The goal of this program is to provide postdoctoral fellows, and in some cases graduate students, the unique opportunity to work in a biotech-like atmosphere and transform their basic neurobiological findings into drug discovery programs.

Funding is available for five fellowships and will cover salary, supplies and a housing allowance for the fellows to reside in Boston area for a period of one year. The proposed drug discovery project should be based on on-going studies of the applicant and mentor, and have clear relevance for neurodegenerative disease. If you are interested, please visit our website (**http://www.hcnr.med.harvard.edu/**) where you will find further details about the program and detailed instructions on how to apply. Applications are due **January 15, 2006**. Decisions will be announced March 2006, for a start date of September 1, 2006. General enquiries can be sent to Eiblis Goldings, Administrative Assistant, LDDN at **egoldings@rics.bwh.harvard.edu**.

Director
Office of Human Research Compliance Review

The Office of the Vice President for Research, the University of Michigan, is seeking candidates for Director of the Office of Human Research Compliance Review (OHRCR). OHRCR is one component of the UM's Human Subject Compliance Initiative. OHRCR will (a) conduct not-for-cause audits of research projects involving human participants for compliance with OHRP, FDA, other federal agencies, and University policies; (b) conduct requested reviews for compliance with OHRP, FDA, and other federal agency policies; (c) conduct periodic reviews of operations of the University's Human Subject Compliance sub-systems (including IRBs, COI committees, Radioactive Drug Review Committee, Investigational Drug Service, the General Clinical Research Center, and the Center for Advancement of Clinical Research) for compliance with OHRP, FDA, other federal agencies, and University policies, in each case reporting findings and recommendations to the Vice President for Research; and (d) direct the initiative leading to accreditation by the Association for the Accreditation of Human Research Protection Programs (AAHRPP). The Director will be a full-time member of the University administrative (non-faculty) staff. Essential qualifications include an advanced bio-medical degree (M.D., D.O., Ph.D., M.P.H. or its equivalent). The ideal candidate will have extensive experience in clinical investigation involving human subjects in greater-than-minimal-risk research, FDA compliance experience with industry (GCP, GMP, or both), prior administrative experience, and knowledge of academic medical centers and university cultures.

Candidates should submit a curriculum vitae, a list of three references, and a letter of application to: **Ms. Jane C. Ritter, PHR, University of Michigan, Office of the Vice President for Research, 4080 Fleming Building, 503 Thompson Street, Ann Arbor, MI 48109-1340; E-mail: ritterj@umich.edu.** Review of applications will continue until the position is filled.

The University of Michigan is an Equal Opportunity/ Affirmative Action Employer.

Faculty Position

Environmental Health Sciences with Emphasis on Spatial and Temporal Aspects of Exposure Assessment

School of Public Health
University of California, Berkeley

The School of Public Health at the University of California, Berkeley plans to appoint an assistant professor (tenure track) specializing in the use of newer technologies such as remote or distributed sensing and geographic information systems in the spatial and temporal aspects of exposure as applied to environmental health research and education for Fall 2006. Duties include developing an original research program, teaching graduate courses, and mentoring doctoral students. Faculty in the School of Public Health also have the opportunity to participate in undergraduate education. We prefer candidates who have begun original research programs focused on relationships in health risk and human exposure arising from toxic and/or infectious agents in the environment and have had experience in the design and implementation of field data collection as in data analysis. Candidates must hold a Ph.D. or equivalent in a relevant subspecialty of public health, environmental sciences, engineering, or geography. Salary will be dependent upon individual qualifications.

The deadline for application and receipt of related materials is **November 28, 2005**. Send a letter of interest, curriculum vitae, sample research publications or manuscripts, teaching experience and ratings, and include 3 reference letters (Refer potential reviewers to the UC Berkeley Statement of Confidentiality found at: **http://apo.chance.berkeley.edu/evalltr.html**): **S. Katharine Hammond, Professor of Public Health, c/o Norma Firestone, School of Public Health, University of California, Berkeley, 140 Warren Hall, Berkeley, CA 94720-7360; 510-642-5815 (Fax).**

The University of California is an Equal Opportunity, Affirmative Action Employer.

POSITIONS OPEN

DEAN, SCHOOL OF SCIENCE

St. Mary's College of California seeks a leader who will build upon a record of success and lead the School of Science to its next level of academic excellence. With strong institutional support, the Dean will continue to develop our outstanding undergraduate science and mathematics programs and our national reputation as a leader in undergraduate science education.

The Dean, as the primary academic advocate and administrative officer of the School, promotes the vitality, integrity, and advancement of all programs and ensures that the programs and the policies of the School are consistent with the College's mission.

The School has a full-time faculty of nearly 50, representing the disciplines of biology, chemistry, computer science, mathematics, physics, psychology, environmental science, and three-plus-two engineering, as well as a consortium arrangement with Samuel Merritt College of Nursing. The faculty is committed to teaching effectiveness and scholarly research; providing our students with outstanding educational experiences; vibrant and innovative teaching; personal contact between professor and student; collaborative research projects that convey the excitement and hands-on nature of all scientific investigations.

Earned doctorate in an appropriate field; distinguished record of teaching, service, and scholarship commensurate with rank of full Professor.

Deadline: Review for the position begins October 15, 2005. The position is opened until filled.

To apply: A complete application includes a letter of application, a current curriculum vitae, the names and contact information of five references, and any other materials the applicant deems relevant. Send to:

Frances Sweeney, Ph.D.
Vice Provost of Academic Affairs
St. Mary's College of California
P.O. Box 4228
Moraga, CA 94575-4228
Website: http://www.stmarys-ca.edu

An independent institution, St. Mary's draws upon three principal traditions: the liberal arts, Catholicism, and the LaSallian education vision of St. John Baptist DeLaSalle.

St. Mary's College of California is an Equal Opportunity Employer, committed to diversity and encourages Christian Brothers, women, minorities, persons with disabilities, and veterans to apply. The College seeks faculty, staff, and administrators who espouse or respect the Catholic tradition.

HARVARD MEDICAL SCHOOL
The Children's Hospital Boston

The Stem Cell Program at Children's Hospital Boston invites applications for two **ASSISTANT PROFESSOR** positions (tenure-track): (1) Joint appointment between the Department of Biological Chemistry and Molecular Pharmacology at the Harvard Medical School (primary faculty appointment) and the Stem Cell Program at Children's Hospital; (2) joint appointment between the Department of Genetics at the Harvard Medical School (primary faculty appointment) and the Stem Cell Program at Children's Hospital. Candidates for either position must hold a Ph.D. and/or M.D. Outstanding scientists with a research interest in stem cells will be given a preference. This could include chromatin or transcriptional regulation, cell cycle biochemistry, chemical biology, cancer, or disease models. Applicants must submit an electronic copy of a current curriculum vitae and a description of current and proposed research plans to **e-mail: ckent@enders.tch.harvard.edu,** and arrange to have three letters of recommendation mailed directly from the references to: **Stem Cell Program Search Committee, Attention Christine Kent, Manager, Stem Cell Program at Children's Hospital Boston, 300 Longwood Avenue/Karp 08215, Boston, MA 02115.** Application review will begin on November 1, 2005, and will continue until both positions are filled. Applications will be reviewed only when all required materials have been received.

FACULTY POSITION
Department of Biology
Duke University

The Department of Biology at Duke University is seeking outstanding candidates for a tenure-track position as Assistant Professor. Exceptional candidates at the Associate Professor level will be considered. We are interested in applicants who investigate the molecular basis of biological function within or between cells. We are particularly interested in research using systems, biochemical, genetic, or other molecular approaches to solve complex mechanistic problems. The successful candidate will be expected to develop a strong independent research program and be fully committed to the graduate and undergraduate education mission of the University. Applicants should submit curriculum vitae, a summary of current and proposed research, a statement of teaching interests, and arrange for three letters of recommendation to be sent to: **Molecular Mechanisms Search, Biology Department, Duke University, Box 90338, Durham, NC 27708-0338.** Application materials may also be submitted electronically to **e-mail: MolecularMechanisms2005@duke.edu.** Applications received by November 15, 2005 will be guaranteed consideration. *Duke University is an Equal Opportunity/Affirmative Action Employer.*

The interdepartmental Computational Biology Program of the University of Colorado School of Medicine is soliciting applications for computational biology and bioinformatics **FACULTY** at the junior and senior levels. The recruitment spans all departments, and is open to scientists doing outstanding computational research relevant to any aspect of human health. Topics of interest include (but are not limited to): whole genome comparison, polymorphism analysis, informatics related to type 1 diabetes or autoimmune diseases, cancer informatics, neuroinformatics, and mass spectrometry informatics. Recruitment packages include substantial startup resources and extensive space at the new Fitzsimons campus. To apply, please send your curriculum vitae, names of at least three references, and a statement of teaching and research interests to: **Bioinformatics Search Committee, c/o Kathy Thomas, University of Colorado Health Sciences Center at Fitzsimons, Mailstop 8303, P.O. Box 6511, Aurora, CO 80045-0511.** Or send to **e-mail: kathy.r.thomas@uchsc.edu.** Review of applications will begin immediately and continue until the position is filled. The University of Colorado offers a full benefits package. Information on University benefits programs, including eligibility, is located at **website: http://www.uchsc.edu/pbs/.** *The University of Colorado is committed to Diversity and Equality in Education and Employment.*

The Department of Chemistry at the University of California, Irvine (UCI) seeks to continue building on its existing breadth and strength in theoretical chemistry by making three new **FACULTY APPOINTMENTS.** Applications are invited from both junior and senior ranks in all areas of theoretical and computational chemistry, including, for example, methods development and application in the traditional areas of electronic structure, statistical mechanics, and dynamics, as well as interdisciplinary areas interfacing with biophysics, chemical biology, chemical engineering, materials science, chemical physics, nanotechnology, and bioinformatics. Candidates should have a visionary research program, and commitments to teaching and to the creation of a center of excellence in theoretical chemistry at UCI. A Ph.D. degree is required. To apply, electronically submit curriculum vitae, statements of research and teaching interests, and at least three letters of recommendation. Application instructions may be found at **website: http://ps.uci.edu/employment/apply.html.** Review of applications will begin November 15, 2005. UCI has an active Career Partners Program and has a National Science Foundation ADVANCE Gender Equity Program. *The University of California, Irvine is an Equal Opportunity/Affirmative Action Employer committed to excellence through diversity.*

FACULTY POSITIONS
Tenure Track
Department of Psychiatry

The Department of Psychiatry and the Center for the Study of Traumatic Stress at the Uniformed Services University of the Health Sciences (USUHS) seeks to fill tenure-track neuroscience laboratory research and teaching positions (**ASSISTANT/ASSOCIATE PROFESSOR**). The Department, 20 full-time faculty, seeks to expand ongoing neuroscience research, animal and human, in: stress, anxiety (particularly acute stress responses, PTSD, and dissociation), depression, behavior, and drug use. Individuals who hold Ph.D. or M.D. degrees and have active, fundable research are invited to apply. Send curriculum vitae, description of current and anticipated research, and three references to: **Robert Ursano, M.D., Chairman, Department of Psychiatry, USUHS, 4301 Jones Bridge Road, Bethesda, MD 20814-4799. E-mail: rursano@usuhs.mil.** Applications should be received before December 1, 2005. *The University is an Affirmative Action/Equal Opportunity Employer.*

TENURE-TRACK FACULTY POSITION
Microbiology

Applications are invited for a tenure-track position in the Biology Department at Humboldt State University (HSU). A Ph.D. in microbiology or related discipline, and some teaching experience are required. We seek a broadly trained Microbiologist with expertise in medical microbiology or microbial physiology. Instructional responsibilities may include: bacteriology, medical microbiology, principles of biology, and additional courses in the candidate's area of expertise. Development of an active research program is expected. For additional information see **websites: http://www.humboldt.edu/~facpers/facvac.html,** and **http://www.humboldt.edu/~biosci/.** Application materials should be sent to: **Chair, Microbiology Search Committee, Biology Department, HSU, Arcata, CA 95521. Job# 7317.** Materials postmarked by December 2, 2005, will receive full consideration. *HSU is an EO/Title IX/ADA employer.*

ASSSISTANT PROFESSOR, GENOMICS

Twelve-month, tenure-track position in the Department of Animal Science, Texas A&M University, available January 1, 2006. The successful candidate will conduct a vigorous extramurally funded research program in bovine functional genomics. Specific research areas might include but are not limited to: QTL trait mapping with SNPs, microarray based analysis of complex traits or modeling of genetic networks underlying metabolic pathways. He/she will also be expected to participate in graduate and undergraduate teaching programs. Send applications/inquiries to: **Dr. Gary Acuff, Professor and Head, Department of Animal Science, 2471 TAMU, College Station, TX 77843-2471. Telephone: 979-845-1543, e-mail: g-acuff@tamu.edu.** A full position announcement is available at **website: http://animalscience.tamu.edu/ansc/index.htm.**

PHYSIOLOGY

ASSISTANT PROFESSOR to teach graduate and undergraduate courses in physiology; develop a strong, independent, and externally funded research program; supervise research by undergraduates, M.S. and Ph.D. students; provide service to the university. Visit **website: http://zoology.muohio.edu/** for further details. Require Ph.D. in physiology or related field. Desire postdoctoral experience and expertise that complement existing research strengths in department. Send letter of application, curriculum vitae, statement of teaching and research interests, and three letters of recommendation to: **Dr. Douglas Meikle, 212 Pearson Hall, Oxford, Ohio, 45056.** Contact telephone number is **513-529-3103.** Screen of applications begins December 1, 2005, and will continue until the position is filled.

Faculty Position in Pediatric Cancer

The UNC Lineberger Comprehensive Cancer Center in association with the Department of Pediatrics at the University of North Carolina at Chapel Hill is searching for individuals with promising or established research relevant to childhood cancers. The cancers include leukemias, neuroblastoma, sarcomas, etc. and the areas of research may include, but are not limited to: cancer genetics, clinical/translational research, experimental therapeutics, animal models of cancer, development, stem cell biology, tumor/stroma interactions, and signal transduction.

Candidates should have an M.D. and/or Ph.D. degree with a strong record of recent accomplishments as a postdoctoral fellow or sustained productivity as an established faculty member. The candidate chosen will be placed in a tenured or tenure-track position in the Dept. of Pediatrics as the G. Denman Hammond Chair in Childhood Cancer. The candidate will also have an appointment and laboratory space in the UNC Lineberger Comprehensive Cancer Center. Curriculum vitae, research plans, and three letters of reference should be sent to:

Melissa Stroud Mack/Pediatric Cancer Search
UNC Lineberger Comprehensive Cancer Center, CB# 7295
University of North Carolina at Chapel Hill
Chapel Hill, NC 27599-7295

Review of applications will begin **December 1, 2005**.

The University of North Carolina at Chapel Hill is an Equal Opportunity/ADA Employer. Women and minorities are encouraged to apply.

RUSH S. DICKSON PROFESSORSHIP IN PROSTATE CANCER

The UNC Lineberger Comprehensive Cancer Center invites applications for the Rush S. Dickson Distinguished Professorship of Prostate Cancer Research. The UNC Lineberger Comprehensive Cancer Center and the University of North Carolina at Chapel Hill provide an outstanding environment for basic, clinical, and population-based research in the field of prostate cancer. The Center has a funded DOD Center of Excellence Grant in prostate cancer, a program project on prostate cancer, and a strong focus on animal modeling and translational research in prostate cancer. A new North Carolina Cancer Hospital will provide state-of-the art facilities for clinical research. Applicants should have an M.D., Ph.D., or M.D.-Ph.D. degree and a strong research program in clinical trials and/or the epidemiology, genetics, or fundamental biology of prostate cancer. Appointments will be made in the department appropriate to the candidate's background and at an academic rank consistent with the candidate's credentials.

Curriculum vitae, research plans, and three letters of reference should be sent to:

Melissa Stroud Mack/Prostate Cancer Search
UNC Lineberger Comprehensive Cancer Center, CB# 7295
University of North Carolina at Chapel Hill
Chapel Hill, NC 27599-7295

Review of applications will begin **December 15, 2005**.

The University of North Carolina at Chapel Hill is an Equal Opportunity/ADA Employer. Women and minorities are encouraged to apply.

ASSISTANT PROFESSOR IN SOIL BIOGEOPHYSICS

The Department of Environmental Science, Policy and Management (ESPM), University of California at Berkeley invites applications for a tenure-track, nine-month (academic year) faculty position in Soil Biogeophysics at the Assistant Professor rank. This position will be available starting July 1, 2006 (pending budgetary approval).

We are seeking a candidate with strong quantitative expertise in the production, transport, and transformations of particles, fluids, or solutes in the Critical Zone, and with a productive research program that bridges geophysical and biological approaches. The candidate also will be expected to teach both an undergraduate and a graduate course on soil biogeophysics.

We particularly encourage applications from women and under-represented ethnic minorities. An application should include a curriculum vitae, separate two-page statements of research and teaching interests, and up to three scientific articles. Three to five letters of recommendation should be requested and sent separately.

Please refer potential reviewers to the UC Berkeley Statement of Confidentiality found at **http://apo.chance.berkeley.edu/evalltr.html**. Applications and letters of recommendation should be sent to:

Ms. Kim Oyler, Soil Biogeophysics Search Committee
Department of Environmental Science, Policy, and Management
137 Mulford Hall
University of California
Berkeley, CA 94720-3114

Applications must be *postmarked* by **December 1, 2005**. Applications submitted after the deadline will not be considered.

The University of California is an Equal Opportunity, Affirmative Action Employer with an abiding institutional commitment to excellence through diversity.

Biology Department Head University of Minnesota Duluth

The Department of Biology at the University of Minnesota Duluth (UMD) invites applications for Department Head as a tenured Associate or Full Professor starting in August 2006. We seek a person who combines research and teaching excellence with strong leadership and administrative skills, who can provide leadership for the department, supervise personnel, oversee the departmental budget, and perform other administrative duties with a reduced teaching load. The successful candidate will have a nationally recognized, externally funded research program that can involve graduate and undergraduate researchers. Opportunities exist to participate in several University of Minnesota graduate programs including the new Integrative Biological Sciences graduate program. Scientific collaboration is also possible with researchers at UMDs School of Medicine, Natural Resources Research Institute, College of Pharmacy, and Large Lakes Observatory in addition to US EPAs Mid-Continent Ecology Division. State-of-the-art research and instructional facilities are available in the new Swenson Science and renovated Life Science buildings. Competitive startup funding is available. Abundant recreational opportunities and a high quality of life complement the thriving intellectual and artistic atmosphere in the region. Qualifications include a Ph.D. or equivalent degree in the biological sciences; peer-reviewed publications; evidence of achievement in teaching and research; strong oral and written communication skills; and demonstrated leadership and administrative abilities.

Review of complete applications will begin on **November 7, 2005** and continue until the position is filled. Submit letter of application, curriculum vitae, reprints of research publications, brief statements of teaching and research interests, and administrative accomplishments. Provide contact information for three to five references who can address the candidates instructional skills, research ability and administrative potential. Send application to: **Chairperson, Department Head Search Committee, Department of Biology, University of Minnesota Duluth, 207 SSB, 1035 Kirby Drive, Duluth, Minnesota 55812**. Visit UMD at **www.d.umn.edu/biology** for a complete position description.

The University of Minnesota is an Equal Opportunity Educator and Employer.

POSITIONS OPEN

FACULTY POSITIONS
Pharmaceutics/Drug Delivery
Department of Pharmaceutical and Biomedical Sciences
College of Pharmacy
University of Georgia

The Department of Pharmaceutical and Biomedical Sciences at the University of Georgia, Athens invites applications for two full-time, tenure-track faculty positions (**ONE ASSISTANT PROFESSOR and ONE ASSOCIATE/FULL PROFESSOR**) in the areas of drug delivery/nanotechnology, drug targeting/ drug transport. Applicants should possess a Ph.D. or Pharm.D./Ph.D. or equivalent degree with pharmaceutical sciences or a closely related area as the focus of their graduate education and research training. Excellent communication skills and the ability to teach basic pharmaceutics and drug delivery concepts at both the Pharm.D. and Ph.D. levels are required. Each successful applicant is expected to have or develop a dynamic, extramurally funded research program in an area identified above. To be assured of full consideration, applications should be received by December 1, 2005. Interested qualified applicants should submit a letter of application, curriculum vitae, a research plan, and three confidential letters of recommendation to: **Chair, Pharmaceutics Search Committee, Department of Pharmaceutical and Biomedical Sciences, R. C. Wilson Pharmacy Building, University of Georgia, Athens, GA 30602-2352.** Applicants may also apply online to **e-mail: pbssearch@rx.uga.edu.** *The University of Georgia is an Equal Employment Opportunity/ Affirmative Action Employer. Applications from qualified women and minority candidates are encouraged.*

GENOMIC APPROACHES TO LEARNING OR BEHAVIOR

The Department of Biology at the University of Kentucky invites applications for a tenure-track **ASSISTANT PROFESSOR** position to investigate the molecular and neurobiological basis of behavior. Of particular interest are programs in learning and memory or behavioral plasticity. Preference will be given to candidates working in genetically tractable systems using genomic, proteomic or bioinformatic approaches. The successful candidate is expected to develop a vigorous, extramurally-funded research program and participate in undergraduate and graduate instruction. The startup package includes a competitive salary, a generous budget, and an outstanding collegial environment. Send curriculum vitae, research statement, and three reference letters to: **Behavior Search, Department of Biology, University of Kentucky, 101 Morgan Bldg., Lexington, KY 40506.** Consideration of applications will begin November 14, 2005. *Equal Opportunity/Affirmative Action Employer. Women and minorities encouraged to apply.*

ASSISTANT PROFESSOR OF PHYSICS

Applications are invited for a full-time, tenure-track position in physics, beginning in September 2006. Candidate should be able to teach General Physics I and II and appropriate lab, as well as upper level pre-engineering courses.

All candidates should have a Ph.D. in Physics (ABD considered) in a field of experimental physics, a commitment to teaching and excellent communication skills.

A letter of application, personal teaching philosophy, a curriculum vitae, (unofficial) graduate transcript, and three letters of recommendation should be sent by November 11, 2005, to:

Dr. Mary Ellen Ferraro
Chairperson, Division of Natural Sciences a Nd Mathematics
St. Thomas Aquinas College
125 Route 340
Sparkill, NY 10976

Visit the St. Thomas Aquinas College website at **website: http://www.stac.edu** for details about our college.

VA DESERT PACIFIC HEALTHCARE NETWORK

The VA San Diego Healthcare System is currently seeking applications for the **ASSOCIATE CHIEF OF STAFF** for Research Service. This position may be filled by an academic physician or a Ph.D.-prepared medical scientist. A medical research background is essential. The Chief of Staff is responsible for the Medical Center's $50 million research program. We offer excellent education, teaching, and clinical practice opportunities in an interdisciplinary collaborative setting. Comprehensive benefits package. Must be U.S. Citizen. Direct questions to: **Jan Stock, telephone: 858-552-8585, ext. 7859.** *Equal Opportunity Employer.*

FACULTY POSITION
Developmental Biology

The Department of Biological Sciences at Clemson University invites applications for a tenure-track position in the area of developmental biology at the Assistant Professor level to begin August 2006. Exceptional candidates of higher rank will be considered and postdoctoral experience is required. The successful candidate will be expected to interact with faculty having diverse interests ranging from cell and molecular biology through organismal biology to ecology and evolution, and to support the continuing development of the Biomedicine and Biotechnology emphasis area at Clemson University. Interactions are also expected with faculty from the Greenwood Genetics Center (GGC), a nonprofit institute conducting research on brain development, limb malformation and other birth defects. The successful candidate will be expected to establish innovative, externally-funded research programs of national distinction using modern cell and molecular techniques and to be an excellent teacher. Primary teaching responsibilities will be an undergraduate developmental biology course for majors and graduate course(s) in one's specialty. Applications should include a curriculum vitae, up to three reprints, a statement of current and planned research, a statement of teaching philosophy and interests, and three letters of recommendation sent directly by the applicant's references to the search committee. Review of applications will begin on November 30, 2005, and will continue until the position is filled. Please mail hard copies of applications materials to: **Ms. Amy Wilson, Search Committee, Department of Biological Sciences, Clemson University, Clemson, SC 29634-0314.** Further information concerning this position, departmental resources, programs, and faculty research interests are available at the departmental **website: http://www.clemson.edu/biosci** as well as the GGC **website: http://www.ggc.org.**

Clemson University is an Affirmative Action/Equal Opportunity Employer. Clemson University does not discriminate against any person or group on the basis of age, color, disability, gender, national origin, race, religion, sexual orientation, or veteran's status.

RESEARCH POSITION
Anti-Viral Activity

Stephen F. Austin State University is seeking a full-time **RESEARCH SCIENTIST** in the identification of anti-viral compounds from plants. Candidates must have a Ph.D. or M.S. degree in a field related to anti-viral bioactivity of natural products and at least two years research experience in the field. The detailed job description is available at **website: http://www.sfasu.edu/personnel/professional.html.** Salary is commensurate with qualifications and experience. Review of applications will begin immediately. Interested individuals should submit a letter of application, curriculum vitae, two or three representative publications, and three letters of recommendation to: **Dr. Shiyou Li, SFA Center for Pharmaceutical Crops, P.O. Box 6109, Nacogdoches, TX, 75962 (E-mail: lis@sfasu.edu).**

The University of Florida McKnight Brain Institute (MBI), UF Shands Cancer Center (UFSCC), the Department of Neurological Surgery, and the Department of Pharmacology and Therapeutics in the College of Medicine are expanding the neuro-oncology program with a focus on molecular therapeutics. Positions are open for tenure-track neuro-oncology researchers having a Ph.D. and/or M.D. degree, at the **ASSISTANT/ASSOCIATE/FULL PROFESSOR** levels. We are especially interested in the fields of cancer stem cell biology, immunology, and cell signaling with an eye toward the development of new cellular and molecular therapeutic approaches for brain cancer. Substantial startup packages and endowments will support the investigators to help build a program dedicated to the development of new therapeutics for invasive brain tumors. Additional information about the research and educational programs in the MBI, UFSCC, and the Department are available at **websites: http://www.mbi.ufl.edu, http://www.ufscc.ufl.edu,** and **http://www.med.ufl.edu/pharm,** respectively. Applications consisting of curriculum vitae and three letters of recommendation will be accepted until December 31, 2005. Please contact: **Dr. Dennis A. Steindler, Executive Director, The Evelyn F. and William L. McKnight Brain Institute of the University of Florida, College of Medicine, P.O. Box 100015, Gainesville, FL 32610. E-mail: steindler@mbi.ufl.edu.** *This is an Equal Opportunity Institute.*

GENETICIST
VERTEBRATE BIOLOGIST
BIOCHEMIST

University of Wisconsin, Eau Claire, a selective, state comprehensive university and Center of Excellence in Undergraduate Research, seeks two tenure-track Assistant Professorships (Geneticist, Vertebrate Biologist) in the Biology Department and one Assistant or Associate Professorship (Biochemist) in the Chemistry Department beginning August 21, 2006. Ph.D. required. Must have demonstrated ability to teach at post-secondary level and have commitment to develop an active research program. Responsibilities include teaching introductory and upper level courses for majors and nonmajors. Detailed description and application information at **website: http://www.uwec.edu/Biology** or **http://www.uwec.edu/Chemistry.** Priority deadline November 7, 2005. For Vertebrate or Geneticist Searches send inquiries to: **Department of Biology, University of Wisconsin, Eau Claire, WI 54702-4004. E-mail: bogstafg@uwec.edu; telephone: 715-836-4166; fax: 715-836-5089.**

For the Biochemist Search send inquiries to: **Department of Chemistry, University of Wisconsin, Eau Claire, WI 54702-4004. E-mail: halfenja@uwec.edu; telephone: 715-836-4360; fax: 715-836-4979.** *Equal opportunity/affirmative action employer.*

INORGANIC CHEMISTRY
University of California, Irvine

The Department of Chemistry at the University of California, Irvine invites applications for a tenure-track position at the **ASSISTANT PROFESSOR** level in the field of inorganic chemistry. We are seeking a Ph.D. level scientist who will establish a vigorous research program related to any aspect of inorganic chemistry. A strong commitment to teach at the undergraduate and graduate levels is also required. Applications should contain a cover letter, curriculum vitae, list of publications, statement of research, and at least three letters of recommendation. Completed applications should be sent electronically, instructions are to be found at **website: http://ps.uci.edu/employment/apply.html.** To ensure full consideration, applications and supporting materials should be received by December 1, 2005. *The University of California, Irvine is an Equal Opportunity/Affirmative Action Employer committed to excellence through diversity.*

POSITIONS OPEN

UNIVERSITY OF BRITISH COLUMBIA
Innate Immunity/Cellular Microbiology

The Department of Microbiology and Immunology, University of British Columbia, has a tenure-track **ASSISTANT PROFESSOR** position available for an investigator whose research interests lie in the area of cellular microbiology and/or innate immunity. The selected candidate would be eligible to apply for a Tier II Canada Research Chair, a prestigious funding program that was created to attract and retain outstanding young scientists. The Department of Microbiology and Immunology has a strong research record and a thriving graduate program. The nominated candidate will benefit from shared departmental equipment and modern laboratory facilities in the newly erected Life Sciences Centre that will be home to more than 100 multidisciplinary research teams. To apply, please send your curriculum vitae and a five year research plan to: **Nancy Kan, Secretary to the Head, Department of Microbiology and Immunology, Life Sciences Centre, 2350 Health Sciences Mall, Vancouver, BC, V6T 1Z3, Canada**, by December 1, 2005. Electronic (PDF) submissions can be sent to: **e-mail: nancyk@interchange.ubc.ca.** Please also arrange to have three confidential letters of recommendation mailed or e-mailed to the same address for receipt by December 1, 2005. The letters should focus on the applicant's potential to develop an independent research program as well as their demonstrated or potential abilities to train graduate students and teach undergraduate students. All positions are subject to review and final approval by the CRC Secretariat. We encourage all qualified persons to apply. Canada Research Chairs are open to individuals of any nationality; offers will be made in accordance with Canada immigration requirements associated with the Canada Research Chairs program. *The University of British Columbia hires on the basis of merit and is committed to employment equity.*

DEPARTMENT OF MEDICINE
Division of Rheumatology Research

Tenure-track faculty positions at the **ASSISTANT PROFESSOR** level are available in the Department of Medicine/Division of Rheumatic Diseases at Case Western Reserve University, Cleveland, OH. We closely collaborate with the large and expanding rheumatology/musculoskeletal research community at Case and at the University Hospitals of Cleveland.

Candidates should employ cellular, molecular, animal model, transgenic/gene knockout, stem cell approaches to investigate important questions related to immunomodulation/cartilage biology in inflammatory or degenerative joint diseases. They will be expected to develop an independent, vigorous, extramurally funded research program in line with our existing interests and studies (signal transduction, cartilage/chondrocyte biology, novel T cell ligands, animal models of arthritis, complement system, phytochemicals). Competitive startup package will be provided.

Applicants (Ph.D., M.D., or M.D/Ph.D.) should have at least three years of relevant postdoctoral research experience and a solid publication record. Some evidence of independent funding is highly desirable and will be an added qualification. Please send curriculum vitae with names, telephone numbers, and e-mail addresses of three referees, and a letter describing your research interests and goals to:

Dr. Tariq M. Haqqi
Professor & Director of Research
Division of Rheumatic Diseases
Department of Medicine
Case Western Reserve University
2109 Adelbert Road, BRB-319
Cleveland, OH 44106-4919

Case Western Reserve University is an Equal/Opportunity/Affirmative Action Employer and encourages applications from minorities and women candidates.

POSITIONS OPEN

POSTDOCTORAL POSITIONS
Membrane Specialization During Epithelial Differentiation

To study the structure and function of the highly specialized mammalian bladder urothelial membrane (**website: http://www.med.nyu.edu/sun/**). Contact: **Tung-Tien Sun, Director Epithelial Biology Unit and Rudolf Baer Professor of Dermatol, Pharmacol, and Urol, NYU Medical School, New York, NY (e-mail: sunt01@med.nyu.edu).**

DIRECTOR OF EXPERIMENTAL PATHOLOGY
Drs. Mae and Anderson Nettleship Chair in Oncologic Pathology

The Department of Pathology at the University of Arkansas for Medical Sciences invites applications from outstanding scientists for the position of Director of Experimental Pathology, Drs. Mae and Anderson Nettleship Endowed Chair in Oncologic Pathology at the Associate or Full Professor rank. This is a 12-month, tenure-track or tenured position. The successful applicant will be expected to have a funded research program compatible with existing departmental strengths in cancer biology and tumor immunology. Specific areas of interest include extracellular matrix, glycobiology, proteases and gene regulation. (For information on cancer-related research see **website: http://www.acrc.uams.edu/cancer_research/**). The University of Arkansas for Medical Sciences campus has experienced remarkable growth over the last decade and offers a modern and highly collaborative environment. Current extramural funding exceeds $100 million annually. Nationally competitive salary and startup packages along with a state-of-the-art research laboratory will be offered to top candidates. Candidates should send curriculum vitae, statement of research interests, and names/addresses of three references to:

Bruce Smoller, M.D., Chair, Department of Pathology, University of Arkansas for Medical Sciences, 4301 West Markham Street, #517, Little Rock, AR 72205.

E-mail: smollerbrucer@uams.edu.

UAMS is an Equal Opportunity Employer, promoting workplace diversity.

FACULTY POSITION
Department of Applied Science
College of William and Mary

The Department of Applied Science at the College of William and Mary, an interdisciplinary Ph.D.-focused department established in 1995, invites applicants for a tenure-track position at the Assistant Professor level in biophysics, neurophysiology, biomedical engineering, biomaterials, or a related field, emphasizing either computational or experimental approaches. The new faculty member will be expected to establish a vigorous, independent, and well-funded graduate research program at the interface of the physical, mathematical, and biological sciences. Excellence and high commitment to the teaching of graduate and undergraduate students is also expected of all faculty at the College. Located two hours south of Washington, DC in Williamsburg, Virginia, the College of William and Mary is the second oldest university in the United States and was recently named by the editors of Newsweek as the "hottest small state school" in the nation. Candidates should submit a complete curriculum vitae, contact information for three letters of reference, and copies of no more than five refereed publications to: **Faculty Search Committee, Department of Applied Science, The College of William & Mary, PO Box 8795, Williamsburg, VA 23187-8795.** Review of materials is expected to begin January 1, 2005, and continue until the position is filled. For more information see **website: http://as.wm.edu.** *The College is an Equal Employment Opportunity/Affirmative Action Employer.*

POSITIONS OPEN

UCLA **TENURE-TRACK FACULTY POSITION,** Department of Anesthesiology: The Department of Anesthesiology at the David Geffen School of Medicine at UCLA invites applications for a tenure-track faculty position in its Division of Molecular Medicine at an academic rank appropriate for qualifications. The position involves cardiovascular research to complement an existing world-class interdisciplinary program in this area, combining molecular biology, genetics, proteomics, imaging, molecular/cellular/systems physiology, biophysics and mathematical modeling. Candidates are expected to have an M.D. and/or Ph.D. degree with a strong background in one or more of these areas. The successful candidate will become a member of the Department's research group as well as the interdepartmental Cardiovascular Research Laboratory, and will be expected to develop an independent research program as well as collaborative interactions. He/she will also participate actively in the teaching mission of the Department, and will facilitate research training of M.D. candidates for academic careers. Applicants should e-mail their curriculum vitae, a letter with a statement of research interests and career goals, and the names of three references to: **Chair, Anesthesiology Search Committee, c/o adetemple@mednet.ucla.edu** *All qualified applicants are encouraged to apply including women and minorities. UCLA is an Equal Opportunity Employer.*

PHARMACOLOGY/PHYSIOLOGY

The Department of Pharmacology and Physiology at Oklahoma State University Center for Health Sciences invites applications for a tenure-track faculty position at the level of **ASSISTANT PROFESSOR.** For all applicants, a Ph.D. is required with at least two years of postdoctoral experience. The successful applicant is expected to develop an extramurally funded research program and contribute to medical and graduate teaching. Individuals with diverse interests in pharmacology, physiology, or toxicology are invited to apply. Those with interests that complement our current strengths in molecular pharmacology/physiology, neuroscience, or cardiovascular/renal physiology are especially encouraged to apply. Applicants should submit curriculum vitae, a brief description of research accomplishments and future research plans, and the names and contact information of three references to: **Human Resources Main Hall 1405, OSU Center for Health Sciences, 700 N. Greenwood Avenue, Tulsa, OK 74106.** Applicant review will start November 1, 2005. The position is available July 2006. **Website: http:// www healthsciences.okstate.edu.** *Oklahoma State University, Center for Health Sciences is an Equal Opportunity/Affirmative Action Employer.*

COLORADO STATE UNIVERSITY
Two Assistant Biology Professors

Behavioral Ecology. We seek a broadly trained animal biologist whose research addresses fundamental questions in behavioral ecology at multiple levels of inquiry.

Animal Systematics. We seek a broadly trained animal biologist who addresses fundamental questions in systematics and molecular evolution.

The successful candidate for each tenure-track position is expected to develop an externally funded research program and contribute to undergraduate and graduate education. Applicants should have a Ph.D. and record of research excellence. Postdoctoral experience is preferred. For full consideration, submit application materials for the relevant position (cover letter, curriculum vitae, statements of research and teaching interests, contact information for three referees, and up to three representative publications) online at: **website: http:// www.natsci.colostate.edu/searches/Biology/** by December 2, 2005. Applicants should provide referee contact information online as early as possible. Detailed descriptions of each position and the Department of Biology can be found at: **website: http:// www.colostate.edu/Depts/Biology/** *CSU is an Affirmative Action/Equal Opportunity Employer.*

URBAN ENVIRONMENT FACULTY POSITION

Yale University's School of Forestry and Environmental Studies (FES) seeks to fill a junior-level faculty position focused on the urban environment. We seek an individual who takes an integrated view of the natural and human aspects of urban systems. Candidates should have an interdisciplinary approach and a capacity to address both natural and social science aspects of the urban environment. Research topics of interest include but are not limited to: urban land use and land cover; urban environmental modeling, transportation and environment linkages; and alteration of urban ecological conditions by development, including waste management, air or water pollution, and habitat fragmentation and destruction. The successful candidate will have an earned doctorate and an active research program that complements those of existing faculty in FES. She or he will demonstrate capacity for excellence in teaching, and will be expected to advise Master's and Doctoral students. We prefer a candidate with formal training in one or more relevant disciplines such as ecological sciences (e.g., ecology, hydrology, chemistry, geoscience), geography, political science, urban planning, or allied fields.

Applicants should send a c.v., a statement of research and teaching interests, two reprints or other professional publications, and a list of three references to:

Eleanor Migliore
Urban Environment Search Committee
School of Forestry and Environmental Studies
Yale University
205 Prospect St.
New Haven, CT 06511 USA

The deadline for receipt of applications is **November 18, 2005**.

Yale University is an Affirmative Action/Equal Opportunity Employer. Men and women of diverse racial/ethnic backgrounds and cultures are encouraged to apply. Women and minorities, as well as individuals from developing countries, are particularly urged to apply.

University of California, Berkeley
Berkeley Nanosciences and Nanoengineering Institute
Assistant Professor Position in Nanoscience and Nanoengineering and Information Science/Technology

The University of California, Berkeley solicits applications for a tenure track, Assistant Professor position beginning in the Fall of 2006. Creative and energetic candidates who have demonstrated extraordinary accomplishment in research and teaching are specifically sought in fields that are at the intersection between nanoscience, nanoengineering, and information science/technology. Areas of consideration include molecular electronics, self- and directed assembly of nanoelectronic devices and circuits, and nanostructured materials/ devices for quantum information processing. This faculty search will be conducted under the auspices of the Berkeley Nanosciences and Nanoengineering Institute, with participation from the Departments of Physics, Chemistry, Chemical Engineering, Materials Science and Engineering, Electrical Engineering and Computer Science, and Mechanical Engineering. Successful candidates will have the opportunity to interact with scientists and engineers across a wide spectrum of disciplines, and to help develop the new interdisciplinary Nanoscience and Nanoengineering Initiative at Berkeley. Applicants should send a complete curriculum vitae, a selection of publication reprints (five or less), a brief statement of future research plans and teaching interests and the names of at least three references to the address below. Refer potential reviewers to the UC Berkeley Statement of Confidentiality found at: **http://apo.chance.berkeley.edu/evalltr.html** .Applicants should request their references forward letters to the same address. These letters will not be requested directly by the department.

Applications should be sent to: **Chair, Faculty Recruitment Committee; Berkeley Nanosciences and Nanoengineering Institute, c/o Department of Electrical Engineering and Computer Science; University of California; Berkeley, CA 94720-1770**. The deadline for receipt of applications, including references, is **January 31, 2006**, but the search committee will begin interviewing candidates on January 1, 2006.

The University of California is an Equal Opportunity/ Affirmative Action Employer.

CNRS CENTRE NATIONAL DE LA RECHERCHE SCIENTIFIQUE

In 2006, CNRS is recruiting 380 tenured researchers in all scientific fields*.

This recruitment campaign is open **to junior and senior researchers from all over the world**. One of the major objectives of this campaign is to encourage international scientists to apply to CNRS.

CNRS researchers work in an enriching scientific environment:

- numerous large-scale facilities
- highly-skilled technical support
- multiple networks throughout Europe and across disciplines
- access to university research and teaching
- lab-to-lab and international mobility

At CNRS, a long-term vision of excellence in basic research provides a solid foundation for the latest technological research. Successful candidates from the CNRS competitive entry process benefit from the dynamics, stability and stimulation of belonging to a major research organization.

***Mathematics; Physics; Nuclear and High-Energy Physics; Chemistry; Engineering Sciences; Communication and Information Technology and Sciences; Earth Sciences and Astronomy; Environmental Sciences: Life Sciences; Humanities and Social Sciences.**

Application deadline: January 2006. Applications available online in December.

www.cnrs.fr

FACULTY POSITION
Department of Materials Science and Engineering
The Johns Hopkins University

The Department of Materials Science and Engineering at the Johns Hopkins University invites applications for a tenure-track faculty position. Preference will be given to applicants at the assistant professor level, but exceptionally qualified candidates at all ranks will be considered. The successful candidate will be expected to establish an independent, multidisciplinary, internationally recognized research program as well as contribute fully to both undergraduate and graduate instruction. Areas of interest include, but are not limited to, the following: materials computation, ceramics, biomaterials, transmission electron microscopy. Applicants should have a PhD in materials science and engineering or related field and must have demonstrated ability to undertake interdisciplinary research. Post-doctoral experience is highly desirable. Information on the Department of Materials Science and Engineering can be found at **www.jhu.edu/~matsci/**.

All applications should be submitted electronically (for full consideration, before **January 16, 2006**) as a single PDF document to: **materials@jhu.edu**. Electronic applications should include a cover letter describing the principal expertise of the applicant, a statement of teaching and research interests and experiences, a complete resume, and the names and contact information for at least three references.

The Department is committed to building a diverse educational environment; women and minorities are strongly encouraged to apply. The Johns Hopkins University is an EEO/AA Employer.

U.S. Environmental Protection Agency
Office of Research and Development
National Center for Computational Toxicology
VACANCIES IN POSTDOCTORAL RESEARCH

EPA's **National Center for Computational Toxicology (NCCT)** is seeking individuals to fill several vacancies in our postdoctoral research program. The NCCT provides scientific leadership, understanding and tools related to the application of mathematical and computer models to technologies derived from computational chemistry, molecular biology and systems biology in order to improve the Agency's data reporting requirements, priority setting approaches to understanding chemical toxicity, and risk assessment approaches.

Current Opportunities: *•Application of Advanced Statistical Methods to Evaluate Complex Relationships between Environmental Factors and Health Outcomes; •Pharmacokinetics and Perfluorinated Compounds; •Application of Ecological Models to Characterize Environmental Exposures and Risks to Human Populations; •Biologically-Based Pharmacodynamic Modeling Linked with Pharmacokinetic Modeling.*

Benefits: These are full-time, excepted-service appointments lasting 2-4 years. Preference is given to U.S. citizens. The selected applicant is eligible for full benefits including relocation expenses, health and life insurance, retirement, vacation and sick leave. **Easy Application Process**. For more information on NCCT, details on these vacancies and how to apply, visit our website at: **http://www.epa.gov/comptox/** or contact: **Ms. Dorothy Carr** at **(800) 433-9633** or via email at **carr.dorothy@epa.gov**.

The U.S. EPA is an Equal Opportunity Employer.

POSITIONS OPEN

CONSERVATION BIOLOGY OF FISHES

The Department of Biology at the University of Central Florida invites applications for an open rank, tenure-track **FACULTY POSITION** in fish conservation biology. Candidates must have a Ph.D. and a demonstrated ability to establish and maintain a vigorous, extramurally funded research program in fish conservation biology. This individual will contribute to our Ph.D. program in conservation biology and M.S. program in biology, and teach a graduate course in ichthyology and other undergraduate and graduate courses. Preference will be given to innovative and productive scientists whose expertise complements those of our active and growing faculty. See **website: http://www.cas.ucf.edu/biology/** for department details. Applicants should send a letter of intent, curriculum vitae, one-page statements of research plans and teaching philosophy, and arrange for three letters of recommendation to be sent directly to: **Dr. John E. Fauth, Chair, Fish Conservation Search Committee, Department of Biology, University of Central Florida, Orlando, FL 32816-2368.** Review of applications will begin November 15, 2005, with an anticipated start date of August 2006. The University of Central Florida is the seventh largest university in the United States and the second largest in the state of Florida. Search documents may be viewed by the public upon request in accordance with Florida statute. *The University of Central Florida is an Affirmative Action/Equal Opportunity Employer.*

Applications/nominations are invited for the position of **CHAIR OF BIOLOGICAL SCIENCES** at East Tennessee State University starting July 1, 2006. The successful candidate will have an earned doctorate in the life sciences, a commitment to teaching and research, sustained extramural research funding, a record that qualifies him/her for tenured full professorship, evidence of strong leadership and administrative capabilities. The Department seeks to expand its research productivity and graduate program building on an exceptionally strong undergraduate program. Area of expertise is open, but candidates who could strengthen the Department's involvement in the Institute for Quantitative Biology, the health or environmental sciences, paleontology, or proteonomics/molecular biology are encouraged to apply. Send a letter of application, curriculum vitae, and statement of teaching, research, service, leadership philosophy, and contact information for at least three references to:

Michael L. Woodruff
Office of the Vice Provost for Research
Box 70565, ETSU
Johnson City, TN 37614

Application materials should be e-mailed to: **woodrufm@etsu.edu**. Application review will begin on November 1, 2005, and continue until the position is filled.

ETSU is an Affirmative Action/Equal Opportunity employer.

CENTER FOR THE PHYSICS OF INFORMATION
California Institute of Technology

The Center for the Physics of Information at the California Institute of Technology will have **POSTDOCTORAL SCHOLAR** positions available beginning September 2006. Researchers interested in all aspects of the interface between information science and physical science are invited to apply.

Please apply online at **website: http://www.ist.caltech.edu/joinus/positions.html.**

Electronic copies of your curriculum vitae, publication list, statement of research interests, and three letters of recommendation are required. The deadline for receipt of all application materials is January 13, 2006. *The California Institute of Technology is an Equal Opportunity/Affirmative Action employer. Women, minorities, veterans and disabled persons are encouraged to apply.*

POSITIONS OPEN

POSTDOCTORAL, RESEARCH, AND CLINICAL FELLOWSHIPS
at the
National Institutes of Health
U.S. Department of Health and Human Services

Website: http://www.training.nih.gov

NIH is dedicated to building a diverse community in its training and employment programs.

IOWA STATE UNIVERSITY
Department of Physics and Astronomy
Physics of Biological Systems

Applications are invited for a tenure-track **FACULTY** position to begin August 2006. We seek candidates with the strongest credentials and promise of future accomplishment in a forefront area of the physics of biological systems. The successful applicant will be expected to interact with researchers within the department as well as researchers in other disciplines. Potential approaches include single molecule studies, spectroscopy, diffraction methods and theoretical biological physics. Candidates at the assistant professor level are expected to have a Ph.D. in physics or a closely related discipline and a demonstrated record of research accomplishments normally achieved through postdoctoral experience. All candidates should demonstrate promise for excellence in teaching at both the undergraduate and graduate levels. Further information about the Physics and Astronomy Department and the life sciences program at ISU are on the web at **websites: http://www.physics.iastate.edu** and **http://www.bioinformatics.iastate.edu/.**

Applicants should send a letter of application, a resume including a statement of research and teaching interests, along with names, and contact information for at least three references. Please arrange for these letters of recommendation to be sent to: **Physics of Biological Systems Search Committee, c/o Ms. Gloria Oberender, Department of Physics and Astronomy, Iowa State University, Ames, Iowa, 50011-3160.** E-mail applications will not be considered. Applications will be accepted until December 15, 2005, or until the position is filled. *Iowa State University is an equal opportunity employer. Women and minorities are encouraged to apply.*

FACULTY POSITION IN NUTRITION AND AGING. The Department of Nutrition and Exercise Sciences and the Linus Pauling Institute at Oregon State University (OSU) invite applications for a tenured or tenure-track, full-time faculty position in the newly created Center for Healthy Aging Research. The successful candidate will be expected to establish or maintain a competitive research program focused on studying the role of diet or micronutrients in influencing cellular and physiological function during aging. Research on the interactive effects of inflammation or immunoscenescence, nutritional factors, and aging are of particular interest. The successful candidate is also expected to contribute to undergraduate and graduate teaching, and academic service appropriate with faculty rank. Send or e-mail a letter of application with research and teaching interests, curriculum vitae, and names of three references by November 15, 2005, to: **Search Committee, c/o Barbara McVicar, Linus Pauling Institute, Oregon State University, 571 Weniger Hall, Corvallis, OR 97331-6512, E-mail: lpi@oregonstate.edu.** For full position announcement see **website: http://oregonstate.edu/jobs.** *OSU is an Affirmative Action/Equal Opportunity Employer.*

POSITIONS OPEN

STATISTICAL GENETICIST
Institute of Medical Sciences University of Tokyo (IMSUT)

IMSUT is collaborating with the RIKEN SNP Research Center on the Japan Biobank Project, a national research programme to identify and to investigate susceptibility genes for diseases of major public health significance. In conjunction with this project, IMSUT intends to create a new group with an international profile in the area of statistical genetics.

IMSUT is now seeking to appoint a statistical geneticist to play a lead role in this development. This is a unique opportunity for a dynamic researcher to participate in a major national programme in disease genetics in Japan. The successful applicant will be responsible for implementing new methodologies for genetic and epidemiological analysis, and for applying these to the analysis of data from the Japan Biobank project. He/she should have a strong background in genetic epidemiology, statistics and software development, and should be capable of obtaining independent support from Japanese and international funding agencies. The appointment is initially for five years at the equivalent of Assistant Professor with the possibility of renewal. A higher-level appointment may be considered for an exceptionally qualified and experienced candidate. Salary will be determined according to the University Corporation standard.

Applicants should submit a curriculum vitae (including the names of two referees). The mailing address is posted at **website: http://www.ims.u-tokyo.ac.jp/imswww/Event/notice050930.htm.**

The closing date for applications is November 30, 2005.

RESEARCH ASSOCIATE positions are available to study vascular wall remodeling and angiogenesis. Experience with balloon injury model of restenosis and/or angiogenesis is highly desirable. Based on experience competitive salaries are offered. Highly motivated candidates with a Ph.D. or M.D. degree should send curriculum vitae and three letters of references to:

Dr. G. N. Rao
Department of Physiology
University of Tennessee
Health Science Center
894 Union Avenue
Memphis, TN 38163
E-mail: grao@physio1.utmem.edu

The University of Tennessee is an Equal Employment Opportunity /Affirmative Action/Title VI/Title IX/Section 504/ADA/ADEA institution in the provision of its education and employment programs and services.

POSTDOCTORAL RESEARCH position to study genes cooperating with AKT in oncogenesis. The ideal candidate would be a recent Ph.D. with experience in mouse genetics, cell signaling, and tumor cell biology. Please send curriculum vitae and the names of three references to:

Dr. Joseph R. Testa,
Fox Chase Cancer Center
Human Genetics Program
333 Cottman Avenue,
Philadelphia, PA 19111-2497.
E-mail: JR_Testa@fccc.edu
Equal Opportunity Employer

Fox Chase Cancer Center has an immediate opening available for a **RESEARCH CYTOGENETICIST** with prior experience with FISH. Training in chromosome analysis and molecular genetics preferred. Please send curriculum vitae and the names of three references to:

Dr. Joseph R. Testa
Fox Chase Cancer Center
Human Genetics Program
333 Cottman Avenue
Philadelphia, PA 19111-2497
E-mail: Joseph.Testa@fccc.edu
Equal Opportunity Employer

Third International Conference
Ubiquitin, Ubiquitin-Like Proteins, and Cancer

February 9-11, 2006

Department of Cardiology
The University of Texas
M.D. Anderson Cancer Center

Organized by Edward T.H. Yeh

Application and Abstract Deadline
November 11, 2005

For more information visit:
www.sentrin.org

THE UNIVERSITY OF TEXAS
MD ANDERSON
CANCER CENTER
Making Cancer History®

Confirmed Speakers

James Chen
Mary Dasso
George N. DeMartino
Raymond J. Deshaies
Ivan Dikic
Ronald T. Hay
Avram Hershko
Erica S. Johnson
Peter-M. Kloetzel
Hsing-Jien Kung
Christopher D. Lima
Leroy F. Liu
Michael J. Matunis
Frauke Melchior
Kim Orth
Michele Pagano
Cam Patterson
Ze'ev Ronai
Brenda A. Schulman
William P. Tansey
Ning Wei
Allan M. Weissman
Yue Xiong
Dong-Er Zhang
Yanping Zhang

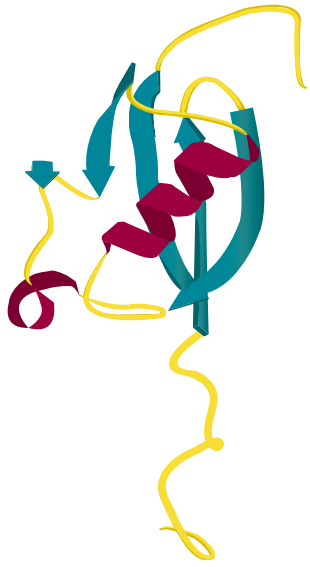

THE UNIVERSITY of York

DEPARTMENT OF BIOLOGY

Lectureship in Mammalian Biochemistry

The Biology Department is large and multidisciplinary, with an outstanding performance in teaching (QAA subject review grade 24/24) and research (RAE grade 5) in one of the UK's leading Universities. A £25m building and refurbishment programme has provided first-rate laboratories and a technology facility housing a full range of state-of-the-art equipment. In addition to recent expansion of cell biology research in York, the biomedical research base is being developed in conjunction with the new and highly successful Hull-York Medical School.

Applicants should have a proven track record of high quality biochemical research in cell-based or organismal systems. Areas of particular interest include lipid-based intracellular signalling, membrane proteins and receptors and vesicle trafficking, although applicants working in other areas of mammalian biochemistry are also encouraged to apply.

Informal enquiries should be directed either to the Chair of Biochemistry, Professor Colin Kleanthous, tel: 01904 328820, email: ck11@york.ac.uk or Head of Department, Professor Dale Sanders, tel: 01904 328650, email: biohod@york.ac.uk

Salary will be within the range £24,820 - £35,883 p.a. (pay award pending).

For further particulars and details of how to apply, please see our website: http://www.york.ac.uk/admin/persnl/jobs/ or write to the Personnel Office, University of York, Heslington, York YO10 5DD, quoting reference number DA05426.

Closing date: 14 November 2005.

The University of York is committed to diversity and has policies and developmental programmes in place to promote equality of opportunity. It particularly welcomes applications from ethnic minority candidates.

www.york.ac.uk

GENETIC ANALYSIS: Model Organisms to Human Biology

GSA Genetics Society of America

GSA MEETING

Genetic Analysis:
Model Organisms to Human Biology

January 5-7, 2006
San Diego, California

Growth, Differentiation and Cancer
Steve Elledge, Charles Sherr, Vicki Lundblad, Titia de Lange, Iswar Hariharan

Gene Interactions and Unraveling Complex Traits
Aravinda Chakravarti, Chuck Langley, Allen Orr, Trudy Mackay, Peter Donnelly

New Insights in Epigenetic Phenomena
Art Beaudet, Barbara Meyer, Vicki Chandler, Steve Henikoff

Stem Cell Genetics
Judith Kimble, Janet Rossant, Allan Spradling, Liheng Li

Neurological Diseases
Susan Lindquist, Jeremy Berg, Li Hui Tsai, Mario Capecchi, Cynthia Kenyon

Comparative Genomics
Maynard Olson, Eric Green, Bill Gelbart, David Kingsley, Richard Durbin

Technology
Stan Fields, George Church, Ron Davis, Lee Hood

KEYNOTE SPEAKERS: PAUL NURSE, MARY-CLAIRE KING, SYDNEY BRENNER

Two poster sessions
PLUS additional speakers chosen from abstract submissions!

Abstract Deadline: November 14

Register for this meeting at
www.GSA-MODELORGANISMS.org

TriFECTa™

IDT's winning Dicer-Substrate RNAi Kit

Why run behind with ordinary 21mer siRNA's? They only mimic Dicer products and bypass interaction with important components of the endogenous RNAi pathway.

Not so with our Dicer-Substrate RNAi. Published experiments show that 27mer siRNA duplex designs can yield up to a 100-fold increase in potency over first-generation 21mer designs [1]. Our RNAi duplexes are HPLC purified and backed by our functional knockdown guarantee.* Tri*FECTa*'s huge performance edge is based on our proprietary Dicer-Substrate technology#. Our unique Dicer cleavage design rules (free to you online) direct the dicing to get the specific results you want for maximum potency [2]. They're flat out winners!

Each Tri*FECTa*™ Dicer-Substrate RNAi kit contains:
3 Dicer-Substrate RNAi duplexes, ESI-MS QC and HPLC purification for each duplex, duplex resuspension buffer, negative and positive control duplexes, and a fluorescent, transfection control duplex.

Order or get the details now at www.idtdna.com.

*Using the IDT design service. IDT guarantees that at least 1 of the 3 duplexes will give a 70% knockdown of the target mRNA (when >90% transfection efficiency and >90% knockdown with positive control is demonstrated).
Patent Pending

THESE PRODUCTS ARE NOT FOR USE IN HUMANS OR NON-HUMAN ANIMALS AND MAY NOT BE USED FOR HUMAN OR VETERINARY DIAGNOSTIC, PROPHYLACTIC OR THERAPEUTIC PURPOSES.

Innovation and Precision in Nucleic Acid Synthesis

IDT
INTEGRATED DNA TECHNOLOGIES, INC.

1710 Commercial Park Coralville, IA 52241 USA
800.328.2661 www.idtdna.com

References:
1. Kim, D.-H., Behlke, M.A., Rose, S.D., Chang, M.-S., Choi, S., and Rossi, J.J. (2005) Synthetic dsRNA dicer substrates enhance RNAi potency and efficacy. Nature Biotechnology, 23:222-226.

2. Rose, S.D., Kim, D.-H., Amarzguioui, M., Heidel, J.D., Collingwood, M.A., Davis, M.E., Rossi, J.J., and Behlke, M.A. (2005) Functional polarity is introduced by Dicer processing of short substrate RNAs. Nucleic Acids Res., 33:4140-4156.